RAiSE

Conference Proceedings

INTERNATIONAL CONFERENCE ON RECENT ADVANCEMENTS IN SCIENCE AND ENGINEERING

(RAiSE '23)

12 - 13 APRIL, 2023

KMCT

COLLEGE OF ENGINEERING FOR WOMEN

International Conference on Recent Advancements in Science and Engineering (RAiSE '23)

KMCT College of Engineering for Women

Published By:

BOOK RIVERS

Website: www.bookrivers.com

Email: publish@bookrivers.com

Place: Lucknow

Year: 2023

ISBN: 978-93-5515-988-5

[PRINTED IN INDIA]

CONTENTS

Mechanical Properties And Bond Behaviour Of Polypropylene Fibers And Nano Silica In Concrete

Haritha Y M
Dept.of Civil Engineering
AWH Engineering College
Kozhikode, Kerala, India
harithaprasanth1998@gmail.com

Sabeena M V
Dept.of Civil Engineering
AWH Engineering College
Kozhikode, Kerala, India
sabeena@awhengg.org

Abstract- Concrete has a substantial impact on the environment as the cement, whose production involves a large amount of CO2, is its main ingredient. Incorporating a small amount of nanoparticles in concrete can modify the nano-structure of cementitious materials, and thus procure high durability. This present work explains the effect of use of nano- silica material and polypropylene fibers with traditional concrete mix. The Nano silica contents of 2,3 and 4 % by replacing cement and polypropylene fiber by 0.1, 0.15 and 0.2% of volume of concrete were considered. Various properties of concrete such as flexural tensile strength, compressive strength, split tensile strength were determined. Pullout test (IS 2770 part 1: 1967) were also conducted to study the effect of nano silica and polypropylene fiber on the bond strength of reinforcement bars and compared with normal concrete. The tests are carried out at the casting age of 28 days. It is concluded that use of nano- material and polypropylene fibers has minute change on its compressive strength. The Split tensile strength, flexural tensile strength gets enhanced by some considerable amount. The results of the study showed that the presence of both nano silica and polypropylene fibers in optimal percentages, can improve the mechanical properties as well as bond strength of reinforcement bars embedded in concrete.

Keywords—Nano silica, Polypropylene fiber, pull out test, Bond strength.

I. INTRODUCTION

The behaviour of reinforced concrete (RC) structures depends up on the type of bond developed between the steel reinforcement and the surrounding concrete. To ensure the integrity of various constituent or composite action of concrete and steel reinforcement, sufficient bond should be developed by the surrounding concrete with the reinforcement.[1]Proper bond between the steel reinforcement and the surrounding concrete is also crucial for the overall strength and serviceability of RC members.

Fibre reinforced concrete is concrete containing fibrous material which increases its structural integrity. It contains discontinuous, discrete, uniformly distributed and randomly oriented fires. Polypropylene fibres used in this study come under synthetic fibres. Polypropylene fibre (PPF) is a kind of linear polymer synthetic fibre obtained from propylene polymerization. It has some advantages such as light weight, high strength, high toughness, and corrosion resistance. The PPF is widely used in chemical industry, energy, clothing, environmental protection, and construction.[2] When PPF is added in concrete, the three-dimensional random distribution network structure can be formed in concrete, which effectively inhibit the microcrack generation and development. As a result, the PPF can prevent water and other harmful ions entering into concrete. The durability of concrete can be improved by adding PPF.[3]

Modern concrete infrastructure requires structural components with higher mechanical strength and greater durability. A solution is the addition of nanomaterials to cement-based materials, which can enhance their mechanical properties. Optimal dosages of these materials can improve the compressive, tensile and flexural strength of cement-based materials, as well as their water absorption and workability.[4] Nano-silica (NS) or silica nanoparticles, also known as silicon dioxide nanoparticles, can be used as additives for improving concrete's mechanical and durability properties. The effect of NS on nanostructure of cement paste also confirmed the improvement in concrete durability. Using NS as a cement replacement makes concrete more cost-effective and reduces the CO2 footprint of the

concrete products.[5] Due to their improved performance in filling effect and particle size distribution, thereby decreasing the porosity in concrete and increasing their pozzolanic reaction.[6]

II. OBJECTIVES

The prime research objectives of this present work are as follows:

- To determine the mechanical properties of concrete specimens
- To obtain optimum combination of nano silica and polypropylene fiber in concrete.
- To determine the bond strength corresponding to the pull-out force in rebar embedded in concrete specimen.

III. EXPERIMENTAL PROGRAMME

This experimental programme was carried out to evaluate the bond stress - slip behaviour and pull-out strength of reinforced bars embedded in fibre reinforced concrete. The main variables considered were: (i) weight percentage of nano silica viz; 2%, 3% , 4% and optimum percentage of nano silica in concrete is calculated (ii) Volume fraction of polypropylene fibres viz; 0.1%,0.15% , 0.2%, is added with optimum percentage of nano silica. Thus, optimum percentage of both is calculated. (iii) diameter of reinforcing steel bars(ϕ) viz;16mm and 20mm. Three specimens were cast for each parameter and the average of the two was taken for analysis.

A. Materials

Ordinary Portland cement of 53 grade confirming to IS: 12269-1987 [7] was used. Test on cement were conducted as per IS 4031-1988 [8]. Fine aggregate passing through 4.75 mm IS sieve confining to grading zone III of IS: 383-1970 [9] was used. Crushed stone with a maximum size of 20 mm were used [9]. CONPLAST SP430 complies with IS: 9103:1999 [10] with specific gravity of 1.2 was used as a water reducing agent. Polypropylene fiber of 12mm length from Cera chemicals (P) Ltd is used in concrete. Pure Nano- Silica was collected and its properties are tested in manufactured company. The properties of fibres and nano silica given by the manufacturer are given in Table 1 and II. Reinforcement bars used is Fe500 of Minar TMT brand.

Fig. 1. Nanosilica

TABLE I. PROPERTIES OF NANOSILICA

Specific surface area (m^2/g)	202
pH	4.12
SiO_2 content (%)	99.88
Specific gravity	2.3
Particle size	17 nm

Fig. 2. Polypropylene fibres

TABLE II. PROPERTIES OF POLYPROPY-LENE FIBRES

Length	12mm
Specific gravity	910 kg/m^3
Diameter	0.01mm
Melting Point	162℃

B. Mix Proportions

In this experimental study concrete of M20 grade is used and for that mix design is done based on IS 10262:2009[11]. The details of mix proportions are given in Table III. Required quantities of cement, fine aggregates and coarse aggregates were first mixed thoroughly in a drum type mixer for a period of 2 minutes. During the mixing operation 80% of water was added first and mixed thoroughly and the remaining 20% water, mixed with superplasticizer was added later. The polypropylene fibres were dispersed by hand to the mixture to achieve a uniform

distribution throughout the concrete. Since the addition of fibres reduced the workability of concrete, the dosage of super plasticizer was adjusted to maintain required workability for the mixes.

TABLE III. MIX PROPORTION FOR M20 GRADE CONCRETE

Cement	315.2 kg/m^3
Fine aggregate	820.27 kg/m^3
Coarse aggregate	1149.64 kg/m^3
Water	157.6 kg/m^3
Admixture	3.78 kg/m^3

C. Specimen Preparation

Concrete cubes of size 150 mm, Prism of size 100 x 100 x 500 mm and cylinders with a size 150 mm x 300 mm was prepared for testing compressive strength, flexural strength and tensile strength respectively.[12] To evaluate workability of concrete standard test with actions described with Indian standards BIS 1199-1959 [13] are conducted. Cast iron mould was used to cast specimens and all specimens were filled in concrete with three layers and tamping rod was used to compact the specimens in each layer. Nano silica were mixed concrete by replacing cement in first stage and optimum percentage is calculated. In second stage, optimum amount of nano silica and different percentage of volume of polypropylene fiber is used. After 24 hours of air curing specimens are demoulded and transferred to curing tank. After curing, the specimens were tested.

Fig. 3. Casting of specimen

D. Casting Of Pull Out Specimens

The pull-out specimens were prepared as per IS 516-1959 (reaffirmed 2004) [14]. The specimen consists of concrete cubes 150mm with a single reinforcing bar (16mm or 20mm dia) embedded vertically along the central axis in each specimen. The bar was projected down by about 10 mm from the bottom of the cube for measuring the slip of the reinforcement bar. Also, the bar was projected upwards by about 85 cm from the top face of the cube to provide an adequate length for gripping the specimen in the testing machine. The end of the reinforcing bars on which the tip of LVDT was fixed during the test was ground to a reasonably smooth surface normal to the axes of the bars. The specimens were also reinforced with a helix of 6mm diameter plain mild steel bar at a pitch of 25mm to prevent splitting failure. Moulds for casting were prepared using plywood. De moulding was carried out after 24 hours and then the specimens were immediately placed into curing tank for 28 days of curing.

Fig. 4. Casting of pull out specimens

E. Testing Of Pullout Specimens

The test was conducted as per IS 2770 Part 1:1967 – (reaffirmed 2002) [14] using a universal testing machine of 600kN capacity. While testing, the pullout specimen was mounted on the testing machine in such a manner that the bar is pulled axially from the specimen. As per IS 2770 the end of the bar at which the pull is applied shall be that which project from the top face of the cube as cast. The test framework setup is shown in Fig. 5. Linear variable differential transformer (LVDT) was used to measure the displacement of the bar. Two LVDT's were fixed one at the loaded end and other at the free end of the bar for measuring the slip of the bar with respect to concrete. The LVDT at the free end was placed such that the pointed tip of the LVDT touches the exposed end of rebar on the back end of the specimen to record bar slip. Load was applied to the reinforcing bars monotonically at a rate not greater than 22.5 kN/min. The loading was continued until the specimen failed. The recording of loads and deformations were carried out. The loads recorded were then converted to bond stress. Assuming a uniform bond stress distribution over the embedment length in concrete, the average bond stress between the reinforcing bar and the surrounding concrete τ_b was calculated as,

$$\tau_b = \frac{P}{\pi d_b l_b}$$

where, τb is the bond stress in (MPa), P is the applied load (N), db is the diameter of bar (mm) and lb is the embedded length of bar (mm).

Fig.5. Pull out test setup

IV. RESULTS AND DISCUSSION

A. Nano Silica In Concrete

Nano silica is added to concrete as 2%, 3% and 4% by replacing percentage weight of cement. Table IV shows the details of specimens. Optimum nano silica content in concrete is calculated by conducting compressive strength test, flexural strength test and split tensile strength test.

TABLE IV. DETAILS OF SPECIMENS

MIX DESIGNATION	% CONTENT OF NANO SILICA
NC	-
NS1	2%
NS2	3%
NS3	4%

1) Compressive strength: From Fig. 5., the compressive strength of 26.44 N/mm2 was obtained for the specimen NS2 which is about 12.27 % higher than the control specimen. Further for NS1 and NS3, the compressive strength is 9.42% and 2.84% higher respectively when compared to the control specimen.

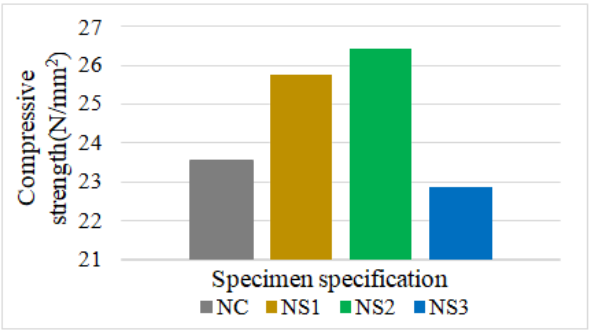

Fig. 5. Compressive Strength

The enhancement of compressive strength is due to the favorable surface physical characteristic that improves the bond between nano silica, fine aggregate and cement paste up to 3 % of nano silica by cement weight.

2) Flexural strength : From Fig. 6., the Flexural strength of 4.68 N/mm2 was obtained for the specimen NS2 which is about 49.04 % higher than the control specimen. Further for NS1 and NS3, the flexural strength is 43.94% and 24.84% higher respectively when compared to the control specimen. It was noted that the flexural behavior of beams containing 3% nano silica behaved in a superior way when compared with corresponding control specimen.

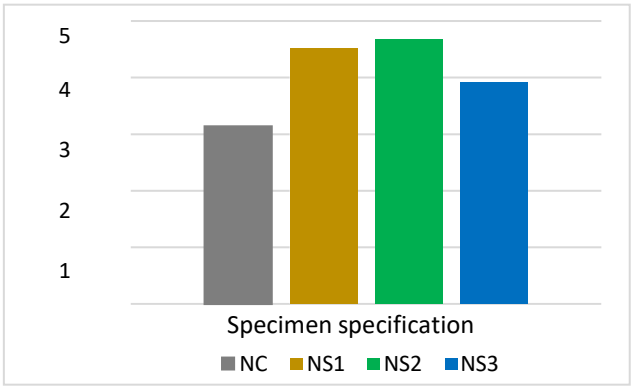

Fig. 6. Flexural strength

3) Split tensile strength: From Fig. 7., the split tensile strength of 2.075 N/mm2 was obtained for the specimen NS2 which is about 8.63 % higher than the control specimen. For NS1 the split tensile strength is 5.49% higher compared to the control specimen. This improvement is because of the more efficient bridging effect across the crack width.

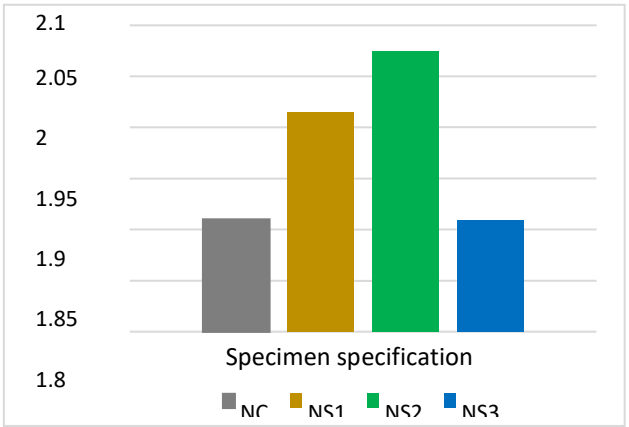

Fig. 7. Split tensile strength

B. Polypropylene Fiber And Nano Silica In Concrete

Polypropylene fiber is added to concrete as 0.1%, 0.15% and 0.2% by percentage volume of concrete. And optimum content of 3% nano silica is added to concrete. Table V shows the details of specimens and variables. By conducting compressive strength test, flexural strength test and split tensile strength test, the optimum content of polypropylene fiber is calculated.

TABLE V. DETAILS OF SPECIMENS AND VARIABLES

MIX DESIGNATION	% CONTENT	
	NANO SILICA	POLYPROPYLENE FIBER
NC	-	-
NSP1	3%	0.1%
NSP2	3%	0.15%
NSP3	3%	0.2%

1) Compressive strength: From Fig. 8., the compressive strength of 26.66 N/mm^2 was obtained for the specimen NSP1 which is about 13.2 % higher than the control specimen. Further for NSP2 and NSP3, the compressive strength is 7.55% and 5.64% higher respectively when compared to the control specimen.

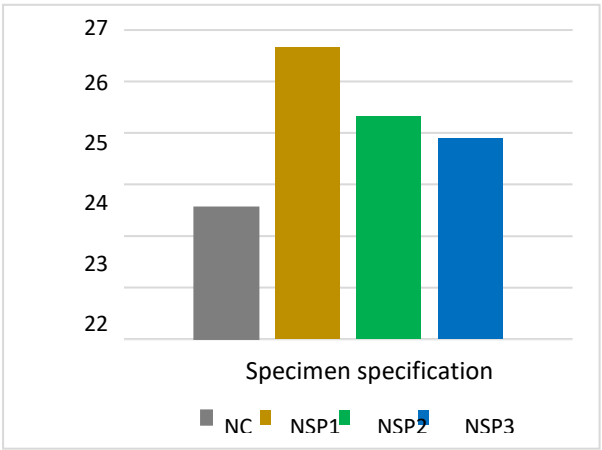

Fig. 8. Compressive strength

2) Flexural strength : From Fig. 9., the Flexural strength of 4.92 N/mm2 was obtained for the specimen NSP1 which is about 56.68 % higher than the control specimen. Further for NSP2 and NSP3, the flexural strength is 50.31% and 47.77% higher respectively when compared to the control specimen.

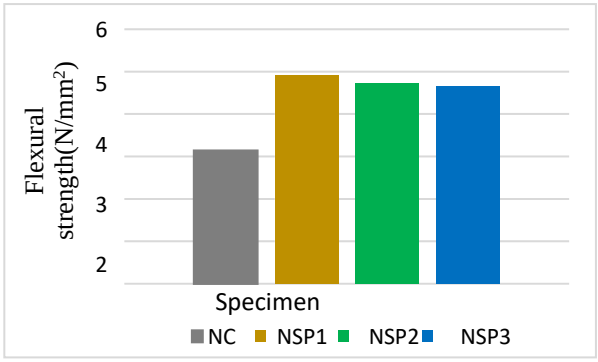

Fig. 9. Flexural strength

3) Split tensile strength: From Fig. 10., the split tensile strength of 2.29 N/mm2 was obtained for the specimen NS2 which is about 19.89 % higher than the control specimen. Further for NSP2 and NSP3, the split tensile strength is 14.65% and 9.47% higher respectively when compared to the control specimen.

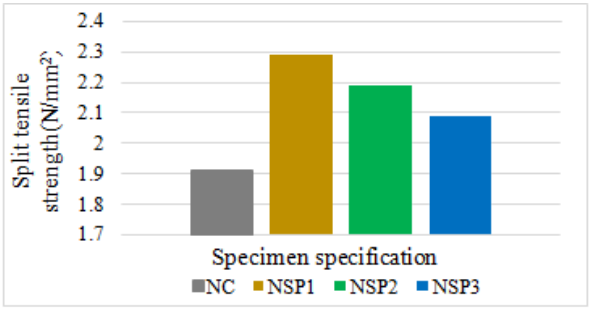

Fig. 10. Split tensile strength

C. Bond Stress

The value of bond stress at a slip of 0.025mm and 0.25mm which is the requirement as per IS 2770 Part (1):1967 (reaffirmed 2002) [14] and the ultimate load and ultimate bond stress of all the specimens which failed due to pullout of reinforcement bars are shown in Table VI. For the comparison of bond stress as per IS 2770 slip at 0.025mm and slip at 0.25mm was noted. The results from table show that the bond stress for Nano silica was more than the control specimen and that for Nano silica and polypropylene fiber was more than control specimen for both 16 and 20mm bars. It can be noted from Table VI that, for a given embedded length and mix the bond stress for smaller diameter bars is more than that of larger diameter bars. This may be because of the larger concrete cover to bar diameter ratio available in the case of small diameter bars which may contribute more to the bond resistance of the bar. When the cover to the reinforcement is

increased, then crack initiation load increases and subsequently bond strength improves.[15]

a) NCΦ16 b) NS2Φ16 c) NSP1Φ16

a) NCΦ20 b) NS2Φ20 c) NSP1Φ20

Fig. 11. Pull out failure

Significant improvement in bond stress was seen in the case of 16 and 20mm bars when the polypropylene fiber and nano silica is added to concrete. In the case of 16mm bar, there was an increase of 15.44% compared to control specimen for 0.1% polypropylene fiber and 3% Nano silica, whereas a significant improvement of 8.94% was seen compared to CS when 3% of nano silica was added. Similarly in the case of 20mm bars, when the polypropylene fiber and nano silica is added to concrete, there was an increase of 13.44% compared to CS. And 4.20% was seen compared to CS when 3% of nano silica was added. For specimens with same bar diameters improvement in bond stress was observed when the polypropylene fiber and nano silica is added.

TABLE VI. PULL OUT TEST RESULTS

Sl.no	Specimen designation	Bond stress at 0.025mm slip (MPa)	% Increase or decrease in bond stress compared to CS	Bond stress at 0.25mm slip (MPa)	% Increase or decrease in bond stress compared to CS	Ultimate load (kN)	Ultimate bond stress (MPa)	Failure mode
1	NCΦ16	12.3	-	11.5	-	121.5	16.07	Pullout
2	NS2Φ16	13.4	8.94	12.3	6.95	128	16.93	Pullout
3	NSP1Φ16	14.2	15.44	13.4	16.52	140.5	18.58	Pullout
4	NCΦ20	11.9	-	11.3	-	130	13.71	Pullout
5	NS2Φ20	12.4	4.20	11.6	2.65	135	14.23	Pullout
6	NSP1Φ20	13.5	13.44	12.6	11.50	150	15.82	Pullout

Bond Stress-Slip Behaviour

Generally bond stress slip relationship represents the bond behaviour in reinforced concrete members. Adhesion of bars to concrete is the principal component that describes the bond performance of the bar at initial loading stages.[16] Once adhesion between bar and concrete breaks, the bar starts to slip and friction between the outer layer of the bar and concrete controls the bond mechanism. The load versus slip values were recorded for all types of specimens during testing and the values were plotted in graph. [17] All curves were found to have almost the same trend. The Fig.12. shows the experimental graph for the bond stress versus slip behaviour of specimens with 16mm bars. Whereas Fig.13. shows the experimental graph for the bond stress versus slip behaviour of specimens with 20mm bars. All curves showed an initial ascending branch up to maximum stress τmax. It also showed a falling branch or softening branch, after the maximum bond stress was attained. This portion of curve was characterized by a significant decrease in the bond stress accompanied by an increase in bar slip.

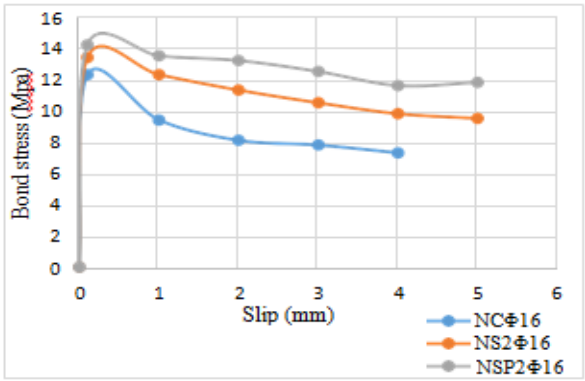

Fig. 12. Bond stress vs slip behavior of specimens withl 6mm bar

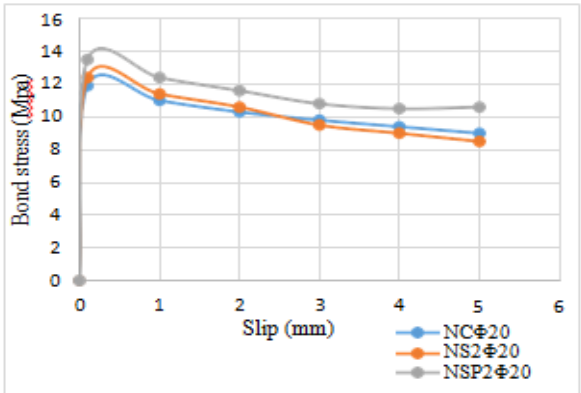

Fig. 13. Bond stress vs slip behavior of specimens with 20mm bar

V. CONCLUSIONS

Based on the experimental results of the study presented in this paper the following conclusions are made.

1. Mechanical properties were found to be maximum for concrete mix containing 3% of nano silica and 0.1% polypropylene fiber.
2. In 1st stage - By addition of 3% nano silica the compressive strength only increased by 12.27% whereas, flexural strength of concrete increased by 49.04%
3. In 2nd stage - By addition of 3% nano silica and 0.1% polypropylene fiber the compressive strength increased by 13.2% and split tensile strength increased by 19.89% whereas, flexural strength of concrete increased by 56.68%.
4. The addition of nano silica and polypropylene fiber improved the bond stress for 16mm and 20mm bar compared to normal concrete specimen.

REFERENCES

1. N. Ganesan, P.V. Indira, M.V. Sabeena "Bond stress slip response of bars embedded in hybrid fibre reinforced high performance concrete" Construction and Building Materials, vol 50, pp. 108–115, 2014.
2. S. Pirotia, M. Najarchia, E. Hezavehib, M.M. Najazadehc, and S.M. Mirhosseini (2020) "The experimental assessment of the effect of polypropylene fibers on the improvement of nano-silica concrete behavior" Scientia Iranica A (2020) 27(2), 682-692
3. S. Pirotia, M. Najarchia, E. Hezavehib, M.M. Najazadehc, and S.M. Mirhosseini (2020) "The experimental assessment of the effect of polypropylene fibers on the improvement of nano-silica concrete behavior" Scientia Iranica A (2020) 27(2), 682-692
4. Mohamed amin, "Effect of using different types of nano materials on mechanical properties of high strength concrete", Construction and Building Materials, No.80 2015,pp. 116–124.
5. Gaurav Tanwar, Rajesh Kumar (2020) "Contrastive Approach to The Use of Nano-Material and Polypropylene Fibers in Reinforced Concrete" International Research Journal of Engineering and Technology, Volume 07, Issue 09, Sep 2020.
6. Abhilash P. P, Dheeresh Kumar Nayak, Bhaskar Sangoju, Rajesh Kumar, Virendra Kumar (2021) "Effect of nano-silica in concrete" Construction and Building Materials - 278 (2021) Pg. No. 122347.
7. IS 12269: 1987 (reaffirmed 2004). Specifications for 53 grade ordinary Portland cement. Bureau of Indian Standards. New Delhi.
8. IS 4031 Part 4, Methods of physical tests for hydraulic cement Determination of consistency of standard cement paste, Bureau of Indian Standards.2004
9. IS 383: 1970 (reaffirmed 2002). Specification for coarse and fine aggregates from natural sources for concrete. Bureau of Indian Standards. New Delhi.
10. IS 9103, Concrete Admixtures Specification,1999
11. IS 10262, Concrete Mix Proportioning Guidelines,2009
12. BIS 1199- 1959, "Methods of Sampling and Analysis of Concrete",2001
13. IS 516-1959 (reaffirmed 2004). Method of test for strength of concrete, Bureau of Indian Standards. New Delhi
14. IS 2770 Part (1):1967 (reaffirmed 2002). Methods of testing bond in reinforced concrete Part I Pull-out Test. Bureau of Indian Standards. New Delhi.
15. N. Ganesan, P.V. Indira, M.V. Sabeena "Bond stress slip response of bars embedded in hybrid fibre reinforced high performance concrete" Construction and Building Materials, vol 50, pp. 108–115, 2014.
16. Sehaj Singha, Arun Shuklaa, Richard Brown (2004) "Pullout behavior of polypropylene fibers from cementitious matrix", Cement and Concrete Research 34 (2004) 1919 – 1925
17. Deepthi. V, Dr Sabeena M. V (2016) "Experimental and Analytical Study on Bond Performance of Reinforced Bars Embedded in Fibre Reinforced Concrete", International Journal of Innovative Research in Science, Engineering and Technology, Vol. 5, Issue 8, August 2016.

Analysis and Design of Multi-Storey Steel Staggered-Truss System

Shanila P
Dept of Civil Engineering
AWH Engineering College
Kozhikode, India
email:shanilanice@gmail.com

Minu U
Dept of Civil Engineering
AWH Engineering College
Kozhikode, India
email:minuawhengg.org

Abstract— A staggered Truss System (STS) is a new concept in the high-rise building construction. It is an effective design technique to improve the efficiency in building construction. It was first developed in Massachusetts Institute of Technology in 1960s. By providing STS we can increase the strength and ductility of the building. It helps to cut down the number of interior columns and thereby reduce the cost of the building construction. In this project analytical investigation on the seismic behaviour of a 16-storey steel staggered-truss system using the ETABS software was conducted. The structural shape of the trusses was varied, and their influences on seismic behaviours of the system were studied. The seismic performance of STS structures by varying the Vierendeel panel width was also evaluated. The models were analysed by using time history analysis method. From the analysis result maximum storey displacement, maximum storey drift and base shear is extracted. From the result it was found that the model with warren trusses showed the highest strength and stiffness to the corresponding earthquake but all other truss shapes were also achieved the target performance level and also the model with less Vierendeel panel width shows higher base shear and lower inter storey drift and displacement.

Keywords—Staggered Truss System, Seismic loading, Time History Analysis, ETABs.

I. INTRODUCTION

The staggered truss system was developed in the USA by the Massachusetts Institute of Technology (MIT) in the 1960s. It was a new concept in the construction of high-rise buildings. A Staggered Truss Framing (STF) system consists of a series of structured trusses, with an opening in the middle of truss span (Vierendeel panel) that serve s as a corridor on the floor. This system is efficient for midrise apartments, hotels, dormitories, hospitals, and other structures for which a low floor to-floor height is desirable. The staggered truss framing system is used in building to improve efficiency of the structure. The staggered -truss framing system is one of the only framing system that can be used to allow column - free areas sized 18 to 21 meter. For achieving a large column- free area twice than column spacing the STS should be provided at an alternate floor level. A staggered truss system was generally suitable for rectangular buildings and is usually provided in the shorter direction. As columns are located only on the exterior faces of the building, large clear span and open areas can be created. Compared with conventional reinforced concrete residential buildings' plan layouts which are divided into many small spaces by vertical shear walls, the residential buildings with staggered trusses placed at alternate levels have enhanced spatial flexibility with the economy and constructability. The vertical loads concentrated at a few columns normally exceed the uplift forces generated by the lateral loads and, as a result, uplift anchors are often not required. The reduced number of columns also results in less foundation formwork, less concrete, and reduced construction time. When used, precast plank is lighter than cast-in-place concrete, the building is lighter, the seismic forces are smaller, and the foundations are reduced. The STS system is normally economical, simple to fabricate and erect, and as a result, is often cheaper than other framing systems. Other benefits include minimum deflection and greater stiffness in the structure. The reduced weight of the superstructure results in reduced seismic loads and substantial cost savings in foundation work. It was reported that the structural costs per unit building area turned out to be relatively low in STS. The STS, however, has not been considered as one of the basic seismic-force-resisting systems in most of design codes, which implies that further research is still necessary for the system to be accepted as a standard structure system for seismic load. For STS guidelines are given in

"Design Guide 14" by AISC (American Institute of Steel Construction) but there is no guideline given by Indian standard. The purpose of this project is analytical investigation on the behaviour of an 16-storey steel staggered-truss system using the ETABS software. The parameters such as the shape of trusses and Vierendeel panel width were varied, and their influences on seismic behaviours of the system were studied. Based on the analysis result storey displacement, storey drift and base shear of the building was extracted and compared.

II. MODELLING

In this project 12 models were designed and analyzed by using ETAB software. Time history method was used for the analysis. The 1940 El Centro earthquake (or 1940 Imperial Valley earthquake) is taken for the time history analysis.

TABLE I. PROPERTIES OF MODEL

Type of building	Steel building with RCslab
No.of stories	G + 15
Dimension of plan area	36×17m
Height of each storey	3m
Bay spacing in x direction	6m
Bay spacing in y direction	3.4m
Column size	WPB 400×400
Beam size	ISMB 600
Slab thickness	0.1m
Grade of steel	Fe 345
Grade of concrete	M 20
Live load	3 kN/m^2
Floor finish	1 kN/m^2
Roof load (flat roof)	0.75 kN/m^2

TABLE II. SEISMIC AND WIND DATA

SEISMIC DATA		WIND DATA	
Code	IS	Code	IS
Zone factor	0.36 (V)	Wind speed	39 m/s
Importance factor	1.2	Terrain category	4
Response reduction factor	5	Windward coefficient	0.8
Soil type	II	Leeward	0.5

A. Model 1

It consists of model with pratt truss arranged in a way that the first floor consist of 4 frames with pratt truss and 3 frames with open truss. It consists of 3 models with varying VP width. Model 1A consist of pratt truss with 2m VP width. Model 1B consist of pratt truss with 2.5m VP width. Model 1C consist of pratt truss with 3m VP width.

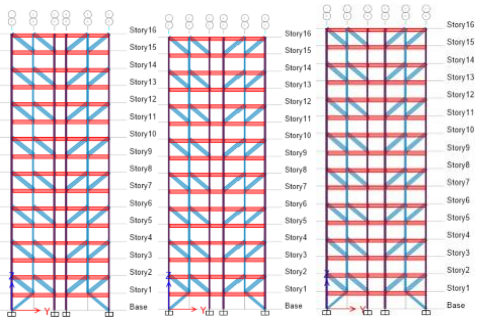

(a) (b) (c)

Fig. 1. Elevation of model (a)1A (b)1B and (c)1C

B. Model 2

It consists of model with howe truss arranged in a way that the first floor consist of 4 frames with howe truss and 3 frames with open truss. It consists of 3 models with varying VP width. Model 2A consist of howe truss with 2m VP width. Model 2B consist of howe truss with 2.5m VP width. Model 2C consist of howe truss with 3m VP width.

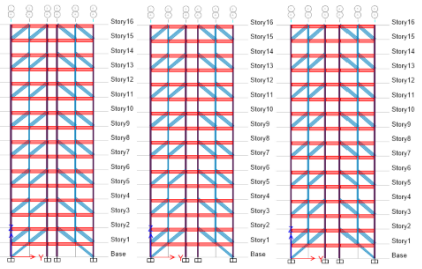

(a) (b) (c)

Fig. 2. Elevation of model (a)2A (b)2B and (c)2C

C. Model 3

It consists of model with warren truss arranged in a way that the first floor consist of 4 frames with warren truss and 3 frames with open truss. It consists of 3 models with varying VP width. Model 3A consist of warren truss with 2m VP width. Model 3B consist of warren truss with

2.5m VP width. Model 3C consist of warren truss with 3m VP width.

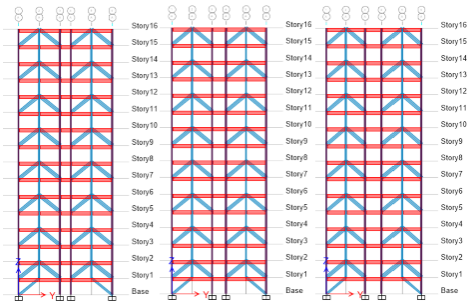

(a) (b) (c)

Fig. 3. Elevation of model (a) 3A (b) 3B and (c) 3C

D. Model 4

It consists of model with K truss arranged in a way that the first floor consist of 4 frames with K truss and 3 frames with open truss. It consists of 3 models with varying VP width. Model 4A consist of K truss with 2m VP width. Model 4B consist of K truss with 2.5m VP width. Model 4C consist of K truss with 3m VP width.

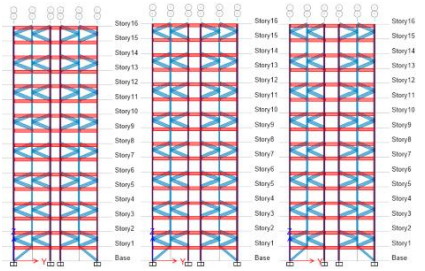

(a) (b) (c)

Fig. 4. Elevation of model (a)4A (b)4B and (c)4C

III. RESULTS AND DISCUSSION

The 12 models were analysed by using time history analysis method. From the analysis results the maximum storey displacement, maximum storey drift and base shear was extracted. The models were compared on the basis of Vierendeel panel width and shape of trusses. The STS were provided in the Y direction hence the analysis results in Y direction is taken for the comparison.

A. Comparison of Virendeel Panel width

In this the models were studied by varying Vierendeel panel width. The comparison of models was done to find the model with which VP width have greater seismic performance.

TABLE III. ANALYTICAL RESULTS

MODEL	MAX STOREY DISPLACEMENT		MAX STOREY DRIFT		BASE SHEAR	
	X direction	Y direction	X direction	Y direction	X direction	Y direction
3PA	1377.233	171.796	0.037155	0.004777	3328.539	14440.88
3PB	1371.395	188.291	0.037004	0.005266	3327.012	13351.49
3PC	1404.672	201.877	0.03784	0.005656	3316.741	12345.58
3HA	1377.121	168.331	0.037152	0.004651	3328.56	15173.07
3HB	1371.261	184.391	0.037002	0.005129	3327.036	13644.72
3HC	1404.542	200.303	0.037838	0.005581	3316.775	12570.74
3WA	1377.051	166.219	0.037151	0.004669	3328.454	15376.38
3WB	1371.211	181.387	0.037	0.005148	3327.049	13796.23
3WC	1404.499	196.224	0.037837	0.005565	3316.79	12870.45
3KA	1407.604	172.963	0.037989	0.004784	3405.792	14616.99
3KB	1400.654	189.978	0.037809	0.00528	3401.696	13499.72
3KC	1432.159	203.492	0.038595	0.00567	3385.188	12475.08

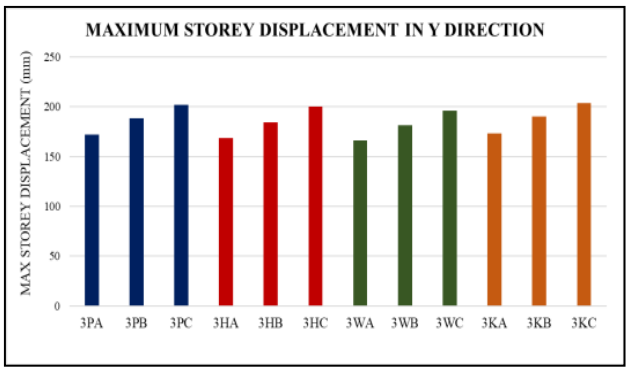

Fig. 5. Maximum storey displacement in Y direction

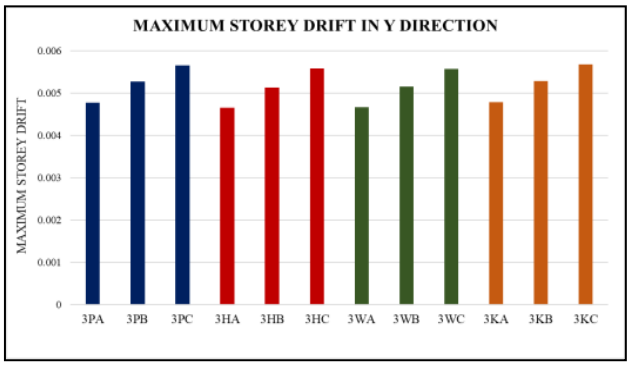

Fig. 6. Maximum storey drift in Y direction

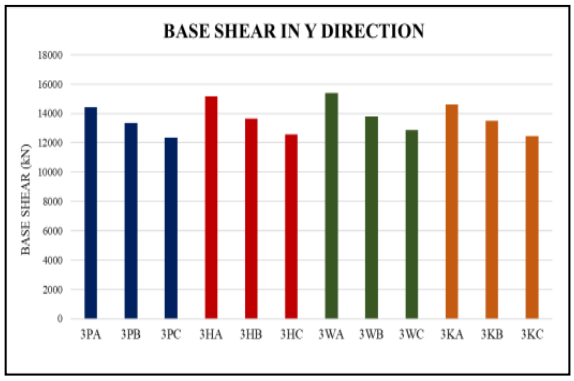

Fig. 7. Base shear in Y direction

From the analysis result, (i.e.; from Fig. 5, 6 and 7) it was observed that for all truss shapes the model with 2m Vierendeel panel have lower maximum storey displacement, inter storey drift and maximum base shear. It was also observed that model with warren truss having 2m VP width shows better seismic performance.

B. Comparison Of Shape Of Trusses

In this the models were studied by varying shape of trusses. The comparison of models was done to find the model with which type of truss have greater seismic performance.

TABLE IV. ANALYTICAL RESULTS

MODEL	MAX STOREY DISPLACEMENT		MAX STOREY DRIFT		BASE SHEAR	
	X direction	Y direction	X direction	Y direction	X direction	Y direction
3PA	1377.233	171.796	0.037155	0.004777	3328.539	14440.88
3HA	1377.121	168.331	0.037152	0.004651	3328.56	15173.07
3WA	1377.051	166.219	0.037151	0.004669	3328.454	15376.38
3KA	1407.604	172.963	0.037989	0.004784	3405.792	14616.99

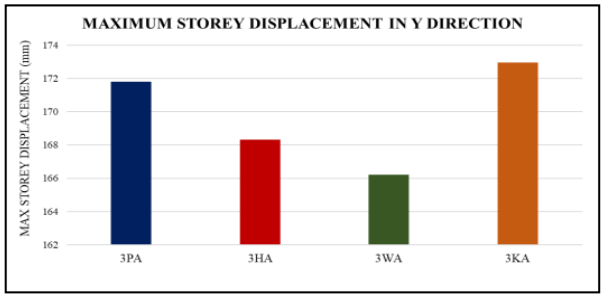

Fig. 8. Maximum storey displacement in Y direction

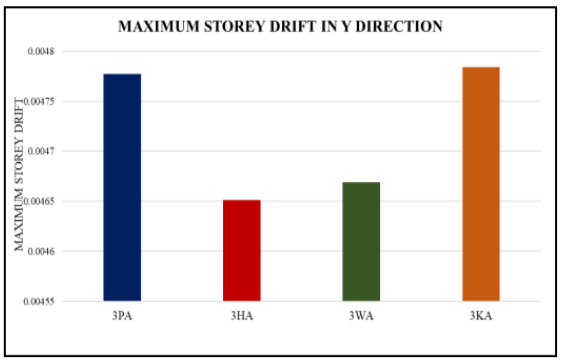

Fig. 9. Maximum storey drift in Y direction

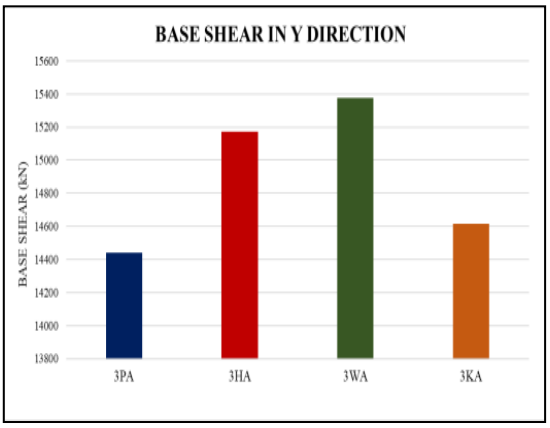

Fig. 10. Base shear in Y direction

From the Fig. 8., it was observed that the model with warren trusses have less maximum storey displacement. From the Fig. 9., it was seen that the model with howe truss shows lower inter storey drift. From the Fig. 10. the model with warren truss shows maximum base shear. So we can say that from the analysis result warren truss shows better seismic performance.

IV. CONCLUSION

The seismic analysis of steel staggered truss system of high-rise building has been completed. From the analysis result it was concluded that the model with warren truss having 2m Vierendeel panel width shows better seismic performance. It is observed that as the Vierendeel panel width increases the stiffness and ductility of the structure decreases. From the comparison of shape of trusses, it was observed that warren trusses show lower displacement, inter storey drift and higher base shear. Because this shape transfers the loads effectively than that of others.

ACKNOWLEDGMENT

I would like to express my acknowledgement to the faculty of civil engineering department of AWH engineering college, Kozhikode, India for providing the computer lab for to accomplish this study.

REFERENCES

1. Awkar J. C. and Lui E.M, "Seismic analysis and response of multistory semi rigid frames", Journal of Engineering Structures, Volume 21, Issue 5, Page no: 425-442, 1997.
2. Durgadas Ashok Rude, Harshvardhan Rangari, "Analysis and Design Multi-storey Steel Staggered-Truss System RC Slab Using ETABs", International Journal for Modern Trends in Science and Technology, 8(06):06-16, 2022.
3. Kim, J., & Jun, Y, " Seismic performance evaluation of partially staggered-wall apartment buildings", Magazine of Concrete Research, 63(12), 927–939,2011.
4. Kim Jinkoo, Joonho Lee, "Seismic behavior of staggered truss system" , First European Conference on Earthquake Engineering and Seismology, Geneva, Switzerland, 2006 .
5. Pradeep, S., & Pradeep, S. "Behaviour of Steel Staggered Truss System Under Seismic Loading" © I a E M E. 1215(July), 177–186. (2015)
6. IS 12778: 2004, "Hot Rolled Parallel Flange Steel Sections for Beams, Columns and Bearing Piles – Dimensions and Section Properties", Bureau of Indian Standards, New Delhi.
7. IS 1893 (Part 1): 2016, "Criteria for Earthquake Resistant Design of Structures", Bureau of Indian Standards, New Delhi
8. IS 800:2007, "General construction in steel – Code of Practice Bureau of Indian standards, New Delhi".
9. IS: 875(Part-1)- 1987 "Code of Practice for Design Loads (Other than Earthquake) buildings and structures", Part-1 Dead load, Unit weight of building materials and stored materials, Bureau of Indian Standards, New Delhi
10. IS: 875(Part-2)- 1987 "Code of Practice for Design Loads (Other than Earthquake) buildings and structures", Part-2 Imposed loads, Bureau of Indian Standards, New Delhi
11. IS: 875(Part-3)- 1987 "Code of Practice for Design Loads (Other than Earthquake) buildings and

Wind Load Analysis Of Rc Structure Resting On Sloping Ground By Using Etabs

Aysha Rashmin
Dept. of Civil Engineering
AWH Engineering College
Kozhikode, India
ayshae34@gmail.com

Priyanka Devan
Dept. of Civil Engineering
AWH Engineering College
Kozhikode, India
priyankadevan777@gmail.com

Abstract—Wind load is regarded as one of the crucial design loads that a structure must withstand throughout its lifetime. The impact of wind speed on the building frame has been investigated in this research. Due to a lack of available land, buildings lying on slopes were taken into consideration for the study. The 40-story, three-dimensional building frame is modelled and examined for wind zones of 33 m/s and 39 m/s, respectively. It rests on slopes of 5°, 10°, and 15°. ETABS software is used to perform the modelling and analysis as necessary. The maximum storey displacement and maximum storey drift are the factors taken into account for the post analysis. For ground slopes and wind speeds, all the parameters have been compared, and the findings have been compiled and graphically shown.

Keywords— sloping ground, displacement, drift,, wind zones, ETABS

I. INTRODUCTION

Modernization, industrialisation, and social rationalisation have all contributed to a growth in urbanisation over the last few decades. More than half of the world population lives in urban areas. In modern days urbanization is considered as a sign of economic progress but at the same time urban areas becoming more populated and dense. On the other hand land scarce and ever growing demand of accommodation also increasing. Therefore Owing to scarce land resources, urbanization and ever-growing demand of accommodation is leading developers into sloping grounds. To overcome this problem the only solution is that to prefer multi-storeyed structural buildings in the current scenario of this world. In this regard realistic analysis and design of these building frames on sloping ground are of paramount importance. Wind is the major factor This has an impact on the structure sitting on sloped ground. Wind load is one of the important design load in civil engineering. Buildings bend and twist elastically under static wind loads, which has an impact on the structure's structural design. Therefore knowledge of the characteristics of structure under wind loading becomes a requirement in engineering design. The goal of structural engineers is for the structure to remain serviceable despite anticipated wind deflections by having sturdy structural components that can resist excess loads over the course of the building's life. This project is based on research on wind and how multi-story buildings behave. Buildings atop hill slopes are typically asymmetrical in design. in this project. In this project, three different height of building frames resting on four different slopes of ground for five different wind speeds are analysed. The study is carried out on software ETABS for effect of wind on building frame resisting on sloping ground. The influence of slope and wind on the building frame will be investigated and analyzed using ETABS software.

The objectives of this work is to study the effect of wind velocity on building with different inclined slope.

II. .METHODOLOGY

The methodology employed for this investigation is explained in depth in this section of the research article. The following stages are used to carry out the entire investigation, from modelling through analysis and result.

Step 1: Choosing the building frame The 40-story building frame is utilised in this study for modelling purposes. The height of each storey is 3.3 metres. Both the x and y directions have five bays.

Step 2: Choosing slope, the three varied ground slopes. The slopes on which the buildings are perched are 5°, 10°, and 15°.

Step 3: Selecting wind zones. As per IS 875:2015 part 3 the wind velocities of 33m\s and 39 m\s are considered.

Step 4: Selecting properties and assigning load. Various material properties and section properties are defined. Wind load and dead load calculated and assigned to the model. Wind load in both x and y direction is assigned as per Indian Standard Code.

Step 5: Linear static analysis of all cases Models are analysed and results are compared, tabulated and graphically represented.

III. MODELLING

The various material and section properties which have to define during modelling in ETABS are tabulated as following

A. Section Properties

There are three different storey or three different height buildings have to modelled. The length and width taken while modelling is 25m. Each storey height is 3.3 m. The size of beam 300mm X 600 mm and 1000 mm X 1000mm coloumn. The thickness of slab which we taken is 150mm. The thickness of interior and exterior walls of building is taken as 160mm and 150mm respectively. All the support fixed.

B. Material Properties

For the structure component like column, beam and slab M45 grade of concrete and Fe550 steel grade are considered. Mild steel is used for confinement bars. The cover considered is 40 mm. The dead load is calculated using 20kN/m³ unit weight of concrete.

C. Load

a) DEAD LOAD

Dead loads are considered for the design of structure as per the Indian standard recommended guidelines for dead loads contained in the Hand book of IS 875:1987(part 1) published by the Indian standards Institution.

- Exterior wall load = (unit weight of brick masonry X wall thickness X wall height) =20*0.160*3.3 = 10.56 kN/m
- Interior wall load = (unit weight of brick masonry X wall thickness X wall height) =20*150*3.3 =9.9 kN/m
- Floor load = floor finish = 1 kN/m²

b) LIVE LOAD

Live loads of 3kN is considered for the design of structure as per the Indian standard recommended guidelines for dead loads contained in the Hand book of IS 875:1987(part 2) published by the Indian standards Institution.

c) Wind Load

Calculation and assigning of wind load is done as per is-code 875 (part-III):2015

Vz= Vb k1 k2 k3

- Vb = design wind speed at any height z in m/s = (39 m/s, 44 m/s, 49 m/s)

- kl= risk coefficient (see 6.3.1)= 0.83 (for 24m) =0.93 (for 30m) =1 (for 36m)

- k2 = terrain, height and structure size factor (see 6.3.2.2) = 1

- k3 = topography factor (see 6.3.3) = 1

- Terrain category = 4

- Structure class = B

Wind load is assigned as per clause 6.2.2.1, table number 5 of IS875:2015 (Part 3).

This table gives the value for external pressure due to wind for wind angle of 90° and 0°. Here we have to calculate the ratio of height to width as well as the ratio of length to width. According to that the external pressure coefficient values have to apply to the buildings.

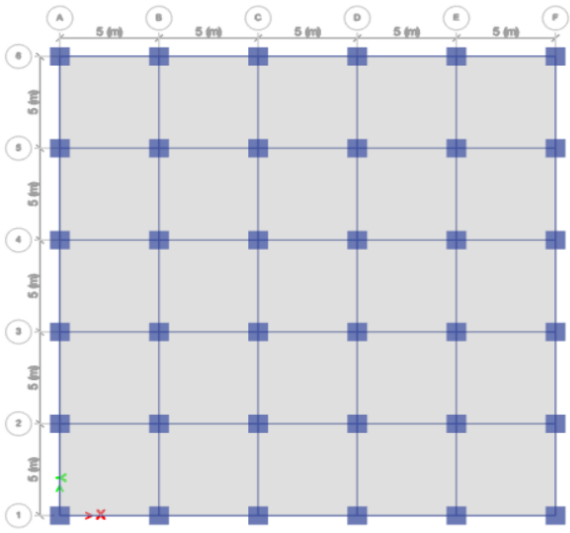

Fig. 1.Plan view

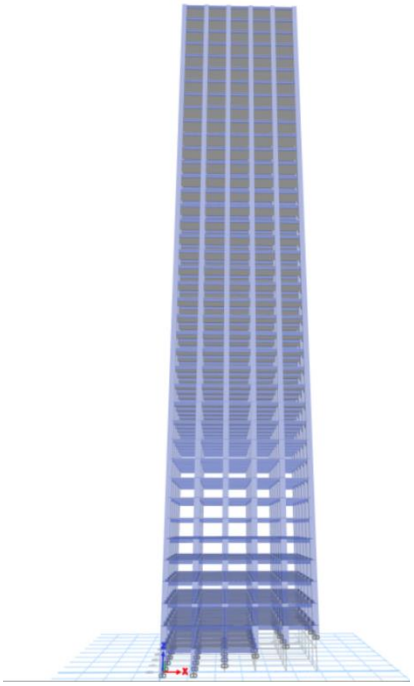

Fig. 2. 3D view of building with 15 degree ground slope

Fig. 3. Deformed shape of 15 degree model with 39 m/s wind speed

II. RESULT AND DISCUSSION

Maximum storey displacement and maximum storey drift of 40 storey building frame on three different slopes are evaluated and compared. Here the results are tabulated and represented.

Fig. 4. Maximum storey displacement for wind velocity 33m/s

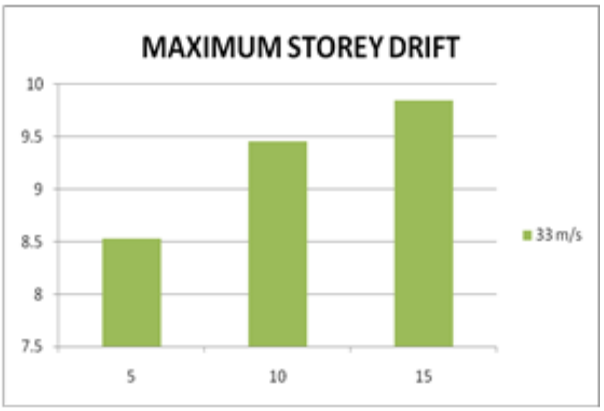

Fig. 5. Maximum storey drift for wind velocity 33m/s

Fig. 6. Maximum storey displacement for wind velocity 39m/s

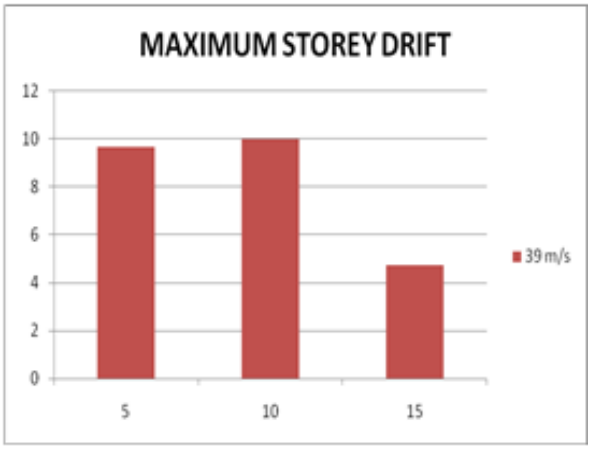

Fig. 7. Maximum storey drift for wind velocity 39m/s

III. CONCLUSIONS

All of the results are tabulated and graphically shown in the previous chapter. Tables display how slope and wind speed affect maximum displacement and maximum drift values. Graphs are used to demonstrate and represent it. Every table and graph is examined to draw conclusions. The conclusion following study of all the cases is provided in this chapter.

The wind speed has more effect on the structure. It was found that as wind velocity was raised for wind loads WLx and WLy, the maximum storey driftt values also rose. Additionally, it is raised by combining loads.It is observed that when we increased the wind velocity, Maximum drift value increased more for considered load combination as compare to wind loads 1.5(SD+LL-WLX).

- It is observed that the values of maximum storey drift for 5 and 10 degree slope differ very less. Therefore it can be said that by changing slope maximum storey drift has only a small change. It did not show a gradual increase or decrease.
- It is observed that the maximum storey drift value increases with increases in slope for 33 m/s wind velocity.
- But for 39 m/s wind velocity, the maximum storey drift increases with increase in slope from 0 to 10 degree and then decreases to 15 degree.
- Like maximum storey drift, maximum storey displacement also have similar observations. It is observed that when we increased the wind velocity, maximum storey drift values increased with that of wind speed for load combination 1.5(SD+LL-WLX).
- Maximum storey displacement increases with increase in group slope from 0 to 15 degree for both cases of 33 amd 39 m/s wind speeds.

References

1. Diksha Gawai and Sarita Harne, Effect of wind on building frame resting on sloping ground and analysis using ETABS, Journal of Emerging Technologies and Innovative Research (JETIR), Volume 9, Issue 5, May 2022.
2. Umesh R Biradar, Shivraj Mangalgi, "Seismic Response of Reinforced ConcreteStructure by Using Different Bracing System", International journal of research and technology, vol 3, Issue 09, 2014
3. G Ajay Kumar ,A.G Seismic Analysis of RC High Rise Building with Shear Walls at Diverse Locations .International Journal of Innovative Technology anfd Engineering ,7,9113-9117, (2019)
4. Apurva Arjun Gaikwad ,D.A.B .P. Sesimic Analysis of Low Rise ,High Rise,Mid Rise Rcc structure on Sloping Ground International Research Journal Of Engineering and Technology. 2019
5. Sachin Kumar Dangi and Saleem Akhtar' Proceedings of the International Conference on Sustainable Materials and Structures for Civil Infrastructures (SMSCI2019) AIP Conf. Proc. 2158, 020030-1–020030-10; https://doi.org/10.1
6. Umakant arya ,Aslam Hussain, Waseem khan, Wind analysis of building frames on sloping ground, International journal of scientific and research publications,vol 4,issue 5 2014
7. Mohit sharma, dr. savita maru Dynamic analysis of multistoried regular building analysis and design of buildings for static force", international journal of research in engineering and technology, vol4, issue 4,2014
8. Varalakshmi V, G Shivakumar and R S Sarma "Designed and d G+5 residential building by ETABS", International Conference on Advance in Engineering and Technology.

9. Mr. Naved Ahmed, Mr. Rajeev Banerjee " Comparison of Different Parameters of a High Rise Building Due to Wind Forces for a Regular 20 Storeyed Building for Lucknow and Bhubaneswar-A Review", International Journal of Engineering Research & Technology (IJERT) ISSN: 2278- 0181 . 2019
10. Roy o. Onoye, kevin c okolie, f. O. Ezekoli, s. C. Ugochukwu):wind analysis of high rise building resting on sloping ground of fedral capital territory, abuja, Nigeria,2020
11. IS 875 Part-2"Code of practice for design loads (other than earthquake) for buildings and structures."
12. IS 875 (PART 1) Code for practise of design loads(other than Earthquake loads, 1987
13. IS 875 (PART 3) Wind loads on buildings and structures, 2015

Analysis Of U – Shaped Damper Using Structural Steel And Shape Memory Alloy As Base Isolators

Sona Jose K
dept.of Civil Engineering
AWH Engineering College, Kozhikode
Kozhikode, Kerala, India
ksonajose@gmail.com

Anila S
dept.of Civil Engineering
AWH Engineering College, Kozhikode
Kozhikode, Kerala, India
anila@awhengg.org

Abstract—Base isolation systems are built to withstand significant ground vibrations during the maximum assessed earthquakes. A novel material called shape memory alloy (SMA) was added to the damping device to increase the limiting capacity of isolation bearings and decrease residual deformation. SMAs are effective materials that are capable of being loaded or heated and then restored to their initial state and preset. The investigation begins with cyclic load test utilizing the ANSYS 2023R1 software on individual steel plate damping systems that include both shape memory alloys and structural steel (SS) for U-shaped dampers. Evaluation of damping systems using SMAs and structural steel at two distinct radii of 85.75 mm and 116 mm was done. Under cyclic loading, U-shaped dampers can sustain significant vertical loads from superstructure. UDs mostly lose energy through hysteresis behavior. The findings demonstrate that great performance was seen for SS UD with an enlarged radius and SMA UD with a decreased radius. SMA UD's hysteresis loop displayed the greatest amount of energy loss and a spring action.

Keywords— U –shaped dampers, shape memory alloys, structural steel, base isolators and hysteresis loop.

I. Introduction

Base isolators have gained popularity over the past few decades as a reliable seismic protection technique for industrial buildings, bridges, and other structures located in seismically active areas. Decoupling a superstructure's response from its foundation or substructure situated on the trembling ground is the basic idea behind base isolators. Elastomeric bearings and sliding isolation systems, both of which exhibit a low lateral stiffness associated with a damping mechanism for lowering the seismic reactions of a superstructure, are the isolation devices most frequently used in engineering practice. As a result, the isolation layer or story experiences the majority of the displacements caused by earthquakes, while the superstructure acts almost like an elastic body. As a result, base isolation systems need to be built to withstand significant displacements during the strongest possible earthquakes.

In order to eliminate post-seismic residual deformations of the base isolators, the self centering capacity of base isolators refers to the ability to return the isolators toward their original locations following earthquake events. The need for high-performing, adaptive, dependable, and cost-effective structural systems has increased interest in the use of intelligent materials in engineering. Shape memory alloys are a particularly intriguing and captivating class of smart materials (SMA).

A novel material called shape memory alloy (SMA) was added to the damping device to increase the limiting capacity of isolation bearings and lessen residual deformation. SMA shape memory materials have shape memory effect, super elastic effect, and damping properties of metal alloys.

II. SHaPe MEMORY ALLOY

The concept of using smart materials in engineering has received significant interest with the growing demand for high performance, adaptive, reliable, and cost-effective structural systems. SMAs are a class of metallic alloys that possess several unique characteristics. The shape memory effect, which is the capacity of the material to return to its original shape after heating, and the super elastic effect, which is the propensity of the material to recover its potentially significant inelastic deformations upon the removal of the load, are two most important characteristics of SMAs. Both of these peculiar capabilities depend largely on diffusion less solid-

to-solid phase change, i.e., martensitic transformations. As a result of these phase transformations, SMAs can produce very high actuation strain, stress, and work output.

In addition, SMAs have excellent self-centering ability, good energy dissipation capacity, high corrosion resistance, and high fatigue life. As a result, SMAs have indeed been applied in a wide range of fields, such as biomedicine, aerospace, the automobile industry, and other fields. Shape memory alloys are materials that can remember their original shape, if deformed they recover the original shape upon heating. They can take large stresses without undergoing permanent deformation. They can be formed into various shapes like bars wires plates and rings thus serving various functions.

SMS shape changes is based on a solid state phase transformation. The shape change mechanism takes place in shape memory alloys by the transition from one form of crystalline structure to another. This change involves transition from a monoclinic crystal form called martensitic form to an order to be crystal form called austenite form.

A. Adaptive U-Shaped damper

The Natural rubber bearings (NRB) equipped with the U-shaped damper are capable of recentring as well as they have high energy dissipation capacity and long service life. The variable characteristics of the shape memory alloy have made them a suitable candidate for seismic isolators subject to earthquake excitations of varying amplitude and frequency. In the case of small loads (wind loads and low-frequency earthquakes), the NRBs equipped with the U-shaped damper serve as a resistant link to minimize damage to expansion joints or other structural supporting elements. In a moderate earthquake, the U-shape damper improves the damping capacity of the NRBs. In the case of strong ground motion, the U-shaped damper not only provides additional hysteresis damping, but it can also can keep relative displacement within the design range. In the present study, U-shaped dampers are used to improve the energy dissipation capacity and residual deformation of NRBs subjected to large shear strain.

III. Modelling And Analysis

A. Model Geometry

U-shaped components are placed between two steel plates to form the U-shaped damping system. These U-shaped dampers can be chosen and fitted to the dimensions as necessary. The UDs are the core components in the proposed base isolators that provide self-centering capability under seismic loading. An UD comprises one semicircular part and two straight parts therefore, the tails of the two straight parts can be easily fixed on the adjacent plates through welded connections. In general, the deformation capacity of the UD is mainly determined by the semicircle diameter and straight part length.

The lateral stiffness and energy dissipation capacity improve as the number of U-shaped dampers rises. Dampers also need to be able to dissipate a lot of energy and have a high lateral relative displacement. Between the bottom and top anchor steel plates are alternate layers of steel shims and rubber layers. The early variants were steel-rubber bearings with varying amounts of layers of steel and rubber. The height of the damping system is determined by the quantity of steel and rubber layers. The table I provide the measurements for the anchor plate, rubber layers, and steel shims.

Table I. Model Dimensions

SECTIONS	DIMENSIONS
Thickness of steel shims (ts)	1mm
Thickness of rubber layers (tr)	4.5mm
Thickness of anchor plate (ta)	20mm
Length and breadth of steel shims & rubber layers (Ds & Dr)	600mm x 600mm
Length and breadth of anchor plate (Da)	1400mm x 1400mm

Figure 1 shows the model geometry of general U-Shaped damper.

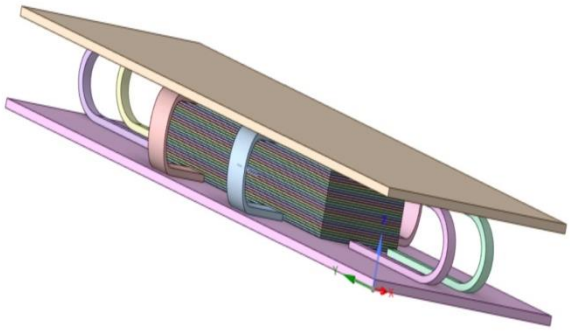

Fig.1. U-Shaped damping system

Modeling and analysis is done for U-Shaped dampers incorporating only structural steel, only SMA and combination of SS and SMA. The UDs are arranged in such a way that for damping system incorporating only SS and SMA they are placed adjacent to each other and for the model with combination the SS and SMA UDs are placed alternatively. Figure 2 illustrates the cross section details of UD.

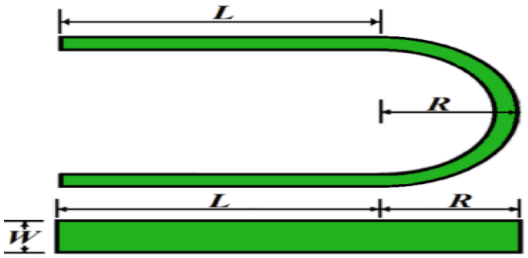

Fig.2. Crossection of a UD

Figure 3 shows the cross section and dimension details of U-Shaped damping system with UDs of radius 85.75mm and model section details are listed in table II.

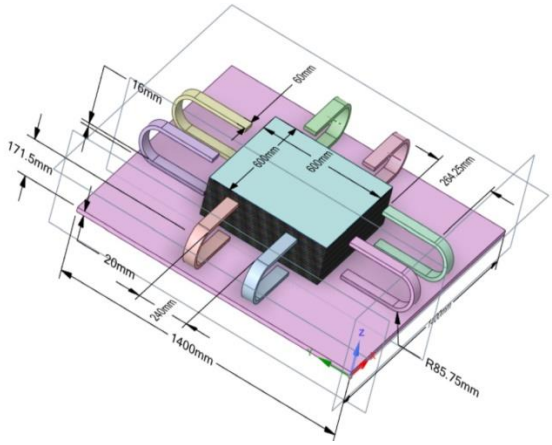

Fig.3.U-Shaped damper with UD radius 85.75mm

TABLE II. Model details of u damper with radius 85.75mm

MODEL SECTIONS	DIMENSIONS
Radius of UD (R)	85.75mm
Length of straight part (L)	264.25mm
Width of the UD (W)	60mm
Spacing btw UDs	240mm
No. Of steel shims	32
No. Of rubber layers	31
Total height of model	211.5 mm

Figure 4 shows the model geometry and of U-Shaped damping system with UD radius 116mm. dimension details of U damper with radius 116mm is mentioned in table III.

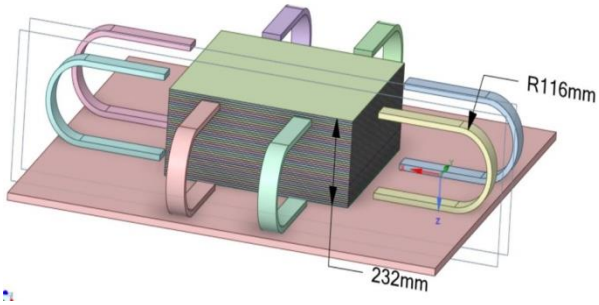

Fig.4. U-Shaped damper with UD radius 116mm

TABLE III. Model Details Of U Damper With Radius 116mm

MODEL SECTIONS	DIMENSIONS
Radius of UD	116 mm
Length of straight part	264.25mm
Width of the UD (W)	60mm
Spacing btw UDs	240mm
No. Of steel shims	43
No. Of rubber layers	42
Total height of model	272 mm

B. Material properties

ANSYS FEA analyses require two material properties to be specified in order to perform the analysis. In the case of non-linear structural steel and rubber, the user will need to specify the Young's modulus, Poisson's ratio, yield strength, and other material properties for each material. Depending on the analysis, additional material properties may also be needed. The material properties are taken from the ANSYS material library. The material used for analysis are neoprene rubber as the rubber material, structural steel is used for anchor plates and steel shims and nitinol as SMA material. Nitinol is an alloy of nickel and titanium. The material properties SMA, neoprene rubber and structural steel are listed in tables IV, V and VI respectively.

TABLE IV Material Properties Of Sma - Nitionl

DECRIPTION	VALUE	UNIT
Density	6450	kg/m^3
Young's modulus	90000	MPa
Poisson's ratio	0.3	
Tensile yield strength	1000	MPa
Tensile ultimate strength	1400	MPa

Table V Material Properties Of Neoprene Rubber

DESCRIPTION	VALUE	DESCRIPTION	VALUE
Young's modulus	4.25 MPa	Minimum service temperature	-60 °C
Tensile strength	20 MPa	Maximum service temperature	100 °C
Elongation	250 %	Density	1250 kg/m^3
Hardness	57.5 Shore	Resistivity	1x 10^{15} Ohm*m m^2/m
Thermal expansion	7.1x 10^{-6}/K	Glass temperature	-47.5 °C

Table VI Material Properties Of Structural Steel

DECRIPTION	VALUE
Young's modulus	2 x 10^5 MPa
Poisson's ratio	0.3
Density	7.85x10^{-6} kg/mm^3
Thermal expansion	1.2x10^{-5} $1/^0C$
Tensile yield strength	250 MPa
Compressive yield strength	250 MPa
Tensile ultimate strength	460 MPa

C. Analysis

The analysis was carried out using the finite element modelling software called ANSYS. A cyclic loading pattern is used to predict the seismic behavior of a damping plate. The load is applied in the axial direction, while the bottom plate is fixed. The cyclic loading pattern is used to simulate the seismic loading conditions, allowing for the evaluation of the damper performance under the expected conditions. Loading cycle is illustrated in figure 5.

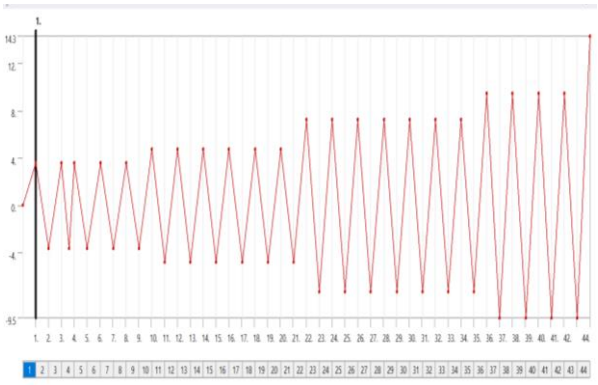

Fig.5. Loading cycle

The bottom anchor plate is fixed and the load is applied on the top anchor plate.

IV. Results And Discussion

FEM analysis was carried out for the models. Total deformation and equivalent stress was determined for the models. The figure 6 and figure 7 shows the total deformation and equivalent stress of u shaped damper with UD radius of 85.75mm incorporating only SS.

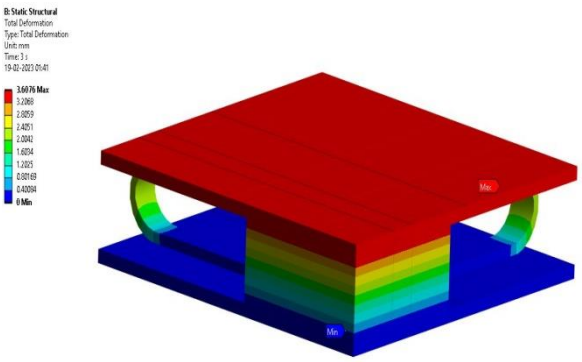

Fig.6. Total deformation of U-Shaped damper with UD radius 85.75mm

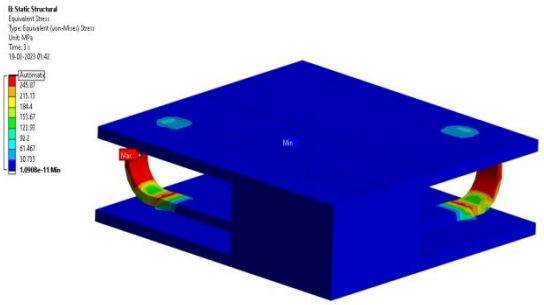

Fig.7. Equivalent stress of U-Shaped damper with UD radius 85.75mm

Hysteresis curve for the models were plotted. Hysteresis loop obtained for the U-shaped damper with UD radius 85.75mm is illustrated in figure 8.

Fig.8. Hysteresis curve for the U-shaped damper with UD radius 85.75mm

The total deformation and equivalent stress obtained for the U-Shaped damper with UD radius 116mm is depicted in figure 9 and figure 10 respectively.

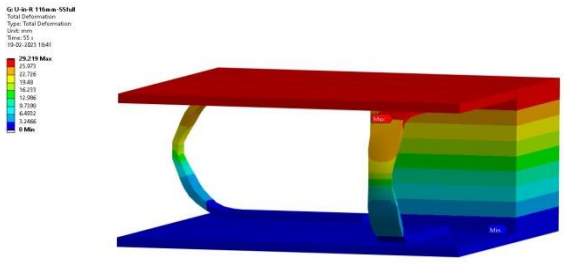

Fig.9. Total deformation of U-Shaped damper with UD radius 116mm

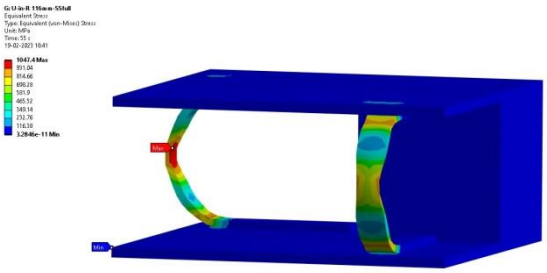

Fig.10. Equivalent stress of U-Shaped damper with UD radius 116mm

Hysteresis curve obtained for U-Shaped damper with UD radius 116mm is illustrated in figure 11.

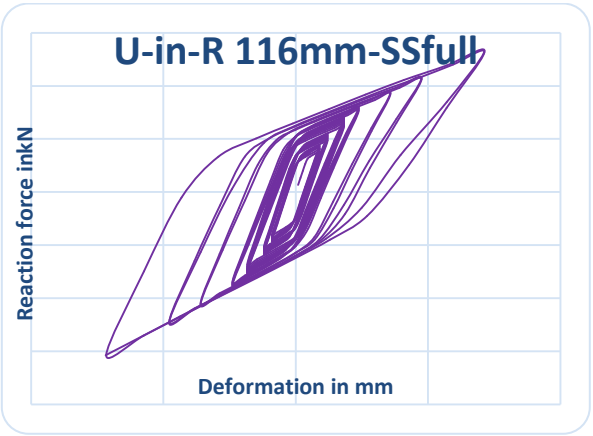

Fig.11. Hysteresis curve for the U-shaped damper with UD radius 116mm

Analysis was carried out for all the models and the results are shown in table VII.

Table VII Results Of Analysis

Model	Total deformation mm	Equivalent Stress MPa
U-R85.75-SS	3.6076	245.87
U-R85.75-SMA	35.597	568.1

U-R85.75-COMB	29.562	1256.3
U-R116-SS	29.219	1047.4
U-R116-SMA	25.409	517.95
U-R116-COMB	28.952	1062.1

V. Conclusions

This study proposed and investigated novel designs of U-Shaped damping system as base isolators by taking advantage of the SMA-UDs comprising super elastic SMA, Structural steel SS under cyclic loading. For the cyclic analysis, ANSYS finite element software was employed. U-shaped dampers made of structural steel and shape memory alloy were employed. For the U-Shaped damping system, the total deformation and equivalent stress have been determined at two different radii.

The findings are summarized as follows:

- Under cyclic loading, the SMA UDs displayed cyclic qualities, including steady and excellent flag-shaped hysteresis loops. The suggested base isolators demonstrated the expected deformation behaviour and typically displayed flag-shaped hysteresis loops associated with greatly reduced residual deformation under cyclic loading.
- For a U-shaped damper with a UD radius of 85.75mm and using only SMA UDs, the maximum total deformation of 35.597mm was obtained.
- For a reduced radius of UDs when SMA UD was replaced with SS UDs and COMB UDs the deformation was decreased by 89.86% for SS and 16.95% for COMB.
- For the case of enlarged radius of 116mm the maximum total deformation of 29.219mm was obtained for U-shaped damper with SS UDs.
- It was observed that the total deformation increased by 15% and 13.9% respectively when SMA UD was replaced with SS UDs and COMB UDs.
- SMA UD with a smaller radius and SS UD with a larger radius both performed more efficiently. The hysteresis loop of SMA UD showed the most energy loss and a spring action.

From a design standpoint, engineers can adapt the component proportions of the isolation bearings to meet various performance goals. The proposed base isolators will offer a potential alternative to current seismic isolation devices or systems for resilient and sustainable high-performance seismic-resistant modern civil infrastructure.

References

1. Javed Sheikhi, Mojtaba Fathi, Rohola Rahnavard, Rebecca Napolitano "Numerical analysis of natural rubber bearing equipped with steel and shape memory alloys dampers," Structure 32, 2021,pp.1839-1855.
2. Bin Wang, Songye Zhu, Fabio Casciati, "Experimental study on novel self-centering seismic base isolators incorporating superelastic shape memory alloys" J. Struct.Eng, 146(7): 04020129, 2020, pp.1-14
3. Sheikhi Javad, Fathi Mojtaba, Rahnavard Rohola. Natural rubber bearing incorporated with high toughness steel ring dampers. Structures 2020; 24:107–23.
4. Sheikhi J, Fathi M. Natural Rubber Bearing Incorporated with Steel Ring Damper (NRB-SRD). Int J Steel Struct 2019. https://doi.org/10.1007/s13296-019-00267-7.
5. Rahnavard Rohola, Thomas Robert J. Numerical evaluation of steel-rubber isolator with single and multiple rubber cores. Eng Struct 2019;198:109532.
6. Rahnavard Rohola, Craveiro Helder D, Napolitano Rebeca. Static and dynamic stability analysis of a steel-rubber isolator with rubber cores. Structures 2020; 26: 441–55.
7. Radkia Sahar, Rahnavard Rohola, Tuwair Hesham, Gandomkar Farhad Abbas, Napolitano Rebecca. Investigating the effects of seismic isolators on steel asymmetric structures considering soil-structure interaction. Structures 2020, 27: 1029–40.
8. Ikeda T, Nae FA, Naito H. Constitutive model of shape memory alloys for unidirectional loading considering inner hysteresis loops. Smart Mater Struct 2004, 13:916–25.

Analysis Of Steel Buildings With Steel Plate Shear Wall At The Corners With Varying Thickness

Aysha Banu
Dept. of Civil Engineering
AWH Engineering College, Kozhikode
Kozhikode, Kerala, India
chikkubanu@gmail.com

Anila .S
Dept. of Civil Engineering
AWH Engineering College, Kozhikode
Kozhikode, Kerala, India
anila@awhengg.org

Abstract- Steel high rise buildings are becoming more prevalent every day. The stability of the buildings is taken into consideration as their height rises. To withstand the lateral loads brought on by wind and seismic activity, shear walls had to be installed in these buildings. Of the several shear wall kinds, steel plate shear walls (SPSW) are the most effective since they are lighter and thinner, increasing architectural space and the rigidity of the buildings. This study uses ETABS software to show the seismic analysis of a 15-storey steel building with steel plate shear walls at the corners and centre that is situated in seismic zone III. The performance of another 15-storey steel building with steel plate shear walls of various thickness (15mm,20mm and 25mm) is also compared in this article. When comparing the results to other buildings, it is found that the steel building with the thicker steel plate shear walls at the corners performs better in terms of storey displacement and storey drift. The models are analyzed by Response Spectrum Method as per IS 1893:2016

Keywords-Steel plate shear wall, rigidity, seismic analysis.

I. Introduction

Shear walls are vertical elements of a force resisting system. They are provided to act against the effects of lateral loads that are acting on the structure. Shear wall mainly increases stiffness in building providing them better way to withstand lateral loads. Steel buildings being more vulnerable to lateral loads respond vey well when Steel Plate Shear Walls (SPSW) are provided. SPSW is more effective for lateral loads as they are more ductile, lighter and also occupy less space. SPSW systems are used in high-rise buildings as a retrofitting method also.

The main function of steel plate shear wall is to resist horizontal story shear and overturning moment due to lateral loads. Steel plate shear wall system consists of a steel plate wall, two boundary columns and horizontal floor beams. The steel plate walls and two boundary columns together act as a vertical plate girder. The columns act as flanges of the vertical plate girder and the steel plate wall acts as its web. The horizontal floor beams act as transverse stiffeners in a plate girder.

L Rahul, et al (2020) analyzed a 6 storey R.C. building frame for seismic zone-III using ETABS. This paper has been described to determine the proper location of shear wall. Dynamic linear analysis using response spectrum method is performed and lateral load analysis is done for structure with RC shear wall and steel plate shear wall. There are some parameters considered such as node displacement, maximum reactions, and total weight of reinforcement. It is inferred that steel plate shear walls are more resistant to lateral loads in an irregular structure. Deflection in the case of without SPSW is very large and in the case of with SPSW, deflection is very less.

Prof. Prashant Topalakatti, et al (2014) analyzed high-rise steel buildings frames with and without SPSW by using STAAD PRO V8i FEA programme. The primary variable in the analysis was the presence of steel plate shear walls thickness of plate (6 mm to 18 mm). The main parameters considered are deflection, shear force, bending moment and axial force. Steel frame building with SPSW has lesser deflection, shear force, bending moment and axial force values compared to steel frame building without SPSW. As the thickness of the steel plate shear wall increases, then the deflection, shear force, bending moment and axial force decreases.

II. Objective

The present study aims at determining the effectiveness in placing the steel plate shear wall

at the corners over centre of a G+15 storied steel building using ETABS software.

To determine the performance of a G+15 storied building with steel plate shear wall placed at the corners of various thickness-15mm, 20mm and 25mm using ETABS software.

III. Model Description

Model I- G+15 storied steel building with steel plate shear wall at the corners.

Model II- G+15 storied steel building with steel plate shear wall at the centre.

Model III- G+15 storied steel building with steel plate shear wall of 15mm thickness at the corners.

Model IV- G+15 storied steel building with steel plate shear wall of 20mm thickness at the corners.

Model V- G+15 storied steel building with steel plate shear wall of 25mm thickness at the corners.

IV. Modelling

In the present study, the building models are analyzed by using ETABS software. The number of bays taken in X and Y directions is 5.Bottom storey height and typical storey height are taken as 3m.The building models are analyzed by using Response Spectrum Method as per IS1893:2016.The details of Model I and Model II are given in Table I. Table II shows the details of Model III, IV and V. Load details and seismic data are same for all models and are shown in Table III.

Table I. Details of model I and II

Beam section	ISLB500
Column section	ISMB400 with M40 encasement
Secondary beam section	ISLB100
Deck slab thickness	100mm
Shear wall thickness	50mm
Grade of steel	Fe345
Grade of longitudinal bars	HYSD500
Grade of confinement bars	Mild Grade 250

Table II Details of Models III, IV And V

Beam section	ISLB600
Column section	ISMB500 with M40 encasement
Secondary beam section	ISLB150
Deck slab thickness	100mm
Shear wall thickness	15mm for Model III 20mm for Model IV 25mm for Model V
Grade of steel	Fe345
Grade of longitudinal bars	HYSD500
Grade of confinement bars	Mild Grade 250

Table III LOAD DETAILS AND SEISMIC DATA

Live load	2kN/m²
Floor finish	1kN/m²
Outer wall load	12kN/m²
Inner wall load	7kN/m²
Roof slab load	1.5kN/m²
Zone	III
Soil type	Type II
Importance factor	1
Response reduction factor	5

V. Structural Details

The plan and three-dimensional views of the steel buildings with steel plate shear walls provided at the corners and centre are shown in Fig. 1-4.

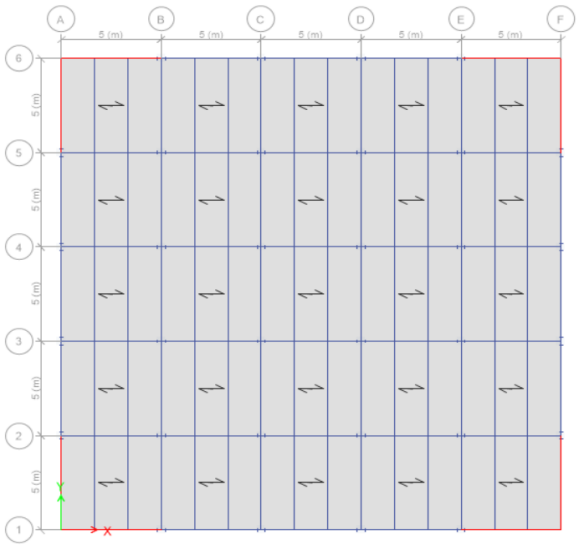

Fig. 1.Plan view of steel building with shear wall at the corners.

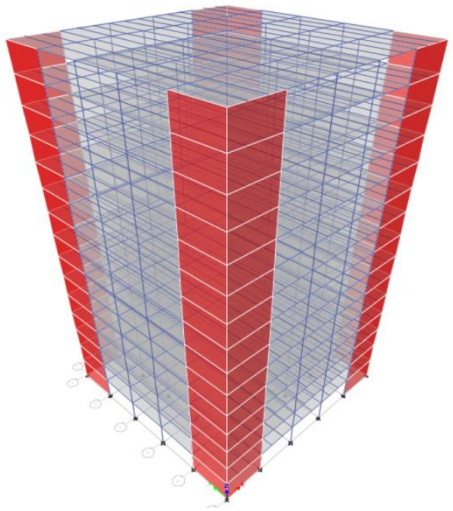

Fig. 2.-3D view of steel building with shear wall at the corners

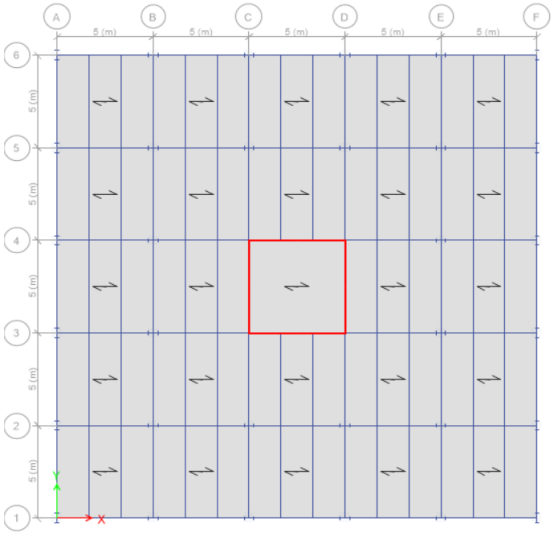

Fig. 3.-Plan view of steel building with shear wall at the centre

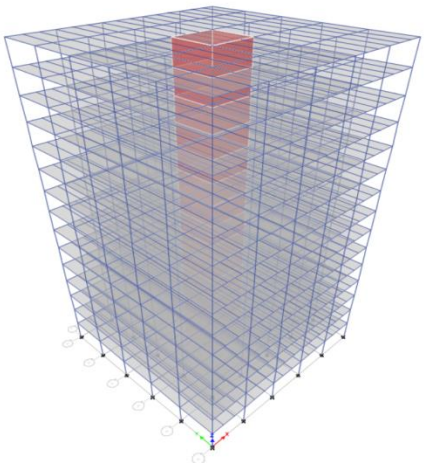

Fig. 4.-3D view of steel building with shear wall at the centre

VI. Results And Dicussions

The models are analyzed by using Response Spectrum Analysis of ETABS software. The performance of Model I and Model II are compared in terms of storey drift and storey displacement to verify the effectiveness of the building when the steel plate shear wall is placed at the corners. Model III, Model IV, and Model V are also compared to determine their performance in terms of the parameters mentioned above when the thickness of the steel plate shear wall changes.

The maximum storey displacement and drift values of Model I and Model II are shown in Table IV and Table V.

TABLE IV. MAXIMUM STOREY DIS-PLACEMENT

STOREY LEVEL	MODEL I (mm)	MODEL II (mm)
15	25.008	30.07
14	22.881	27.591
13	20.729	25.065
12	18.563	22.512
11	16.393	19.943
10	14.239	17.379
9	12.124	14.848
8	10.073	12.381
7	8.117	10.015
6	6.287	7.791
5	4.617	5.752
4	3.144	3.943
3	1.905	2.414
2	0.939	1.214
1	0.29	0.399
Base	0	0

TABLE V MAXIMUM STOREY DRIFT

STOREY LEVEL	MODEL I (mm)	MODEL II (mm)
15	0.000709	0.000826
14	0.000717	0.000842
13	0.000722	0.000851
12	0.000723	0.000856
11	0.000718	0.000855
10	0.000705	0.000844
9	0.000684	0.000822
8	0.000652	0.000789
7	0.00061	0.000741
6	0.000557	0.00068
5	0.000491	0.000603
4	0.000413	0.00051
3	0.000322	0.0004
2	0.000216	0.000272
1	0.000097	0.000133
Base	0	0

It is found that the performance of Model I is better than Model II. Therefore, it is evident that the steel building with steel plate shear wall performs better when placed at the corners than at the centre.

The maximum storey displacement for Model I is 25.008mm and that of Model II is 30. 07mm.The maximum storey displacement for Model I is found to be 20.24% less than that of Model II. According to Indian standard code, maximum permissible displacement is 110 mm. It can be observed from the results that it is under permissible limit.

The maximum storey drift for Model I is 0.00072 and that of Model II is 0. 000856.The maximum storey drift of Model I is 18.88% less than that of Model II. The results found are also compared with the help of graphs as shown in Fig. 5-6

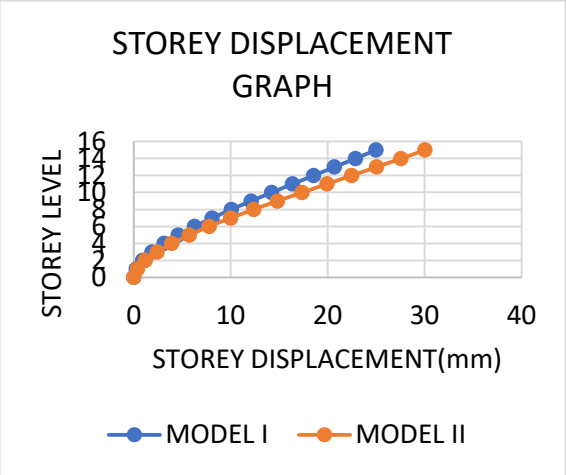

Fig. 5.-Comparison of storey displacement of Model I and Model II

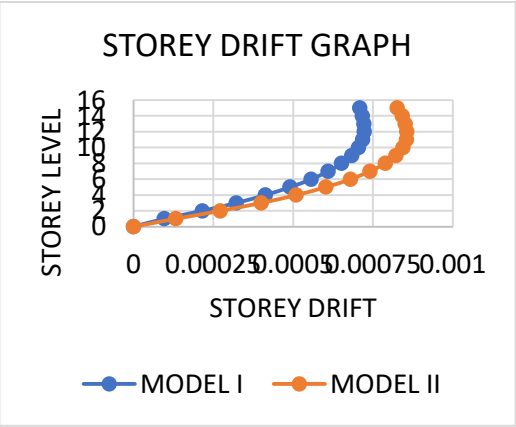

Fig .6.-Comparison of storey drift of Model I and Model II

The maximum storey displacement and drift values of Model III, Model IV and Model V are shown in Table VI and Table VII. It is already mentioned that the thickness of steel plate shear wall of Model III, Model IV and Model V are 15mm, 20mm and 25mm, respectively. From the results, it is inferred that the Model V performs better and are also within the limits prescribed by Indian Standard Codes. The maximum storey displacement and drift values of Model III, Model IV and Model V are shown in Table VI and Table VII.

TABLE VI MAXIMUNM STOREY DISPLACEMENT

STORY LEVEL	MODEL III (mm)	MODEL IV (mm)	MODEL V(mm)
15	26.656	22.886	19.963
14	24.723	21.178	18.425
13	22.669	19.403	16.838
12	20.611	17.578	15.216
11	18.464	15.712	13.564
10	16.279	13.819	11.898
9	14.082	11.922	10.235
8	11.901	10.046	8.599
7	9.772	8.22	7.013
6	7.733	6.478	5.506
5	5.824	4.854	4.108
4	4.091	3.388	2.851
3	2.582	2.119	1.77
2	1.351	1.094	0.904
1	0.457	0.362	0.294
Base	0	0	0

TABLE VII MAXIMUM STOREY DRIFT

STORY LEVEL	MODEL III	MODEL IV	MODEL V
15	0.000644	0.000569	0.000512
14	0.000675	0.000592	0.000529
13	0.000696	0.000608	0.000541
12	0.000715	0.000622	0.00055
11	0.000728	0.000631	0.000555
10	0.000733	0.000632	0.000554
9	0.000727	0.000625	0.000546
8	0.00071	0.000608	0.000529
7	0.00068	0.000581	0.000502
6	0.000636	0.000541	0.000466
5	0.000578	0.000489	0.000419
4	0.000503	0.000423	0.00036
3	0.00041	0.000342	0.000289
2	0.000298	0.000244	0.000203
1	0.000152	0.000121	0.000098
Base	0	0	0

It is found that the performance of Model V is better than Model III and Model IV. Therefore, it is evident that the steel building with thicker steel plate shear wall performs better when placed at the corners.

The maximum storey displacement for Model III is 26.656mm and that of Model IV and Model V are 22.886mm and 19.963mm, respectively. The maximum storey displacement of Model V is less than 33.52% and 12.77% that of Model III and IV, respectively.

The maximum storey drift for Model III is 0.000733 and that of Model IV and Model V are 0.000632 and 0.000554, respectively. The maximum storey displacement of Model V is less than 32.31% and 15.88% that of Model III and IV, respectively. All the values of storey displacement and storey drift are within the limits provided in Indian Standard Codes. The results found are also compared with the help of graphs as shown in Fig. 7-8.

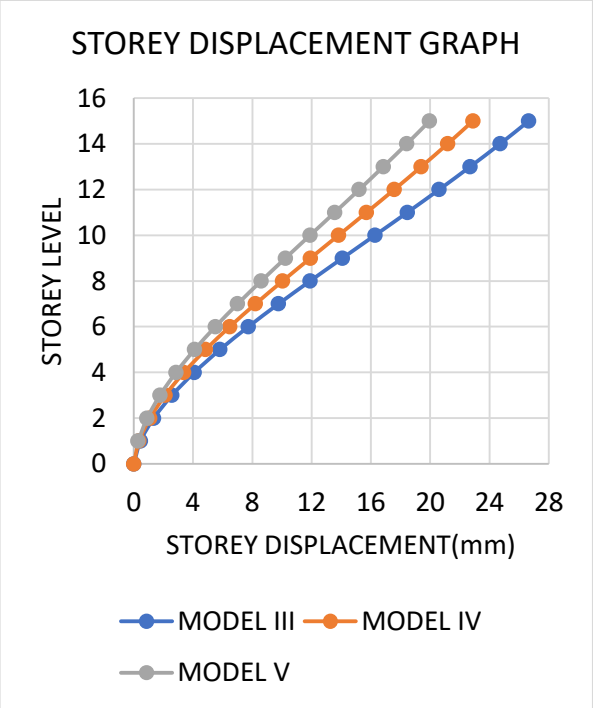

Fig. 7- Comparison of storey displacement of Model III, Model IV and Model V

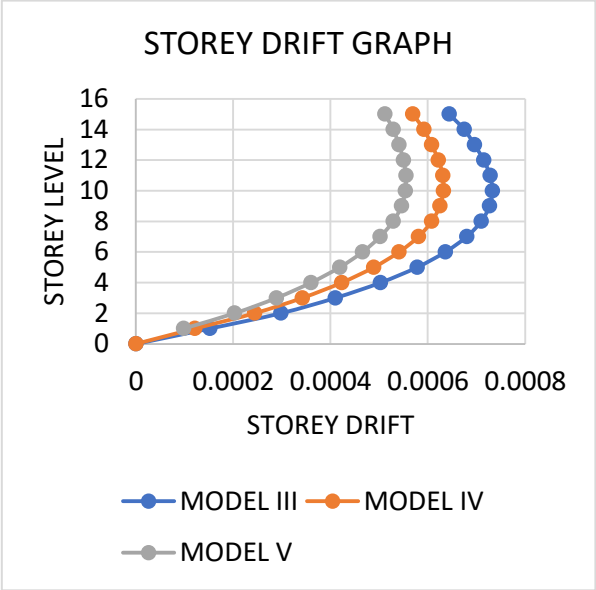

Fig. 8.- Comparison of storey drift of Model III, Model IV and Model V

VII. Conclusion

Based on the present study for comparison of steel plate shear walls at corners and centre and with varying thickness when placed at the corners in 15 storied steel buildings, we can conclude that:

1. Steel plate shear wall placed at the corners performs well as compared to that of at the centre.
2. By providing shear wall at the corners, torsional stability can be achieved in the building.
3. It is found that as the thickness of the steel plate shear wall increases, storey displacement and storey drift decreases. This is because as the thickness of steel plate shear wall increases, the stiffness of the structure also increases.
4. Steel plate shear walls occupy much less space due to the relatively small thickness of SPSW compared to reinforced concrete shear walls and aesthetic good from architectural point of view. Therefore, steel plate shear walls are preferred over reinforced concrete shear wall.

REFERENCES

1. Prof. Prashant Topalakatti and Prabhu M. Kinagi, "Parametric Study of Steel Frame Building with and without Steel Plate Shear Wall", Civil and Environmental Research, Volume 6, 2014

2. L.Rahul, M.Akbar and M.Sriraman, "Design Optimization and Earthquake Analysis of Shear Wall in High Rise Building", Journal of Xi'an University of Architecture and Technology,2020
3. Misbah Danish Sabri and Ankit Rawat, "Performance Based Analysis of Building with Steel Plated Shear Wall", International Journal of Modern Developments in Engineering and Science, 2022,Vol 1
4. Kavin Y. Patel and Dipali Y. Pate, " A Comparative Study of Effectiveness of Steel Plate Shear Wall Patterns in Steel Building", International Conference on Research and Innovations in Science, Engineering and Technology, 2021, Volume 1
5. Londhe R.S and Chavan A.P, "Behaviour of building frames with steel plate shear walls", Asian journal of civil engineering. 2010 ,Vol. 11, no. 1 Pages 95-10

Experimental Study On The Mechanical Properties And Cracking Characteristics Of Bacterial Concrete

Ansal A
Dept.of Civil Engineering
AWH Engineering College Kozhikode,
Kerala, India
ansalkhader@gmail.com

Sabeena M V
Dept.of Civil Engineering
AWH Engineering College Kozhikode,
Kerala, India
sabeena@awhengg.org

Abstract— Concrete is a material that is used worldwide for centuries as a construction material. Exposure to extreme conditions and adverse effects of corrosion of reinforcements leads to cracking of concrete. Compressive strength, Flexural strength, and permeability can be affected by these cracks, which in turn reduces the useful life of the concrete. Repairing and maintenance of these infrastructures needs higher cement consumption and expenses. Self-healing concrete by microbially induced calcite precipitating bacteria is an economical and sustainable solution, as it repairs small cracks. This paper discusses the mechanism and performance of bacterial concrete. The Bacillus species is proven to be an effective microbial agent for self-healing concrete. The sample preparation is done using Bacillus Subtilis. The concentration adopted for sample preparation is **105** cells per milliliter. The mechanical properties and durability of bio concrete are evaluated to check the possibility of the same as a building material. While assessing the strength of reinforced concrete sections, the tension in the concrete is usually ignored because it contributes little to member strength. However, it provides an important contribution to the performance of members at service loads. In this project, tension stiffening properties of bacterial concrete is experimentally evaluated on concrete prismatic members made of M20 grade concrete reinforced with bars of 8mm and 12mm in diameter. The length of the concrete prism in all the direct tension specimens is 600 mm. The specimens are 60 mm square in cross-section. The total length of the steel reinforced specimens, including the bars is 900 mm. The tension stiffening properties of bacterial concrete are compared with that of conventional concrete.

Keywords— bacillus subtilis, bacterial concrete, tension stiffening

I. INTRODUCTION

Due to its numerous performance features, concrete remains as the most used materials in nowadays and it will undoubtedly remain as the most manufactured and consumed construction material in the long run [2]. Concrete is distinguished by numerous cracking behaviour because of low tensile strength and brittleness. Cracks can weaken the integrity and bearing capacity of structure[1]. Due to volume instabilities or other external reasons such as excessive loads, severe strength environmental exposure, or design error, cracks can develop at any point of a concrete structure's service life [9]. Bond of reinforcing bars to the surrounding concrete influences the behaviour of reinforced concrete structures in many ways. It can be a key element for the ultimate load carrying capacity of reinforced concrete structures since it affects the anchorage of bars. The deformation of a rebar embedded in concrete is significantly influenced by the bond between the two materials. In fact, it is well known that, after cracking, bond transfers tensile stresses from the rebar to the surrounding concrete (between cracks) that stiffen the response of a RC member subjected to tension; this stiffening effect is referred to as "tension stiffening". Tension stiffening refers to tension carrying ability of concrete between cracks, contributing to the stiffness of a reinforced concrete member before the reinforcement yields. Cracking causes a softening behaviour in plain concrete. As cracking progresses, concrete loses its stiffness at a relatively high rates[12]. Micro-cracks in concrete allow water and contaminants to enter, causing matrix degradation and corrosion of embedded steel reinforcement, compromising the structure's strength and endurance[3].

Steel reinforcement is used to avoid cracks. New environmentally friendly and self-healing

procedures must be developed to protect existing and future structures and increase their durability. Microbiologically Induced Calcite Precipitation (MICP), a type of mineral precipitation induced by the metabolism of bacteria in concrete, it is recently discovered to increase the performance of concrete[4].

A. MICP – Microbially Induced Calcite Precipitation

Biomineralization is accomplished by a process known as Microbiologically Induced Calcite Precipitation (MICP). The microbial urease hydrolyses urea to form ammonia along with carbon dioxide. As a result of the ammonia released into the environment insoluble calcium carbonate is deposited. [6]. MICP is a practical, and sustainable alternative for repairing the cracks. Microbially induced calcium carbonate precipitation (MICP) is a part of various geological habitats like soils, limestone caves. Calcium carbonate (CaCO3) crystals can be formed via biological mechanism in two ways: autotrophic and heterotrophic pathways. Biotechnological approaches to innovation of a type of bio concrete have been proposed based on micro -organisms inherent ability to produce calcium carbonate precipitation [8]. When a crack forms, the bacteria imbedded within it becomes active, and calcium carbonate minerals are produced and fills the cracks. In comparisonto ordinary self-healing concrete, the MICP-based self-healing technique provides a long-term and ecologically sustainable solution to cracking.

The number and quality ofinduced minerals have a significant impact on the MICP process efficiency [10]. Ammonium and carbonate formed by hydrolysis of urea, catalysed by urease. One mole of carbamic acid is formed from hydrolysed ammonia and Carbamic acid, which further hydrolysed to ammonia and carbonic acid.

The products, Ammonia and Carbonic acid produces bicarbonate, ammonium and hydroxide ions. This change will then cause the precipitation of the metal ions. The reaction continues to produce calcium carbonate [11].

II. OBJECTIVES

The objectives of this present work are as follows:

- To determine the mechanical properties of bacterial concrete specimens
- To evaluate the tension stiffening properties of bacterial concrete.

III. EXPERIMENTAL PROGRAMME

This experimental programme was carried out to investigate the mechanical properties and tension stiffening effect on the bacterial concrete. The experimental work consisted of casting and testing 16 reinforced concrete prismatic tension members made of M20 grade concrete having cross-sectional dimensions of 60 x 60 mm and a length of 600 mm. 8 numbers of specimens were reinforced with 8 mm diameter bar and 8 numbers of specimens were reinforced with 12 mm diameter bar of grade Fe 500.The reinforcing bar was extended 150 mm on either side for proper gripping in the testing equipment. Standardized cracks were also introduced in some of the concrete prism specimen to evaluate the self-healing property of bacterial concrete. Cubes, cylinders, and beams were cast for finding the mechanical properties of bacterial concrete. The concentration of bacteria selected for sample preparation is 105 cells per milli litre [5].

A. Materials

Ordinary Portland cement of 53 grade confirming to IS: 12269-1987 [13] was used. Test on cement were conducted as per IS 4031-1988 [14] Fine aggregate passing through 4.75 mm IS sieve confining to grading zone III of IS: 383-1970 [15] was used. Crushed stone with a maximum size of 20 mm and 12 mm were used. 20mm aggregates were used for making cubes, beams and cylinders. 12mm aggregates were used for making direct tension specimen. CONPLAST SP430 complies with IS: 9103:1999 [18] with specific gravity of 1.2 was used as a water reducing agent. The bacteria used for the sample preparation is bacillus subtillis. The concentration of bacteria adopted for the sample preparation is 105 cells per millilitre. The bacterial strain details are provided in the Table I. Reinforcement bars used is Fe500 of Minar TMT brand. Table II gives the properties of reinforcement bars obtained by doing tension tests.

TABLE 1 BACTERIAL STRAIN DETAILS

Fields	Detailed information
Taxonomic designation	Bacillus Subtilis
Medium name	Nutrient agar

pH	11.8
Temperature of growth	30°C
Incubation period	24 to 48 hours
Subculturing period	2 months
Additional information	Efficient alkali protease and amylase producer, alka-lophilic and thermos tolerant, used in compost accelerator

TABLE II REINFORCEMENT BAR DETAILS

Properties	12mm	8mm
Yield point stress(N/mm^2)	504.24	517.5
Ultimatestress (N/mm^2)	633.401	537.14

B. Mix Proportions

In this experimental study M20 grade concrete is used and the mix design is done based on IS 10262:2009The details of mix proportions are given in Table III. Mix design for normal concrete and bacterial concrete were done. For tension stiffening specimen the maximum size of coarse aggregate used is 12mm.

TABLE III MIX PROPORTION

Item	Quantity
Cement	315.2 kg/m^3
Fine aggregate	820.27 kg/m^3
Coarse aggregate	1149.64 kg/m^3
Water	157.6 kg/m^3
Admixture	3.78 kg/m^3

C. Specimen Preparation

Concrete cubes of size 150mm were cast for finding the compressive strength, prism of size 100x100x500mm were cast for finding flexural strength and concrete cylinder of diameter 150mm with a depth of 300mm were cast for finding split tensile strength. Test were also conducted to find the workability of concrete. Cast iron mould was used to cast specimens, concrete was filled in the mould in layers and each layer was tamped by a tamping rod. In case of bacterial concrete around 10% of total water was taken out and used for mixing the bacterial solution. Remaining 90% of water was added and mixed with dry aggregates and cement for 1 minute, the diluted bacterial solution was then mixed with concrete for another 3 minutes.

Fig. 1. Specimen for finding mechanical properties

D. Casting Of Direct Tension Specimen

Fig.2 shows the reinforcement details of the direct tension specimens and in Fig.3 cast direct tension specimen are shown. For both 8 mm and 12 mm bar specimens, wooden formwork was prepared by using wooden plywood and they were fixed using nails and screws for the required dimension. Holes were provided on the side faces of the formwork so that they accommodate the reinforcing bars. The concrete used for casting of specimen were mixed in a concrete mixer. In Table IV the details of tested specimens and variables are given.

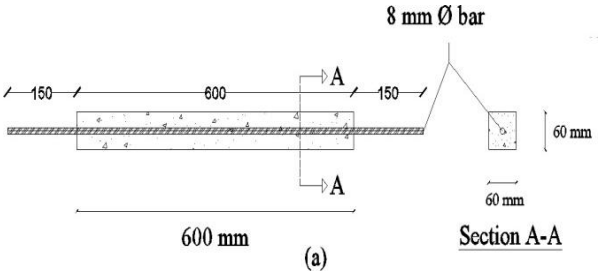

Fig. 2. Sketches for reinforced specimen

TABLE IV DETAILS OF DIRECT TENSION SPECIMEN

Serial no.	Specimen designation	Rebar diameter	details
1	NC8	8	Normal concrete
2	NCC8	8	Normal concrete withcrack
3	BC8	8	Bacterial concrete

4	BCC8	8	Bacterial concrete withcrack
5	NC12	12	Normal concrete
6	NCC12	12	Normal concrete withcrack
7	BC12	12	Bacterial concrete
8	BCC12	12	Bacterial concrete with crack

Fig. 3. Direct tension specimen

E. Casting Of Direct Tension Specimen With Standardised Cracks

Standardized cracks were realized in the specimen investigate the crack healing property of bacterial concrete. A thin plate of 0.3mm thickness and a length of 300mm were introduced in the direct tension specimen up to a depth 20mm. The plates were removed during demolding, resulting in prisms with a narrow groove on their upper surface with a thickness of 0.3mm. Direct tension specimen with standardized cracks is shown in Fig.4.

Fig. 4 . Specimen with standardised cracks

F. Test Setup And Instrumentation.

After 28 days of curing, the specimens were coated with white paint so that the cracking pattern is clearly visible during the time of conducting the test. Fig. 5 shows the test setup. The specimens were tested under uniaxial tension in a universal testing machine (UTM) with a capacity of 600 kN. The axial elongation of the specimen was monitored by a linear variable differential transducer (LVDT), fixed on the face of the specimen over a gauge length of 550 mm. The displacement was noted using a digital displacement indicator. A grid with a spacing of 100 mm was drawn on the front face of the specimen before testing to identify the crack locations continuously during the test. The location of each visible crack was marked on the specimen immediately after its appearance during the test. The testing was done under a load-control condition and continued until yielding occurred. In Table IV the details of tested specimens and variables are given.

Fig. 5. Test setup

IV RESULTS AND DISCUSSIONS

A) Compressive strength: On the 7th and 28th days three cubes of normal concrete were tested and average of the compressive strength were obtained as 16.98 N/m $m2$ and 23.55 N/$mm2$. TableV shows that bacterial concrete cubes have a higher compressive strength than the conventional concrete.

TABLE V COMPRESSIVE STRENGTH

Compressive strength	7^{th} day (N/mm^2)	28^{th} day (N/mm^2)
Normal concrete	16.98	23.55
Bacterial concrete	20.6	33.8

B) Flexural strength : From Table VI, the Flexural strength of bacterial concrete was obtained as 4.08 N/*mm*2.the flexural strength of bacterial concrete showed an increase of 29.93%.

TABLE VI FLEXURAL STRENGTH

Mix designation	Flexural strength (N/mm^2)
Normal concrete	3.14
Bacterial concrete	4.08

C) Split tensile strength: After 28 days 3 normal concrete cyinders were tested for fiding the split tensile strength. The averge of the result of split tensile strength were obtained as 1.91 N/ mm2. The results in table VII shows that the bacterial concrete has a better tensile strength than normal concrete.

TABLE VII SPLIT TENSILE STRENGTH

Mix designation	Split tensile strength (N/mm^2)
Normal concrete	1.91
Bacterial concrete	2.11

D) Tension Stiffening

Crack pattern of direct tension specimen are shown in fig.6

NC8&BC8 NC12&BC12

NCC8&BCC8 NCC12&BCC12

Fig. 6. Cracked specimen

In all specimen first crack appeared near the middle portion of the specimen. The first cracks widened, and additional cracks appear. Longitudinal splitting cracks were also developed in some of the normal concrete specimen. Bacterial concrete specimen showed less crack with reduced crack width. The test results are given in table VII

TABLE VIII TEST RESULTS

SPECIMEN	FIRST VISIBLE CRACK (KN)	YIELD LOAD (KN)
NC8	12	28
BC8	15	32
NCC8	10	24
BCC8	12	29
NC12	23	61
BC12	27	70
NCC12	18	55
BCC12	16	60

From the direct tension test the better results were shown by bacterial concrete specimen. In all the cases the yield load of bacterial concrete is more than that of the conventional concrete. In case of 8mm diameter bar specimen the yield load of bacterial concrete specimen is 14.28%. In the case of 12 mm diameter bar specimen the yield load of BC12 is 14.75% more than that of NC12. In the case of cracked specimen better result is observed in bacterial concrete specimen. The yield load of BCC12 is 9.09% more than that of NCC12. The yield load of BCC8 is 20.83% more than that of NCC8.

E) Load Deformation Behaviour : the load deformation response of entire specimen can be obtained by plotting axial load with member strain. The Fig. 7. shows the experimental response of all specimens containing 8 mm diameter bar compared with bare bar. Fig. 8. shows the experimental response of all specimen containing 12 mm diameter bar compared with bare bar. Fig. 9. shows the response of all cracked specimen containing 8mm diameter bar compared with bare bar. Fig. 10. shows experimental response of all cracked specimen containing 12mm diameter bars compared with bare bar. When considering the experimental test result for all specimen, the behaviour was linear up to first crack and initial stiffness of specimen was higher than the stiffness of bare bar. It can be noted that bacterial concrete specimens exhibited more stiffness compared to conventional concrete.

Among the pre cracked specimen the better results where shown by the bacterial concrete specimens. This may be due to the crack healing property of bacterial concrete. The better results of bacterial concrete cracked specimen may be because of the microbially induced calcite precipitation. The bacteria used for sample preperation (Bacillus Subtilis) is a ureolytic bacteria, which precipitates calcite.

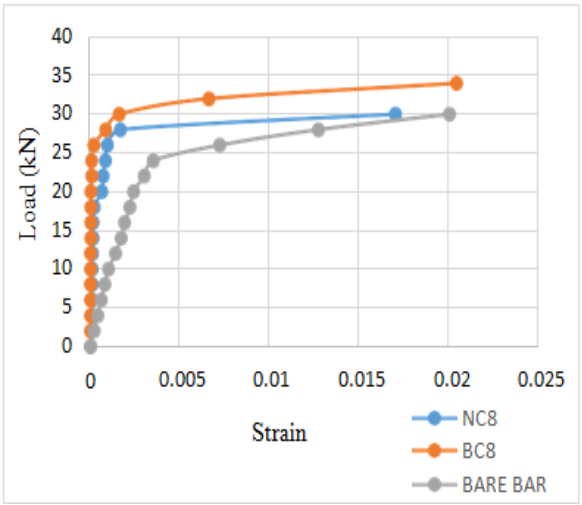

Figure 7 load deformation behaviour of nc8, bc8 and 8mm diameter bare bar

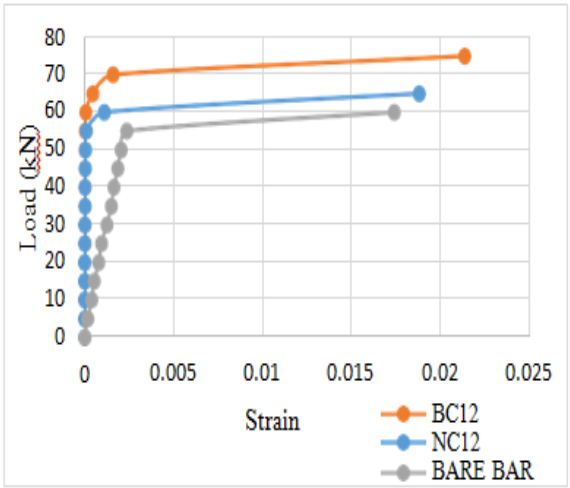

Fig. 8. Load deformation behavior of NC12, BC12 and 12mm diameter bare bar

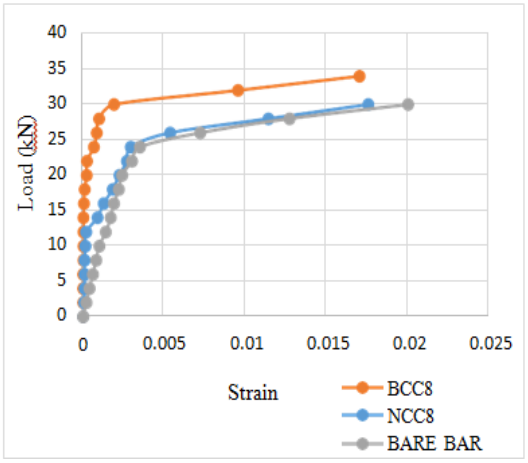

Fig. 9. Load deformation behavior of BCC8, NCC8 and 8mm diameter bare bar

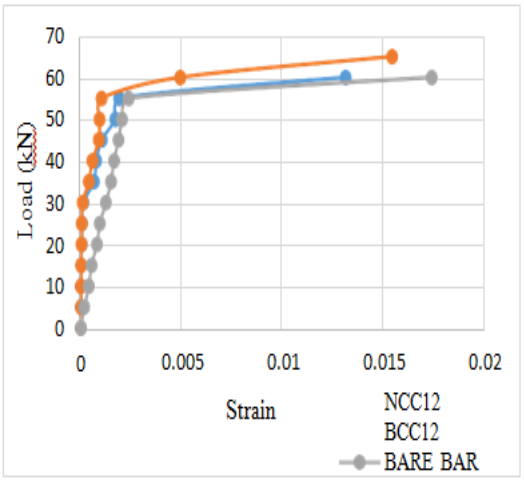

Fig. 10. Load deformation behaviour of NCC12, BCC12 and 12mm diameter bare bar

V CONCLUSIONS

Based on the experimental results of the study presented in this paper the following conclusions are made.

1. Bacillus subtilis is a soil bacterium with a safer bio safety value of 1 and it can be prepared in a laboratory.
2. The result of compressive strength indicates that the introduction of bacteria in concrete cubes increases the strength compared to conventional cubes. Early age strengthening is observed. The 7th an 28th day compressive strength after curing shows that the strength increased by 21.3% and 43.5%
3. Flexural strength results of bacterial concrete is increased by 29.93%. Likewise

split tensile strength of bacterial concrete is 10.47% more than that of conventional concrete.

4. Improvement in strength was visible from initial stage in all cases. It shows that the bacteria activities were on peak on the initial days.
5. The stiffness of all the direct tension specimen is more than that of bare bar.
6. While considering the bar diameters, the prism specimen containing 12mm diameter reinforcement bar shows more tension stiffening behaviour than that of specimen containing 8mm diameter bars.
7. The tension specimen with bacterial concrete shows more stiffness than the conventional concrete.

REFERENCES

1. Sandip Mondal, Aparna Ghosh (2019) "Review on microbial induced calcite precipitation mechanisms leading to bacterial selection for microbial concrete" Construction and Building Materials 225(2019) 77-75.
2. Kim Van Tittelboom, Nele De Belie, Willem De Muynck, and Willy Verstraete. (2010) "Use of bacteria to repair cracks in concrete" cem.conc.res; 40(1) 157-156
3. Henk M. Jonkers, Arjan Thijssen, Gerard Muyzer, Oguzhan Copuroglu, and Erik Schlangen. (2010). "Application of bacteria as self-healing agent for the development of sustainable concrete." Ecol. Eng., 36(2), 230–235
4. Mostafa Seifan, Ali Khaje Samani, Aydin Berenjian, (2016) "Bio concrete; next generation construction material." Construction and building materials 100: 2591–260polypropylene fiber on fresh, mechanical and durability properties of concrete" Journal of King Saud University – Engineering Sciences, 75 (2015) 15245
5. Sandip Mondal, Aparna (Dey) Ghosh (2018) "Investigation into the optimal bacterial concentration for compressive strength enhancement of microbial concrete" Construction and Building Materials, 183 (2018) 203-214
6. Akshay J P, Basil Baby, T Palanisamy (2021) "Experimental Study on Durability and Mechanical Properties of Lightweight Mortar with Encapsulated Spore Forming Bacteria" international conference on structural engineering and construction management springer link volume 284
7. Mingyue Wu , Xiangming Hu, Qian Zhan, Weimin Cheng , Di Xue, Yanyun Zhao (2015) "Application of bacterial spores coated by a green inorganic cementitious material for the self-healing of concrete cracks", cement and concrete composites 113(2020) 103718
8. Tanvir Manzura, Rafid Shams Huq , Ikram Hasan Efaz, Sumaiya Afrozd , Farzana Rahmane, Khandaker Hossain (2019) "Performance enhancement of brick aggregate concrete using microbiologically induced calcite precipitation" case studies in construction material 11(2019) e00248
9. Chandni Kumari; Bhaskar Das ; R. Jayabalan; Robin Davis; and Pradip Sarkar (2016) "Effect of Nonureolytic Bacteria on Engineering Properties of Cement Mortar toughness" journal of material in civil engineering 2016
10. Hui Rong, Guanqi Wei, Guowei Ma, Ying Zhang, Xinguo Zheng, Lei Zhang, Rui Xu (2020) "Influence of bacterial concentration on crack self-healing of cementbased material" Construction and building materials, 244(2020) 118372 65
11. Mitchell, A. C., Espinosa-Ortiz, E. J., Parks, S. L., Phillips, A. J., Cunningham, A. B., & Gerlach, R. (2019). Kinetics of calcite precipitation by ureolytic bacteria under aerobic and anaerobic conditions. Biogeosciences, 16(10), 2147–2161.
12. Sooraj Chandra R.S, Dr. Sabeena M.V "Experimental and Analytical approach to Study the Effect of Tension Stiffening and Cracking in Fibre Reinforced Concrete" International Journal of Innovative Research in Science, Engineering and Technology, Vol. 5, Issue 8, August 2016.
13. IS 12269, Specification 53 grade ordinary Portland cement specification, Bureau of Indian Standards,1997
14. IS 4031 Part 4, Methods of physical tests for hydraulic cement Determination of consistency of standard cement paste, Bureau of Indian Standards.2004
15. IS 2386. Methods of test for aggregates for concrete, Bureau of Indian standards,1986
16. IS 383, Specification for Coarse and Fine aggregate from natural sources for concrete, 1970

17. Henk M. Jonkers, Arjan Thijssen, Gerard Muyzer, Oguzhan Copuroglu, and Erik Schlangen. (2010). "Application of bacteria as self-healing agent for the development of sustainable concrete." Ecol. Eng., 36(2), 230–235
18. IS 9103, Concrete Admixtures Specification, 1999

Progressive Collapse Analysis by Comparing Intermediate Moment Resisting Frames and Dual Systems with Buckling Restrained Braces

Christina Bobby P
Dept.of Civil Engineering
AWH Engineering College, Kozhikode
Kozhikode, Kerala, India
christinasiyon@gmail.com

Priyanka Dilip
Dept.of Civil Engineering
AWH Engineering College, Kozhikode
Kozhikode, Kerala, India

Abstract— Progressive collapse refers to the phenomenon in which the local damage of a primary structural element leads to total or partial structural system failure. In the present study, the progressive collapse potential of steel dual systems with buckling restrained braces was evaluated and compared with those of the conventional intermediate moment resisting frames. The study was conducted on 5- storey frames by applying the alternate path method and the critical columns and adjacent braces, if present were instantaneously removed as per the GSA guidelines and the ability of the structure to successfully absorb member loss was investigated. The structures were modelled and analysed using ETABS software and non- linear dynamic analysis was carried out. The results showed that the dual systems showed better progressive collapse capacity when compared to intermediate moment resisting frames.

Keywords— Progressive Collapse, Dual Systems, Buckling Restrained Brace, Moment Resisting Frame, Alternate Path Method, Nonlinear Dynamic Analysis.

I. INTRODUCTION

Progressive collapse is a dynamic failure process in which loss of local load carrying capacity propagates through a system, precipitating widespread collapse. The process evolves from a local triggering event for which the structure was not designed, such as gas explosions, vehicular impact, blast effects, etc.

They can also be induced deliberately as a demolition method, specifically that of building implosion, or caused by acts of terrorism or war. Any collapse in a way could be regarded as progressive collapse, but it should be of special concern if the collapse is disproportionate to its original cause. The disproportionality refers to the situation in which failure of one member causes a major collapse of larger magnitude compared to initial event. Progressive collapse analysis and design guidelines provided by General Service Administration (GSA) employ the alternate path method to evaluate a structural system in order to compute its vulnerability to progressive collapse.

Dual systems with Buckling Restrained Braces (BRBs) are primarily employed as lateral load resisting systems in the structures located in seismic-active areas. These systems consist of buckling restrained braces arranged in various configurations, such as diagonal, Inverted-V (chevron), Double-story X, etc. in conformity with their heights and have the advantages of both moments resisting frames and buckling restrained braced frames. The main characteristics of BRBs are the high ductility, excellent energy dissipation, and nearly symmetrical hysteretic response in tension and compression. The core segment of a BRB is filled with unbounded concrete (mortar) that offers resistance to both in-plane and out of plane buckling of the steel plate inside, thereby boosting the axial resistance and energy dissipation potential of BRBs under the compressive axial loading. The modern buckling restrained braces are called all-steel BRBs, are entirely made up of steel components. The buckling restraining mechanism in this type of BRBs are usually steel hollow structural members as an alternative for conventional mortar or concrete filled steel tubes.

II. BUCKLING RESTRAINED BRACE

A buckling-restrained brace (BRB) is a structural brace in a building, designed to allow the building to withstand cyclical lateral loadings, typically earthquake-induced loading. It consists of a slender steel core, a concrete casing designed

to continuously support the core and prevent buckling under axial compression, and an interface region that prevents undesired interactions between the two. Braced frames that use BRBs – known as buckling-restrained braced frames, or BRBFs – have significant advantages over typical braced frames. Three major components of a BRB can be distinguished are its steel core, its bond-preventing layer, and its casing. The steel core is designed to resist the full axial force developed in the bracing. Its cross-sectional area can be significantly lower than that of regular braces, since its performance is not limited by buckling. The core consists of a middle length that is designed to yield inelastically in the event of a design-level earthquake and rigid, non-yielding lengths on both ends. Increased cross-sectional area of the non-yielding section ensures that it remains elastic, and thus plasticity is concentrated in the middle part of the steel core. Such configuration provides high confidence in prediction of the element behavior and failure. The bond-preventing layer decouples the casing from the core. This allows the steel core to resist the full axial force developed in the bracing, as designed. The casing – through its flexural rigidity – provides the lateral support against flexural buckling of the core. It is typically made of concrete-filled steel tubes. The design criterion for the casing is to provide adequate lateral restraint (i.e., rigidity) against the steel core buckling.

III. Modelling and analysis

In this work, the analysis based on non-linear dynamic method is used to compare the progressive collapse capacity of Intermediate Moment Resisting (IMF) frames and Buckling Restrained Braced (BRB) frames. The removal of critical columns is governed by GSA (general service administration)

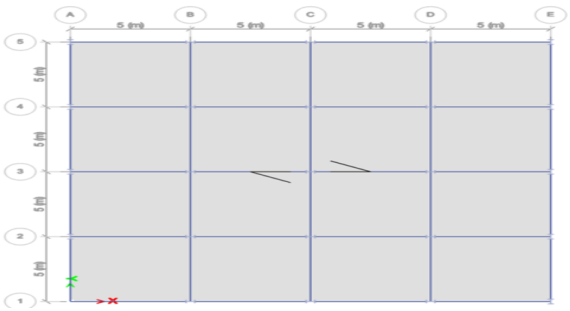

Fig.1. Plan of the model- column removal positions

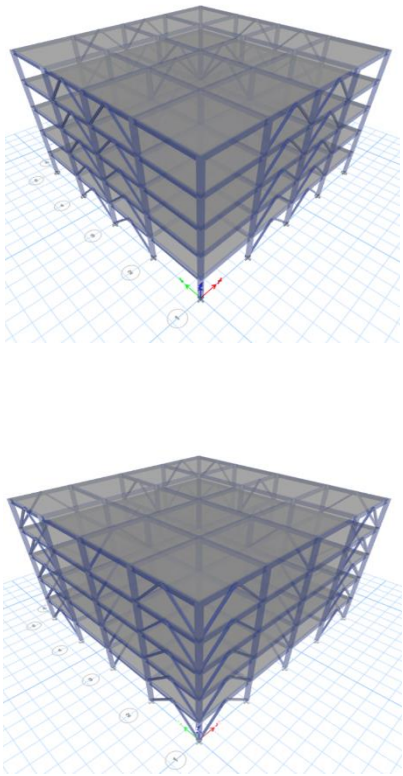

Fig.2. Dual system 1 and 2

TABLE I. PROPERTIES OF 5 STOREY IMF AND DUAL SYSTEMS

Parameters	**Values**
Typical Storey Height	3
Base Storey Height	3
No. of Bays along X-Direction	5
No. of Bays along Y-Direction	5
Bay Length along X-Direction	4
Bay Length along Y-Direction	4
Columns	W14X74, W14X82(bottom)
Beams	W14X 48
Slab Thickness (deck slab)	85 mm
Bottom Support Conditions	Fixed
Grade of steel	Grade 50
Area of brace	970mm^2

TABLE II. LOAD CALCULATIONS

Parameters	Values
Live Load - Floor	2.5 kN/m^2
Live Load - Roof	1.5 kN/m^2
Dead load	3.5 kN/m^2

Dual system 1 and 2(DS1 and DS2) vary in the position of bracing. Columns were removed from three positions i.e., exterior, interior and corner positions as per GSA guidelines. Non-linear time history analysis using El Centro data is conducted. Column forces adjacent to the removed column in all directions are analysed and maximum values were taken. The maximum storey displacement in each storey is also taken and compared the progressive collapse capacity of dual system and IMF.

IV. RESULT AND DISCUSSION

1) Corner column removal ground storey

Corner column C1 from ground storey of both IMF and dual systems were removed and parameters of C2 and C6 were analysed.

a) Column forces

TABLE III. RESULTS COLUMN C2

Parameter	IMF		DS1		DS2	
	Intact	Damaged	Intact	Damaged	Intact	Damaged
Axial load (kN)	911.22	1183.09	1058.08	1265.17	1370.33	1124.94
Shear force (kN)	214.37	229.11	135.55	140.52	133.93	158.23
Bending moment (kNm)	542.02	572.19	307.9	317.45	307.81	355.45

TABLE IV. RESULTS COLUMN C6

Parameter	IMF		DS1		DS2	
	Intact	Damaged	Intact	Damaged	Intact	Damaged
Axial load(kN)	787.34	1109.86	1041.72	1217.14	1024.47	1079.08
Shear force(kN)	274.19	264.71	163.36	155.19	161.73	172.74
Bending moment(kNm)	593.76	611.48	331.95	331.92	331.86	376.82

b) Maximum Storey displacement

Parameter	IMF		DS1		DS2	
	Intact	Damaged	Intact	Damaged	Intact	Damaged
Axial load(kN)	1463.99	1746.39	1714.69	1770.8	1617.19	1854.94
Shear force (kN)	271.47	294.04	163.29	220	162.6	169.46
Bending moment(kNm)	591.4	629.77	331.9	429.32	332.61	344.07

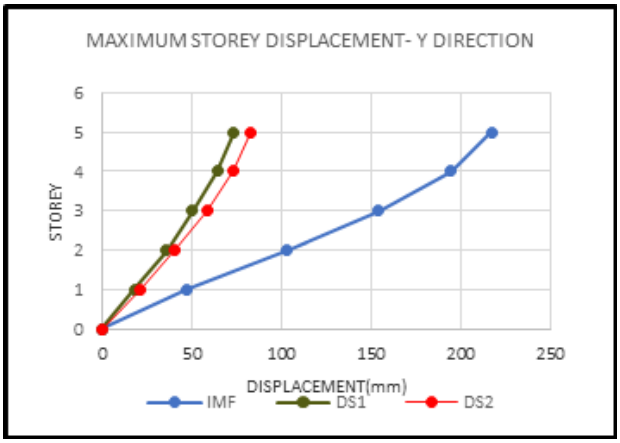

Fig.2. Maximum storey displacemet in Y direction

From corner column removal, except for the shear force of DS1 and axial load of DS2, all other parameters are increasing in damaged condition. The decrease in axial load is due to the removal of two braces.

Exterior column removal ground storey

Exterior column C11 from ground storey of both IMF and dual systems were removed and parameters of C6, C12 and C16 were analysed.

a) Column forces

TABLE V. RESULTS COLUMN C12

TABLE VI. RESULTS COLUMN C6 and C16

Parameter	IMF		DS1		DS2	
	Intact	Damaged	Intact	Damaged	Intact	Damaged
Axial load(kN)	787.34	1117.21	1041.72	1714.69	1024.47	1032.05
Shear force(kN)	274.19	302.5	163.36	163.29	161.73	168.11
Bending moment(kNm)	593.76	646.02	331.95	331.9	331.86	344.99

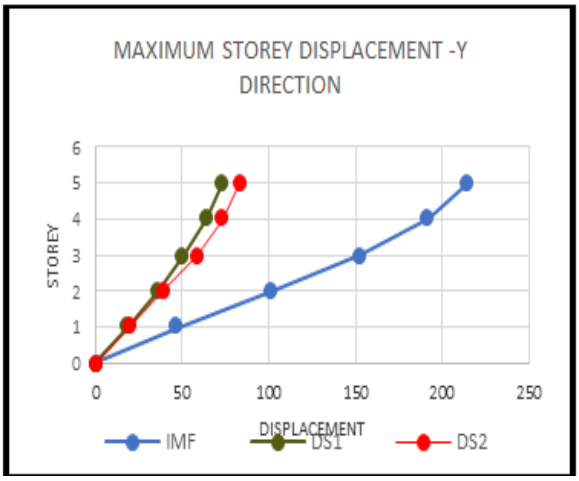

Fig. 3. Maximum storey displacemet in Y direction

For exterior column removal, most of the parameters are increasing in damaged condition. The parameters are increasing and shows the maximum values for column C12.

3) Interior column removal ground storey

Interior column C12 from ground storey of both IMF and dual systems were removed and parameters of C7, C11, C13 and C17 were analysed.

a) Column forces

TABLE VII RESULTS COLUMN C7 and C17

Parameter	IMF		DS1		DS2	
	Intact	Damaged	Intact	Damaged	Intact	Damaged
Axial load(kN)	1528.48	1965.93	1525.02	1733.68	1517.68	1714.92
Shear force (kN)	274.2	285.81	164.89	167.19	163.85	166.12
Bending moment(kNm)	593.76	617.18	333.28	339.66	333.69	339.98

TABLE VIII RESULTS COLUMN C11

Parameter	IMF		DS1		DS2	
	Intact	Damaged	Intact	Damaged	Intact	Damaged
Axial load(kN)	798.34	1077.44	740.62	896.62	1527.83	1539.89
Shear force(kN)	271.47	292.63	163.82	170.5	165.13	171.73
Bending moment(kNm)	591.4	627.31	332.36	349.52	334.81	345.82

TABLE IX RESULTS COLUMN C13

Parameter	IMF		DS1		DS2	
	Intact	Damaged	Intact	Damaged	Intact	Damaged
Axial load (kN)	1488.7	1902.72	1395.42	2146.64	1542	1731.93
Shear force (kN)	271.47	282.61	163.81	167.95	165.07	169.13
Bending moment(kNm)	591.4	610.18	332.35	339.32	334.74	341.58

b) Maximum Storey displacement

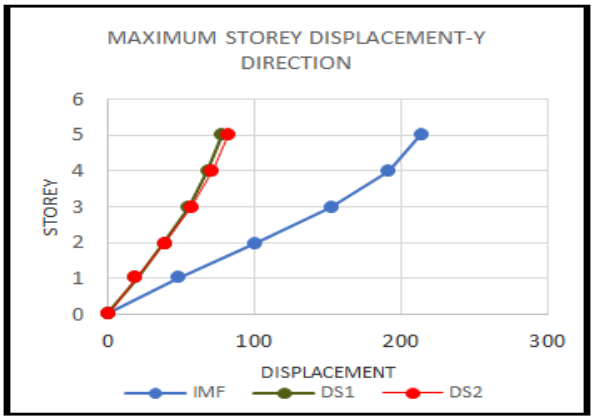

Fig.4. Maximum storey displacement in Y direction

For interior column removal all the parameters are increasing in damaged condition. Column C13 shows the maximum values of axial load. In the case of shear force and bending moment column C11 shows the maximum values.

V. Conclusions

This study was conducted to find the progressive collapse capacity of buckling restrained braced frames as dual systems and to compare with conventional steel moment resisting frames. Nonlinear dynamic analysis were conducted. The alternate path method was employed and first storey column was detached from the structural models. Based on the study following conclusions were made:

- The IMF shows more storey displacement than dual systems. So dual systems are better than IMFs.

- In most of the cases, DS1 shows less displacement than DS2. So, DS1 has better progressive collapse capacity.
- When comparing axial load, interior column removal is the most critical for ground storey removal and third storey removal.
- When comparing shear force and bending moment, IMF shows the maximum values than the dual systems.

Acknowledgment

I am sincerely grateful for all the guidance and help I received from the professors and staff at the institution.

References

1. Khandelwal, K., El-Tawil, S. and Sadek, F., "Progressive collapse analysis of seismically designed steel braced frames", Journal of Constructional Steel Research, Vol. 65, No. 3, (2009), pp 699-708.
2. Liu, M., "Progressive collapse design of seismic steel frames using structural optimization", Journal of Constructional Steel Research, Vol. 67, No. 3, (2011), pp 322-332.
3. Ruth, P., Marchand, K.A. and Williamson, E.B. (2006), "Static equivalency in progressive collapse alternate path analysis: Reducing conservatism while retaining structural integrity", Journal of Performance of Constructed Facilities, Vol. 20, No. 4, (2006), pp 349-364.
4. Chen, Ch.H., Zhu, Y.F., Yao, Y., Huang, Y. and Long, X., "An evaluation method to predict progressive collapse resistance of steel frame structures", Journal of Constructional Steel Research, Vol. 122, (2016), pp 238–250.
5. Tavakoli, H. and Kiakojouri, F., "Influence of sudden column loss on dynamic response of steel moment frames under blast loading" International Journal of Engineering-Transactions B: Applications, Vol. 26, No. 2, (2013), pp 197-206.
6. Parsaeifard, N. and Nateghi-A, F., "The effect of local damage on energy absorption of steel frame buildings during earthquake", International Journal of Engineering-Transactions B: Applications, Vol. 26, No. 2, (2012), pp 143-152.
7. GSA, Progressive collapse analysis and design for new federal office buildings and major modernisation projects, The US General Services Administration, Washington, DC (2013).
8. AISE360-10, "Specification for structural steel buildings", American Institute of Steel Construction Inc. Chicago, (2010).

Seismic Analysis Of Buildings Using Water Tank As Tuned Liquid Mass Damper

Sadha Parveen P
dept.of Civil Engineering
AWH Engineering College, Kozhikode
Kozhikode, Kerala, India
sadhaparveen.p@gmail.com

Anila S
dept.of Civil Engineering
AWH Engineering College, Kozhikode
Kozhikode, Kerala, India
anila@awhengg.org

Abstract— A Tuned mass damper (TMD) is a device consisting of a mass, and spring that is attached to a structure in order to reduce the dynamic response of the structure. The frequency of the damper is tuned to a particular structural frequency so that when that frequency is excited, the damper will resonate out of phase with the structural motion. Therefore, various types of dampers are being developed at present to reduce the vibration in those structures. Amongst the Tuned Mass Dampers, the usage of Liquid Tuned Mass Damper is more encouraged due to their relative advantages. Since the overhead water tanks are integral part of a structure, they can serve as Tuned Liquid Mass Dampers. In this study the liquid tuned mass dampers are modeled making use of the overhead water tanks in buildings. The effect of Multiple Liquid Tuned Mass Dampers on the unsymmetrical buildings with and without tuned liquid mass damper is to be studied. The study is carried-out on Hexagonal and rectangular shaped buildings by using response spectrum analysis. The studies are repeated by varying the water level in tanks as empty, one-third full, two-third full and full water tank conditions. The performance of tuned liquid mass dampers is demonstrated by comparing the values of Maximum storey deflection and the magnitude of Base shear of the building for different tank capacities.

Keywords— Tall structures, Tunes Mass Liquid Damper (TLMD), Water Tank, Seismic Vibration

I. INTRODUCTION

Urbanization of a metropolis is in general reflected by tall buildings all around and improvised infrastructure. For a structural designer, tall structures pose design challenges as they are highly vulnerable to natural calamities like Cyclones and Earthquakes. Excessive use of shear walls in buildings is not always acceptable as their placement infringes with the vehicular movement and the architectural features of the building. As the next alternative, the base isolators are tried at to reduce both base shear and the lateral displacements of the buildings. Though the idea appears to be acceptable, it is a costly proposition, hence it is not a desirable alternative. In this backdrop, introduction of Tuned Mass Dampers is considered the most effective alternative. The TMDs are both economical and are effective in reducing both base shear and amplitude of vibrations of the building subjected to dynamic causes. As well as providing passive or active counter forces, structural vibrations generated by earthquakes or wind can be controlled by modifying rigidities, masses, damping, and form. Efficiency,2 compactness, weight, capital cost, operating cost, maintenance needs, and safety are all factors that influence the choice of vibration dampening equipment. On excitation of a certain structural frequency, the damper's frequency is changed, causing the damper to oscillate out of phase with structural motion. By attaching a spring-dashpot to the mass, energy is released as a result of its relative movement with respect to the building.

Amongst the Tuned Mass Dampers, the usage of Liquid Tuned Mass Dampers are more encouraged. Since the overhead water tanks are integral part of a structure, they can serve as Tuned Liquid Mass Dampers and are considered a very cost- effective solution in seismic design. The mass of water in the tank plus the mass of the water tank constitute the total mass of the Tuned Mass Damper. The structural damping due to the concrete structure constitutes the damping of the Tuned Mass Damper. By suitably altering the mass of liquid in the water tank, the size of the water tank and the number and size of the columns supporting the water tank, the mass, the

damping and the stiffness of the Tuned Liquid Damper are tuned.

A. Tuned Liquid Mass Damper

The passive device, tuned liquid damper (TLD), is a type of tuned mass damper (TMD) where the mass is replaced by liquid (generally water). A conventional TMD needs frictionless rubber bearings, special floor for installation, springs, dashpots and other mechanical components which increase the cost of this device. It dissipates vibration energy through sloshing.

Although TLD is usually a rigid tank with shallow water in it, it promises to be most suitable, since existing water tanks in buildings may be used as TLD without adversely affecting its functional use and also include low cost, easily adjustable natural frequency, suitability for temporary use, easy installation and maintenance. The working principle of TLD is based on sloshing of the liquid to absorb a portion of the dynamic energy of the structure subjected to seismic motion and thus controlling the structural vibration. Tuned liquid damper (TLD) is a device which absorbs energy of structural vibration through sloshing of fluid when sloshing frequency is tuned to the structural frequency. TLD is widely used to control wind-induced vibrations in civil structures.

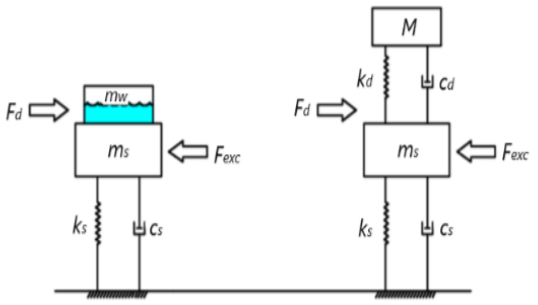

Fig. 1. Representation of a TLMD

II. OBJECTIVE

The objective of the present study is to find effectiveness of TLMD for different building plans with and without TLMD. To study the effective of multiple TLMDs in a buildings. To study effect of TLMD by varying the water level in tanks as empty, one-third full, two-third full and full water tank conditions.

III. LITERATURE REVIEW

Rajashekhar S. Talikoti et. al. had studied the effectiveness of TMD in controlling the vibrations of structure. A building structure was modelled with and without TMD and Response spectrum analysis was carried- out. From the study, it was found that TMD was more effective when it is attached at the top floor of building and the presence of TMD resulted in gradual decrement of the displacement, the storey drift and the fundamental period of the structure [1].

Manjusha M had carried out the analytical investigation to study the feasibility of implementing water tank as a passive Tuned Mass Damper (TMD) using ETABS 2015. Multi- storey concrete building structure was taken for the study and a water tank was placed on the roof. The mass and frequency of both were tuned to the optimized values. The behavior of the tank under full and empty tank condition subjected to earthquake data was studied. It was concluded that TMD had effectively reduced the overall behavior of the structure resulting in economic and safe design and can successfully be used to control the response of the structure [2].

Dorothy Reed et al analyzed Time histories of the base shear force and water-surface variations by shaking table tests and compared with a numerical model investigating behavior of tuned liquid dampers (TLD) with the help of laboratory experiment and numerical modelling. It was found that the response frequency of tuned liquid dampers increased as excitation amplitude increased, and the TLD behaved as a hardening spring system. The design frequency damper should be set at the value lower than that of the structure response frequency if it is computed using the linearized water-wave theory by which the actual nonlinear frequency of the damper matched with the structural response. It was found that, even if the damper frequency had been mistuned slightly, the TLD always performed favourably [3].

IV. MODELLING

A. MODEL DETAILS

The buildings considered for the study are RC ordinary moment resisting space frames of G+10 storey located in IV of seismic disturbances. The analysis is carried-out on a rectangular shaped building and hexagonal shaped building. The study is conducted by varying the

water level in water tank by considering, 1. Empty water tank, 2. One-third, 3. Two-third's full and 4. Full water tank conditions using ETABS software.

The plan configuration consist of

1. Hexagonal shaped building with one water tank (V1=13500m3), Two water tank using half volume (V2= 6750m3), Two water tank using double volume (V3= 2V1).
    1. Model 1- Empty water tank
    2. Model 2- One-third water tank
    3. Model 3- Two-third water tank
    4. Model 4- Full water tank
2. Rectangle shaped building with one water tank (V1=13500m3), Two water tank using half volume (V2= 6750m3), Two water tank using double volume (V3= 2V1).

    5. Model 1- Empty water tank

    6. Model 2- One-third water tank

    7. Model 3- Two-third water tank

    8. Model 4- Full water tank

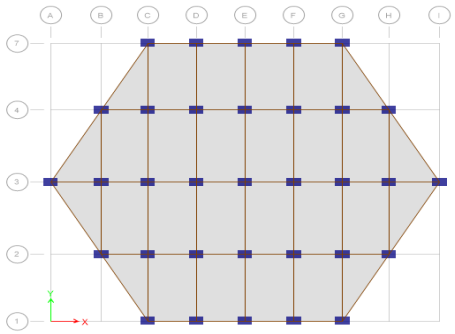

Fig. 2. Plan view of hexagonal shaped building

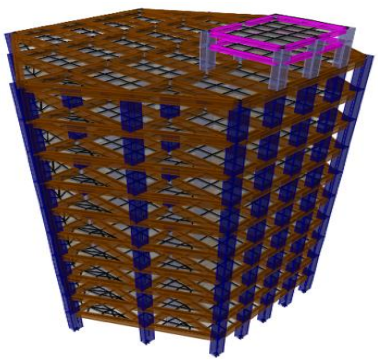

Fig. 3. 3D view of hexagonal shaped building of one water tank (V1=13500m3).

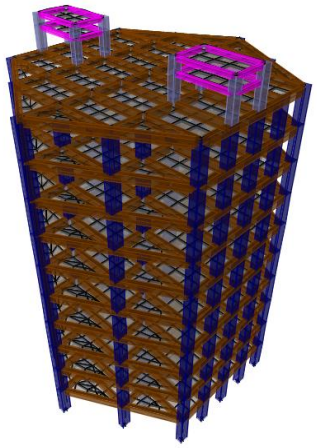

Fig. 4. 3D view of hexagonal shaped building of two water tank using half volume (V2=6750m3).

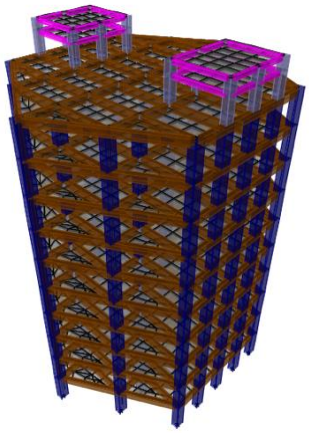

Fig. 5. 3D view of hexagonal shaped building of two water tank using double volume((V3= 2V1).

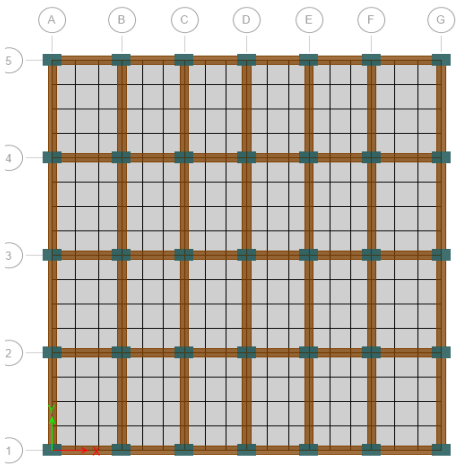

Fig. 6. Plan view of rectangle shaped building

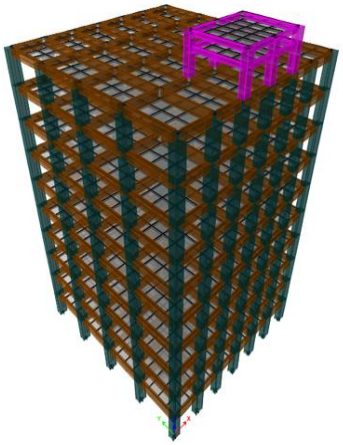

Fig. 7. 3D view of hexagonal shaped building of one water tank (V1=13500m3).

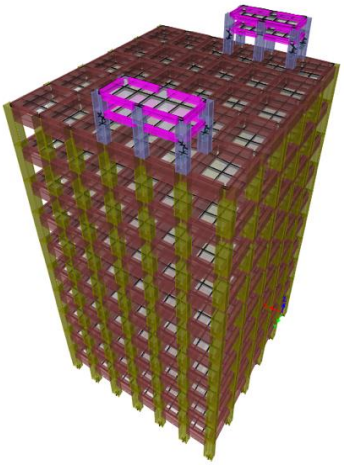

Fig. 8. 3D view of rectangle shaped building of two water tank using half volum((V2= 6759m3).

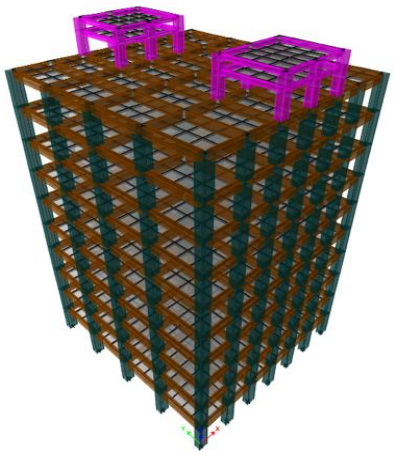

Fig. 9. 3D view of rectangle shaped building of two water tank using double volume((V3= 2V1).

V. SPECIMEN CALCULATION

The preliminary data for the analysis of the frame in ETABS is considered as per the prevailing construction practices which is presented below.

TABLE I. DETAILS OF BUILDING

MODEL DETAILS OF BUILDING	
Material	M30, Fe-500
Size of beam	400x600mm
Size of column	600x900mm
Depth of slab	150mm
Live load	4kN/m
Dead load	2kN/m
Seismic zone factor	0.24
Response reduction factor	5
Importance factor	1

A. Calculation Of Water Tank

TABLE II. DETAILS OF WATER TANK

DETAILS OF WATER TANK	
Total Mass of hexagonal building	4482481.895kg
Total mass of rectangle building	3803450.409kg
Dead load of water tank	386.24KN
Live load of water tank	132.39KN
Length of water tank	6m
Breadth of water tank	5m
Height of water tank	1m
Dead load of water tank V_2	225KN
Live load of water tank V_2	66.195KN

B. Calculation Of Tuned Liquid Mass Damper

TABLE III. CALCULATION OF TLMD PARAMETERS FOR VARYING WATER LEVEL IN THE TANK (V1) FOR HEXAGONAL BUILDING

Hexagonal shaped (V_1)	**Empty water tank**	**One-third level water**	**Two-third water level**	**Full water level**
Mass ratio	0	0.0097	0.0107	0.0117
Tuning ratio	1	0.99	0.9894	0.9884
Optimum damping ratio	0	0.06	0.063	0.0658
Optimum stiffness (KN/m)	0	1314.98	1448.79	1580.99
Optimum damping (KN-s/m)	0	85.91	99.509	113.64

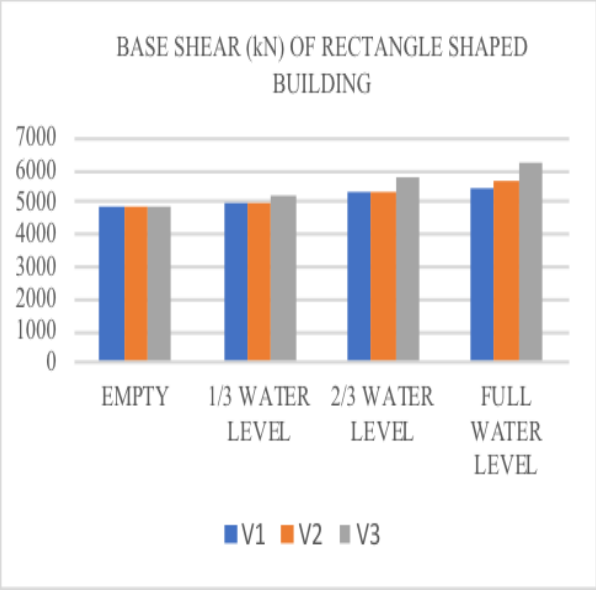

Fig. 10. Base shear of rectangle shaped building

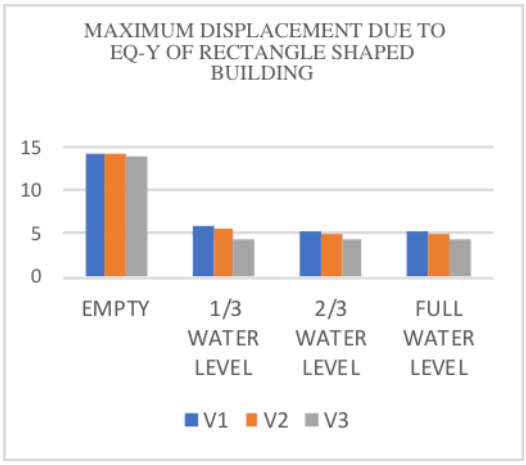

Fig. 11. Maximum displacement due to EQ-X of rectangle shaped building

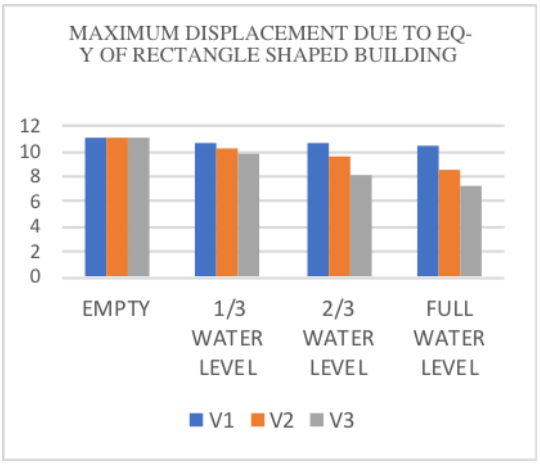

Fig. 12. Maximum displacement due to EQ-Y of rectangle shaped building

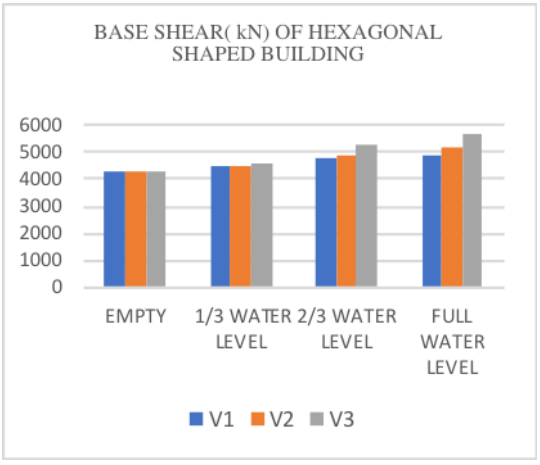

Fig. 13. Base shear of hexagonal shaped building

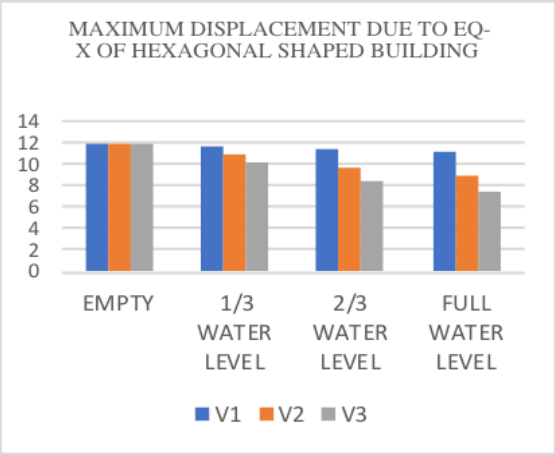

Fig. 14. Maximum displacement due to EQ-X of hexagonal shaped building

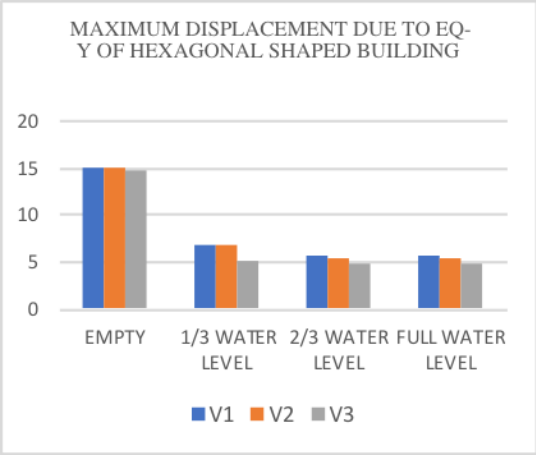

Fig. 15. Maximum displacement due to EQ-Y of hexagonal shaped building

VI. RESULTS AND DISCUSSIONS

The studies are carried-out for water tank empty, one-third full, two-third full and full tank conditions. The information from graphs shows the percentage reduction in the magnitudes of maximum storey displacement and percentage increase in base shear due to the increase of volume of water level. From the graph its obvious that rectangle shaped building with two water tank by using double volume outperforms out of all

- The magnitude of base shear for rectangle shaped building with two water tank using double volume (V3) found to be increased by 23.12% for full water tank with the action of tuned liquid mass damper.
- The magnitude of base shear of hexagonal shaped building with two water tank using double volume(V3) is found to be increased by 25.26% for full water tank by comparing with empty water tank, 19.09% with two-third water level, 7.41% with one-third water level.
- The maximum displacement of X-direction is found to be reduced by 35.26% for full tank condition for rectangle shaped building with two water tank using double volume (V3) with the action of tuned liquid mass damper.
- The magnitude of base shear of rectangle shaped building with two water tank using half volume(V2) is found to be increased by 16.45% for full water tank by comparing with empty water tank, 7.002% with two-third water level, 17.41% with one-third water level.
- The Max storey displacement for X and Y direction is found to be reduced by 25.14% and 55.77 % with hexagonal shaped building with 2 water tank using half volume(V2).
- The maximum displacement of X-direction is found to be reduced by 58.62% for full tank condition for hexagonal shaped building with two water tank using double volume (V3)with the action of tuned liquid mass damper.
- The magnitude of base shear of rectangle shaped building with two water tank using half volume is found to be increased by 9,92% with rectangle shaped building with two water tank using double volume(V3).
- The maximum displacement of Y-direction is found to be reduced by 18.53% for full tank condition for rectangle shaped building with two water tank using double volume (V3) with the action of tuned liquid mass damper.
- The Max storey displacement for X and Y direction is found to be reduced by 19.21% and 35.33 % with rectangle shaped building with 2 water tank using half volume(V2).

VII. CONCLUSION

Based on the studies carried out on different shapes of buildings in different seismic zones, the following conclusions are made:

- It is observed that a structure equipped with Tuned Liquid Mass Damper (TLMD) is effective in controlling the Maximum storey displacements of the structure when compared to a structure without Tuned Liquid Mass Damper.

- The magnitude of Max storey displacement is found to reduce in about 34.23% respectively in X-direction and 28.99% respectively in Y-direction for rectangle-shaped building when equipped with Tuned Liquid Mass dampers.
- The magnitude of base shear is found to be increased by 23.12% for full water tank for rectangle shaped building with two water tank using double volume with the action of tuned liquid mass damper.
- Rectangle shaped building with 2 water tank using double volume (V3) for full water level outperforms out of all
- Based on the conclusions, the present study clearly demonstrates that there is a substantial reduction of amplitude of vibration in tall buildings especially in the direction of weak axis, when the overhead water tanks are modelled as Tuned Liquid Mass Dampers.

ACKNOWLEDGMENT

The support of the authorities of AWH engineering college for the successful completion of project is gratefully acknowledged.

References

1. Mudabbir Imran, Dr. B. K. Raghu prasad "Seismic Response of Tall Structures Using Tuned Mass Dampers", IJREAS (2017)
2. A. Lucchini, R. Greco, G. C. Marano and G. Monti "Robust Design of Tuned Mass Damper Systems for Seismic Protection of Multi-storey Buildings", ASCE (2014)
3. S.M.Zahrai, A. Ghannadi-Asl "Seismic Performance of TMDs in Improving the Response of MRF Buildings", Scientia Iranica (2008)
4. Ashish A. Mohite, G.R. Patil "Earthquake Analysis of Tall Building with Tuned Mass Damper", IOSR (2015)
5. Saurabh Chalke, P.V. Muley "Vibration Control of Framed Structure Using Tuned Mass Damper" International Journal of Engineering Development and Research (2017)

.

Non Linear Static Progressive Collapse Analysis Of A Multi-Storey RC Framed Structure

Nayana Sivadas
Dept. of Civil Engineering
AWH Engineering college,Kozhikode
Kozhikode,Kerala,India
nayanasivadas1998@gmail.com

Minu.U
Dept. of Civil Engineering
AWH Engineering College, Kozhikode
Kozhikode,Kerala,India
minu@awhengg.org

Abstract—Progressive collapse is the process of extensive failure initiated by local structural damage or a chain reaction of failures. This is due to some reasons like fire, gas explosion, terrorist attack etc structures undergoes some major component failure. The main objective of this project is to assess the progressive collapse of RC structures by nonlinear static analysis under column removal scenario using ETABS software. Pushover analysis was performed on a G+11 RC framed rectangular commercial building designed as per Indian Building Code. The removal process of identified critical columns was initiated for progressive collapse and the various parameters like story displacement and column forces were calculated. Thus, the influence of removal of critical elements has been discussed here by comparing the parameters before and after the progressive collapse. From the analysis corner column and middle of long edge column removal shows more critical results.

Keywords—Progressive collapse, Push over analysis, Storey displacement, Column forces, ETABS

I. INTRODUCTION

When the interior load-bearing structural element fails due to any number of means such as blast activity or vehicular accident which results in the failure of a structure or component to maintain its structural integrity this phenomenon is called collapse phenomena. This situation may be initiated by an earthquake, interior or exterior explosions and construction activities.

The classification of the causes of the building collapse is specified under general headings given below:

1. Faulty Construction
2. Unexpected Failure Modes
3. Extraordinary Loads
4. Foundation Failure
5. Column and beam failure

The worldwide problem of ensuring the stability of structures of high-rise buildings against progressive collapse as a result of fire and blasts is becoming more urgent because, leads to very serious consequences. Wear and tear of fixed assets of the country, increasing the rate and density of construction in urban areas, an increase in recent years, the number of terrorist acts (bombings, arson, etc.). The progressive collapse of building structures is a complicated mechanical behaviour of entire structural systems under large deformation. However, limited researches have been conducted to investigate this issue at the last century due to the lack of the experimental technique and numerical simulation for entire structural systems under large deformation. In recent years, with the development of the experimental technique and numerical simulation, the progressive collapse of building structures is studied in depth and the exciting progresses have been reported. A progressive collapse of a building is initiated by an unexpected event that causes local damage and subsequently propagates throughout the structural system, leading to a final damage state in largescale or entire collapse of the building. A progressive collapse can be triggered by accident actions, including fire hazard, gas explosion, terrorist attack, vehicle collision, design and construction errors, and environmental corrosion. With the development of industrialization, the buildings with multifunction and high complication become more common of which the safety and stability are far more concerned. However, the current ultimate limit state design based on the structural reliability theory is commonly used for regular structures to ensure their safety. On the other hand, during the

long-term use, the structure may suffer unexpected accidental actions, causing local damage or failure. Hence if the remaining structural system cannot absorb or contain the internal force variation caused by the initial failure, it will lead to a further damage even the collapse of whole structure, causing huge loss of life and property. The local failure of one or many structural elements creates the additional load in surrounding elements that leads to steady progressive collapse initially and then to the total failure. Therefore the remaining portion of the building is required to redistribute the loads applied to it through the alternate load paths provided for the purpose. This process may continue further till the equilibrium condition of the structure is reached either by provision of loadbearing bracing, or by stable alternative load paths. Progressive collapse is a natural nonlinear event, in which structural components are stressed beyond their elastic limit to occur the failure. The progressive collapse of the building has started gaining attention after the partial collapse in London (Roman point apartment building structure) and the collapse of the Alfred p. Murrah Federal Building structure (Oklahoma City, 1995) and the structure collapse of the World Trade Centre Towers, caused due to the terrorist attacks

II. ASSESSMENTS

A. Pushover Analysis

When a structure is subjected to earthquake, it responds by vibrating. An example force can be resolved into three mutually perpendicular directions two horizontal directions (X and Y directions) and the vertical direction (Z). This motion causes the structure to vibrate or shake in all three directions; the predominant direction of shaking is horizontal. All the structures are primarily designed for gravity loads-force equal to mass time's gravity in the vertical direction. Because of the inherent factor used in the design specifications, most structures tend to be adequately protected against vertical shaking. Vertical acceleration should also be considered in structures with large spans those in which stability for design, or for overall stability analysis of structures. The basic intent of design theory for earthquake resistant structures is that buildings should be able to resist minor earthquakes without damage, resist moderate earthquakes without structural damage but with some non-structural damage. To avoid collapse during a major earthquake, members must be ductile enough to absorb and dissipate energy by post elastic deformation. Redundancy in the structural system permits redistribution of internal forces in the event of the failure of key elements. When the primary element or system yields or fails, the lateral force can be redistributed to a secondary system to prevent progressive failure. The structural model is prepared and pushover analysis has been carried out. The parameters such as storey displacement, storey drift, storey shear, and base shear have been founds so as to check whether the structure is safe in pushover analysis.

B. Progressive Collapse

The expression "Progressive Collapse" can be just characterized as a definitive disappointment or proportionately enormous disappointment of a bit of a structure because of the spread of a neighbourhood disappointment from component to component all through the structure. Dynamic breakdown happens when moderately neighbourhood basic harm, causes a chain response of structure components disappointments, unbalanced to the underlying harm, causing in halfway or full breakdown of the structure. Near by harm that starts dynamic breakdown of structure is called starting harm. When all is said in done, dynamic breakdown happens in a brief time frame right away. It is additionally conceivable that it very well may be described by the loss of burden conveying limit of a moderately little segment of a structure because of a normal burden which, thusly, starts a fall of disappointments influencing a primary segment of the structure. A dynamic breakdown is commanding occasion as it involves the vibrations of auxiliary segments and results in powerful interior powers. These inside powers could be, for example,

Inactivity powers and so on, whose force isn't consumed bythe structure. Dynamic breakdown is a characteristic non-direct occasion, in which auxiliary segments are worried past their versatile point of confinement to happen the failure. Progressive breakdown is are liable annihilation of the bearing structures of the (structure) because of the underlying. Near by harm to the individual transporters of basic segments and prompting the breakdown of the whole building or significant part .

III. MODEL DESCRIPTION

A G+11 storey RC (Reinforced Concrete) multi-storey structure with plan dimension 28×24 m considered. The structure is then designed for the Seismic loads as per IS:1893:2016. The gravity load and wind load acting on building structure is carried out as per IS 875 part 1 & 2 and IS 875 Part 3. The 2D and 3D model generated in ETABSv18.2.1

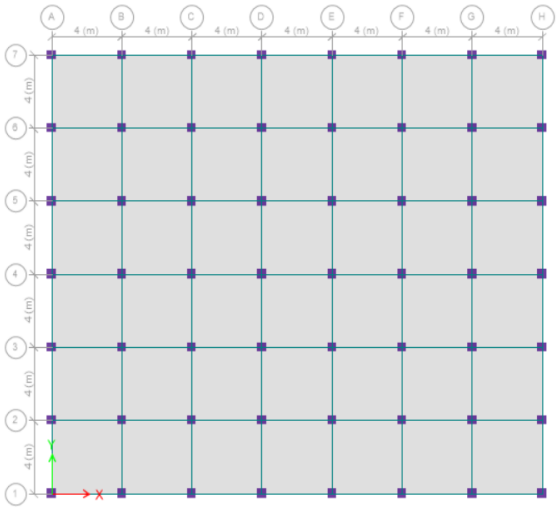

Fig. 1. Plan of the structure

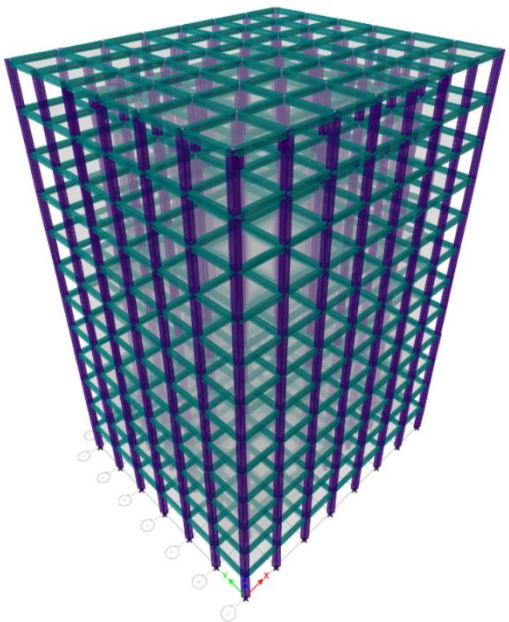

Fig. 2. 3D view of structure

A. Model Dimension

TABLE I. MODEL DETAILS

Dimension	Values
Span in X direction	4 m
Span in Y direction	4 m
Storey height	3.5 m
Beam size	300×400 mm
Column size 1-4 storey	450×450 mm
Column size 5-8 storey	400×400 mm
Column size 9-12 storey	350×350 mm
Slab thickness	150 mm
Grade of concrete	M30
Grade of steel	Fe415

B. Loading Considerations

TABLE II. LOADING DETAILS

Dead load	
Self weight	1 kN/m^2
Wall load on exterior beam	21 kN/m^2
Wall load on interior beam	12.06 kN/m^2
Parapet load	2.06 kN/m^2
Floor finish	1 kN/m^2
Live load	
On floor	4kN/m^2
On roof	1.5 kN/m^2
Wind load	
Wind speed	39 m/s
Terrain category	4
Importance factor	1.2
Response reduction factor	5
Seismic load	
Seismic zone	V
Zone factor	0.36

IV ANALYSIS

Initially, the plan of the building is developed using ETABS v18.2.1 software along with the provisions of IS 1893 for design and load combinations. Then the Non-linear static analysis is carried out separately for each case of column removal and check the structure for progressive Collapse potential.

Identification Of Critical Columns:

Four column removal conditions have been considered as mentioned in GSA 2016 Guidelines to evaluate the potential for progressive collapse of G+11 reinforced concrete structure and the method of analysis used here is Non-linear static analysis techniques.

Thus, there are four cases under consideration.

1. Removal of a column A1 on GF situated at the corner position

2. Removal of column D1 on GF situated at the exterior middle side position.

3. Removal of column D2 GF situated at the interior position.

The building combination analysis is carried out according to the load of IS 1893:2016.

V RESULTS AND DISCUSSIONS

TABLE IV. MAXIMUM STORY DISPLACE-MENT (mm)

Cases	X Direction	Y direction
Case 1	105.61	0.54
Case 2	101.10	0.48
Case 3	100.65	0.42

TABLE V. MAXIMUM BASE SHEAR (kN)

Cases	Base shear
Case 1	5967.23
Case 2	6281.46
Case 3	6325.3

TABLE VI. Comparison of the Values of the Axial Load (AL), Bending Moment (BM), and Shear Force (SF) Results for the case of removal of critical Column A1 (case 1).

Column forces	Intact condition	Damaged condition
Column forces related to column A2		
AL (kN)	1371.99	1598.9
SF (kN)	139.29	141.25
BM (kNm)	282.42	285.4
Column forces related to column B1		
AL (kN)	1381.98	1523.5
SF (kN)	117.3	120.3
BM (kNm)	268.25	290.25

TABLE VII. Comparison of the Values of the Axial Load (AL), Bending Moment (BM), and Shear Force (SF) Results for the case of removal of critical Column D1 (case 2).

Column forces	Intact condition	Damaged condition
Column forces related to column C1		
AL (kN)	1489.34	1667.43
SF (kN)	78.45	81.34
BM (kNm)	189.53	192.4
Column forces related to column D2		
AL (kN)	1134.5	1431.4
SF (kN)	90.45	98.41
BM (kNm)	200.34	202.67
Column forces related to column E1		
AL (kN)	1465.78	1578.3
SF (kN)	75.4	78.5
BM (kNm)	154.78	155.3

TABLE IX. Comparison of the Values of the Axial Load (AL), Bending Moment (BM), and Shear Force (SF) Results for the case of removal of critical Column D2 (case 3).

Column forces	Intact condition	Damaged condition
Column forces related to column D1		
AL (kN)	1057.34	1573.5
SF (kN)	87.31	88.72
BM (kNm)	150.71	152.81
Column forces related D3		
AL (kN)	1778.64	1898.34
SF (kN)	70.83	71.64
BM (kNm)	184.73	185.69
Column forces related C2		
AL (kN)	1564.98	1688.9
SF (kN)	70.71	70.08
BM (kNm)	164.59	164.13
Column forces related E2		
AL (kN)	1425.89	1589.4
SF (kN)	70.82	71.18
BM (kNm)	174.72	178.24

A. Base Shear And Story Displacement

From the results obtained, Base shear decreases and Story displacement increases after column removal. In case of Base shear value corner column removal shows more decrease and Storey displacement shows increase.

B. Column Forces

Column forces like Axial load, Bending moment and Shear force are mostly increasing after column removal and in rare cases decreasing. Decrease in column forces shows that load is transferring to the adjacent column more while removing the column. Axial load shows more increases in all adjacent columns after column removal.

VI CONCLUSIONS

While removing column from the Corner, Interior and middle of exterior edge in the ground storey, Corner column removal shows more critical.

Interior column removal shows least critical

Base shear decreases and Storey displacement increases after column removal.

While removing the column, Column forces are increased in the adjacent column due to the transfer of loads to the adjacent column.

VII REFERENCES

1. S. Mohan Kumar, R. Jeyanthi – "ProgressiveCollapse Analysis of a Multi-storey RCC Building using Pushover Analysis" MNM Jain Engineering College Chennai,March 2016, Vol.No.- 5, ISSN: 2278-0181
2. Shaikh Akhibuddin, L.G.Kalurkar– "Evaluation of Progressive Collapse Resistance of Multi-Storey RC Building by Linear Static Analysis Method" JNEC College, Aurangabad,India, Jul. – Aug. 2016, Volume 13, Issue 4 Ver. VII, e-ISSN: 2278-1684
3. A.Choubey and M.D. Goel – "Progressive Collapse Analysis of Rcc Structures" 2016; 6(2): 287-301
4. Shaikh Akhibuddin, L.G.Kalurkar – "Progressive Collapse Assessment of Reinforced Concrete Framed Structure" JNEC College, Aurangabad, India, 4th Sep.2016, ICRTSTM – 16 , ISBN : 978-93-86171-05-4.
5. S. M. Marjanishvili, - "Progressive Analysis Procedure for Progressive Collapse", Vol. 18, No. 2, May 1, 2004. ©ASCE, ISSN 0887-3828/2004/2-79–85
6. Shefna L Sunamy, Binu P, Dr.Girija K – "Progressive Collapse Analysis Of a Reinforced Concrete Frame Building" Volume 5, Issue 12, December (2014), ISSN 0976 – 6316(Online).
7. Miss. Preeti K. Morey and Prof S.R.Satone –"Progressive Collapse Analysis of Building" KDKCE, RTM University, Nagpur-09, Vol. 2, Issue 4, June-July 2012, ISSN: 2248-9622

Comparative Analysis Of Y Column And Oblique Column By Using Etabs

Shonisha Ajith[1]
Dept of civil Engineering
AWH Engineering college
Kozhikode,India
Shonishaajithaminu@gmail.com

Priyanka Devan[2]
Dept of civil Engineering
AWH Engineering college
Kozhikode,India
priyankadevan777@gmail.com

Abstract— Now a day's utility or floor area of Residential RC Structure is very costly. Any analysis and design approach which enhances the utility area of residential or commercial buildings is highly appreciable. Many researchers/design engineers attempted to achieve it. Strategies like floating columns, central core columns and cantilever beam structures are one of the usual techniques. In the present study, oblique columns and Y-shaped columns are adopted instead of conventional (rectangular or square) columns, 7 storied structures are considered for analysis and comparative study between oblique columns and Y-shaped columns is to be adopted. All the analysis and design work are conducted using ETABS 2018 version. It needs optimum design procedure to proceed for further studies and also for construction. The oblique columns and Y-shaped columns can be used for architectural purpose by giving the pleasing appearance to inclined support members, which increases the aesthetic appearance of the structure. Using ETABS 2018 version for all analysis and design work. In order to move on with more research and construction, the best design process is required. By giving inclined support components an appealing look, oblique columns and Y-shaped columns can be employed for architectural purposes, enhancing the structure's aesthetic appeal.

Keywords—Residential building, Y column, Oblique column, ETABS 2018

I. INTRODUCTION

High rise structures are an important indicator of a country's economic and technological strength. In recent years, countries going for tall buildings, because of material, technology, progress of economy and continued development. Large populations and per capita are the main reasons for the need of ultrahigh rise buildings. Due to various architectural features and style, more and more complex high rise buildings are appearing. Facing a large number of new type complex structural system and progressively consummate earthquake resistant theories, the conventional software can no longer meet the needs of calculation and analysis. Meanwhile some international finite element program such as ETABS, were updating themselves bu remained respective limitations. The fast increment of the urban populace in creating nations, for example, India has constrained the revaluation of the significance of tall structures with various size and shape which prompts distinctive perspective proportion of the structures.

The basic frame work of tall structures are normally not very efficient with the impact of wind and tremor, the breeze seismic tremor structure connections and afterward decides the wind loads and earthquake forces as proportional static loads. It has been demonstrated that the angle proportion of building influences the impact of wind and seismic tremor powers on building .These postulation study the various instances of viewpoint proportion of the structure and impact of wind and earthquakes are occasional forces on structures that may occur rarely during the lifetime of buildings. It is also likely that a structure may not be subjected to severe earthquake forces during its design lifetime .Reinforced Concrete Multi-storied buildings (RCMS) are supposed to be of engineered construction in the sense that they might have been analysed and designed to meet the provisions of the relevant codes of practice and building by laws: The construction might have been supervised by trained persons .In such cases, even if earthquake forces have not been considered precisely, the structures would have adequate in built strength and ductility to

withstand some level of earthquake intensity. In India, in recent decades, the use of civil engineering is becoming more and more popular and the technological situation has improved considerably.

The wind engineering needs a way to get information solution to various critical wind problems .Including various fields such as (i) Fluid energy (ii)potential once calculations and (iii) structural properties. The spirit, generally has two main effects on long structures :First ,they are strong too design times and installations ,second distributes wind into and around a building is called wind pressure. The wind pressure in the building are influenced building geometry, angle of wind events surrounding and signs of wind flow. There are many situation where database , codes / standard and analysis are available. Methods cannot be used to measure wind pressure coefficients and windloads on the claddings and support system of structures, for example ,aerodynamic formation of the structure is unusual.

Various world wide structure and examination programming, for example ETABS, SAP2000, MIDAS/Gen and SATWE are continually developing themselves ,yet stayed individual impediments . In this paper ,reaction range, time history and connecting piece in-plan stresses examination was executed joined with areasonable task ,by the project referenced above, which were additionally looked at following the investigation results.

II. TYPES OF COLUMNS

A. Oblique Column

The new construction method to increase the seismic performance of the multi-storied building is the use of oblique columns instead of normal columns. Oblique column is a column which is not constructed vertical. The oblique columns can be adopted in high-rise, mid-rise and low-rise buildings. The position, arrangement, and angle of inclined columns makes different types of oblique columns in buildings. The angle may vary and this affects the performance of the building. For oblique column of below 90° ,there will be decrease in plan dimensions and for above 90°, there will be increase in plan dimensionsas we reach upper floors. It affects the lateral stiffness of the buildings. But the seismic responses may vary in each case. The dynamic analysis is done to quantify the storey responses in each type of buildings. Here ETABS software is used for the response spectrum analysis. It is a complex structural analysis package. It can be used for the analysis and deisgn of buiding and its components

B. Y Shaped Column

Nowadays utility or floor area of residential building is very costly. Any analysis and design approach which enhances the utility or floor area of residential or commercial building is highly appreciable. Strategies like floating column center core columns and cantilever core structures are the usual techniques. Y shaped column can also be used to increase the utility area. It is adopted where there is a no chance of building square or rectangular or circular type of column. It is rarely used as it possess very difficulty in casting. These types of columns are generally used in the construction of bridges, flyovers, etc.

III. OBJECTIVES

- To analyse the seismic performance of G+7 building with oblique column of 80 degree inclination
- To analyse the seismic performance of G+7 building with Y column of 1.2 m minor leg length.
- To compare the performance of multi-storey structural bulding with oblique and Y column.

IV. METHODOLOGY

- Various literature were made to understand more about oblique and Y column
- Validation of the journal is done to acquire more knowledge about ths topic.
- A G+7 building with oblique column and Y column are modelled
- Analysis and comparison results are made .
- Conclusion about the thesis is made

IV. LITERATURE REVIEW

Harshada Ashok Targe, Utkarsha Dilip Bhadane, Gauri Madav Derle (2022) studied about oblique and Y column which are adopted instead of conventional rectangular column in a 6 storied building are considered for analysis and comparative study between oblique and Y column. All the analysis and d esign work are conducted using ETABS 2013 version. Maximum storey displacement ,Maximum storey drift, Base

shear , storey stiffness and time period are analysed and compared. The results obtained showed that maximum storey displacement is increased in Y shaped column by 697.94 %.In case of storey drift y column shows higher value of 53.08%.Moreover the lower baseshear is obtained in oblique column. It means that base shear value is increased by 32.07 % in Y shaped column as compared to oblique column. The joint of Y shaped column holds to be weak under seismic loading. Neccessarily requires strengthening the joints of Y shaped column. Maximum storey stiffness is decreased by 58.25% in Y columns.. Oblique column offers best resistance to lateral loads. Hence it needs optimum design procedure to proceed for further studies and also for construction. In time period there is no change in oblique and Y column. By the analysis we can conclude that the overall performance of structure is increased when the oblique shape dcolumns are used for construction instead of Y shaped columns. Hence, oblique column is more sustainable than Y columns.

Rohan Singh, Vikas Prabhakhar ,(2018) studied about oblique column which is inclined at 80 ,82,84,86,88 and 90 degrees on a 12 storied building. Static and dynamic analysis should be finished in these columns. Ground motion performance of oblique column are analysed by response spectrum method .The analysis of building is performed by using ETABS software and the performance will be analysed by same building with oblique column replaced with normal vertical columns. The structural system with oblique column is one of the most unique lateral load resisting system for todays building. As the lateral loads are resisted by structures with oblique column, topstorey displacement is very much less in blique structure as compared to simple RC frame building. As time period is less in oblique column, lesser is mass of structure and more is the stiffness. The timeperiod is observed less in structure with oblique columns. This reflects more stiffness of the structure and lesser mass of structure. Structure provides more resistance in the oblique column building which makes the structural system mre effective. The overall results suggested that oblique column is excellent seismic control for high –rise symmetric buildings upto certain angle of inclination.

Geethu Krishna K V and Lekshmi L (4) (2018) studied the performance of building having oblique columns of different angles and to compare different parameters by response spectrum analysis using ETABS software. For this project, total 9 models were studied. The modelling was done by using ETABS software. The buildings were modelled with concrete structural elements. High-rise building - Gt19 Stories, Mid -rise building - G+9 stories, Low-rise building - G+3 stories were used for making models. The buildings with oblique column at different angles such as 80°, 85° and 90° were studied. It was found that in high-rise building, the storey displacement was 40% lesser for 80° columns and 27% lesser for 85° column than the normal column. In low-rise building, the displacement for 80° and 85° columns were about 48% and 18% respectively compared to normal column construction. In the low-rise building, the drift was reduced 24% for 80° and 85° respectively than 90° columns. The storey shear decreased when the column angle decreases than 90°. In mid-rise building, when the column was at 80°, the storey shear decreased about 34% than the normal column. By the use of 80° oblique columns, the stiffness was increased 60% in high-rise, 34% in mid-rise and 89% in low-rise buildings than the normal column having 90°.

Geethu Krishna K V and Lekshmi L (4) (2018) studied the performance of building having oblique columns of different angles and to compare different parameters by response spectrum analysis using ETABS software. For this project, total 9 models were studied. The modelling was done by using ETABS software. The buildings were modelled with concrete structural elements. High-rise building - Gt19 Stories, Mid -rise building - G+9 stories, Low-rise building - G+3 stories were used for making models. The buildings with oblique column at different angles such as 80°, 85° and 90° were studied. It was found that in high-rise building, the storey displacement was 40% lesser for 80° columns and 27% lesser for 85° column than the normal column. In low-rise building, the displacement for 80° and 85° columns were about 48% and 18% respectively compared to normal column construction. In the low-rise building, the drift was reduced 24% for 80° and 85° respectively than 90° columns. The storey shear decreased when the column angle decreases than 90°. In mid-rise building, when the column was at 80°, the storey shear decreased about 34% than the normal column. By the use of 80° oblique columns, the stiffness was increased 60% in high-

rise, 34% in mid-rise and 89% in low-rise buildings than the normal column having 90°.

Kapil Dev Mishra et al [14], (2018), In this paper, a multi storied Plaza building of storey (G+5) having different position of oblique columns (4 columns of mid ordinate axis or 4 columns of diagonal axis at different height of building (at the level above second floor) at 16 two different zones (ZONE Ill and ZONE IV) are considered for analysis. The plan area of building up to second floor was 30m×30m and above this floor area was reduced to 20m ×20m.Height up to second floor of the building was used for parking or commercial shops having floor height of 4m and above this it was used for residential and office purpose. Different combinations of office and residential floors were considered. Floating columns were provided at office floor. These were the following consideration where comparison was done based on results from the software, Support reaction at the base, maximum moment at the joint. On the results mentioned above of study the following conclusions were made; Maximum Bending Moments as well as Maximum Support Reaction for the structures having oblique columns were higher than that of structures without oblique columns. Maximum Bending Moments at seismic Zone IV were 16% greater than that of Zone III. Structures having oblique column constructed in Zone IV are more affected by earthquake than Zone III.

V. MODELLING

TABLE I. MODEL DETAILS

Plan Area	144 sq.m
Bay length	3 m
Storey height	3.2 m
Thickness of slab	150 mm
Column size	450 mm x 450mm
Beam size	230 mm x 450 mm
Concrete grade	M40
Grade of steel	Fe 500
Live load	3 kN/m^2
Floor Finish load	1 kN/m^2
Windspeed Vb	39 m/s
Zone factor	0.36
Importance factor	1
Response reduction factor	5

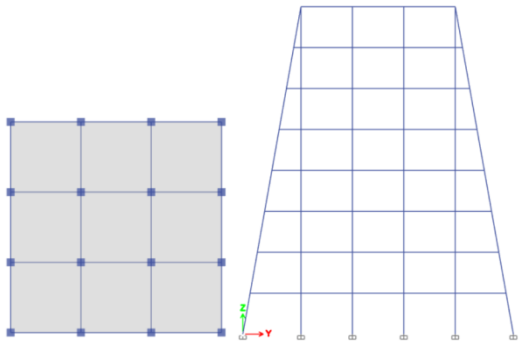

(a) (b)

Fig. 1.Oblique Column(a) Plan (b) Elevation

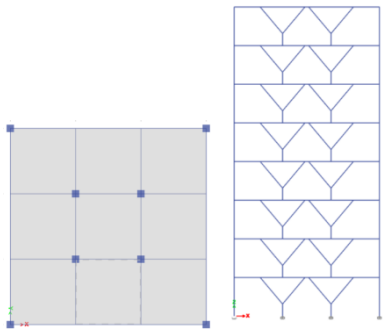

(a) (b)

Fig. 2.(a)Y column (a)Plan (b)Elevation

VI. RESULT

TABLE I. RESILTS OF OBLIQUE AND Y COLUMN

Column Type	Displacement	Drift	Base shear	Timeperiod
Oblique	21 mm	0.001	2416.96	0.3 sec
Y shape	47.38 mm	0.002	2214 kN	0.3 sec

VII. CONCLUSION

Following are the conclusions drawn by comparing oblique and Y column:

1) Maximum displacement is shown by building with Y shaped column ie 47.38 mm.In Y shaped column the displacement is increased by 55.67 % as compared to building with oblique column
2) Maximum drift is shown by building with Y shaped column ie 0.002.The drift has

shown an increse of 50 % in Y shaped column.

3) Maximum base shear is shown in Oblique column ie 2416.96 kN.As compared to Y column the base shear has shown a decrease of about 8.3%.
4) Time period remains unchanged in both building with oblique and Y column.
5) The number of Y column used is very less as compared to oblique column.Therefore we can conclude that building with Y column offers more carpet area.
6) Oblique column is more seismic resistant than Y column.

VII. REFERENCES

1. Abhilash A.S. ,Keerthi Gowda B.S.(2016) A "Comparative study of Multi-storied RC structures with Y column."
2. Rohan Singh ,Vikas Prabhakhar ,(2020) "Study of multi-storied building with Oblique Column."
3. Shivaranjitha T H ,Naveen Kumar S (2017) "Comparative study of Y shaped column with conventional rectangular column."
4. Harshada Ashok Targe ,Utkarsha Dilip Bhadane,Gauri Madav Derle (2022) "Comparative analysis of oblique column and Y shaped column by using ETABS"

Seismic Performance Of Beam-Column Joint With Different Compressive Strength Ratio's

SAHNA
Dept. of Civil Engineering
AWH Engineering College
Kozhikode, Kerala, India
sahnaalmana@gmail.com

SABEENA M V
Dept. of Civil Engineering
AWH Engineering College
Kozhikode, Kerala, India
sabeena@awhengg.org

Abstract— This study analysed the seismic performance of beam-column joint with different concrete compressive strength. A total of three exterior beam-column joints were designed and analysed under reverse cyclic loading using ANSYS. The effects of the concrete compressive strength ratio in column to beam joints were noted. The specimens with the column to beam concrete compressive strength ratios of 1, 2 and 3 are modelled and analysed under reverse cyclic loading, keeping the concrete compressive strength of beam constant. According to the results, the overall performance of the beam-column joint was improved as the compressive strength of the concrete in the column is increased.

Keywords— Exterior beam-column joint, Compressive strength ratio, ANSYS

I. INTRODUCTION

Beam-column joint is one of the most important structural components in the lateral load path of the structure. The failure of beam-column joint can be very disastrous because it can destroy column that is necessary to support gravity loads. Severe reverse cyclic loading due to earthquakes causes large inelastic deformations in the beam column joints of high-rise buildings. If the joints are not designed and detailed properly, their performance can significantly affect the overall response of the moment-resisting frames.

With the advancement of concrete mixing technology, the strength of concrete used on construction sites continues to increase [1, 2] and high-strength concrete (HSC) is widely used in columns subjected to high levels of axial load ,while the floor system (slab and beam) is often made with normal-strength concrete (NSC). The load transfer performance of the HSC column may decrease based on the interference of the NSC floor system [5-9]. Therefore, current design codes specify that specific measures be taken when the column and floor system have different compressive strengths.

Seung-Ho Choi et.al [3] they studied the effective compressive strength of the column-slab connection with different compressive strengths between the column and slab concrete, and the test results were compared to the existing design codes. The specimen with its slab-column connection zone reinforced by steel fibers showed an increased effective compressive strength compared to that of the specimen without the reinforcement, and the interior column specimens restrained with slabs reached the compressive strength of the column. Seung-Ho Choi et.al [1] studied the compressive strengths of HSC columns with intervening NSC slabs, and a simplified equation for estimating the effective compressive strength of the column was proposed, based on the analytical research. Bindhu K R [4] studied the behavior of exterior columns joints under seismic type loading. Cross inclined bars were provided as a replacement of ties in the joint region for the joints having transverse reinforcement detailed as per IS 13920:1993. The specimens having special confining reinforcement as Per IS 13920:1993 showed improved ductility and energy absorption capacity than the specimens detailed as per IS 456:2000 and SP34.The performance of the specimens with non-conventional confinement reinforcement had exhibited higher ultimate strength with minimum cracks.

II. OBJECTIVE

- The present study aims at analyzing on the overall seismic performance of beam-column joint with different compressive strength ratio
- To determine the load-deformation relationships, energy absorption capacity,

envelope curves, and shear stress of the joint.

III. DETAILS OF THE SPECIMEN

The model prepared is detailed as per IS 456:2000 (Fig.1.). All the beam- column joint models prepared had identical beam and column sizes. The beams are 200mm deep by 150 mm wide and columns are 150 mm deep by 200 mm wide. The specimen is one-third of full scale with 1015 mm long beams measured from column face with an inter-storey height of 1560 mm. Three exterior beam-column joint is prepared changing the concrete compressive strength of column ie,20N/mm2 , 40 N/mm2, and 60 N/mm2 (as shown in Table I) .The concrete compressive strength of beam for all model is 20 N/mm2 and Fe 415 grade steel were used. Development length of 532 mm is provided as per IS 456:2000.

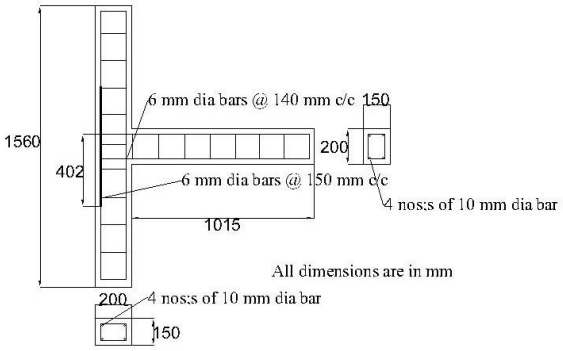

Fig. 1. Reinforcement Detailing of Model

TABLE I. COMPRESSIVE STRENGTH RATIO'S OF MODELS

Model	Compressive strength of column (MPa)	Compressive strength of beam (MPa)	Compressive strength ratio (f_{cc}/f_{cb})	
CM20-BM20	20		20	1
CM40-BM20	40		20	2
CM60-BM20	60		20	3

IV. Modeling

For the present study ANSYS workbench 2023/R1is being used. Modeling of the beam-column joint with different compressive strength ratio's is done. The material properties of the beam-column joint is given as shown in Table II. Both ends of the column are fixed and the reverse cyclic load is applied to the end of the beam. 20 mm mesh size is provided to the specimen

TABLE II. MATERIAL PROPERTIES OF THE SPECIMEN

Material Model No:	Element Type	Material Properties
1	Reinforcement	Linear Isotropic Elastic Modulus 2.1×10^5 MPa Poisson's Ratio 0.3 Bilinear Kinematic Shear Modulus 76923 MPa
2	Concrete	Linear Isotropic EX 22360 MPa Poisson's ratio 0.18 Bulk modulus 11646 MPa Shear modulus 9474.6 MPa

Finding an appropriate mesh size has less computational cost and reasonable accuracy by mesh-dependent study. Here 6 elements are tested and the mesh is converged at size 20mm. The mesh data is given as per the Table III.

TABLE III. MESH DATA OF THE MODELS

Material Model No:	Element Type	Material Properties
1	Reinforcement	Mesh size 20 mm Element: Hex 20 Element order: Linear
2	Concrete	Mesh size 20 mm Element: Hex 20 Element order: Linear

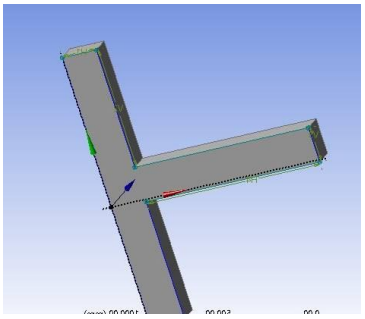

Fig. 2. ANSYS Model of specimen

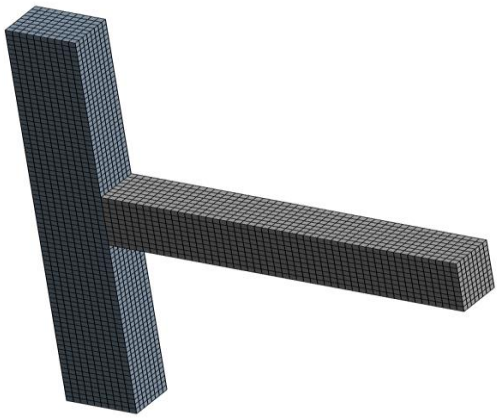

Fig. 3. Model after Meshing

The loading of the model is done as per the Fig.4. The specimen was subjected to an maximum load of 55 kN .

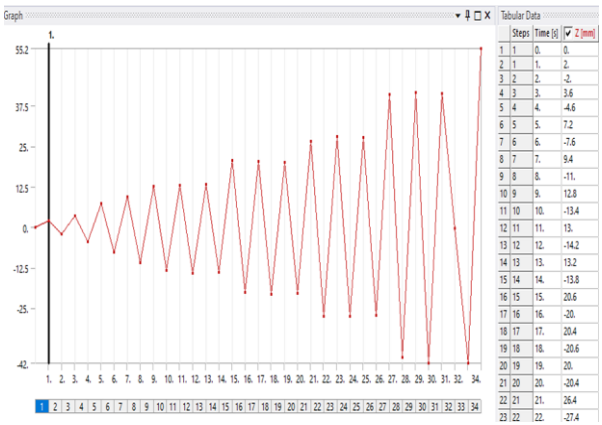

Fig. 4. Load pattern

V. ANALYSIS OF MODELS

Model is analysed using ANSYS 2023/R1 workbench. Deformation and stress on the application of load is found out. The effect increased concrete compressive strength in column than the beam in the three exterior beam column joint is found out in the case of both upward and downward loading.

TABLE IV. MAXIMUM SHEAR STRESS OF MODELS

Model	Shear Stress (MPa)
CM20-BM20	5.9646
CM40-BM20	8.3354
CM60-BM20	12.102

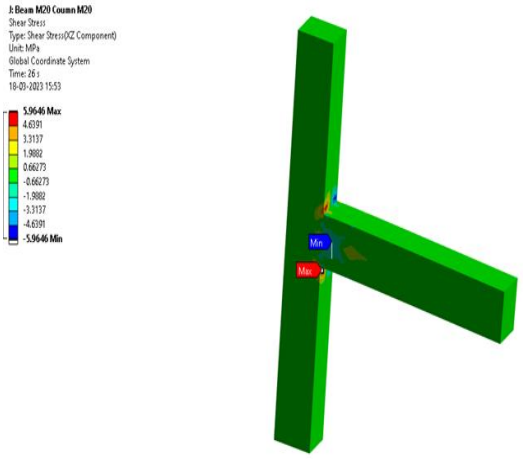

Fig. 5. Shear stress of CM20-BM20 model

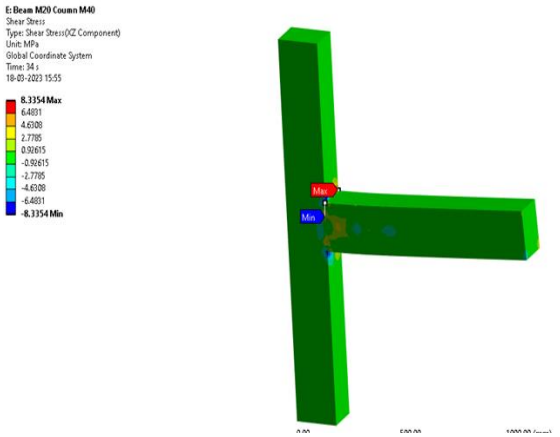

Fig. 6. Shear stress of CM40-BM20 model

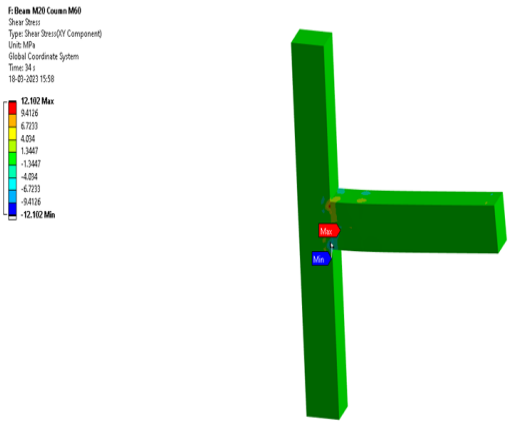

Fig.7. Shear stress of CM60-BM20 model

From TABLE IV, it can be seen that the increase in the compressive strength ratio increased the shear bearing capacity of the joint. From Fig. 5-7, it is clear that the max shear stress is formed at the region were the beam connect with the column.

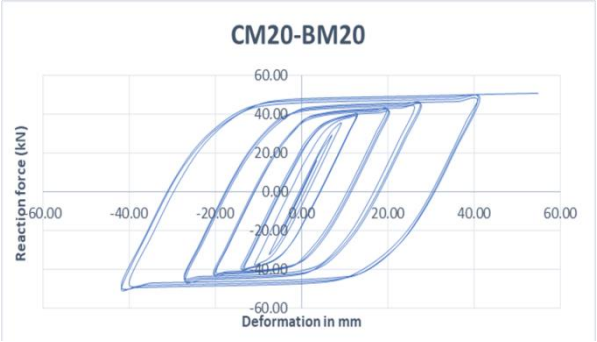

Fig.8. Hysterisis loop of CM20-BM20 model

Fig .9. Hysterisis loop of CM40-BM20 model

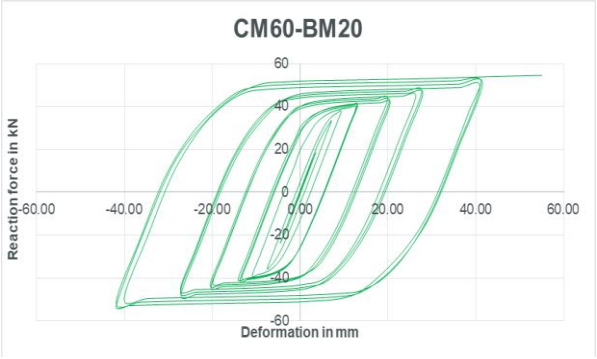

Fig. 10. Hysterisis loop of CM60-BM20 model

The hysteresis loop of models CM20-BM20, CM40-BM20, and CM60-BM20 is shown in Fig. 8-10. The pattern of the loop is almost same for the three models. The ultimate load of the model is increased as the concrete compressive strength of the column increased.

TABLE V. COMPARISON OF THE ULTIMATE LOAD CARRIED BY THE BCJ WITH DIFFERENT COMP.STRENGTH RATIO'S

Model	Ultimate Load (kN)
CM20-BM20	50.72
CM40-BM20	54.05
CM60-BM20	54.57

TABLE V shows the comparison of the ultimate load carried by the beam-column joint with different compressive strength ratio's. As the concrete compressive strength of column increased the load carrying capacity of the model also increased, i.e, 6.56% and 7.59% respectively for the models with concrete compressive strength ratio of column to beam 2 and 3, when compairing with the monolithically designed model.

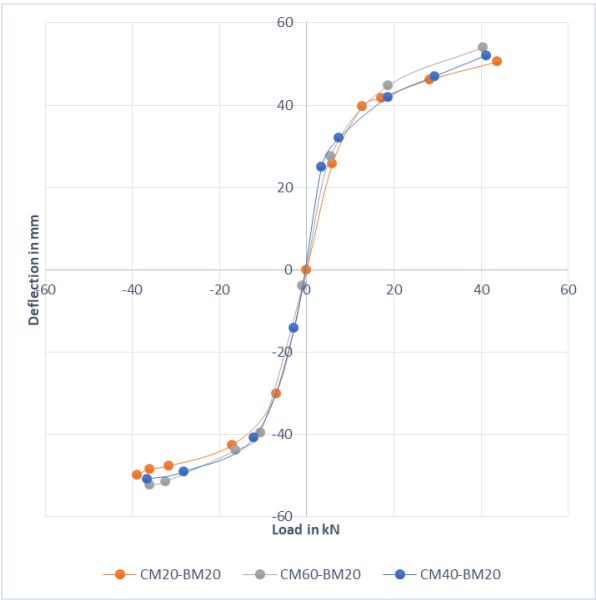

Fig. 11. Envelope curves of models

From Fig 11, it can be seen that the models with the compressive strength of the concrete in the column to beam ratios 2 and 3 (CM40-BM20 & CM60-BM20) showed better load bearing capacity than the one with a monolithic joint (CM20-BM20).

TABLE VI. ENERGY ABSORTION CAPACITY OF MODELS

Energy absorption (kN-mm)		
Specimen	**Forward cycle**	**Reverse cycle**
CM20-BM20	613.13	592.21
CM40-BM-20	676.3	613.41
CM60-BM-20	685.24	623.43

From the TABLE VI, it can be seen that the compressive strength of the concrete in the column to beam ratios 2 and 3 (CM40-BM20 & CM60-BM20) showed better energy absorption capacity than the one with a monolithic joint (CM20-BM20). In forward cycle 10.13% and 11.76% of energy absorption capacity is increased in models with concrete compressive strength ratio 2 and 3, when compared with the monolithic model . About 3.758% and 5.27% energy absorption capacity is increased in CM40-BM20 and CM60-BM20 models respectively, when compairing with the CM20-BM20 model.

VI. SUMMARY AND CONCLUSION

This study analysed the seismic performance of exterior beam-column joint considering the compressive strengths of the column to beam (fcc/fcb ratio) as a variable. The overall behavior, energy dissipation, envelope curves, and shear stress were analysed in detail. The following conclusion were derived from this study.

- The overall seismic performance of the exterior beam-column joint was improved as the fcc/fcb ratio increased.
- The maximum loads of the specimen CM40-BM20 and CM60-BM20 with fcc/fcb ratio 2 &3 is increased by 6.56 % and 7.59 % respectively, compared to CM20-BM20 which was cast monolithically with the same compressive strength of concrete.
- The energy absorption capacity of the CM40-BM20 and CM60-BM20 is increased by 3.5%-10.3% and 5.27%-10.5% in forward and reverse loading than the monolithically framed BCJ.
- The shear capacity of the specimen CM40-BM20 and CM60-BM20 have increased by 35.78% and 96.45% respectively, compared to CM20-BM20 which was cast monolithically with the same concrete compressive strength.

References

1. S.H. Choi, Jin-Ha Hwang, Sun-Jin Han1, Hae-Chang Cho, Jae Hyun Kim1 and Kang Su Kim, "Effective Compressive Strengths of High Strength Concrete Columns Intersected by Normal Strength Concrete Slab", Dissertation, Department of Architectural Engineering, University of Seoul, 2019. Ph.D.
2. S.H. Choi, D.H. Lee, K.S. Kim, "Effective compressive strength of RC columns with intervening floor slab", ACI Struct. J. 119 (1) (2022) 183–198, https://doi.org/ 10.14359/ 51733005.
3. S.H. Choi, J.H. Hwang, S.J. Han, H. Kang, J.Y. Lee, K.S. Kim, Failure characteristics of columns intersected by slabs with different compressive strengths, Struct. Eng. Mech. 74 (3) (2020) 435–443, https://doi.org/10.12989/sem.2020.74.3.435.
4. Bindhu K R (2009), "Behaviour of columns and exterior joints under Seismic type loading", PhD thesis at Anna Univeristy. http://home.iitk.ac.in/~vinaykg/Iset503.pdf.
5. H.C. Cho, S.H. Choi, S.J. Han, S.H. Lee, H.Y. Kim, K.S. Kim, Effective compressive strengths of corner and edge concrete columns based on and adaptive neurofuzzy inference system, Appl. Sci. 10 (10) (2020) 1–11, https://doi.org/ 10.3390/app10103475.
6. S.H. Choi, J.H. Hwang, S.J. Han, I.W. Heo, D.H. Lee, K.S. Kim, Axial behavior of full-scale sandwich columns with different compressive strengths, Struct. Concr. 21 (6) (2020) 2782–2794, https://doi.org/10.1002/suco.202000405.
7. Fu, Jianping, Tao Chen, Zheng Wang, and Shaoliang Bai. "Effect of axial load ratio on seismic behavior of interior beam–column joints." In Proc. 12th world conf. earthquake eng. 2000.

8. Jung Yoon Lee, Jongwook park, Deformation of reinforced concrete beam-column joint assemblies (2017) https://www.icevirtuallibrary.com/doi/10.1680/jmacr.18.00368
9. Burak, B. U. R. C. U., and JAMES K. Wight. "Experimental investigation of eccentric reinforced concrete beam-column-slab connections under earthquake loading." In Proceedings of the 13th World Conference on Earthquake Engineering, Paper, no. 2150. 2004.

Buckling Analysis of Cold-Form Steel Built-Up Column with Two Sections

Fathima sherin
Dept of Civil engineering
Awh engineering college,
Kozhikode, India sherin9349@gmail.com

Minu U
Dept of Civil engineering
Awh engineering college, Kozhikode, India
minu@awhengg.org

Abstract—Cold-formed steel have a high strength ratio, high corrosion resistance, and ease of fabrication. So, their range of applications has rapidly expanded as a primary structure for flexural and compression members due to its varieties of advantages. The increased load-carrying capacity and span length can be achieved by the built-up of the section connecting two or more individual sections together by self-drilling screws or spot welds. This project deals with the buckling analysis of cold-form built-up sections using ANSYS software. The sections were made by connecting two sections using self-drilling screws. The sections used for the study were channel sections without lips. This project mainly aims to study the effect of buckling loads by changing the screw spacing. According to the findings, buckling load increases as screw spacing decreased. In contrast to open sections, closed sections display variable findings.

Keywords—Cold-form sections, Buckling analysis.

I. INTRODUCTION

Cold-formed steel (CFS) section is the term used for products that are made by rolling or pressing thin gauges of steel sheets into goods. CFS construction materials differ in many respects from other steel construction materials like hot rolled steel. The manufacturing of CFS products occurs at room temperature with the use of rolling/pressing. The main advantage of cold-formed steel are lightness, high strength and stiffness, easy prefabrication, uniform quality, and economy in transportation and handling. Built-up of cold-form sections can give favourable results of compression members in cold- formed steel construction, which can achieve higher load-carrying capacity than a single section.

The main issue faced while using Built-up members is the effect of partial composite action on the other hand if the sections are not linked effectively, they will bend separately and there will be no composite action. A proper connection should be provided to avoid this issue. For long columns providing screws along the length is not possible. Screws can be provided with a definite spacing value. The main objective of this study are to investigate the buckling behaviour of cold-formed steel built-up compression members. The buckling property is used to analyse the strength of elements.

Finite element analysis (FEA) is an effective method for studying the buckling effect and forecasting the ultimate strength of cold-formed steel structural components due to its high efficiency and low cost. Several studies have reported on the effective use of the FEA to forecast the structural performance of cold-formed steel components. Jessica Whittle et al. conducted buckling capacities tests of cold- form built-up c- channels [1]. The member is discretized both within the cross-section and throughout its length in the finite element approach, necessitating a considerable number of degrees of freedom in order to accurately estimate the buckling stresses. This suggests that several possible buckling modes which can be formed.

M Anbarasu et al. [2] studied the behaviour of cold-form steel built-up of I section composed of four U profiles. In this study, FE model was developed and compared with the numerical study from the literatures. Jia-hui zhang et al. [3] experimentally investigated the ultimate strength of cold- form steel built-up closed-section columns having stiffeners. The experimental values were compared with the direct strength method showing that design strengths using 1.2, 1.5 and 2 times the nominal plate thickness in the contact area as one rigidly connected section are generally unconservative and unreliable, while the modified design strength, assuming the thickness

at the contact area to be the nominal plate thickness, are conservative and reliable for the cold-formed steel built-up closed sections with web stiffeners.

Kim J.R. Rasmussen et al. [4] studied the effect of discrete locations of fasteners. The paper studies the mechanics of the composite action of sections. A closed-form solution was derived for the effective torsion rigidity which shows that the rigidity varies with the square of the enclosed area. Most of the studies in cold form built-up sections are conducted according to ACI code I. Georgieva et al. [5], Sivaganesh S et al. [6], considered direct strength method to evaluate the strength of the built-up cold form sections.

II. MODELLING

A. Model Details

The material properties used are provided in Table I. The sections for the built-up column were taken according to the IS code 811:1987. Channel sections without lips were considered for the study the section details are shown in Table II. The dimensions of the channel section are 120×60×5mm, length of the column is kept as 3m. The column is built-up in two ways. First is an open section by connecting the channels back-to-back. The second model is a closed section obtained by connecting columns face-to-face by overlapping one over the other (Fig 1). Screws of 4.5mm diameter and 19mm long were used for connecting the sections.

TABLE I . MATERIAL PROPERTIES

Young's modulus	2.033×10^5 MPa
Poison's ratio	0.3

TABLE II . SECTION DETAILS

Model Name	Connection Type	Spacing(mm)
CO960	OPEN	960
CO720	OPEN	720
CO320	OPEN	320
CC960	CLOSE D	960
CC720	CLOSE D	720
CC320	CLOSED	320

B. FEA modelling

FE software ANSYS workbench (2021) was used to develop the FE model for the CFS built-up columns. The finer the mesh, the more accurate the findings will be in finite element analysis. Mesh size is given as finer to obtain accurate results. The boundary condition applied is one end fixed and the other end load is applied as shown in Fig 2. Tracks are provided at the ends of the column to uniformly apply load to the column. The load applied is according to Euler's buckling equation

$$P = \frac{\pi^2 EI}{4L^2}$$

where P is the buckling load; E is young's modulus of the cold form section; I is the min moment of inertia of the section; L is the total length of the section. This equation provides an approximate value of the buckling load, which can be different as screws are provided in the section. So, the actual value of the buckling load can be obtained from the analysis.

Fig. 1. Sections of channel back-to-back model and channel face-to-face model.

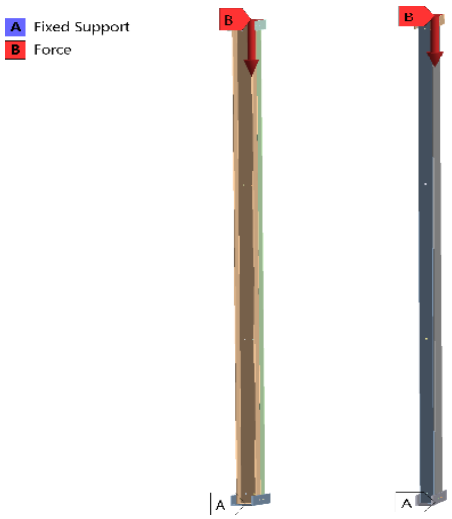

Fig. 2. Boundary conditions of the model

III. RESULTS AND DISCUSSION

Different buckling modes of CFS built-up back-to-back and face-to-face with the same cross sections and varying screw spacings were investigated. The results of columns are summarized in Table III and Table IV. Figures of buckling modes of back-to-back built-up and face-to-face columns are shown in Fig 3 and Fig 4.

TABLE III . BUCKLING MODES OF BACK-TO-BACK MODELS

Model Name	Load Multiplier for Buckling Mode				
	Mode 1	*Mode 2*	*Mode 3*	*Mode 4*	*Mode 5*
CO960	0.85572	5.6352	13.074	19.216	29.759
CO720	0.86423	5.6697	13.795	19.547	30.302
CO320	0.88463	5.77	15.015	20.443	31.22

Mode 1 represents the maximum load value at which the column first buckles. The buckling loads are calculated from the equation [7],

$$P = (1+\text{load multiplier}) \times \text{load applied}$$

The load multiplier value was taken from the results of buckling. The values of critical loads for the different modes of back-to-back columns are given in Table V. From the critical load values, we can obtain the effective length of the modes (TABLE VI).

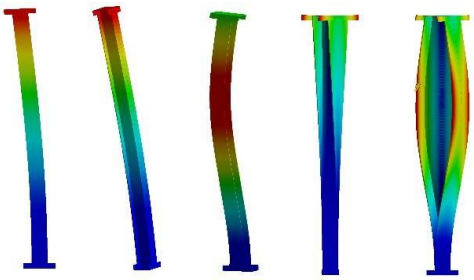

(a) Buckling modes of CO960

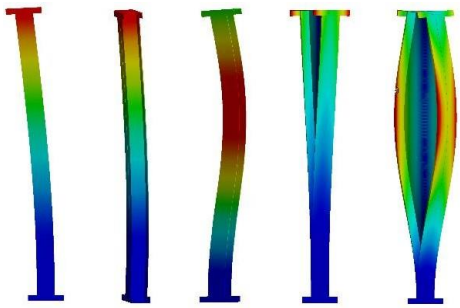

(b) Buckling modes of CO720

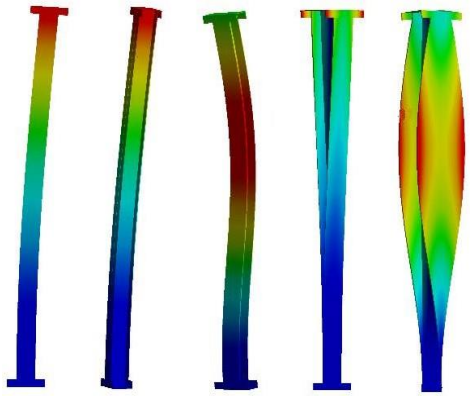

(c) Buckling modes of CO320

Fig. 3. Buckling modes of back-to-back

TABLE IV. BUCKLING MODES OF FACE-TO-FACE MODELS

Model Name	Load Multiplier for Buckling Mode				
	Mode 1	*Mode 2*	*Mode 3*	*Mode 4*	*Mode 5*
CC960	0.56199	5.4439	8.8451	14.836	15.355
CC720	0.56228	5.4438	8.8457	14.848	15.365
CC320	0.56205	5.4414	8.7407	14.73	15.235

TABLE V. BUCKLING LOADS OF BACK-TO-BACK MODELS

Model Name	Buckling Loads				
	Mode 1	*Mode 2*	*Mode 3*	*Mode 4*	*Mode 5*
CO960	79.8kN	285.3kN	605.2kN	869.3kN	1322.6kN
CO720	80.2kN	286.8kN	636.2kN	896.2kN	1346kN
C0320	81kN	291.1kN	688.6kN	922kN	1385.5kN

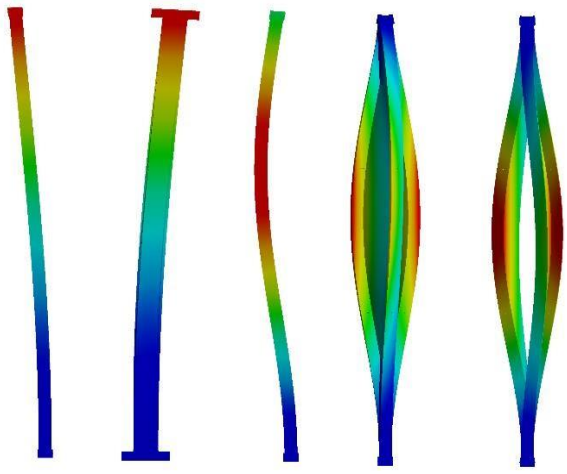

(a) Buckling modes of CC960

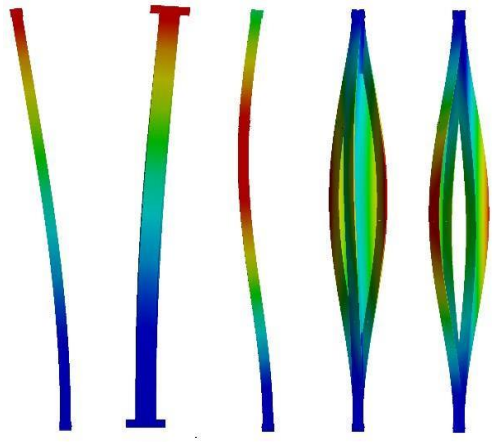

(b) Buckling modes of CC720

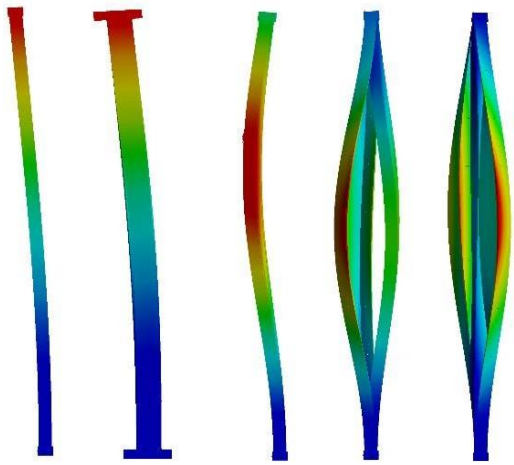

(c) Buckling modes of CC320

Fig. 4. Buckling modes of face-to-face

TABLE VI . BUCKLING LOADS OF FACE-TO-FACE MODELS

Model Name	Buckling Loads				
	Mode 1	*Mode 2*	*Mode 3*	*Mode 4*	*Mode 5*
CC960	67.16 kN	277.09 kN	423.3 kN	680.95 kN	703.26 kN
CC720	67.17 kN	277.08 kN	423.36 kN	681.46 kN	703.69 kN
CC320	67.16 kN	276.98 kN	418.85 kN	676.39 kN	698.10 kN

From the results obtained from the analysis of the back- to-back column models the buckling loads increase with increasing screw spacing. The critical buckling load of the back-to-back section is 79.8kN which is increased by 0.5% and 0.98% when the screw spacing is increased to 720mm and 320mm. The closed section has a different pattern as screw spacing increases 720mm spacing has a large value of buckling load than 960mm and 320mm spacing models. The closed section has more overlapping between the flanges so the resistance is provided. This reduces the action of screws to an extent. The effective length can be calculated from buckling loads the results are given in Table VII.

TABLE VII. EFFECTIVE LENGTH OF MODELS

Model Name	Effective length				
	Mode 1	*Mode 2*	*Mode 3*	*Mode 4*	*Mode 5*
CO960	2197.19 mm	1162.03 mm	797.84 mm	665.70 mm	539.70 mm
CO720	2181.70 mm	1158.98 mm	778.16 mm	655.64 mm	534.99 mm
CO320	2180.85 mm	1150.39 mm	747.97 mm	646.40 mm	527.30 mm
CC960	2395.04 mm	1179.12 mm	953.99 mm	752.16 mm	740.13 mm
CC720	2394.86 mm	1179.14 mm	953.92 mm	751.88 mm	739.90 Mm

Model Name	Effective length				
	Mode 1	*Mode 2*	*Mode 3*	*Mode 4*	*Mode 5*
CC320	2365.29 mm	1179.35 mm	959.04 mm	754.69 mm	742.86 mm

IV CONCLUSIONS

Finite element modelling and analysis of two types of models were performed. All the models were having the same dimensions only varying in screw spacing and connection style. Buckling analysis of the models was done to obtain values of buckling loads at different modes. The effective length of the column at different modes was calculated.

- The following conclusions were drawn from the study of buckling analysis of cold-form steel built-up
- The critical buckling load of each models were 79.8kN, 80.3kN, 81kN, 67.16kN, 67.17kN and 67.1kN corresponding to CO960, CO720,CO320, CC960, CC720 and CC320 respectively.
- The buckling loads increase with the increase in screw spacing for back-to-back connected models by 0.5% and 0.98%.
- Loading area for the open section can be higher than closed as closed sections have interconnection between flanges.

- Total width of the built-up column has an effect in buckling loads, as compared with closed and open sections open section has higher buckling loads than closed sections.

REFERENCES

1. Jessica Whittle, Chris Ramseyer, "Buckling capacities of axially loaded, cold-formed, built-up C-channels," University of Oklahoma, Oklahoma City,USA, Thin-Walled Structures 47 pg 190-201 May 2009
2. M Anbarasu, M Venkatesan "Behaviour of cold-formed steel built-up I-section columns composed of four U-profiles" govt college of engineering Salem, Tamil Nadu India, Advances in Structural Engineering p 1–13 (2018)
3. Jia-Hui Zhang, Ben Young "Experimental investigation of cold-formed steel built-up closed section columns with web stiffeners" University of Shanghai for Science and Technology, Shanghai, China, Journal of Constructional Steel Research 147, Pg 380–39 (2018)
4. Kim J.R. Rasmussen, Mani Khezri, Benjamin W. Schafer, Hao Zhang "The mechanics of built-up cold-formed steel members" University of Sydney, Sydney, NSW, 2006, Australia, Johns Hopkins University, Baltimore, MD, 21218, USA, Thin-Walled Structures 154, (2020)
5. I Georgieva*, L. Schueremans, L. Vandewalle, L. Pyla, "Design of built-up cold-formed steel columns according to the direct strength method," Procedia Engineering 40 pg 119 – 124 (2012)
6. Sivaganesh Selvaraj, Mahendrakumar Madhavan, "Design of Cold- formed Steel Built-Up Closed Section Columns using Direct Strength Method," Thin-Walled Structures171 (2022)
7. Ansys users guide pg 327 (2021)

Seismic Analysis Of High-Rise Buildings Considering Aerodynamic Effect

Sakira Nasla P V
Department of Civil Engineering
AWH Engineering College
Kozhikode, India
sakiranaslapv@gmail.com

Jisha. P
Department of Civil Engineering
AWH Engineering College
Kozhikode, India

Abstract— High-rise buildings with irregular shapes are gaining popularity in creating vertical cities around the world. A high-rise building is a wind-sensitive structure and its shape plays a major role in determining wind loads, which usually govern the design of its lateral resisting system. Therefore, aerodynamic treatments on high-rise buildings must also be considered, because even a small amount of geometrical shaping modifications can provide considerable damping against wind loads which in turn disturbs the mechanism of the vortex shedding phenomenon. Computational fluid dynamic (CFD) simulations are currently an effective tool for the aerodynamic study of buildings in conjunction with wind tunnel investigations. This paper presents the analysis of a 50-storey and 100-storey building considering aerodynamic modifications, which is firstly achieved by creating a digital system of computational fluid dynamic (CFD) analysis of buildings with the different minor and major aerodynamic shape modifications and hence evaluating aerodynamic forces on the buildings, subsequently the seismic assessment of a 50-storey regular and irregular building by response spectrum and time history analysis is also studied.

Keywords— Aerodynamic shape modification, CFD, Wind tunnel setup, Drag force, Seismic analysis, response spectrum, time history analysis

I. INTRODUCTION

For high-rise structures, the structural design, in general, begins to be controlled by wind loads. These buildings are subject to complicated loading conditions, particularly urban aerodynamics created by neighboring clusters of high-rise structures. They are wind-prone structures due to their great flexibility and low natural frequency, and their response to wind loads is a critical parameter in their structural design. Additionally, the dramatic increase of wind speed with building height, and combined increases in slenderness ratios make them more flexible and therefore more susceptible to wind loads. In this sense, in supertall building design, to guarantee the functional performance and occupancy comfort, selection of proper structural system selection, aerodynamic modifications, and supplementary damping devices plays an important role.

Aerodynamic modifications can alter the wind pattern around structures by suppressing the uniformity of vortex shedding, thereby effectively mitigating wind loads on buildings . In addition, vortex shedding poses a significant danger to the serviceability issue, especially when it reaches the natural frequency of the structure. Aerodynamic design considerations can be divided into two groups: major and minor modifications. Major modifications, which play a critical role in mitigating the wind effect on supertall towers, include building orientation, aerodynamic form, plan variation, and the aerodynamic top that have a significant impact on the overall architectural design. On the other hand, minor modifications including corner modifications and air passes do not significantly change the overall architectural design.

II. MODELLING

For the modeling and analysis, a 50 and 100 storied building are selected. Modeling of the structure is done in ANSYS FLUENT 2019 R3 and CSI ETABS version 18.0 software. RCC building with a plan area 1400m2, is modeled as per IS 1893:2016 for seismic zone V with soil type III. As the modelling is done in ANSYS and ETABS they are named as type 1 and type 2 models respectively. The details of modeling and analysis is described below.

A. TYPE 1

The dissertation work is concerned with the study of drag force on a regular and irregular buildings while modifying the buildings with aerodynamic modifications. 9 models of regular building with different minor shape modifications (basic, recessed, chamfered, curved, double recessed) and major shape modifications (setback, tapering, varying cross section and twist) each of 150 m and 300 m were modelled and processed separately for 1000 iterations. After that 4 models of 50 storey irregular buildings (plus, L, T & I) were prepared and analyzed in ANSYS 2019 R3 to find better aerodynamic shape considering drag coefficient and drag force. The best two irregular shape building which shows better performance in aerodynamic force optimization is chosen for further seismic analysis. Modifications are done by fixing base floor area as 1400m2 and for minor modification the corner modification is done in 5m from the corner. The velocity magnitude of air in wind tunnel setup is 30m/s and the mesh method adopted is hex dominant method. For all the type of models CFD test will be done in ANSYS 2019 R3.

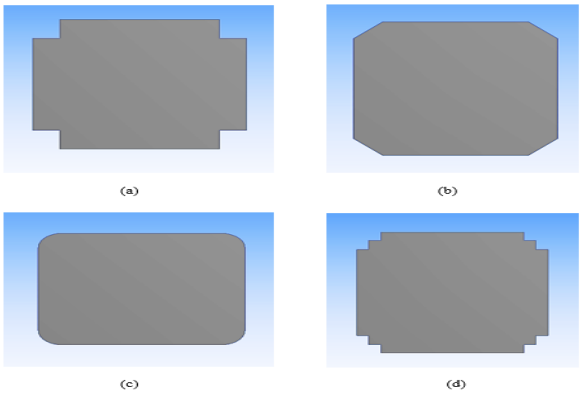

Fig. 1. Regular rectangular building model with basic corner (a) plan view (RBB) (b) wind tunnel setup

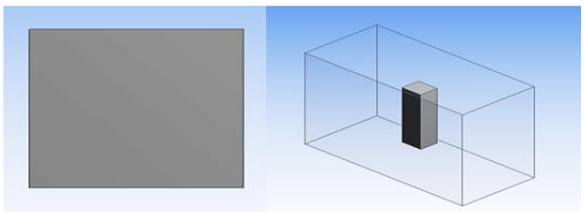

Fig. 2: Plan view of Regular rectangular building model with minor corner modifications (a) recessed (RBR) (b) chamfered (RBF) (c) curved (RBC) (d) double recessed (RBD)

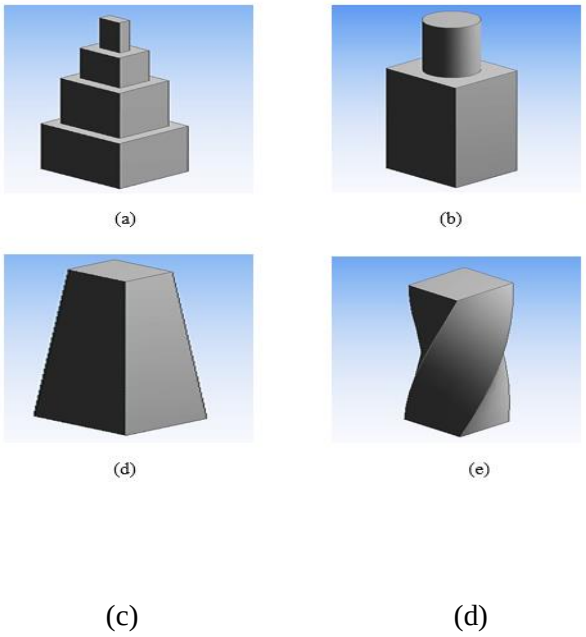

(c) (d)

Fig .3: Regular rectangular building model with major modifications (a) setback (RBS) (b) varying c/s(RBV) (c) tapered (RBT) (d) twist (RBW)

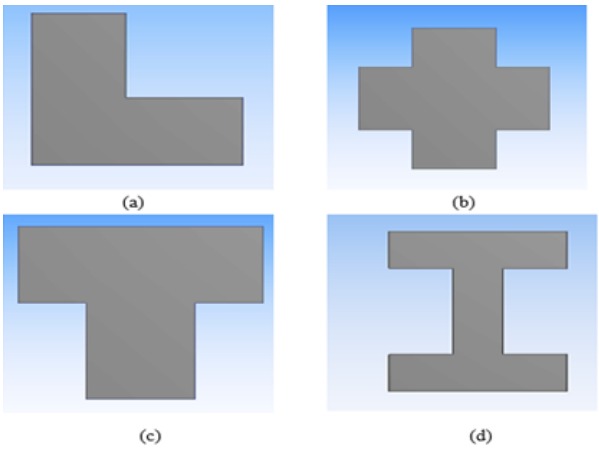

Fig .4: Plan view of irregular building models (a) L shape (IBL) (b) Plus shape (IBP) (c) T shape (IBT) (d) I shape (IBI)

B. TYPE 2

The building was created with 50 storey RCC frame as per IS 1893:2016 for seismic zone V with soil type III. 15 models namely 5 regular rectangular building models with minor corner modifications (basic, recessed, chamfered, curved, double recessed), 5 plus-shape building models with minor corner modifications and 5 L-shape building models with minor corner modifications are modelled with fixing the floor area as 1400m2. The base is restrained with fixed support. For the modelling of building in ETABS, shell loads on slabs of DL=2.5kN/m2,

LL=3kN/m2 except on roof and LL =2.5kN/m2 were assigned to the slabs on roof and frame loads of DL=18 kN/m2 was assigned to all the frames. Seismic loads are considered according to code IS: 1893-2016 and wind loads according to IS: 875- 2015. For seismic zone V, the seismic zone factor 0.36 with importance factor 1 and response reduction factor 5 is considered. The mass source includes total self-weight and 25% live load. Response function has been defined using IS1893: 2016 for a damping of 5% and Time history function has been defined using Elcentro Earthquake (1940) data from the program file. For all the types of models response spectrum analysis and time history analysis was done in ETABS2018.

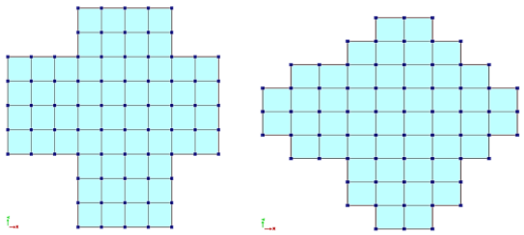

(a) (b)

Fig. 5: Regular rectangular building model with basic corner (RBB) (a) plan view (b) 3d model

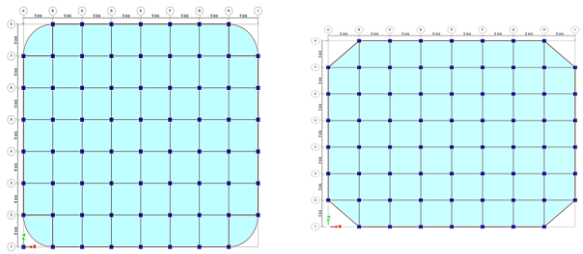

(a) RBR (b) RBF

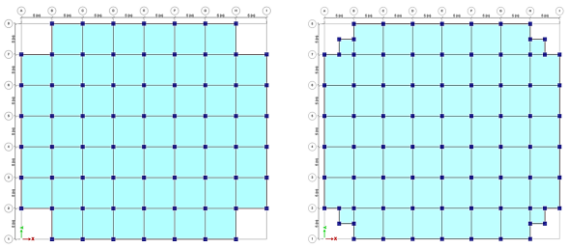

(c) RBC (d)RBD

Fig. .6: Plan view of Regular rectangular building model with minor corner modifications (a) recessed (b) chamfered (c) curved (d) double recessed

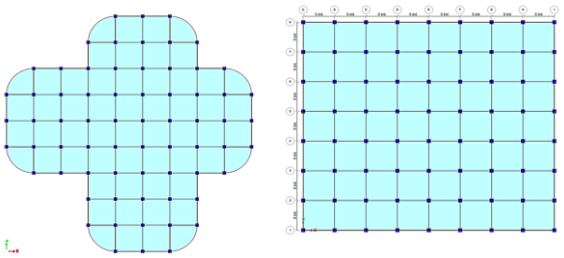

(a) PBB (b)

Fig. 7: Irregular Plus-shape building model with basic corner (a) plan view (b) 3d model

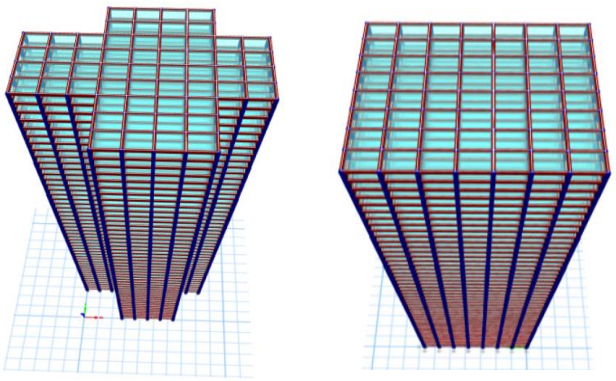

(a)PBR (b)PBF

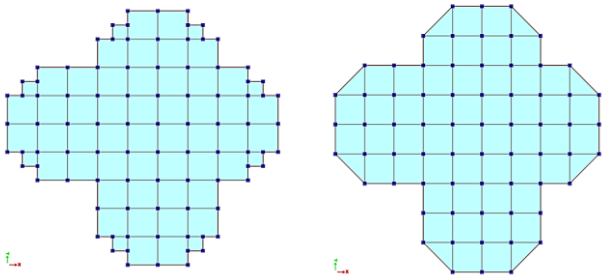

(c) PBC (d) PBD

Fig .8: Plan view of irregular Plus-shape building model with minor corner modifications (a) recessed (b) chamfered (c) curved (d) double recessed

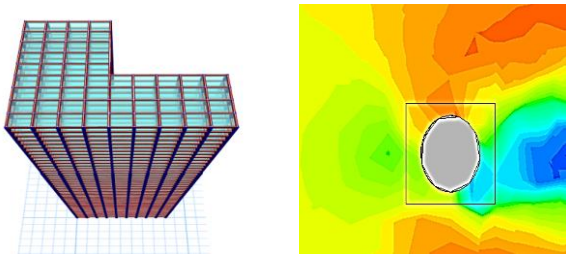

(a) LBB (b)

Fig .9: Irregular L-shape building model with basic corner

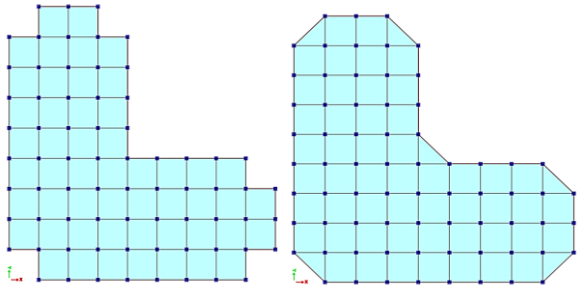

(a) plan view (b) 3d model

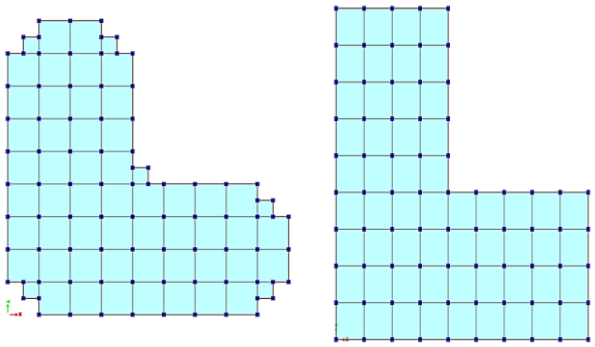

(a) LBR (b) LBF

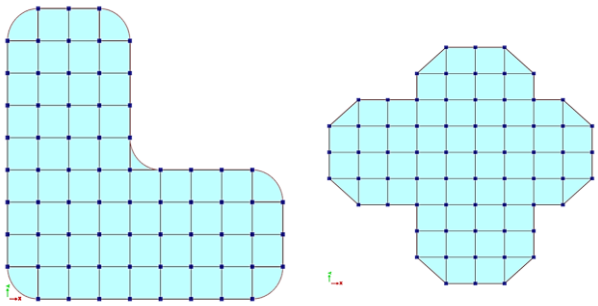

(c) LBC (d) LBD

Fig .9: Plan view of irregular L-shape building model with minor corner modifications (a) recessed (b) chamfered (c) curved (d) double recessed

III RESULTS

A. Type 1

The building models created in Ansys is applied with a wind of velocity 30 m/s. And for each model the velocity contours and drag force studied for understanding the effect wind on the vortices of building which may cause vortex shedding phenomenon in buildings.

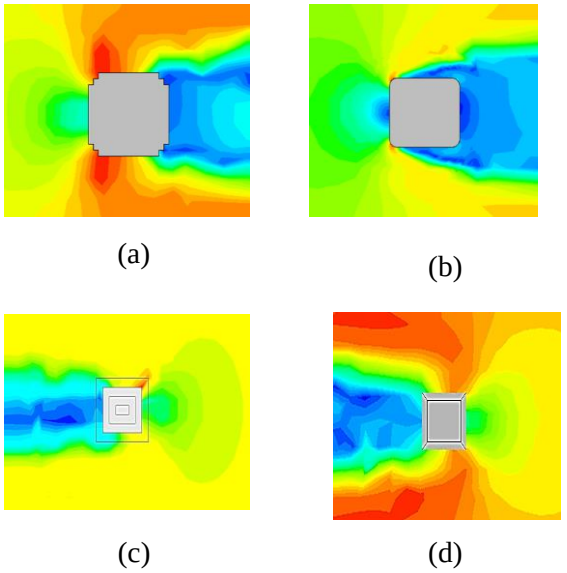

(a) (b)

(c) (d)

Fig 10: Velocity contour of regular rectangular-shape building model with minor corner modifications (a) basic (b) recessed (c) chamfered (d) curved (e) double recessed

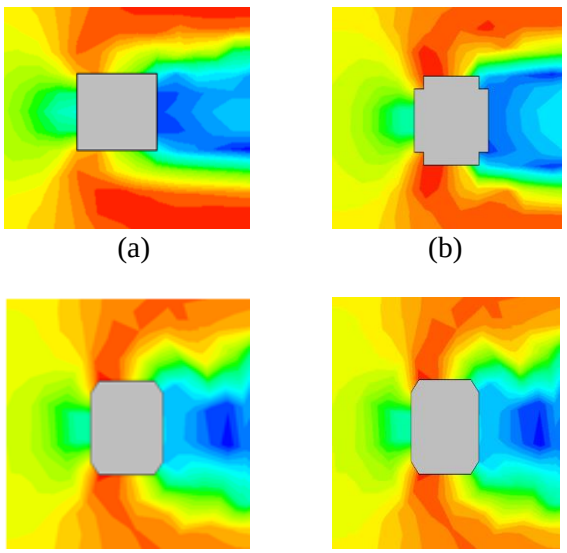

(a) (b)

(c) (d)

Fig 11: Velocity contour of regular rectangular-shape building model with major corner modifications (a) setback (b) varying c/s (c) tapering (d) twist

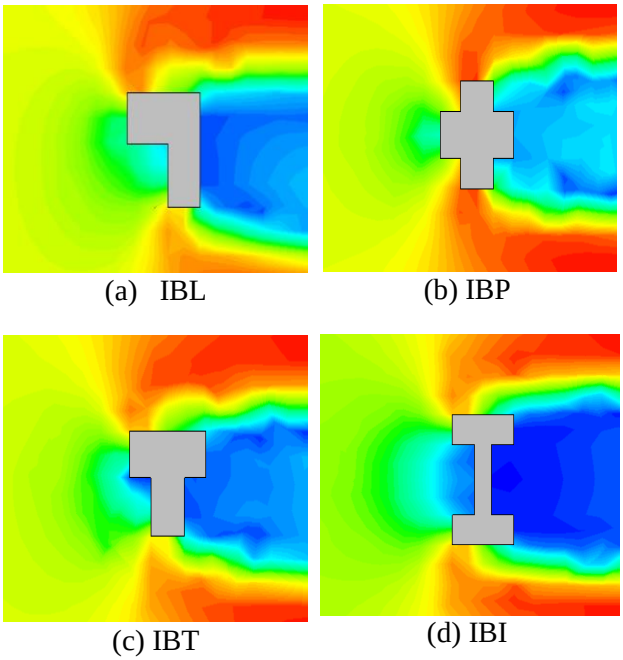

(a) IBL (b) IBP

(c) IBT (d) IBI

Fig 12: Velocity contour of irregular building model (a) L shape (b) Plus shape (c) T shape (d) I shape

From the contour velocity diagrams we can see that wind affecting at the corners of the building in regular rectangular and irregular buildings are high compared to minor and major shape modifications. In order to understand the effect of aerodynamic forces, the drag force on these buildings is computed and given in table 1. from the table we can say that as we give aerodynamic shape modifications the drag force affecting on the building decreases. For 50 storey buildings minor modifications provides best reductions in drag force. But as the height increases the major modifications have more effect in reducing the drag force.

TABLE I : DRAG FORCE IN REGULAR RECTANGULAR BUILDINGS WITH AERODYNAMIC MODIFICATIONS

models	***Drag force (kN)***	
Height of building	150 m	300 m
RBB	297.683	422.373
RBR	269.852	385.301
RBF	253.365	370.369
RBC	243.142	363.950
RBD	258.368	376.042
RBS	276.865	329.127
RBV	288.928	356.472
RBT	289.507	358.399
RBW	324.610	410.979

TABLE 2 : DRAG FORCE IN IRREGULAR BUILDINGS

models	***Drag force (kN)***
RBB	297.683
IBL	316.898
IBP	312.352
IBT	325.245
IBI	352.628

In regular rectangular buildings while giving aerodynamic minor shape modifications we can see, for recessed corner the drag force is reduced by 9.34% and 8.77%, for chamfered corner the drag force is reduced by 14.88% and 12.31%, for curved corner the drag force is reduced by 18.32% and 13.83% and for double recessed corner the drag force is reduced by 13.20% and 10.96% in 50 storey and 100 storey respectively. And for major shape modification we can see for setback building the drag force is reduced by 6.99% and 19.33%, for building with varying cross section the drag force is reduced by 2.94% and 13.66 %, for tapered building the drag force is reduced by 2.74% and 13.26% in 50 storey and 100 storey respectively. For building with twist the drag force is increased by 9.04% and decreased by 2.3% in 50 storey and 100 storey respectively.

From minor shape modifications, the model with curved corner (RBC) and chamfered corner (RBF) increased the reduction of drag force in 50 storey and 100 storey building. Building with curved corner (RBC) shows maximum percentage reduction when comparing 50 and 100 storey building. And from major shape modifications, the model with setback (RBS) increased the reduction of drag force in building. For minor shape modifications the percentage increase in

reduction of drag force as height increases is in between the range of 1 to 5%. For major shape modifications the percentage increase in reduction of drag force as height increases is in between the range of 5 to 15%.

Irregular buildings are more affected by drag forces compared to a regular building. The increase in drag force for a L shape, plus shape, T shape & I shape building is 6.4%, 4.9%, 9.2% and 18.4% respectively. The model with plus shape and L shape have comparatively less increase in drag force. Maximum increase in drag force is found in building with I shape. From this we can conclude that aerodynamic forces can reduces the effect of drag force on building and there by vortex shedding phenomenon can also be avoided. In order to understand the seismic performance of this buildings further analysis are done in Etabs.

TABLE 3 : MODAL PROPERTIES OF THE BUILDINGS

Models	*Max. storey displacement (mm)*		*Max. storey drift*		*Base shear* (kN)
	X axis	Y axis	X axis	Y axis	
RBB	165.81	169.40	0.00239	0.00241	21970.56
RBR	166.26	170.13	0.00240	0.00242	21970.56
RBF	166.03	169.87	0.00238	0.00240	20961.95
RBC	166.34	170.21	0.00239	0.00241	20945.51
RBD	100.17	102.32	0.00140	0.00141	14117.52
PBB	193.44		0.00276		22418.26
PBR	198.36		0.00282		19566.85
PBF	194.96		0.00275		20395.67
PBC	198.15		0.00281		20704.13
PBD	161.98		0.00218		21193.70
IBB	212.06		0.00291		22418.26
IBR	221.11		0.00302		20636.12
IBF	214.49		0.00292		21230.26
IBC	217.02		0.00296		21353.33
IBD	178.36		0.00236		21842.53

The building models created in Etabs is defined with a response function using IS1893: 2016 for a damping of 5% and time history function Elcentro Earthquake (1940) data from the program file And for each model the displacement, storey drift and base shear has been studied. For rectangular, Plus shape and L shape building with basic, recessed, chamfer and curved corner shows similar values of displacement and storey drift. The model with double recessed corner shows reduction in maximum storey displacement, storey drift &Base shear. Minor shape corner modification in rectangular building reduces base shear of building.

In rectangular building models, Max storey displacement and storey drift in double recessed building reduced by 39.58% and 41.5% respectively. Base shear in double recessed building reduced by 35.74%. In P shape building models, Max storey displacement and storey drift in double recessed building reduced by 16.26% and 21.29% respectively. The model with recessed corner shows reduction base shear by 12.71%. In L shape building models, Max storey displacement and storey drift in double recessed building reduced by 15.89% and 18.89% respectively. The model with recessed corner shows reduction in base shear by 7.94%.

Irregular buildings are more affected by drag forces compared to a regular building. The increase in drag force for a L shape, plus shape, T shape & I shape building is 6.4%, 4.9%, 9.2% and 18.4% respectively. The model with plus shape and L shape have comparatively less increase in drag force. Maximum increase in drag force is found in building with I shape. From this we can conclude that aerodynamic forces can reduces the effect of drag force on building and there by vortex shedding phenomenon can also be avoided. In order to understand the seismic performance of this buildings further analysis are done in Etabs.

B. Type 2

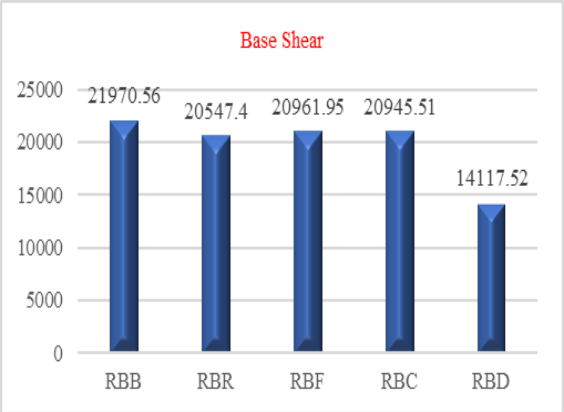

Fig 13: Comparison of base shear of regular rectangular-shape building model with minor corner modifications

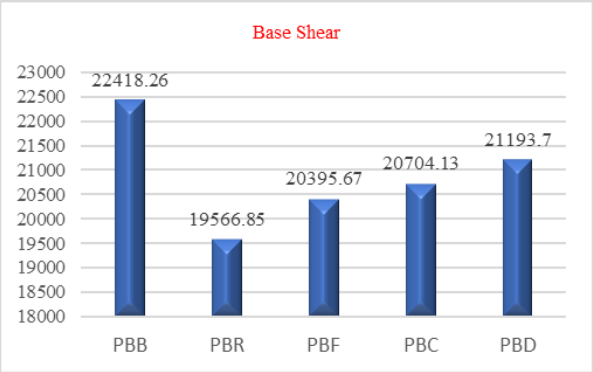

Fig 14: Comparison of base shear of irregular Plus-shape building model with minor corner modifications

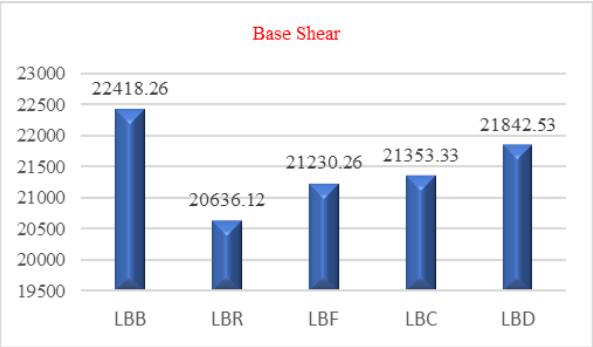

Fig 15: Comparison of base shear of irregular L-shape building model with minor corner modifications

IV. CONCLUSION

Aerodynamic modifications can reduce the drag force acting on the building. In case of regular building, while giving minor aerodynamic shape modification curved corner shows maximum reduction in drag force whereas in major modification the setback building shows maximum reduction in drag force. For 50 storey buildings minor modifications are dominant in reducing the drag force. As the height increases the major modifications are dominant than minor modification in reducing drag force acting on the building. Irregular buildings are more affected by drag force compared to a regular rectangular building. The increase in drag force is highest in building with I shape and lowest in building with Plus shape.

From seismic analysis, rectangular building with basic, recessed, chamfer and curved corner shows similar values of displacement & storey drift. The model with double recessed corner shows reduction in maximum storey displacement, storey drift & Base shear. From seismic analysis of irregular shape building, the models with basic , recessed, chamfer and curved corner shows similar values of displacement & storey drift. The model with double recessed corner shows reduction in maximum storey displacement & storey drift. The model with recessed corner shows reduction in base shear.

Acknowledgment

The support of the authorities of AWH Engineering College for the successful completion of project is gratefully acknowledged.

References

1. Gavane Vaishali, Prof. A.N. Shaikh (2022) "Analysis of high rise buildings with different shapes by corner modification & considering aerodynamic effect" e-ISSN : 2582-5208 Volume:04/Issue:08/August-2022
2. Maryam Asghari Mooneghi, Ramtin Kargarmoakhar (2016) " Aerodynamic Mitigation and Shape Optimization of Buildings: Review" http://dx.doi.org/10.1016/j.jobe.2016.01.009 2352-7102/& 2016 Elsevier Ltd.
3. G.W. Alminhana, A.L. Braun, A.M. Loredo-Souza (2018) "A numerical-experimental investigation on the aerodynamic performance of CAARC building models with geometric modifications" https://doi.org/10.1016/j.jweia.2018.07.001 © 2018 Elsevier Ltd.
4. Fadi Alkhatib ,Narimah Kasim, Shaker Qaidi, Hadee Mohammed Najm and Mohanad Muayad Sabri (2022)"Wind-resistant structural optimization of irregular tall building using CFD and improved genetic algorithm for sustainable and cost-effective design"doi 10.3389/fenrg.2022.1017813
5. Akhtarpour, A., & Mortezaee, M. (2019, June). "Dynamic response of a tall building next to deep excavation considering soil–structure interaction". Asian J Civ Eng (2019). doi:https://doi.org/10.1007/s42107-018-0078-4
6. Bobby, S., & Spence, S. .. (2014). "Performance-based topology optimization for wind-excited tall building- A framework". Engineering Structures doi:10.1016/j.engstruct.2014.05.043

7. Li, Y., & Tian , X. (2018, November). "Aerodynamic treatments for reduction of wind loads on high-rise buildings. Journal of Wind Engineering & Industrial Aerodynamics. doi:10.1016/j.jweia.2017.11.006
8. Kim, Y. C., & Kanda, J. (2013). "Wind pressures on tapered and set-back tall buildings. Journal of Fluids and Structures" doi:10.1016/j.jfluidstructs.2013.02.008
9. Abdollah Baghaei Daemei, Elham Mehrinejad Khotbehsara , Erfan Malekian Nobarani, Payam Bahrami (2019). "Study on wind aerodynamic and flow characteristics of triangularshaped tall buildings and CFD simulation in order to assess drag coefficient" https://doi.org/10.1016/j.asej.2018.08.008.
10. Laura Micheli, Jonathan Hong, Simon Laflamme, Alice Alipour(2020) "Surrogate models for high performance control systems in wind-excited tall buildings" https://doi.org/10.1016/j.asoc.2020.106133 1568-4946/© 2020 Elsevier B.V.
11. Jerzy Szolomicki and Hanna Golasz-Szolomicka (2019) "Technological Advances and Trends in Modern High-Rise Buildings" Buildings 2019, 9, 193; doi:10.3390/buildings9090193
12. Huseyin Emre Ilgın (2022) "Use of aerodynamically favorable tapered form in contemporary supertall buildings" Volume 3, Issue 2, (183-196), 2022DOI: 10.47818/DRArch.2022.v3i2052
13. Yanyu Ke, Guohui Shen, Hangcong Yu and Jiming Xie (2022) "Effects of Corner Modification on the Wind-Induced Responses of High-Rise Buildings" Appl. Sci. 2022,12, 9739. https://doi.org/10.3390/app12199739
14. Zhendong Xu, Jiming Xie(2018) "Application of Wind Fairings for Building Aerodynamic Optimization" Downloaded from ascelibrary.org
15. Matin Alaghmandan, Payam Bahrami, Mahjoub Elnimeiri(2014) "The Future Trend of Architectural Form and Structural System in High-Rise Buildings" Architecture Research 2014, 4(3): 55-62 DOI: 10.5923/j.arch.20140403.01

Seismic Analysis of a Multi- Storey Building with Different Types of Slabs

Smrithi K V
Department of Civil Engineering
AWH Engineering College, Kozhikode
Kerala, India
kvsmrithi2112@gmail.com

Jisha. P
Department of Civil Engineering,
AWH Engineering College, Kozhikode
Kerala, India
jishasunil10@gmail.com

Abstract— Earthquake plays an influential role in the analysis and design of structures. Unless the structures are designed and constructed to withstand seismic forces, failure cannot be avoided. Buildings can be made seismically sound with proper structure design, detailing and construction practice. The configuration of a building is very much important for the seismic performance of buildings. The important aspects that affect the seismic configuration of a building are overall geometry and structural system. This parameter varies in their behaviour in the flat slab, waffle slab and conventional slab. Therefore introducing different types of slabs becomes very crucial for a structural engineer when it comes to better performance of RC structure. The objective of this paper is to study the seismic behaviour of multi-storeyed buildings with different types of slab systems. The study is done by considering the varying number of stories i.e. low-rise, mid-rise and high-rise buildings. The study aims to find an effective slab system for both regular and irregular structures. The different types of slabs considered are flat plate system, flat slab with drop system and waffle slab system which is compared with the conventional slab system. Seismic assessment using response spectrum analysis is done. For low rise to high rise buildings, the seismic behaviour of waffle slab is more effective.

Keywords— Seismic analysis, Conventional slab, Flat plate, Flat slab with drops, Waffle slab

I. Introduction

The population of the world is increasing day by day. Besides this increase in population, housing requirements are also increasing. Nowadays, people are facing problems due to land scarcity and the cost of land. Therefore, there is required for vertical development of the building. But, the tall buildings are not properly constructed and designed for the resistance of earthquake loads. In earlier days, only gravity loads are considered for the design of buildings, but nowadays both gravity and lateral loads are considered for the design of buildings. Before the actual erection of the high-rise buildings, it should be analytically or numerically analyzed for seismic loads. Earthquake load is the most important reason for the failure of many tall building structures worldwide.

Earthquake resistant design of RC buildings is a continuing area of research since the earthquake engineering has gained prominence across the globe. Earthquakes occurring in recent past have shown that poorly designed and constructed structures result in great destruction. Hence, there is a need to determine seismic response of tall buildings for designing earthquake resistant structures. The seismic behavior of the structure during the earthquake depends critically on parameters like shape of the structure, size of the structure, intensity of the earthquake along with the type of slab. This paper is focused on the analysis and design of a multi-storey building with different slab arrangements. The function of slab is to prepare a flat surface for loads to be placed on, to act as a sound, fire, and heat insulator or resistance and to use the space between the floor and ceiling for construction equipment and supplies. The different types of slabs considered in the study are conventional slab, flat slab with drops, flat plate and waffle slab.

II. Modelling of Buildings for Analysis

ETABS 2018 has been used for this study. The regular and irregular buildings were designed as per IS 1893:2016 for seismic zone V with soil type III. The irregular building plans, considered for the analysis are of T and S shape. For all the building plan, the study is done for 5, 10 and 15

storey structure with different types of slab i.e. conventional slab, flat slab with drops, flat plate and waffle slab. The description of models are provided in table 1.

TABLE 1 DESCRIPTION OF MODELS

Plan area	576 m^2	
Height of each storey	3 m	
Bay width in X and Y direction	4 m	
Column size	5 storey	450 mm X 450 mm
	10 storey	550 mm X 550 mm
	15 storey	800 mm X 800 mm, 700 mm X 700 mm, 450 mm X 450 mm
Beam size	350 mm X 350 mm	
Shell loads	FF	1.2 kN/m²
	LL	3 kN/m²
	Roof live	1.5 kN/m²
Wall load	External	14 kN/m
	Internal	10.5 kN/m
Mass source	DL+ 0.5 LL	
Seismic zone	V	
Zone factor	0.36	
Response reduction factor	5	
Importance factor	1	
Soil Type	III	

Fixed restraints and rigid diaphragms are provided for the structure. Response function has been defined using IS1893: 2016 for a damping of 5%. For the slabs except conventional slab, the external and internal wall loads are provided using null beams. For all the 36 models, response spectrum analysis was done in ETABS 2018.

TABLE II. THICKNESS OF SLAB

Parameter	Conventional slab	Flat slab with drops	Flat plate	Waffle slab
Slab thickness	150 mm	150 mm	160 mm	100 mm
Drop panel thickness	–	250 mm	–	300 mm
Overall depth of waffle slab	–	–	–	300 mm
Width of rib	–	–	–	100 mm

A. Regular buildings

A square building of 24 m X 24 m is used for the analysis (i.e. having a plan area of 576 m2). The plan of the building with different types of slabs are as provided in Fig. 1.

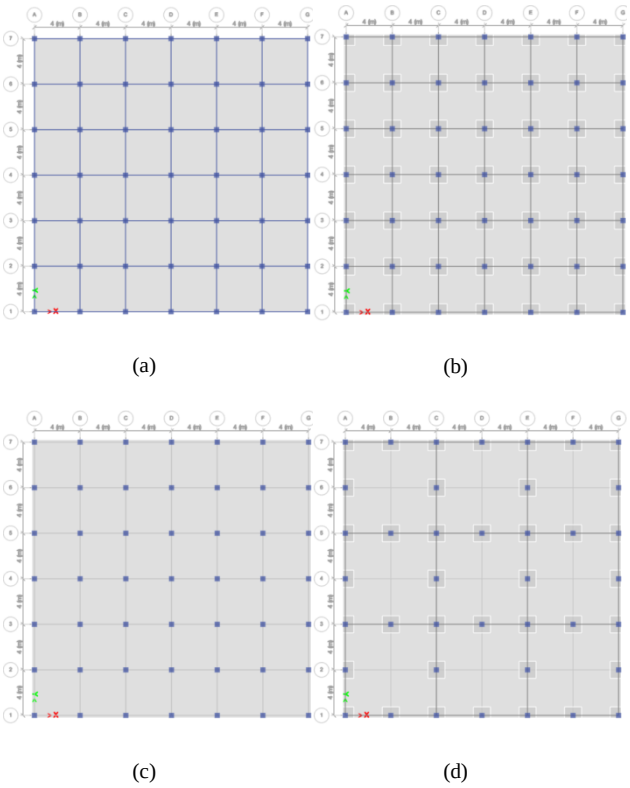

Fig. 1. Plan of building with (a) conventional slab, (b) flat slab with drops (c) flat plate and (d) waffle slab

B) Irregular buildings

Irregular buildings can be either due to plan irregularity or vertical irregularity. In our study, plan irregularity has been considered. The plan area of the building is kept constant to that of regular buildings i.e. 576 m2. The different shapes of building considered are the T shape and S shape buildings. To have an insight about the shape of the building, the plan of the irregular buildings with conventional slabs is provided (as shown from Fig. 2).

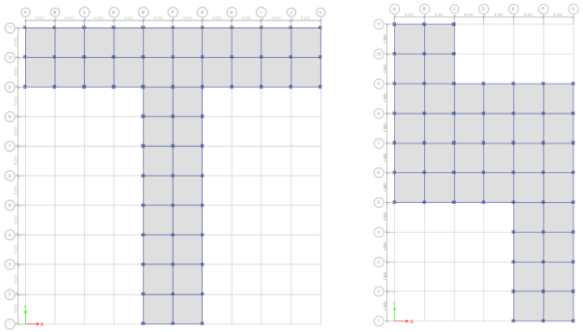

(a) (b)

Fig. 2. Plan of (a) T shape and (b) S shape building with conventional slab

III. Results and Discussion

Response spectrum analysis is done for 5, 10 and 15 storey buildings with the 4 types of slabs (mentioned earlier), for both regular and irregular buildings. The results in terms of storey displacement, inter storey drift ratio, base shear and time period are discussed further.

A. Regular buildings

The results obtained from the analysis of regular square shape buildings using ETABS 2018 are provided in table 3 and table 4.

TABLE III. The Maximum Storey Displacement, Inter-Storey Drift Ratio and Base Shear

Type of slab	No. of stories	Max. storey displacement (mm)		Max. inter storey drift ratio		Base shear (kN)
		X	*Y*	*X*	*Y*	
Conventional slab	G+4	40.49	40.49	0.00364	0.00364	3813.73
	G+9	82.61	82.61	0.00382	0.00382	4206.74
	G+14	121.9	121.9	0.00395	0.00395	4979.54
Flat slab with drops	G+4	40.18	40.18	0.00362	0.00362	3511.04
	G+9	82.97	82.97	0.00385	0.00385	3872.37
	G+14	122.8	122.8	0.00398	0.00398	4642.09
Flat plate	G+4	57.71	57.71	0.00506	0.00506	2632.33
	G+9	124.5	124.5	0.00574	0.00574	2741.09
	G+14	179.9	179.9	0.00589	0.00589	3289.83
Waffle slab	G+4	34.42	34.42	0.00309	0.00309	3253.96
	G+9	68.01	68.01	0.00310	0.00310	3750.01
	G+14	101.9	101.9	0.00336	0.00336	4533.62

1) Story displacement: Maximum displacement (i.e. roof displacement) is as shown in table 3. Since the building is a square shaped regular building, we can see that the storey displacement in X and Y axis are found to be same. This is due to the symmetry of structure in both X and Y direction. It is also observed that as the storey level or as the height of the building increases, the roof displacement also increases. Graphs are plotted for storey displacement in each building as shown in Fig. 3. The conventional slab and flat slab with drops show similar results, so the lines are coinciding in the graphs plotted showing the maximum storey displacement. The storey displacement is least for buildings with waffle slab and maximum for buildings with flat plate. The flat plate system storey displacement is about 50.17% higher than that of conventional slab. The waffle slab storey displacement is about 17.68% lesser than that of conventional slab.

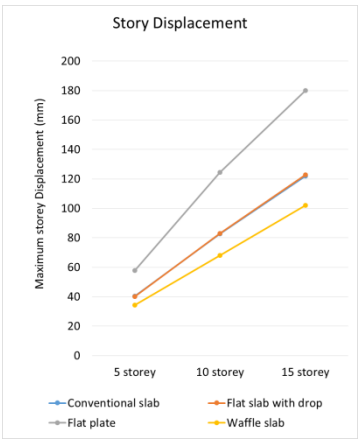

Fig. 3. Maximum storey displacement in 5, 10 and 15 storey building

2) Inter-Story drift ratio: It is defined as the relative translational displacement between two consecutive floors divided by the storey height. The graphs plotted for each models as shown in Fig. 4.

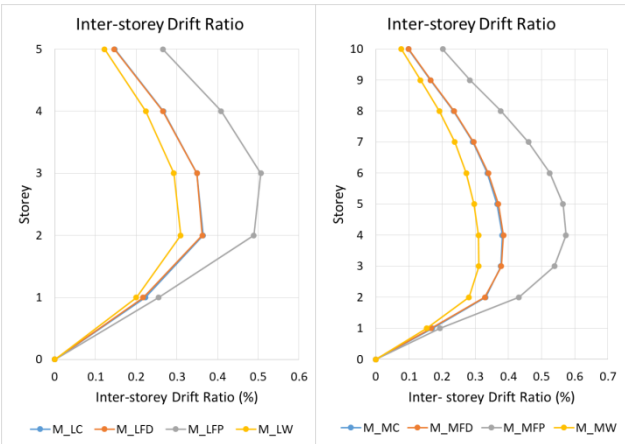

(a) (b)

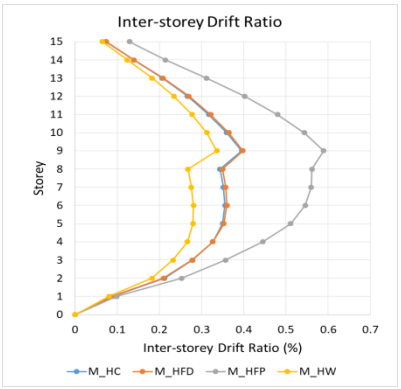

(c)

Fig. 4. Inter-storey drift ratio in (a) 5, (b) 10 and (c) 15 storey building

From the IDR graph, we can see that the maximum Inter-storey drift is seen in the models with flat plate slab. And the waffle slab experiences the least drift. The sudden variation of the inter-storey drift in 9th storey of 15 storey buildings are due to change in building geometry.

3) Base shear: Base shear is an estimate of the maximum expected lateral force on the base of the structure due to seismic activity. The graphical representation of base shear for G+4, G+9 and G+14 storey buildings are shown in Fig.5.

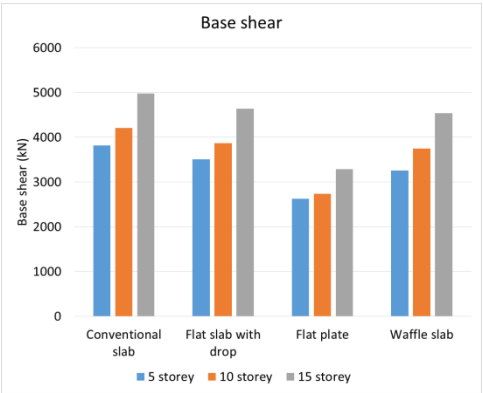

Fig. 5. Base shear of G+4, G+9 and G+14 storey building

The above graphs indicate that the base shear of the building with conventional slab is more when compared to the models with other slab. This is because the seismic weight of the building is more compared to the others due to the presence of beams. And as the seismic weight of the building increases the base shear value also increases. This is also the reason why the models with flat plate slab have the least base shear. The base shear is reduced by about 33% compared to the conventional slab.

4) Time period: It is the time required by the building to undergo one complete cycle of oscillation. Table 4 shows the time period of the structure for first 3 modes.

TABLE IV. Time Period

Type of slab	No. of stories	Time Period (sec)		
		Mode 1	*Mode 2*	*Mode 3*
Conventional slab	G+4	0.982	0.304	0.167
	G+9	1.949	0.614	0.336
	G+14	2.582	0.885	0.494
Flat slab with drops	G+4	0.966	0.296	0.161
	G+9	1.948	0.610	0.331
	G+14	2.566	0.882	0.489
Flat plate	G+4	1.315	0.378	0.189
	G+9	2.806	0.835	0.423
	G+14	3.689	1.202	0.645
Waffle slab	G+4	0.848	0.268	0.151
	G+9	1.621	0.518	0.289
	G+14	2.113	0.753	0.421

The maximum time period is for structure with flat plate, and it is about 43.9% more than that of conventional slab system. The time period of the waffle slab is the least. It is about 18.16% less than that of conventional slab.

B. Irregular buildings

The analysis results are provided from table 5 to table 6.

TABLE IV.The Maximum Storey Displacement, Inter-Storey Drift Ratio and Base Shear

Shape of building	Type of slab	No. of stories	Max. storey displacement (mm)		Max. inter storey drift ratio		Base shear (kN)
			X	*Y*	*X*	*Y*	
T	Conventional slab	G+4	42.01	40.51	0.00374	0.00363	4141.26
		G+9	88.61	83.84	0.00406	0.00387	4530.48
		G+14	132.2	124.1	0.00423	0.00400	5374.05
	Flat slab with drops	G+4	40.59	40.31	0.00363	0.00362	3838.45
		G+9	86.63	84.19	0.00398	0.00390	4204.91
		G+14	129.9	125.1	0.00417	0.00404	5067.53
	Flat plate	G+4	57.95	57.54	0.00508	0.00504	2888.38
		G+9	125.3	125.1	0.00576	0.00574	3005.22
		G+14	181.2	181.1	0.00594	0.00593	3629.01
	Waffle slab	G+4	35.53	34.59	0.00318	0.00311	3613.30
		G+9	73.06	69.62	0.00331	0.00318	4128.87

		G+14	111.0	104.6	0.00359	0.00342	5020.81
S	Conventional slab	G+4	41.08	40.36	0.00368	0.00363	4000.25
		G+9	85.66	82.73	0.00394	0.00382	4401.68
		G+14	127.0	122.2	0.00408	0.00395	5221.58
	Flat slab with drops	G+4	40.32	40.21	0.00363	0.00362	3673.88
		G+9	84.55	82.97	0.00390	0.00385	4035.19
		G+14	126.4	123.5	0.00407	0.00400	4879.36
	Flat plate	G+4	57.86	57.73	0.00507	0.00506	2755.45
		G+9	124.2	124.1	0.00572	0.00571	2864.20
		G+14	180.5	180.3	0.00591	0.00590	3459.05
	Waffle slab	G+4	34.89	34.40	0.00313	0.00309	3448.24
		G+9	70.47	68.04	0.00320	0.00311	3946.39
		G+14	106.7	102.5	0.00348	0.00337	4822.76

1) Story displacement: The waffle slabs shows least displacement when compared to the models with other slabs. It is also notable that for T and S shape buildings, the flat slab with drops performs better than the conventional slab building when considering both X and Y directions. The graphs plotting the maximum displacement of 5, 10 and 15 storey buildings for both X and Y directions are shown in Fig. 6 and Fig. 7. The story displacement of waffle slab is 17.5% lower than that of conventional slab. The storey displacement of models with flat slab with drops is seen to be reduced upto 4% than that of conventional slab. Least roof displacement is seen in waffle slab system, and it is reduced upto 17.75% than that of conventional slab system.

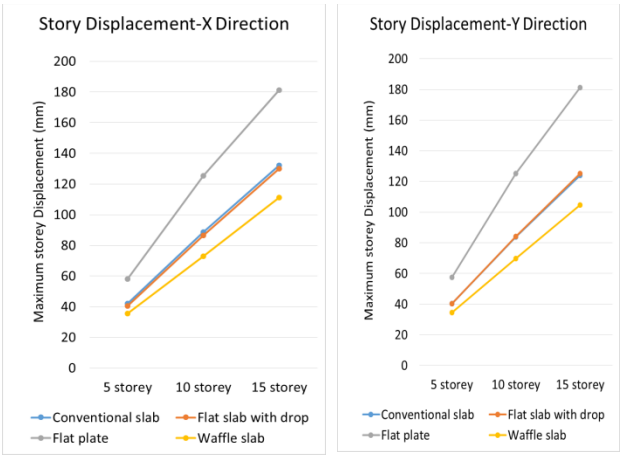

Fig. 6. Maximum storey displacement in 5, 10 and 15 storey- T shape building

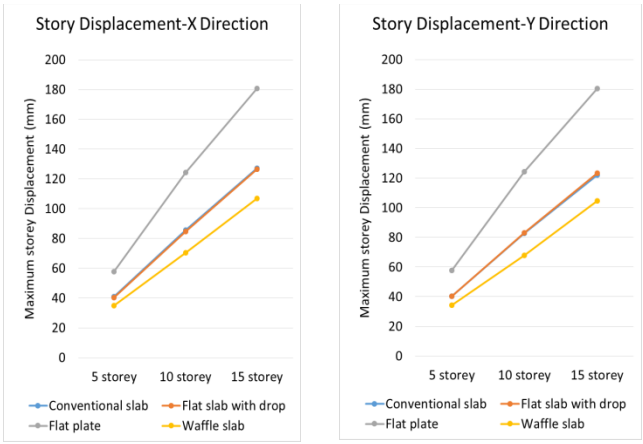

Fig. 7. Maximum storey displacement in 5, 10 and 15 storey- S shape building

2) Inter-Story drift ratio: Since more prominent change is seen in X directtion, the inter- storey drift ratio graphs of T and S shape buildings along the X direction are provided (Fig. 8 to Fig. 10.) as reference. The same trend is seen in the Y direction.

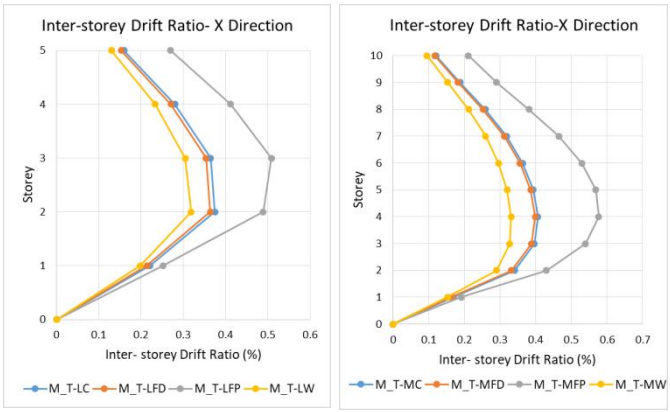

(a) (b)

Fig. 8. Inter-storey drift ratio in (a) 5 and (b) 10 storey- T shape building

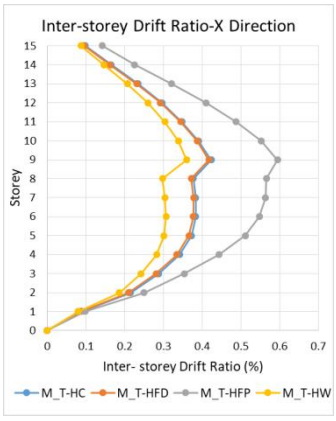

Fig. 9. Inter-storey drift ratio in 15 storey- T shape building

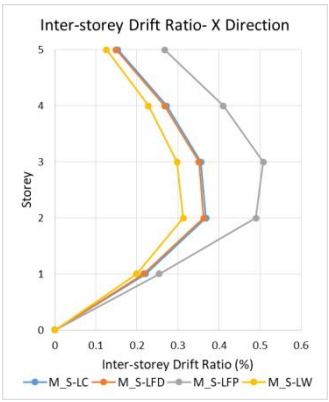

(a)

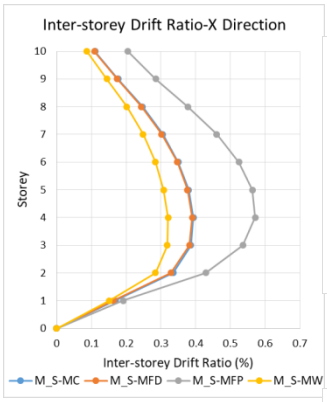

(b)

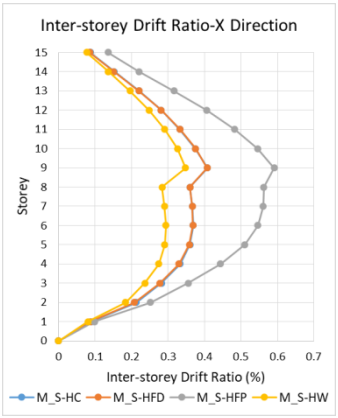

(c)

Fig. 10. Inter-storey drift ratio in (a) 5, (b) 10, and (c) 15 storey- S shape building

From the IDR graph, we can see that the maximum inter-storey drift is seen in the models with flat plate slab. And the waffle slab experiences the least drift. Since the T shape building is only symmetrical along the Y axis and unsymmetrical along the X axis, the storey drift variation of conventional and flat slab with drops is more and hence in Fig. 8 we could see the IDR curves more clearly. The sudden variation of the inter-storey drift in 9th storey of 15 storey buildings are due to the change in building geometry.

3) Base shear: The base shear of the T and S shape buildings are shown in Fig. 11 and Fig. 12. The base shear is minimum for flat plate slab models and is maximum for conventional slab models. Since the self weight of the conventional slab models are more due to the presence of beams, the base shear is more.The base shear of flat plate slab models were reduced by almost 32.47 % for T shape buildings and 33.75% for S shape models when compared to the conventional slab models.

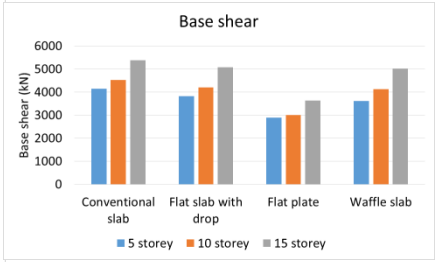

Fig. 11. Base shear of G+4, G+9 and G+14 storey- T shape building

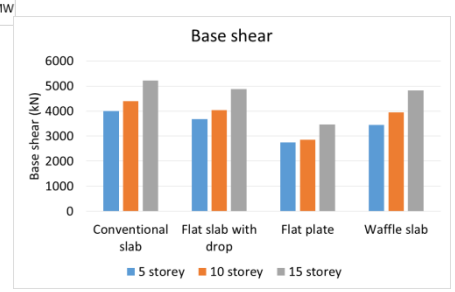

Fig. 12. Base shear of G+4, G+9 and G+14 storey- S shape building

4) Time period: The table 6 and 7 shows the time period of the T shape and S shape models. The flat plate slab system shows more time period. The time period required by the waffle slab is the least.

TABLE VI. Time Period of T Shape Building

Shape of building	Type of slab	No. of stories	Time Period- X dir (sec)			Time Period- Y dir (sec)		
			Mode 1	*Mode 2*	*Mode 3*	*Mode 1*	*Mode 2*	*Mode 3*
T	Conventional slab	5	0.98	0.30	0.16	0.97	0.30	0.16
		10	1.99	0.62	0.33	1.96	0.61	0.33
		15	2.62	0.89	0.49	2.60	0.88	0.49
	Flat slab with drops	5	0.96	0.29	0.15	0.96	0.29	0.15
		10	1.97	0.61	0.33	1.96	0.61	0.33
		15	2.59	0.88	0.48	2.58	0.88	0.48
	Flat plate	5	1.30	0.37	0.18	1.30	0.37	0.18
		10	2.79	0.82	0.41	2.79	0.82	0.41
		15	3.66	1.19	0.63	3.66	1.19	0.63
	Waffle slab	5	0.84	0.26	0.14	0.84	0.26	0.14
		10	1.66	0.52	0.29	1.64	0.52	0.29
		15	2.16	0.76	0.42	2.14	0.76	0.42

TABLE VII. Time Period of S Shape Building

Shape of building	Type of slab	No. of stories	Time Period- X dir (sec)			Time Period- Y dir (sec)		
			Mode 1	*Mode 2*	*Mode 3*	*Mode 1*	*Mode 2*	*Mode 3*
S	Conventional slab	5	0.98	0.30	0.16	0.97	0.30	0.16
		10	1.97	0.62	0.33	1.94	0.61	0.33
		15	2.61	0.89	0.49	2.56	0.87	0.49
	Flat slab with drops	5	0.96	0.29	0.15	0.96	0.29	0.15
		10	1.96	0.61	0.32	1.94	0.60	0.32
		15	2.58	0.88	0.49	2.56	0.88	0.48
	Flat plate	5	1.30	0.37	0.18	1.30	0.37	0.18
		10	2.80	0.83	0.41	2.79	0.82	0.41
		15	3.67	1.2	0.64	3.67	1.2	0.63
	Waffle slab	5	0.85	0.26	0.15	0.84	0.26	0.14
		10	1.64	0.52	0.28	1.62	0.51	0.28
		15	2.14	0.76	0.42	2.10	0.75	0.42

For the T and S shape models the time period of flat plate is about 40% and 42% more (respectively), than that conventional slab models. And the time period of waffle slab is about 17.5% and 18% less than that of conventional slab system for the T and S shape buildings respectively.

IV. Conclusion

Storey displacement is maximum for flat plate slabs and minimum for waffle slabs for all the models. Inter-storey drift ratio is maximum for flat plate slab models. Base shear is maximum for conventional slab and minimum for flat plate slab. The conventional slab and the flat slab with drops performs similarly in terms of storey displacement and storey drift. The time period of the waffle slab system is minimum compared to the other models. The waffle slabs shows better performance. And since the flat slab with drops model and the conventional slab models are showing almost similar results, the flat slab with drops or waffle slab should be preferred over the conventional slab. Considering the economical aspect, the quantity of concrete required for the buildings with flat slab with drops or waffle slab will be less compared to the building with conventional slab. The waffle slab is economical and safer when compared to the buildings with other types of slab.

Acknowledgment

The support of the authorities of AWH Engineering college for the successful completion of project is gratefully acknowledged.

References

1. C. L. Nishanth, Y. Sai Swaroop, D. C. K. Jagarapu et al., "Analysis and design of commercial building with different slab arrangements using ETABS," Materials Today: Proceedings, https://doi.org/10.1016/j.matpr.2020.05.823 , April 2020.
2. G. Sridevi , Antaratana Shivaraj , Gouda Sudarshan and Umesh Biradar, "Comparative Study on Dynamic Behaviour of RC Building With Conventional and Flat Slab," Advances in Structural Engineering and Rehabilitation, Lecture Notes in Civil Engineering 38, https://doi.org/10.1007/978-981-13-7615-3_18, 2020.
3. Chintha Santhosh, Venkatesh Wadki, S.Madan Mohan and S.Sreenatha Reddy, "Analysis and Design of Multistory Building with Grid Slab Using ETABS," International Journal of Innovative Research in Science, Engineering and Technology, Vol. 5, Issue 9, 2016.
4. Abhijit K Sawwalakhe and Prabodh D Pachpor, "Comparative Study Of Conventional Slab, Flat Slab And Grid Slab Using ETABS," ICACE, doi:10.1088/1757-899X/1197/1/012020, 2020.
5. R.S.More, V. S. Sawant and Y. R. Suryawanshi, "Analytical Study of Different Types of Flat Slab Subjected to Dynamic Loading," IJSR, Vol. 4 Issue 7, 2015.
6. Shital Borkar, Kuldeep Dabhekar, Isha Khedikar and Santosh Jaju, "Analysis of Flat Slab Structures in Comparison with Conventional Slab Structures," International Conference on Contemporary and Sustainable Infrastructure, IOP Conf.

Series: Earth and Environmental Science 822 (2021) 012049, 2021.

7. Latha M.S and Pratibha K, "Analysis and comparison of conventional slab and grid slab for symmetric and asymmetric structures," Materials Today: Proceedings, https://doi.org/10.1016/j.matpr.2020.12.1245, 2020.
8. S. Lakshmi Kiran, Sri Raghu M.E, "Comparative Analysis Of Conventional Slab And Flat Slab System Of Commercial Building On Different Zones And Heights By Using Etabs," IRJET, Vol. 7, Issue 8, 2020.
9. Sudhir Singh Bhaduria, Nitin Chhugani, "Comparative Analysis And Design Of Flat And Grid Slab System With Conventional Slab System," IRJET, Vol. 4, Issue 8, 2017.
10. Mrs. Sarita R. Khot, Mr. Kumar T. Bharekar, Mr. Vishwajit V. Jadhav, Mr. Himanshu V. Mahajan, Mr. Purval D. Shiram, Mr. Siddharth V. Tupe, "Comparative Study Of Waffle Slabs With Flat Slabs And Conventional RCC Slabs," IJERT, Vol.5, Issue 4, 2016.
11. Amaresh Chaturvedi, Rajeev Singh Parihar, Abhay Kumar Jha, Barun Kumar, Rajesh Misra, "Seismic Analysis and Modelling of Grid Slab and Flat Slab of G+14 R.C. Framed Structure using ETABS," IJRASET, Vol.10, Issue 9, 2022.
12. Dr Ramakrishna Hegde, Chethana, Nanditha Vinod Kumar, "Comparative Study On Seismic Analysis Of Conventional Slab, Flat Slab And Grid Slab System For A R.C Framed Structures," IRJET, Vol.5, Issue 8, 2018.
13. Vishesh P. Thakkar, Anuj K. Chandiwala, Unnati D. Bhagat, "Comparative Study Of Seismic Behavior Of Flat Slab And Conventional RC Framed Structure," IJERT, ISSN: 2278-0181, Vol.6, Issue 4, 2017.

Seismic Analysis Of Irregular Buildings With And Without Lead Plug Rubber Bearings (LPRB)

Shadiya P V
Department of Civil Engineering
AWH Engineering College
Kozhikode, India
shadiyakabir@gmail.com

Priyanka Dilip P
Dept of Civil Engineering
AWH Engineering College
Kozhikode, India

Abstract—Base isolation has proven to be an effective technique that aids in earthquake hazard mitigation and has been in use for the past decade. The isolation system decouples the structure from the horizontal components of the ground motion, consequently reducing the possibility of resonance. Isolators are provided at the base of the structures, and decoupling is achieved by altering the flexibility of the system, together with appropriate damping. Structures with irregular plans are gaining popularity owing to their aesthetic appearance as well as architectural designs. The response of such structures to seismic action will be different from conventional structures. This paper aims to study the effect of base isolators on structures with irregular plans, while simultaneously observing the changes occurring when height of the structures is increased. Three unique plans are chosen, namely plus, L and T shapes, whose responses are studied on 5, 10 and 15 storeyed structures. All the columns in the base isolated structures are equipped with lead plug rubber bearing base isolators which is the chosen isolator for the purpose of this study. The base isolators are designed for each structure specifically, so that the behavioral patterns observed are as accurate as possible. From the results obtained, it is discerned that base isolated buildings exhibited better performances in comparison with fixed base buildings, and as height of the structure increases the effect of the base isolator tends to decrease.

Keywords—Base Isolation, Lead Plug Rubber Bearing, Seismic Analysis, Mode Period

I. Introduction

Earth quake is a shaking of the ground caused by movement of the tectonic plates relative to each other, both in direction and magnitude. A large part of the world people lives in area of seismic hazard at risk from earthquake of varying harshness and varying frequency of existence. Earthquake cause significant loss of life and destruction to property every year. Several seismic construction designs and technologies have been developed over the years in efforts to reduce the effect of earthquakes on structures, bridges and potentially susceptible contents. Seismic isolation is relatively recent and growing technology of this kind.

II. Base isolation

A. General

Seismic isolation also known as base isolation is an earthquake resistant design concept in which a building is decoupled from the earthquake ground motion or seismic waves. When a building is decoupled from ground motion it significantly reduces response in the structure which would have affected building if it is fixed base. Base isolation decouples the building from ground motion by decreasing the fundamental frequency when compared to fix-based building. This concept of base isolation also makes to remain building elastic during an earthquake. Base isolation concept is also used in bridges, nuclear power plants and liquid storage tanks etc.

B. Lead plug rubber bearing isolators (LPRB)

Lead plug rubber bearing, applied to building and bridge constructions, is a practical and cost-effective choice for seismic isolation. It is composed of laminated elastomeric bearing pad, top and bottom sealing & connecting plates and lead plug inserted in the middle of the bearing as shown in fig 1. The steel shims provide vertical stiffness to the LRB and layers of rubber provide lateral flexibility or horizontal stiffness. Lead core of the LRB provides damping to the structure. It has low maintenance when compared to other types of isolators.

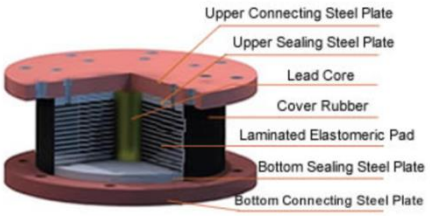

Fig. 1. Typical lead plug rubber bearing isolator

During the earthquake, the un-isolated building will vibrate back and forth in varying directions due to the inertial forces and result in deformation and damages of the building. In contrast, the base isolated building will also displace but remains its original shapes and avoid damages - that is because the lead rubber bearing effectively dissipates the inertial force upon the building, extends the building's period of vibration and decrease the acceleration of the building. The lead plug will slide with laminated rubber during earthquake but convert this energy of movement to heat so that it efficiently reduces the inertial force upon the building, which slow the vibration of the building. Meanwhile, the rubber part will preserve its original shape due to high elasticity.

III.ANALYSIS AND DESIGN

In this study, G+4, G+9 and G+14 structures were modelled and later analysed using the ETABS software. Irregularity in the structures was studied by providing plus, H and T shaped plan to the structures. Hence, a total of 18 structures were studied, out of which 9 structures had fixed bases and 9 were base isolated. Base isolation was incorporated into the structures by providing them with base isolators under all the columns of the structures. Initially, a fixed base structure was modelled and analysed, after which the maximum column support reaction of the structure was obtained. Using this, the base isolator was designed and was then provided to the same structure. The seismic response of the two structures were then studied and compared. The seismic analysis was carried out as per IS 1893:2016 and loads were provided in accordance with IS 875:2015.

A. Model specifications:

Type of building: Reinforced Concrete Building

Plan area: 320 m2

Each bay width: 4m

Height of each storey: 3m

B. Load specifications:

Live load on floors: 3 kN/m2

Floor finish: 1.2 kN/m2

Live load on roof: 1.5 kN/m2

External wall load: 14 kN/m2

Internal wall load: 10.5 kN/

C. Sectional properties:

TABLE I. SECTIONAL PROPERTIES OF MODELS

Storey	Size of beam	Size of column	Slab thickness	Grade of concrete	Grade of concrete
G+4	0.36 m X 0.36 m	0.45 m X 0.45 m	0.15 m	30 MPa	415 MPa
G+9	0.45 m X 0.45 m	0.55 m X 0.55 m	0.15 m	30 MPa	415 MPa
G+14	0.45 m X 0.45 m	0.65 m X 0.65 m	0.15 m	40 MPa	500 MPa

D. Seismic data:

Seismic Zone: V

Zone factor: 0.36 (for Zone V)

Soil Type: Soft (III)

Response Reduction Factor: 5

Importance Factor: 1

Damping: 5%

E. LPRB characteristics:

Isolators were designed for all the models and the corresponding values are given in TABLE II, TABLE III AND TABLE IV.

TABLE II. ISOLATOR PARAMETERS OF G+4 MODELS

Input Parameters	**LPRB Values of models**			
	P5B	**L5B**	**T5B**	
U1 Effective Stiffness	1117903.357 kN/m	1120611.552 kN/m	1120600.671 kN/m	
U2 and	10301.03434 kN/m		10325.98	10325

U3 Stiffness		932 kN/m	.89 kN/m
Yield strength	58.67967 kN	58.82182 kN	58.82 kN
U2 and U3 Effective Stiffness	1117.9033 kN/m	1120.611552 kN/m	1120.6 kN/m

TABLE III. ISOLATOR PARAMETERS OF G+ MODELS

Input Parameters	**LPRB Values of models**		
	P10B	**L10B**	**T10B**
U1 Effective Stiffness	2453580.2 kN/m	2421534.7 kN/m	2453495.1 kN/m
U2 and U3 Stiffness	22608.76462 kN/m	22313.4807 kN/m	22607.98117 kN/m
Yield strength	128.79 kN	127.1082 kN	128.7589 kN
U2 and U3 Effective Stiffness	2453.58	22313.4807 kN/m	2453.4951 kN/m

TABLE IV. ISOLATOR PARAMETERS OF G+14 MODELS

Input Parameters	**LPRB Values of models**		
	P15B	**L15B**	**T15B**
U1 Effective Stiffness	3856182.29 kN/m	3715632.9 kN/m	5256829 kN/m
U2 and U3 Stiffness	35533.19 kN/m	34238.078 kN/m	48439.58802 kN/m
Yield strength	202.4142 kN	195.03658 kN	275.9352 kN
U2 and U3 Effective Stiffness	3856.182 kN/m	3715.6329 kN/m	5256.829 kN/m

All the structures were modelled using ETABS software and are shown in Fig. 2, Fig. 3, and Fig. 4. given below.

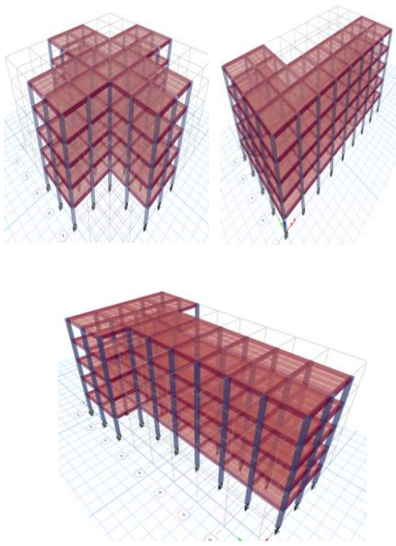

Fig. 2. 3D views of plus, L and T shaped G+4 models

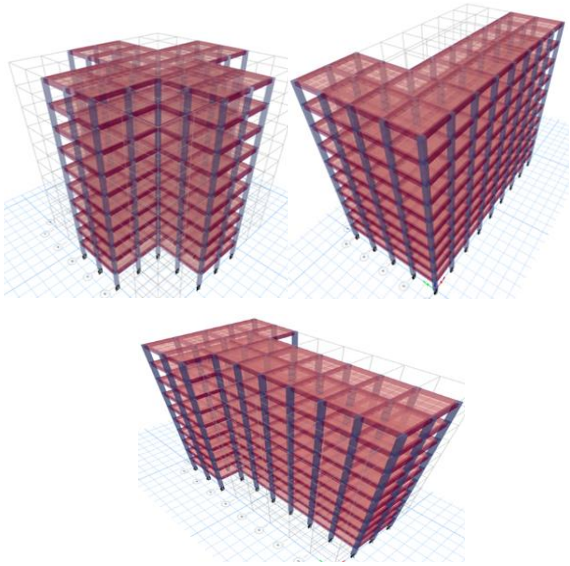

Fig. 3. 3D views of plus, L and T shaped G+9 models

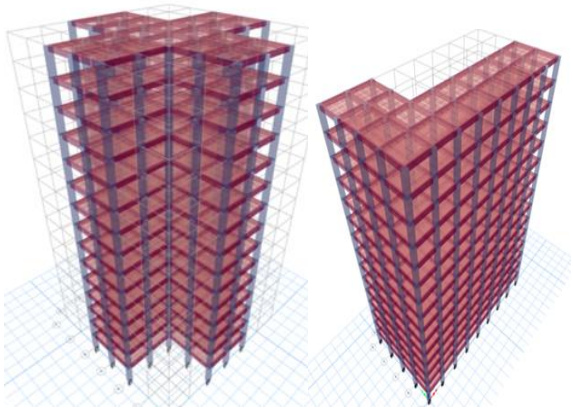

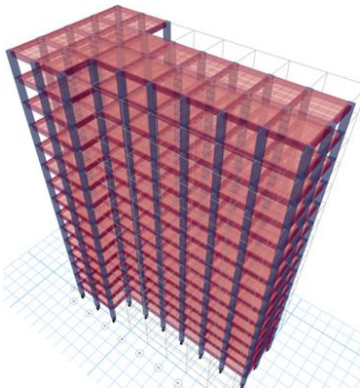

Fig. 4. 3D views of plus, L and T shaped G+14 models

IV. RESULTS AND DISCUSSSION

The results obtained from the seismic analysis of the structures with different plans were discussed. The results of parametric study by varying the height of the structure were included. The storey displacement, storey drift, mode period and base shear vales were noted and comparison graphs were plotted for all eighteen models.

A. Storey displacement

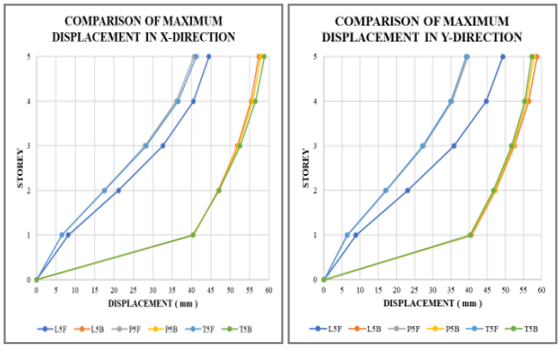

Fig. 5. Storey displacement comparison for G+4 models in X and Y directions

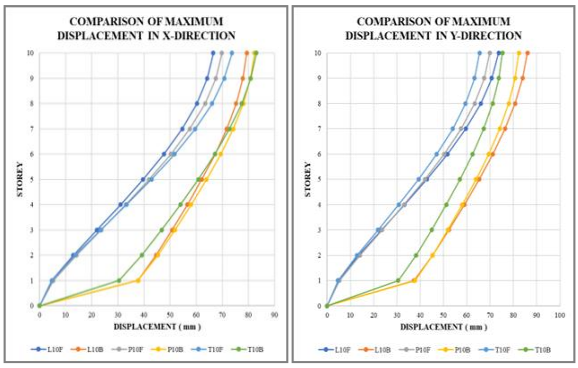

Fig. 6. Storey displacement comparison for G+9 models in X and Y directions

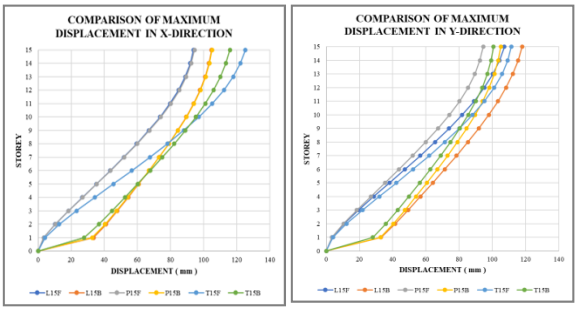

Fig. 7. Storey displacement comparison for G+14 models in X and Y directions

The presence of base isolator in the structure resulted in an increase in the displacement values compared to the fixed base structures. The interstorey displacements were smaller for isolated structures compared to fixed base buildings. This means that once the base isolator came into action, lesser amount of seismic energy was passed onto the structure, hence the smaller interstorey displacement values. Increase in interstorey displacement was found to be the lowest in the case of T5B model. As the number of stories increased, the reduction of displacement values decreased, i.e. the percentage of displacement reduction between the top and bottom storey was found to be the lowest in the case of G+14 structures. Also as the height of the structure increased, the effect of irregularity of the structure increased. This was observed in the 10 and 15 storeyed structures where the top storey displacement of base isolated structure was lesser than fixed base structure.

B. Storey drift:

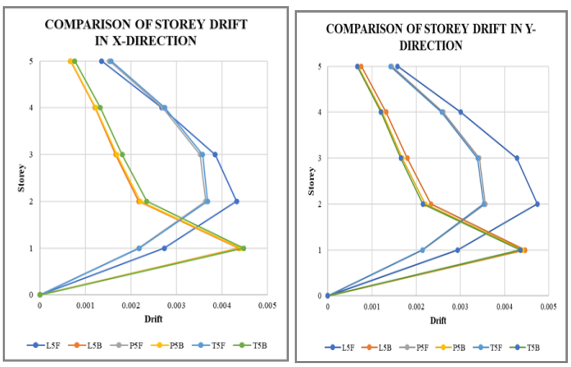

Fig. 8:.Storey drift comparison for G+4 models in X and Y directions

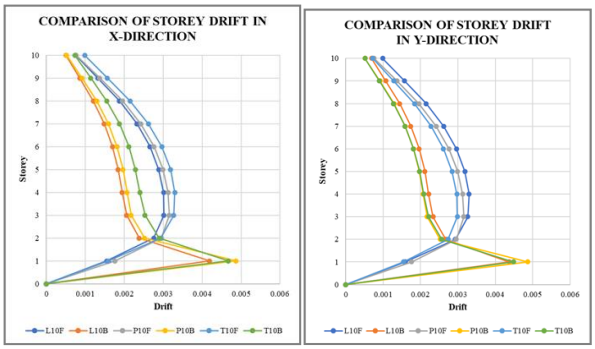

Fig. 9. Storey drift comparison for G+9 models in X and Y directions

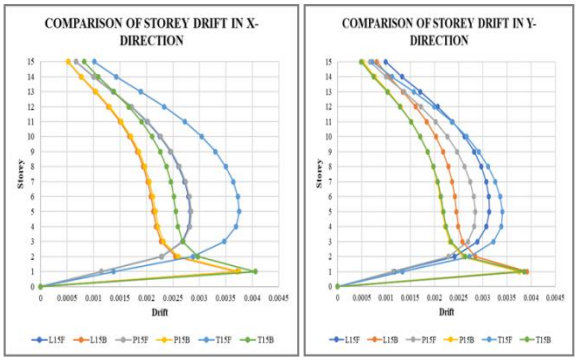

Fig. 10. Storey drift comparison for G+14 models in X and Y directions

In the case of base isolated structures, the highest drift value was obtained at storey one in all of the cases. This was due to the presence of base isolators in the structure. The base isolator imparts a certain displacement at storey one which will was the highest interstorey displacement in that structure. Hence the highest value of drift also occurred at the same storey. But like the fixed base structures, in the base isolated structures the storey drift decreased thereafter as the height of the structure increased.

C. Base shear:

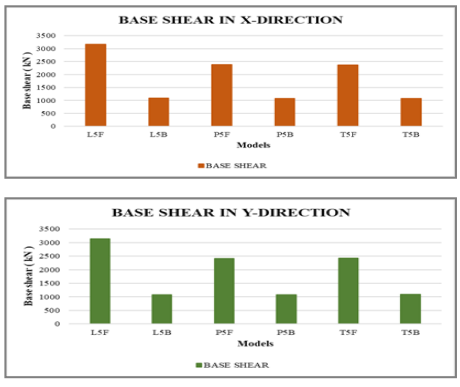

Fig. 11. Base shear comparison for G+4 models in X and Y directions

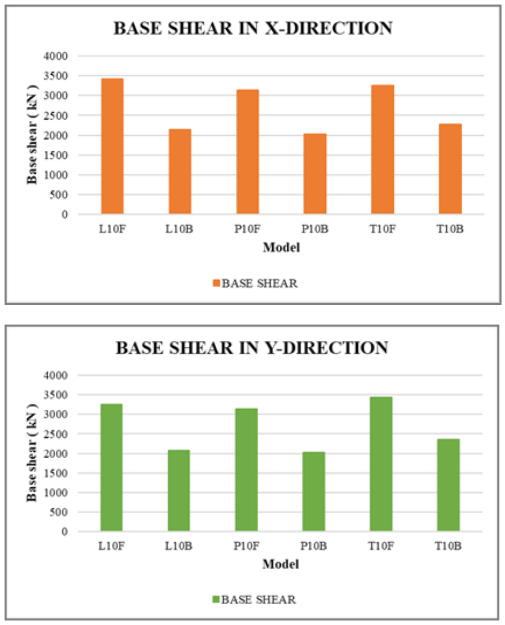

Fig. 12. Base shear comparison for G+9 models in X and Y directions

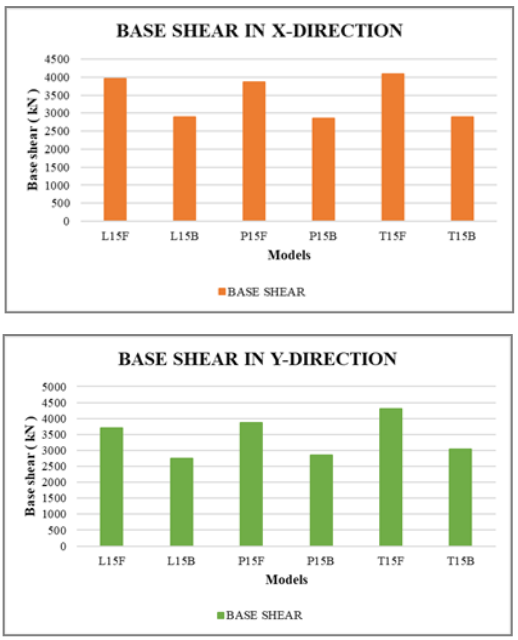

Fig. 13. Base shear comparison for G+14 models in X and Y directions

The above graphs indicate that when base isolator was provided to a structure the base shear of the structure decreased. Hence, the base shear of the fixed models was greater than that of base isolated models. Among the models L5B indicated highest value of base shear reduction.

D. Mode period:

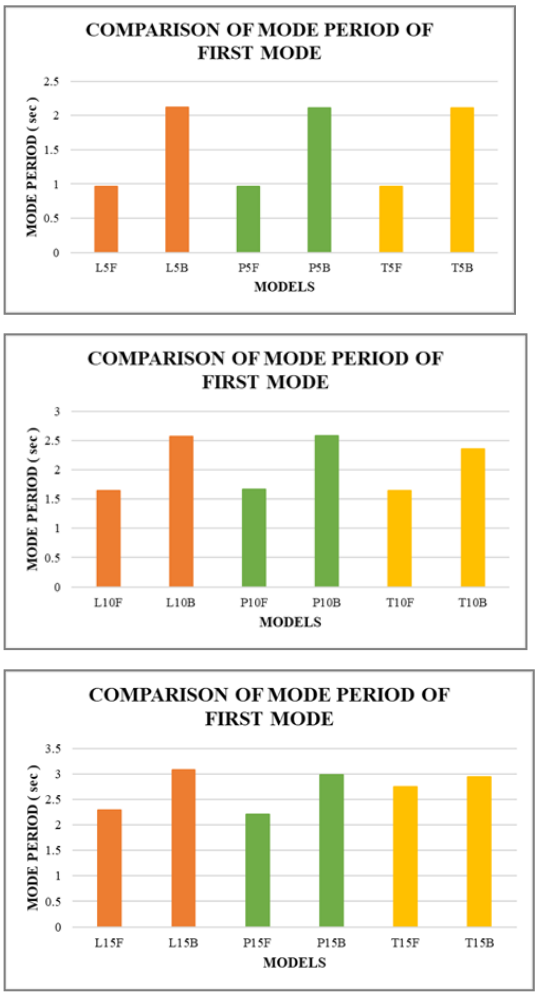

Fig. 14. Mode period comparison for G+4, G+9 and G+14 models

For all the base isolated models the mode period was greater than the base isolated models in the case of the first mode. The first mode of a building is considered as critical and hence, the increase in these mode periods indicates better response of the base isolated structures. As the mode period increased the chances of resonance occurring was reduced. Model L5B indicated greater increase in first mode period compared to the other models.

V. CONCLUSION

The initial displacement of base isolators structures was greater than fixed base structures. This was due to the sliding effect of the isolator on the structure.

- The interstorey displacement of the base isolated models, however, were lesser compared to fixed base models. This ensured that lesser displacements occurred in the upper stories.
- As height of the storey increased the effect of irregularity of the structure increased.
- Base isolated models were observed to have lower drift values compared to fixed base model. The highest drift value was found to be at storey 1 in base isolated models, due to higher displacement at that storey.
- Base shear of the models reduced when isolators were provided to the structures. The reduction in base shear however decreased as the number of stories increased.
- The first mode period of all the isolated structures were greater than the corresponding fixed base structures. As a result, only a reduced amount of energy was transferred to the structure.
- The percentage of increase in mode period decreased as height of the structure increased.

Acknowledgment

I am sincerely grateful for all the guidance and help I received from the professors and staff at the institution.

References

1. James M.Kelly and Farzad Naeim, Design of Seismic Isolated Structure from stheory of practice, John Wiley and sons, 1999.
2. Vinod Kumar Parma, G.S.Hiremath, " Effect Of Base Isolation In Multistoried RC Irregular Building Using Time History Analysis " International Journal of Research in Engineering and Technology, Volume 04, Issue 06, June 2015.
3. Prof. Anubhav Rai, Sandeep Kumar Sahu, Prof. Vedant Shrivastava, " Static Analysis of Asymmetric Reinforced Concrete Structure with Lead Rubber Bearing " International Research Journal of Engineering and Technology, Volume: 07 Issue: 11 Nov 2020.
4. Venkatesh, Mr.Arunkumar H.R " Dynamic Analysis Of 11 Storey RC Structure By Providing Lead Rubber Bearing As Base Isolation System " International Research Journal of Engineering and Technology (IRJET), Volume: 03 Issue: 07, July-2016

5. Swapnil Ambasta, Dushyant sahu, G.P. Khare " Analysis Of The Base Isolated Building (Lead Plug Bearing) In Etabs " International Research Journal of Engineering and Technology (IRJET), Volume: 05 Issue: 01, Jan-2018.
6. Bommena Karthik, E.Rani, Dr M.S.V.K.V.Prasad, Mr. K. Shanthakumar, Dr. K. Mohan Das "Seismic Analysis Of A Multistoried Rc Structure With And Without Lead Plug Rubber Bearing(LPRB)" UGC Care Group I Journal, Vol-12 Issue-08,August 2022
7. Sonali Anilduke, Amay Khedikar, (2015).Comparision of building for sesmic response by using base isolation, International Journal of Research in Engineering and Technology (IJRET), 2321-7308
8. Shirol,S. and Kori, J. G. (2017). "Seismic Base isolation of RC Frame Structures with and without Infill" International Research Journal of Engineering and Technology (IRJET), 4(6), 1783-1792
9. IS 875 (Part 2):1987, Indian Standard "CODE OF PRACTICE FOR DESIGN LOADS (OTHER THAN EARTHQUAKE) FOR BUILDING AND STRUCTURES", PART 2 IMPOSED LOADS (Second Revision), BUREAU OF INDIAN STANDARDS, NEW DELHI
10. Ghodke, R.B. and Admane, S.V. (2015). "Effect of Base-Isolation for Building Structures." International Journal Science, Engineering and Techonology Research (IJSETR), 4 (4), 971-974.
11. Amer Hassan, Ahmed Saeed (2018)."Design Of Lrb Isolatros For Seismic Resistant", Proceedings Of Arsss International Conference, 01st April, 2018, New Delhi, India.
12. Mounika,Dr.,B.L.Agarwal (2016) "Seismic Analysis Of Fixed Base And Base Isolated Building Structures" International Journal of Advanced Technology In Engineering And Science,volume-4,issue-8,277-288.
13. Ashish R. Akhar, Tejas R.Wankhade (2014) "Seismic Performance of RC Structure Using Different Base Isolator" International Journal Of Engineering Sciences&Research,volume-3,issue-5,724-729.
14. Anusha R Reddy, Dr. V Ramesh (2015) "Seismic Analysis of Base Isolated Building in RC Framed Structures" International Journal of Civil and Structural Engineering Research, Vol. 3, Issue 1, pp: (170-176).
15. Md. Arman Chowdhury and Wahid Hassan, Comparative study of the Dynamic Analysis of Multi-storey Irregular building with or without Base Isolator, Proc of IJSET, Volume No.2, Issue No.9, 1.Sept.2013, pp : 909-912.

Investigation of Temperature Variation in Kozhikode District, Kerala

Mufeeda NK
Dept of Civil Engineering, KMCT College Of Engineering For Women Kozhikode 673601, Kerala, India
mufeedaaly@gmail.com

Dr. Dinesan VP
Dept of Civil Engineering, KMCT College Of Engineering For Women Kozhikode 673601, Kerala, India
dinesanvp2019@gmail.com

Abstract— Kerala is situated on the Western Ghats' southern edge. Kerala has a topography that is asymmetrical. Its landform is characterized by steep slopes and rolling, quiet hills. Kerala has been experiencing temperature rise, irregular monsoons, and water scarcity for the past few years. The present study includes an investigation of temperature variations in the Kozhikode district, Kerala by examining the Maximum, Minimum, and Average Temperature in annual, seasonal, and monthly variations by time series of meteorological stations in the Kozhikode district. Gridded data of temperature prepared by the Indian Meteorological Department (IMD) and Centre for Water Resources Development and Management (CWRDM) for the Kozhikode region have been used in the study. The temperature data is collected from three meteorological stations in the Kozhikode district. The variation of temperature was analyzed by linear regression method. The statistical significance of the trend can be tested by a non-parametric test, such as the Mann-Kendall Trend Test.

Keywords- Climate change, Temperature trend, Linear regression method, Mann-Kendall trend test

I. INTRODUCTION

Long-term changes in temperature and weather patterns are referred to as climate change. These changes may be natural, but since the 1800s, human activities, particularly the combustion of fossil fuels have been the primary drivers of climate change. One of the main contributors to the current climate issue is the carbon that people have released into the atmosphere since the Industrial Revolution. However, the effects of climate change have been amplified by human activity.

The goal of this study is to look into the temperature variability in the district of Kozhikode in the Indian state of Kerala. This involves being aware of patterns or changes in temperature. Recognizing the uncertainty related to temperature. Being aware of the mitigation strategies used to lessen the effects of climate change on people and the environment.

The present study includes an investigation of temperature variations in the Kozhikode district by analyzing the maximum, minimum, and average temperature by annual, seasonal, and monthly temperature variation time series of meteorological stations in the Kozhikode district. This study uses daily time series data obtained from 1969 to 2021, 1996 to 2021, and 1983 to 2021 for long-term investigation of temperature variability. In the Kozhikode district, temperature data is gathered from three meteorological stations. The Mann-Kendall Trend Test, which is frequently used to evaluate the statistical significance of trends, is employed to investigate temperature. In this study, future temperature patterns were also evaluated, and suggestions for mitigating temperature change effects were made.

II. METHODOLOGY

A. Study area

The study is conducted in Kerala's Kozhikode district. One of Kerala's 14 districts, Kozhikode or Calicut, is located along the Malabar Coast in the state's southwest. The district's administrative center is located at Kozhikode, often referred to as Calicut. On India's southwest coast sits the Kozhikode district. The district is bounded to the north by the district of Kannur, to the east by the district of Wayanad, to the south by the district of Malappuram, and to the west by the Arabian Sea.

The district is divided into three separate topographical areas: the lateritic midland, the rocky highlands created by the steep Western Ghats, and the sandy coastal belt. The rocky

highlands cover 637.65 m2, the lateritic midlands 1343.50 m2, and the sandy coastal belt 362.85 m2 of the overall area of 2344 m2. The district's coastline spans roughly 80 kilometers. The lowland region makes up 15.55 percent of the district's total area, while the highland region makes up 26.80 percent.

The district experiences a highly hot season from March to May and a usually humid environment overall. The South West Monsoon, which begins in the first week of June and lasts through September, is when it rains. The second half of October through November is the North East Monsoon month. In December and January, when the skies are clear and the air is crisp, you'll find the greatest weather of the year.

Fig. 1 shows the location map of the Kozhikode district.

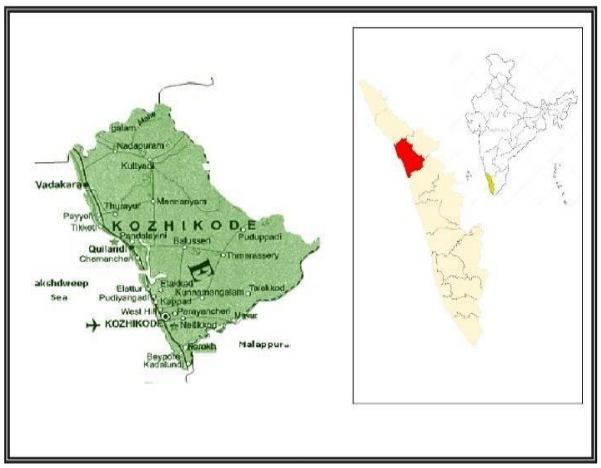

Fig. 1 Location map of kozhikode district

B. Data collection

The data for minimum and maximum temperature data were collected in different meteorological stations in the Kozhikode district. The minimum and maximum air temperature (°C) were recorded daily basis. The data were collected from IMD Pune and the Centre for Water Resources and Management (CWRDM). Here also include data from Karipur station. Which is located in the Malappuram district. It is the border area of Kozhikode district. the temperature data is collected from Kozhikode station from 1969 to 2021. The availability of temperature data for Karipur Station is from 1996 to 2022 and Kunnamangalam station from 1983 to 2021. Minimum and maximum daily temperature data were collected from these stations.

C. Data analysis

The magnitude of the trend was determined using statistical software such as the Mann-Kendall trend test (non- parametric method). these methods assume a linear trend in the time series. The trend analysis was carried out for the temperature data using the Mann-Kendall test. In order to understand the Temperature variability and change throughout the period of 1969-2021, 1996-2022, and 1983-2021. the analysis work was used to recognize the recent trend of variation of each temperature parameter (maximum and minimum and average temperature).

The trend was analyzed to understand the trend of annual maximum, minimum, and average temperature also monthly and seasonal (southwest monsoon, northeast monsoon, winter, summer) variations through the period of 1969-2021, 1996-2022, and 1983-2021.

Materials and method

The magnitude of trends can be determined regression (parametric test) method, whose statistical significance can be obtained by Mann–Kendall test.

Linear regression method

Temperature and time can be used as the independent and dependent variables in a regression analysis. Here use regression analysis to fit a linear equation,

$$y = mx + c \qquad (1)$$

Where c is the intercept and m is the slope. The rate of rise or decline in the variable was provided by the linear trend value represented by the slope of the simple least-square regression line.

Mann-Kendall test

A non-parametric statistical technique called the Mann- Kendall test is effective at spotting trends in data that span extensive time periods. The Mann-Kendall Trend Test also called the M-K test, is used to look for persistently rising or falling trends in data gathered over time.

The Mann-Kendall test can be used to assess the statistical significance of the trend in rainfall and temperature variables. The test compares the alternative hypothesis of no trend.

The definition of the statistic S is;

$$S = \sum_{i=2}^{n} \sum_{j=1}^{i-1} sign(x_i - x_j) \quad (2)$$

The standardized test statistic Z is given by:

$$z = \begin{cases} \frac{S-1}{\sqrt{Var(S)}} & if\ S > 0 \\ 0 & if\ S = 0 \\ \frac{S+1}{\sqrt{Var(S)}} & if\ S < 0 \end{cases} \quad (3)$$

The test statistics Z is used a measure of significance of trend. A positive Z indicates anincreasing trend in the time- series, while a negative Z indicates a decreasing trend. If the computed value |Z| >Zα/2, where α represents the chosen significance level (eg:5% with Z0.025 = 1.96) then the null hypothesis (H0) is rejected in a two-sided test. The statistical significance level of 5 percent has been chosen for the study. Addinsoft XLSTAT 2022 has been used for performing Mann-Kendall test.

III. RESULT AND DISCUSSION

A. Long term trend in temperature

The trend analysis of temperature (maximum, minimum, average) is carried out using linear regression method; whose statistical significance is tested by Mann- Kendall Trend Test. The analysis is carried out in three stations such as Kozhikode, Karipur, Kunnamangalam.

Maximum Temperature

The regression analysis shown an increasing trend in maximum temperature for Annual, monthly and four seasons for station at Kozhikode. The Mann-Kendall Test Shows that this trend has statistical significance at 95% confidence. On the basis of trend line the Annual maximum temperature at Kozhikode station in 1969 is 33.3oC and in 2021 is 36.7. So, there is an increasing 3oC of maximum temperature at Kozhikode for the total period analysed. The seasonal (southwest, northeast, winter, summer) maximum temperature at Kozhikode station in 1969 is 31.5, 32.4,32.6,33.3 Degree Celsius and in 2021 is 34.9,35.4,35.78, 36.9. so there is an increase in 3.4, 3, 3.1 ,3.6 Degree Celsius of seasonal maximum temperature at Kozhikode for the total period analysed. The monthly maximum temperature at Kozhikode station is increasing 2.6, 3.4, 3.5, 4.4, 3.1, 3.2, 3.6, 3.9, 3.1, 3.2, 2.7, 3.3 Degree Celsius for the total period analysed.

The regression analysis shown an increasing trend in maximum temperature at Karipur station for annual, winter and in months of February, March, May, July, August, September, October, November. But the Mann-Kendall Test shows that this trend has no statistical significance.

The regression analysis shows an increasing trend in maximum temperature, during the annual, monthly, southwest monsoon, the northeast monsoon, winter, and summer seasons at Kunnamangalam station. The Mann- Kendall Test Shows that this trend has statistical significance at 95% confidence except northeast monsoon and in the month of June. On the basis of trend line the Annual maximum temperature at Kunnamangalam station in 1969 is 33.3oC and in 2021 is 36.7. So, there is an increasing 3oC of maximum temperature at Kunnamangalam for the total period analysed. The seasonal (southwest, northeast, winter, summer) maximum temperature at VVSSSS station in 1969 is 31.5, 32.4,32.6,33.3 Degree Celsius and in 2021 is 34.9,35.4, 35.78, 36.9. so there is an increase in 3.4, 3, 3.1 ,3.6 Degree Celsius of seasonal maximum temperature at Kozhikode for the total period analysed. The monthly maximum temperature at Kozhikode station is increasing 2.6, 3.4, 3.5, 4.4, 3.1, 3.2, 3.6, 3.9, 3.1, 3.2, 2.7, 3.3 Degree Celsius for the total period analysed.

Minimum Temperature

The regression analysis shown an increasing trend in minimum temperature for all the seasons for the station at Kozhikode. The Mann-Kendall Test Shows that this trend has statistical significance at 95% confidence. On the basis of the trend line the Annual minimum temperature at Kozhikode station in 1969 is 18.7oC and in 2021 is 21oC. So, there is an increasing 2.3oC of minimum temperature at Kozhikode for the total period analyzed. the seasonal (southwest, northeast, winter, summer) minimum temperature at Kozhikode station in 1969 is 17.8, 19.4,19.2,22 Degree Celsius and in 2021 is 21, 18.3, 21.5, 21.5, 23.2. So there is an increase in 0.5, 2.1, 2.3, 1.2 Degree Celsius of minimum temperature at Kozhikode for the total period analysed. The monthly minimum temperature at c station is increasing in the order of 2.4, 2.01, 1.8, 1.5, 1.5, 0.6, 0.7, 0.6, 1, 2.1, 2.1 for the total period analysed.

The regression analysis shows an increasing trend in minimum temperature at Karipur station in annual and in months of June, September and December. But the Mann- Kendall Test shows only annual minimum temperature has statistical significance at 95% confidence. On the basis of the trend line the Annual minimum temperature at Karipur station in 1996 is 24.2oC and in 2021 is 25.2oC. So, there is an increasing 1oC of minimum temperature at Karipur for the total period analyzed.

The regression analysis shown an increasing trend in minimum temperature in the month of March and decreasing trend in annual,sw monsoon, May, June, July, August, September and October months and shows no trend in NE monsoon, winter, summer, January, February, April, November, and December for the station at Kunnamangalam. The Mann-Kendall test shows Annual, southwest monsoon, March, May, June July, August, and September trend has statistical significance at 95% confidence. On the basis of the trend line the southwest monsoon minimum temperature at Kunnamangalam station in 1983 is 22.15oC and in 2021 is 20.2oC. So, there is an decrease in 1.95oC of minimum temperature at Kunnamangalam for the total period analyzed. the monthly (June, July, August, September) minimum temperature at Kunnamangalam station in 1983 is 22.5, 22.3, 22.6, 22.5

Degree Celsius and in 2021 is 21.2, 20.5, 21.5, 21.05 . So there is an decrease in 1.33, 1.77, 1.59, 1.5 Degree Celsius of minimum temperature at Kunnamangalam for the total period analysed.

Average Temperature

The regression analysis shows an increasing trend in average temperature in the annual, monthly, southwest, northeast, winter, and summer seasons at Kozhikode station. The Mann-Kendall Test Shows that this trend has statistical significance at 95% confidence. On the basis of the trend line the Annual Average temperature at Kozhikode station in 1969 is 27.1oC and in 2021 is 29oC. So, there is an increasing 1.9oC of average temperature at Kozhikode for the total period analyzed. the seasonal (southwest, northeast, winter, summer) average temperature at Kozhikode station in 1969 is 25.9, 26.9, 26.8, 28.8 Degree Celsius and in 2021 is 29, 27.6, 28.9, 29.2, 30.7 Degree Celsius. So there is an increase in 1.7, 2, 2.4, and 1.9 Degree Celsius of average temperature at Kozhikode for the total period analysed. The monthly Average temperature at Kozhikode station is increasing in the order of 1.9,1.7, 2, 2.4, 1.9, 2.5, 2.3, 2.3, 1.8, 1.7, 1.5, 1.7, 2, 1.6, 1.8, 2, 2.3 Degree Celcius for the total period analysed.

The regression analysis shows an increase in trend in average temperature at Karipur station in winter and in the months of May, July, October, and December. average temperature at Karipur station. The Mann-Kendall test shows that this trend has no statistical significance.

The regression analysis shows an increasing trend in average temperature in the annual, northeast, winter, and summer seasons at Kunnamangalam. Also shows increasing trend in the months of January, February, March, April, May, September, November, December. The regression analysis shows decreasing trend in the months of July and August. The regression analysis shows no trend in southwest monsoon, June and October. The Mann- Kendall Test Shows only in the season of summer, February, March, and November trend has statistical significance at 95% confidence.

On the basis of the trend line the Summer Average temperature at Kunnamangalam station in 1983 is 29.3oC and in 2021 is 30.1oC. So, there is an increasing 0.8oC of average temperature at Kunnamangalam for the total period analyzed. The monthly (February, march, November) average temperature at Kunnamangalam station in 1983 is 27.64, 28.8, 27.2 Degree Celsius and in 2021 is 28.5, 30.1, 27.72 Degree Celsius. So there is an increase in 0.86, 1.31 and 0.44 Degree Celsius of average temperature at Kunnamangalam for the total period analysed.

A. Future trend Kozhikode station

The increasing trend in the Annual maximum temperature at Kozhikode station shows that by 2050 it may reach to 38.1 degree Celsius. The increasing trend in the Seasonal (southwest monsoon, northeast monsoon, winter, summer) maximum temperature at Kozhikode station shows that by 2050 it may reach to 36.7, 36.2, 36.6, and 38.8 degree Celsius. The increasing trend in the Monthly (January to December) maximum temperature at Kozhikode station shows that by 2050 it may reach to 35, 37.6, 38.4, 39, 37.9,36.3, 35.3, 35.4 35.2, 36.3,36.3, 36.9 degree Celsius.

The increasing trend in the Annual minimum temperature at Kozhikode station shows that by 2050 it may reach to 22.2 degree Celsius. The increasing trend in the Seasonal (southwest monsoon, northeast monsoon, winter, summer) minimum temperature at Kozhikode station shows that by 2050 it may reach to 18.5, 22.6, 22.7, and 23.8 degree Celsius. The increasing trend in the Monthly (January to December) minimum temperature at Kozhikode station shows that by 2050 it may reach to 23, 22.9, 23.4, 24.7, 24.4, 23, 22.7 22.9, 23.3, 23.5, 24.3, 22.7 degree Celsius.

The increasing trend in the Annual average temperature at Kozhikode station shows that by 2050 it may reach to 30 degree Celsius. The increasing trend in the Seasonal (southwest monsoon, northeast monsoon, winter, summer) average temperature at Kozhikode station shows that by 2050 it may reach to 28.5, 29.9, 30.5, and 31.7 degree Celsius. The increasing trend in the Monthly (January to December) average temperature at Kozhikode station shows that by 2050 it may reach to 30.1, 30.6, 31.9, 32, 31.3, 28.7, 28.2, 28.5, 28.8, 29.5, 30.1,30 degree Celsius.

Karipur station

The increasing trend in the Annual minimum temperature at Karipur station shows that by 2050 it may reach to 26.4 degree Celsius.

Kunnamangalam station

The increasing trend in the Annual maximum temperature at Kunnamangalam station shows that by 2050 it may reach to 40.3 degree Celsius. The increasing trend in the Seasonal (southwest monsoon, winter, summer) maximum temperature at Kunnamangalam station shows that by 2050 it may reach to 36.57, 38.6, and 40 degree Celsius. The increasing trend in the Monthly (Except June) maximum temperature at Kunnamangalam station shows that by 2050 it may reach to 36.4, 38.5, 38.5, 39.8, 38.7, 33.6, 33.6, 35.8, 35.5, 35.1, 35.8 degree Celsius.

The decreasing trend in the southwest monsoon minimum temperature at Kunnamangalam station shows that by 2050 it may reach to 18.7 degree Celsius. The decreasing trend in the monthly (June, July, August, and September) minimum temperature at Kunnamangalam station shows that by 2050 it may reach to 20.8, 19.2, 19.8, and 19.9 degree Celsius.

The increasing trend in the summer average temperature at Kunnamangalam station shows that by 2050 it may reach to 30.6 degree Celsius. The increasing trend in the monthly (February, March, and November) average temperature at Kunnamangalam station shows that by 2050 it may reach to 29.1, 31.1, and 28 degree Celsius.

IV. CONCLUSION

The study focused on the investigation of temperature changes in the Kozhikode district of Kerala. The parametric ordinary least square fits have been used to estimate the magnitude of trend in three temperature variables (maximum, minimum, and average) in various seasons (annual, monthly, seasonal) whose statistical significance was assessed by nonparametric Mann-Kendall test.

The investigation on the long-term trend of three temperature variables (maximum, minimum, average) at Kozhikode station in Kozhikode district, using the linear regression method shows an increasing trend for temperature for all the seasons (annual, monthly, and seasonal). The statistical test by Mann-Kendall test reveals that this increasing trend has statistical significance at 95% confidence level.

The investigation on the long-term trend of maximum and average temperature at Karipur station shows no statistical significance and shows trend in annual minimum temperature with 95% of statistical significance.

The investigation on the long-term trend of maximum temperature at Kunnamangalam station in Kozhikode district, using the linear regression method shows an increasing trend for temperature for all the seasons (annual, monthly, and seasonal). The statistical test by Mann- Kendall test reveals that this increasing trend has statistical significance (except in the month of June) at 95% confidence level. The investigation on the long-term trend of minimum temperature at Kunnamangalam station shows a decreasing trend in southwest monsoon, in the months of February, March, and November with 95% of statistical significance. . The investigation on the long-term trend of average temperature at Kunnamangalam station shows an increasing trend in summer, February, March, and November with 95% of statistical significance.

In summary, the temperature in Kozhikode District shows major changes in Kozhikode

station and Kunnamangalam station. The maximum temperature at Kozhikode and kunnamangalam stations show an increasing trend. The minimum and average temperatures at Kozhikode station shows also an increasing trend. In karipur station there no trend is detected for the temperature parameters. Which may be due to the insufficient temperature data at the station. Trend analysis needs long- term data for the investigation of climate change. So in the Kozhikode and Kunnamangalam stations, there is an increasing temperature in every year. It will affect the whole environment. Hence, an early implementation of mitigation measures to reduce the adverse impact of temperature change.

REFERENCES

1. K. Venkata Sai and Asha Joseph. Trend Analysis of Rainfall of Pattambi Region, Kerala, India. International Journal of Current Microbiology and Applied Sciences. SSN: 2319-7706 Volume 7 Number 09 (2018)
2. B.U. Choudhury et al. Trend Analysis of Long-Term Weather Variables in Mid Altitude Meghalaya, North-East India. Journal of Agricultural Physics. ISSN 0973-032X Vol. 12, No. 1, pp. 12-22 (2012)
3. Zeineddine Nouaceur1 and Ovidiu Mursrescu. Rainfall Variability and Trend Analysis of Annual Rainfall in North Africa. International Journal of Atmospheric Sciences. Volume 2016K. Elissa, "Title of paper if known," unpublished.
4. Abel Girma et al. Study on Recent Trends of Climate Variability Using Innovative Trend Analysis: The Case of the upper Huai River Basin. Pol. J. Environ. Stud. Vol. 29, No. 3 (2020), 2199-2210
5. Kalidoss Radhakrishnan et al. A Climate Trend Analysis of Temperature and Rainfall in India. Climate Change and Environmental Sustainability (October 2017) 5(2): 146-153.
6. Keredin Temam Siraj et al. National Monthly Refereed Journal of Research in Science & Technology. Volume no.2, Issue NO.7 ISSN 2277-1174
7. Benjamin Nnamdi Ekwueme and Jonah Chukwuemeka Agunwamba. Trend Analysis and Variability of Air Temperature and Rainfall in Regional River Basins. Civil Engineering Journal. E-ISSN: 2476- 3055; ISSN: 2676-6957 Vol. 7, No. 05, May, 2021
8. Akinsanola A. A & Ogunjobi K. Analysis of Rainfall and Temperature Variability Over Nigeria. Global Journal of Human-Social Science (2018)
9. Ihimekpen Ngozi Isioma et al. Non-parametric Mann-Kendall Test Statistics for Rainfall Trend Analysis in Some Selected States within the Coastal Region of Nigeria. Journal of Civil, Construction and Environmental Engineering 2018; 3(1): 17-28
10. E P Agbo et al. Trend Analysis of the Variations of Ambient Temperature Using Mann-Kendall Test and Sen's Estimate in Calabar, Southern Nigeria. Journal of Physics: Conference Series 1734 (2021) 012016

Feasibility Study Of Wastewater Treatment By Soil Aquifer System

Nimna Nasar
Dept.Civil Engineering
KMCT College of Engineering for Women
Kozhikode, Kerala, India
nimnanasar.clt@gmail.com

Harsha P
Dept. Civil Engineering
KMCT College of Engineering for Women
Kozhikode, Kerala, India
harshap@kmctcew.ac.in

Abstract— The treatment of wastewater is very important prior to disposal into various water bodies. But, the sustainability of the water treatment method is challenging for the environment. Soil Aquifer Treatment (SAT) is a controlled aquifer recharge system that further improves the quality of the feed water as it passes through the soil. This paper provides an overview of SAT systems for wastewater treatment and reuse. Wastewater samples are collected from the college canteen. Initially, canteen wastewater without pre-treatment was analyzed after that pre-treatment such as coagulation using neem leaves powder was carried out for canteen wastewater and then introduced into SAT system.

Keywords—wastewater treatment, SAT system, reuse of water, coagulant, environmentally friendly.

I. INTRODUCTION

The lack of clean water is a growing problem and natural water resources are inadequate to meet their needs, as cities become more and more populous and industrialized, and important to improve the environment. Wastewater treatment includes the conversion of wastewater into an effluent which is in disposable form or reusable form, that can be returned to the water cycle with minimal impact on the environment. The problem with current treatment technology is that they are not sustainable.

Wastewater treatment through land use is an alternative technology to purify the water. The land treatment method to be adopted is SAT, i.e., soil aquifer treatment. It is easy to operate, easy to maintain, and aesthetic in nature. SAT is an artificial groundwater recharge technology that is more suitable for augmenting water resources. It is a low-cost sustainable water and wastewater treatment technology. During SAT, the saturated and unsaturated zones of natural soil and groundwater act as a medium for physical, chemical, and biological processes to improve the quality of wastewater, improve the quality of wastewater through soil layers, and provide water of acceptable quality for reuse purposes. SAT is the only process used to recharge groundwater aquifers from outside or below the surface. In this way, wastewater infiltrates through soil and aquifers and is used to enter stormwater or pre-treated wastewater through recharge basins, which can significantly improve quality. Biodegradation occurs mainly within the top meter of the SAT system, by bacterial biofilms attached to the media, as well as through bacterivores and grazers that can be found in the pore water. Then the purified water is stored in the underlying unconfined aquifer for subsequent reuse, such as irrigation or drinking water, it can undertake considerable quality improvement. Processes and parameters that govern biodegradation efficiency include residence time, hydraulic loading rate, and microbial activity.

Experiments were carried out here to test the implications of the soil aquifer treatment system for the treatment of canteen wastewater at KMCT college and a study of the effectiveness of campus top soil to substantially enhance the biodegradation rates and removal efficiency of an operational SAT. The project was done in intermediate scale columns by comparing the campus soil from two sampling points where one soil is gravely laterite and one sample is clay laterite. The study carried out samples with and without absorbent.

II. OBJECTIVES OF THIS STUDY

- Treatment of canteen wastewater in a sustainable manner.
- Evaluate the biodegradation and filtration efficiency of the soil aquifer treatment system.

- Check the suitability of campus soil for SAT system
- Evaluate the coagulation process's effectiveness in improving the SAT system.

III. METHODOLOGY

A. Collection Of Soil Samples

This project was conducted to check the suitability of campus soil for a soil aquifer treatment system to treat canteen wastewater. A column study is adopted for this project, and soil was collected from two sampling points in KMCT college. One soil sample is collected near the canteen and the soil has a property like gravely laterite (station 1) and the second sample is collected some distance away from the canteen (back side of KMCT college of engineering for women) and the soil has clay laterite property (station 2). Before the collection of a soil sample from the stations, the field density of the sample is checked to maintain the same density in the columns where the experiments are conducted.

B. Preparation Of Column Study Setup

Column study setup is made with two PVC pipes having a length of 1.5m and a diameter of 4 inches. A filter cloth is used to cover the bottom of the pipe to eliminate the discharge of finer material along with effluent. Both pipes are filled with two soil samples up to 1m in height.

C. Working

Canteen wastewater is collected in the sterile can and water quality parameters before treatment were analysed and stored in a beaker connected with corresponding pipes. The valve of the storage beaker is opened in such a way that the ponding depth of water in the pipe is maintained at 30cm. The wastewater is infiltrated into two columns and effluent is collected from the bottom beaker, and effluent parameters are analysed.

Fig. 1. column study setup

D. Coagulant Preparation

Neem leaves were collected and washed with distilled water to remove dust and impurities and dried naturally under the sunlight for 5 days. The dried neem leaves were crushed and powdered using the home grinder and sieved. Finally, this powder is used as a natural coagulant in wastewater treatment.

Fig. 2. Neem leaves

IV. RESULT AND DISCUSSION

A. Phase 1

Treatment of canteen wastewater (without primary treatment) by column study setup. Soil property such as field density is maintained in two columns. The density soil sample used in phase 1 is given below.

Field density of clay laterite soil = 1.7 g/cc

Field density of laterite soil = 1.4 g/cc

TABLE I. WATER QUALITY PARA-METERS BEFORE AND AFTER TREATMENT

Samples	Parameters						
	Turbidity (NTU)	pH	DO (mg/l)	BOD (mg/l)	COD (mg/l)	Alkalinity (mg/l)	Acidity (mg/l)
Influent	178	5.56	4.8	190	259	204	415
Effluent (CLS)	115	6.89	5.6	123	188	127	260
Effluent (LS)	124	6.67	5.4	127	198	118	284

When comparing the clay laterite and laterite soil used in the SAT, better treatment efficiency is shown by clay laterite soil. The below graph represents treatment efficiency v/s water quality parameters in phase I.

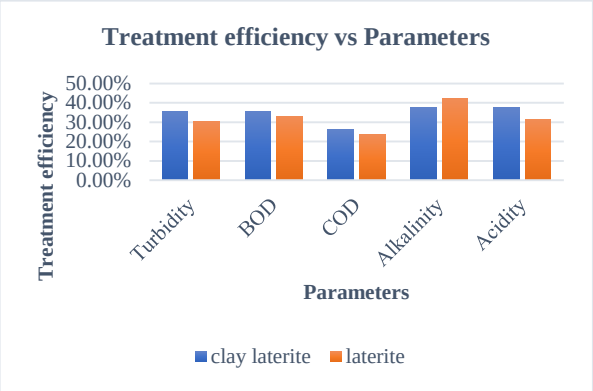

Fig. 3. Comparative study in phase 1

From the graph, it is clear that clay soil has slightly higher treatment efficiency than laterite soil. The greater difference is shown by turbidity and acidity. In the case of turbidity, the treatment efficiency for laterite soil is 30.3% and for clay laterite soil, it is 35.3%. In the case of acidity around 6% higher treatment efficiency is shown by clay laterite soil. But, there is a slight difference in trend in the case of alkalinity. Alkalinity is more reduced through the laterite soil column than clay laterite soil.

B. Phase 2

To enhance the effluent water quality obtained in phase I analysis, the second phase of the project includes a preliminary treatment of canteen wastewater prior to the SAT. Preliminary treatment such as coagulation is conducted for canteen wastewater by a natural coagulant such as neem leaves powder (Azadirachta indica) to settle down suspended particles. Primarily treated water is allowed to flow through the SAT setup with new soil samples.

Field density of clay laterite soil = 1.7 g/cc
Field density of laterite soil = 1.4 g/cc
Optimum coagulant dosage = 0.6 g/L

TABLE II. EFFLUENT WATER QUALITY PARAMETERS IN PHASE II

Samples	Parameters						
	Turbidity (NTU)	pH	DO (mg/l)	BOD (mg/l)	COD (mg/l)	Alkalinity (mg/l)	Acidity (mg/l)
Influent	184	5.46	4.6	190	281	200	422
New influent	112	5.41	4.8	128	199	130	310
Effluent (CLS)	76	6.85	5.7	87	143	88	209
Effluent (LS)	81	6.77	5.3	91	161	86	220

The below graph represents treatment efficiency v/s water quality parameters in phase II.

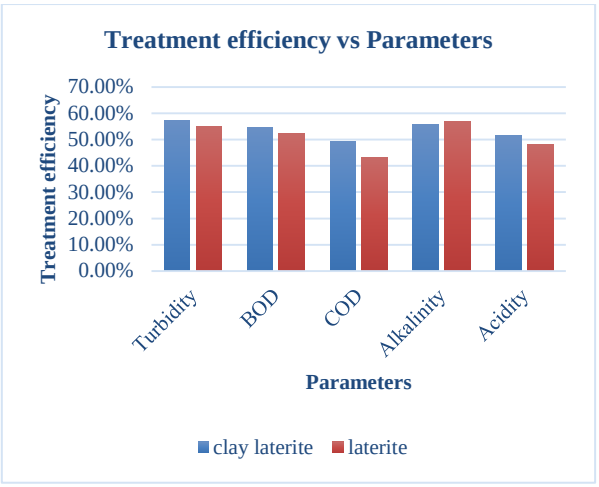

Fig. 4. Comparative study in phase 2

From the graph, it is clear that clay soil has slightly higher treatment efficiency than laterite soil. Water flow through laterite soil is higher than the clay laterite soil, maybe this is the one reason that clay soil shows better treatment efficiency than pure laterite soil. The detention time of wastewater in the pore space of the clay matrix enhances several filtration mechanisms.

V. CONCLUSIONS

In this paper, we analyze the effectiveness of campus soil for canteen wastewater treatment through SAT system. From the above results, we can conclude that both soil samples were effective for wastewater treatment. But, clay laterite soil shows slightly better treatment efficiency than laterite soil. Water discharge from the laterite soil column is higher than compared to the clay laterite soil column. The detention time of wastewater in clay laterite column is higher hence several filtration mechanisms such as straining, sedimentation, impaction, interception, adhesion, and adsorption effectively occur in the pore space of the clay matrix. When comparing phase 1 and phase 2, the treatment efficiency is highly improved through the primary treatment of canteen wastewater. Neem leaves as a natural coagulant improvise the water quality parameters in phase 2. Treatment efficiency in phase 1 is around 30-35 % which is improved in to 50-55% in phase 2. Hence it is clear that the primary treatment of canteen wastewater prior to SAT system by using a natural coagulant (neem leaves) is highly effective for canteen wastewater treatment.

References

1. K.H Rekha and D.P Nagarajapa, "Toxic wastewater treatability study by SAT with adsorbent", Environmental development and studies, Springer, June 2020, (22)1.
2. Saroj K. Sharma and Maria D. Kannedy, "Soil aquifer treatment for wastewater treatment and reuse", ScienceDirect, International biodetoriation and degradation, vol: 19, April 2017.
3. Aniket V. Patil1, Tejaswini S. Mankar,and Shilpa S. Motegaonkar, "Wastewater Renovation using Soil Aquifer Treatment (SAT) System :Case Study of Latur District (Marathwada)", International Research Journal of Engineering and Technology (IRJET) e-ISSN: 2395 -0056 Vol: 04, Issue: 04, Apr -2017.
4. Joshua Brooks, Noam Weisbrod, and Edo Bar-Zeev, "Revisiting Soil Aquifer Treatment: Improving Biodegradation and Filtration Efficiency Using a Highly Porous Material", Water 2020, 12, 3593; doi: 10.3390/w12123593.
5. Wendesen Mekonin and DestaMillion Ebba Bote, "Wastewater treatment using a natural coagulant (Moringa oleifera seeds): optimization through response surface methodology", ScienceDirect, Heliuon 7, 2021.
6. S. Gautam and G. Saini, "Use of natural coagulants for industrial wastewater treatment", Global Journal of Environmental Science and Management, 6(4)-2020, 553-557.
7. S. Mohan, K.Vidhya, C.T. Sivakumar, M.Sugnathi1, V. Shanmugavadivu1and M.Devi, "Textile Waste Water Treatment by Using Natural Coagulant (Neem-Azadirachta India)", international research journal of multidisciplinary technovation (irjmt), 2019, 1(6), 636-642.
8. Jyoti Rana, Gyanendra Goindi and, Navneet Kaur, "Neem Leaves as Adsorbent for Dye Waste water Treatment", International Journal of Innovative Technology and Exploring Engineering (IJITEE) ISSN: 2278-3075, Volume-8 Issue-9, July 2019.
9. Sankeeth.K.V and Asha Rani.N.R, "Use of Neem Leaf Powder as Natural Coagulant to Treat Industrial Wastewater", IJIRT, Volume 8 Issue 1, june 2021, ISSN: 2349-6002.
10. Saravanan, Priyadharshini, Soundammal, Sudha and Suriyakala, "Wastewater Treatment using Natural Coagulants", SSRG International Journal of Civil Engineering (SSRG - IJCE) – Volume 4 Issue 3 – March 2017.
11. Muruganandam, M P Saravana Kumar, Amarjit Jena, Sudiv Gulla and Bhagesh Godhwani, "Treatment of waste water by coagulation and flocculation using biomaterials", IOP Conf. Series: Materials Science and Engineerin1g 23246536 (72809107) 032006.
12. Erick Butler, Yung-Tse Hung , Ruth Yu-Li Yeh and Mohammed Suleiman Al Ahmad, "Electrocoagulation in Wastewater Treatment", Water 2011, 3, 495-525; doi:10.3390/w3020495.
13. Alsumayya Latheef, Sahad M Saheed, Aneesha K Basheer, Amjed P. S1, Jobin Johnson, " water treatment using natural coagulants", International Research Journal of Engineering and Technology (IRJET) e-ISSN: 2395-0056, vol-6,issue-6,june 19.
14. Krishnapriya G Nair1, Mingul Pertin1, Prince Philip Kadavil1, Jency Nadayil, "Emerging trends in the usage of bio-coagulants in waste Water treatment", International Research Journal of Engineering and Technology (IRJET) e-ISSN: 2395-0056, vol-6, issue-4, April2019.
15. Saravanan J, Priyadharshini, Soundammal, Sudha G, Suriyakala, "Wastewater Treatment using Natural Coagulants", SSRG International Journal of Civil Engineering (SSRG-IJCE) – volume 4 Issue 3 – March 2017.

Feasibility Study on Wastewater Treatment and Production of Livestock Feed by Azolla Pinnata

Sreelekha T S
Student
Dept.Civil Engineering
KMCT College of Engineering for Women
Kozhikode, Kerala,
India sreeluts@gmail.com

Harsha P
Assistant Professor
Dept. Civil Engineering
KMCT College of Engineering for Women
Kozhikode, Kerala, India
harshap@kmctcew.ac.in

Abstract— Pollution of water is a major threat we face today. Increased population and industrialization are the common factors that fasten the water pollution rate. Here pollution due to Canteen wastewater is taken into account and a solution to it by a modern cheapest method known as phytoremediation is studied here. Here Azolla pinnata plant is used to find the feasibility of phytoremediation over canteen wastewater. Also the production of livestock feed by azolla pinnata at the end of treatment. Parameters like pH, Turbidity, COD, DO and BOD was analyzed before and after treatment.

Keywords—Phytoremediation, Wastewater treatment, Azolla Pinnata, Canteen wastewater, Dairy wastewater

I. INTRODUCTION

One of the major problems India faces is water pollution. The major reason for it is urbanization. Water pollution is one of the biggest issues India facing right now. The waste generated from the dairy industry and canteen kitchen is potential pollutant. Dairy industries are well established in India.

Phytoremediation is used to better the water quality. Here Assessing the effectiveness of Azolla (plant) in treating Canteen wastewater. Azolla is used for livestock feed and as bio-fertilizer for agricultural purposes.

II. OBJECTIVES OF THIS STUDY

- To check the feasibility of phyto-remediation technique to treat canteen wastewater
- To check the potential of the Azolla pinnata plant for phytoremediation.
- Testing of parameters like pH, Turbidity, DO, BOD, and COD in effluents and treated water.
- To identify the optimum conditions for better performance of Azolla pinnata in the treatment of wastewater.

III. METHODOLOGY

A. MATERIALS USED

1. Rectangular glass trough
2. Azolla pinnata
3. Sucker
4. PVC net
5. Circular trough used for culturing
6. Sterilized cans for collecting wastewater
7. Wastewater used for treatment
8. Buckets

B. EXPERIMENTAL LAYOUT

The experiment was conducted for wastewater obtained from dairy and canteen wastewater and Azolla pinnata was the plant used for the experimental study. Azolla pinnata species were collected from an aquarium shop in Kozhikode. 20 g of Azolla was collected in a plastic bag as shown in Fig. 1.

Fig. 1. Azolla

Azolla is cultured in a trough by mixing cow dung and phosphorous lightly with water. The arrangement is kept under light shade for 7 days and the growth of Azolla has increased.

C. COLLECTION OF SAMPLES

Canteen wastewater is collected from the college canteen of KMCT Engineering College, Kozhikode. Dairy wastewater from Dairy wastewater treatment plant, Kozhikode.

IV. RESULTS AND DISCUSSION

A. PHYTOREMEDIATION POTENTIAL IN THE TREATMENT OF WASTEWATER

1. Effect of contact time

The wastewater is treated for different contact times such as 2,4,6 days. Similarly, a blank is set up to study the effect of time on the degradation of contaminants.

2. Effect of dilution

Collected samples are treated with different dilutions such as 25%, 50%, and 75%.

B. CANTEEN WASTE WATER

1) Effect of contact time on sample with azolla

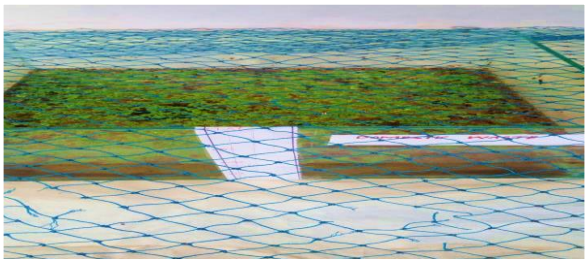

Fig. 2. Initial stage of filling azolla in the trough

Fig. 3. Growth of azolla in sixth day

30g of azolla was filled in the trough as shown in Fig. 2. When weight of azolla was taken on sixth day it has become 64g as shown in Fig. 3. This can be utilized as livestock feed and as bio-fertilizer for agricultural purposes. Similarly a blank is also set up for contact time of six days. The effect of variation of parameters for phytoremediation system and that of blank is shown in Table1 & Table 2 respectively.

TABLE 1 EFFECT OF VARIATION OF PARAMETERS FOR PHOTO REMEDIATION SYSTEM

Parameters	Before treatment	Days			
		2	4	6	7
pH	6.5	6.6	6.8	6.83	6.98
Turbidity (NTU)	83	61	18.3	11	9
DO (mg/l)	3.6	3.4	3.1	2.8	2.6
BOD (mg/l)	178	146	95	58	51
COD (mg/l)	784	638	522	439	386

TABLE 2 EFFECT OF VARIATION OF PARAMETERS FOR BLANK

Parameters	Before treatment	Days			
		2	4	6	7
	6.5	6.63	7.2	7.4	7.3
pH	83	52	12	4.1	4.6
Turbidity(NTU)	3.6	4.1	4.6	5.5	4.8
DO(mg/l)	178	87	58	32	39
BOD(mg/l)	784	593	313	198	223
COD(mg/l)	6.5	2	4	6	7

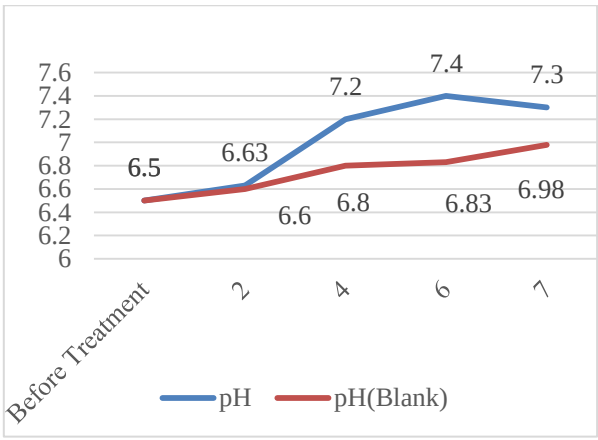

Fig. 4. Variation of pH

Fig 4 shows the variation of pH of phytoremediation system and that of blank. There is a fast increase in the pH for phytoremediation system than blank.

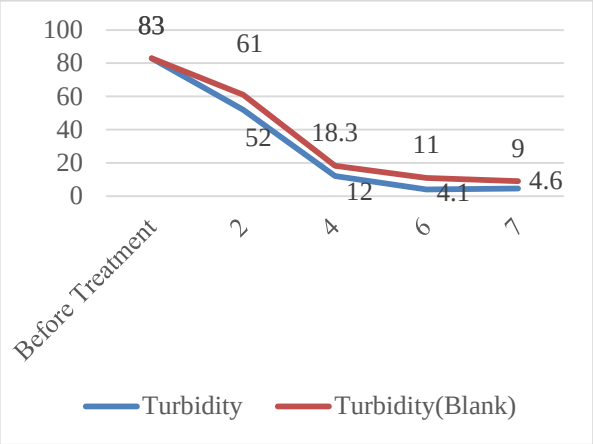

Fig. 5. Variation of Turbidity

In Fig. 5 there is a fast reduction in the turbidity value for phytoremediation system than blank.

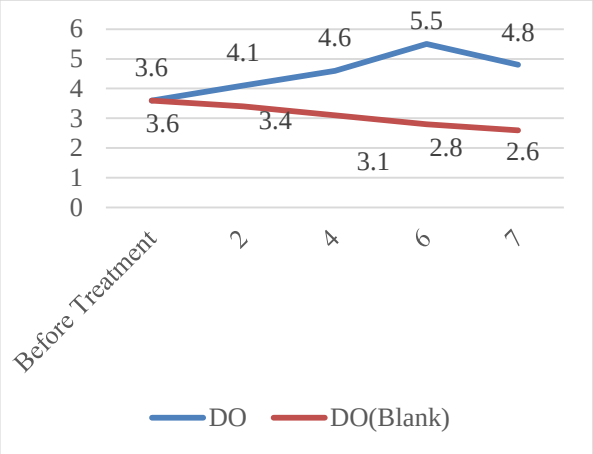

Fig. 6. Variation of DO

In Fig. 6 for phytoremediation system DO is increasing till 6th day contact time.DO is reduced for blank.

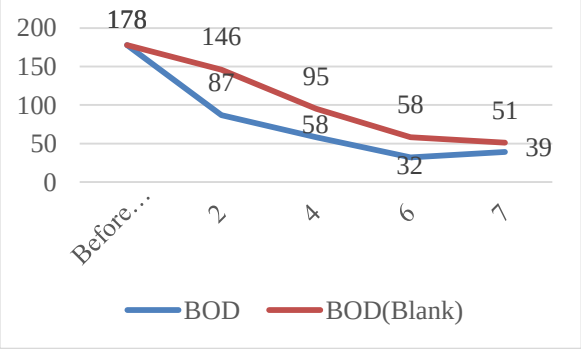

Fig. 7. Variation of BOD

Fig. 7 shows variation of BOD of phytoremediation system and blank. There is a fast reduction of BOD of phytoremediation system than blank.

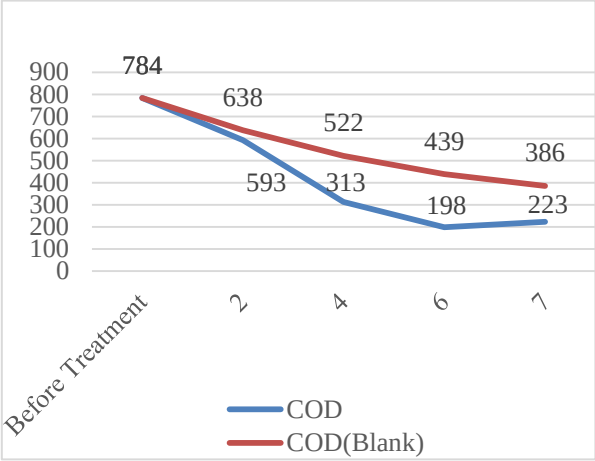

Fig. 8. Variation of COD

In Fig. 8 there is steep reduction of COD for phytoremediation system than blank.

2) Effect of Dilution

Different dilutions such as 25%, 50% & 75% are used. Canteen waste water is diluted with distilled water. Table 3 and 4 shows variation of parameters with different dilutions before treatment and after treatment respectively.

TABLE 3 VARIATION OF PARAMETERS WITH DIFFERENT DILUTIONS BEFORE TREATMENT

Dilution	25%	50%	75%
pH	6.4	6.2	6.1
Turbidity	49	54	68
DO	3.2	2.8	2.4
BOD	142	167	174
COD	484	632	756

TABLE 4 EFFECT OF VARIATION OF PARAMETERS AFTER TREATMENT

Dilution	25%	50%	75%
pH	7.2	6.9	6.6
Turbidity	2.4	2.8	3.2
DO	6.7	6.1	5.4
BOD	17	23	28
COD	56	124	187

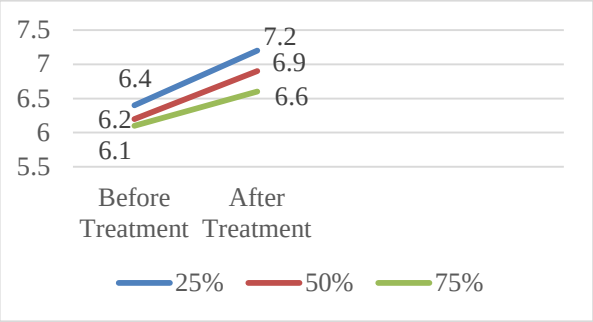

Fig. 9. Variation of pH with different dilution

In Fig. 9 pH value after treatment is more at 25% dilution than 50% and 75% dilutions.

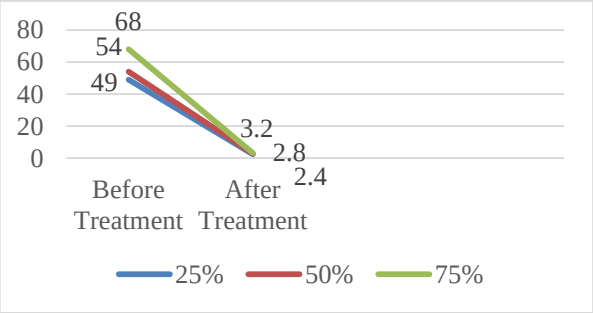

Fig. 10. Variation of Turbidity with different dilution

In Fig. 10, turbidity value has decreased more at 25% dilution than at 50% and 75% dilutions.

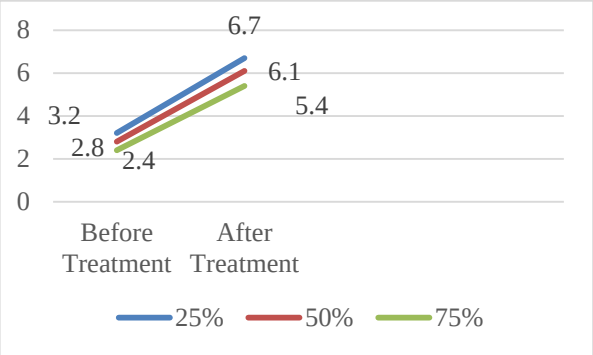

Fig. 11. Variation of DO with different dilution

In Fig. 11, DO value has increased more at 25% dilution than at 50% & 75%.

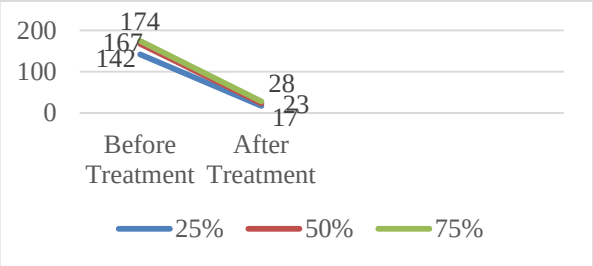

Fig. 12. Variation of BOD with different dilution

In Fig. 12, BOD value after treatment has decreased more at 25% dilution than at 50% & 75%.

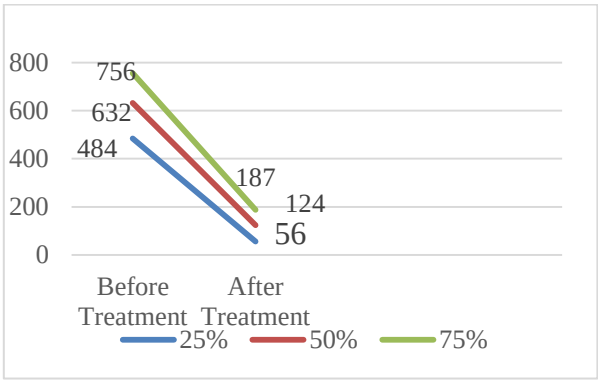

Fig. 13. Variation of COD with different dilution

In Fig. 13. there is a great reduction in the COD value at 25% dilution than at 50% & 75%.

V. CONCLUSIONS

In this paper, we analysed the feasibility of phytoremediation technique to treat canteen wastewater using aquatic pteridophyte Azolla pinnata and thus identifing the optimum conditions for better performance of Azolla pinnata in the treatment of wastewater. From the above results, we can conclude that treatment of canteen waste water using Azolla pinnata is more at 25% dilution at optimum contact time of 6 days. Thus we can say that optimum condition is at 25% dilution. Phytoremediation system is also tested against blank. It showed that there is a great reduction in the variation of parameters in phytoremediation system than blank. At the end of treatment, there is an abundant production of azolla pinnata, which can be used as livestock feed for high milk production and as bio-fertilizer. The effluent after phytoremediation can be used for irrigation and agricultural purposes. Large scale treatment using azolla pinnata requires large area but this treatment method is ecologically sound, economically viable, low capital cost and an attractive alternative to the current clean up methods. Hence this treatment method can be adopted.

REFERENCES

1. Golzary, A. Et.Al (2021),"wastewater treatment by azolla filiculoides (A study on color, odor, cod, nitrate and phosphate removal)",j.Pollution, 4(1): 69-76, winter

2018 DOI: 10.22059/poll.2017.236692.290J.
2. C. O. Akinbile et.Al (2020), "development and performance evaluation of low-cost wastewater treatment plan", journal on sustainable water resources management, https://doi.Org/10.1007/s40899-018-0295-8K. Elissa, "Title of paper if known," unpublished.
3. M Murali Krishna et.Al (2019), "wastewater treatment from the dairy farm by using azolla (azolla pinnata)", the pharma innovation journal 2022, ISSN (P): 2349-8242.
4. Pandey, C.V and Bajpai O (2019) Phytoremediation: From Theory Towards Practice, Phytoremediation of polluted sites, 1-49
5. Sudiarto, S.I.A., Renggaman, A and Choi, H.L (2019) Floating aquatic plants for total nitrogen and phosphorous removal from treated swine wastewater and their biomass characteristics, Journal of Environmental Management, 231, 763-769
6. Ting, W.H.T., Tan, I.A.W., Salleh, S.F and Wahab, N.A (2018) Application of water hyacinth (Eichhornia crassipes) for phytoremediation of ammoniacal nitrogen: A review, Journal of Water Process Engineering, 22, 239-249
7. Baldawi, A.I., Abdullah, S.R.S., Anuar, N and Hasan, A.H (2018) Phytotransformation of methylene blue from water using aquatic plant (Azolla pinnata), Environmental Technology and Innovation, 11, 15-22
8. Jeevanantham, S., Saravanan, A., Hemavathy, V.M., Kumar S.P., Yaashikaa, R.P and Yuvaraj(2018) Removal of toxic pollutants from water environment by phytoremediation: A survey on application and future prospects, Environmental Technology and Innovation, 13, 264-276
9. Zhou, W., Wang, Z., Xu, J. and Ma, L.(2018) Cultivation of microalgae Chlorella zofingiensis on municipal wastewater and biogas slurry towards bioenergy, Journal of Bioscience and Bioengineering, 15, 1-5
10. Lu B., Xu Z., Li J and Chai X (2018) Removal of water nutrients by different aquatic plant species: An alternative way to remediate polluted rural rivers, Ecological Engineering, 110, 18-26
11. Naghipour, D., Ashrafi, S.D., Gholamzadeh, M., Taghavi, K and Joubani, M.N. (2018) Phytoremediation of heavy metals (Ni, Cd, Pb) by Azolla filiculoides from aqueous solution, Data in Brief, 21, 1409-1414
12. Biswas, B., Singh, R., Krishna, B.B., Kumar, J. and Bhaskar, T. (2017) Pyrolysis of azolla, sargassum tenerrimum and water hyacinth for production of bio-oil, Bioresource Technology, 242, 139-145.
13. Neethu V.C., Prof. M.A. Chinnamma (2017) Phytoremediation Effect In Dairy Wastewater And Domestic Wastewater Using Constructed Wetlands Of Azolla Pinnata, IJRSET
14. Gomes, P.M., Brito, M.C.J., Carneiro, C.L.M.M., Cunha, R.R.M., Garcia, S.Q and Figueredo, C.C (2017) Responses of the nitrogen-fixing aquatic fern Azolla to water contaminated with ciprofloxacin: Impacts on biofertilization, Environmental Pollution, 232, 293-299

Comparison Of Garbage Enzyme Solutions In Treating Domestic Waste Water

Fathima Henan E
Department of civil engineering
KMCT College of engineering, Kallanthode, Calicut
fathimehenan685@gmail.com

Reena Abraham
Department of civil engineering
KMCT College of engineering, Kallanthode, Calicut
reenacr5@gmail.com

Abstract—Garbage enzyme solutions are prepared by fermentation of kitchen waste mainly vegetable and fruit peeled wastes by adding jaggery and water in to it. In this paper solutions made in three different compositions are taken one with only vegetable peels and one with only fruit peel and last one with a mix of vegetable and fruit peeled waste and add it in to domestic water which is collected from kitchen of own house in three different percentages and find the best enzyme solution and its optimum percentage and analyzing its various applications.

Keywords—Garbage enzyme solution, domestic waste wastewater quality parameters

I. INTRODUCTION

India is a developing country. The population in India is increases in day by day and due to this the waste generation also increases as same. The increase in waste creates more complex situations in waste disposal too. The main options that we take for waste disposal is landfills, which are open dumps, were trashes are disposed in sites without any further treatment. The wastes which are included in this are mainly of domestic wastes such as peels of vegetables and fruits which are less harmful for the environment but in some cases the leachate percolated from these wastes may contaminate the nearby surface or ground water streams. So one of the best solutions against this is treating those wastes in economical and efficient ways for example these wastes can be used to make garbage enzyme solutions which have a lot of applications.

The technology in wastewater treatment is improving day by day. Domestic wastewaters are the one which incorporates of waste waters from washrooms and kitchen sinks etc. Which are not at all destructive and can be disposed effectively. In case treated at first, they can be utilized in different purposes such as cultivation, vehicle washing etc. And it will be greatly helpful for the people who live in heavily populated cities such as Delhi, Kolkata etc. where the availability of water is time limited. The most objective in residential wastewater treatment is expulsion of supplements and organic natural pollutants.

II. LITERATURE REVIEW

Jyotiprakash G et.al (2022)In this journal a study was conducted by making four different enzyme solutions with orange,tomato,tamarind and lemon by mixing them with jaggery and water with a ratio of 1:3:10 and they kept it for three months for the production of enzyme solutions. It explained that the degradation of particles obtained due to microbial activity. The main findings showed that garbage enzyme was acidic in nature, with citric acid being a significant component. Citric acid, sugars, proteins, alcohol, and enzyme activity such as protease, amylase, lipase, and papain were found in biochemical analyses of garbage enzyme solution preparations. As a result, this investigative support the use of garbage enzyme solution as a multipurpose liquid.They analysed the degradation of agricultural waste with enzyme solution by observing the height of garbage heap. The other applications of garbage enzyme solutions are also discussed for example to deodorize air, floor cleaning, cleaning kitchen and toilet, fertilizer and pesticide. They analysed the cost of materials and discussed about its application in various sectors such as agricultural and domestic uses. The advantages and disadvantages also discussed together with explaining do's and don'ts while making garbage enzyme solutions.

B.L Pranav S Bhunje et.al (2019) in this journal it is explaining about the enhancing property of river water while adding garbage enzyme solutions to it.The major point of wastewater treatment is to realize most extreme productivity with steady enhancements in

utilizing the most reduced cost, time and region. In wastewater treatment framework, added substances may be included into so that particular pollutants may be degraded to the next degree inside a shorter time. Added substances within the wastewater treatment are those accessible as organic and chemical. Chemical added substances may be hurtful to the environment.. Here they selected a river nearby and made eco enzyme which can be said as a biological additive using fruit and vegetables peels, jaggery and water and after allowing fermentation for a period of three months they analysed the properties such as BOD, COD, DO of river water by adding enzyme solution in to it in various concentration and found out the optimum dosage and compared it with the results obtained before adding enzyme solutions. They concluded that the water treatment with eco enzyme is the treatment which require lesser experts and less cost. Ms Samiksha Sridhar Kerkar et.al (2018) this is a review journal which explains about applications of eco enzymes to the environment.

This journal detail explains about what is an enzyme and Eco enzyme also it says about the origin of eco enzyme its functions and how it is prepared. And they also discuss about the advantages and applications of eco enzymes in agricultural sector, livestock farming drainage system and for eco living. And they concludes that garbage enzyme may be an item made with the utilization of rough fabric, for case, natural product peeled and vegetable waste, jaggery or dull colour sugar and water and they have the diverse application in cultivation, domesticated creatures developing, household cleaning etc. In any case, sometime recently greatest capacity of garbage enzyme can be known. A few critical issues remain to be tended to. For case, depiction of Eco chemical, Evaluation of their impact on the soil, recognizable confirmation of methodologies for exchange of solid build-up cleared out after the filtration of test.

III. OBJECTIVES

- Preparation of eco enzymes from fruit peeled wastes and vegetable wastes separately and together
- To apply the arranged garbage enzymes to waste water collected kitchen of own house
- To analyse the optimum amount of garbage enzymes needed in treatment of domestic waste water
- To compare the enzyme solutions
- To analyse the use of treated water

IV. SCOPE OF THE STUDY

- All the parameters of the water can be studied to know the quality of waste water
- By understanding the values of water quality parameters it can be suggested does it fit for the mentioned purposes after treatment with enzyme solution or not
- To use the waste effectively
- To reduce load on sewage treatment plant
- To compare the enzyme solutions to know which is more economical and efficient

V. LIMITATIONS

- Fermentation is depending upon the activities of microorganisms
- Encompassing environment and its condition will affect e enzymatic activities of respective solutions
- Amount of fruit peeled or vegetable peeled waste may influence the behaviour of garbage enzyme solutions

VI. METHODOLOGY

1. Preparation of garbage enzyme solutions.

➢ **Materials needed**
- Fruit peeled wastes, vegetable peeled wastes, jaggery, fresh water, plastic containers, measuring cup

➢ Procedure of the preparation of garbage enzyme solution
- In a plastic container which is airtight, measure and add 1 part Jaggery and 3 parts vegetable or fruit peels and 10 parts water. Example: 400g Jaggery + 1200 g of veggie/fruit peel + 4000g of water. Here prepared six containers in which two container consist of 400g jaggery,1200g veg peeled waste and 4L water and another two containers with 400g jaggery, 1200g fruit peeled waste and 4L water and the remaining two containers having 400g jaggery,600g fruit peel waste and 600g veg peel waste and 4L water.

Fig. 1. Preparation of garbage enzyme solution

- Shake the mixture well, and screw the lid tightly. Fermentation takes a time period of 3 months. Label the container with date. After 3 months of fermentation the residue is filtered out to get a clear liquid

Fig. 2. Garbage enzyme containers

1. Testing of domestic waste water before adding garbage enzyme solution

- In this project the waste water is collected from kitchen of own house and analysed its drinking water quality parameters such as electrical conductivity, turbidity, pH, Total hardness, Total dissolved solids, DO, BOD & COD, found out in all samples as per procedures

2. Testing of domestic waste water after adding the enzyme solution

- Here consider 10%, 20% and 30% of trash chemical measurement with residential wastewater was chosen 9 measuring utensils

Those are filled with one litre residential waste water test and the particular dilutions of trash enzyme arrangement were included into these containers individually.

- These measuring utensils were secured and were cleared out for 5 days digestion period.
- The parameters such as electrical conductivity, turbidity, pH, Total hardness, Total dissolved solids, DO, BOD & COD, found out in all samples as per procedures

VII. RESULT AND DISCUSSIONS

Parameters before adding enzyme solution

TABLE I. WASTE WATER QUALITY PARAMETERS BEFORE ADDING ENZYME SOLUTION

PARAMETERS	VALUE	UNITS
pH	5.41	-
EC	900	µs/cm
Turbidity	70	NTU
Total hardness	75	mg/l
TDS	495	mg/l
DO	3.8	mg/l
BOD	198	mg/l
COD	413	mg/l

B. waste water parameters after adding fruit peel based enzyme solution in three different percentages

TABLE II. WASTE WATER QUALITY PARAMETERS AFTER ADDING FRUIT BASED ENZYME SOLUTION

PARAMETERS	10%	20%	30%
pH	5.68	6.86	5.49
EC	850	800	760
Turbidity	49.2	48	50
Total hardness	67	65.2	68
TDS	423	442	484
DO	4.6	4.8	4.4
BOD	25	20	28
COD	95	90	92

C. Waste water parameters after adding veg based enzyme solution in three different percentages

TABLE III. WASTE WATER QUALITY PARAMETERS AFTER ADDING MIXED ENZYME SOLUTION

PARAMETERS	10%	20%	30%
pH	6.0	5.9	5.1
EC	910.5	920.4	930
Turbidity	68.5	69	68
Total hardness	76	74	71
TDS	545	550	561
DO	4	4.2	4.4
BOD	35	42	40
COD	132	158	145

- pH:

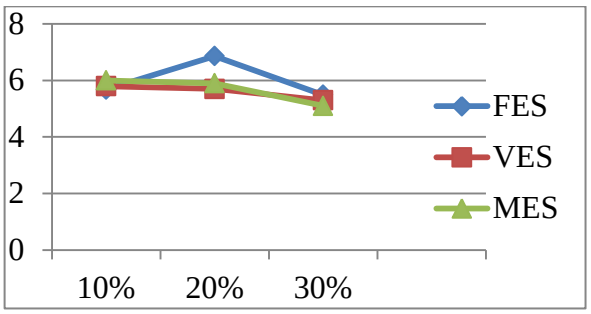

Fig. 3. Variations in Ph

The acceptable range of pH is 6.5-8.5.pH of the waste water sample added with fruit based enzyme is more on compared to another two enzymes in 20&30 percentages. pH of the kitchen waste water sample added with fruit based enzyme solution shows a pH value of 6.86 which is acceptable limit under drinking water and irrigation water quality standards.20% addition of fruit based enzyme solution is optimum in this case.

- Waste Electrical conductivity

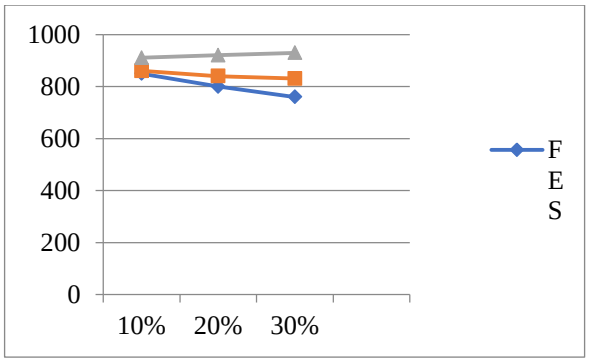

Fig. 4. Variations in electrical conductivity

Electrical conductivity of drinking water samples has no limits. But in case of water used for irrigation purposes it should be below 2000 µmole/cmFor all samples the electrical conductivity is within the acceptable limit.

- Turbidity

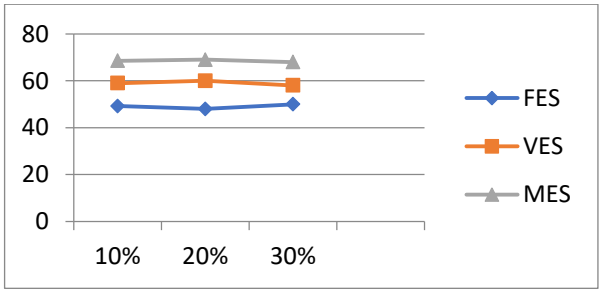

Fig. 5. Variations in turbidity

The limit of turbidity in drinking water is 5NTU.Turbidity is more in the case of waste water added with mixed enzyme solution followed by veg based one and then fruit based. Among three of these the waste water added with fruit based enzyme solution is less turbid.

- Total hardness

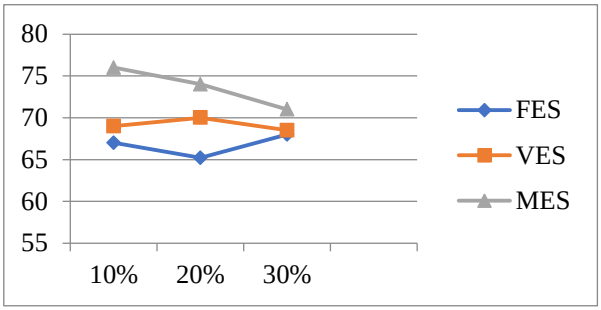

Fig. 6. Variations in total hardness

Limit of hardness in drinking water is 600mg/l.All samples are in acceptable ranges.

- Total dissolved solids

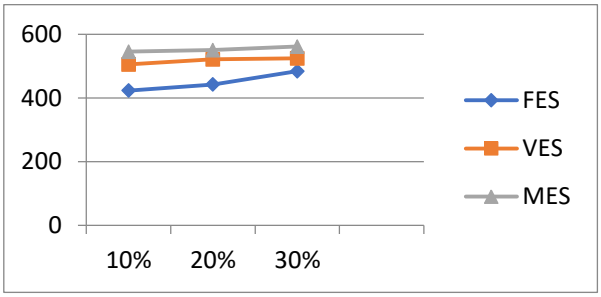

Fig. 7. Variations in total dissolved solid content

The limit of total dissolved solids in water used for irrigation purpose in less than 1300 mg/l .The enzyme solutions added in the kitchen waste water sample is within the limit for its total dissolved solid content when analyzing its use in irrigation as well as drinking purposes.

- DO

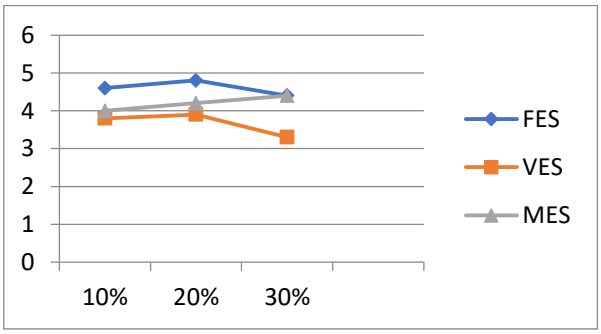

Fig. 8. Variation in DO

DO should be in range of 4-8 mg/l in drinking water and should lay in range below 100mg/l for irrigation purposes.DO content when waste water added with fruit based enzyme solution and mixed enzyme solution shows that it can be used for irrigation purposes.

- BOD

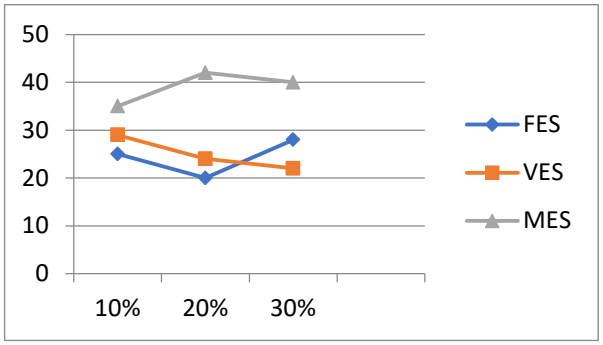

Fig. 9. Variation in BOD

The range of BOD for drinking water purpose is less than 2 mg/l and for irrigation purpose is less than 20 mg/l.Here the value of fruit based enzyme solution when added to waste water as 20% shows the BOD value within its acceptable limit for irrigational purposes.

- COD

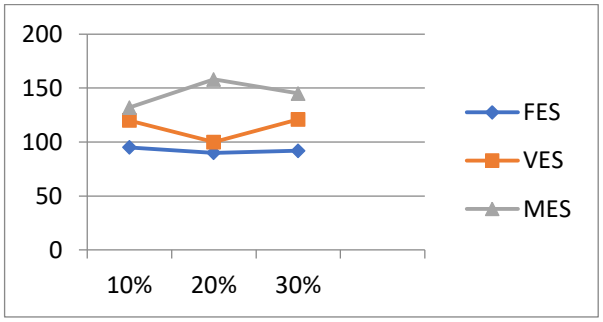

Fig.10. Variation in COD

The limit of COD in drinking as well as irrigation water was less than 100mg/l.In waste water added with fruit based enzyme solution in all percentages. in veg based enzyme solution added to waste water in 20% showed COD values are within the acceptable range.

VIII. CONCLUSIONS

The waste water collected from kitchen of own house gives an acceptable pH while adding 20% fruit based enzyme solution in it.In all samples electrical conductivity was in acceptable limit for irrigation purpose. Turbidity of all the waste water added with and without enzyme solution was not in the limit for drinking purpose. All the values for hardness were within the acceptable limit for drinking purpose.The all enzyme solution added waste water sample is within the limit for its total dissolved solid content when analyzing its use in irrigation purposes.The DO content became acceptable for drinking as well as irrigation purposes if the kitchen waste water is added of 20% fruit based enzyme solution.BOD of the kitchen waste water is in its acceptable range for irrigation purposes if it is added with 20% fruit based enzyme solution.COD of the kitchen waste water is in its acceptable range for irrigation purposes if it is added with 20% fruit based enzyme solution. The kitchen waste water added with 20% fruit based enzyme solution was founded as best to use for irrigation purposes.Eco enzyme is cheap and cost effective. Hence they can be utilized as a low cost alternative tool for the treatment of domestic waste water. It cost only 10rs/litre for the preparation of eco enzymes. The Eco enzyme can be used in decentralized treatment aid in domestic waste water treatment for treating effluent and also maintaining neutral pH range of effluent in sewer [10].

REFERENCES

1. Aishwarya Rani, Suraj Negi, Athar Hussain, Sunil Kumar (2019). "Treatment of Urban Municipal Landfill Leachate Utilizing GE". Journal of Bio-resource Technology. Volume 297, February 2020, 122437
2. Amee Patolia., Charvi Pandya and Archana Mankad(2021) "Production and utilization of bioenzyme using fruits and vegetables peels: a review"International Journal of Recent Scientific Research Vol. 12, Issue, 04 (A), pp. 41463-41465, April, 2021
3. Anshal Kumar1, Himanshu Kumar Sadhya2, Dr. Esar Ahmad3, Shashivendra Dulawat(2020) "Application of Bio-Enzyme in Wastewater (Greywater) Treatment" International Research Journal of Engineering and Technology (IRJET) e-ISSN: 2395-0056 Volume: 07 Issue: 05 | May 2020
4. Bharvi S. Patel , Bhanu R. Solanki and Archana U. Mankad(2021) "Effect of eco-enzymes prepared from selected organic waste on domestic waste water treatment" World Journal of Advanced Research and Reviews, 2021, 10(01), 323–333

5. Bhavani Penmatsa, D Chandra Sekhar, Bhagavathula S Diwakar, TV Nagalakshmi(2019) "Effect of Bio-Enzyme in the Treatment of Fresh Water Bodies" International Journal of Recent Technology and Engineering (IJRTE) ISSN: 2277-3878, Volume-8 Issue-1S3, June 2019
6. FaznaNazim , Dr. Meera.V(2017)" Comparison of Treatment of Greywater Using Garbage and Citrus Enzymes"International Journal of Innovative Research in Science, Engineering and Technology Volume 6, 4, March 2017
7. Harkeerat Singh, Aarti Prasad K V NAL (2019) "Study and analysis of bio-enzyme based natural product" International Journal of Engineering Applied Sciences and Technology, 2019 Vol. 4, Issue 8, ISSN No. 2455-2143, Pages 205-20
8. Hasanah, Y., Mawarni, L., Hanum, H. (2020). "Eco enzyme and its benefits for organic rice production and disinfectant" Journal of Saintech Transfer, 3(2), 119-128. doi:10.32734/jst.v3i2.4519
9. Janarthanan, M., Mani, K., & Raja, S. R. S. (2020, November). "Purification of Contaminated Water Using Eco Enzyme" In IOP Conference Series: Materials Science and Engineering (Vol. 955, No. 1, p. 012098)
10. Javalkar Sayali D, Shinde Shruti C , Savalkar Shweta S, Pawar Sudarshan E , Dhamdhere Akash , Patil Shrikant (2019) "Use of Eco Enzymes in Domestic Waste Water Treatment" International Journal of Innovative Science and Research Technology Volume 4, Issue 2, February – 2019
11. Jyotiprakash G. Nayak1, K. L. Bidkar1, Dinesh Yeole, Shubham Sonawane, Shubham Punde, Sachin Mhalaskar (2022) "Garbage Enzyme Solution – An Effective Alternative As A Surface Cleanser" International Research Journal of Engineering and Technology (IRJET) Volume: 09 Issue: 06 | June 2022
12. Kerkar, S. S., & Salvi, S. S. (2020). "Application of eco-enzyme for domestic waste water treatment" International Journal for Research in Engineering Application and Management, 5(11), 114-116. doi:10.35291/2454- 9150.2020.0075
13. Kumar A., Sandhya H., Ahmad E. and Dulawat S,(2020) Application of bio-enzyme in waste water(Greywater) treatment, International Research Journal of Engineering and Technology (IRJET.), 8(3), 2886-2890 (2020).
14. Li, T., Shen, P., Liu, W., Liu, C., Liang, R., Yan, N., & Chen, J. (2014). "Major polyphenolics in pineapple peels and their antioxidant interactions" International Journal of Food Properties, 17(8),
15. Mercy John P, Ranjana Singh* Dr. Ranjana Singh(2022) "Production of Enzyme Bio-cleaner from Fruit Waste by Yeast" International Journal of Creative Research Thoughts IJCRT © 2022 IJCRT | Volume 10, Issue 3 March 2022 | ISSN: 2320-2882
16. Muliarta, I. N., & Darmawan, I. K. (2021). "Processing Household Organic Waste into Eco-Enzyme as an Effort to Realize Zero Waste". Agriwar Journal, 1(1), 6-11. doi:10.22225/aj.1.1.3658.6-11
17. Nazim, F., & Meera, V. (2013). "Treatment of synthetic greywater using 5% and 10% garbage enzyme solution." International Journal of Industrial Engineering and Management Science, 3(4), 111-117. doi:10.9756/BIJIEMS.4733
18. Novianti, A., & Muliarta, I. N. (2021)." Eco-Enzym Based on Household Organic Waste as Multi-Purpose Liquid". Agriwar Journal
19. Nurlatifah, I., Agustine, D., & Puspasari, E. A. (2022, July). "Production and Characterization of Eco-Enzyme from Fruit peel waste" Biochem Technol (2022) 13(3): 32
20. Olgalizia Galintin , Nazaitulshila Rasit , Sofiah Hamzah (2021) " Production and Characterization of Eco Enzyme Produced from Fruit and Vegetable Wastes and its Influence on the Aquaculture Sludge" bio interface research in applied chemistry Volume 11, Issue 3, 2021, 10205 – 10214
21. Parul Lakra1 , Dr. Sunil Kumar Saini2 and Dr. Ankita Saini (2022) "Synthesis, Physio-Chemical Analysis and Applications of Bio-Enzymes Based on Fruit and Vegetable Peels" 3 2022 JETIR September 2022, Volume 9, Issue 9 Journal of Emerging Technologies and Innovative Research (JETIR)
22. Pranav S. Bhunje , Deepak Ambulge , Pramod Bhutte , Akash Bokade , Amit

Ghorpade , Ankur Burade (2019) "Enhancing property of river water with eco-enzyme solution" JETIR April 2019, Volume 6, Issue 4

23. Samriti, Sajal Sarabhai, Arti Arya (2019) "Garbage enzyme: A study on compositional analysis of kitchen waste ferments" The Journal of Pharma Innovation. 8(4), 1193-1197.
24. Samiksha Shridhar Kerkar, P (2018) "Application of Eco-Enzyme to the Environment - A Review" International Journal for Research in Engineering Application & Management (IJREAM) ISSN : 2454-9150 Vol-04, Issue-02, May 2018
25. Srimathi.N, Subiksha.M, Abarna.J, Niranjana.T (2020) "Biological Treatment of Dairy Wastewater using Bio Enzyme from Citrus Fruit Peels" International Journal of Recent Technology and Engineering (IJRTE) ISSN: 2277-3878 (Online), Volume-9 Issue-1, May 2020
26. Swarndeep Kaur Sethi1, Kiran Soni2, Neha Dhingra3, Gita Batra Narula(2021) "Bringing Lab to Our Home: Bio-Enzyme and its Multiutility in Everyday Life" International Research Journal of Engineering and Technology (IRJET) e-ISSN: 2395-0056 Volume: 08 Issue: 03 | Mar 2021
27. Syakdani, A., Zaman, M., Sari, F. F., Nasyta, N. P., & Amalia, R. (2021). "Production of Disinfectant by Utilizing Eco-enzyme from Fruit Peels Waste". International Journal of Research in Vocational Studies (IJRVOCAS), 1(3), 01-07. doi:10.53893/ijrvocas.v1i3.53
28. Tang, F. E., & Tong, C. W. (2011)" A study of the garbage enzyme's effects in domestic wastewater" International Journal of Environmental and Ecological Engineering, 5(12), 887-892. doi:10.5281/zenodo.133298
29. T Fazna Nazim and V. Meera(2013) "treatment of Synthetic Greywater Using 5% and 10% Garbage Enzyme Solution" International Journal of Industrial Engineering and Management Science Vol. 3, No. 4, December 2013
30. Vishakha V. Pawar1 , Vaishnavi G Kulkarni2 , Prerana N. Chavan3 , Gayatri E. Kanse4 , Mayuri B.Bhadange5(2022) "Citrus Bio-enzyme production and Application for waste water treatment" Vol-8 Issue-3 IJARIIE-ISSN(O)-2395-4396 16737

Spatial Water Quality Characteristics Of Kallayi River Basin In Gis Platform

Nadeeda
Dept. Civil Engineering
KMCT College of Engineering for Women
Kozhikode, Kerala, India
nadeedarasheed@gmail.com

Binisha P
Dept. Civil Engineering
KMCT College of Engineering for Women
Kozhikode, Kerala, India
binishap@kmctcew.ac.in

Abstract— Kallayi River is a small river situated in the Kozhikode district of Kerala.it is well known for its timber business. This river is being polluted by these timber businesses and other human activities. This paper deals with the water quality analysis of river Kallayi in post-monsoon and premonsoon seasons and assesses the water quality index using the CCME method and GIS mapping. The parameters analyzed are pH, turbidity, chloride, DO, BOD, COD, E coli, total coliform

Keywords—— Kallayi River, pH, turbidity, chloride, DO, BOD, COD, E coli, total coliform, GIS mapping, water quality index, CCME method.

I. INTRODUCTION

Kallayi is one of the rivers in Kerala, India which is known for its timber businesses. It is 22 kilometers (13.7 mi) long and it originates from Cherikkulathur in the Western Ghats, at an elevation of 45 meters (148 ft). It is linked to the Chaliyar River by a man-made canal (canoli canal) on the south side of the small timber village of Kallayi lying on its banks. Because of the rapid industrialization and discharge of sewage and other effluents into the river have made more changes in many of its water quality parameters .now a day's people living in and around that region don't take water from it for any of their purposes.

Fig.1 Kallayi River

II. OBJECTIVES OF THIS STUDY

- To assess the surface water and groundwater quality of River Kallayi at three different stations
- To analyze the water quality at two different seasons (post-monsoon and premonsoon) using the WQI method and GIS mapping.
- To check whether the water quality is within the standards, and hence suitable or not for domestic and other purposes.

III. SCOPE OF THIS STUDY

- It provides an overview of surface and groundwater quality. Hence it helps in identifying whether the quality of water is low or high.
- To access the impact on the water quality of the various activities performed by human beings.
- To obtain definitive and useful data on water quality as a whole and to adopt corrective measures to ensure a safe supply of drinking water.

IV. METHODOLOGY

A. Sample Collection

- The water samples are to be collected from the different groundwater sources and surface water sources of the kallayi river basin
- Surface water from Mampuzha bridge(S1), Pantheeramkavu(S2), Kunnath bridge(S3), Mankave bridge(S4), Mooriyad(S5), Kallayi bridge (S6) and Kothi bridge(S7)
- The ground water are from Nallalam(G1), Meenchandha(G2), Payyanakkal(G3), Kuttichira (G4), Palayam(G5) and Mankave (G6), Puthoor (G7).

B. Tests Performed

- The water was tested for pH, turbidity, chloride, DO, BOD, COD, E coli, total coliform.

TABLE I. DESIRABLE LIMITS OF THE PARAMETERS TO BE TESTED

parameters	Desirable limits
pH	6.5-8
turbidity	1NTU
electrical conductivity	No limit
chloride	250mg/l
hardness	200mg/l
DO	6mg/l
BOD	5mg/l
COD	4mg/l
E coli	Zero
total coliform	Zero

C. Water Quality Index

- After finding out the value for each parameter the water quality index is found by the CCME method

TABLE II. WATER QUALITY INDEX

CCME-WQI Value	Water quality
95-100	Excellent
80-94	Good
60-79	Fair
45-59	Marginal
0-44	Poor

D. GIS Mapping

- GIS mapping is done using Arc GIS
- IDW interpolation is used as we donot have all the points of the basin, to get a map we use this method.

V. RESULT AND DISCUSSION

A. Test Results

- The test results of water samples collected from different stations of the kallayi river basin post monsoon are shown in Table 3

TABLE III. TEST RESULTS DURING POST MONSOON SEASON

station	pH	turbidity	chloride	DO	BOD	COD	E coli	total coliform
S1	7.1	2	40.1	5.2	1.2	2.5	4500	1700
S2	6.5	2	57.2	5.8	.12	3.3	7000	5500
S3	6.7	2	42.9	5.7	11	2.2	10000	8000
S4	7.3	2	53.7	9.8	7.6	7.3	11000	10000
S5	7.1	4	1920	8.2	.2	2.8	51000	12000
S6	7.7	3	3400	2.9	2.4	9.8	90000	60000
S7	7.3	4	5400	8.2	.1	3.2	4300	1200
G1	6.8	2	22.3	2.3	1.1	2	3	0
G2	7.2	1	45.2	1.4	.2	4.2	5	1
G3	7.2	1	45.2	1.4	.2	1.1	4	0
G4	6.6	1	12.8	1.5	.5	7	9	0
G5	7.7	1	43.5	2.4	.3	3.5	6	0
G6	7.3	3	23.9	7.6	9.8	7.2	8	0

- The lower pH is in surface water which is 6.3 and the high pH is 7.7. all the value of pH is within the limit.
- The maximum permissible limit of turbidity is 5NTU all are within the maximum permissible limit but may exceed the desirable limit which is 1NTU.
- The maximum value obtained for chloride is 5400 mg/l which exceeds the limit, the minimum value obtained is 22.3mg/l which is within the limit the desirable limit of chloride is 250mg/l.all the groundwater sources show that the chloride is within the desirable limit.
- Every source i.e, the surface water and groundwater has the presence of total coliform
- Ecoli is present in all samples of the surface water and one groundwater sample.

TABLE IV. TEST RESULTS DURING PRE-MONSOON SEASONS

station	pH	turbidity	chloride	DO	BOD	COD	E coli	total coliform
S1	6.77	1	50.13	4.3	2.1	3	1700	4600
S2	7	2	57.25	5.1	1.5	3.5	5500	7200
S3	6.9	2	62.98	5.6	0.25	3.4	8000	10500
S4	6.5	2	43.7	5.7	11.15	7.5	10000	11000
S5	7.1	3	2500	5.2	7.68	3.2	12000	52000
S6	7.2	4	14700	6.6	5.9	10	60000	90000
S7	7.23	4	14691	8	6	5.2	59000	95000
G1	7.38	1	12.99	2	2	1.5	0	56
G2	7.2	1	45.23	2.3	1.9	1	0	20
G3	7.6	1	20.12	1.43	1.7	0.2	0	45
G4	7	1	52.16	1.57	2	0.11	0	11
G5	7.5	2	25	2.4	1.9	0	25	22

- The pH is within the limit the lower pH IS 6.77 and the higher value is 7.6.
- The turbidity of the water is within the limit no sample exceeded its limit.
- The downstream of the river has a higher chloride content .the ground water sources shows a lower chloride content and those are within the limits.
- The number of E coli and total coliform has increased in the surface water comparing to the post monsoon season.

B. Water Quality Index

TABLE V. WATER QUALITY INDEX

Sl.NO	STATIONS	WQI POST MONSOON	WQI PREMONSOON
1	S1	38.12	38.11
2	S2	34.36	34.055
3	S3	33.94	33.93
4	S4	33.91	33.906
5	S5	24.34	18.95
6	S6	24.3	18.875
7	S7	24.941	12.846
8	G1	74.401	74.82
9	G2	89.247	82.6336
10	G3	100	82.95
11	G4	83.62	91.81
12	G5	89.02	79.455
13	G6	83.42	83.44

- The surface water of Kallayi river has a poor water quality in premonsoon and post monsoon it shows that the surface water of the river is not fit for domestic purpose
- The groundwater quality of Kallayi river basin which is away from the river shows a fair, good and excellent quality.
- The ground water near to the river shows a poor quality in both the post monsoon and premonsoon seasons.
- The water quality index of the of the Kallayi river shows that the river and the ground water very near to the river is polluted and not fit for domestic purpose and the ground water away from the river does not have a much effect of the pollution of the river.

C. GIS Mapping

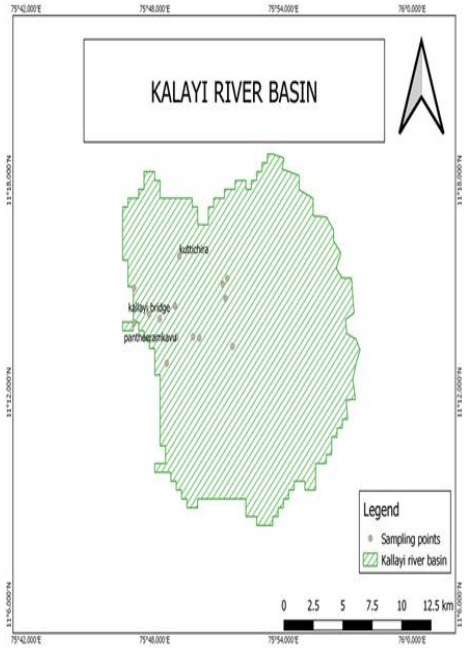

Fig. 2. Kallayi river basin map

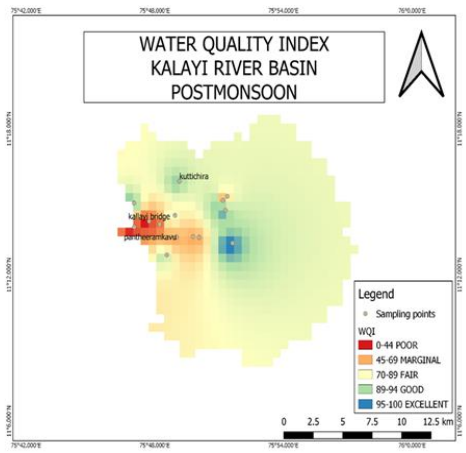

Fig. 3. Water quality index map post monsoon

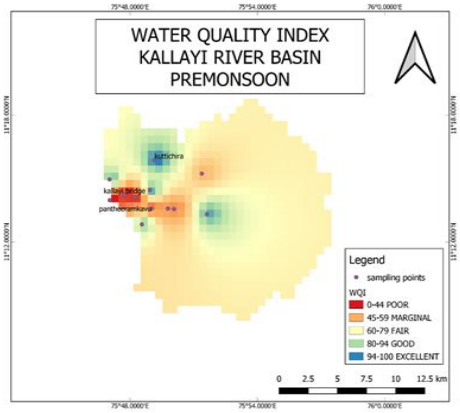

Fig.4. Water quality index map premonsoon

- The above map shows the variation of water quality index in kallayi river basin in postmonsoon and premonsoon.

VI. CONCLUSIONS

In this paper, we have studied about the Kallayi river basin, it shows that the river is highly polluted .the number of E coli and total coliforms are very high it shows that the water is highly polluted. The main reason of the pollution are the wastes dumped into the river, the timber business, dumping of septic wastes, the polluted canals, ponds linking to the river all these are the causes of the pollution of the river.in all the seasons the surface water of the river has a poor water quality index .in postmonsoon there is a small variation of water quality index comparing to premonsoon but still the water quality is poor.

Remedies to reduce the level of pollution:

- Proper collection and management system for different types of waste generated.
- No septic wastes to be dumped into the river.
- Proper disposal of septic wastes.
- Cleaning and maintaining canals and other water resources linking to the river
- Proper guidelines and awareness should be given to those who are using river for timber business.
- We can use some plants which can be used for removing bacterias and pollutants (phytoremediation).

References

1. Navamuniyammal M, Vidhya , Sivakumar ,M Saravanan K," Surface Water Quality Analysis in Thamirabarani River Using Remote Sensing And GIS " ,SSRG International Journal of Geo-informatics and Geological Science Volume 8 Issue 1, 2021
2. Subha Lekshmi , Athira Somarajan, Merlin Daniel, Vishak Sasidhar "Water Quality Analysis of River PAMBA using WQI Method and GIS Mapping ", International Journal of Engineering Research & Technology (IJERT) IERTV9IS060349 2020
3. Anoop Kumar Shukla, C. S. P. Ojha and R. D. Garg "SURFACE WATER QUALITY ASSESSMENT OF GANGA RIVER BASIN, INDIA USING INDEX MAPPING",Researchgate 2017
4. Mity Thambi, Tom Cherian, Anju Therese Jose, Sunaina Jamal "PHYSICO-CHEMICAL CHARACTERISTICS OF GROUND WATER SAMPLES FROM DIFFERENT AREAS OF THRISSUR DISTRICT, KERALA STATE, INDIA", INTERNATIONAL JOURNAL OF ENVIRONMENT Volume-4, Issue-2, March-May 2015
5. Anirudh Ramaraju1 and Giridhar M.V.S.S. " Spatial Analysis of Surface Water Bodies Quality using GIS ",HYDRO 2015 INTERNATIONAL IIT Roorkee, India, 17-19 December, 201520th International Conference on Hydraulics,Water Resources and River Engineering
6. Ganpat B. More, Kailas P. Dandge and Sanjaykumar R. Thorat ," Spatial Distribution Analysis of Surface Water Quality Index Using Remote Sensing and GIS: A Case Study of Erandol (Maharashtra, India) ",International Journal of Advanced Remote Sensing and GIS, 2019

A Comparative Study of Vetiver Grass and Lemon using Phytoremediation Technique for Waste Water Treatment

Anjana Paramesh
Dept. of Civil Engineering
KMCT college of Engineering for women
Kozhikode, India
anjanaparamesh97@gmail.com

Reena Abraham
Dept. of Civil Engineering
KMCT college of Engineering for women
Kozhikode, India
reenacr5@gmail.com

Abstract — Increase in population led to scarcity of water. To avoid this situation there is a solution to solve this problem, using vetiver grass and lemon grass to treat waste water. In this method we are finding various parameters such as Ph., Turbidity, Conductivity, Alkalinity, DO, BOD, COD, T.T Coliform are analyzed to identify the changes & condition before and after treatment.

Keywords— Pyto-remediation, Waste water, Lemon grass, Vetiver grass.

I. INTRODUCTION

There are lots of environmental hazards as well as Health hazard are increasing day by day. One of the major problem happening in our country is scarcity of water. Due to the increase in population and their human activities fresh water deficiency is increasing. To overcome these situations, the most effective and cost effective method is using vetiver grass and lemon grass for the water treatment. This method is mainly focusing to find out the efficiency and quality of waste water.

Vetiver and Lemon grass are effective for various purpose, the oil from these plants are extracted and used for medicinal, Ayurveda, Food items, Pest reduction etc. These plants have lots of importance in our environment. To reduce the scarcity of water, these plants are using to treat the waste water and the treated water can be used for many purposes like agriculture etc.

II. MATERIALS USED

A. Waste water

The waste water is collected from Pond near Chathamangalam Panchayat. We are taking 30 Liters of waste water for treatment. Waste water from pond is collected.

B. Vetiver grass

Vetiver grass is collected from Silent valley gardens Kozhikode, Kerala. We are taking 4 vetiver grass for treatment.

C. Lemongrass

Lemon grass is collected by ordering through online website (India Mart). We are taking 4 Lemon grass for treatment.

D. Sand

The sand is collected from near river. We are taking 5cm in depth and approximately 7kg sand in each container for treatment.

E. Gravel

The aggregates in the size of 6mm and we are taking 8cm in depth and approximately 15 kg of gravel is using in each container for treatment.

F. Soil

Soil provides plants with the foothold for their roots. Here we are using Laterite soil. This is provided at the depth of 6cm of the container that is about 10 kg of soil is using in both the container for treatment.

III. METHODOLOGY

Experimental setup and Treatment

This experiment required 2 trays. In each tray 10 kg of soil, 7 kg sand and 15 kg gravel is taken. The Size of 6 mm of gravel and 0.3 mm to 0.5 mm of fine aggregate is taken. Then take 10 kg of laterite soil is taken. After this process the Vetiver grass and Lemon grass are planted separately in each tray. In this experiment each tray contains 4 vetiver and 4 Lemon Grasses. 15-liter capacity of waste water is poured into this tray for the treatment process. After the treatment process waster is collecting in the collection tank. The waste water was treated, will be tested in the 5-day gap in a month (5,10,15,20). Various Test are conducted COD, DO, BOD, Ph., Alkalinity, Conductivity. Total coliform of present sample is tested. The final Test is completed after taking 4 samples in each tray. The test is conducted in

KMCT College of Engineering. At last, the root of vetiver and Stem part of Lemon grass is measured using measurement.

Fig 1 Experimental setup

IV. FIGURES AND TABLES

TABLE I. ROOT LENGTH OF VETIVER AND LEMON GRASS

SI No.	Initial and Final root length of vetiver and lemon grass				
	Type	*Initial figure*	*Final figure*	*Initial Root length*	*Final Root length*
1	Vetiver Grass			2 cm	14 cm
2	Lemon Grass		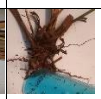	1.30 cm	4 cm

TABLE II. SHOOT LENGTH OF VETIVER AND LEMON GRASS

SI No	Initial and Final shoot length of vetiver and lemon grass				
	Type	*Initial figure*	*Final figure*	*Initial Shoot length*	*Final Shoot length*
1	Vetiver Grass			7 cm	12.5 cm

SI No	Initial and Final shoot length of vetiver and lemon grass				
	Type	*Initial figure*	*Final figure*	*Initial Shoot length*	*Final Shoot length*
2	Lemon Grass			6 cm	9 cm

V. RESULTS AND DISCUSION

TABLE III. VETIVER GRASS BEFORE AND AFTER TREATMENT

SI No	Parameter	Initial Test	Day5	Day10	Day15	Day20
1	PH	6.5	6.7	6.91	6.98	6.99
2	Turbidity (NTU)	30	26	24	23	22
3	Conductivity (µs/cm)	320	270	230	200	200
4	E. coli (mg/l)	TNTC	TNTC	Present	Absent	Absent
5	DO(mg/l)	3.54	3.9	4.53	5.32	5.35
6	BOD(mg/l)	9	7.93	6.89	4.85	4.03
7	COD(mg/l)	221.16	213.23	206.34	201.49	201.19
8	Total Coliform (CFU/l00ml	TNTC	TNTC	177	50	40

TABLE IV LEMON GRASS BEFORE AND AFTER TREATMENT

SI No	Parameters	Initial Test	Day5	Day10	Day15	Day20
1	PH	6.5	6.8	6.78	6.82	6.82
2	Turbidity (NTU)	30	27	25	20	20
3	Conductivity (µs/cm)	320	260	235	210	207
4	E. coli (mg/l)	TNTC	TNTC	TNTC	Present	Present
5	DO(mg/l)	3.54	3.74	4.82	5.92	5.93
6	BOD (mg/l)	9	8.87	6.90	5.93	5.08
7	COD (mg/l)	221.16	212.29	205.39	203.32	203.12
8	Total Coliform (CFU/l00ml)	TNTC	TNTC	TNTC	TNTC	TNTC

TABLE V. REMOVAL EFFICIENCY IN VETIVER GRASS

Sl no.		parameters			
		Day 5	Day 10	Day 15	Day 20
1	BOD	11.88	23.44	46.11	55.22
2	COD	3.58	6.70	8.89	9.02
3	Turbidity	13.33	20	23.33	26.66

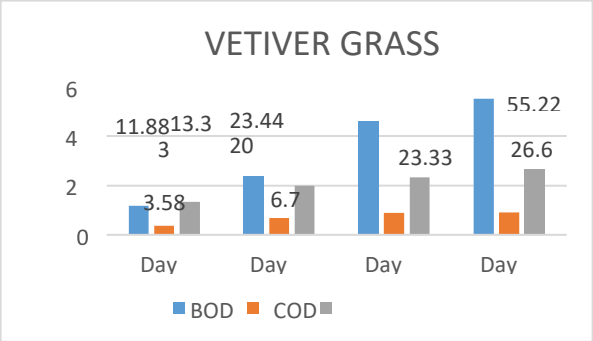

Fig 2. Removal efficiency in Vetiver grass (%).

Fig. 2. Indicates the percentage removal efficiency in vetiver grass for the parameters Bod, Cod, Turbidity is increased at Day 20

TABLE VI. REMOVAL EFFICIENCY IN LEMON GRASS

		Removal efficiency (%)			
SL.NO	PARAMETERS	DAY 5	DAY 10	DAY 15	DAY 20
1	BOD	1.44	23.33	34.11	43.55
2	COD	4.01	7.13	8.06	8.15
3	Turbidity	10	16.66	33.33	33.33

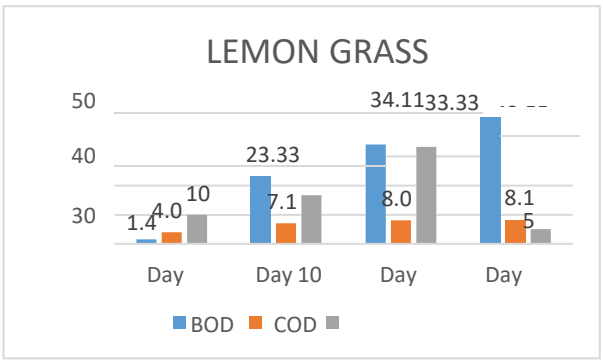

Fig 3. Removal efficiency in Lemon grass (%).

Fig. 3 indicates the percentage removal efficiency in Lemon grass for the parameters Bod, Cod, Turbidity is increased at Day 20.

VI. CONCLUSION

This study deals with the treatment of waste water by using vetiver grass and lemon grass. Various parameters are used in this method to find whether the waste water is treated or in this method to find whether the waste water is treated or not. The parameters like PH, Conductivity, Turbidity, DO, BOD, COD, E-Coli, T.T Coliform are tested. After completing Fourth stage of these test, we find that Vetiver grass is more effective than Lemon grass.

ACKNOWLEDGEMENT

We would like to thank the KMCT college of engineering for women, for its constant support all the way through our work.

REFERENCES

1. Ngisa darageh, Paul pruong and Hossein alizapeh "Effectiveness of vetiver grass versus other plants for pyto-remediation of contaminated water," August 2019.
2. Pradeep kumar, Joice k joseph and Amrutha haridasan A P, "Application of vetiver grass in eco system based disaster risk reduction- studies from kerala state of india," vol. 7, 2017.
3. Mini mathew, "effectiveness of vetiver system for the treatment of waste water from an institutional kitchen." Vol 10, 2015.
4. Rinitha P, (2022). "Grey Water Treatment by Phytoremediation Technique-A Comparative Study using Vetiver Grass and Lemon Grass" International Journal of Engineering Research & Technology, Vol.10, Issue 06 ISSN: 2278-0181.
5. Anugraha A (2022). "Salinity Removal Efficiency of Vetiver Grass from Laterite Soil'' International Journal of Engineering Research & Technology, Vol.10, Issue 06 ISSN: 2278-01.
6. Alina maharajan (2017)."Potential of vetiver grass for waste water treatment" Environment and ecology research, 489-494.
7. Jalal N F (2013)."Water quality assesment of pumba river of kerala" International journal research chemistry environment, 3: 341-347.
8. Gupta A K (2012)."Ecosystem approach to disaster risk reduction new delhi" National Institute of disaster management.

Clay Soil Stabilisation Using Bioenzyme

Sufana Ahammed
Dept. Civil Engineering
KMCT College of Engineering for Women
Kozhikode, Kerala, India
sufanaahammed@gmail.com

Shamila T
Dept. Civil Engineering
KMCT College of Engineering for Women
Kozhikode, Kerala, India
shamilat12@gmail.com

Abstract— The engineering properties of the soil can be improved, higher soil compaction densities are possible, and soil stability is increased by use of bioenzyme. It is a naturally obtained, non-toxic, non-flammable, and non-corrosive liquid enzyme formulated from fermented from vegetable, fruit, and sugarcane extracts and so. It is possible to employ bioenzymes like ecozyme too. It is possible to determine the stability by varying the bioenzyme addition rates to soil. Liquid limit, California Bearing Ratio, and Compaction other tests can be carried out, and the findings are compared to the typical soil strength.

Keywords— CBR, UCC, Compaction, Clay soil

I. INTRODUCTION

A better and more efficient vehicle operation is now necessary due to the growing population, which calls for adequate highways with suitable geometric design, pavement quality, and maintenance. In Kerala, areas with clay soil predominate include Pathanamthitta, Alappuzha, Thrissur, etc. Due to its high fertility, clay soil is beneficial for agriculture. However, due to its instability, it is unsuitable for the construction of foundations and roads. The ability of soil to contract and expand is very high. The kind and quality of the particles found in the material can be typically blamed for these poor soil performance characteristics. The best course of action whenever there is improperly graded soil on a construction site is to change the soil's characteristics so that it can meet the pavement. This might stabilize the creation of methods for stabilizing soil. Since natural soil has different characteristics around the world, a practical stabilising strategy must be chosen for a specific context after taking the soil characteristics into account. It is common to practise to enhance soil using mechanical or chemical methods. Bio-Enzymes have recently gained stabilization as a fresh chemical for stabilization. Chemicals, organic compounds, and liquid concentrated materials called "bio-enzymes" are employed to increase the durability of the soil, especially in the sub-base of pavement systems. Bio-enzymes are very easy to use, reliable, and could significantly enhance the condition of roads.

II. OBJECTIVES OF THIS STUDY

Worldwide, expansive soils (clay) are widely dispersed and are significant sources of damage to infrastructure. This kind of problematic soil must be remedied for an effective purpose of usage by enduring various ground improvement approaches and stabilization because it may result in significant economic losses and other risk factors to the surrounding environment. Examine how adding bio enzymes in various dosages affects the designed behavior of problematic soils in the current experimental investigation.

III. MATERIALS USED

A. Clay Soil

It is smaller than 0.002mm in size. More than 25% of it is clay. These, also known as heavy soils, can be fruitful because they contain various nutrients that are found in the clay minerals in the soil. But due to the capillary pull of the microscopic crevices between the numerous clay particles, they also contain a small amount of water. In comparison to sandy soils, they can drain slowly and take much longer to warm up in the spring. Clay soils are easily compacted whenever wet and bake harder in the summer, frequently could split up visibly. These soils thus keep frequently put the gardener to the limit, but they may be quite gratifying to deal with whenever correctly managed with cultivation and plant selection. When wet, it smears and becomes sticky. It can be readily flattened with a finger to get a polished appearance and rolled into a long, thin sausage. It won't get quite as shiny\ier or be as simple to form a sausage if it's not at all thick clay. If the organic matter can be added to clay soil to break up its cloudiness, it can be

exceedingly fruitful and rich in nutrients. This separates the clay into little pieces, allowing plant roots to access the water and nutrients it contains more easily. Making the clay crumble also makes it easier to the soil warmer, more easily workable, and less prone to compaction.

TABLE I. PROPERTIES OF CLAY SOIL AT MAVOOR

Property	Value
Specific gravity	2.6
Plastic limit in %	24
Liquid limit in %	36
Plasticity index in %	12
Maximum dry density in KN/m^3	2.01
Optimum moisture content in %	12
CBR in %	2.4
UCC in KN/m^3	4.4

TABLE II. PROPERTIES OF CLAY SOIL AT MUKKAM

Property	Value
Specific gravity	2.5
Plastic limit in %	26
Liquid limit in %	36
Plasticity index in %	10
Maximum dry density in KN/m^3	2.03
Optimum moisture content in %	12
CBR in %	2.9
UCC in KN/m^3	4.41

TABLE III. PROPERTIES OF CLAY SOIL AT KUTTIADI

Property	Value
Specific gravity	2.72
Plastic limit in %	4.76
Liquid limit in %	19.8
Plasticity index in %	15.04
Maximum dry density in KN/m^3	1.71
Optimum moisture content in %	12
CBR in %	1.5
UCC in KN/m^3	7.2

B. Terrazyme

Terrazyme is a dark, non-flammable liquid made from the extract of several fruits and vegetables. It is simple to combine with water, and for best effects, should be diluted with the soil's ideal moisture level. To create cementitious material, it reacts with the soil's organic materials. Enhancing the chemical interaction between the soil particles can be created a permanent structure, lowering the swelling capacity of the soil particles, and also lowering permeability.

Property	Value
Specific gravity, G	1.05
pH	3.5
Appearance	Dark brownish
Total dissolved salts, TSS	19.7ppm
Hazardous content	None
Boiling point	212 ˚F
Evaporation rate	Same as the water
Solubility in water	Completely
Reactivity data	Stable

IV. METHODOLOGY

In the present investigation, different laboratory and experimental works will be carried out. I first determined all index and engineering properties of Clayey soil such as moisture content, specific gravity, liquid limit, plastic limit, compaction and also the CBR test was performed for the stabilization process by taking different dosages of Terrazyme i.e, 0.3%, 0.6%, & 0.9% at 0.3% interval till optimum strength is attained, the enzymes get added per kg soil sample respectively. This project was conducted on clay soils for the determination of geotechnical properties (collected from Mavoor (Paddy field), Mukkam and Kuttiadi of Kozhikode district). The project is to study carefully the change in geotechnical properties of clay soil with the presence of Terrazyme. Terrazyme is collected from the Avijith Enzyme agency in Chennai. Initially, the basic properties of clay soil are determined, and later its strength properties are also evaluated. Basic properties test includes specific gravity, maximum dry density, Compaction values, Liquid limit, and plastic limit. Strength test includes the CBR test, Compaction test, and UCC. Later strength test was performed on Terrazyme added soil mixture.

V. EXPERIMENTAL WORK

A. California Bearing Ratio Test

Clay soil samples were treated with various dosages of 0.3 % interval untill the optimum strength is attained. Here optimum moisture content was taken 12%. Here with 3 dosages of terrazyme was done with clay collected from Mavoor.

TABLE IV. CBR TEST RESULTS (%)

Soil enzyme Dosage	CBR value
1.5ml/5m^3	7.95
3ml/5m^3	15.87
4.5ml/5m^3	10.83

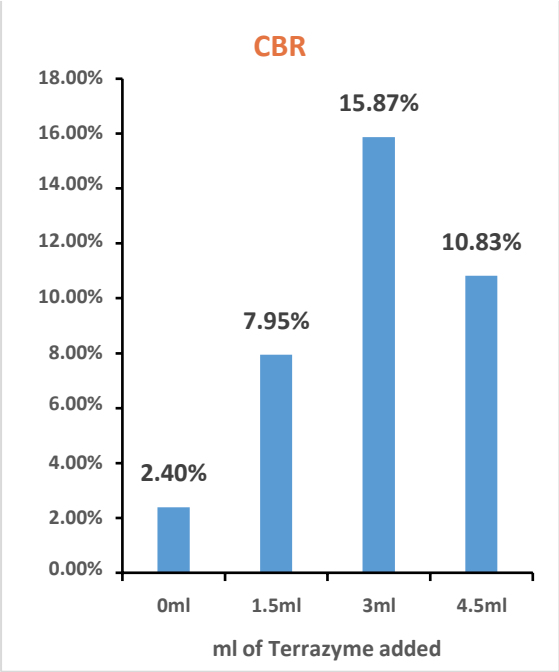

Fig. 1. CBR test

B. Unconfined Compression Test

The materials that is used for the test includes clay sample collected and Terrazyme (Bioenzyme). Here the sample collected from paddy field was tested under laboratory condition for the Unconfined Compressive Strength. The Unconfined Compressive Strength was conducted by stabilisation with varying dosages of enzyme. The test results is been given in table.

TABLE V. UNCONFINED COMPRESSIVE TEST IN KN/M2

Soil enzyme Dosage	UCC value
1.5ml/5m^3	6.92
3ml/5m^3	15.87
4.5ml/5m^3	10.83

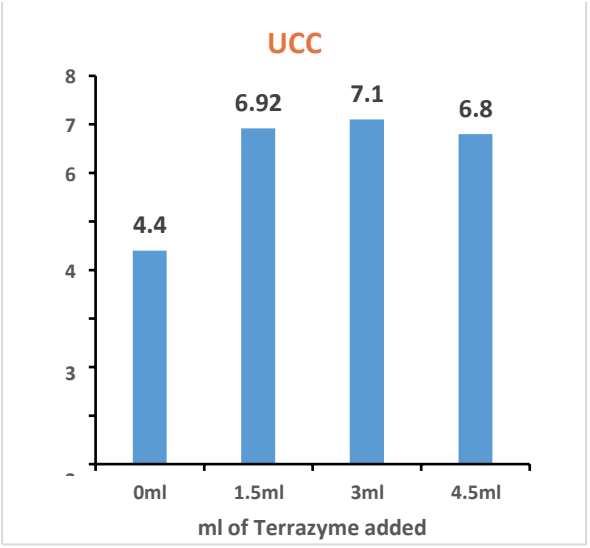

Fig. 2. Unconfined compression test

VI. CONCLUSION

The performance of Bioenzyme stabilised soil is been investigated in this work. Based on the experiments conducted in the laboratory, the following conclusions were made:

- The best result of CBR value was observed with 3ml/5m3.
- With the application of Terrazyme best result for UCC values was observed with the dosage of 3ml dosage.

REFERENCES

1. Rakesh A.H et al.,(2022) "Soil stabilization of BC Soil using Bio enzymes and Ferric chloride" International Journal of Engineering Research & Technology
2. Esthetic Mekonen et al., (2020) "Application of Microbial Bioenzymes in soil stabilization" International Journal of Microbiology
3. Athira S et al., (2017) "Soil Stabilization using Terrazyme for Road Construction" International Journal of Engineering Research & Technology
4. Amith kadaba sheshadri (2016) "Compressive Strength of a Black Cotton Soil", Anveshana's international Journal of Research in Engineering and Applied sciences, Volume 1, issue 10.
5. Akshya Raghwa, Er. Vinod Kumar Sonthwal (2016), "Bearing capacity", International Research Journal of

Engineering and Technology, Volume: 08, Issue: 01.

6. Joydeep Sen, Jitendra Prasad Singh (2015), "Bearing capacity and deformation increases in stabilized soil", International Journal of Innovative Research in Science, Engineering and Technology, Volume. 4, Issue 12.
7. Kowalski et al., (2007) "Stabilization with lime", International Journal of Civil engineering and Technology.

Melanoma Detection Using Deep Learning Techniques

Anupama J
Dept.of Biomedical Engineering
KMCT College of Engineering for Women Calicut, India
anupamaj68@gmail.com

Sreelakshmi A K
KMCT College of Engineering for Women Calicut, India
sreelakshmisatheesh856@gmail.com

Sawfa Mazna T P
KMCT College of Engineering for Women Calicut, India
sawfamazna5468@gmail.com

Nafeesathul Misriya
KMCT College of Engineering for Women Calicut, India
kmw19bm027@gmail.com

Mini Lal M
KMCT College of Engineering for Women Calicut, India

Abstract— One of the most fatal forms of skin cancer, carcinoma, begins in the cells (melanocytes) that produce melanin, the pigment that gives your skin its colour. The exact cause of all tubercles is unknown, however being exposed to ultraviolet (UV) radiation from the sun, sun exposure, or tanning lights raises your risk of contracting the condition. However, there's a substantial mortality rate, If cancer isn't treated at an early stage. A prompt and accurate opinion can ameliorate the case's chances of survival. Directly relating skin cancer at an early stage can save the cases' lives. therefore, the creation of a computer-backed support system for the opinion of carcinoma is necessary.

Our study presents a novel deep transfer learning approach for diagnosing melanoma that employs Alexnet to detect whether the sample skin lesions are either benign or malignant. Our model uses a convolution neural network. In order to identify whether the sample skin lesions are malignant or benign, deep convolutional neural networks are utilised. The effectiveness of the suggested deep learning model is evaluated using the ISIC Archive dataset, that contains fewer than 2% malignant samples. This worsens the disparity between classes. A variety of data augmentation methods were used to increase the dataset's diversity and address the issue of class imbalance. The experimental results demonstrate that the suggested deep learning approach outperforms cutting-edge deep learning algorithms in both precision and computational effectiveness.

Keywords—deep learning, convolutional neural network , keras package, tensorflow, alexnet

Melanoma is brought on by melanocytes, that are skin cells. These cells create melanin, the dark pigment that gives our skin its colour. On the other hand, some melanomas are flesh- or pink-colored. Melanomas are usually seen in brown or black. Most melanomas start in normal skin, but about 30% start in existing moles.

Because most melanomas don't start as birthmarks, it's very important to look out for skin changes. However, your skin's susceptibility to melanoma can be partially predicted by the number of moles you have. If diagnosed early, the cure rate is 99%. Early detection is of the utmost scientific importance, since the depth of tumor development directly affects the effectiveness of treatment. Melanoma is the most common cause of mortality from skin cancer even though it only makes up around 1% of all cases.

One of the most prevalent forms of cancer among people who are under the age of 30, particularly among young women, is this one. Melanoma incidence has significantly grown during the past 30 years. It is commonly acknowledged that the rise in UV exposure is one of the primary causes of this rise in melanoma occurrences. Cutaneous (skin) melanoma is one of the most prevalent melanoma types. There are two varieties of cutaneous melanoma: Melanoma may only develop in situ in the epidermis, or skin's outermost layer.

Once deleted, a change is not maintained. Invasive melanoma has impacted the dermis and subcutaneous tissue, two of the deepest layers of skin. A melanoma is often more prone to spread to other places of the body the more prevalent it is. When melanoma starts to spreads to other

regions of the body, it frequently affects the lymph nodes, lungs, brain, liver, bones, and gastrointestinal system. Nevertheless, any organ in the body might be impacted.

The four forms of cutaneous melanoma are:

a) Superficial melanoma: Although it can spread to other cells, superficial melanoma remains on the skin's surface. 70% of all cases of melanoma are the type that typically affects young people. It appears as a tan, tan, black, red, blue, or white patch of skin that is flat or slightly raised, discolored, and has jagged edges. Typical localizations for superficially spreading melanomas are the trunk, the legs or the upper back.

b) Lentigo maligna: It is a flat or slightly raised growth that varies in color from light brown to dark brown and stays close to the skin's surface. Elderly persons have skin damage from the sun, mainly to the upper torso, ears, arms, and face. This particular form of cancer, lentigo maligna, has the potential to spread.

c) Acral lentigo: It usually appears under the nails, on the hands or feet or on the soles of the feet as a black or brown discoloration. This type of melanoma can spread fairly quickly and is sometimes seen in black people.

d) Nodular Melanoma: An aggressive form of the disease that usually appears as a black bump on the skin but can sometimes take on shades of blue, gray, white, brown, tan, or red. it even corresponds to the shadow of a nearby body. This form of melanoma frequently affects the chest, legs, and arms of older patients as well as the scalp in male patients.

A suspicious region will be excised and sent to a lab to be examined under a microscope if the doctor suspects it may be a melanoma. It is called skin biopsy and it can be performed in several methods. Depending on the size of the damaged region, where it is on your body, and other considerations, the doctor will decide which one to use. Any biopsy will almost certainly leave at least a little scar. Before the biopsy, inquire with your doctor about scarring since different procedures can produce different kinds of scars. No matter what kind of biopsy is performed, the questionable area should be as thoroughly removed as possible to allow for a precise diagnosis.

In addition to biopsy methods, several medical imaging techniques, such as dermatoscopy, CT scans, and ultrasound, have been used to diagnose melanoma. Major testing are not necessary for early-stage melanomas among these assays. Dermatoscopy, particularly for melanomas and nevi, is typically used to examine skin lesions for the early identification of skin cancer. To identify melanomas in their earliest stages, dermatologists must be knowledgeable and trained. A skilled dermatologist could still make a mistake due to human error, misdiagnosing, which can be a significant, even fatal, issue. Computer- aided diagnostic (CAD) systems have been offered by several researchers as a solution to this problem. Dermoscopic pictures are examined using the CAD system in research that frequently makes use of image processing and machine learning approaches. This aids dermatologists in making quick decisions and guards against incorrect diagnoses. To categorise and detect skin cancer, traditional machine learning approaches use extracted features. This feature extraction procedure is time- and labor-intensive, nevertheless. Deep learning techniques for lesion analysis and feature extraction have been developed to circumvent this feature engineering process. The primary advantage of employing deep learning techniques is that the algorithms already extract dermoscopic information, thus this step may be skipped.

I. LITERATURE SURVEY

In the year 2019 proposal of employing image processing to detect skin cancer lesions using digital images was proposed. Using probabilistic neural networks and the GLCM algorithm for feature extraction, the suggested strategy is put into practise. It included steps like pre processing of input dermoscopy images by using median filters ,transforming it into an HIS image ,segmentation of the image using sharp and texture segmentation methods, feature extraction implemented by GLCM algorithm and finally PNN classification which is used to classify the lesions ascancerous or normal. PNN classifier not only helps to classify the lesions but also specifies the type of cancer. This technique can serve the purpose of automous diagnostics of skin cancer. The main disadvantage of this network is that it is slower than other networks like multilayer perceptron network at classifying new cases and it requires more space to store the model [1].

A deep learning-based method for automatically identifying melanoma was put forth in a publication in 2019 that employed a fully automated way to find the disease using dermoscopic pictures. The proposed strategy improves the state of the art and is especially designed for melanoma diagnosis. This method uses a multistage, multiscale technique with the Softmax classifier to categorise melanoma lesions at the pixel level. It is a powerful system that can do real-time medical diagnosis tasks while using the fewest amount of computer resources possible. [2].

A comparison of the diagnosis of melanoma skin cancer using old and modern methods of image processing was carried out in 2020. Several image processing methods for skin cancer picture categorization, preprocessing methods, feature extraction, and image segmentation were examined in a comparison of classic and modern technology [3].Using a skin cancer image as an input, image segmentation, applying intelligent algorithms, and lastly image classification employing machine learning and deep learning-based algorithms like CNN, ANN, and Support Vector Machine (SVM) are some of the current methodologies. It is implied that modern image processing techniques perform better than old ones and that old image processing techniques take a lot of time.

Skin cancer cell identification via image processing was the subject of a study article published in 2020, and different strategies, including ANN, feed forward ANN, BPN, CNN, and SVM evaluation matrix of classification algorithms, were reviewed.4].

In 2020 a paper was established for deep convolutional neural network for melanoma detection using dermoscopy images. In the proposed methodology, dermoscopic images collected from open sources are used for training the network[5]. It helps DCNN to execute many complex operations simultaneosly. But it failed to achieve adequate diagnostic accuracy for melanoma.

Two cancer types, along with one non-cancer type, were classified using a skin classification model built on VGG19 and transfer learning. The data came from the HAM10000 dataset. Autonomous feature extraction capability of VGG19 makes it simple to find the traits that set each different cancer type apart without having to spend time manually inspecting them. By using a suggested VGG19 with finely tuned parameters, this VgG19 model was used for the classification of skin cancer. [6].It is an effective tool with excellent accuracy for diagnosing skin cancer. One disadvantage is that additional pre-processing procedures must be conducted in order to increase accuracy.

A work on melanoma lesion recognition and segmentation utilising YOLOv4- Darknet and acuive contour was presented in 2020. The methodology they used includes sharpening the image regions and removing artefacts from the dermascopic images by using morphological processes. [7].The infected region is then identified by tuning the YOLO v4 object detector for melanoma detection to be able to differentiate between inseparably linked infected and non-infected regions. Finally, utilising active contour segmentation for Texture extraction, the affected melanoma patches are obtained. The results of segmentation aid in the creation of a clinical support system for melanoma detection There is greater localization inaccuracy in YOLOv4, which is one of its drawbacks.

For the early diagnosis of skin lesions, machine learning algorithms for skin cancer detection can also be based on feature extraction utilising the ABCD rule, GLCM, and HOG [8]. The process involves converting the RGB image to grayscale and then subjecting it to noise median filtering. Using region filling morphology, detected hair will be eliminated before segmentation is carried out utilising GAC. The GAC detects fluctuations in total skin lesions, and SVM, KNN, and Nave Bayes are used for feature extraction and classification. The main benefits of employing this technique are its high computational complexity and improved accuracy after augmentation.

A research on employing neural networks on an embedded device to detect skin cancer in real time was published in 2021. The method was designed to provide real-time skin cancer detection on a smart phone, allowing users to simultaneously scan several tumours. In order to detect skin cancer, embedded technologies and artificial intelligence are used[9].The two models for detecting images are the model for image categorization and the model for detecting images. Because of the absence of data on the

body, such as age or the location of tumours, this technique's accuracy is a severe flaw.

II. METHODOLOGY

In order to categorise skin cancer melanoma, this study introduces a deep transfer learning method. At the first level, pre-processing and other augmentation techniques are used to create diversity and solve the issue of class imbalance in the dataset. Auto features are extracted at the second level and then utilised with a trained "Alexnet" model to distinguish between a malignant melanoma and a benign skin lesion.

A. Introduction to Deep Learning

Deep learning can be said as a form of artificial intelligence (AI) that uses numerous layers of a neural network to analyse data to mimic pattern recognition in the human brain. The straightforward machine learning algorithms are very effective at solving numerous crucial issues. The fundamental issues with AI, like the ability to recognize speech and objects, have not yet been resolved. Deep learning was created to get around these problems as well as others.

The application of deep-learning architectures like deep neural networks, deep belief networks, recurrent neural networks, and convolutional neural networks has been beneficial in a number of fields, which include computer vision, machine vision, language understanding, language processing, audio acknowledgement, social network filtering, machine translation, bioinformatics, drug design, medical image analysis, material inspection, and board game programmes.

The operation and information processing of neurons and neural networks in the brain strongly influences all deep learning methods.

B. Convolutional Neural Network

In order to segment, classify, and process pictures, convolutional neural networks (CNNs), which are neural networks containing one or more convolutional layers, are predominantly employed. An algorithm for deep learning that could identify different features and objects in an input image, assign them learnable weights and biases, and then make a distinction between them. In comparison to other classification methods, a ConvNet needs substantially less pre-processing. A ConvNet's design is comparable to the connectivity pattern of neurons in the human brain and was influenced by how the Visual Cortex is structured.

C. Introduction to Python

Python is a high-level scripting language used for a diverse variety of text processing, system administration, and internet-related tasks. Compared to many other languages of a similar nature, its core language is significantly smaller and easier to learn, and it enables the creation of modules to do an almost unlimited variety of jobs. A true object-oriented language that runs on a variety of platforms is Python. The fact that there's a Python interpreter developed entirely in Java further solidifies Python's status as a top-notch alternative for internet problems. Python was developed in the early 1990s by Guido van Rossum, who is now at CNRI in Virginia but was previously at CWI in Amsterdam. A project to develop a programming language that could be easy for beginners to learn yet robust sufficient to satisfy advanced users might be claimed to be the source of Python. Reflections of this lineage can be seen in Python's succinct, straightforward syntax and the rigor with which ideas including object- oriented programming are executed while still allowing for the use of more traditional programming methods. Python keeps the power and complex capabilities that users will gradually need, making it a fantastic choice for new programmers.

Python has a few features that set it apart from other programming languages. The existence of a newline, which is created whenever you hit the "Return" key on your keyboards, signals to the Python interpreter that you have done with a particular statement. Python statements don't have to conclude with a particular character. If a statement extends more than one line, it is recommended that you employ a backslash (/) to tell Python that you intend to continue it on that line.

Python offers some flexibility when writing programmes, but there are fundamental rules that must be adhered to at all times. One of these principles indicates that, contrary to numerous other languages, Python employs indentation to signal the presence of loops, although some people find to be quite shocking. Statements that aren't indented must begin in the first column, despite the fact that the degree of indentation used within a given composition of a loop is not critical.

Most Python developers prefer to employ an editor like emacs, which automatically offers constant indentation. Your programmes will likely be simpler to maintain if you employ regular indentation across every loop, at all depths. In order to do this, an intelligent editor is quite beneficial. Many features in Python are typically only found in languages that are much more difficult to learn and use.

Instead of building up to a final product, as is the case with many other scripting languages, these features were built into Python from the very beginning.

Using the import command, you can call modules— programmes that run independently and define a number of functions and data kinds—in Python to perform operations that fall outside the purview of the language's core functionality. Python's core distribution, for instance, includes modules for processing files, connecting to the internet and your computer's operating system, manipulating strings, writing CGI scripts (which deal with interfacing with web pages shown in web browsers), and many more activities. For creating graphical user interfaces, interacting with databases, processing image files, and other tasks, the Python website provides extra modules.

In order to categorize skin cancer melanoma, this study introduces a deep transfer learning system. Pre-processing and a range of augmentation techniques are used at the first level to introduce diversity and address the issue of unequal class distribution in the dataset. To distinguish a malignant melanoma from a benign skin lesion, auto features are extracted at the second level, and an "Alexnet" model that has already been trained is then used.

D. Introduction to Keras

Many types of neural networks can be easily built, trained, tested, and used thanks to a Deep Learning API Keras.

It abstracts away the implementation details of many Machine - learning libraries, such as TensorFlow, Microsoft Cognitive Toolkit (CNTK), and Theano.

On top of which Keras operates are open source machine libraries like Theano, Tenser flow or Cognitive Toolkit (CNTK).TensorFlow or Theano-based deep learning models may be easily and quickly built thanks to Keras's basic framework.

With Keras, deep learning models could be rapidly defined. The best choice for applications which require deep learning is Keras, obviously. As a python-based neural network library, Keras requires Python to be installed on your machine. The following features are supported by it:

- An extensible, simple, and consistent API.
- Simple structure that makes it simple to achieve the desired result.
- It accommodates various backends and platforms.
- It is an easy to use framework with highly scalable computation that runs on both CPU and GPU.

The perks of Keras, a very flexible and robust framework, include:

- Broader community support
- Easy to test
- Keras support both Recurrent networks and CNN.
- Deep learning models are composed of discrete components that can be coupled in a variety of ways.

E. Tensor Flow

It is a deep learning library that also offers a vast array of tools for large-scale machine learning and computation. In addition, it offers TensorBoard for model visualization, TensorFlow Extended (TFX) for scaling up TensorFlow projects, and a lot more.

Key characteristics of TensorFlow:

- It contains a capability that employs multi-dimensional arrays considered as tensors to simply design, fine tune, and calculate mathematical expressions.
- It supports both Deep neural networks and machine learning programming.
- It has a flexible and scalable computation feature that performs with various sets of data.
- It allows us to train multiple neural networks simultaneously on multiple GPUs, TensorFlow's Parallel Neural Network Training makes models for large-scale systems extremely efficient.
- Through GPU computing TensorFlow automates management. It also has unique

feature that optimizes how to utilise the same memory and data.

- Flexible,one of the key characteristics of Tensorflow is its operability flexibility; this feature refers to the fact that it is modular and gives you the option of making any part of it stand alone.
- Access to Summary Statistics; the library provides distribution functions such as Bernoulli, Chi2,Beta, Uniform, and Gamma, which seem to be especially important when using probabilistic approaches such as Bayesian models.

F. Flowchart

The flow diagram for the suggested method is depicted in the figure below.

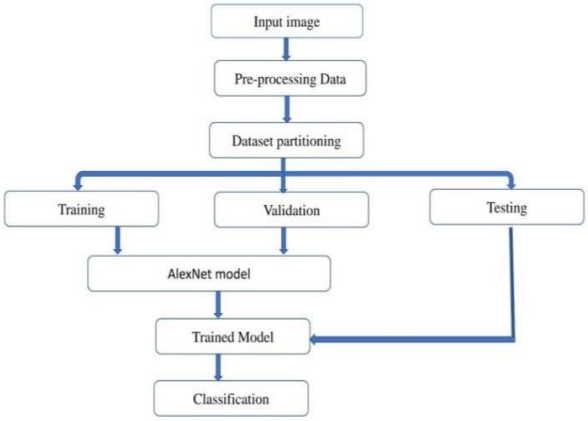

Fig. 3.1 Flow chart of the proposed model

A) Dataset

The effectiveness of deep learning techniques depends on a valid and appropriate dataset being available. Processed Skin Cancer pictures of the ISIC Archive Skin Cancer: Malignant vs Benign is used as dataset in the proposed research.This dataset contains a well-balanced mix of benign and malignant skin moles.

- **Image Pre-Processing**

Preprocessing is applied to all ISIC-2020 input images so that it can produce classification results which has better features and are more consistent. To avoid over-fitting, the CNN approach's massively repetitive training required a large-scale image dataset.

- **Data Augmentation**

Various data augmentation techniques were applied to the training set to reduce overfitting and increase dataset diversity using the Python image data generator function from the Keras library. A scaling transform was used to reduce computational overhead by using smaller pixel values within the same range.

B) Training, Validation and Testing

There were three parts to the ISIC dataset: training, testing, and validation. The test and validation datasets were used to gauge how well the new model was performing once the Alexnet model had been trained. As a result, we split the dataset into training, testing, and validation groups, which accounted for 70%, 15%, and 15% of the total, respectively.

C) Alexnet Architecture

AlexNet was the first convolutional network to use GPUs to improve performance. Five convolutional layers, three max pooling layers, two normalization layers, two fully connected layers, and one softmax layer make up the AlexNet architecture. A convolutional filter and a nonlinear activation function called ReLU make up each convolutional layer. Since we have a fully connected layer, max pooling is performed using pooled layers and the input size is fixed. ReLu activations are performed at the end of each shift except the last shift. This produces a softmax distribution over 1000 class labels. According to AlexNet, deep CNNs can be trained much faster using ReLU nonlinearity than saturation activation functions such as Tanh or Sigmoid.

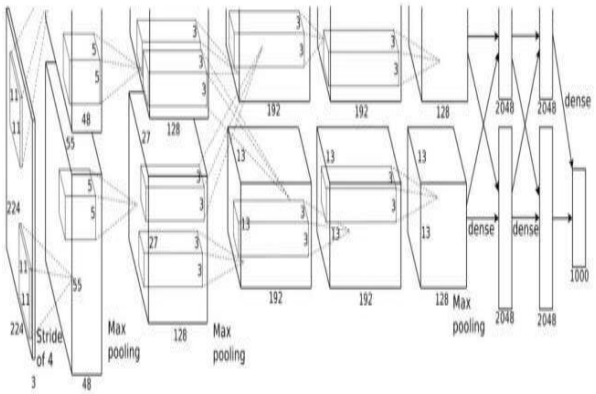

Fig. 3.2 Alexnet Architecture

III. CONCLUSION

Subsequently, it is critical to utilize complementary imaging thinks about that have been appeared to bolster conclusion. These methods were created by therapeutic experts to identify melanoma some time recently it spreads

to adjacent lymph nodes. To investigate any troubling lesion, we arrange to send a exchange learning demonstrate for melanoma and benign skin injuries conclusion based on AlexNet architecture in this study. The proposed strategy is utilized to classify infections as kind or harmful utilizing photographs from an ISIC dataset of skin cancer clutters. To grow the dataset and improve the accuracy of the AlexNet design, a number of information increase approaches are utilized. Through this plan, we expect a symptomatic exactness of more than 90%. Moreover, we need to test the exactness of a few cutting-edge models to the proposed system through this consider.

REFERENCES

1. M. Waghulde, S. Kulkarni and G. Phadke, "Detection of Skin Cancer Lesions from Digital Images with Image Processing Techniques," 2019 IEEE Pune Section International Conference (PuneCon), 2019, pp. 1-6, doi: 10.1109/PuneCon 46936. 2019.9105886.
2. A. Adegun and S. Viriri, "Deep Learning-Based System for Automatic Melanoma Detection,"in IEEE Access, vol. 8, pp. 7160-7172, 2020, doi: 10.1109/ACCESS. 2019.2962812.
3. B. Sreedhar, M. Swamy B.E and M. S. Kumar, "A Comparative Study of Melanoma Skin Cancer Detection in Traditional and Current Image Processing Techniques," 2020 Fourth International Conference on I-SMAC (IoT in Social, Mobile, Analytics and Cloud) (I-SMAC), 2020, pp. 654-658, doi: 10.1109/I-SMAC49090.2020.9243501.
4. E. Jana, R. Subban and S. Saraswathi, "Research on Skin Cancer Cell Detection Using Image Processing," 2017 IEEE International Conference on Computational Intelligence and Computing Research (ICCIC), 2017, pp. 1-8, doi: 10.1109/ICCIC.2017.8524554.
5. K. R., G. H. and S. R., "Deep Convolutional Neural Network for Melanoma Detection using Dermoscopy Images," 2020 42nd Annual International Conference of the IEEE Engineering in Medicine & Biology Society (EMBC), 2020, pp. 1524-1527, doi: 10.1109/ EMBC44109. 2020.9175391.
6. Nour Abuared etal; "Skin cancer classification model based on VGG19 and transfer learning". 2020 3rd International Conference on Signal Processing and Information Security (ICSPIS), 2021 ,DOI: 10.1109/ICSPIS51252.2020.9340143
7. S. Albahli, N. Nida, A. Irtaza, M. H. Yousaf and M. T. Mahmood, "Melanoma Lesion Detection and Segmentation Using YOLOv4-DarkNet and Active Contour," in IEEE Access, vol. 8, pp. 198403-198414, 2020, doi: 10.1109/ ACCESS. 2020.3035345.
8. M. Vidya and M. V. Karki, "Skin Cancer Detection using Machine Learning Techniques," 2020 IEEE International Conference on Electronics, Computing and Communication Technologies (CONECCT), 2020, pp. 1-5, doi: 10.1109/ CONECCT50063.2020.9198489
9. Rowin Veneman, "Real time skin cancer detection using neural networks on an embedded device", 2021
10. R. R. Subramanian, D. Achuth, P. S. Kumar, K. Naveen kumar Reddy, S. Amara and A. S. Chowdary, "Skin cancer classification using Convolutional neural networks," 2021 11th International Conference on Cloud Computing, Data Science & Engineering (Confluence), 2021, pp. 13-19, doi: 10.1109/Confluence 51648.2021. 9377155.
11. Wang, Shi & Hamian, Melika. (2021). "Skin Cancer Detection Based on Extreme Learning Machine and a Developed Version of Thermal Exchange Optimization". Computational Intelligence and Neuroscience. 2021. 10.1155/2021/ 9528664.
12. Girdhar, Nancy & Sinha, Aparna & Gupta, Shivang. (2022). "DenseNet-II: An Improved Deep Convolutional Neural Network for Melanoma Cancer Detection". Soft Computing. 10.1007/s00500-022-07406-z.

Multiple Lung Diseases Classification System Using DWT, Based On Deep Learning

Abhirami B A
Dept. of Biomedical Engineering
Kmct College of Engineering for Women Calicut, India
abhiramiba2018@gmail.com

Dilsha V M
Dept. of Biomedical Engineering
Kmct College of Engineering for Women Calicut, India
dilshavm2002@gmail.com

Meghna Lakshmi M
Dept. of Biomedical Engineering
Kmct College of Engineering for Women Calicut, India
meghnalakshmim@gmail.com

Andriyo Royee
Dept. of Biomedical Engineering
Kmct College of Engineering for Women Calicut, India
andriyoroszario@gmail.com

Mini lal M
Dept. of Biomedical Engineering
Kmct College of Engineering for Women Calicut, India
minilal@kmctcew.ac,in

phini Ann Philip
Dept. of Biomedical Engineering
Kmct College of Engineering for Women Calicut, India
phiniannphilip@gmail.com

Abstract- An exceptional pandemic that has economically, and socially impacted billions of lives has stimulated the clinical network to supply techniques for prognosis, prevention, and prediction of this pandemic that are primarily based on personal system virtual technology. To reduce the exposure to health, computerized and powerful techniques are necessary because the unfolding of COVID-19 is continuously increasing. Although restricted to specific visualisation images, X-ray imaging can be used for prognosis. Some of those efforts basically focus on statistical and artificial intelligence, primarily based on the evaluation of the COVID-19 information. The goal of this is to predict a lung disorder, either COVID-19 or pneumonia. This is implemented via means of remotely monitoring the X-ray picture of the lungs. The X-ray picture information is obtained from an open-source repository. It includes approximately 5000 normal, COVID-19, and pneumonia X-ray pictures for each class. With the aid of wavelet-based image segmentation, feature extraction strategies, knowledge of machine learning, and neural networks, one such system may be produced.

Keywords—DWT, CNN, COVID-19.

I. INTRODUCTION

Lung disease is a common disease in the world .It comprises of pulmonary fibrosis, lobar pneumonia, Covid-19, tuberculosis disease etc. The Covid-19 and preceding lung disorder pneumonia are strongly associated because numerous individuals died from severe chest congestion (pneumonic condition).For medical professionals , it can be difficult to distinguish between pneumonia and Covid-19 lung illnesses .The most accurate way to diagnose lung illness is by chest x-ray imaging. Appropriate prognosis of lung disease is necessary. A lot of image processing and machine learning models have been established for the purposes.

In this paper , we propound a structure for the pulmonary disease prognostication like pneumonia, Covid-19,and pulmonary fibrosis from the chest X-ray images of patients. The framework comprises of dataset capture, Feature extort, training, testing and prediction. We used two publicly accessible chest x-ray imaging datasets for the data acquisition. The given data is divided into 80% training and 20% testing data . The discrete wavelength transform - based image decomposition technique is used for feature extraction as it gives all-inclusive and approximate coefficients at horizontal, vertical and diagonal approaches at each level of decomposition. A vast labelled dataset of extracted features with the identification of all four classes .The data does not need pre-processing or cleaning as it already comprise of all the the extracted features. Then these features are used to train classifier models for testing and prediction.

We are using different machine learning algorithms like Random forest , SVM algorithm, KNN, and deep learning algorithms like CNN,

and ANN for training and evaluating the performance of each algorithm by using accuracy, precision and recall. By comparing this algorithm, we can develop a system that will give accurate prediction on user input. The unprecedented pandemic that has affected millions of people moderately , ethically and humanly has instigated the clinical network to provide methods for prediction ,prevention, and Covid-19 prediction and also identifies the stage of the patient's lung condition which is classified as HIGH,MEDIUM and LOW. It is made mostly using personal data helped by a system virtual technology.

This system suggests a non-intrusive method for examining and keeping track of the patients. The project's objective is to design a system that can identify COVID-19, or pneumonia, as a lung condition. This is done by using a method for remotely observing the radiogram illustration of the respiratory organ. Information about the radiogram image is collected from open-source storage facilities. It contains roughly 5000. For each class: normal, COVID-19, and pneumonitis, radiogram images. With feature extraction and wavelet-based picture segmentation techniques, understanding of neural networks, and machine learning One such system could be built. This study suggests a non-intrusive method for examining and keeping track of patients.

II. LITERATURE SURVEY

In [1] 2017, Abhishek Sharma proposed the discovery of pneumonia shadows in casketx-ray using an image processing approach. It's an image processing approach which chance ways to automate diagnostics from medical images and has been one of the most intriguing areas of software development. It helps to pressure a new approach for detecting the presence of pneumonia shadows in casket x-rays(CXR) by using only image processing ways.

The term "computed tomography," or CT, refers to a computerized x-ray imaging procedure in which a narrow beam of x-rays is aimed at a patient and quickly rotated around the body, producing signals that are processed by the machine's computer to generate cross-sectional images, or "slices." These slices are called tomographic images and can give a clinician more detailed information than conventional x-rays. Once a number of successive slices are collected by the machine's computer, they can be digitally "stacked" together to form a three-dimensional (3D) image of the patient that allows for easier identification of basic structures as well as possible tumors or abnormalities.

About 40 analogs of casket CXRs pertaining to normal and pneumonia infected cases have been worked on. Indigenous algorithms have been developed for cropping and for the birth of the lung region from the images.

In [2] 2019, Md Mehdi Hasanet. al proposed A combined approach using image processing and deep literacy to descry pneumonia from a casket-ray image. Inorder to help unfortunate deaths of patients having pneumonia which is an epidemic complaint, it is demanded to be detected in it's early stage. By using traditional styles the detection of the complaint may take more time. The detection of the complaints has been accelerated by using caskets x-ray images . For that an expert and a radiologist for interpreting the x-ray image is necessary. In the countries like Bangladesh, where the failure of expert and a medical person is persisting, it is very difficult to chancing a professed and educated radiologist especially in certain areas.

In [3] 2019, Diego Arditaet. al proposed end-to-end cancer webbing with 3-dimensional deep literacy on low cure casket reckoned tomography. With a estimate of 1000 deaths on 2018, lung cancer is the most common cause of cancer deaths in the United States. Lung cancer is the leading cause of cancer deaths worldwide.

People who smoke have the greatest risk of lung cancer, though lung cancer can also occur in people who have never smoked. The risk of lung cancer increases with the length of time and number of cigarettes you've smoked. If you quit smoking, even after smoking for many years, you can significantly reduce your chances of developing lung cancer.

Computed tomography (CT) is an imaging procedure that uses special x-ray equipment to create detailed pictures, or scans, of areas inside the body. It is sometimes called computerized tomography or computerized axial tomography (CAT).

Lung cancer webbing using low-cure reckoned tomography has been shown to reduce mortality by 20-43 and is now included in the US webbing guidelines 1-6.

Being challenges including inter-grader variability and high false - positive and false - negative rates 7-10 we propound a deep literacy algorithm which uses a case's current and previously reckoned tomography volumes to prognosticate the threat of lung cancer.

In [4] 2019, Enes AYAN proposed opinion of Pneumonia from casket X-Ray Images using Deep literacy. pneumonia is a kind of lung disease caused by bacterial infection. For a successful treatment pre opinion leads an vital role. With the help of an expert radiologist the complaints from the casket radiogram images can be diagnosed. In the cases of an unclear casket radiogram images or confused with other conditions the consultation can be private. Inorder to guide the clinicians ,computer backed opinion systems were demanded. This gives the result as the Vgg16 network exceed the exception network at the delicacy with 0.87,0.82 independently. Even though in the case of detecting pneumonia cases the exception network has a high rate of success. So that we conclude the result that every network has its own special capabilities on the same dataset.

In[5] 2020 liqaA. Rousanet.al proposed casketx-ray findings and temporal lung changes in cases having Covid- 19 and Pneumonia. Coronavirus disease (COVID-19) is an infectious disease caused by the SARS-CoV-2 virus.

Most people infected with the virus will experience mild to moderate respiratory illness and recover without requiring special treatment. However, some will become seriously ill and require medical attention. Older people and those with underlying medical conditions like cardiovascular disease, diabetes, chronic respiratory disease, or cancer are more likely to develop serious illness. Anyone can get sick with COVID-19 and become seriously ill or die at any age.

Pneumonia is an infection that inflames the air sacs in one or both lungs. The air sacs may fill with fluid or pus (purulent material), causing cough with phlegm or pus, fever, chills, and difficulty breathing. A variety of organisms, including bacteria, viruses and fungi, can cause pneumonia.

Computed tomography (CT) is a diagnostic imaging test used to create detailed images of internal organs, bones, soft tissue and blood vessels. The cross-sectional images generated during a CT scan can be reformatted in multiple planes, and can even generate three-dimensional images which can be viewed on a computer monitor, printed on film or transferred to electronic media. CT scanning is often the best method for detecting many different cancers since the images allow your doctor to confirm the presence of a tumor and determine its size and location. CT is fast, painless, noninvasive and accurate. In emergency cases, it can reveal internal injuries and bleeding quickly enough to help save lives.

Casket CT checkup and casket x-rays show characteristic radiographic findings in cases with COVID-19 and pneumonia. caskets-ray can be used in opinion and follow-up in cases with COVID-19 and pneumonia. The study aims at describing the caskets-ray findings and temporal radiographic changes in COVID-19 cases. From March-15 to April 20, 2020, cases with positive rear recap polymerase chain response (RT-PCR) for COVID-19 were retrospectively studied. Case's demographics, clinical characteristics, and caskets-ray findings were reported. Radiographic findings were identified with the course of the illness and case's symptoms.

III. METHODOLOGY

The lives of billions of people have been affected adversely on both an economic and social level. COVID-19 diagnosis, prevention and prediction has developed by the medical world which are completely based on the individual system-aided virtual technology. As the COVID-19 is spreading rapidly, modern, computerized, and potent procedures for the error-free spotting are required to decrease the uncovering of healthcare professionals to the outbreak. Radiogram imaging, however, narrowed to conception, could be helpful for predicting. Certain of these initiatives concentrate on the graphical as well as the AI techniques, largely based upon the analysis of the available pandemic data. This project's objective is to design a system that can identify COVID-19 or pneumonia as a lung condition. It also identifies the stage of the patient's lung condition which is classified as HIGH, MEDIUM and LOW. This is done by using a method for remotely monitoring the radiogram images. The radiogram images data is sourced from publicly accessible repositories. It contains over 5000 images of normal, covid-19

and pneumonia radiogram images. One such system might be created using wavelet-based picture segmentation, feature extraction techniques, an understanding of machine learning, and neural networks. This study suggests a non-intrusive method for examining and keeping track of the patients.

A.CNN ARCHITECTURE

This model is known as a sequential CNN model since each layer is connected to the layers above and below it. Three dense layers and five convolutional layers make up the suggested model. The input layer receives input images with a size of 48x48x1.There are 64 filters in the conditional layer. Each typical layer is followed by a reactivation to enhance learning. An additional layer called maxpooling follows the activation function ReLU. After calculating data for producing a down sampled feature map, the average of two conventional layers is pooled, after two levels of average pooling. There is a dense layer with 1024 neurons that uses the output from the convolutional layer to classify images. Dropout and dense layer come after ReLU activation fiction. Dropout is a method for avoiding a model from over fitting drop out works by randomly setting input units zero with a frequency of rate of each step during training time. Four neurons in the third dense layer, which is supplied to SoftMax, are present. Which is a multinomial probability distribution activation function in the neural network's output layer Here, CNN design is based on the sequential data technique. Using X-ray images of diverse lung diseases, including fibrosis, pneumonia, covid-19, this model was trained from scratch.

B. DISCRETE WAVELET TRANSFORM

Discrete Wavelet Transform to extract features from time series and then build a classification model. Wavelet transform provides a multi-resolution area representation. The lower frequency sub bands have finer frequency resolution and coarser time resolution than the higher frequency sub bands as a result of the DWT's decomposition of a digital signal into several sub bands. Time series of coefficients describing the time evolution of the signal in the corresponding frequency band. The distinct Digitally altered signals are the focus of the discrete wavelet transform.

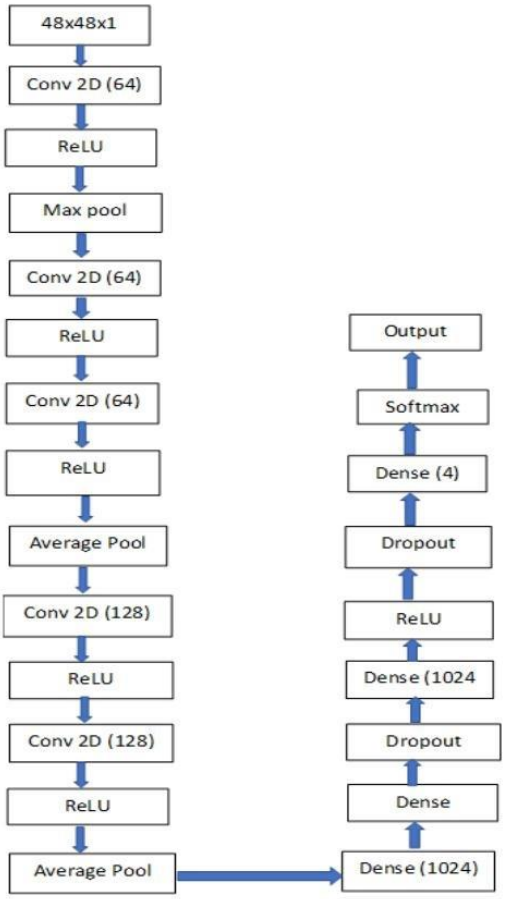

Fig.1 Architecture of CNN

The sibling continuous wavelet transform, which handles analogue signals, is not at all covered in this article. A mathematical procedure known as the wavelet transform (DWT) measures the amount of energy present in a signal at different times and frequency bands. A non-mathematician can gain a conceptual understanding of the DWT and its significance by comparing it to the more well-known Fourier transform and examining how they vary. Picture compression, picture reduction, and picture separation are at the cutting edge of image processing applications.

As a result, the field of image processing is constantly developing, and new applications are being developed at an increasing rate. It is a stimulating and stimulating environment to be in. These days, the application areas range from the entertainment sector to the space programme. among the leading Interestingly, one aspect of this data transformation is the ability to send and receive sophisticated information beyond the simple written material. Picture data, which is

delivered as digital images, has emerged as one of the most popular methods to Conversation in the twenty-first century. The original image is passes through the low pass filter on rows and we get the horizontal approximation and horizontal details .Then this details will passes through the low pass filter on columns from here we get approximate image, vertical details, horizontal details, diagonal details. the approximate image contains more features of the original image.

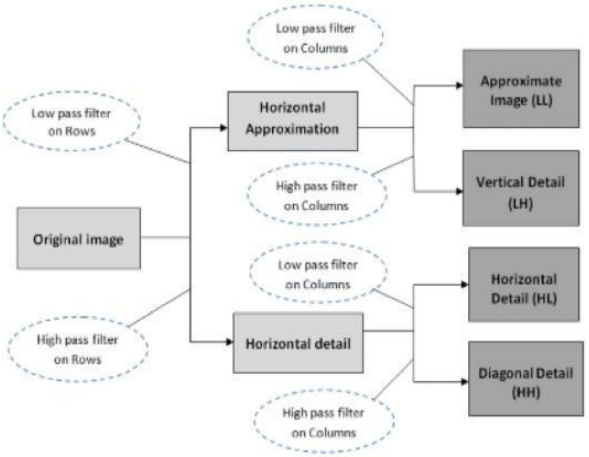

Fig .1 DWT Working

C. BLOCK DIAGRAM

There are three subsections in this section.

1. Data capture.

2. Feature Extort

3. Prognosis

- The first stage implies the need for an X-ray picture dataset. A Kaggle no. of typical, covid infected and as well as pneumonic radiogram images are present.
- The data divided into 34% of testing data and 66% of training data.
- The DWT based image perishing method is utilized for the feature extort because it provides accurate and detailed coefficients at each level of decomposition for the horizontal, vertical, and diagonal modes.

A sizable, labelled data set of features that have been extracted and all three classes have been identified. As all the retrieved features are already there. No pre-processing or cleaning is necessary for this data.

Classifier models are then trained using this data set. For testing the patient for covid-19 or pneumonia or other lung diseases the procedural work includes an x-ray. So that this particular feature gives a non-invasive ability to the proposed system.

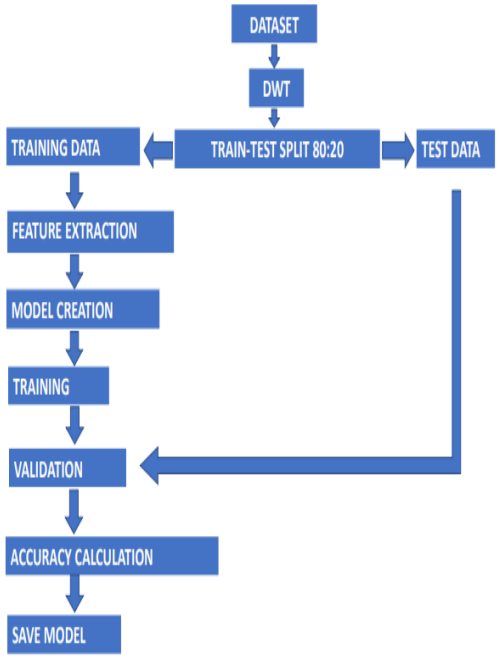

Fig.3 Block daigram

Data Capture:

There are some open-source respositories from which the data can be easily obtained which is created especially for biomedical images and signal.

The major 2 sources inludes;

*Arxiv.org:covid-19 image dataset acquisition *Kaggle.com:covid-19 and pneumonia chest radiogram images.

A total of 15,089 images were presented in the data.

Feature Extort:

For the different feature extraction of each image, a DWT based image decomposition method is used. The Daubechies (db3) [21][22] wavelet and decomposition up to level 4 are utilized as the benefits includes orthogonal set of functions, stability and finite vanishing moments. For training a multilayer perceptron model for the classification task it is necessary to extract properties such as energy retention, mean, standard deviations, So the goal is to construct a massive dataset of photos of all types and extract properties.

Prognosis:

DWT can be using dto2-D signals or pictures. According to this method, 1 dimensional discrete wavelet transform can be applied to each row and columns of a picture separately.

D. FLOWCHART

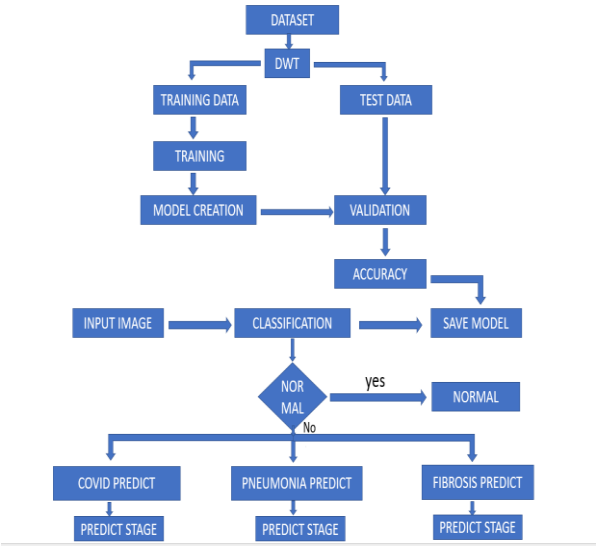

Fig.4 Flow chart

a) Training section

b) Prediction section

The input of the training session is the dataset.

The features are extracted, and the images are normalized by DWT. In numerical analysis and

Any wavelet transform that is discrete in functional analysis is one where the wavelets are discretely sampled. It incorporates both frequency and location information, which gives data of the whole dataset remarkable advantage over Fourier transforms. Test data is used in order to measure the precision of the system.80% data of the hole dataset is used for the preparing or training and the remaining20% is for prediction in order to measure the accuracy. From the data train data, the features are extracted. The creation of the architecture of the neural network is well known as model creation and also done after feature extort.

III. RESULT

The proposed medical image classification and implementation results are discussed in this section. This research presents an intelligent model of deep neural network for prediction and classification of various lung diseases. A prediction is made by comparing the radiogram images to the saved model once it has been uploaded to the website. This is done with the intention of making it simpler for people to comprehend the different lung issues utilizing an x-ray image without first seeing a doctor. On average, the model's accuracy is assessed to be 99%.

IV.CONCLUSION AND FEATURE SCOPE

The discrete wavelet transform of the radiogram images and the feature extent are the 1st 2 important elements that highlight the project's outcomes. The outcomes from the 2 trained classifiers models and their comparison are another crucial element. A special technique for classifying medical images that uses the best features currently available is optimal feature selection. A unique system of clinical picture classification based on dataset is introduced in order to enhance execution in terms of accuracy, precision, and classification. To get the required results, a collection of records with diverse image types was added to the study. Using textural deep learning techniques, such as CNN and PyCharm, the most pertinent subset of features is extracted from preprocessed medical images. Usually, the recovered features are taught and used in the categorization procedure. The application makes use of Python. The presented medical image was then classified using the approach into further categories, including Normal, viral pneumonia, Covid-19, and fibrosis. Also, the congruent performance of the proposed model was verified, and its correctness was assessed; both were largely successful. Deep learning discovers a number of opportunities and hidden patterns that can help the medical industry deliver high-quality patient care. Artificial intelligence and machine learning have received a lot of attention in recent years. Even deep learning has now established a commercial niche in this sector and is slowly growing its share. Deep learning's function in healthcare is amply proved by its current and upcoming uses, and additional study may broaden the field's possible application areas. By this work, even without a medical professional, we can quickly and readily diagnose the lung disease.

With a better outcome of more than 95% accuracy on prediction, this initiative suggests a

non-invasive method of examining and monitoring the patient's lung status.

REFERENCES

1. Anthimopoulos (2016) 'Lung pattern classification for interstitial lung diseases using a deep convolutional neural network'. (IEEE - Journal)
2. Abhishek Sharma (2017) 'Detection of pneumonia clouds in chest X-ray using image processing approach'. (IEEE - Conference)
3. Sana and Abedi (2019) 'Coronavirus disease 2019 (COVID-19): a systematic review of imaging findings in 919 patients'. (Journal)
4. Md Mehedi and Hasan (2019) 'A combined approach using image processing and deep learning to detect pneumonia from chest X-ray image'. (IEEE - Conference)
5. Ardila Diego (2019) 'End-to-end lung cancer screening with three-dimensional deep learning on low-dose chest computed tomography'. (Nature Publishing Group - Journal)
6. Wang and Linda (2019) 'Covid-net: A tailored deep convolutional neural network design for detection of covid-19 cases from chest x-ray images'. (Nature Publishing Group - Journal)
7. Ayan Enes (2019) 'Diagnosis of pneumonia from chest X-ray images using deep learning'. (IEEE)
8. liqa A Rousan (2020) 'Chest x-ray findings and temporal lung changes in patients having Covid-19 and Pneumonia'. (BioMed Central – Journal)
9. [9] Ming yun Ng et.al (2020) 'Imaging profile of the Covid-19 infection: radiologic findings and literature review'. Radiological Society of North America - Journal)
10. Loannis Apostolopoutos et.al (2020) 'deep covid: predicting covid-19 from chest c-ray images using deep transfer learning'. (Springer - Journal)
11. Sherbin Minace (2020) 'Deep covid: predicting covid-19 from chest c-ray images using deep transfer learning'. (Elsevier - Journal)

Symptom Based Explainable Artificial Intelligence Model For Leukemia Detection And CNN Based Image Processing

Geethu S Anand
Dept. of Biomedical Engineering
KMCT College of Engineering for Women Calicut, India
kmw19bm020@gmail.com

Nimisha KV
Dept. of Biomedical Engineering
KMCT College of Engineering for Women Calicut, India
nimishakv99@gmail.com

Akshaya P
Dept. of Biomedical Engineering
KMCT College of Engineering for Women Calicut, India
akshayagireesh9@gmail.com

Nafeesathul Nasariya
Dept.of Biomedical Engineering
KMCT College of Engineering for Women Calicut, India
nasriyanazar0987@gmail.com

Shibitha K P
Dept.of Biomedical Engineering
KMCT College of Engineering for Women Calicut, India
shibithakp@kmctcew.ac.in

Abstract— Leukemia is a disease that is fatal by nature and is also exceedingly expensive to treat. However, early leukemia discovery can save lives and money for those affected, particularly youngsters, for whom leukemia is a relatively prevalent cancer type. In this study, we propose a supervised machine-learning model that accurately predicts the probability of early-stage leukemia based solely on symptoms. The suggested model is built using original data gathered from two significant hospitals in Bangladesh. With the help of a specialised doctor, a survey of leukemia and non-leukaemia patients is used to collect sixteen dataset features. Our explainable supervised model uses a decision tree classifier as its foundation to generate explainable rules and many superior results to those of existing methods.

Keywords-DT; CNN; FC

I. INTRODUCTION

Blood cancer (leukemia) is one of the leading causes of human death. The speed of recovery depends largely on early detection and diagnosis of the disease. The main cause of leukemia is that the bone marrow produces too many abnormal white blood cells. Imaging microscopy is performed by a hematologist using a sample of human blood. From there, microscopic colour imaging, image segmentation, clustering and classification are required. Microscopic imaging can detect blood cancer with visible immature white blood cells in several different ways. Early and rapid detection of leukaemia can significantly help doctors provide appropriate treatment for their patients. First, the segmentation step is achieved by separating leukocytes from other blood components. H. Red blood cells and Platelets, can be distinguished using statistical parameters such as mean and standard deviation. Geometric features such as the area and circumference of the leukocyte nucleus are studied to predict the diagnosis of leukemia. The proposed methodology uses decision trees to detect cancer stages and detect them early. The tests and results showed promise in detecting cancer cells with 90% accuracy. A decision tree classifier creates a structured decision flow by making decisions based on selected characteristics at each decision node. Features are selected based on data content. DT classifiers are used to generate appropriate rules for explainable AI. Different types of properties have been found in leukaemia prediction and leukaemia screening. It should be noted that early detection of leukaemia is possible only based on symptoms. The relationships between symptoms and cancer types have been analyzed using many methods, but most often they are used together with advanced features of other predictive models. Leukaemia is a blood cancer characterized by the rapid growth of abnormal blood cells. This uncontrolled growth occurs in the bone marrow, where most of the body's blood is formed. Leukemic cells are usually immature (still developing) white blood cells. The term leukemia comes from the Greek words white (euros) and blood (pancreas). Unlike

other cancers, leukaemia does not usually form a mass (tumour) that shows up on imaging tests such as X-rays and CT scans. There are many types of leukemia. Some are more common in children, while others are more common in adults. Bone marrow is a soft, spongy tissue within the lumen where the body's blood cells form. Blood cells go through several stages before they reach their fully mature form. Mature normal blood cells are Red blood cells: Cells that carry oxygen and other vital substances to all body tissues and organs. White blood cells: cells that fight infection. Platelets are cells that help blood clotting. These blood cells become hematopoietic stem cells (hero = blood, priests = to make). Stem cells arise from either myeloid (MAI-uh-loyd) or lymphoid (LIM-food) cells. If the development of blood cells continues normally, the mature forms of these cells are Bone marrow cells develop into red blood cells, Platelets, and some types of white blood cells (basophils, eosinophils and neutrophils). Lymphocytes develop into certain types of white blood cells (lymphocytes and natural killer cells). But in leukemia, one of the developing blood cells begins to grow out of control. These abnormal cells, called leukemia cells, begin to take up space in the bone marrow.

II. LITERATURE SURVEY

In 1992 Naomi S Altman proposed The creation of kernel and nearest-neighbour nonparametric regression Nonparametric regress of strategies for estimating a regression curve without making sturdy assumptions approximately the form of the real regression feature. These strategies are consequently beneficial for constructing and checking parametric models, in addition to for records description. Kernel and nearest-neighbour regression estimators are nearby variations of univariate place estimators, and to be able to without problems be added to starting college students and consulting customers who're acquainted with such summaries because the pattern suggests and median[1].

In 2005, TMarkiewicz, S.Osowski et al proposed Automatic Recognition of the blood molecular of myelogenous leukaemia through the usage of SVM. In this gadget routinely figuring out leukaemia blast molecular the usage of a photo of the bone marrow aspirate is defined with inside the have a look at. Support Vector Machine is utilized by the popularity because the classifier and it takes gain of the feel geometry, and histogram associated traits of the blood molecular photo. The studies targeted the manufacturing and choice of the characteristic for the satisfactory popularity exams figuring out 17 kinds [2].

In 2005 Va Briggitte Leunoe et al Br J Haematol proposed a Prediction of haemorrhage withinside the early level of acute myeloid leukaemia via way of means of float cytometric evaluation of platelet feature Haemorrhage is regularly accountable for the deadly direction of acute myeloid leukaemia (AML). Previously, a couple of platelet feature defects have been diagnosed via way of means of float cytometric evaluation of platelet activation markers in AML. The position of float cytometric evaluation of platelet features in the characterization of prognostic markers of haemorrhage in AML sufferers has now no longer been nicely elucidated. The goal of this potential has a look examine platelet features in 50 AML sufferers at analysis and to evaluate effects with a scientific bleeding score, graded via way of means of not unusual place toxicity criteria [3].

In 2010 Subrajeet Mohapatra and Dipti Patra proposed Automated leukaemia detection through the usage of Hausdorff size in blood microscopic photos A lovely lymphocytic leukaemia (ALL) is a malignant ailment characterised via way of means of the buildup of lymphoblast withinside the bone marrow. An stepped forward scheme for ALL detection in blood microscopic photos is supplied right here. In this have a look at capabilities i.e. Hausdorff size and contour signature are hired to categorise a lymphocytic molecular withinside the blood photo into ordinary lymphocyte or lymphoblast (blasts). In addition form and texture capabilities also are extracted for a higher category. Initial segmentation has executed the usage of K-manner clustering which segregates leukocytes or white blood cells (WBC) from different blood additives i.e. erythrocytes and platelets. The effects of K-manner are used for comparing a person's mobileular form, texture and different capabilities for the very last detection of leukaemia. Fractal capabilities i.e. Hausdorff size applied for measuring perimeter roughness and for this reason classifying a lymphocytic molecular nucleus. A general of 108 blood smear photos have been taken into consideration for characteristic extraction and the very last overall performance

assessment is demonstrated with the effects of a haematologist [4]

In 2010 S-H Hsieh , Z Wang, P -H Cheng I Shun Lee Proposed Leukemia most cancers category primarily based totally on the guide gadget right here classify most cancers with Leukemia most cancers of clinical diagnostic records. Information benefit has been tailored for characteristic selections. A Leukemia most cancers version that makes use of Information Gain primarily based totally on Support Vector Machines (IG-SVM) strategies and upgrades to evaluate, and interpret the most cancers category. The experimental effects imply that the SVM version illustrates the best accuracy of classifications for Leukemia and most cancers [5].

In 2011, Udi Zelig, Shaul Mordechai, and George Shubinsky, Early Screening and Monitoring of Childhood Acute Leukemia Using Infrared Biochemical Analysis of Peripheral Blood Mononuclear Cells, designed Recent advances in the chemotherapy treatment of childhood acute leukaemia have improved remission rates by about 80%. When developing new drugs and treatment protocols tailored to specific individual patients, a simple diagnostic tool is needed to update patient responses. In this clinical study, we investigated the utility of Fourier transform infrared microscopy (FTIR-MSP) in the prescreening and monitoring of leukaemia patients receiving chemotherapy. It is a simple diagnostic tool to monitor the patient's response. the daily basis is necessary. Later, new drugs and therapeutic areas were developed that were tailored to the specific, unique patient. In this study, Fourier transforms infrared microscopy (FTIR-MSP) was used to examine and monitor a leukaemia patient. Thus, the method involves samples taken from a leukaemia patient before treatment. Decreased lipid and increased DNA absorption in PBWC and other groups of the disinfection spectrum. These are powerful indicators of leukaemia. In addition, FTIR-MSP offers a pre-indicator of patient response compared to current technology [6].

In 2011, Mohammad Sorowar Hossain, and Mohd S Iqbal proposed a retrospective analysis of more than 500 cases of haematological malignancies diagnosed in Bangladesh from 10 speciality hospitals. The global burden of cancer is increasing, especially as poor countries like Bangladesh experience rapid ageing. To date, comprehensive descriptions of diagnosed cancer groups including haematological malignancies in Bangladesh are lacking. This indicates differences in population distribution compared to other situations where the incidence of non-Hodgkin lymphoma may be lower. Affected women may be too few. Further research is needed on the epidemiology, genetics and potential environmental risk factors in this rapidly ageing country [7].

In 2014 Mashiat Fatma and Jaya Sharma Proposed the Identification and classification of acute leukaemia using neural network Leukemia, a subdivision of cancer, develops in human blood and the bone marrow. The reason behind this is the expeditious and sudden formation and accumulation of WBCs in blood. Identification & diagnosis of these types of abnormalities by humans is difficult and may lead to misidentification. Therefore an automatic system for the identification and classification would be of great help. For this, different features are extracted from the input images and then based on these features a data set for the input image is created. This data set is then utilized as input data to a neural network for training purposes. This neural network is designed and created to categorize the images according to their corresponding leukaemia type [8].

III.METHODOLOGY

Leukemia cells are blood cells that are underdeveloped and show abnormal behaviour of growing and dividing in an indomitable manner. Based on the cell types leukemia is broadly categorized in to two types: lymphocytic (or lymphoblastic) and non-lymphocytic (or myeloid). They can occur in chronic or acute form. A body with leukaemia cells develops signs and symptoms. However, often it is diagnosed at a later stage, thus making the treatment more difficult. An early screening of leukaemia can make a great difference by reducing the cost and related fatality rate and also improving the quality of life among the patients. This work proposes a symptom-based early detection of leukaemia.

Decision tree algorithms fall into the category of supervised learning. Decision trees use a tree representation to solve the problem where each leaf node corresponds to a class label and attributes are represented by the inner nodes of the tree. Decision trees allow individual attributes to represent arbitrary Boolean functions.

Decision trees are considered widely used in data science. It is an important and proven tool for making decisions in complex scenarios. Ensemble techniques such as decision trees and random forests are commonly used In machine learning. A decision tree is a type of supervised learning algorithm that continuously classifies data into different categories based on certain parameters. A decision tree, as the name suggests, is like a tree structure in which flow operates on the principle of conditions. It is efficient and has powerful algorithms used for predictive analytics. It mainly has attributes including internal nodes, branches, and leaf nodes. Each inner node contains an attribute "test", branches contain test conclusions, and each leaf node represents a class label. This is the most commonly used algorithm when it comes to supervised learning techniques.

CNN BASED IMAGE PROCESSING

A convolutional neural network (CNN) is a special architecture of artificial neural networks, proposed by Yann LeCun in 1988. CNN uses some features of the visual cortex.

One of the most popular uses of this architecture is image classification. For example Facebook uses CNN for automatic tagging algorithms, Amazon for generating product recommendations and Google for search through among users photos. Data set according to the World Health Organization (WHO) stroke is the 2nd leading cause of death globally, responsible for approximately 11% of total deaths. This dataset is used to predict whether a patient is likely to get stroke based on the input parameters like gender, age, various diseases, and smoking status. Each row in the data provides relavant information about the patient. Yann LeCun invented the convolutional neural network (CNN) in 1988 as a unique architecture for artificial neural networks. Some visual cortex properties are used by CNN. Image categorization is one of the most widely used applications for this architecture. For instance, Facebook employs CNN for its automatic tagging algorithms, Amazon for its product suggestion engine, and Google for its user photo search. According to data from the World Health Organization (WHO), stroke is the second most common cause of death worldwide, accounting for around 11% of all fatalities. Based on inputs including gender, age, numerous diseases, and smoking status, it his dataset is used to determine whether a patient is likely to get a stroke. Each row of the data contains pertinent patient information.

IV. BLOCK DIAGRAM

The block diagram consists of the following steps:

- Data collection
- Data preprocessing
- Split data
- Evaluate model
- Feature selection

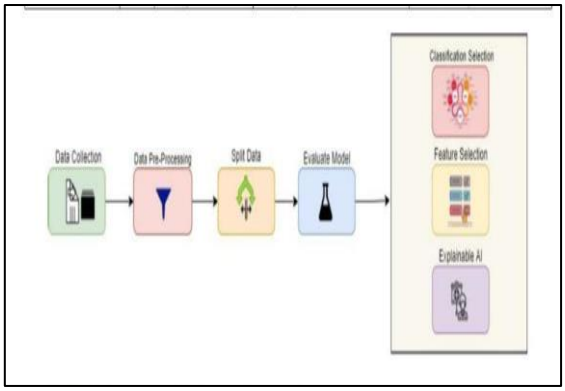

Fig.1 Block diagram

To answer specified research questions, test hypotheses, and assess results, data collection is the act of acquiring and measuring information on variables of interest in a systematic and defined manner. A paper questionnaire or a system for computer-assisted interviews are examples of the types of tools/devices that are used to collect data and are referred to as "data gathering tools." Case studies, checklists, interviews, sporadic observation, surveys, and questionnaires are some of the instruments used to collect data. To ensure accuracy and facilitate data analysis, the primary goal of data collection is to gather information in a measured and systematic manner.

Step 1: Identify the purpose of your study.

Step 2: Select the data collection strategy.

Step 3:Plan your data collection methods in step three.

Step 4: Gather the information

V . FLOW CHART

The flow chart represents two sections:

a.Training data

b. Test data

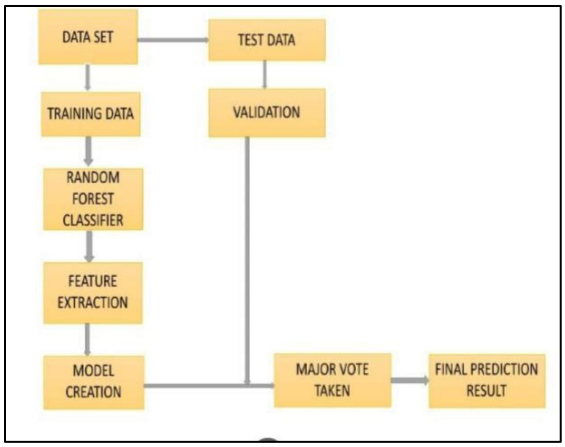

Fig. 2 . Flowchart of decision tree

The data set is first preprocessed and divided into two halves. Random Forest Classifier has trained on the training set of data. The model will then predict leukaemia. A large number of decision trees are built during the training phase of the random forests or random decision forests ensemble learning approach, which is used for classification, regression, and other tasks. The class that the majority of the trees chose is the output of the random forest for classification problems. The mean or average prediction of each tree is returned for regression tasks. The tendency of decision trees to overfit their training set is corrected by random decision forests. Although they frequently outperform decision trees, gradient-boosted trees are more accurate than random forests.

Flow Chart of CNN

CNN's image classifiers process and assign a category to each input image after processing it. An input image is viewed asdepending on the resolution of the image, a collection of pixels. Technically, each input image will be passed through a series of convolution layers with filters (Kernals), Pooling, fully connected layers (FC), and apply Softmax function to classify an object with probabilistic values between 0 and 1.

The input image should be loaded first, followed by image processing and prediction using the loaded model. If the value is zero, it will indicate that the leukaemia is benign. And the benefit is that it anticipates the early stage. And when the number is two, leukemia's early stages are predicted. and if the value is three, leukaemia is predicted to be in the pro stage. then comes a standstill.

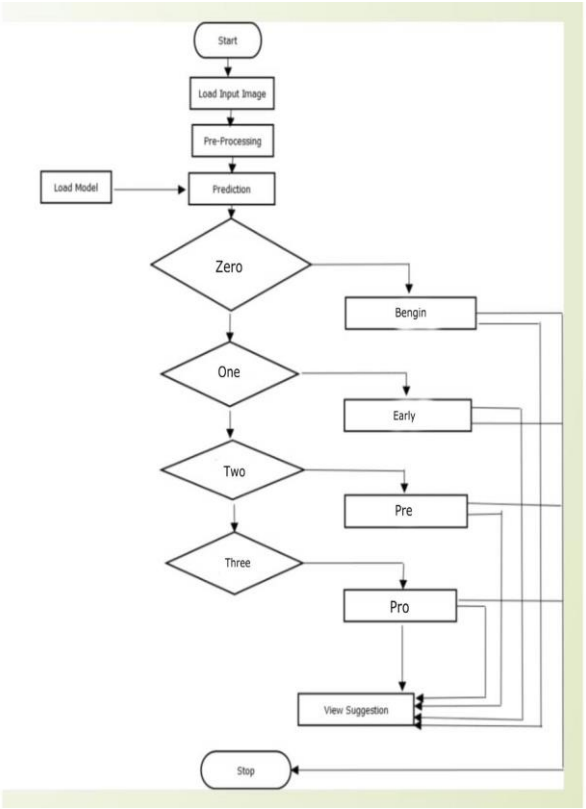

Fig. 3. Flowchart of CNN

LAYERS OF CNN

Convolution Layer: The first layer to extract features from an input image is convolution. Convolution keeps the connection. By identifying visual features using small input data squares, between pixels. It is a mathematical process that requires two inputs, such as an image matrix and a kernel or filter.

In convolution, the first layer to extract features from an input image is convolution. Convolution learns visual features from small input data squares, preserving the link between pixels. It is a mathematical operation that takes two inputs such as image matrix and a filter or kernel. Pooling Layer: When the photos are too huge, the section on pooling layers would lower the number of parameters. Spatial pooling, also known as sub sampling or down-sampling, lowers the dimensionality of each map while preserving crucial data. Space pooling can take many distinct forms.

Types:

i) Max Pooling

ii) Average Pooling

iii) Sum Pooling

The largest element in the corrected feature map is selected using max pooling. The average pooling could be taken instead of just the largest element. Sum pooling is the term used to describe the total of all feature map elements are fully connected layer .We flattened our matrix into a vector and fed it into a fully connected layer like a signal. This layer is known as the FC layer network of neurons. Choose your parameters, apply filters in steps, and add padding if necessary. Apply ReLU activation to the image and perform convolution on the matrix. Reduce the size of the dimensionality through pooling. Convolutional layers can be added till you're happy. Feed the output into a fully linked layer after flattening it (FC Layer). Classify photos by utilising an activation function and logistic regression with cost functions. function

VI. RESULT AND CONCLUSION

In this paper, we have presented an explainable machine-learning model for leukemia detection. In our experiments, we have seen that simple and explainable model like the decision tree classifier performs the best results when compared to the other more sophisticated methods. The decision tree analysis is used as the last phase to forecast leukaemia. For the detection of leukemia we are collecting 16 symptoms like fever, shortness of breath, bleeding, fatigue, etc A non-parametric supervised learning algorithm called a decision tree is used for tasks involving classification and regression. It is therefore more precise than other algorithms.. Decision tree algorithm shows 99% of accuracy and CNN shows 86%accuracy. In this paper CNN algorithm is used for image prediction. It is used to predict the 4 stages of patients are benign, early stage, pre, pro.

Deep learning discovers a number of opportunities and hidden patterns that can help the medical industry deliver high-quality patient care. Artificial intelligence and machine learning have received a lot of attention in recent years. Even deep learning has now established a commercial niche in this sector and is slowly growing its share. Deep learning's function in healthcare is amply proved by its current and upcoming uses, and additional study may broaden the field's possible application areas.

REFERENCES

1. N. S. Altman,(1992), ''An introduction to kernel and nearest-neighbor nonparametric regression,'' Amer. Statist., vol. 46, no. 3, pp. 175–185.
2. T. Markiewicz, S. Osowski, B. Marianska, and L. Moszczynski,(2005) ''Automatic recognition of the blood cells of myelogenous leukemia using SVM,'' in Proc. IEEE Int. Joint Conf. Neural Netw., vol. 4, pp. 2496–2501.
3. E. B. Leinoe, M. H. Hoffmann, E. Kjaersgaard, J. D. Nielsen, O. J. Bergmann, T. W. Klausen, and H. E. Johnsen,(2005), ''Prediction of haemorrhage in the early stage of acute myeloid leukaemia by flow cytometric analysis of platelet function,'' Brit. J. Haematol., vol. 128, no. 4, pp. 526–532.
4. S. Mohapatra and D. Patra, (2010), ''Automated leukemia detection using Hausdorff dimension in blood microscopic images,'' in Proc. INTERACT, pp. 64–68.
5. S.-H. Hsieh, Z. Wang, P.-H. Cheng, I.-S. Lee, S.-L. Hsieh, and F. Lai, (2010)''Leukemia cancer classification based on support vector machine,'' in Proc. 8th IEEE Int. Conf. Ind. Informat., pp. 819–824.
6. U. Zelig, S. Mordechai, G. Shubinsky, R. K. Sahu, M. Huleihel, E. Leibovitz, I. Nathan, and J. Kapelushnik, (2011),"Pre-screening and followup of childhood acute leukemia using biochemical infrared analysis of peripheral blood mononuclear cells", Biochim. Et Biophys. Acta (BBA) Gen. Subjects, vol. 1810, no. 9, pp. 827–835.
7. M. S. Hossain, M. S. Iqbal, M. A. Khan, M. G. Rabbani, H. Khatun, S. Munira, M. Miah, A. L. Kabir, N. Islam, T. F. Dipta, and F. Rahman, (2014),''Diagnosed hematological malignancies in Bangladesh—A retrospective analysis of over 5000 cases from 10 specialized hospitals,'' BMC Cancer, vol. 14, no. 1, pp. 1–7.
8. M. Fatma and J. Sharma, (2014), ''Identification and classification of acute leukemia using neural network,'' in Proc. Int. Conf. Med. Imag., m-Health Emerg. Commun. Syst. (MedCom), pp. 142–145.

Image Processing Based Intelligence Stroke Prediction Using CNN

Krishnendu M A
Dept. of Biomedical Engineering
KMCT College of Engineering for Women Calicut, India
krishnenduma542@gmail.com

Sneha P K
Dept. of Biomedical Engineering
KMCT College of Engineering for Women Calicut, India
pksneha282@gmail.com

Hina Ayisha V
Dept. of Biomedical Engineering
KMCT College of Engineering for Women Calicut, India
hinaayisha8@gmail.com

Fathima Nourin A K
Dept. of Biomedical Engineering
KMCT College of Engineering for Women Calicut, India
nourinfathima541@gmail.com

Abstract—Active primary prevention and early identification of prognostic signs are crucial since stroke disease frequently results in death or major disability. Ischemic and hemorrhagic strokes are two types of stroke disorders that should be avoided. By form of emergency treatment, such as the delivery of thrombolytic or coagulants. First and foremost, it's critical to recognize the early warning signs of stroke in real time, which vary from person to person, and to receive expert care from a medical facility within the appropriate treatment window. Prior research, however, has concentrated on creating guidelines for clinical or acute treatment following the onset of stroke rather than identifying its predictive symptoms. Recent investigations, in particular, have used image analysis techniques including Magnetic Resonance Imaging (MRI) and Computed Tomography (CT), which are expensive and difficult to use for real-time diagnosis. Since stroke is a dreadful disease the early detection as well as prediction of level of stroke is important. The CNN model using raw data of ECG and PPG showed satisfactory prediction accuracy, Electrocardiogram (ECG) images used here as dataset have an accuracy of 93% and Photoplethysmography (PPG) images have an accuracy of 100 %. As a result, the real-time prediction of the elderly stroke patients simultaneously showed high prediction accuracy and performance.

Keywords- CNN;LSTM;PPG;ECG;AI;BMI

I. INTRODUCTION

The greatest cause of disability in adults and the elderly including many social and financial challenges is stroke. As stroke happens when a blood vessel in the brain bursts and bleeds or when the blood supply to the brain is cut off. It is impossible for blood and oxygen to reach the brain tissues because of the rupture or obstruction. Stroke frequently results in death or severe disability.

There are two main causes of stroke, a blocked artery (ischemia stroke) or leaking or bursting of a blood vessel (hemorrhagic stroke) . Due to the fact that it might, in extreme situations, result in death in today's society and could induce physical and mental diseases like hemiparesis, apraxia of speech, ataxia, visual impairment, consciousness impairment, and dementia are some of the symptoms. In most cases, patients with stroke have been observed 3 to have abnormal bio-signals (i.e., ECG). Stroke diseases can be minimized by emergency treatment such as thrombolytic or coagulant administration. In recent studies,[2] image analysis such as MRI or CT has mostly been used to detect and predict prognostic symptoms in stroke patients, which are expensive and difficult to use for real-time diagnosis. With the help of this paper, thus created a stroke prediction system that uses real-time use of artificial intelligence in biosignals (AI). The multi-modal bio-signals ECG and PPG measured in real-time for elderly people are used in our proposed system, which can predict stroke

prognostic symptoms based on machine learning. This system can also predict the stroke level using age, gender, Body Mass Index (BMI) ratio, living conditions etc.

The proposed project is designing and implementing a stroke disease prediction system with an ensemble structure by using CNN. The level prediction is more accurately done by the Random Forest Classsifier. The real-time prediction of the elderly stroke patients simultaneously showed high prediction accuracy and performance. This device might be viewed as an alternative, inexpensive, real-time diagnostic tool that like heart disease.

II. LITERATURE REVIEW

In [1] Mike Schuster et.al proposed Bidirectional Recurrent Neural Networks .In this research focus an investigating ANN structure for a specific class of issues that are modelled a temporal sequence of input output data pairs . The methodology used here is RNN and BRNN . Advantages of this paper is that through a series of extensive experiments it has been shown that BRNN structure leads to better result than the other ANN structure. The paper investigated that faster development of usual application with better result. The disadvantages of the proposed project is that it does not provide the class sequence with highest probability Over the past few decades, machine learning has gained popularity in areas like as self-driving automobiles, effective web search, speech and image recognition. Successful outcomes slowly permeate our daily lives. A group of artificial intelligence techniques known as machine learning enable the computer to function in a self-learning manner without being explicitly programmed. It is a fascinating and complicated subject that may influence how technology develops in the future.

In [2] Alex Graves et al proposed bidirectional LSTM networks for improve phoneme classification and recognititon. They conducted experiments on both framewise phoneme categorization and identification to further prior work on bi-directional LSTM. They employ a hybrid technique for phoneme recognition, integrative hidden Markov models (HMMs) and recurrent neural network(RNNs) in an iterative training procedure. This enables to compare their results directly and those of a conventional HMM system and provides with insight into the expected effects of bi-directional training on speech recognition. methodology used here is LSTM . It's advantage is they are faster ad more accurate than conventional RNNs.

In [3] J.Allen et.al proposed photoplethy smography and its application in clinical physiological measurement by this the assessment of the cardiovascular system. It has widespread clinical application. By this study they conclide current and potential clinical application in physiological monitoring vascular assesment and autonomic function. Disadvantages of this study are blending the standardization of measurements, improving repeatability and establishing comprehensive normative data ranges for comparison with patients and for evaluating response to therapy.

In [4] Aditya khoshla et.al proposed an integrated machine learning approach to stroke prediction on the Cardiovascular Health Study (CHS) dataset. Compare the COX proportional hazards model with a machine learning strategy in this study to predict stroke with regard to particular issues, we focus on the feature selection prediction and data imputation issues that frequently arise in medical datasets. The learning methods utilized for stroke prediction are support vector machines and margin-based censored regression (MCR). Thus conducedt a thorough comparison of machine learning techniques with the COX proportional hazards model and demonstrate that for both binary stroke prediction and stroke risk estimate, the machine learning techniques significantly outperform the COX model. It can be used for identifying potential risk factors for disease without performing clinical trial.

In [5] Shu Zhang et.al proposed Bidirectional Long Short-Term memory Networks for relation classification. Here proposed bidirectional Long Short-Term Networking, (BLSTM) to model the sentence the complete and sequential information about all the words. The methodology include initial feature extraction , future embedding, BLSTM based sentence level representation, constructing feature vector ,classifying, The experiments findings demonstrate that state of-the art performance can be attained even with just words embedding as an input feature. The performance of the relationship classification could be further enhanced by importing more features.

In [6] Jinli Ite et.al proposed p wave indices and risk of ischemia stroke in this paper atrial cardiomyopathy is associated with an increased risk of ischemia stroke. Electroencephalographic measurements such as p wave terminal force in level v1,p wave deviation and maximal p-wave are have been utilized to evaluate left atrial anomalous connected to the emergence of atrial fibrillation . The methodology used here is the relationship between p-wave indices and stroke risk are looked up in the databases. The disadvantages are systematic review and meta-analysis has same potential limitations.

In [7] Joseph M Bumgarner et.al proposed" smart watch algorithm for automated detection of atrial fibrillation". The purpose of this study is to examine whether, the KB could accurately differentiates since rhythm (SR) from AF compared with physician- intrepreted 12 lead ECG, and KB recordings. Patients with AF who had previously sought cardioversion(CV) were included. Patients underwent a KB recording and pre-CV ECG if CV was done, a post-CV ECG and KB recording were both obtained physician reviewed ECGs were contrasted them with ECG reading. K, specificity and sensitivity.

In [8] Tae-Young Kim et al. proposed a method for "Predicting Residential Energy Consumption Using CNN-LSTM Neural Networks." The authors propose a combination of Convolutional Neural Networks (CNNs) and Long Short Term Memory (LSTM) networks to predictresidential energy consumption. The algorithm is able to forecast complex electric energy usage with the best performance in all situations at the minute, hour, and daily level compared to other strategies. The authors also report that their weekly unit resolution analysis reveals that air conditioners and electric water heaters have the most significant impact on the prediction model. The proposed method has the advantage of minimizing energy waste and economic loss caused by unplanned power plant operation through the management of increasing energy consumption. Overall, the policy aims to introduce a power consumption prediction method to minimize costs.

In [9] M. Grandini et.al proposed matrices for multi-class classification an overview classification tasks in machine learning involving more than two classes are known by the name of "multi-class classification. By this they review a list of the most promising multi-class calssification matrices. A classification model gives as the probability of belonging to a specific class for each possible units.in order to remove any intrinsic characteristic of the dataset, cohens kappa uses the expected accuracy, which is a measure representing the dependence derived by chance between the predicted and the true classification measure. The value represents the dependence between the predicted and the true classification. This makes is possible to compare various models used on various data samples.

In [10] Minhaz Uddin Emon et.al performed performance analysis of machine learning approaches in stroke prediction .We suggest an early stroke illness prediction utilising several machine learning methods with the hypertension occurrence age, body mass, average glucose level, smoking status, index level, heart disease, and history of stroke. Here, the section is divided into three parts they are Data description, machine learning classifiers and evaluation matrices, implementation procedures. The performance evaluation reveals that weighted voting, provided as the highest accuracy of about 97% compared to the commonly used other machine learning algorithms. It will help to reduce stroke in our life.

In [11] Sejin Park et.al proposed Machine-Learning-Based elderly stroke monitoring system using electroencephalography vital signs .In this paper they designed and implement a health monitoring system that can predict the precursors of stroke diseases in the elderly in real time during daily walking. The methodology used here is machine learning . The raw EEG data from six channels were preprocessed via fast Fourier transform. From the raw spectra, the raw EEG power values are extracted. The extracted raw spectrum includes alpha, beta, gamma, delta, theta , low beta, high beta, and theta to beta ratio. These are taken from six measurement locations(Fz,Oz,T1,T8,C1 and C2). That means here 66 important attributes were used in total. By this prediction and analysis model in machine-learning attempts to analyze the results of real time predictions and experiments of stroke disease in order to people. In this study, they developed and put into use a health monitoring system that can foretell real-time detection of older patients' stroke-related disorders while routine walking. Here, machine learning is the methodology. The raw EEG power levels are taken from the raw

spectra. Alpha, beta, gamma, delta, theta, low beta, high beta, and theta to beta ratio are all included in the retrieved raw spectrum. These were obtained from six different measuring sites (Fz, Oz, T1, T8, C1 and C2). This suggests that a total of 66 significant qualities was employed here. This prediction and analysis model for machine learning makes an effort to examine the outcomes of real-time predictions and tests for stroke disease.

In [12] Jong Arun Jun et.al proposed deep learning based stroke disease prediction system using real time Bio signals .By doing so, they provided a fresh approach that enables the immediate implementation of deep learning models on unstructured data. EEG data not using the EEG's frequency characteristics. The suggested deep learning based model for predicting the occurrence of stroke disease was created and trained using real-time EEG sensor data. Different deep-learning models (LSTM, Bidirectional LSTM, CNN-LSTM) were implemented and compared. The experimental outcomes shown that the CNN, Bidirectional LSTM model can predict stroke with 94.0% accuracy, and low FPR(60%) and FNR(5.7%) using the raw EEG data , demonstrating great trust in our system. These research findings show that non-invasive technique that can quickly assess brain waves alone can be used to forecast and monitor stroke disorders in real time, while people are going about their normal lives.

III. METHODOLOGY

Over the past few decades, machine learning has gained popularity in areas like as self-driving automobiles, effective web search, speech and image recognition. Successful outcomes slowly permeate our daily lives. A group of artificial intelligence techniques known as machine learning enable the computer to function in a self-learning manner without being explicitly programmed. It is a fascinating and complicated subject that may influence how technology develops in the future.

A) Techniques and Tools

For this project, Python syntax was used hence utilised Keras, a Python-based high-level neural network API, as my framework. But for Keras to function, it needs alow-level operations backend Consequently, Google's Tensor Flow software library was deployed here used PyCharm as a development environment. For visualisation, used Matplotlib. A machine learning technique called a neural network is based on the organisation and operation of biological systems.

Neural systems in an effort to imitate the functions of the brain, Warren McCulloch and Walter Pitts developed this idea in 1943. Neurons are small, discrete units that make up neural networks. A number of groupings of strata make up the location of neurons. Each layer's neurons are interconnected with those in the following layer.

Along these molecules, data travels from the input layer to the output layer. Every node works on a straightforward mathematical calculation individually. The data is then sent to all of the nodes to whom it is connected. The last wave of neural networks came in connection with the increase in computing power and the accumulation of experience.

Deep learning resulted from this, and more advanced technical neural network structures complicated and able to successfully complete a variety of activities that were previously impossible. A good illustration is image classification.

B) Convolutional Neural Networks And Image Classification

A convolutional neural network (CNN) is a special architecture of artificial neural networks, proposed by Yann LeCun in 1988. CNN uses some features of the visual cortex.

One of the most popular uses of this architecture is image classification. For example Facebook uses CNN for automatic tagging algorithms, Amazon for generating product recommendations and Google for search through among users photos. Data set according to the World Health Organization (WHO) stroke is the 2nd leading cause of death globally, responsible for approximately 11% of total deaths. This dataset is used to predict whether a patient is likely to get stroke based on the input parameters like gender, age, various diseases, and smoking status. Each row in the data provides relavant information about the patient. Yann LeCun invented the convolutional neural network (CNN) in 1988 as a unique architecture for artificial neural networks. Some visual cortex properties are used by CNN. Image categorization is one of

the most widely used applications for this architecture.

For instance, Facebook employs CNN for its automatic tagging algorithms, Amazon for its product suggestion engine, and Google for its user photo search. According to data from the World Health Organization (WHO), stroke is the second most common cause of death worldwide, accounting for around 11% of all fatalities. Based on inputs including gender, age, numerous diseases, and smoking status, it his dataset is used to determine whether a patient is likely to get a stroke. Each row of the data contains pertinent patient information.

C) Flow Chart

CNN's image classifiers process and assign a category to each input image after processing it. An input image is viewed asdepending on the resolution of the image, a collection of pixels. Technically, each input image will be passed through a series of convolution layers with filters (Kernals), Pooling, fully connected layers (FC), and apply Softmax function to classify an object with probabilistic values between 0 and 1.

This is done in order to train and test deep learning CNN models.

Convolution Layer: The first layer to extract features from an input image is convolution. Convolution keeps the connection. By identifying visual features using small input data squares, between pixels. It is a mathematical process that requires two inputs, such as an image matrix and a kernel or filter.

In convolution, the first layer to extract features from an input image is convolution. Convolution learns visual features from small input data squares, preserving the link between pixels. It is a mathematical operation that takes two inputs such as image matrix and a filter or kernel.

Pooling Layer: When the photos are too huge, the section on pooling layers would lower the number of parameters. Spatial pooling, also known as sub sampling or down-sampling, lowers the dimensionality of each map while preserving crucial data. Space pooling can take many distinct forms.

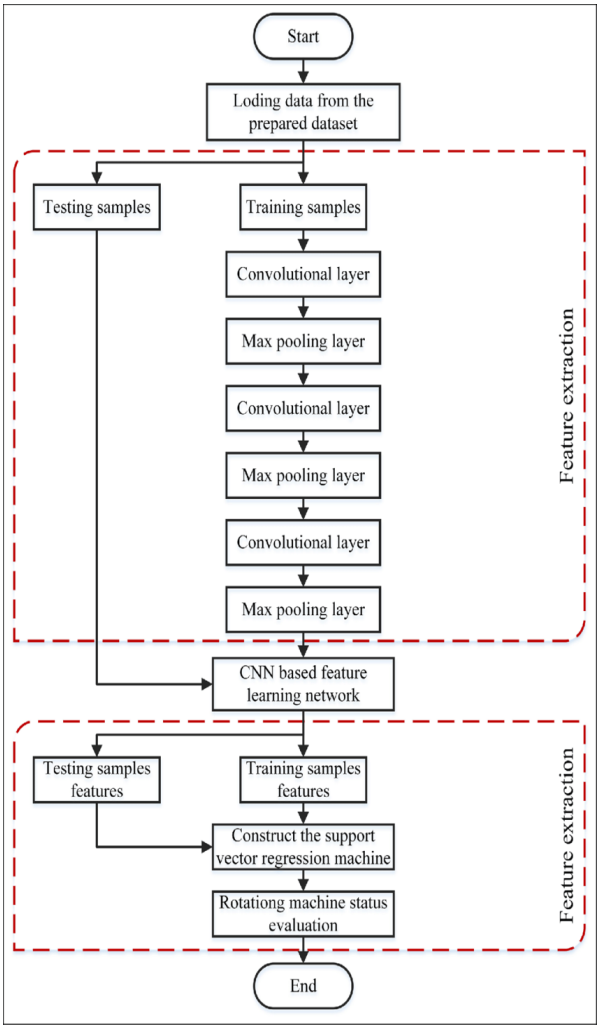

Fig. 1. Architecture of CNN

Types:

i) Max Pooling

ii) Average Pooling

iii) Sum Pooling

The largest element in the corrected feature map is selected using max pooling. The average pooling could be taken instead of just the largest element. Sum pooling is the term used to describe the total of all feature map elements are fully connected layer .We flattened our matrix into a vector and fed it into a fully connected layer like a signal. This layer is known as the FC layer network of neurons. Choose your parameters, apply filters in steps, and add padding if necessary. Apply ReLU activation to the image and perform convolution on the matrix. Reduce the size of the dimensionality through pooling. Convolutional layers can be added till you're happy. Feed the output into a fully linked layer after flattening it (FC Layer). Classify photos by

utilising an activation function and logistic regression with cost functions.

D) Block diagram

The block diagram of the proposed technique is presented in the figure below:

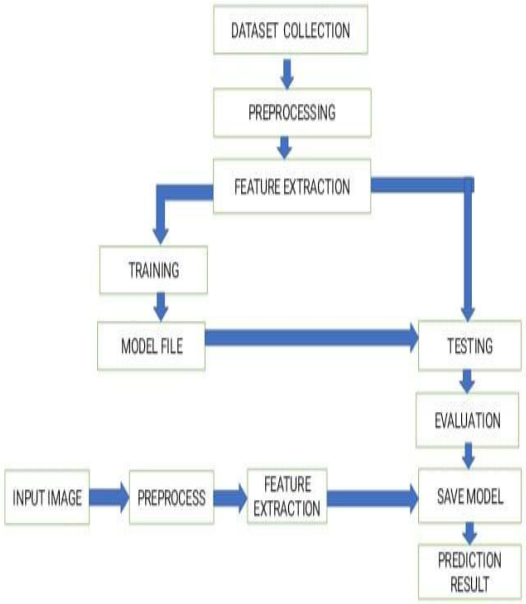

Fig. 2. Blockdiagram

a) Dataset

The ECG and PPG biosignal images are taken as dataset. Dataset are collected from website kaggle.

- **Dataset for ECG testing:**

Fig. 3. Dataset for testing

- **Dataset for ECG training:**

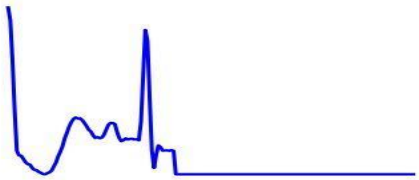

Fig. 4. Dataset for training

- **Dataset for PPG:**

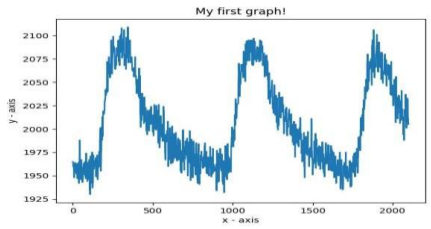

b) Preprocessing

In this stage image undergoes normalization, segmentation, noise reduction, etc. Data preprocessing can refer to manipulation or dropping of data before it is used in order to ensure or enhance performance, and is an important step in the data mining process.

c) Feature Extraction

Preprocessed images are used as the input for feature extraction.Feature extraction helps to reduce the amount of redundant data from the data set.Extracted feature is divided into 40 % of training data and 60% of testing data.

d) Machine Learning and Deep Learning

Give computers "the ability to learn without being explicitly programed". Teaches computer to do what comes naturally tohumans: Learn by example. The 40% of features extracted undergoes training and the 60% of features extracted undergoes testing. After undergoing various processes it shows the result which will display whether the patient is having stroke or not.

FLOW CHART

The flow chart of the proposed technique is presented in the figure below:

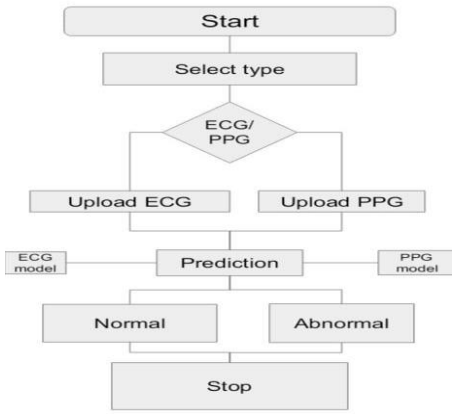

Fig. 5. Flowchart for stroke prediction

V. DECISION TREE

A large number of decision trees are built during the training phase of the random forests or random decision forests ensemble learning approach, which is used for classification, regression, and other tasks. The class that the majority of the trees chose is the output of the random forest for classification problems. The mean or average prediction of each tree is returned for regression tasks. The tendency of decision trees to overfit their training set is corrected by random decision forests. Although they frequently outperform decision trees, gradient-boosted trees are more accurate than random forests.

VI. RESULT AND CONCLUSION

In this paper an approach is used to predict stroke by using CNN algorithm and decision tree algorithms. CNN algorithm is used to predict whether the condition of patient is normal or abnormal. Random forest classifier is used to predict the level of stroke by giving patient datas such as age, gender, BMI ratio, living environment, occupation, blood glucose level etc. The system proposed in this paper has great academic value. It accurately predicts the stroke by measuring ECG and PPG at low cost. Various bio-signal datas collected in daily life can provide objective interpretation information to stroke patients or medical staff with a high recurrence rate. The experimental results verified that this method can be used for practical healthcare services which reduce the after effects of stroke and prevent emergency situations through constant monitoring. A machine learning-based prediction model study was performed using multiple biosignal data, which involves dividing the signal waveform into specific sections, and relatively accurate prediction results and semantic interpretations were obtained using this model.

A system that provides the semantic analysis of diseases in the elderly using multiple biological signal images of ECG and PPG are proposed. Since the system suggested in this research can precisely anticipate the stroke by measuring, it has significant academic significance, low-cost PPG and ECG. Various bio-signal data gathered in daily life can give stroke patients or medical professionals with a high recurrence risk objective interpretation information. According to the experimental findings, this approach can be utilised to provide realistic healthcare services by continuously monitoring patients, lessen the symptoms of stroke and avert emergencies. Multiple biosignal data were used in a machine learning-based prediction model study, which involves segmenting the signal waveform into distinct parts. Relatively accurate prediction results and semantic interpretations were obtained using this model. The approach suggested in this paper allows the semantic analysis of diseases .

REFERENCES

1. M. Schuster and K. K. Paliwal, (1997)"Bidirectional recurrent neural networks," in IEEE Transactions on Signal Processing, vol. 45, no. 11, pp. 2673-2681, Nov. 1997, doi: 10.1109/78.650093.
2. Graves, Alex, Santiago Fernández, and Jürgen Schmidhuber. (2005). "Bidirectional LSTM networks for improved phoneme classification and recognition." International conference on artificial neural networks. Springer, Berlin, Heidelberg,
3. Allen J. Photoplethysmography and its application in clinical physiological measurement. Physiological measurement. 2007 Feb 20;28(3):R1.
4. Aditya khosla,Yu Cao,Cliff Chilung-Yu Lin,Hsu-Kuang Chiu,Junling Hu,Honglak Lee(2010),"Integrated machine learning approach to stroke prediction on the cardiovascular Health Study (CHS) dataset ".
5. Shu Zhang, Dequan Zheng, Xinchen Hu, and Ming Yang. (2015)." Bidirectional Long Short-Term Memory Networks for Relation Classification'. In Proceedings of the 29th Pacific Asia Conference on Language, Information and Computation, pp. 73–78, Shanghai, China.
6. J. He, G. Tse, P. Korantzopoulos, K. P. Letsas, S. Ali-Hasan-Al-Saegh, Kamel, G. Li, G. Y. H. Lip, and T. Liu, ''P-wave indices and risk of ischemic stroke: A systematic review and meta-analysis,'' Stroke, vol. 48,no. 8, pp. 2066–2072, Aug. 2017.
7. Bumgarner, J.M., Lambert, C.T., Hussein, A.A., Cantillon, D.J., Baranowski, B., Wolski, K., Lindsay, B.D., Wazni, O.M. and Tarakji, K.G., 2018. Smartwatch algorithm for automated detection of atrial fibrillation. Journal of the American

College of Cardiology, 71(21), pp.2381-2388.

8. Kim, Tae-Young, and Sung-Bae Cho.(2019). "Predicting residential energy consumption using CNN-LSTM neural networks." Energy 182 pp.72-81.
9. [9] Grandini, Margherita, Enrico Bagli, and Giorgio Visani. "Metrics for multi-class classification: an overview." arXiv preprint arXiv:2008.05756 (2020).
10. M. U. Emon, M. S. Keya, T. I. Meghla, M. M. Rahman, M. S. A. Mamun and M. S. Kaiser, "Performance Analysis of Machine Learning Approaches in Stroke Prediction," 2020 4th International Conference on Electronics, Communication and Aerospace Technology (ICECA), Coimbatore, India, 2020,PP.14641469,doi:10.1109/ICECA49313.2020.9297525.
11. Choi, Yoon-A, Sejin Park, Jong-Arm Jun, Chee Meng Benjamin Ho, Cheol-Sig Pyo, Hansung Lee, and Jaehak Yu. 2021. "Machine-Learning-Based Elderly Stroke Monitoring System Using Electroencephalography Vital Signals" Applied Sciences 11, no. 4: 1761. https://doi.org/10.3390/app11041761.
12. Choi YA, Park SJ, Jun JA, Pyo CS, Cho KH, Lee HS, Yu JH Deep Learning-Based Stroke Disease Prediction System Using Real-Time Bio Signals. Sensors (Basel). 2021 Jun 22;21(13):4269. doi: 10.3390/s21134269. PMID: 34206540; PMCID: PMC8271462.

Early Prediction of Chronic Kidney Disease Using Convolutional Neural Network

Aysha Ashraf
Dept. of Biomedical Engineering
KMCT College of Engineering for Women Calicut, India
ayshaashrafodkd@gmail.com

Fathima Hiba T
Dept. of Biomedical Engineering
KMCT College of Engineering for Women Calicut, India
fathimahiba.19@gmail.com

Jifana Melethil
Dept. of Biomedical Engineering
KMCT College of Engineering for Women Calicut, India
jifanajiff@gmail.com

Varsha K
Dept. of Biomedical Engineering
KMCT College of Engineering for Women
Calicut, India
varshakolliyil00@gmail.com

Nutan Hegde
Dept. of Biomedical Engineering
KMCT College of Engineering for Women
Calicut, India

Abstract-- Chronic kidney disease (CKD), despite advancements in surgical treatment and therapy, is still a health concern. Due to the increased prevalence of Chronic Kidney Disease (CKD), researchers from around the world are actively working to develop effective methods for detecting the condition and creating therapies and preventative measures. The advancement of this chronic condition to the point at which a kidney transplant or dialysis are the sole options for saving the patient's life can be stopped or delayed with early identification and treatment. Thus, the need of precise automated methods to recognize various forms of renal illness has grown critical in recent years. A Sequential CNN has been proposed here to investigate the potential of several deep learning techniques for the early detection of CKD (such as tumor, stone, cyst, and normal) efficiently. The study of the results demonstrates that applying advanced deep learning algorithms is advantageous for clinical decision-making and can help in the early detection of CKD and its linked phases, which slows the course of kidney damage.

Keywords— CKD; CNN; Kidney Diseases; Deep Learning

I. INTRODUCTION

Chronic kidney disease is one of the most severe conditions, where the introduction of an accurate diagnosis should be introduced as soon as possible. Machine Learning technique has been one of the most reliable methods for medical treatment. The doctor can promptly diagnose the ailment with the use of machine learning techniques. Kidney disease is defined as a diverse group of illnesses that impair the urinary organ's function and structure [17]. Here chronic kidney diseases are mainly categorized into four stages, which are normal, cyst, stone, and tumor[3]. If the GFR (Glomerular Filtration Rate) is 60 or greater, that falls within the normal range. A GFR below 60 means kidney disease.

A. KIDNEY CONDITIONS

The two basic types of kidney disease are acute renal injury and chronic kidney disease. Although it can raise a person's chance of developing chronic kidney disease in later life, short-term renal illness typically results in full recovery. Chronic renal disease happens when your kidneys have experienced irreparable damage. To be classified as a chronic kidney disease, the condition must have persisted for at least three months. You may live a normal life with chronic renal illness for a very long time. As the kidney function deteriorates, patients may require kidney replacement therapy such as dialysis or kidney transplantation. These options may become necessary if the kidneys are no longer able to filter the blood effectively. [16]. Numerous factors, including genetics, infections, immune disorders that affect the kidneys, diabetes, and high blood pressure, can contribute to chronic kidney disease. Examples include cystinosis, diabetes, glomerular disease, kidney stones, tumors, and other chronic kidney illnesses. Here, we're considering typical renal problems as

well as chronic kidney diseases including tumors, stones, and cysts.

Kidney cysts are spherical fluid pockets that can develop on or inside the kidneys and are linked to illnesses that may impair kidney function. Kidney cysts, or round fluid pouches, can form on or inside the kidneys. Kidney cysts may be brought on by conditions that may impair kidney function. Simple kidney cysts, on the other hand, are a kind of kidney cyst that develops more commonly. Simple kidney cysts are not cancerous and seldom cause problems. Simple kidney cysts almost seldom provide a threat. They are termed to as "simple" since there is little chance that they will develop into anything more serious. However, certain cysts do have thicker walls, might seem abnormal on X-rays, and can be related to kidney cancer.

kidney stones are the name for the hard deposits of minerals and salts that develop inside your kidney. These deposits are also referred to as "renal calculi." Hard deposits made up of minerals and salts that form inside your kidneys are known as kidney stones. They are also referred to as nephrolithiasis, renal calculi, or urolithiasis. Kidney stones can be caused by a variety of factors such as diet, obesity, certain health conditions, specific supplements, and medications.

A tumor or mass in the kidney is an abnormal growth there. There are benign (non-cancerous) and malignant kidney masses (cancerous). benign kidney masses make up one in four. A greater likelihood of benignity is associated with smaller lumps.

B. DIAGNOSIS

Early detection of renal illness shields the patient from potentially fatal repercussions. To accurately forecast renal disorders, the factors that contribute to them—such as obesity and hypertension, family history, medications and race—must be thoroughly investigated. Typically, standard medical imaging methods like CT scans, bone scans, magnetic resonance imaging (MRI), PET, etc., are used to diagnose kidney illness. This study suggests the use of the Convolutional Neural Network (CNN) for the detection and diagnosis of chronic kidney disease. By employing the convolutional neural network algorithm on the chronic picture data set from the Kaggle respiratory, predictions are produced using this technique [18].

The method involves gathering data, pre-processing, feature extraction, classification, and evaluation. To make the dataset suitable for training, the raw data are first gathered and then pre-processed to remove any unnecessary image data and transform the pictures into the same format in terms of size, kind, etc. The preprocessed data is then used to extract features, which are then split into training and testing data. Test data are used to assess the model's performance and gauge how effectively our preprocessing approach worked after the CNN model has been trained and developed using training data.

II. LITERATURE REVIEW

Numerous researchers are interested in CKD prediction. To create a productive and precise prediction system, they used various classification algorithms.

Basma Boukenze et al. [22] stated a system for the prediction of kidney disease by using multiple machine learning algorithms that are Support Vector Machine (SVM), Multilayer Perceptron (MLP), Decision Tree (C4.5), Bayesian Network (BN) and K-Nearest Neighbor (K-NN). This technique seeks to examine such algorithms that allow you to decide which is the best based on a number of different factors. The most effective algorithms for predicting renal failure in this situation are MLP and C4.5. Making decisions requires the use of data mining tools in the medical industry.

Graham W. Taylor et al. [23] proposed RBMs, or restricted Boltzmann machines, have been applied as generative models for a wide range of data sources. Typically, the contrastive divergence learning approach is used to train RBMs. Choosing how to set the values of numerical meta-parameters takes some actual knowledge. This tutorial is an attempt to share the enormous knowledge in training RBMs that the University of Toronto's machine learning group has gathered over the previous few years with other machine learning researchers.

C. Parker [16] proposed an investigation of binary classifiers' performance indicators. Given a set of test data and two binary classifiers, it should be easy to determine which is superior. Though many of the methods that were previously thought

to be excellent practices for this endeavor have been called into doubt by recent studies. In this work, we compare the effectiveness of classifiers utilizing the same test data using seven different approaches. While the other two are relatively new, the other five have a long history. We look at and extend work showing that one of these strategies is manifestly erroneous before evaluating the applicability of our theoretical approach. The real analysis is then performed utilizing a sizable number of datasets. Our theoretical and empirical research firmly backs one of the more effective strategies.

Hossin M and Sulaimn M N [4] evaluated how important matrices are in choosing and differentiating the best classifier. In general, many classifiers use accuracy as a criterion to determine the best candidates during training. However, a number of characteristics, including bias to majority data, lack of distinctiveness, discrimination, and informativeness, have an impact on accuracy. This essay also merits consideration for various matrices, their flaws, and solutions. Data collection, evaluation, employment, and classification are done in order to choose the right matrices and create an optimized classifier. Here are some more advantageous aspects for matric construction.

Ani R et al. [10] had proposed Decision Support system for diagnosis and prediction of Chronic Renal Failure using Random Subspace Classification. Renal function loss begins the phases of CRF, which progresses to total failure of all kidney functions. If a kidney transplant or the artificial filtering procedure known as dialysis is not performed, this illness will eventually be fatal. collected data set with 400 instances and 25 attributes from the UCI repository. The algorithm that produced the best results from the results was used to construct the clinical decision support system.

Milandeep Arora et al. [12] had proposed Chronic Kidney Disease Detection Analyzing Medical Dataset in weka. In this study, we provide appropriate methods and findings for the precise and early detection of this potentially fatal condition. Although it won't guarantee complete immunity from sickness, it will give you enough time to get treated if you catch it early. With the use of three classification algorithms—naive bayes, J48, and SMO—and the data mining tool WEKA, we were able to reliably identify 24 signs of chronic kidney disease. The medical datasets are introduced to each of the three algorithms separately using the WEKA data mining tool's knowledge flow interface, and the parameters used to compare the outcomes of these three different algorithms are mean absolute error, kappa statistics, and the total number of instances studied correctly or incorrectly.

Veenitha kunwar et al. [9] Proposed CKD analysis using data mining classification technique. The purpose of the project is to use artificial neural networks and Navie Bayes classification methods to predict CKD. According to experimental data utilized in the Rapidminer programme, navie bayes produces results that are more accurate than ANN. Data is gathered from many sources and transformed into the proper format for further processing during data mining. Using data mining techniques, relevant information is retrieved from the data, and assessment is finished in the end.

Bhavya Gudeti et al. [5] had proposed A Novel Approach to Predict Chronic Kidney Disease using Machine Learning Algorithms. Humans develop nephropathy between the ages of 48 and 70 on average. Males are more likely than females to have CKD. India has unfortunately been included in the list of top 17 countries with a high prevalence of Chronic Kidney Disease (CKD) since 2015. CKD is a condition that is characterized by a gradual loss of excretory organ function over time.Early sickness detection and effective treatment may help keep this dreadful disease at bay. Machine learning is finding practical uses in fields like interpreting results from medical research and detecting fraud, among others. The major goal is to compare how well different machine learning algorithms perform, which are mainly based on accuracy. Rcode has been praised in this study's analysis of performance. This study's primary goal is to classify cases of CKD and non-CKD using an analysis of the Chronic Kidney Disease dataset.

Qiuling Suo, et al [24] proposed a system for personalized disease prediction using the CNN-Based Similarity Learning Method. This study focuses on recognizing and ranking patient similarity based on medical information in order to create a model or several models for individuals. Here, the pairwise similarity is measured while simultaneously learning patient representations using a unique time fusion CNN

framework. This approach does customized prediction and measures patient similarity in two stages. Similar to ICD coding, matrix formatting is used to represent patient medical histories. Researchers embed each code into a vector space using a fully linked network layer to learn reduced feature dimensions and interactions between codes.. The sequential relation between subsequent visits is then captured via a process of one-side convolution in the time dimension. The degree of similarity between two patients is evaluated using the similarity score that was acquired. Each patient's unique tailored model is created based on their similarity cohorts. The goal of personalized predictive modeling in healthcare is to identify distinctive patient features and create focused, patient-specific forecast.

Jing Zhaoa, Shaopeng Guc, Adam McDermaidc [1] stated prediction of CKD from EMR data based on Random forest regression. Here, information on demographics, clinical care, and laboratory testing was gathered from primary care clinics. A model using a random forest regression model was then built, and its performance was assessed using discrimination metrics and goodness-of-fit statistics. 61,740 patient cases were examined and analyzed in this instance. Based on the eGFR readings, the patients were divided into groups. Using actual data from electronic medical records (EMRs), this model was created to accurately predict future kidney functions and offer clinical decision support. This model has a great chance of becoming a clinical decision support tool to help clinicians.

Himanshu Kriplani et al. [2]proposed a system for the Prediction of Chronic Kidney Diseases Using Deep Artificial Neural Network Technique. 224 records of chronic renal disease from the UCI machine learning repository were examined in this case. Deep neural networks are used for detection, and they have a 97% accuracy rate when predicting the presence or absence of chronic renal disease. Cross-validation methods are used to put this idea into practice. Here, additional information is necessary for better outcomes. Clinics and hospitals can utilize this technology to predict chronic kidney disease more quickly and digitally.

Ahmed Abdul azeez Et al. [11] Proposed a machine learning model for predicting chronic kidney disease based on internet of things used cloud computing in smart lines In particular, the prediction of diseases in smart cities' IOT devices can be used to convey massive data on chronic kidney diseases and store it in the cloud. Cloud computing and the internet of things play an essential role in health care services. The focus of this paper is on the cloud computing environment's usage in the prediction of CKD as an illustration of health care services. A hybrid intelligent model, combining linear regression (LR) and neural network (NN), has been proposed for predicting Chronic Kidney Disease (CKD) based on cloud-IOT. The hybrid intelligent model has demonstrated an impressive CKD prediction accuracy of 97.8%.

Aditya khamparia ,Gurinder Saini Et al. [6] Proposed chronic kidney disease classification with multimedia data and learning using deep stacked autoencoder network. A novel deep learning framework for categorizing chronic kidney illness is presented in this paper employing multi-media data, stacked encoder models, and a softmax classifier. After the stacked autoencoder assists in collecting the dataset's crucial properties, the softmax classifier is then used to anticipate the final class. This method involves preprocessing the input CKD dataset before using a deep learning trained model and a softmax classifier to train the data. A excellent tool for CKD prognosis with improved accuracy, precision, and specificity will be the developed deep stacked encoder version for CLD classification, keeping in mind that they are critical and clinical domains. This version can be used to classify diseases in big data sets, and the back propagation algorithm can also be utilized to achieve the optimum tuning.

SMK Chaitanya and P. Rajesh Kumar [7] proposed chronic Kidney disease by using Artificial Neural networks and gravitational search algorithm. The diagnosis of this chronic Kidney illness can be made using artificial neural networks and the gravitational Search algorithm, an optimization technique.The data for this study was collected using an MR image from the UCI machine learning repository. To train the neural networks, 80% of the acquired data was used, while the remaining 20% was reserved for testing. This study makes use of the methods K closest neighbor and Artificial Neural Network (ANN+GA), which is similar to gravitational search algorithm (KNN). When these three algorithms are merged, the (GSA+ANN)

technique outperforms the other methods in terms of accuracy, sensitivity, and specificity for classification training performance.

In their study, Ankit and colleagues [8] put forth an analysis of a prediction system for chronic kidney disease (CKD), which involved data cleaning, preprocessing, and effective classification.It introduces a procedure that will result in a more accurate prediction of kidney damage after a diagnosis of CKD. Pre-processing processes are the first step, followed by classification, identification of the instances that were collected, and determination of the glomerular filtration rate (GFR) value. The fact that it has a high accuracy level between 98.30 and 99.5% is one of its key advantages. Additionally, it can forecast a patient's prognosis for CKD based on the test results. GFR value that could help physicians diagnose and treat patients more thoroughly and accurately

Hamida Ilyas, Sajid Ali, et al. [25] introduced chronic kidney disease diagnosis using decision tree algorithms. According to the severity of the condition, they divided CKD into six phases based on the Glomerular Filtration Rate (GFR), which in turn takes into account factors including age, sex, race, and serum creatinine. Using datasets compiled from the medical records of those who have the condition, this study seeks to predict the different stages of CKD. Here, the Random Forest and J48 algorithms are specifically employed to create a model that may be used to detect different stages of CKD with complete medical accuracy. After data analysis, it was discovered that J48 had an accuracy of 85.5% in predicting CKD in all phases, outperforming a random forest.

Fuzhe Ma,Tao Sun, Lingyun Liu and Hongyu jing [19] Proposed detection and diagnosis of chronic kidney disease using deep learning-based heterogeneous modified artificial neural network. This research utilizes the Internet of Medical Things (IoMT) platform to introduce the Hydrogenous Modified Artificial Neural Network (HMANN) for the early detection, segmentation, and diagnosis of Chronic Kidney Disease (CKD). Support vector machines and multilayer perception (MLP) with backpropagation algorithms are the categories under which HMANN falls (BP). The segmentation of the area of interest for the kidneys in the ultrasound image serves as the sole basis on which the suggested algorithm operates. The proposed HMANN technique for kidney segmentation achieves good accuracy while significantly reducing the time to outline the counter. Here, the most popular approach for treating CKD is ANN. Then, digital photos are analyzed using computer vision and machine learning techniques to extract the relevant semantics. The abdomen's images were further divided into left and right components by a radiologist in order to create the reference data set, which is well known for segmentation from the validation and training data sets. The HMANN Method reduces loudness, aids in clearly identifying kidney stones, and reduces excessive exercise.

Gazi Mohammed Ifraz, Muhammad Hasnath Rashid, Tahia Tazin, Sami Bourouis, and Mohammad Monirujjaman Khan[20] proposed a Comparative Analysis for the Prediction of Kidney Disease Using Intelligent Machine Learning Methods. This system offers a framework that makes use of the dataset for CKD prediction. The DT, KNN,

and logistic regression techniques have been applied after feature selection and preprocessing. KNN's total performancein this case falls short of expectations. The final F1 score obtained in this case is 71%. Individual F1-scores are 69 percent for non-CKD and 73 percent for CKD. The study's conclusions suggest that the decision tree method and logistic regression can be used to forecast chronic renal disease more precisely.

Anjan Gudigar,U Raghavendra Et al. [21] Proposed automated detection of chronic kidney disease using Image fusion and graph embedding technic with ultrasound images. According on the estimated glomerular filtration rate (GFR)value echocardiography images of huge hemodynamic change which are secondary to CKD inside the shape of extent, they divided the CKD into five stages here. In order to forecast the various stages of CKD, this study analyses ultrasound pictures of the heart. This technique uses an image and feature fusion approach based on a graph embedding framework to classify the characteristics of the heart chamber. An automated CAD system using a graph embedding framework preprocesses the input ultrasound pictures, extracts the features, and then classifies the features into normal and CKD phases while

taking into account local inherent properties. Additionally, it removes the difficulty of the unbalanced class frequency issue and offers great classification accuracy.

Shahinda Mohammed Musthafa et al. [3] proposed the early prediction of Chronic Kidney Disease (CKD) using a deep belief network. An intelligent categorization and prediction model is suggested in this paper. It employs a modified Deep Belief Network (DBN) classification algorithm, the Softmax activation function, and the Categorical Cross-entropy loss function to forecast kidney-related disorders. In comparison to existing models, the evaluation of the proposed model reveals that it can predict CKD with an accuracy of 98.5% and a sensitivity of 87.5%.

III. METHODOLOGY

Convolutional neural networks are a part of machine learning known as Deep Learning. Because the human brain is too complicated, deep learning systems analyze information on a considerably smaller level than the human brain does (we have about 86 billion neurons in our brain.). For image classification, features must be extracted from a picture in order to identify certain patterns in the dataset. Using an ANN for photo categorization might probably end up being quite costly in terms of computation because of the relatively large trainable parameters. The trainable parameters would be, for example, if we wanted to train the conventional ANN on a 50 * 50 image of a cat to determine if it was a dog or cat. (50*50) 100 visual pixels multiplied by a concealed layer, a bias, a multiplier of two, and 100 output neurons all add up to 2,50,302 . We implement filters while using CNNs. There are several unique categories of filters, each serving a particular function. The sequential data approach is the foundation of this CNN architecture.. Using CT scan images of diverse kidney diseases, including tumor, stone, cysts, and normal, this model was trained from scratch.

A. CNN ARCHITECTURE

This model is known as a sequential CNN model since each layer is connected to the layers above and below it. Three dense layers and five convolutional layers make up the suggested model. The input layer receives input images with a size of 48x48x1.

There are 64 filters in the conditional layer. Each typical layer is followed by a reactivation to enhance learning. An additional layer called maxpooling follows the activation function ReLU. After calculating data for producing a down sampled feature map, the average of two conventional layers is pooled, after two levels of average pooling. There is a dense layer with 1024 neurons that uses the output from the convolutional layer to classify images. Dropout and dense layer come after ReLU activation fiction. Dropout is a method for avoiding a model from over fitting drop out works by randomly setting input units zero with a frequency of rate of each step during training time. Four neurons in the third dense layer, which is supplied to SoftMax, are present. Which is a multinomial probability distribution activation function in the neural network's output layer

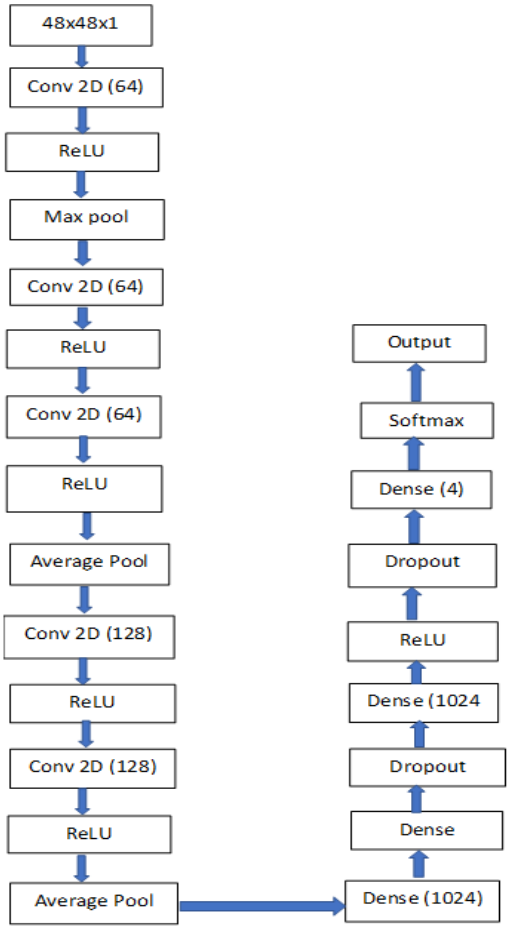

Fig. 1. Architecture of CNN

Here, CNN design is based on the sequential data technique. Using CT scan images of diverse kidney diseases, including tumor, stone, cyst, and normal, this model was trained from scratch.

B. BLOCK DIAGRAM

The input CKD dataset, which includes numerous photographs of both healthy and sick kidneys, goes through a preprocessing step called greyscale conversion. 20% of the data are used for testing, and the remaining 80% are used to train the set. The is educated using CNN initialization. One kind of deep learning network architecture that directly learns from data is convolutional neural networks (CNN or ConvNet). CNNs are especially useful for spotting picture patterns that distinguish objects, groups, and classes. They can be very helpful for classifying signal, time series, and aural data.. The test results are used to develop a model, which is then evaluated. When an input is provided to the Save model that specifies the disease as Stone, Tumor, or Cyst.

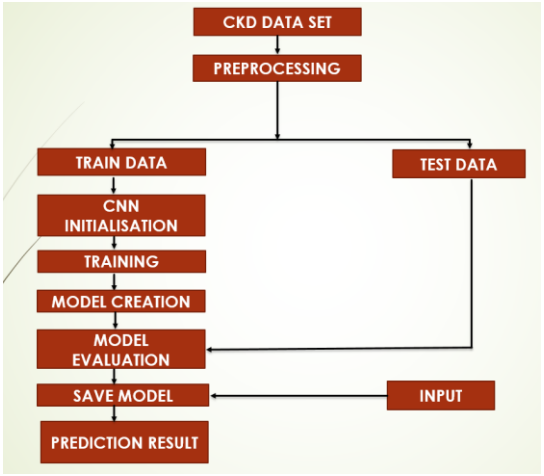

Fig. 2. Block diagram

C. FLOWCHART

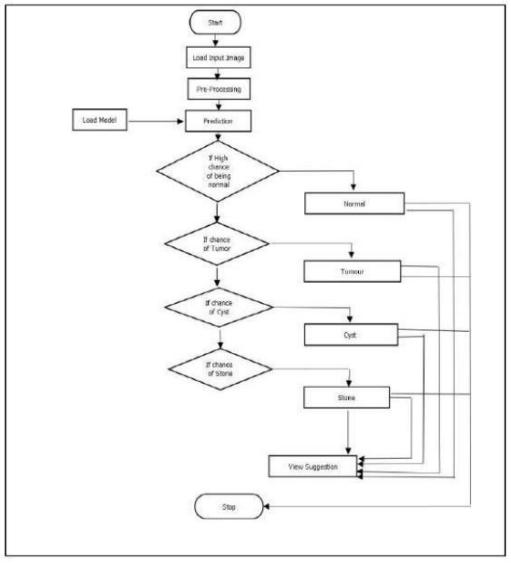

Fig. 3. Flowchart of proposed model

The flowchart above illustrates the training and prediction sections of the proposed model. The loading of the raw picture, further preprocessing, and prediction using a load model come after the first step. Every condition, including normal, cyst, tumor, and stone, is subjected to this procedure with the goal of predicting the outcome if there is a high probability that it will be normal. The representation above illustrates the recommended method's flowchart. .

IV. RESULT

The proposed medical image classification and implementation results are discussed in this section. This research presents an intelligent model of deep neural network for prediction and classification of chronic kidney disease. A prediction is made by comparing the CT scanned picture to the saved model once it has been uploaded to the website. This is done with the intention of making it simpler for people to comprehend the many kidney issues utilizing a CT image without first seeing a doctor. On average, the model's accuracy is assessed to be 96%.

TABLE. 1 Accuracy Detection

	precision	recall	f1-score	support
Cyst	0.99	0.99	0. 99	729
Normal	0.96	0.99	0.98	1022
Stone	0.93	0.99	0.96	292
Tumor	0.99	0.90	0.94	447

V. CONCLUSION AND FUTURE SCOPE

A Medical Image Classification method based on optimum feature selection, by categorizing images at the best characteristics present. To improve execution in terms of accuracy, precision, and classification, a novel system of clinical image classification is being presented depending on dataset. A collection of records containing various photographs was introduced into the study in order to obtain the desired results. The most appropriate subset of features is retrieved from pre-processed medical pictures using texture deep learning features, such as CNN and PyCharm. The retrieved features are

typically learned and sent into the classification process. Python is used to aid with the application. Subsequently, the method was used to classify the provided medical picture into other categories, such as Normal, Cyst, tumor, or stone. Additionally, the suggested model's congruent performance was confirmed, and its accuracy was evaluated, which was successful to a significant degree. Deep learning captures a variety of hidden patterns and opportunities that can assist the medical sector in providing quality patient care. Over the past few years, artificial intelligence and machine learning have drawn a lot of attention. Even deep learning has now carved out a niche for itself in this industry and is steadily expanding its market share. Deep learning's role in healthcare is very clearly demonstrated by its present and future applications, and more research could expand its potential applications to a variety of different branches.

REFERENCES

1. kidney disease from EMR data based on random forest regression,'' Math. Biosci., vol. 310, pp. 24–30, April 2019.
2. H. Kriplani, B. Patel, And S. Roy, ''prediction of chronic kidney dis- eases using deep artificial neural network technique",in Computer Aided Intervention and Diagnostics in Clinical and Medical Images, pp. 18–179, 2019.
3. Shahinda Mohammed Mostafa Elkholy,Amira Rezk,Ahamed Abo El Fetoh Saleh ,"Early prediction of chronic kidney disease using deep belief network",IEEE Access,Vol.9, September 2021.
4. H. M And S. M. N,'a review on evaluation metrics for data classification evaluations,' Int. J. Data Mining Knowl. Manage. Process, vol. 5, no. 2, pp. 1–11, 2015
5. Gudeti, Bhavya and Mishra, Shashvi and Malik, Shaveta and Fernandez, Terrance Frederick and Tyagi, Amit Kumar and Kumari, Shabnam,"A Novel Approach to Predict Chronic Kidney Disease using Machine Learning Algorithms",Fourth International Conference on Electronics ,Communication and Aerospace Technology,2020
6. 6 A. Khamparia, G. Saini, B. Pandey, S. Tiwari, D. Gupta,A. Khanna,''kdsae: chronic kidney disease classification with multi- media data learning using deep stacked autoencoder network,'' Multime-dia Tools Appl., vol. 79, nos. 47–48, pp. 35425–35440,2020
7. S. M. K. Chaitanya and P. R. Kumar,''Detection of chronic kidney disease by using artificial neural networks and gravitational search algorithm,'' in Innovations in Electronics and Communication Engineering (Lecture Notes in Networks and Systems), vol. 33, 2019
8. Ankit, B. Besra, and B. Majhi, ''An analysis on chronic kidney disease prediction system: Cleaning, preprocessing, and effective classification of data,'' in Recent Findings in Intelligent Computing Techniques (Advances in Intelligent Systems and Computing), vol. 707,2019
9. V. Kunwar, K. Chandel, A. S. Sabitha, and A. Bansal,''Chronic kidney disease analysis using data mining classification techniques,'' in Proc. 6th Int. Conf.-Cloud Syst. Big Data Eng. (Confluence), pp. 300–305,2016
10. R. Ani, G. 10Sasi, U. R. Sankar, and O. S. Deepa,''Decision support system for diagnosis and prediction of chronic renal failure using random sub- space classification,'' in Proc. Int. Conf. Adv. Comput., Commun. Informat,(ICACCI), pp. 1287–1292,2016
11. A. Abdelaziz, A. S. Salama, A. M. Riad, and A. N. Mahmoud,''A machine learning model for predicting of chronic kidney disease based Internet of Things and cloud computing in smart cities,'' in Security in Smart Cities: Models, Applications, and Challenges (Lecture Notes in Intelli- gent Transportation and Infrastructure), pp. 93–114, 2019.
12. 12 M. Arora and E. A. Sharma, 'Chronic kidney disease detection by ana- lyzing medical datasets in weka,'' Int. J. Comput. Appl., vol. 6, no. 4, pp. 1797–2250,2016
13. A. Khamparia, B. Pandey, S. Tiwari, D. Gupta, A. Khanna, and. J. P. C. Rodrigues,''An integrated hybrid CNN-RNN model for visual description and generation of captions,'' Circuits Syst., Signal Process., vol. 39, pp. 776–788,2020
14. M. Sharma, B. Jain, C. Kargeti, V. Gupta, and D. Gupta,,'Detec- tion and diagnosis of skin diseases using residual neural

networks (RESNET),'' Int. J. Image Graph., Art. no. 2140002, 2020
15. G. Hinton, ''A practical guide to training restricted Boltzmann machines",UTML TR., Tech. Rep., 2010.
16. C. Parker,''An analysis of performance measures for binary classifiers,''Proc. IEEE 11th Int. Conf. Data Mining, pp. 517–526,2011
17. S. M. M. Elkholy, A. Rezk and A. A. E. F. Saleh, ("Early Prediction of Chronic Kidney Disease Using Deep Belief Network," in IEEE Access, vol. 9, pp. 135542-135549, doi: 10.1109/ACCESS.2021.3114306.
18. 18 Z. Xue, S. Rajaraman, R. Long, S. Antani and G. Thoma, (2018)"Gender Detection from Spine X-Ray Images Using Deep Learning," 2018 IEEE 31st International Symposium on Computer-Based Medical Systems (CBMS), pp. 54-58, doi: 10.1109/CBMS.2018.00017.
19. 19 Ma, Fuzhe and Sun, Tao and Liu, Lingyun and Jing, Hongyu, (2020),"Detection and diagnosis of chronic kidney disease using deep learning-based heterogeneous modified artificial neural network" Future Generation Computer Systems,vol.111,pp.17-26.
20. Ifraz, Gazi Mohammed and Rashid, Muhammad Hasnath and Tazin, Tahia and Bourouis, Sami and Khan, Mohammad Monirujjaman ,("Comparative analysis for prediction of kidney disease using intelligent machine learning methods",Computational and Mathematical Methods in Medicine,vol.2011,2021
21. Anjan Gudigar,U Raghavendra,Jyothi samanth,Mokshagna Rohit Gangavarapu,Abhilas Kudva,Ganesh Paramasisam,Krishnananda Nayak,Ru-San Tan,Filippo Molinari,Edward J.Ciacco, Rajendra Acharya,(2021), "Automated Detection of chronic kidney disease using image fusion and embedding techniques with ultrasound images",in biomedical signal processing and control,
22. Basma Boukenze,Abdelkrim Haqiq and Hajar Mousannif, "Predicting Chronic kidney Failure Diseases Using Data Mining Techniques",(2004),Advances in Ubiquitous Networking,pp.701-712
23. Graham W. Taylor, Geoffrey E. Hinton,"Factored Conditional Restricted Boltzmann Machines for Modeling Motion Style", International Conference on Machine Learning, pp. 1025–1032 ,2009
24. Q. Suo et al., "Personalized disease prediction using a CNN-based similarity learning method, IEEE International Conference on Bioinformatics and Biomedicine (BIBM), pp. 811-816,2017
25. Hamida Ilyas, Sajid Ali, Mahvish Ponum, Osman Hasan, Muhammad Tahir Mahmood, Mehwish Iftikhar, Mubasher Hussain Malik,"Chronic kidney disease diagnosis using decision tree algorithms" BMC Nephrol,2021.

Smart Sleep Monitoring System

Akshari KP
KMCT College of Engineering for Women, Kalanthode 673601, Kerala. India
aksharikp89@grnail.com

Fidha fahmi MC
KMCT College of Engineering for Women, Kalanthode 673601, Kerala. India
fidhafahmimc@gmail.com

Huda Assootty
KMCT College of Engineering for Women, Kalanthode 673601, Kerala. India
Hudaassootty()@gmail.com

Varsha P
KMCT College of Engineering for Women, Kalanthode 673601, Kerala. India
varshathazhe@gmail.com

Abstract - Sleep monitoring is really crucial in determining the health status of a human being. In sleep monitoring process we measure the individual's vital parameters like Heart Rate (HR), Respiration Rate to define their sleep quality. Sleep monitoring is usually done by making use of different devices to measure parameters. They typically collect data about your movement and heart rate and access our sleep status. Aproper sleep is really important in one's health if deprivation of sleep persists then it can add to serious problems. Over time, lack of sleep can lead to health issues like diabetes, hypertension, weight gain, Mental health issues like depression, anxiety problems.

We measure the people's vital and important parameters like Heart Rate (HR), Respiration Rate (RR) and change in body postures. The proposed methodology makes use of ESP32module, Pulse Sensor, Breath Sensor, ADXL335 Sensor to measure the vital parameters. The proposed system will help to monitor sleep quality and conditions without creating any discomfort to user .Another feature of this system is, the proposed system continuously monitors sleep status. An embedded system collects real-time data from sensors attached to frame. A robust HR and RR estimation method is also proposed to obtain stable vital parameters. The proposed system has more features than similar existing ones. The system will serve as an effective solution for monitoring sleep quality and circumstances. It helps in accessing persons sleep without causing any hindrance and makes the process troublefree.

1. INTRODUCTION

Sleep monitoring helps people track their health. It is an important human activity monitor. Heart rate (HR) is typically measured by wearables and wearable devices such as chest and wrist sensors like the Apple Watch. It requires physical contact and is powerful. Many people find it uncomfortable or forget to put it on before going to bed.Having a security camera can pose a problem of invasion of privacy. Sleep monitoring is important because it allows you to monitor your sleep patterns and see how well you are getting quality sleep. This kind of information i.e valuable information to help you take control of your sleep and optimize your sleep experience. The four main reasons our bodies and minds need sleep are to aid brain function, control emotions, reduce disease risk, and control sleep. Sleep deprivation is what happens to your brain when you don't get enough sleep. The brain becomes exhausted and unable to perform tasks or functions well. You may also find it difficult to concentrate or learn new things. Our body sensations can also be delayed, affecting coordination and increasing the risk of accidents. So sleep quality is of utmost importance. Sleep quality can be defined as an individual's satisfaction with all aspects of their sleep experience. There are four attributes of sleep quality: sleep efficiency, sleep latency, sleep duration, and wakefulness after sleep onset. There are many devices that have been proposed for sleep tracking or sleep monitoring in a realworld context, and these devices are called sleep trackers that can track a person's sleep activity. Therefore, here we proposed a bed-mounted vibration sensor-based system for monitoring vital signs during sleep such as heart rate (HR) and respiratory rate (RR), body movements, and sleep posture. . This system enables smart healthcare to monitor daily sleep ubiquitously and non-invasively. Additionally, the vibration based approach also prevents security cameras from invading our privacy. A robust, robust and stable signal mode decomposition-based HR and RR estimation method for complex and noisy vibration signals was designed and developed for

effective sleep monitoring. In addition, body motion and detection algorithms based on the demonstration of the vibration signal characteristics of the prototype system were also proposed and the details of the system were presented. It has great potential for user-friendly real-time sleep monitoring. Here we provide an innovative and holistic method of human approach. H. A vibration-based sleep monitoring system that not only estimates vitals and key parameters, but also identifies sleep postures. This is a novel approach that uses human body vibration sensors to determine sleep position. Extract and use advanced vibration functions and features. The proposed HR/RR estimation method shows better result performance in terms of accuracy and robustness compared with previous domain, envelope and frequencydomain-based methods. The system produces instant sleep monitoring results in real time.

II. METHODOLOGY

This paper uses both software and hardware setups. Its main functions include heart rate estimation, sleep posture detection, and breathing rate detection. The system provides immediate real-time sleep monitoring results, which requires computationally efficient algorithms. Our continuous monitoring system measures changes in heart rate and breathing rate.

A. HARD WARE SET-UP

The hardware set up is done on a board with facilities to attach to the side of a bed. And there will be connection to the individual's body in order to track the patient's condition.

It has been built around ESP 32 NODE VICU Microcontroller unit. It controls the peripherals like sensors, server and android application that act as an interface between the system and the user. Sensor based readings are implemented in this project to carry out sleep monitoring d accessing. As shown in the project setup mainly three sensors are made use to calculate the vital parameters of the patient. The parameters that are measured in this system are Heart Rate, Respiration Rate and change in body postures of one's during sleep. The heart of the system is ESP32 NODE MCU microcontroller unit. The feature of this microcontroller unit is that, it has got inbuilt wi-fi and Bluetooth module. The proposed system is a bed side prototype that helps in continuous sleep monitoring process. The sensors used for measuring the individual's vital parameters are affixed on patient's body. These bodily placed sensor helps in measuring Heart Rate (HR), Respiration Rate (RR), change in bodily movements during sleep which are integrated on NODE MCU.

The microcontroller is programmed accordingly for carrying out the process. The main sensors used for this process are ADXL335 Sensor, Pulse Sensor and Breath Sensor. The sensors measure the parameters and readings are taken for monitoring sleep conditions of a person. Additional feature of the proposed system is readings are send or shared to server for future use or reference and by using an Android Application we can view the persons readings and sleep study even from afar location using the app. LED indications are also used check the working condition of component and process of the system. The proposed system do not cause any discomfort or hindrance to patient during the process and is user friendly. Thus we can access the person sleep quality and monitor them efficiently.

BLOCK DIAGRAM

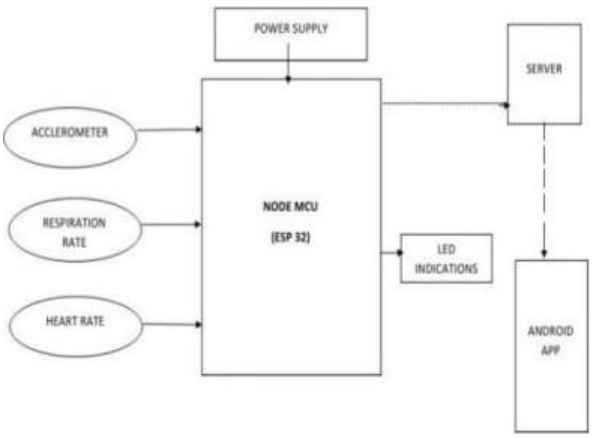

The project has been built around ESP 32 NODE MCU Microcontroller unit. It controls the peripherals like sensors, server and android application that act as an interface between the system and the user. Sensor based readings are implemented in this project to carry out sleep monitoring and accessing. As shown in the project setup mainly three sensors are made use to calculate the Vital parameters of the patient. The parameters that are measured in this system are Heart Rate, Respiration Rate and change in body postures of one's during sleep. The heart of the system is ESP32 NODE MCU microcontroller unit. The feature of this microcontroller unit is

that, it has got inbuilt wifi and Bluetooth module. The proposed system is a bed side prototype that helps in continuous sleep monitoring process. The sensors used for measuring the individual's vital parameters are affixed on patient's body. These bodily placed sensor helps in measuring Heart Rate (HR), Respiration Rate (RR), change in bodily movements during sleep which are integrated on NODE MCU. The microcontroller is programmed accordingly for carrying out the process. The proposed system do not cause any discomfort or Hindrance to patient during the process and is user friendly. Thus we can access the person sleep quality and monitor them efficiently.

CIRCUIT DIAGRAM

In this system proposed we are making use of different components. So for the working we require a DC input supply. The heart of the system is ESP32 NODE MCU Microcontroller unit. Microprocessor used inside it is IOSilicaExtensaLX6, which is a 32 bit processor. Led indications like power led is used to check whether conversion process is taking place or not and to check working condition of components, they are connected across a resistor.

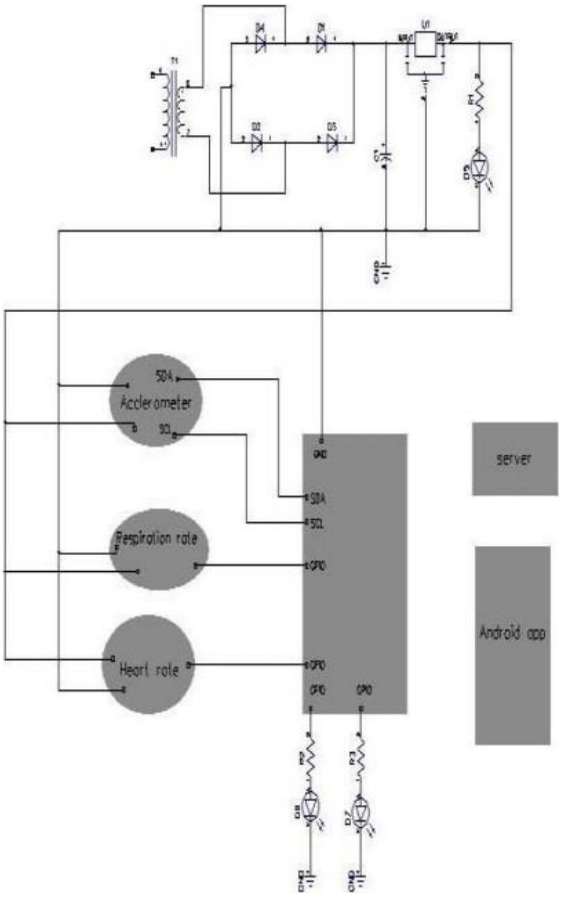

We are making use of sensors to calculate vital parameters. Mainly 3 sensors are used for this process and they are Accelerometer sensor or ADXI_ß35 Sensor to measure the change in persons position or posture during sleep. A Breath sensor mainly a sound based sensor used for detecting Respiration or Breathing Rate. Pulse Sensor is also made used in system for measuring the Heart Rate (RR)

Additionally there is a server we can share the data of sleep study and monitoring, server is developed using python and also an Android application is also generated to view the sleep study details even from afar location. Android application using developed Java software. By making use of the proposed system we can monitor sleep quality and parameters without causing any discomfort to user.

B. SOFTWARE

After finalizing the design and components, the next stage is the software section. In this stage, smart sleep monitoring system is provided with programming code or algorithm that is designed to be programmed into the microcontroller which in this case is nodemcu ESP 32. It is important for the algorithm to be simple and easy and user friendly without enor occurrence.

FLOWCHART

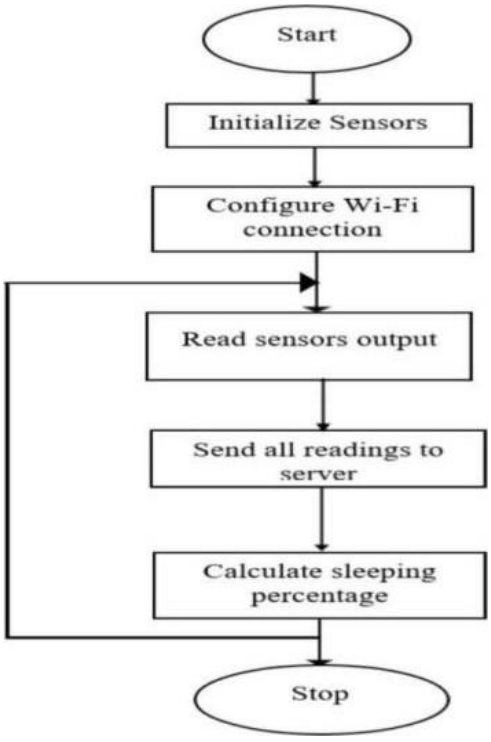

ALGORITHM

Step l : Start

Step 2: Initialise Accelerometer sensor, Respiration sensor and Pulse sensor for sleep monitoring system.

Step 3: Connect and configure Wi-Fi connection with ESP 32.

Step 4: Output readings of Accelerometer sensor, Respiration sensor and Pulse sensor is generated

Step 5: Send all the reading of sensors to the server connected with ESP 32.

Step 6: Calculate sleeping percentage and go to step 4.

Step 7: Stop

CONCLUSION

Sleep tracking is the process of monitoring a person's sleep, most commonly by measuring inactivity and movement. By monitoring your sleep patterns, you]l know how much quality sleep you're getting. This kind of valuable information allows you to take control of your sleep and optimize your sleep experience. Sleep is an important part ofhuman daily life. Adequate sleep is closely associated with improved physical, cognitive and mental health. On the other hand, poor or disturbed sleep can lead to impairment of cognitive and psychological functioning and deterioration of overall physical health. It can be concluded that our project proposes a comprehensive sleep monitoring system based on bed-mounted vibration sensors. The approach is intrusive and the key contribution is a new estimate of only the HF and RR oscillations excited by subjects during sleep. On the other hand, the first attempt to identify sleeping posture using human body vibration is presented. The proposed system can accurately measure HR and RR and identify changes in sleep posture with low error, resulting in a promising sleep monitoring system. The project could be improved in the future with additional features and then advanced sensor technology to bridge the gap between traditional clinical approaches and commercial home sleep-tracking devices. This goal is ambitious and could lead to improved human well-being in the short and long term.

REFERENCES

1. A. Crivello, P. Barsocchi, M. Girolami and F. Palumbo, "The Meaning of Sleep Quality: A Survey of Available Technologies," in IEEE Access, vol. 7, pp. 167374-167390, 2019, doi: 10.1109/ACCESS.2019.2953835.
2. S. Jeon, T. Park, A. Paul, Y. -S. Lee and S. H. Son, "A Wearable Sleep Position Tracking System Based on Dynamic State Transition Framework," in IEEE Access, vol. 7, pp.
3. A. Zaffaroni et al., "Sleep Staging Monitoring Based on Sonar Smartphone Technology," 2019 41 st Annual International Conference of the IEEE Engineering in Medicine and Biology Society (EMBC), 2019, pp. 22302233, doi: 10.1109/EMBC.2019.8857033
4. A. Zhao, J. Dong and H. Zhou, "SelfSupervised Learning From Multi-Sensor Data for Sleep Recognition,"in IEEE Access, vol. 8, pp. 93907-93921, 2020, doi: 10.1109/ACCESS.2020. 2994593.
5. T. Lauteslager, S. Kampakis, A. J. Williams, M. Maslik and F. Siddiqui, "Performance Evaluation of the Circadia Contactless Breathing Monitor and Sleep Analysis Algorithm for Sleep Stage Classification," 2020 42nd Annual International Conference of the IEEE Engineering in Medicine Biology Society (EMBC), 2020, pp. 5150-5153, doi: 10.1109/EMBC44109.2020.9175419.
6. 1. Fener-L1uis, Y. uusti110-Escario, J. M. Montserrat and R. Jané, "Analysis of Smartphone Triaxial Accelerometry for Monitoring Sleep-Disordered Breathing and Sleep Position at Home," in IEEE Access, vol. 8, pp. 71231-71244, 2020, doi: 10.1109/ACCESS.2020.2987488.
7. X. Jiao, X. Wang, X. wang and Z. Liu, "Noncontact Sleep Monitoring System Under a Mattress," in IEEEAccess,v01.9,
8. T. Nakamura, V. Goverdovsky, M. J. Morrell and D. P. Mandie, "Automatic Sleep Monitoring Using Ear-EEG," in IEEE Journal of Translational Engineering in Health and Medicine, vol. 5, pp. 1-8, 2017, Art no.
9. [9]Qiang Pan, Damien Brulin, Eric Campo*LAAS-CNRS, University of

Toulouse, 7 avenue du Colonel Roche, 31400, Toulouse, France,2021.
10. Barsocchi, M. Bianchini, A. Crivello, D. La Rosa, F. Palumbo and F. Scarselli, "An unobtrusive sleep monitoring system for the human sleep behaviour understanding," 2016 7th IEEE International Conference on
11. Cognitive Infocommunications (Cog1nfoCom), 2016, pp. 000091000096, doi: 10.1109/Cog1nfoCom.2016.7804531.
12. N. Surantha, O. K. Utomo and S. M. Isa,
13. "High-Performance and Resource-Efficient 10Tbased Sleep Monitoring System," 2020 IEEE 91 st Vehicular Technology
14. Conference (VTC2020Spring), 2020, pp. 15, doi: 10.1109/VTC2020 Spring 48590. 2020.9129521.
15. Y. Ren, C. Wang, Y. Chen, J. Yang and H. Li, "Noninvasive Fine-Grained Sleep Monitoring Leveraging Smartphones," in IEEE Internet of Things Journal, vol. 6, no. 5, pp. 8248-8261, Oct. 2019, doi: 10.1109/JIOT.2019.2922283.
16. F. Li, M. Valero, J. Clemente, Z Tse and W. Song, "Smart Sleep Monitoring System via Passively Sensing Human Vibration Signals," in IEEE Sensors Journal, vol. 21, no. 13, pp. 1446614473, 1 Julyl, 2021, doi: 10.1109/JSEN.2020.3013435.
17. N. Surantha, O. K. Utomo, E. M. Lionel, 1. D. Gozali and S. M. Isa, "lntelligent Sleep Monitoring System Based on Microservices and Event-Driven Architecture," in IEEE Access, vol. 10, pp. 42069-42080, 2022, doi: 10.1109/ACCESS.2022.3167637.
18. S. Lee, L. Yan, T. Roh, S. Hong and H. -J. Yoo, "The Smart Patches and Wearable Band (W-Band) for comfortable sleep monitoring system," 2011 Annual International Conference of the IEEE Engineering in Medicine and Biology Society, 2011, pp. 6915-6918, doi: 10.1109/ 1EMBS.2011. 6091741.
19. Y. Yamana, S. Tsukamoto, K. Mukai, H. Maki, H. Ogawa and Y. Yonezawa, "A sensor for monitoring pulse rate, respiration rhythm, and body movement in bed," 2011 Annual International Conference of the IEEE Engineering in Medicine and Biology Society, 2011, pp. 5323-5326, doi: 10.1109/1EMBS.2011.6091317.
20. [171M. H. Li, A. Yadollahi and B. Taati, "Noncontact Vision-Based
21. Cardiopulmonary Monitoring in Different Sleeping Positions," in IEEE Journal of Biomedical and Health Informatics, vol. 21, no. 5, pp. 1367-1375, sept. 2017, doi: 10.1109/JBH1.2016.2567298.
22. [181B. Yu et al., "WiFi-S1eep: Sleep stage Monitoring Using Commodity Wi-Fi Devices," in IEEE Internet of Things
23. Joumal, vol. 8, no. 18, pp. 13900-13913, 15 Sept. 15, 2021, doi: 10.1109/JIOT.2021.3068798.
24. [19]H. Korkalainen et al., "Detailed Assessment of Sleep Architecture With Deep Learning and Shorter Epoch-to-Epoch Duration Reveals Sleep Fragmentation of Patients With Obstructive Sleep Apnea," in IEEE Journal of Biomedical and Health
25. Informatics, vol. 25, no. 7, pp. 25672574, July 2021, doi: 10.1109/JBH1. 2020.3043507.
26. [201M. van Gastel, S. stuijk, S. Overeem, J. P. Van Dijk, M. M. Van Gilst and G. De Haan, "Camera-Based Vital Signs Monitoring During Sleep — A Proof of Concept Study," in IEEE Journal of Biomedical and Health Informatics, vol. 25, no. 5, pp. 1409-1418, May 2021, doi: 10.1109/JBH1.2020.3045859.
27. [211M. Laurino, L. Arcarisi, N. Carbonaro, A. Gemignani, D. Menicucci and A. Tognetti, "A Smart Bed for Non-Obtrusive Sleep Analysis in Real World Context," in IEEE Access, vol. 8, pp. 45664-45673, 2020, doi:
28. S. Akbarian, G. Deifi, K. Zhu, A. Yadollahi and B. Taati, "Automated Non-Contact Detection of Head and Body Positions During Sleep," in IEEE Access, vol. 7, pp. 72826-72834, 2019, doi: 10.1109/ ACCESS.2019.2920025.

A. Choi, S. Noh and H. Shin, "lnternet Based Unobtrusive Tele-Monitoring System for Sleep and Respiration," in IEEE Access, vol. 8, pp. 76700-76707, 2020, doi: 10.1109/ACCESS.2020.2989336.

29. [24]TY - JOUR Tl - Wearable Sleepcare Kit: Analysis and Prevention of Sleep Apnea Symptoms in Real-Time T2 - IEEE Access SP 60634 EP - 60649
30. AU - Y. J. Jeon AU - S. J. KangPY2019doi:10.1109/ACCESS.2019.2 9138 49 JO - IEEE Access IS -SN - 2169-3536 VO 7 VL-7 JA -IEEE Access

31. A-W. Wang, A. Hunter, N. Gravill and S. Matusiewicz, "Unconstrained Video Monitoring of Breathing Behavior and Application to Diagnosis ofSleep Apnea," in IEEE Transactions on Biomedical Engineering, vol. 61, no. 2, pp.

Artificial Eye For Blind Person

Aiswariya P
Dept.of Biomedical Engineering
Kmct College of Engineering for Women Calicut, India
aiswariya2401@gmail.com

Athira A
Dept.of Biomedical Engineering
Kmct College of Engineering for Women Calicut, India
athiraharidas5424@gmail.com

Mary Suji
Dept.of Biomedical Engineering
Kmct College of Engineering for Women Calicut, India
ousephsuji@gmail.com

Saniya P T
Dept.of Biomedical Engineering
Kmct College of Engineering for Women Calicut, India
saniyanasir05@gmail.com

Irfana Izzath O P
Dept.Of Biomedical Engineering
Kmct College of Engineering
for Women Calicut, India

Abstract—Visually impaired people face many difficulties in their daily lives. Many times, they rely on others' help. There are numerous technologies available to help persons who are blind. The blind person faces difficulties with traveling to a desired distance and finding the desired object. This paper solves this problem by providing a visual assistant for blind people to avoid difficulties in their daily activities. The system proposes an algorithm based on the use of CNN that can improve the features of the assisting system and give more information about the environment to visually impaired persons. Here, the CNN algorithm preprocesses the image captured by the camera, extracts features, and then classifies it. Then the preprocessed data from CNN is processed by D lib for face recognition. D lib can recognize the face from every angle. Using the YOLO algorithm helps detect the object, avoid obstacles, and thereby process every object in front of the blind person, who will then receive all output as a voice through their hearing aid. When a user faces an emergency situation, the user can send an alert to the caretaker as a voice input to overcome emergencies. This system also helps to know all the details about offers at particular shops. It helps to know which types of offers are available, their starting and ending dates, and also discount details from the shop and offer databases. The proposed system has a simple architecture and is user-friendly, making the user independent of his surroundings. The objective is to create a system that will guide visually impaired people so they can engage in both indoor and outdoor activities without running into problems.

Keywords—Visually impaired, convolutional neural network, YOLO algorithm, Dlib Algorithm, hearing aid.

I. INTRODUCTION

The eye is a sensitive organ, and vision is crucial to our survival because it gives us a connection to our environment and ensures our safety. Everybody has a distinct perspective, which is what distinguishes each person. The close bond is described by the proverb "the eyes are the windows to the soul". When looking into another person's eyes, one feels Vision also enables us to evaluate the current situation. It keeps your eyesight healthy so you can stay connected to the outside world and quickly analyze any situations that may arise. The mind, a part of the brain, interprets these images through vision. The idea of seeing is metaphysical. Vision enables a person to comprehend the meaning of an event and make interpretations, whereas vision may enable a person to observe an event. Both are in perfect harmony and play significant roles in our daily lives. The colors, forms, and patterns in our environment are incredibly diverse. We are able to perceive movement through sight, and we are able to judge that movement through vision. Sight and vision are crucial because they enable us to appreciate and comprehend the world.

The human eye functions similarly to a camera, gathering, focusing, and transmitting light through a lens to produce an image of the world around it. Visual impairment, also known as "vision loss," is a reduction in vision to the point where it causes issues that are not flexible by conventional means, such as glasses and lenses. World Health Organization (WHO) claims that

globally, there are over 1.3 billion people who are considered to be disabled, of whom 43.3 million are blind. Blind persons encounter several different obstacles when doing daily tasks. The visually impaired person finds it challenging to self-navigate outside in the familiar area, even while just strolling down a busy street.[1] They are unable to make judgements about their surroundings. According to numerous studies, visual impairment significantly reduces mobility and increases the risk of falling or colliding.[2] Depression, anxiety, and other psychological illnesses are more likely to occur in people with vision impairment. Compared to people of similar ages with other chronic illnesses such as asthma, chronic bronchitis, heart disease, or hypertension, visually impaired people have much greater rates of depression and anxiety.

In this paper, we provide a method for helping those who are blind using machine learning approaches. Machine learning, a subset of artificial intelligence, allows systems to learn from data and spot patterns with little to no human input. Machine learning algorithms perform a wide range of tasks, including email filtering, object recognition in photos, and the analysis of massive amounts of steadily more complicated data sets. Machine learning systems are used by computers to automatically scan emails for spam, identify objects in photographs, and handle large amounts of data. The importance of a smartphone to modern life cannot be overstated. Therefore, this endeavor involves creating a smartphone application that can help blind people with daily tasks. This study involves creating software that helps the blind individual recognize objects and obstacles, understand documents, and manage emergency situations. Through a hearing aid, the user may hear all of the vocal output. Additionally, this system aims to recognize important signboards like those for restrooms, traffic signals, etc.

II. LITERATURE SURVEY

In 2005, John Zelek, Richard Audette, Jocelyn Balthazaar, and Craig Dunk proposed a stereo vision system for visually impaired people.One key obstacle for those with vision problems is navigation. In order to overcome this hurdle, a wearable stereo-vision system has been researched and built. The effectiveness of this device for navigating through straightforward hallway structures has been demonstrated by preliminary experiments. The low-cost prototype includes a wearable computer, a virtual touch input system, and two USB cameras (on an inexpensive laptop or embedded platform). In order to calculate depth uses pixel-to-pixel correlation.The feedback system uses tactile feedback provided by the user's fingertips to transmit visual information.[3]

In 2007, Jonathan D. Anderson, Dah-Jye Lee, and James K. Archibald proposed an embedded stereo vision system providing visual guidance to the visually impaired. This paper has presented an embedded stereo vision technology that will help the blind. In order to create dense disparity maps, stereo vision correlation is carried out using spline and genetic algorithm techniques. In turn, these disparity maps provide the user with rough distance estimations, enabling them to move about the scene. This work offers a way for realizing a stereo vision algorithm using 1D signal processing, as well as an embedded stereo vision system that makes use of specialized hardware and software. Stereo vision is a poorly presented problem, and limitations must be applied to provide a good outcome without regularization.

In 2009, Asim Iqbal, Umar Farooq, Hassan Mahmood, and Muhammad Usman Asad proposed a low-cost artificial vision system for the blind and partially sighted. It uses ultrasonic sensors to measure the distance between obstacles around the blind person and guide them on public roads. Visually impaired people may hear voice prompts for right, left, etc. In advanced mode, the system can identify objects through image processing techniques.[4]

In 2016, Sandeep Shantharam proposed a "bionic eye"—an artificial vision and comparative study based on different implant techniques. This paper provides an overview of alternative retinal implant procedures that, if marketed, might allow blind people to see and understand the colorful world by channeling their vision through artificial intelligence. The bionic eye with retinal, ocular, and subretinal implant techniques appears promising as it is an integration of electronics, biomedicine, and embedded engineering that acts as the artificial eye in interpreting the materialistic images of the world and plays the active role of natural cones and rods for brain image interoperability. Therefore, the recent advancement in technology has driven mankind

towards various approaches, like artificial implants for those blind subjects.[5]

In 2019, Dante Muratore, Subhasish Mitra, Boris Murmann, and E.J. Chichilnisky proposed an artificial retina that could help the blind to restore sight. An extremely tiny computer chip with several protruding metal electrodes is needed for the artificial retina. To construct a map of different cell types, the electrodes first capture the activity of the nearby neurons. The visual data from a camera is then sent to the brain using this information. Unfortunately, when recording, the eye generates so much data that the electronics get unbearably hot. For the purpose of communicating visual information to the brain, retinal neuronal spikes are sent. The problem is that the digitization process still generates a lot of heat even with just a few hundred electrodes used in today's prototypes since the digital retina needs to gather and decode those spikes in order to understand the properties of the neurons.[6]

In 2020, b. Ragini, n. Bliss shiny v. Hemamalini, s. Ranjani, k. Reshma, and r. Vikneshkumar proposed a pseudo-eye for the visually impaired using an artificial intelligence prototype. The paper depicts an intelligent electronic tool for blind people. In order to provide comprehensive measures, the system includes artificial vision, object identifications, and real-time position tracking with an emergency alarm. Blind people frequently lack awareness of external hazards and require assistance to reduce the risk of a collision. The development of a system to aid blind people with outdoor navigation is the goal of this study. By allowing users to move outside without bumping into anything while using voice awareness, the suggested system will be able to lower the chances of obstacle contact. The whole system's goal is to provide blind people with a low-cost, effective navigation tool that simulates artificial vision by informing them about an object's surrounding surroundings using artificial intelligence (ai). An ultrasonic sensor is used to determine the distance of the objects surrounding the blind person in order to direct the user's voice and vibration, which the blind person can hear and feel. When an item is detected in front of a blind person, the camera alerts them using the apr speech module. This project uses machine learning to teach pre-trained objects in an image artificial intelligence (ai) system using the image ai dataset. A computer system that has the object recognition capability to perform real-time object detection receives input from a camera that is oriented according to the system's predetermined orientation. The network's output may then be analyzed and presented to the blind individual as audio.[7]

In 2020, Niveditha K, Pooja B, Kavya P. D, Nivetha P, and Lakshmikantha G. C. proposed an IoT-based virtual eye for the blind. It entails the creation of a system that makes use of the Raspberry Pi camera for text detection and identification from images, which is made feasible by the OpenCV Tesseract OCR package. This makes it easier to turn a camera-taken image of a chosen page into the appropriate text. The TTS engine is then used to turn this text into a voice that can be heard through headphones. It also assists people with vision impairments in moving safely and avoiding accidents caused by potential roadblocks. In order to identify impediments and their proximity to the user, this research suggests wearable technology that comprises ultrasonic sensors. This study outlines a system that would notify their guardian through SMS if a visually impaired person encountered an emergency. Current position data is extracted using a GPS module, and SMS messages are sent to a guardian using a GSM module. While traveling and informing guardians of emergency situations by SMS, a visually impaired person can feel like they are not visually impaired.[8]

In 2020, Emanuele Cardillo, Changzhi Li, and Alina Caddemi proposed a millimeter-wave radar cane: a blind person's aid with moving human recognition capabilities. It is an advanced system that can distinguish between human and nonhuman targets in addition to alerting the user of potential difficulties. A new range alignment technique has been presented with the goal of identifying the minute chest displacement caused by physiological activity as the primary indicator of human presence because real-world scenarios are likely to involve moving objects. The suggested method can accurately identify people in surroundings with many moving targets and complex layouts, giving the user a full set of information about the presence, location, and type of accessible targets.The system's efficacy and working theory are demonstrated through both simulated case studies and the use of a 122 GHz radar board to do the necessary measurements.[9]

In 2020, Shirly Edward proposed a text-to-speech device for the visually impaired. They require a tool to assist them in reading. Therefore, we created a device that can read any type of text by converting it to voice messages. This device's function is to convert the input of images, pdf files, documents, textbooks, and news articles into vocal output. The gadget has each module needed for both voice and picture processing. While reading, it can also play and pause the output. It is more cost-effective, has a lower error rate, and takes less time to process. The device was created using a Raspberry Pi 3. For those who are blind, this apparatus truly serves as an artificial eye. It doesn't require any oversight from people.[10]

In 2021, Ritik Singh, Rishi Kumar Kamat, and Faraj Chisti proposed a third eye for blind people that will enable the blind to explore with confidence and speed by using ultrasonic waves to detect adjacent impediments and alerting users with a beeping sound and audio aid. A number of fields, including software engineering and hardware design, have contributed to the development of this technology. Ultrasonic sensors will be built into this using Raspberry Pi 4 modules with cameras. People with visible disabilities can use sensors to sense their surroundings, and cameras can recognize items to facilitate effective mobility. When the sensors identify any queries, the client will be informed through a headset. The camera will also pick up the name of the person or item, and the headset will broadcast it so the client can comprehend what is in front of them.[11]

II. METHODOLOGY

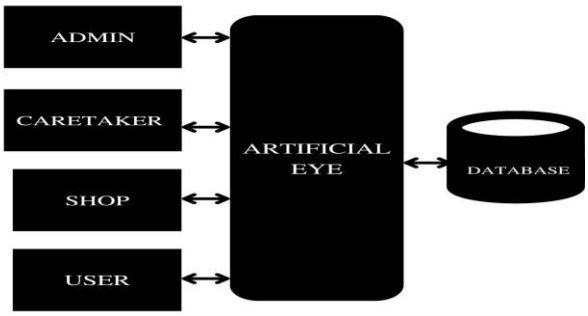

Fig. 1. Architecture of Artificial Eye

In this project, we introduce visual assistance software for blind people. People with blindness or a visual impairment not only compromise their autonomy in any daily living activities, such as selecting color-matched clothes or identifying a desired product in the supermarket, but it also leads to lower workforce participation rates and higher risks of falls. So, here we propose an artificial eye that utilizes machine learning techniques for giving guidance to blind people. The system utilizes CNN-based algorithms, which take the input from an image and extract features to efficiently do classification, detection, and other tasks. The system helps users detect objects, detect obstacles, navigate, and identify familiar and strange people. The software also helps to access the shop to view its offers based on location. Finally, users can hear outdoor and indoor information with earphones.

A. Architecture

This system introduces machine learning for providing environmental information to blind people. The architecture of the artificial eye is shown in fig.1. Firstly, the image is captured by the camera, the image is processed, and features are extracted by the CNN. Then, the various objects are detected using the YOLO algorithm. By using the Dlib Face algorithm, the user can easily recognize the faces of familiar and strange people in their surroundings. In an emergency situation, the user can send emergency messages to the caretaker by giving voice input. Finally, the user can view the offer based on the shop's location.

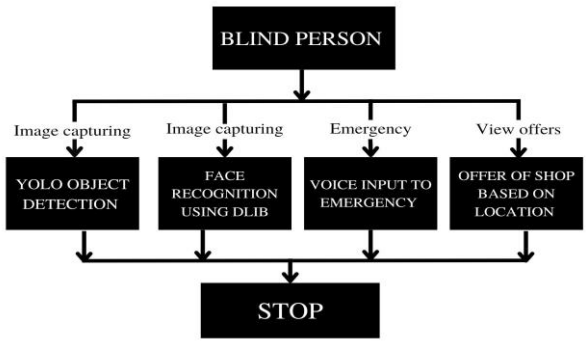

Fig. 2. Data flow diagram of Artificial Eye

B. Data Collection

The system stores the data in various databases, which are organized collections of data stored and accessed electronically. In the database, we store various information about the user, caretaker, and shop. In this project, the database contains various datasets for login, access user, caretaker, shop, familiar person, etc.

The data flow diagram of the artificial eye is shown in Fig.2; the data flow diagram represents the flow of information within the system. It shows how the data enters and leaves the system, what changes the information, and where the data is stored. A data flow diagram graphically represents the function that stores and distributes data to and from the system. Admin can store and retrieve information about users, shops, and caretakers from the database. The caretaker can store the information about themselves. The shop can store information about their shop and offers. Users can get information about the object's location and characteristics from the dataset.

Functions of Modules

Fig. 2. shows the data flow diagram of four modules such as admin, user, caretaker and shop. The modules can store and retrieve data from and to various databases. The login database contains the username and password for admins, caretakers, and shops. The information about the users, caretakers, and shops, such as name, address, contact details, and other personal details, is stored and retrieved from the user database, caretaker database, and shop database, respectively. The emergency database collects and stores the emergency messages, which can be seen by admin. The feedback database used to collect and store feedback received from caretakers and admins can be viewed. The complaint database was used to collect and store complaints. The offer database is used to store offer information, such as the starting and ending dates of offers and discounts at the shops.

The familiar database collects and stores pictures or other details of familiar people.

D. Algorithm

We mainly use the CNN algorithm, the YOLO algorithm, and the Dlib algorithm to implement the system.

Convolutional neural networks (ConvNets or CNNs) are one of the main categories in image recognition and classification. Object recognition, face recognition, etc. are some of the areas where CNNs are widely used. A convolutional layer is always the first layer in a convolutional neural network. Its main function is to look for a set of features in the photos it receives as input. A convolution layer that does the convolution of each filter is exactly what we are looking for in our photos. For each combination of image and filter, we get a feature map showing where the image features are located. A pooling process is applied to each feature map sent through this layer. Pooling technology reduces photos without losing important features. An input vector is fed to this layer to produce an output vector. Classification is done in the final, fully connected layer. This layer provides her N-dimensional vectors based on the number of classes for the image classification task. Each vector element indicates the probability that the image belongs to a particular class.

"You Only Look Once" is referred to as "YOLO" generally. This algorithm identifies and classifies various things in images (in real-time). YOLO performs object detection as a regression problem and outputs the class probabilities of the identified photos. Convolutional neural networks (CNN) are used in the YOLO algorithm to quickly identify items. The approach just involves one forward propagation through a neural network, as the name might imply, to detect objects. This implies that a single algorithm run is used to peform full image's prediction. CNN is employed to forecast multiple class probabilities and bounding boxes concurrently.

Dlib is a toolbox for creating practical C++ applications for data analysis and machine learning. The library provides good, user-friendly Python bindings, although it was originally written in C++. Dlib is mostly used for face and facial landmark detection. Dlib's frontal face detector performs excellently.It is based on the CNN algorithm because the CNN-based detector can detect faces practically from any angle.

E. Flow Chart

Fig. 3. shows the flow chart of the artificial eye. Firstly, the system checks the type, i.e., if it is a user (a blind person), admin, caretaker, or shop. If it is a user, it enters the user platform. Then the user can identify the objects by the YOLO algorithm, so whatever objects are in front of the user can be detected by this algorithm. Next, any familiar or unfamiliar person in front of the user can be detected using the D lib algorithm. The user can read all the text using optical character recognition (OCR), which is a form of technology that identifies the characters like numbers and letters included in an image. The user can send

emergency messages or make a video call to the caretaker using voice input. Finally, users can view all the offers from shops, which helps them purchase whatever they need without anyone's help. The user can get all the output as a voice through a hearing aid.

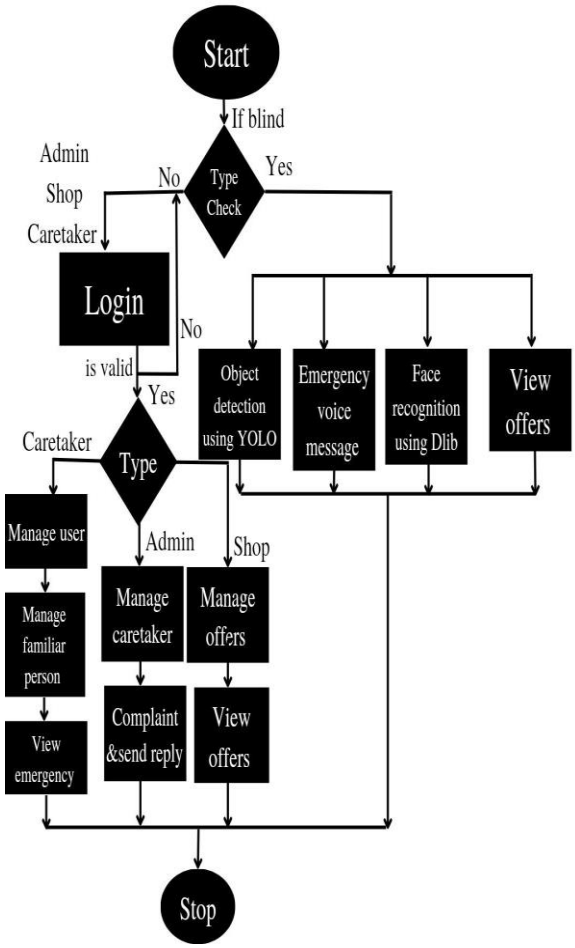

Fig. 3. Flow chart of Artificial Eye

Secondly, if it is not a user, go to log in and check whether it is an admin, caretaker, or shop. If it is an admin, it enters the admin platform. Admins can view users, approve and manage caretakers, and manage shops. Admins can view complaints and feedback from caretakers. If it is the caretaker, then he or she enters the caretaker platform. The caretaker can view and manage the user, view emergencies and add an emergency number, add a familiar person, and send complaints and feedback to the admin. Finally, if it is a shop, they enter the shop platform. Shops can add their own locations and manage their offers and discounts. Therefore, this software provides a platform for blind people to view their indoor and outdoor environments and make them feel more secure and independent while doing their daily activities.

IV. RESULTS

The software provides all kinds of information to the blind person (the user) about his surroundings and the objects in front of him. As the user signs up, he gets the overall effect of artificial vision. When the user opens the app, it provides information about the location, familiar and unfamiliar people, obstacles, and he can make calls and send emergency messages to the caretaker. The user can identify familiar people based on details added by the caretaker, and he can hear their names. The user can also identify any unfamiliar person in front of him. The location of the user is recorded in the background, and the user can hear his location by saying "location". The user can also get information about obstacles near him via voice, and he can move away from those obstacles. The user can identify the objects by saying "recognize" and he can hear the names of all the objects near him. Here we are using Optical Character Recognition (OCR) technology, which helps users read the writings on any papers, in shops, etc. When the user faces any emergency situations, he can make a video call and, when he says "emergency" send emergency messages to the caretaker. The user gets information about the shops and their offers based on their location. Overall, this software provides a visual aid that makes the user feel secure and confident while walking and communicating with his surroundings. So whatever a normal person can see can also be seen by a blind person by hearing it.

When the admin signs up for the website, he can view details of users, caretakers, and shops. Admin can approve or reject the caretaker. They can view the complaints from the caretaker and send a reply. Also, they can view feedback.This software helps the caretaker keep an eye on the user, a blind person. As the caretaker logs in, he can add user details and manage them. The caretaker can add an emergency number for users to avoid emergency situations by sending an alert message or video call. They can also see the emergency messages from the user. The caretaker can add familiar people's details for the user. They can send complaints about the software to the admin and also view the reply. They can also send feedback to the admin. And mostly, the caretaker can know

the location of the user and help the user in emergency situations.

The shops can sign up on the website and add details such as the name and location of the shops and a small description of their shop. The shop can also add offers, such as the starting and ending dates of offers and discounts. From this, the user knows all the information about the shop and its offers. Based on the location of the user, the user can do shopping without the help of anyone.

V. CONCLUSION

This system presents a technique for assisting visually impaired people. The proposed system has a simple architecture and is user-friendly, making the user independent in surrounding areas. In this system, we are mainly using three algorithms. First is CNN, which is used to process images and is specialized for image and video recognition. The second is YOLO, which is used to detect objects and obstacles for easy navigation in outdoor and indoor areas. The third is Dlib, which is used to recognize the face and helps to identify a familiar person. Both the YOLO and Dlib algorithms are based on the CNN algorithm. The user can provide voice commands when it needs to overcome emergencies and make calls to a particular person. The user can receive all output as a voice through a hearing aid. This system makes the surrounding areas user-friendly and makes it easy to avoid obstacles. It is portable and helps to identify the shops and their offers. The shortcoming of the system is that we can't use wide-range cameras, and the output may depend on the network. In the future, we can develop the existing project on a hardware platform to avoid network issues, and we can use wide-range cameras to avoid other issues. The system can provide an overall effect of artificial vision, not only in navigation but also in obstacle detection and spatial recognition, and help users feel more secure and independent while walking. Whatever a normal person can see, a blind person can also see by hearing it. So, find happiness by hearing the view.

REFERENCES

1. Padma Shneha, Prathyusha Reddy, V.M.Megala "Artificial Intelligence for vision impaired people",2018.
2. Yunjia Lei, Son Lam Phung , Abdesselam Bouzerdoum,Hoang Thanh Le And Khoa Luu "Pedestrian Lane Detection for Assistive Navigation of Vision-Impaired People: Survey and Experimental Evaluation ",2022.
3. John Zelek, Richard Audette, Jocelyn Balthazaar, Craig Dunk "A Stereo-vision System For the Visually Impaired", 2005.
4. Jonathan D. Anderson, Dah-Jye Lee, and James K. Archibald, "Embedded Stereo Vision System Providing Visual Guidance to the Visually Impaired", 2007.
5. Sandeep Shantharam, "Bionic eye – An artificial vision and comparative study based on different implant technique",2016.
6. Dante Muratore, Subhasish Mitra, Boris Murmann, E.J. Chichilnisky, "An artificial retina that could help restore sight to the blind",2019.
7. B. Ragini, N. Bliss ShinyV. Hemamalini, S. Ranjani, K. Reshma, R. Vikneshkumar "Pseudo eye for visually impaired using artificial intelligence prototype", 2020.
8. Niveditha K, Pooja B, Kavya P D, Nivetha P, Lakshmikantha G C"Virtual Eye for Blind Using IOT", 2020.
9. Emanuele Cardillo, Changzhi Li, Alina Caddemi,"Millimeter-wave radar cane: A blind People aid with moving human recognition capabilities",2020.
10. Shirly Edward,"Text-to-Speech Device for Visually Impaired People", 2020.
11. Ritik Singh, Rishi Kumar Kamat, Faraj Chisti" Third Eye for Blind Person",2021.

Smart Cities With Smarter Healthcare

Mini Lal
Dept. of Biomedical Engineering
KMCT College of Engineering for Women
Kerala, India

Thushara JS
Dept. of Biomedical Engineering
KMCT College of Engineering for Women
Kerala, India
thusharajs258@gmail.com

Huda Fathima TR
Dept. of Biomedical Engineering
KMCT College of Engineering for Women
Kerala,India
hudafathimatr17@gmail.com

Fathimathul Afhida
Dept. of Biomedical Engineering
KMCT College of Engineering for Women
Kerala,India
kmw19bm018 @gmail.com

Abstract—With the aid of current innovations like 5G and the Internet of Things, creating a smart city has advanced swiftly (IoT). Also being developed are the terms "smart city," "smart traffic systems," and "smart health." Using the two aforementioned, an intelligent ambulance navigation system is being developed. Information transmission takes longer than anticipated when an ambulance sends severely ill patients, and the hospital is completely ignorant of this as well as the patient's unique characteristics and why they are arriving sooner. Therefore, using a patient monitor and ambulance tracking system is a good strategy. Thirty-second diagnosis uses sensors to measure patient parameters that clinicians must first take into account before starting any treatment, such as respiration rate, temperature, and heartbeat. And even before the ambulance is dispatched, wirelessly transmit these parameters to the hospital. Additionally, the patient is given a simple way to summon an ambulance at the touch of a button without first dialing the medical facility. Send a short message service (SMS) with all the hospital's emergency information to a contact significantly earlier in the event of an emergency. This saves a tonne of time, and when the patient's life is at stake, every second counts. The patient can monitor the ambulance's location, which gives them an idea of when it will arrive. If they choose, they can also receive immediate navigation to the closest hospital.

Keywords—IoT, sensors, smart city, ambulance tracking, patient monitoring, emergency service

I. INTRODUCTION

A technologically advanced area that makes use of many electrical devices and sensors to gather data is known as a "smart city." In turn, the information is applied to enhance citywide operations. In order to successfully manage assets, resources, and services, information gained from those data is employed. Data from inhabitants, devices, buildings, and assets is used to monitor and manage traffic and transportation systems, power plants, utilities, water supply networks, waste, criminal investigations, information systems, schools, libraries, hospitals, and other community services. Smart cities are ones that make creative use of technology and have efficient planning, regulating, and monitoring systems.The quality of healthcare provided can be raised by applying the smart city concept to the industry. As a result, we have developed a system that primarily consists of three components: an Android app, a patient monitoring system, and an ambulance tracking system. It is a particularly challenging task in the regularly hectic work to consistently monitor the health of the home patient. Elderly individuals, in particular, should routinely have their health status assessed and reported to the doctor in order to preserve their lives in life-threatening situations. Health monitoring is a significant problem in contemporary culture. Due to inadequate health monitoring, many people experience the harmful repercussions of medical problems.To solve this issue, there are numerous IOT devices on the market today that can independently monitor patient health. This smart health monitoring

system monitors the user's health by using heart rate, temperature, and breath sensors connected to a node MCU board. Just like any other system for patient monitoring, the system will periodically check the patient's health parameters. Additionally, in the event of any changes to the parameters, such as during an emergency, these parameter data and the patient's medical history file will be instantly communicated with the local hospital. The Android app can be used to track the ambulance in addition to sharing the data indicated above. The key benefit of using this app is that, even before the patient arrives at the hospital, the hospital or doctor will be well aware of their status. As a result, the time needed for diagnosis will be shorter, and the likelihood of survival and recovery will also rise. The device also includes a motion sensor, which is useful for monitoring patients who are paralysed. Therefore, the suggested system enables thorough patient health monitoring and aids the physician in providing prompt treatment during an emergency.

Fig. 1. Smart City Concept

II. CONTRIBUTION

The following factors can be used to quantify the proposed framework's commitment:

• The use of mobility, temperature, breath rate, and heart-beat sensors allows for a quick two-dimensional (2D) diagnosis using the patient monitor and ambulance tracking system. The data from these sensors is used to record crucial persistent parameters before starting any therapy and transmit the data through a distance-learning medium so that the doctor may assess the patient's condition before the patient even arrives at the hospital.

• The patient also has a quick means to request ambulance service at the touch of a button. An ambulance monitoring facility is also offered, and the app instantly sends an SMS to the neighborhood hospital.

• Ambulance tracking facility also provided

III. PROBLEM STATEMENT AND SYSTEM MODEL

The current procedure for summoning an ambulance and admitting the patient is incredibly time-consuming because there is no prior transfer of any kind of essential information to the hospital. In an emergency, every second counts, and getting access to the right emergency care could mean the difference between life and death. The hospital is absolutely uninformed of the important patient features the doctor needs before starting any extra therapy for critically ill patients who are evacuated by ambulance prior to their arrival.In some circumstances, methodologies can be useful for making predictions; logistic regression is one such methodology, with its dependent variables being categorical (for example, success or failure). A maximum maximum likelihood estimate is used to formulate the probabilities in which logistic regression will apply to a specific class using an iterative procedure in order to determine the likelihoods that logistic regression will occur.The decentralized autonomous organization (DAO) works to improve the financial situation of everyone who is formally connected to the company in some way, including the residents, and to create truly sustainable, clean community development throughout the world. The linear SVM technology can be repurposed or retransformed using the prediction of any two provided data rather than the observations themselves when the patients are unable to maintain track of the desired ambulance. Every second of this delay hurts the patient, who needs therapy as quickly as possible.When medical data is scattered across two or more servers in a cloud architecture, which is prone to security issues, the risk that an attacker will target all the servers hosting this information, which is encrypted using the Bastion method, increases.The patients may also act in ways that are suggestive of the user's trustworthiness, depending on a number of factors based on the purchase and review history of the user in question. These parameters are used to standardize all of the submitted ratings before being applied by the recommendation algorithm.

DESIGN AND METHOD

An Internet of Things-based smart healthcare system, the proposed patient monitor with ambulance tracking system needs the following parts

- NodeMCU
- Power supply
- Heartbeat sensor
- Temperature sensor
- Breath sensor
- Motion sensor
- GPS
- Button

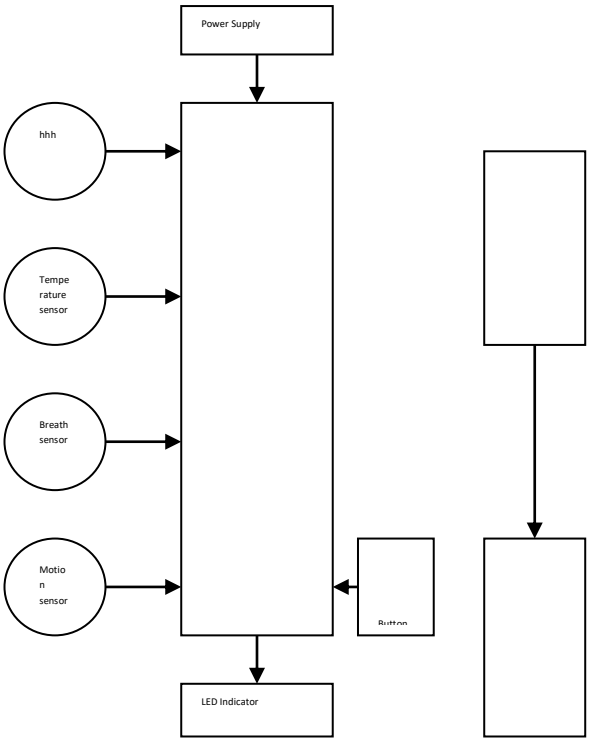

Fig. 2. Block Diagram

V. SOFTWARE

The software step comes next once the design and component stages are complete. The algorithm, or programming code, for the patient monitoring and ambulance tracking system is delivered at this step and is intended to be installed into the microcontroller, in this case the Nodemcu ESP 32. The algorithm must be straightforward and simple to comprehend in order to make it simpler to identify and fix problems.

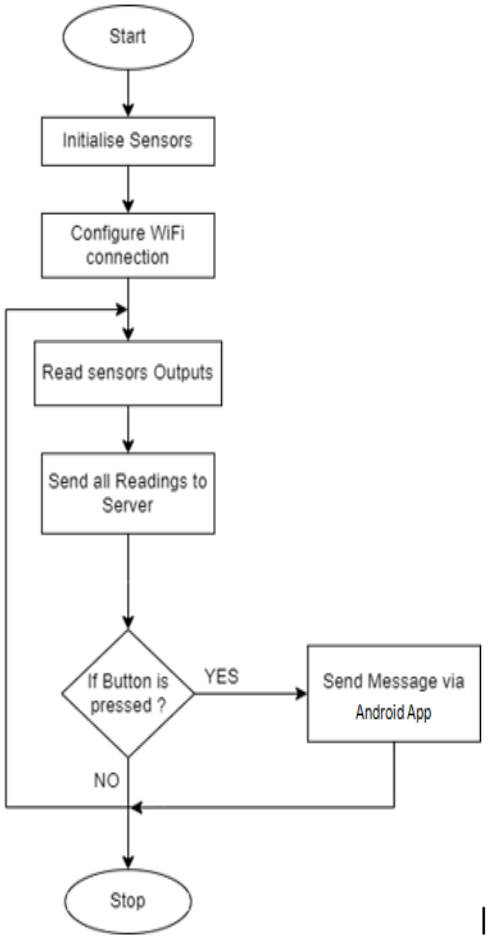

Fig. 10. Flow Chart

ALGORITHM

Step 1: Start.

Step 2: Initialize the Accelerometer sensor, Heart beat sensor, Temperature

Sensor and Breath sensor for patient monitoring.

Step 3: Connect and configure Wi-Fi connection with ESP32.

Step 4: Output readings of accelerometer sensor heart beat sensor, temperature sensor, breath sensor is generated.

Step 5: Send all readings of sensors to the server connected with esp32.

Step 6: Read button value.

Step 7: Check whether the button is pressed or not.

Step 8: If the button is pressed go to step 9 else go to step 10.

Step 9: Send a message to the android application.

Step 10: Go to step 4.

Step: Stop.

V1. RESULT

Developed an intelligent ambulance navigation system. Sensors measure and detect patient parameters such as respiratory rate, temperature, heart rate and movements. Send all these parameters wirelessly to the hospital cloud even before the ambulance is dispatched. In addition location tracking system and android app which makes patients can easily call emergency with the press of a button without having to dial.instant navigation to the nearest hospital is also made possible.

VII. CONCLUSION

Due to the development and progress of technology, the healthcare sector is a hub for technology application. As a result, this work has detailed and put into reality the use of Android and IoT devices for remote patient health parameter monitoring. In this study, we suggest a smart ambulance tracking and patient monitoring system. The suggested system may always remain with the patient to monitor them, which cuts down on the time that would have been missed in the current method. A motion sensor is also incorporated, which is very beneficial for patients who are bedridden or immobile.

References

1. Santinha G,Dias A,Rodrigues M,Queirs A,Rodrigues C,Rocha NP (2019) How do smart cities impact on sustainable urban growth and on opportunities for entrepreneurship? Evidence from Portugal: the case of gueda. In: Carvalho LC, Rego C, Lucas M, Sanchez-Hernandez M, Viana ABN (eds) New paths of entrepreneurship development. Springer, Cham, pp 31–53
2. AlDairi A (2017) Cyber security attacks on smart cities and associated mobile technologies. Procedia Comput Sci 109:1086–1091
3. Lazaroiu GC, Roscia M (2012) Defnition methodology for the smart cities model. Energy 47:326–332
4. Vanolo A (2014) Smartmentality: the smart city as disciplinary strategy. Urban Stud 51:883–898
5. Gifnger R,Gudrun H (2010) Smart cities ranking: an efective instrument for the positioning of the cities? ACE Archit. City Environ. 4:7–26
6. [6]. Marcos-Pablos S,Garca-Pealvo FJ (2019) Technological ecosystems in care and assistance: a systematic literature review. Sensors 19:708
7. Inan, ahin, and Arzu Eren enaras. An application for routing ambulance via ACO in home healthcare. In: Transportation, logistics, and supply chain management in home healthcare: emerging research and opportunities, pp. 102-110. IGI Global, 2020
8. Skarlatidou A, Hamilton A, Vitos M, Haklay M (2019) What do volunteers want from citizen science technologies? A systematic literature review and best practice guidelines. JCOM J Sci Commun 18:A02
9. Sharma Ashutosh, Rathee Geetanjali, Kumar Rajiv, Saini Hemraj, Varadarajan Vijayakumar, Nam Yunyoung, Chilamkurti Naveen (2019) A secure, energy-and SLA-efcient (SESE) E-healthcare framework for quickest data transmission using cyber-physical system. Sensors 19(9):2119
10. [10]. Queirs A, AlvarelhoJ, Cerqueira M, Silva A, Santos M, Rocha NP (2018) Remote care technology: a systematic review of reviews and meta-analyses. Technologies 6:22
11. Ali F, Shaker El-Sappagh SMR, Islam A Ali, Attique M, Imran M, Kwak K-S (2021) An intelligent healthcare monitoring framework using wearable sensors and social networking data. Future Gener ComputSyst 114:23–43
12. Irshad, M. A systematic review of information security frameworks in the internet of things (iot). In Proceedings of the 2016 IEEE 18th International Conference on High Performance Computing and Communications; IEEE 14th International Conference on Smart City; IEEE 2nd International 1 3 Smart healthcare in smart cities: wireless patient monitoring… Conference on Data Science and Systems (HPCC/SmartCity/DSS), Sydney, Australia, 12-14 December 2016
13. Petersen, Fazlyn, Mariam Jacobs, and Shaun Pather. Barriers for user acceptance of mobile health applications for diabetic

patients: applying the UTAUT model. In: Conference on e-Business, e-Services and e-Society, pp. 61-72. Springer, Cham, 2020
14. Tao Da, Wang Tieyan, Wang Tieshan, Zhang Tingru, Zhang Xiaoyan, Xingda Qu (2020) A systematic review and meta-analysis of user acceptance of consumer-oriented health information technologies. Comput Human Behav 104:106147
15. Alazzam Malik Bader, Sibghatullah Abdul Samad, Ramli Mohamad Razif, Jaber Mustafa Musa, Naim Mohd Hariz (2016) Pilot study of EHRs acceptance in Jordan hospitals by UTAUT2. J Theor Appl Inf Technol 85(3):378

Medical Image Classification Based On Optimal Feature Selection For Brain Cancer Detection

Anishma Krishnadas
Dept.of Biomedical Engineering
KMCT College of Engineering for Women Calicut, India
anishmakrishnadas01@gmail.com

Ayisha Hanan M
Dept.of Biomedical Engineering
KMCT College of Engineering for Women Calicut, India
ayishahananm@gmail.com

Fathima Jabin M
Dept.of Biomedical Engineering
KMCT College of Engineering for Women Calicut, India
fathimajabin121@gmail.com

Bareera EM
Dept.of Biomedical Engineering
KMCT College of Engineering for Women Calicut, India
bareeraem@gmail.com

Remya V
Assistant Professor
Dept.of Biomedical Engineering
KMCT College of Engineering for Women Calicut, India
remyav@kmctcew.ac.in

Abstract— This world was in search of simplified and time- consuming methods in every field. Image classification is such type of method in the medical field such as CT, MRI, etc. Image classification helps in the early diagnosis of cancer. The developing technology was influencing everywhere. In the medical or clinical field, image classification technique was common. But it is something difficult in computer-aided diagnosis. Hence, optimal feature selection-based image classification incorporates preprocessing. By analyzing features like image texture, shape, and size image can be classified as benign or malignant. Optimal feature selection-based image classification helps to get accurate and increased classification according to the dataset. In this paper Convolution Neural Network (CNN) was used as the algorithm for the classification. It increases the accuracy of image recognition and also detects the important feature of an image. The Opposition Based Crow Search (OCS) algorithm is implemented to improve the performance of this classifier.

Keywords—preprocessing, feature extraction, optimal feature selection, histogram equalization, crow search algorithm, image classification

I. INTRODUCTION

Where information technology meets the needs of human health care, medical informatics has emerged as a popular academic area. In the field of "medical imaging", many research activities are being carried out for the purpose of diagnosis and clinical research. A key stage in medical image analysis, medical image classification seeks to separate medical images based on specific parameters such as clinical pathology and imaging modality. Doctors can rapidly and accurately evaluate medical images with the aid of a trustworthy medical image classification system. A dependable medical image classification system helps doctors interpret medical images quickly and precisely. Images are collected from computer-aided examination analysis by various imaging systems such as magnetic resonance imaging (MRI), computed tomography (CT), and ultrasound B-scans. When tackling issues with image classification, both descriptive power and power of extracted features are crucial for improving classification performance. Due to its numerous applications in data mining, predictive modelling, media information recovery, and other areas, this branch of machine learning is in high demand. Databases of medical images are used for teaching and classifying images. They frequently include brief descriptions and photographs of variable quality and circumstances. Along with disease identification, it's critical to understand the most significant risk variables in medical diagnosis. The basic features of traditional medical image classification algorithms are many features such as color, texture, and shape. When managing high-dimensional feature spaces through

optimization, a subset of the best features is specified in a way that enhances classification or regression model performance. New issues are created by an optimized representation of a selected subset of features. The implementation of one of the recently suggested swarm intelligence-based algorithms. Manual selection of the best features becomes important therefore, optima l feature selection is used.

II. LITERATURE REVIEW

In [1] is primarily concerned with the study of deep learning and its applications to image analysis. In the field of medical image analysis, convolutional neural networks and its derivatives have emerged as the most popular and commonly applied deep learning models. In this study, brief introductions to contemporary deep-learning models used in medical picture processing are given. provides a thorough discussion of the primary functions of deep learning models, including classification, segmentation, retrieval, detection, and registration. Recent studies have demonstrated that deep learning models can do better than medical specialists in several tasks. With the substantial advancements achieved in deep learning techniques, it is anticipated that patients will soon be able to engage with AI-based medical systems in a safe and convenient manner, and that such intelligent systems will really improve.

In [2], Abdu Gumei, et.al. proposed a method for accurately classifying brain tumors using a hybrid feature extraction technique and a regularized extreme learning machine (RELM). The approach begins by improving the contrast of brain images through normalization. Features are then extracted from the images using a combination of PCA and the Normalized GIST descriptor, without the need for image segmentation. The RELM is used to classify the tumors and to prevent overfitting. The method was tested using a public dataset of brain images and was found to be more effective than existing approaches, with an improvement in classification accuracy from 91.51% to 94.233%.

According to [3], technology and the rapidly expanding field of brain imaging technologies have played a crucial part in assessing and honing the new perspectives on the structure and functioning of the brain. In the field of medical science, image processing is frequently used to enhance the early detection and treatment stages. Deep neural networks (DNN) have so far shown excellent performance in classification and task segmentation. Taking this into account, the deep wavelet autoencoder (DWA) technique for image compression is suggested in this study. DWA combines the basic feature reduction function of the autoencoder with the picture decomposition capability of wavelet transform. The size of the feature set for enduring future classification tasks utilizing DNN is greatly sunk by the combination of both. The suggested technique outperforms the existing methods when the performance criterion for the DWA-DNN classifier is compared to those of other existing classifiers, such as autoencoder-DNN or DNN.

Convolution neural networks based on complicated networks (CNNBCN) with modified activation functions for brain tumour classification using magnetic resonance imaging are described in [4]. Three techniques are offered for randomly generating graphs in the first stage of construction: the Erdos- Renyi (ER), Watts-Strogatz (WS), and Barabasi-Albert (BA) algorithms. In order to give the network generator structure and completion, the created graph is transformed into a trainable network. The graph's complexity is reflected in the graph's mode and edges. The direct graph was then changed into a direct acyclic graph (DAG). then created a trainable network by mapping the straight DAG. For image classification, the CNNBCN model is employed, and it is compared to a modified CNNBCN. The improved model has higher accuracy.

In [5], a single universal network may simultaneously address the segmentation and classification challenges by segmenting several organs using various modalities. With two output heads, one for segmentation and the other for classification, this network architecture is based on the Unet architecture. A concatenating path and an expanding path make up the network. Two layers are optimized by the network. The network's accuracy in classifying modality and viewpoints is 99%. The key benefit is that, in contrast to the conventional approach, error propagation is prevented.

III. METHOD

In this medical image classification process consists of four main stages, which are pre-processing, feature selection, optimal feature extraction and image classification.

1. Preprocessing: The image preprocessing stage helps to improve the quality of images. To enhance the input image quality, here use histogram equalization.

2. Feature selection: Feature selection is the method of reducing the input from the dataset for acquiring maximum accuracy.

3. Optimal Feature Selection (OCS): The selection of features is one of the key stages in image processing, and it simplifies the process of classifying images.

4. Classification: This stage aims to classify medical images as benign or malignant based on the best features that were chosen.

A. Pre-processing

A medical image quality is described in terms of spatial resolution, contrast, image noise, and artefacts. Medical images are distorted by many noise types during the processing of medical imaging. For the specific use, it is crucial to make precise observation easier. When the dose added to the image is larger, image noise is reduced, and low- contrast structures are easier to perceive. Reconstruction filter significantly affects both image noise and resolution, and sampling effectively limits spatial resolution. In order to achieve diagnostically acceptable image quality at reasonable radiation doses, well defined clinical procedures are required. These protocols should include the kilovolt peaks, slice thicknesses, amperages and reconstruction filters.

1) Histogram equalization

To improve the quality of the images, histogram equalization (HE) is performed. In order to continuously reposition the image pixels in space, this is accomplished by levelling the grey levels of the pixels. When the foreground and background of an image are both black or bright, the approach works well. Before being transformed into an output image, the input image's histogram is assessed, normalized for sum evaluation, and analyzed.

2) Median filter

To remove noise from an image or signal, this method uses a digital filtering technique known as median filtering. This type of noise reduction is a common preprocessing method to improve the results of subsequent processing (such as image edge detection). This filter can be used to preserve edges while reducing noise and can be used for signal processing. Median filtering is very common in digital imaging.

B. Feature selection

A dimensionality reduction technique used in datasets called feature selection removes superfluous or unessential features from the preprocessed image. Fewer data must be transmitted, according to the feature selection technique. In the course of data mining, many feature extraction models are frequently used. The suggested method employs two techniques, GLCM and GLRLM, to extract the desired features.

1) Gray-level Co-occurrence Matrix (GLCM)

A statistical method for evaluating textures considering the spatial relationships of pixels is the gray-level co- occurrence matrix (GLCM), often referred to as the gray-level spatial dependency matrix. The GLCM function computes the GLCM, extracts statistical measures from this matrix, and then examines the frequency of occurrence of groups of pixels with different values in a particular spatial relationship in an image. For photos with slow texture changes, the diagonal value of the grey-level co-occurrence matrix is higher; for images with fast texture changes, the diagonal value is smaller. The amount is greater. Since the grey-level co-occurrence matrix has a large amount of data, it's usually not used to directly detect textures.

2) Gray-level Run Length Matrix (GLRLM)

A common technique for extracting statistics from medical images is the Gray-level Run Length Matrix (GLRLM). Entries in this matrix contain statistics that reflect the distribution and connectivity of image pixels. GLRLM construction and feature extraction is complex and computationally intensive because the images are too large for high resolution or there are too many small regions of interest (ROI) to process in one image. This makes the preprocessing phase a lengthy process. The statistics of interest in a gray- level run length matrix (GLRLM) are the number of pairs of gray-level values and their run lengths in a particular region of interest (ROI). A group of pixels with the same gray level value distributed continuously and colinearly along a particular direction within the ROI is called a "gray level run". This particular set of pixels is called the length of the

gray level run. This allows such sets to be described by grayscale values and their lengths. The occurrence of all possible combinations of grayscale values and gradients within an ROI in a given direction are captured by GLRLM, a type of 2D histogram in matrix form. To aggregate the network, the image is commonly lowered in maximum grey dimensions G by preceding re-quantizing. Table 1 lists the features that were isolated with the aid of GLRLM and GLCM.

TABLE 1.

Feature description	Feature	Description
GLCM Features		
F1	Energy	Provides the GLCM's element squared sum. additionally referred to as uniformity or the angularsecond moment.
F2	Contrast	Evaluates the local variations in the gray-level co- occurrence matrix.
F3	Homogeneity	Measures the proximity of the scattering of elements in the GLCM to the GLCM diagonal.
F4	Correlation	Measures the joint probability occurrence of the specified pixel pairs.
GLRLM Features		
F5	Short Run Emphasis (SRE)	The SRE is often large for fine surfaces and is highly dependent on the occurrenceof short runs.
F6	Long run Emphasis (LRE)	Long runs are computed by LRE. LRE is based on the long run that are intended to target maximum textures.

C. Optimal feature selection based on OCS Algorithm

The optimal subset of features was selected from the pre- processed medical image utilizing texture characteristics like GLCM and GLRLM. Since it takes a longer calculation time to complete, the retrieved features were not directly fed into the classification process. To identify the most significant features, the optimal feature selection module, also known as OCS, was selected.

1) Crow search algorithm

The crow search algorithm is the basis of idea that crows are scavengers who like to hide and grab food. By emulating the crow's behavior, the characteristics of CSA are demonstrated since the crow finds food hiding spots, forms a flock, and follows other crows by probability to steal. Typically, CSA can solve various complex engineering problems in the direction of optimal solutions in the search space. It works based on the location and memory update. Based on the feasibility of each crow's location, the memory is updated, correspondingly. The solution is sorted based on the number of iterations.

2) Opposition based crow search (OCS) algorithm

The contrast operation was added to increase the efficiency of the conventional CS technique, which is called the OCS algorithm. The adjacent opposite operation also begins to function for each began solution. Once solutions are considered, better alternatives can be selected in order to arrive at the optimal solution.

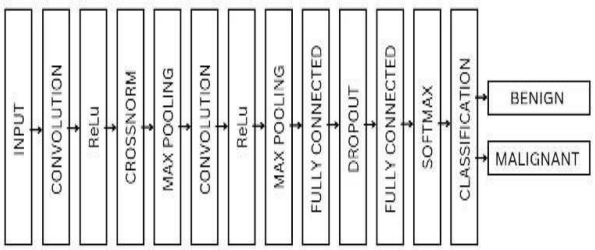

Fig.1.CNN Architecture

D. Image classification

After selecting the best features, the image was divided into two classes, benign and malignant, using the DL approach. The classification algorithm was induced using the relieved feature set. CNN performs feature extraction and classification through sequentially trainable layers placed one after the other. For giving a classified output, we have to give the image as well as the feature set to the following architecture (Fig.1).

This CNN model has 13 weighted layers (1 input, 2 convolutions, 2 ReLu, 2 fully connected, 2 max pooling, 1 normalization, 1 softmax, 1 dropout, and 1 classification) to classify a given image into 2 classes, the output layer has 2 neurons. The softmax classifier retrieves the

output of the final fully connected layer, a two-dimensional feature vector, and makes the conclusive determination of whether or not there is a tumour.

IV. RESULT AND CONCLUSION

In this paper, we proposed a medical image classification system to classify brain tumor as benign and malignant from MR images. This classification method helps in selecting the best features from the images. Thus, a new system of clinical image classification was based on the soft set to achieve better execution in terms of accuracy. The performance measures of the proposed DL achieved 96% accuracy in DL classifier with optimal features (OCSA) model. Current strategies can be modified to include other measurable features to enhance robustness in classifying difficult medical images. The technology presented here causes the greatest cost. We obtained optimal results, but accuracy should be improved using large feature deletion and training set extension. Future investigations should use segmentation systems and some automated classification techniques to identify tumor parts in medical images.

REFERENCE

1. Hafiz Mighees Ahmad. Adeel Yousaf . Sajid Ghuffar. Khurram Khurshid . "Deep Learning: A breakthrough in Medical Imaging." Medical Imaging. Curr Med Imaging. pp. 946-956. 2020.
2. A. Gumaei, M. M. Hassan, M. R. Hassan, A. Alelaiwi and G. Fortino, "A Hybrid Feature Extraction Method With Regularized Extreme Learning Machine for Brain Tumor Classification," in IEEE Access, vol. 7, pp. 36266-36273, 2019.
3. Khan MA, Lali IU, Rehman A, Ishaq M, Sharif M, Saba T, Zahoor S, Akram T. Brain tumor detection and classification: A framework of marker-based watershed algorithm and multilevel priority features selection. Microsc Res Tech. 2019 Jun;82(6):909-922. doi: 10.1002/jemt.23238. Epub 2019 Feb 23.
4. Z. Huang et al., "Convolutional Neural Network Based on Complex Networks for Brain Tumor Image Classification With a Modified Activation Function," in IEEE Access, vol. 8, pp. 89281- 89290, 2020.
5. Harouni, A. Karargyris, M. Negahdar, D. Beymer, and T. Syeda-Mahmood, ''Universal multi-modal deep network for classification and segmentation of medical images,'' in Proc. IEEE 15th Int. Symp. Biomed. Imag. (ISBI), Apr. 2018, pp. 872–876.
6. Chetana Srinivas, et.al., "Deep Transfer Learning Approaches in Performance Analysis of Brain Tumor Classification Using MRI Images", Volume 2022 , 2022.
7. Ker D J, L. Wang, J. Rao, and T. Lim (2018) Deep learning applications in medical image analysis, IEEE Access, vol. 6, pp. 9375– 9389, 2018.
8. Affonso C, A. L. D. Rossi, F. H. A. Vieira, and A. C. P. de Leon Ferreira de Carvalho (2017) Deep learning for biological image classification, Expert System Application Journal vol. 85, pp. 114– 122C

Smart Assistive System for Visually Impaired People

Devika K
Dept. of Biomedical Engineering, KMCT College of Engineering for Women, Kozhikode
devikasumal@gmail.com

Fathima Noula
Dept. of Biomedical Engineering, KMCT College of Engineering for Women, Kozhikode
fathimanoula11@gmail.com

Shahana Fathima K
Dept. of Biomedical Engineering, KMCT College of Engineering for Women, Kozhikode
shahanafathimak567@gmail.com

Anagha N
Dept. of Biomedical Engineering, KMCT College of Engineering for Women, Kozhikode
anagha946@gmail.com

Anusha E P
Dept. of Biomedical Engineering, KMCT College of Engineering for Women, Kozhikode
anushachandran08@gmail.com

Sivanath P I
Dept. of Biomedical Engineering, KMCT College of Engineering for Women, Kozhikode
sivanathpi@gmail.com

Abstract-The eyes are our body's extraordinarily evolved sensory organ, as they provides an accurate and complex representation of the environment that can be processed to glean valuable information. Visually impaired people sense their lifestyle is incomplete as they are able to simply touch, feel and smell matters however, can't see them. Daily activities are hampered due to their inability to conceive their surroundings. In this paper, our main aim is to improve the lives of the visually impaired people by among those who are blind by providing mobility and safety measures without depending on others. We help them reduce the suffering of everyday life by developing a hardware prototype and create appropriate software. The suggested approach makes use of a raspberry-pi, camera, speaker, bluetooth and buzzer. Comparable systems lack some of the qualities that the suggested system possesses. This system will help and serve as an effective solution for people with visual impairments. It would enable them to move around with the same ease and confidence as sighted people. It makes the existence prosperous, less complicated and less difficult for visually impaired people.

Keywords- Raspberry-pi, GPS, OCR.

I. INTRODUCTION

A much larger element of the brain is devoted to imagination and prescient than to hearing, taste, touch or smell combined. The malfunction of the eyes might have negative impact on the ability to adapt the information from the outside atmosphere. Conditions affecting the visual system may result in visual impairments, and in the worst cases, blindness, which may make it difficult for people to carry out daily activities like working, studying, and participating in sports. Most visually impaired people require assistance in recognizing barriers, and frequently receive it from others.

The problem of visual impairment is becoming more serious as the world population ages. According to the World Health Organization (WHO), 285 million people worldwide suffer from vision impairment. There are 39 million blind people in worldwide, among them. In the US, there are about 1.3 million people with visual issues. 100,000 of them are students, according to the National Federation for the Blind and the American Foundation for the Blind. The success of public health initiatives has led to a decrease in disease related blindness in recent years. However, every decade, there are 2 million more blind adults over the age of 60.

The term "assistive technology" refers to any program, services, and equipment utilized by persons with disabilities to support their everyday life, ease their activities, and ensures safe mobility. It was created to address common issues with informational transmission, navigation, and mobility-related orientation aids. Through electronic gadgets that enable users to employ object recognition and location to help blind individuals sense the surrounding environment, this assistive technology has been made accessible to blind people.

In this technological age, where everyone is striving to be self-sufficient in order to competitive in a competitive world, being self-sufficient is a key goal for virtually everyone. Due to technological advances in hardware and software, many intelligent alternatives have been created that enable the blind to move freely. The RESIMA architecture to help people with sensory disabilities in indoors has been proposed in [1]. A feedback mechanism based on a model is used to adapt the sensor detection angles and reduce user false alarms in a multi sensor smart cane obstacle detection system [2]. Smart assistive stick for obstacles, holes, water, stairs and other hurdles detection [3]. An assistive technology based on deep learning is used to improve visually impaired people's ability to perceive their surrounding (VI) [4].

However,former exploration has handed colorful results to overcome the problem faced by visually disabled people and give them more independence. But these results have not fully taken into account the safety measures and many of them are limited in scope. They are often both expensive and difficult.

In this work, we suggest a multifeatured system that allows visually impaired people to move around safely and autonomously. The technique for the proposed project is a human-useable camera-based assistive system. The framework is used to integrate image capture technology into an embedded Raspberry-Pi-based system. The system is used to detect objects, optical character recognition, and face recognition, to send an emergency message to the caretaker with the user GPS location and to alert the surrounding people when the user needs help. The visually impaired network will surely benefit from the widespread adoption of this innovative system, as well as model improvements.

II. METHODOLOGY

Smart assistive system is an intuitive combined hardware and software product that would serve as a helping or assistive technologies for those who are blind or have vision problems. The created product will be able to assist those who are visually impaired in simple daily tasks and express all the results or the outputs of the processes. All of these functions would be available for them by pushing a button on a system that corresponds to a specific function. The various functions are processed and executed on the Raspberry Pi processor.

A. Hardware Specifications

In order to efficiently build and use the application, the necessary hardware components are required:

- Raspberry Pi
- Pi camera
- Bluetooth module (HC05)
- Buzzer
- Speaker
- Button

B. Block Diagram

The Raspberry Pi processor board served as the foundation for this suggested system. It regulates the auxiliary devices that serve as a user system interface, such as the camera, speaker, and Android apps. A power supply of 5V DC is given to raspberry pi. The distance to an object is find by using ultrasonic sonic sensor. This system consists of four buttons. Each of the buttons performs its own specific function.

Button 1 is assigned for obstacle detection. If we press the button, the input is given to Raspberry Pi. Then the camera will capture the image and send it for processing. The image will be processed by Raspberry Pi and the object name will be spoken out via speaker. Button 2 is assigned for face recognition. If we press the button, then the camera will capture the frame and send it for processing. The captured frame will be processed by raspberry pi. If the name of the detected person is stored in our database, then it will speak out via speaker. Button 3 is assigned for optical character recognition, or OCR, to identify characters that are subsequently read out by the system over a speaker. The camera will take the picture if we press the button. OCR is used to process the acquired picture and convert it to text. In this manner, a blind person can read a document using a Raspberry Pi based reader for the blind without the use of a human reader or a tactile writing system. Another feature of this device is that we included a help button to send an emergency message to caretaker using the user's GPS location coordinates via. So the caretaker can track the blind very easily. When the user needs help, a buzzer is utilized to inform those in the area.

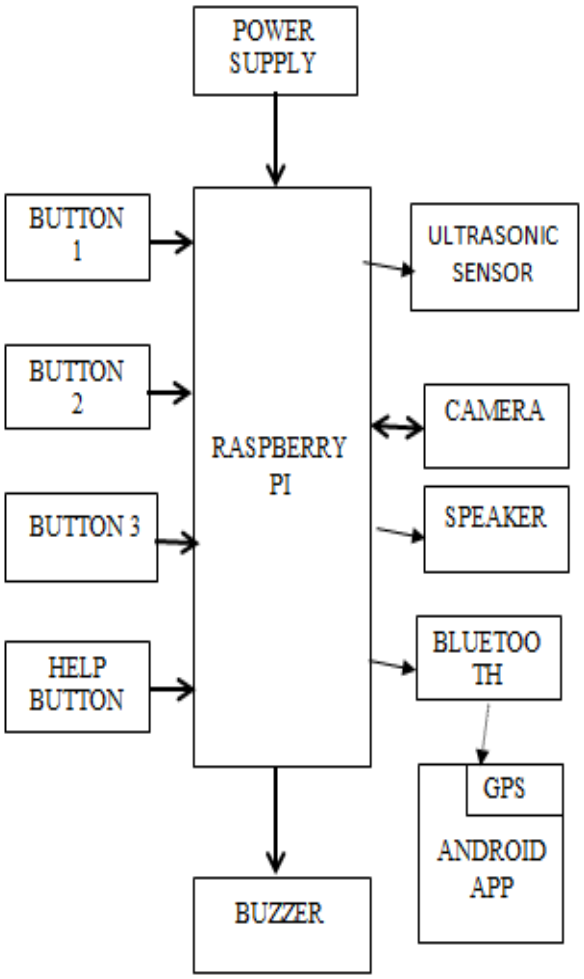

Fig.1. System block diagram

C. Circuit Diagram

The controlled power source provides the circuit with its input. The transformer steps down the mains supply's AC input, or 230V, to 12V, which is then sent to a rectifier. A pulsing DC voltage is produced by the rectifier as its output. Therefore, the output voltage from the rectifier is passed through a filter to eliminate any ac components present even after rectification in order to obtain a clean DC voltage.The rectifier's output is DC voltage, which is what it produces. In order to remove any ac components, the rectifier's output voltage is passed through a filter. The power from the 7805 is now sent via a voltage regulator to provide a clean, consistent DC voltage. Utilizing it is easy. When we switch on the power, we receive a 5 volt supply from the output pin after first connecting the positive lead of our unregulated DC power source input pin and the negative lead to the common pin.

Here, a LED is being used to display the power. A buzzer is connected to a NPN transistor. The system consists of four switches. One end of each switch is connected to Raspberry Pi using a resistor, and other end is grounded. The echo and trigger pins of ultrasonic sensor are connected to Raspberry pi The camera, speaker and bluetooth module are directly connected to Raspberry Pi. The programming LED's are connected to Raspberry Pi by using resistors.

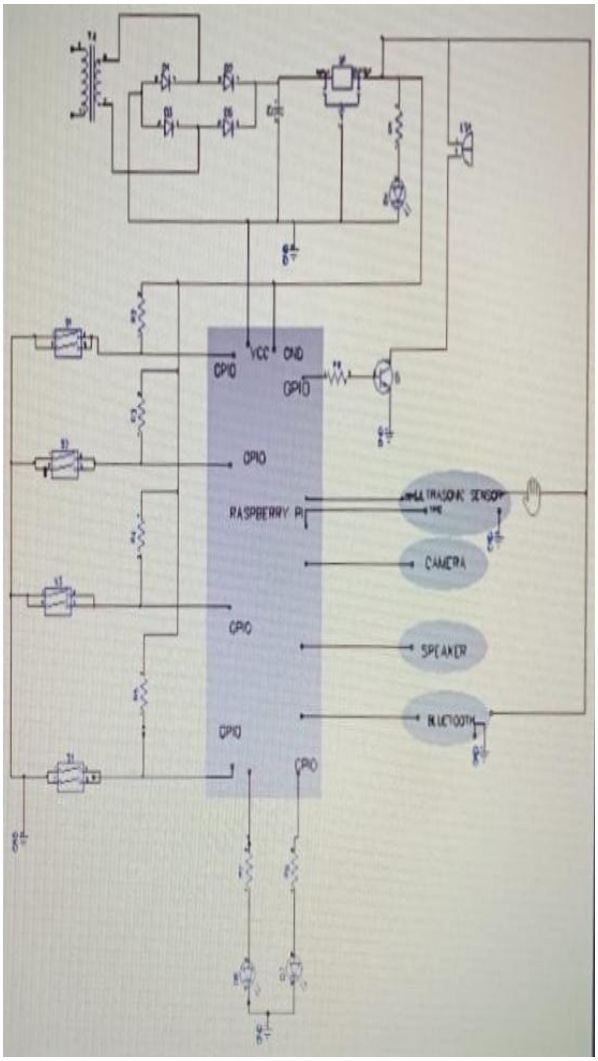

Fig. 2. Circuit diagram for hardware design

D. Software

Software Requirements deals with the prerequisites and resource requirements of software that must be installed on the computer for the application to function optimally.

- Raspberry Pi – Python
- Android app – Java.

1. Flow chart

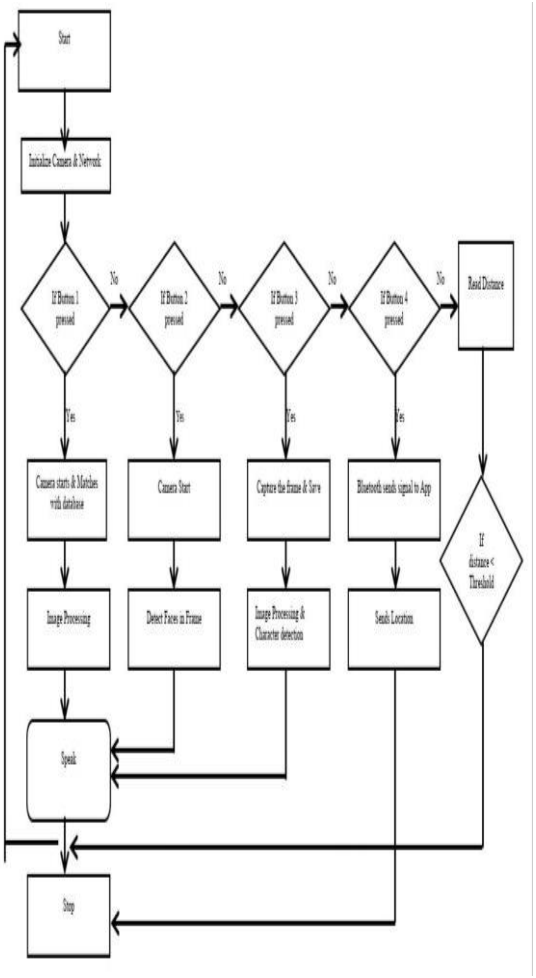

Fig. 3. Flow chart for system operation

2. Algorithm

Step 1: Start.

Step 2: Initialise camera and network (raspberry is powered on).

Step 3: System is ready to process our commands and perform necessary actions.

Step 4: Program is directed to checking the status of the "press button".

Step 5: If yes, it flows goes to detecting obstacles and distance. After the flow is directed towards button pressed block system will out the voice.

Step 6: If no, then it flows goes to detecting faces (button 2).

Step 7: If yes, which is work by invoking to detecting faces.

Step 8: The system will capture the frames, then perform the face detection on the captured frame and if it detects a person whose data is stored in our database.

Step 9: It will speaks name of person.

Step 10: If no, then it flows goes to OCR (button 3).

Step 11: Asks for user input in the form of image which is converted to text by OCR.

Step 12: If the system finds pdf text in the scene (i.e. frame) then it finds the texts and save it in .cv file format inside SD card.

Step 13: Along with saving the image, the system will create the text which is present in the frame.

Step 14: The processed text is converted to audio which enables the blind to hear the text using speakers or earphones.

Step 15: If no, then it flows goes to button 4.

Step 16: Helps the visually impaired to get help in case of emergencies by sending the location of the blind to the emergency number via blind emergency app.

Step 17: If no, Back to Step 3.

Step 18: Stop.

III. CONCLUSION

Technology has played a very important role in our lives. We use it almost everywhere and always. The clear and rapid development that we discover every day proves to us that there is no point in giving up and struggling with our obstacle in life. Technology offers us many sensible solutions to our problems. Our role is to use them properly to achieve success that benefits individuals, society and the country as a whole.

We can conclude that our project can reduce the number of risks and injuries for visually impaired people. The system has a simple architecture that converts visual information captured with a camera into speech information using the Raspberry Pi. The proposed system is cheap and configurable.Additionally, compared to other systems of a similar kind, the system architecture offers increased efficiency.

This project may be improved in the future to add more features and close the accessibility gap between persons with vision impairments and rest of society.

REFERENCES

1. A. A. Nada, M. A. Fakhr and A. F. Seddik, "Assistive infrared sensor based smart stick for blind people," 2015 Science and Information Conference (SAI), 2015, pp. 1149-1154, doi:10.1109/SAI.2015.7237289.
2. N. S. Ahmad, N. L. Boon, and P. Goh, ''Multi-sensor obstacle detection system via model-based state-feedback control in smart cane design for the visually challenged,'' IEEE Access, vol. 6, pp. 64182–64192, 2018, doi:10.1109/ACCESS.2018.2878423.
3. H. Sharma, M. Tripathi, A. Kumar, and M. S. Gaur, ''Embedded assistive stick for visually impaired persons,'' in Proc. 9th Int. Conf. Comput., Commun. Netw. Technol. (ICCCNT), Jul. 2018, pp. 1–6, doi: 10.1109/ICCCNT.2018.8493707.
4. Y. Lin, K. Wang, W. Yi, and S. Lian, ''Deep learning based wearable assistive system for visually impaired people,'' in Proc. IEEE/CVF Int.Conf. Comput. Vis. Workshop (ICCVW), Oct. 2019, pp. 2549–2557, doi:10.1109/ICCVW.2019.00312.
5. S. Srinivasan and M. Rajesh, "Smart Walking Stick," 2019 3rd International Conference on Trends in Electronics and Informatics (ICOEI), 2019, pp. 576-579, doi:10.1109/ICOEI.2019.8862753.
6. Z. Bauer, A. Dominguez, E. Cruz, F. Gomez-Donoso, S. Orts-Escolano, and M. Cazorla, ''Enhancing perception for the visually impaired with deep learning techniques and low- cost wearable sensors,'' Pattern Recognit. Lett., vol. 137, pp. 27–36, Dec. 2020, doi:10.1016/j.patrec.2019.03.008.
7. Z. Xu, H. Chen, and Z. Li, ''Blind image deblurring using group sparse representation,'' Digit.SignalProcess.,vol.102,Oct.2020, Art. No. 102736,doi:10.1016/j.dsp.2020.102736.
8. Z. Li, F. Song, B. C. Clark, D. R. Grooms, and C. Liu, ''A wearable device for indoor imminent danger detection and avoidance with region-based ground segmentation,'' IEEE Access, vol. 8, pp. 184808–184821, 2020, doi: 10.1109/ACCESS.2020. 3028527.
9. W. -J. Chang, L. -B. Chen, M. -C. Chen, J. -P. Su, C. -Y. Sie and C. -H. Yang, "Design and Implementation of an Intelligent Assistive System for Visually Impaired People for Aerial Obstacle Avoidance and Fall Detection," in IEEE Sensors Journal, vol. 20, no. .....17, pp. 10199-10210, 1 Sept.1, 2020, doi: 10.1109/JSEN.2020.2990609.
10. S. Vaidya, N. Shah, N. Shah, and R. Shankarmani, ''Real-time object detection for visually challenged people,'' in Proc. 4th Int. Conf. Intell. Comput. Control Syst. (ICICCS), May 2020, pp. 311–316, doi: 10.1109/ICICCS48265.2020.9121085.

Analysis of SMS Spam Classification Learning and Deep Learning Using Machine

Ayishath Rifa
Dept. of CSE
KMCT College of Engineering for Women, Kozhikode
Kozhikode, India
ayishathrifa5716@gmail.com

Safna Hanan
Dept. of CSE
KMCT College of Engineering for Women, Kozhikode
Kozhikode, India
safnavm123@gmail.com

Rena Salim P
Dept. of CSE
KMCT College of Engineering for Women, Kozhikode
Kozhikode, India
renasalim5@gmail.com

Anagha Ashokan
Dept. of CSE
KMCT College of Engineering for Women, Kozhikode
Kozhikode, India
anaghaashokan504@gmail.com

Aysha Nafla P
Assistant Professor
Dept. of CSE
KMCT College of Engineering for Women
ayshanaflaparoth@gmail.com

Abstract— People who use mobile devices are becoming more numerous every day. Both smartphones and basic phones support message service.

As result, SMS traffic dramatically rose. There were also more spam messages. The spammers attempt to send spam communications in order to benefit financially or commercially, such as market expansion, collection of personal financial card information, etc. Thus, spam-ham classification is given considerable consideration. Here this study, used a variety of machine learning and deep learning techniques to identify SMS spam. We created a spam detection model using data from UCI. With an accuracy of 98.5%, our experimental findings demonstrate that our long short term memory (LSTM) model beats earlier models in spam identification. For all of our implementations, we used Python.

Keywords— Message Service, Spam-ham, Machine Learning, Deep Learning, LSTM, UCI.

I. INTRODUCTION

In five years, there will be 3.8 billion smartphone users, up from uni billion [1]. China, India, and the United States are the most top countries terms of mobile usage. Message Service, is a text messaging service that has been around for a while. You can use message services even without an internet connection. SMS service is thus accessible on both smartphones and low-end mobile devices. Although there are numerous text messaging applications on smart phones, such as WhatsApp, this service can only be used online. However, SMS is available at all times. As a result, SMS service traffic is growing daily. A spammer are person or group of persons that sends unsolicited messages. Spammers bombard people with numerous messages for the advantage of their businesses or for personal gain. Spam messages are what these are known as. Even though there are several SMS spam filtering solutions available [2], more sophisticated methods still need to be used to address this issue. Because of spam texts, mobile users could become irritated. There are two forms of spam messages: SMS spam and email spam. The objective of email SMS spam is the same as spam. In most cases, spammers use these mails to advertise their services and businesses. The users may occasionally suffer financial loss as a result of these spam mails. Machine learning is a technology that make works the computers to learn from the past and makes prediction about the future. In today's environment, machine learning and deep learning can be used to address the majority of real-world issues in all fields, including security, market research, and health. Machine learning uses a variety of techniques, including supervised learning, unsupervised learning, semi supervised learning, and others.

Unsupervised-learning deals with datasets without labels, whereas supervised learning uses output labels on the dataset. We applied multiple supervised learning techniques to a labelled dataset from UCI.

II. LITERATURE REVIEW

Spam detection using ML and DL methods is nothing new. In the past, numerous academics used ML approaches to categorize SMS spam. Amir Nilam With the use of a random forest classifier and the TF-IDF approach, Sjarif[3] et. al. were able to attain an accuracy of 97.5%.A document's words can be quantified by using two metrics - Term Frequency and Inverse Document Frequency - through the TF-IDF method. For email spam filtering, In this study, A. Lakshmanarao [4] et al used four machine learning classification algorithms: Random Forest, Naive Bayes, Decision Trees and Logistic Regression. And utilized a random forest classifier to attain 97 percentage of accuracy. With support vector machines, In a study conducted by Pavas Navaney[5] et al., the accuracy of the predictions was 97.4% using a number of machine learning techniques. By using a logistic regression classifier, Luo GuangJun [6] et. al. were able to attain a high accuracy rate using a variety of shallow machine learning techniques. The Hidden Markov Model was suggested by Tian Xia[7] et. al. for the in an SMS. Their model addressed problems with low term frequency by making use of the word order information. They obtained a 98% accuracy with their suggested HMM. model. With a deep neural network, M. Nivaashini [8] et. al. were able to detect SMS spam with an accuracy of 98%.

Random Forest NB, and KNN and SVM, performance were also contrasted with DNN performance. Mehul Gupta[9] et al. evaluated By using deep learning models and demonstrated techniques for machine learning had a high accuracy rate for detecting SMS spam. For spam identification in an SMS, Gomatham Sai Sravya[10] et al. examined a number of machine learning techniques and found that it was most accurate with He classification model using Naive Bayes. With the aid of a support vector machine, M. Rubin Julis[11] et al. were able to obtain an accuracy of 97%. Recurrent Neural Networks were proposed by K. Sree Ram Murthy [12] et al. for spam identification in an SMS, and they had a decent accuracy rate. S. Sheikh[13] developed the neural network and feature selection model for SMS spam identification and reported a higher percentage of spam detection . For SMS spam identification, Adem Tekerek[14] et. al used a variety of a support vector machine classifier and machine learning classification models to get 97 Percentage of accuracy.

III. METHODOLOGY

The SMS spam dataset was first obtained from the UCI ML repository. Later, we cleaned the dataset using several text preparation methods. Then, using LSTM and other machine learning techniques, figure 1 shows the suggested model.

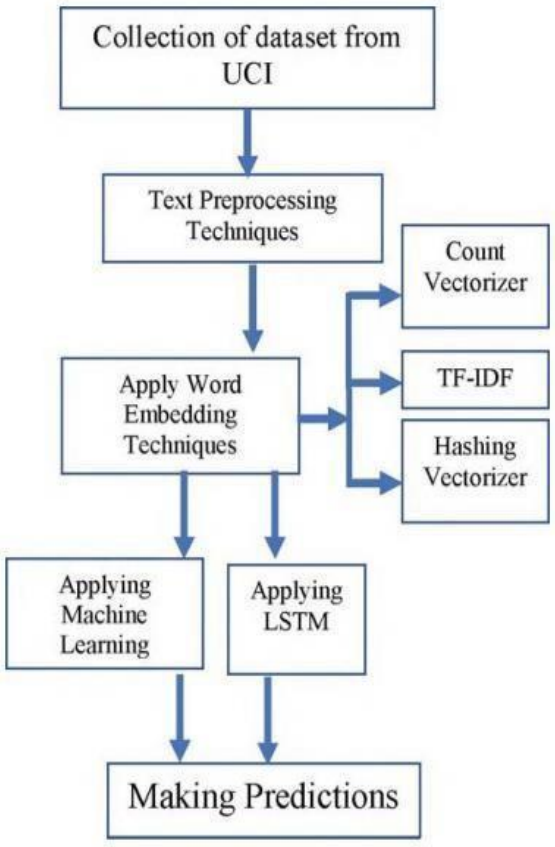

Fig. 1. Proposed Framework for SMS Spam Detection

A. Dataset

A dataset was downloaded from the UCI repository. There are two columns and 5572 rows in the dataset. The message's status as "ham" or "spam" is indicated in the first column. Here, "ham" stands for a typical message while "spam" refers to an uninvited message. The message itself is found in the second column.

Table. 1. Dataset details

Dataset	Number of Training samples	Number of Testing Samples	Total
Dataset-(UCI)	4746	986	5572

B. Text Preprocessing

Vectorized text data can be represented in various ways. There are many NLP (Natural Language

Processing) techniques that can be used for text preprocessing. Algorithms for machine learning only use numbers. Therefore, text data must be encoded into a numeric representation. Tokenization is a method for breaking up text data into smaller chunks. Stop words from in-text preprocessing are eliminated. Stop words are terms that are useless for text data analysis. For instance, stop words include the terms is, was, and that. Stemming can also be used after removal. The process of stemming involves stripping a word down to its stem. The word "playing," for instance, can be altered to "play." The words can then be transformed into vectors of real values in word embedding.

Three different word embedding methods were used. They are;

- Count Vectorizer
- TF-IDF Vectorizer
- Hashing Vectorizer.

I) Counting Vectorizer

All pre-processing such as removing special characters, converting to lower case, etc. is done in this first. Later, it identifies unique words throughout the text and creates an array of zeros for each sentence. Then add the word count to each sentence. The resulting vector is a vector representation of the given text.

II) TF-IDF Vectorizer

The model uses two measures: Term Frequency and Inverse Document Frequency. TF is the frequency with which the sentence appears. IDF is the inverse document frequency. IDF(i)=log2(number of documents / number of sent documents

III) Hashing Vectorizer

A hash vectorizer converts text into a vector using a hashing algorithm. This algorithm can be applied to all sentences in the document.

C) Machine learning techniques

After converting the text to real-valued vectors, we applied various machine learning classifiers such as naive Bayes and random forest decision trees. Apply deep learning model "LSTM".

I) Naive Bayes Classification

The Naïve Bayes Classification algorithm is based on Bayes' theorem. This theorem is based on probability theory.

II) Logistic Regression

Logistic regression uses logit and sigmoid functions for classification tasks. Output variables are predicted based on sigmoidal curves.

III) K Nearest Neighbor

K-NN is a simple but efficient machine learning classifier based on distance computation. It identifies the k nearest neighbours and new data points are classified based on the number of neighbouring classes.

IV) Decision tree classification

A decision tree classifier creates a tree on which to base classification. The tree is built recursively up to a fixed minimum number of nodes.

V) Random Forest Classification

A Random Forest Classifier uses the opinions of multiple decision trees to determine the class of a new data point. It's an ensemble approach.

VI) Support Vector Machine

SVM constructs a hyper plane and performs classification based on it. Some data points are used as support vectors to find hyper planes.

VII) LSTMs

An iterative neural network is a type of artificial neural network. In RNN, the current status input is taken from the previous status output. However, traditional recurrent neural networks have a zero-gradient problem. To solve the traditional RNN problem, descent. LSTM

(Long Short Term Memory) was introduced. LSTM is better suited for text mining problems.

IV EXPERIMENTATION AND RESULTS

A. Evaluation Metrics

The three metrics used to compare classifier performance are precision, recall, and accuracy.

Precision=True Positives/(True Positives + False Positives)

Recall=True Positives/(True Positives + False Negatives)

Accuracy= (TP + TN) /(TP+TN+FP+FN).

B. Results of the experiments with Count Vectorizer Six machine learning techniques for categorization were used: Logistic Regression, K-NN, DT, SVC, Naive Bayes, and Random Forest.

The best accuracy we could get with logistic regression was 94%.

REFERENCES

1. Online:https://www.statista.com/statistics/330695/ number-ofsmartphone-users-worldwide/
2. S. M. Abdulhamid, M.S.Abd Latif, Haruna Chiroma, "Robust Heart Disease Prediction A Review on Mobile SMS Spam Filtering Techniques", EEE Access, vol. 5, pp. 15650-15666, 2017, doi: 10.1109/ ACCESS. 2017.2666785
3. Nilam Nur Amir Sjarif, N F Mohd Azmi, Suriayati Chuprat, "SMS Spam Message Detection using Term Frequenct-Inverse Document Frequency and Random Forest Algorithm," in The Fifth Information Systems International Conference 2019, Procedia Computer Science 161 (2019) 509- 515,ScienceDirect.
4. A.Lakshmanarao,K.Chandra Sekhar, Y.Swathi, "An Efficient Spam Classification System using Ensemble Machine Learning Algorithm," in Journal of Applied Science and Computations, Volume 5, Issue 9, September/2018.
5. Pavas Navaney, Gaurav Dubey, Ajay Rana, "SMS Spam Filtering using Supervised Machine Learning Algorithms.," in 8th International Conference on Cloud Computing, Data Science & Engineering, 978-1- 5386-1719-9/18/ 2018 IEEE.
6. Luo GuangJun,, Shah Nazir, Habib Ullah Khan, Amin Ul Haq, "Spam Detection Approach for Secure Mobile Messgae Communication using Machine Learning Algorithms.," in Hindawi,Security and Communication Netwroks,Volume 2020, Articleid: 8873639.July-2020.
7. Tian Xia, Xuemin Chen, "A Discrete Hidden Markov Model for SMS Spam Detection.," in Applied Science,MDPI, Appl. Sci. 2020, 10, 5011; doi:10.3390/ app10145011.
8. M. Nivaashini, R.S.Soundariya, A.Kodieswari, P.Thangaraj, ": SMS Spam Detection using Deep Neural Network.," in International Journal of Pure and Applied Mathematics, Volume 119 No. 18 2018, 2425-2436.
9. Mehul Gupta, Aditya Bakliwal, Shubhangi Agarwal,Pulkit Mehndiratta, ": A Comparative Study of Spam SMS Detection using Machine Learning Classifiers.," in 2018 Eleventh International Conference on Contemporary Computing (IC3), 2-4 August, 2018.
10. Gomatham Sai Sravya, G Pradeepini, Vaddeswaram, ": Mobile Sms Spam Filter Techniques Using Machine Learning Techniques.," International Journal Of Scientific & Technology Research Volume 9, Issue 03, March 2020.
11. M.Rubin Julis, S.AIagesan:, "Spam Detection In Sms Using Machine Learning through Textmining", International Journal Of Scientific & Technology Research Volume 9, Issue 02, February 2020.
12. K. Sree Ram Murthy,K.Kranthi Kumar, K.Srikar, CH.Nithya, S.Alagesan:, "SMS Spam Detection using RNN", : International Research Journal of Engineering and Technology (IRJET), Volume: 07 Issue: 05,May 2020.
13. S. Sheikhi,M.T.Kheirabadi,A.Bazzazi, "An Effective Model for SMS Spam Detection Using Content- based Features and Neural Network", : International Journal of Engineering, IJE TRANSACTIONS B: Applications Vol. 33, No. 2, (February 2020) 221-228.
14. Adem Tekerek "Support Vector Machine Based Spam SMS Detection", Journal of Polytechnic, 2019; 22 (3): 779-784.
15. https://archive.ics.uci.edu/ml/datasets/SMS +Spam+ Collection

Leukemia Detection Using The K-Means Algorithm

Ayisha Amreena P
Dept. of CSE
KMCT College of Engineering for Women, Kozhikode
Kozhikode, India
amreenaayisha@gmail.com

Fahmidha K
Dept. of CSE
KMCT College of Engineering for Women, Kozhikode
Kozhikode, India
fahmidha001@gmail.com

Anu K S
Assistant Professor
Dept. of CSE
KMCT College of Engineering for Women
anuksoman@gmail.com

Shamna Nourin
Dept. of CSE
KMCT College of Engineering for Women, Kozhikode
Kozhikode, India
shamna3371@gmail.com

Abstract--- Leukemia, a type of blood cancer, is one of the leading causes of death in people. The speed of recovery largely depends on the early diagnosis and detection of a disease. The major cause of leukemia is when the bone marrow creates an excessive amount of abnormal white blood cells. Hematologists employ human blood samples for their microscopic image analysis, which necessitates the use of the subsequent techniques, including microscopic color imaging, image segmentation, clustering, and classification. These techniques make it simple to identify patients with this condition. Various techniques for detecting blood cancer in visible and immature white blood cells are made possible by microscopic imaging. Early and prompt detection of leukemia substantially aids doctors in giving patients the right care.

I. INTRODUCTION

The most common cause of mortality in people is blood cancer. One in six fatalities are caused by cancer. Leukemia is also referred to as "blood cancer." The only source of cancer cells in every part of the body is white blood cells, yet many cancer cells contain dividing cells. As the old cancer cells are destroyed, new cancer cells take their place. They are producing a new generation of cancer cells that are lifeless and cause blood cancer. The expansion of blood cells results in the death of other bodily cells. Additionally, it results in increased orgasms, severe anemia, bleeding, and infection as the pain or swelling spreads to the lymph nodes.

They were therefore useful for detecting cancer at various stages. Imaging techniques can identify patterns in huge data sets while reliably predicting blood cancer outcomes in the future and the patient's present condition. using a sample set of openly available data to examine and assess segmentation and classification algorithms. In order to allow users to assess how well different algorithms work, each image in the data set has a number of merit values provided in the cell rating.

An entire amount of blood cells is used to compute the percentage of blood cells. There are two distinct types of blood cancer: acute and chronic. Using images from an electron microscope, we treat lymphocytic and acute leukemia. Approaches for enhancing contrast and segmentation are used for detection. The photo was used as a compilation of data to forecast lung cancer. The Bayesian Network and the J8 algorithms are equivalent to different classification methods like Naive Bayes for the prediction of lung cancer. The Nave Bayes algorithm outperformed other algorithms. On MATLAB, the diagnosis of blood cancer can be aided by imaging cancer, including enhancement, clustering, mathematical processing, and labelling.

For the identification and classification of blood cancer, algorithms like SVM and KNN have produced trustworthy findings. It has been

investigated how to detect calcifications with the benefits of anisotropic diffusion. It has been attempted to increase the sensitivity and promptness of the detection of various cancers using hepatocellular carcinoma (HCC), a prevalent kind of liver cancer diagnosed by thresholds for particular circulating blood biomarkers. Cancer is divided into learning approaches that are supervised and unsupervised using single layer feed forward in the hidden layer. Fuzzy methodologies and methods are used in unsupervised learning for non-fuzzy classification. Backward propagation training combined with a single hidden layer of NN power is used in supervised learning to remove errors.

By using various variables as inputs to the network, such as cell size, strength, texture, form factor, and DNA, this yields 96.9 accurately calculated outcomes. Conventional cancer prediction approaches frequently exhibit inaccuracy or deception, however a molecular diagnosis using micro-array gene expression technology is extremely trustworthy and frequently successful. Fuzzy Neural Network (FNN) technology is employed to detect cancerous cells. For classification (SVM) and FNN, vector machine methods are employed (Fuzzy Neural Network). To classify and compare cancer cells with other types of cells for research purposes, imaging data is collected.

Gene selection provides a list of various typing methods. Cancer data have very high dimensions, therefore the features are chosen, and accuracy ranges from 92 to 96 percent. CT scans of tumors are diagnosed with an accuracy of 60% using the Particle Swarm Optimization (PSO) method and the Search Engine Optimization (SOA) algorithm. Edge detection segmentation is used to identify and assess the liver tumor using several imaging segmentation techniques such region, threshold, level set, and clustering. This helps identify and categorize the tumor.

Breast cancer is discovered through the ART1 network. There are three steps: recognition, comparison, and search. Error minimization and network design training are two uses for the back propagation method. This demonstrates the accuracy of the ART1 network to a 92% level. Neural network technologies have so far been applied for cancer classification in the unsupervised learning pattern.

The K-means grouping approach is used to research the characteristics of breast cancer, and comparisons have been conducted using various distance measures, scoring methodologies, and comparing the average likelihood that offers a 100% accurate categorization. In order to evaluate centroid initialization, distance measurements, and the division method, the K-mean methodology for clustering was used to analyze the data collection on breast cancer in Wisconsin.

The K-Means algorithm was used to reach the conclusion while taking into account several situations with varied parameters. Taking into account the blood sample data set, blood cancer can be detected using the decision tree method, which looks for previously unidentified patterns in the data. By taking the data set to be analyzed into account, blood cancer can be more easily detected. A dataset with plenty of transactions is used to apply the a priori algorithm. The algorithm picks up the corresponding rules. Associated rules are methods for discovering connections and correlations between database variables.

The clustering technique Maximizing Expectations [EM] is used in data mining to find knowledge. The K-means method and this one are comparable. The EM algorithm maximizes the likelihood of observing the data by analyzing the parameters of a statistical model with unseen variables. The KNN algorithm is used to generate the observed data, which is processed using blood samples, according to the statistical model. The CLAH method boosts the image's contrast. By utilizing the processed image to train the model with the KNN method, the patient's lung cancer status can be determined.

II. RELATED WORK

[A] Image Analysis of Peripheral Blood Smear Slides for Cell Segmentation and Border Identification

For images captured from peripheral blood smear slides, an unsupervised blood cell segmentation algorithm is shown here. All object cells, cell groups, and cell fragments are located using this procedure. Describes the internal points of each object. Identifies an exact border that is one pixel wide for each object. Two sets of photos were used to test the entire method. 97.3% of the 2962 picture objects in the initial set of 47 images were properly segmented. The success percentage

for the second test set, 51 photos from a different source, contained 5417 items, with a 99.0% success rate.

A shortest path tree (SPT) is created via the Graph Algorithm and Dijkstra's Shortest Path Algorithm from one starting vertex to all other vertices. To do this, find the shortest total path iteratively between the beginning vertex and a vertex that is already in the SPT, and then add the new vertex to the SPT. By stopping the SPT build before the target vertex is located, this approach can be used to identify the shortest path between two particular vertices.

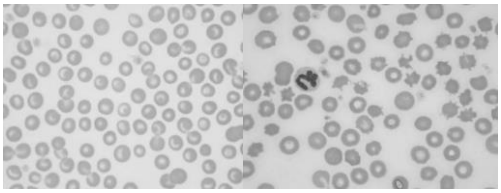

Normal blood Abnormal blood

Fig. 1. images of canine blood smears made from slides of peripheral blood.

[B] The Acute Lymphoblastic Leukemia Image Database For Image Processing

The visual examination of peripheral blood samples is a crucial step in the leukemia diagnosis process. Public blood sample dataset created especially for assessing and contrasting segmentation and classification methods Artificial vision-based automated solutions can expedite this process. Additionally, they can improve response accuracy in telemedicine applications. Here we suggest a brand-new blood sample public dataset.

This is intended primarily for evaluating and contrasting segmentation and classification techniques. In the dataset, the classification of cell is provided for each image. In order to accurately compare various algorithms when dealing with the suggested dataset, a certain set of merit figures must be handled. The dataset can process the selection of lymphocytes, the characterization of tumor cells, and the identification of white cells in the image.

Red and white blood cells make up the majority of the peripheral blood's cells (leucocytes). Granulocytes are leucocyte cells that include granules (composed by neutrophil, basophil, eosinophil). Agranulocytes are cells that lack granules (lymphocyte and monocyte). The peripheral and bone marrow lymphocytes play a role in the all ill ness .The blood preparation colorant primarily concentrates in white blood cells.

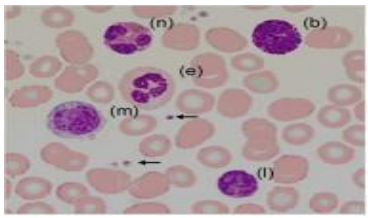

Fig. 2. Basophil (b), eosinophil (e), lymphocyte (l), monocyte (m), and neutrophil are the white blood cells in blood that are colored (n). Platelets are denoted by arrows. Red cells are other components.

C] Detection of Cancer Cells Using Digital Image Processing Techniques

The processes for image processing are widely used in several medical fields to advance earlier detection and therapy stages. It is crucial to diagnose the patient as soon as possible especially when it comes to cancer tumors like lung cancer, where time is of the essence. Due to its high prevalence and challenging treatment options, lung cancer has recently come to the attention of the medical and scientific community. Techniques are:

A. Image Capture

B. Image preparation

C. Processing

D. Segmentation of Images

E. Post-Processing

The two segmentation techniques, thresholding and watershed, are utilised to identify cancer cells and choose the best course of action.

[D] A Review of Blood Cell Image Segmentation

The segmentation of the image is the most important stage of image processing. In essence, segmentation of the image separates the entire image into a number of distinct disconnected parts. The entire procedure is crucial because the segmented image should keep the most relevant information possible while removing unnecessary information. Images obtained during a diagnostic procedure are used in the majority of the proposed approaches. This approach entails

A. image acquisition

B. image preprocessing

C. image segmentation

D. image post-processing

E. image analysis

For automatic cell analysis, segmenting blood cell pictures is an essential stage because accurate image segmentation is largely what determines whether the final classification is successful. The microscopic images have a lot of uncertainty, making this the most challenging component of automatic cell analysis. The foundation for cell phase identification and tracking is cell segmentation, and because cells can cluster or overlap, cell detection before segmentation is incredibly simple. Thus, a three-step detection algorithm is suggested. Binarization technique is used to first achieve cell structure during creation. Second, for the development of local maxima, both intensity and shape information are employed.

The nuclei's pixels are then free to wander about inside the gradient vector field until they eventually meet at these neighbourhood maxima, at which point the discovered in chambers divided using a stream with seeds technique. For image segmentation, a number of all-purpose algorithms and methods have been created. These strategies frequently eed to be combined with domain expertise in order to effectively address an image segmentation problem for a problem domain because there is no generic solution to the picture segmentation problem. The ultimate purpose of blood cell segmentation is to separate each blood cell into its many morphological components, including its nucleus, cytoplasm, holes, and organelles.

III. PROPOSED METHOD

For identifying malignant phases and their early identification, the suggested approach uses K-means. With a 90% accuracy rate in identifying cancer cells, the experiment and results were judged to be encouraging.

IV. CONCLUSION

The dataset obtained from the Kaggle public dataset is made available to researchers for experimental purposes in the proposed approach of diagnosing blood cancer. One of the simple ways to extract the function from the image is through image processing. MATLAB 2018a is used to implement the suggested system. The suggested technique has a 90% accuracy rate and can stage blood cancer.

V. RESULT

The accuracy rate is 98% and can see the stages of blood cancer

REFERENCES

1. Blood Cancer Detection Using Image processing shivkumar Chatarwad,Pratik Bansode, Amar Burade, Prof.T.S Chaware
2. R. Adollah, M.Y. Mashor, N.F.M. Nasir, H. Rosline, H. Mahsin & H. Adilah (2008), "Blood Cell Image Segmentation: A Review", Proceedings of Biomed, Pp. 141–144.
3. N. Ritter & J. Cooper (2007), "Segmentation and Border Identification of Cells in Images of Peripheral Blood Smear Slides", 30th Australasian Computer Science Conference, Conference in Research and Practice in Information Technology, Vol. 62, Pp. 161–169.
4. R. D.Labati, V. Piuri, F. Scotti, "All-Idb: the acute lymphoblastic leukemia image database for image processing",2011.
5. Bhagyashri G. Patil, Prof. Sanjeev N. Jain," Cancer Cells Detection Using Digital Image Processing Methods", International Journal of Latest Trends in Engineering and Technology (IJLTET),vol.3 ISSN: 2278-621X, 2014d for early detection of cancer in blood cells.
6. Christopher, T., & Jamera, J. (2016). Study of Classification Algorithm for Lung Cancer Prediction. A. IJISET - International Journal of Innovative Science, Engineering & Technology.
7. Abdul Nasir, N. Mustafa & Mohd Nasir (2009), "Application of Thresholding in Determining Ratio of Blood Cells for Leukemia Detection", Proceedings of International Conference on Man- Machine system (ICoMMS).
8. Hu.Y., Ashenayi K., Veltri, R., O'Dowd G., Miller G., Hurst R. Bonner. A comparison of neural network and fuzzy c-means methods in bladder cancer cell classification; In Proceedings of IEEE World Congress on Computational Intelligence; 6; 1994; p. 3461 – 3466.

9. Hiro Takahashi, Yasuyuki Murase , Takeshi Kobayashi , Hiroyuki Honda. New cancer diagnosis modeling using boosting and projective adaptive resonance theory with improved reliable index; Biochemical Engineering Journal 33; 2007; p. 100– 109.
10. Yuchun Tang, Yan-Qing Zhang, Zhen Huang, Xiaohua Hu, Yichuan Zhao. Recursive Fuzzy Granulation for Gene Subsets Extraction and Cancer Classification; IEEE Transactions on Information Technology in Biomedicine; 2(6); 2008; p. 723 – 730.
11. Sharma Akanksha, Kuar Parminder. Optimized Liver Tumor Detection and Segmentation Using Neural Network; In Proceedings of International Journal of Recent Technology and Engineering (IJRTE); 2(5);2013;p. 7-10.
12. S. Swathi, G. Anjan Babu, R. Sendhilkumar, Sreenu , Naik Bhukya. Performance of ART1 Network in the Detection of Breast Cancer; In Proceedings of International conference on Comput er design and Engineering (ICCDE2012); 49; 2012 ;DOI:10.7763/IPCSI T.2012.V49.19; p.100-105.
13. Alaa M. El-Halees and Asem H. Shurrab, Blood tumor prediction using data mining techniques. An International Journal (HIIJ) Vol.6, No.2, May 2017 .
14. M. Durairaj and V. Ranjani, "Data Mining Applications in Healthcare: A Study," Int. J. Sci. Technology Res., vol. 2, no. 10, pp. 29– 35, 2013.
15. M. Abdullah and S. Al-Asmari "Anemia types prediction based on data mining classification algorithms," Communication, Management and Information Technology – Sampaio de Alencar (Ed.) 2017.
16. D. Ravi, C. Wong, F. Deligianni, M. Berthelot, J. Andreu Perez, B. Lo, and G.-Z. Yang, "Deep Learning for Health Informatics," IEEE J. Biomed. Heal. Informatics, vol. 21, no. 1, pp. 1–1, 2016.
17. M. Abdullah and S. Al-Asmari "Anemia types prediction based on data mining classification algorithms," Communication, Management and Information Technology – Sampaio de Alencar (Ed.) 2017.
18. A. Sindhu & S. Meera (2015), "A Survey on Detecting Brain Tumor in MRI Images using Image Processing Techniques", International Journal of Innovative Research in Computer & Communication Engineering. Vol. 3, No. 1.
19. Niranjan Chatap & Sini Shibu (2014), "Analysis of Blood Samples for Counting Leukemia Cells using Support Vector Machine and Nearest Neighbor", Vol. 16, No. 5, Ver. III, Pp. 79-87.
20. Arjun Nelikanti, Narasimha LV Prasad, and Naresh M. Goud. "Colorectal Cancer MRI Image Segmentation Using Image ProcessingTechniques."International Journal on Computer Science and Engineering 6.7 (2014) [1].
21. Sungheetha, Akey, and Rajesh Sharma. "GTIKF-Gabor Transform Incorporated K-Means and Fuzzy C Means Clustering for Edge Detection in CT and MRI." Journal of Soft Computing Paradigm (JSCP) 2, no. 02 (2020): 111-119 .
22. Bindhu, V., and Villankurichi Saravanampatti PO. "Semi-Automated Segmentation Scheme for Computerized Axial Tomography Images of Esophageal Tumors." Journal of Innovative Image Processing (JIIP) 2, no. 02 (2020): 110-120.
23. Suresh K and Praveen O, "Extracting of Patterns Using Mining Methods Over Damped Window," 2020 Second International Conference on Inventive Research in Computing Applications (ICIRCA), Coimbatore, India, 2020,pp. 235-241, DOI: 10.1109/ ICIRCA48905. 2020.918289

Easy Learn Using Ml

Akshaya V
Dept of CSE
KMCT College of Engineering For Women, Kozhikode
Kozhikode, India
akshayavp2001@gmail.com

Aswathi Rajagopal
Dept of CSE
KMCT College of Engineering For Women, Kozhikode
Kozhikode, India
aswathirajagopal08@gmail.com

Jumana Haseen K
Dept of CSE
KMCT College of Engineering For Women, Kozhikode
Kozhikode, India
jumanahaseen555@gmail.com

V M Aysha Ishika
Dept of CSE
KMCT College of Engineering For Women, Kozhikode
Kozhikode, India
ayshaishika123@gmail.com

Drishya S.G
Dept of CSE
KMCT College of Engineering For Women, Kozhikode
Kozhikode, India
drishyasg60@gmail.com

Abstract—In the present scenario students faces a number of challenges, including the traditional education system's rigidity, a lack of time to learn about and implement e-learning tools into teaching practise, a shortfall of recognition, Low self-efficacy of teachers in educational technology knowledge, a lack of information and drive among students. The current system converts audio speech into text. There is no combined system for summarization, augmentation and Question-Answer generation. Our system Easy Learn focuses on recording the lecture, summarize and data is augmented along with questionnaire generation thereby improving the teaching and learning process. To implement this, we implemented automated speech recognition, text summarization, chat bots with intelligent educational assistants, and autonomous question generation techniques.

I. INTRODUCTION

As a way to strengthen the methods used in learning and teaching, innovative teaching strategies are gaining popularity all over the world. The term "smart learning" describes how advanced technology help students acquire concepts and skills more swiftly and easily. Researchers are continuously searching for fresh methods and technologies to further the ideas behind smart learning. Exams despite the fact that the global movement towards smart learning is causing a huge change in the way that education is now provided, many people are still perplexed by these ideas. Society typically resists change. Traditional education's rigidity, a shortage of time to learn and use e-learning technologies into teaching practice, with failure to acknowledge teachers' poor self-efficacy in their knowledge of educational technology, and students' lack of understanding and willingness, and other issues are some of the challenges smart learning still faces because it is still in its early stages.

On the other side, smart learning has a number of advantages for the academic community. The benefits include improved productivity, a more engaging and dynamic learning experience, simpler instruction, and cost savings. Smart learning should be embraced by both the academic community and the general public as a solution to numerous issues. Despite all of the difficulties and complexity, research into smart learning and e-learning, as well as related applications, are rapidly growing Automatic speech transcription, automatic text summarization, intelligent chatbots for teaching assistants, and automatic question formulation are some of the examples of trials that have been carried out and others Assisting students with their daily work are a number of smart learning apps, including LinguaKit, GoConqr, Slide Player, and others.

II. LITERATURE SURVEY

Exams have an important role in teaching and learning at all educational levels. Effective assessment activities support students' enthusiasm in learning the subject matter. Exams have

historically been a successful way to evaluate student understanding and help them grow. Examinations are a quick and convenient approach to regularly assess a student's potential. Examinations promote student rivalry. They work harder to develop their skills and expertise. In this way, they learn more. The preparation of the exam's questions and answers is a crucial duty. Manually creating questions is an extremely challenging undertaking. The examiner must consider the entire context before formulating any questions.

According to our research, the majority of examiners claim that this is a time-consuming activity and that, as humans, they run the risk of forgetting some crucial information. We have developed an automated question and answer generation system as a response to these issues. This algorithm analyzes the text sentence by sentence using a natural language processing approach to come up with every question conceivable. Several English grammar variables will be taken into account when validating these questions. After questions have been verified, the text input will be used to select the appropriate replies. From the user's point of view, the user must input text material, after which all possible questions and answers are generated, and the user must select the appropriate questions from the list. Enhanced learning opportunities, Enhanced productivity, and Easier.

Language model pre-training has been shown to be beneficial for several tasks involving natural language processing. These include tasks like named entity recognition and question answering (Tjong Kim Sang and De Meulder, 2003; Williams et al., 2018; Bowman et al., 2015; Williams et al., 2018), which seek to predict the relationships between sentences by analyzing them comprehensively. These tasks call for models to produce fine-grained output at the token level. Rajpurkar and other people (2016). Today, downstream tasks are applied to trained language representations using feature-based and fine-tuning techniques. The pre-trained representations are included as additional features in the task-specific architectures utilized in the feature-based approach, such as ELMO (Peters et al., 2018a). One example of a fine-tuning technique is the Generative Pre-trained Transformer (Open AI GPT) (Radford et al., 2018), which adds only a small number of task-specific parameters and trains on downstream tasks by simply fine-tuning all pretrained parameters. The same objective function applies to both approaches during pretraining, where they both employ unidirectional language models to learn large language representations. We argue that current practices restrict the power of the pre-trained representations, especially for fine-tuning approaches.

The main drawback is that pre training can only use a limited number of designs because conventional language models are unidirectional. For instance, in OpenAI GPT, the authors employ a left-to-right design, where each token can only pay attention to earlier tokens in the Transformer's self-attention layers (Vaswani et al., 2017). Such limitations are not ideal for sentences. Many natural language processing tasks have been proven to benefit from language model pre-training. Sentence-level assignments are among them.

Token-level tasks, such as named entity recognition and question answering, require models to produce fine-grained output at the token level (Tjong Kim Sang and De Meulder, 2003; Rajpurkar et al., 2016). These tasks include natural language inference (Bowman et al., 2015; Williams et al., 2018) and paraphrasing (Dolan and Brockett, 2005), which aim to predict the relationships between sentences by analyzing them holistically. Pretrained language representations can be applied to downstream tasks using either the feature-based approach or the fine-tuning approach. The task-specific architectures used by the feature-based approach, such as ELMO (Peters et al., 2018a), contain the pre-trained representations as additional features.

The Generative Pre-trained Transformer (Open AI GPT) (Radford et al., 2018) uses the fine-tuning technique, which introduces very few task-specific parameters and trains on downstream tasks by simply fine-tuning all pretrained parameters. Pre-training, where both strategies use unidirectional language models to learn broad language representations, has the same purpose as pre-training.

We contend that, particularly for fine-tuning approaches, current strategies limit the effectiveness of the pre-trained representations. The main drawback is that pre-training architectural options are limited due to the unidirectional nature of standard language models. For instance, in Open AI GPT, the

authors employ a left-to-right design, where each token can only pay attention to earlier tokens in the Transformer's self-attention layers (Vaswani et al., 2017). Such limitations are not ideal for activities at the sentence level and could be particularly destructive when applied to token-level-tasks, like question answering, where it is essential to take into account context from both directions. In this study, we propose BERT: Bidirectional Encoder Representations from Transformers, which enhances the fine-tuning-based techniques.

By utilizing a "masked language model" (MLM) pretraining target, which was modeled after the Cloze problem (Taylor, 1953), BERT reduces the previously noted unidirectionality requirement. The goal of the masked language model is to predict the original vocabulary id of the masked word solely from its context after randomly masking some of the tokens from the input. In contrast to pretraining for left-to-right language models, the MLM aim enables the representations to continue the left and right context.

We employ a "next sentence prediction" task that jointly pretrains text-pair representations in addition to the masked language model. BERT uses masked language models to enable pre trained deep bidirectional representations, in contrast to Radford et al. (2018),who pre-train using unidirectional language models. Peters et al. (2018a), on the other hand, employ a shallow concatenation of separately trained left-to-right and right-to-left LMs. We demonstrate how the use of pre trained representations can eliminate the requirement for numerous elaborate task-specific designs. BERT is the first finetuning-based representation model to outperform numerous task-specific architectures and attain state-of-the-art performance on a broad range of sentence-level- and token-level tasks.

For eleven NLP tasks, BERT advances the state of the art.

You may find the source code and pre-trained models at https://github.com/google-research/bert. The same designs are utilized for pre-training and fine-tuning, with the exception of output layers. Models are initialized for various downstream tasks using the same pre-trained model parameters.

All parameters are adjusted during fine-tuning, every input example now has the special symbol [CLS] before it, and [SEP] is a special token that separates questions and answers. , Due to the small amount of training data, deep neural network-based models are prone to overfitting and lose their ability to generalize. Data augmentation techniques are frequently used to produce more training samples in order to address the problem. Data augmentation techniques have been used with remarkable success in the fields of speech recognition and computer vision in recent years. Transformations like scaling, mirroring, random cropping, and color shifting make it simple to add data to these areas. It is impossible to guarantee the semantic invariance and label correctness since the application of these universal modifications to texts is mostly arbitrary and unpredictable.

For instance, given a movie review with the phrase "The actors is good", mirroring produces the nonsensical phrase "doog si srotca ehT" or random cropping produces the useless phrase "actors is".

Existing text data augmentation techniques frequently suffer from loss of generality because they were created with custom rules or pipelines for certain industries. Replacement-based method, which creates new sentences by swapping out the words in the sentences with appropriate ones, is a common strategy for text data augmentation (e. g, .synonyms).

The replacement-based augmentation with synonyms can only yield a small number of diverse patterns from the source texts because the words with synonyms from constructed lexicon databases likes are quite limited.

Kobayashi suggested contextual augmentation for labeled sentences, which offers a variety of substitute words that are predicted by a label-conditional bidirectional language model in accordance with the context, to overcome the drawback of replacement-based approaches. Contextual augmentation however has two

By jointly conditioning on both left and right context in all layers, BERT, which stands for Bidirectional Encoder Representations from Transformers, pre-trained deep bidirectional representations. BERT proposed a "masked language model" (MLM) objective to overcome the unidirectional limitation by randomly masking

a portion of the input tokens and predicting the masked words based on their context. The replacement words are predicted in a manner that is strikingly similar to contextual augmentation. Still, BERT was intended to pre-train text representations, thus the MLM task is carried out in an unsupervised manner with no regard for marker friction.

This exploration proposes a new data addition fashion nominated tentative BERT contextual addition with an emphasis on relief-grounded strategies. The technique uses conditional BERT, which is BERT-tuned, to apply contextual augmentation. For two reasons, BERT was selected as a pre-trained language model in this case. To begin with, BERT is based on Transformer. To handle large dependencies in the text, Transformer gives us a more organized memory. Second, BERT is strictly more efficient than a shallow cascade of left-to-right and right-to-left patterns. since it is a deep bidirectional model. By providing a greater range of replacement words made by the masked language model task, BERT was then applied to contextual augmentation for tagged sentences.

The words may conflict with source sentence annotation tags because the hidden language model only predicts hidden words based on their context. We propose a new objective called "Conditional Masked Language Model" (C-MLM) to overcome this problem. The goal of a conditional masked language model is to randomly select some tokens from the input for masking, with the aim of predicting words compatible with the label given the context and label of the phrase.

By simultaneously adjusting the left and right contexts at all levels, the C-MLM objective—in contrast to Kobayashi's work—allows a deep bidirectional representation. According to Kobayashi, we experimented on the two most popular neural network topologies, LSTM-RNN and CNN, on the text classification task to assess how effectively our augmentation strategy enhances performance of deep neural network models.

We demonstrate through experiments on six different text classification tasks that the proposed conditional BERT model improves sentences better than baselines, and that the conditional BERT contextual improvement method can be easily applied to convolutional neural network classifiers and recurring. The connection between the conditional MLM task and the style transfer task was further studied in this study to show that the conditional BERT can be used to change styles as well. Contextual augmentation by BERT is possible under certain conditions without compromising label compatibility. It can also be used for tasks involving style transfer. Our methodology clearly beats other methods for text data augmentation, according to experimental results. This is the first attempt, as far as we are aware, to convert BERT into a conditional BERT or to use BERT for text production jobs.

At the intersection of computer vision and natural language processing, problems that combine image and language understanding, such as image captioning and visual question answering (VQA), continue to stimulate important research. To produce high-quality results in each of these tasks, it is often necessary to perform elaborate visual processing and even multi-level reasoning. Therefore, image captioning and VQA have widely adopted visual attention strategies. These methods are currently based on deep neural network designs that improve performance by learning to focus on salient regions of images. The top down signals generated by the current task (such as looking for something) attention can be directed in the human visual system, while upward cues from unexpected, abnormal, or salient stimuli can automatically direct attention. Similar language is used in this study to refer to nonvisual or task-specific attentional processes as "top down" mechanisms and specialized visual feedback mechanisms as "bottom-up" mechanisms. The majority of traditional top-down visual attention techniques employed in picture captioning and VQA. These methods are typically trained to selectively process the output of one or more layers of a convolutional neural network, using a representation of a partially completed caption output or an image query (CNN) as context.

This method, however, pays little attention to how the visual portions that are the subject of attention are chosen. Regardless of the image's content the resulting input regions correspond to same size and shape, as schematically shown in Fig. 2.5. Objects and other image regions provide a more naturally for attention, resulting in captions and question answers that are more like human.

We propose a hybrid mechanism of bottom-up and top-down visual attention in this study. A sequence of salient visual regions is represented by a bottom-up approach, each region being represented by a concatenated convolutional feature vector. faster R-CNN, which is a true representation of the bottom-up mechanism, is how we practically implement bottom-up attention. A top-down process predicts the distribution of attention between visual regions using task-specific context. The average of picture feature over all areas is then used to calculate the attended feature vector. Here, it assesses the results of combining two tasks with top-down and bottom-up attention.

First, an image captioning model was described that creates captions by repeatedly scanning salient portions of an image. According to empirical research, adding bottom-up attention has a very favorable impact on image captioning. It also presents a VQA model using the same bottom-up attention features, demonstrating the method's broad applicability. On the VQA v2.0 benchmark server, this model won the 2017 VQA Challenge with an overall accuracy score of 70.3%. Spatial image feature V is defined in a general way. However, we use bounding boxes to designate spatial regions in this study and Faster RCNN to implement bottom-up attention. An object identification model called Faster R-CNN is made to locate instances of objects that belong to particular classes by using bounding boxes. As an attentive mechanism, additional region suggestion networks could also be trained. R-CNN detects faster.

Object proposals are anticipated at the first stage, which is known as a Region Proposal Network (RPN). A CNN's intermediate level features are passed over by a tiny network. The network forecasts a class-agnostic abjectness score and a bounding box refinement for anchor boxes of various scales and aspect ratios at each spatial point. With the intersection-over-union (IoU) criterion and greedy no maximum suppression, the top box proposals are selected as input to the second stage. In the second stage, region of interest (RoI) pooling is used to extract a minute feature map (for instance, 1414) for each box proposal. A batch of these feature maps is then delivered to the CNN's final layers.

To create an output set of image features V for use in image captioning or VQA, we take the model's final output and perform no maximum suppression for each object class using an IoU threshold. After that, we select all regions where any class detection probability is higher than a predetermined degree of confidence. The size D of the image feature vectors is 2048 due to the mean-pooled convolutional feature from each selected region, I, being provided as vi. When utilized in this manner, faster R-CNN effectively functions as a "hard" attention mechanism since only a small portion of picture bounding box features are selected from a large number of alternative configurations.

In order to pretrain the bottom-up attention model, we first initialize Faster R-CNN with ResNet101, which has been pre trained for classification on ImageNet. Then, train using the Visible Genome data. To aid in the learning of efficient feature representations, we include a second training output for predicting attribute classes (in addition to object classes). Concatenate the ground-truth object class learnt embedding with the mean pooling convolutional feature vi, then input this into a second output layer that establishes a SoftMax distribution over each attribute class as well as a class for "no attributes" to forecast attributes for region.

Concatenate the ground-truth object class learnt embedding with the mean pooling convolutional feature vi, then input this into a second output layer that specifies a SoftMax distribution over each attribute class as well as a class for "no attributes" to forecast attributes for region i. The original Faster R-CNN multitask loss function has four components. These components are defined over the classification and bounding box regression outputs for the RPN and the final object class suggestions, respectively. Keep these components and add a second multi-class loss component to train the attribute predictor.

III. EXISTING SYSTEM

Software that converts speech to text currently exists. It functions by playing the audio and providing a verbatim transcript that can be edited on a specific device. The software uses speech recognition to accomplish this. Each language has its own set of voice characteristics. Although though everyone speaks the same language, they all speak at a distinct pace and in a different dialect. This makes it challenging to read conveyed messages with various rates,

pronunciations, etc. The development of technologies for speech recognition and text translation is supported by the interdisciplinary field of speech recognition within computational linguistics. Another system carries out text summarization, pulls the most crucial details from the original text, and then offers a suitable summary of the same. The complexity of abstraction-based summation exceeds that of abstraction-based summation. Replace the original, crucial sentences in text documents with the right synonyms. In this manner, it will appear to be a whole different text but retain the original text's meaning. It is challenging to find the appropriate synonyms and rephrase sentences while maintaining the sense, which is why it is difficult. For example in the case, if the original text reads, "Peter was hurriedly climbing down the stairs.

He tripped and tumbled down and fractured his ankle", then the abstraction summary would be "Peter broke his ankle when he slipped from sprinting down the stairs". The final system is an online question paper generator software, which is a condensed method with unique mathematical symbols and a predefined template that aids in creating exam test papers for various boards, including CBSE, ICSE, ISC, State and Open Boards, and Mock test papers of various educational institutions and competitive exams, including IIT, SSC, NEET, etc.

Disadvantages:

- Time consuming
- No integrated system

IV. PROPOSED SYSTEM

The system focuses on the lecture, compiles the data into summaries, and adds surveys to the data to supplement it. The system converts text files from audio, PDF, and DOC files. Testify the live classes as well. Deep Learning, Natural Language Processing, Machine Learning, and Data Augmentation technologies are applied in these circumstances.

The system is composed of two parts. The Admin and the User. The admin module can log in to the website and look over customer reviews and system issues. Suggestions and complaints can be addressed by administrators. Users can register, log in, upload documents in the voice, DOC, and PDF formats, as well as record live classes and convert them to text. The system takes the keywords and extracts them using the Wikipedia and Yake algorithms. Then summarize the material using the BERT approach. The Transformers Pipeline is used to generate the question and answer sets.

In Fig. 1, the system architecture is illustrated. The inputs come in the form of speech, Word, and PDF files. For PDF and DOC to text conversion, Google is used first, followed by PyPDF and PyDOC. YAKE algorithm is used for key extraction.

It is a straightforward unsupervised keyword extraction method that utilizes text statistical data gathered from a single document to pinpoint the most important terms in the text. Yake is independent of language and domain. Yake can be installed, and it works. BERT is a free machine learning framework for dealing with natural language (Bidirectional Encoder Representation from Transformers). By providing context through the use of neighboring text, it is meant to help computers interpret ambiguous words in text.

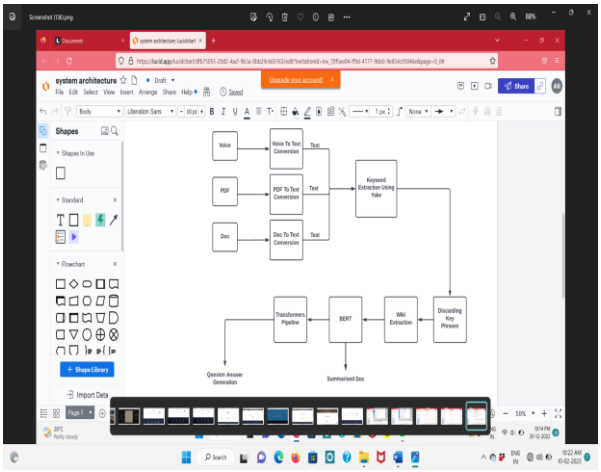

Fig. 1. System Architecture

V. CONCLUSION

This system is designed for the specified condition and works effectively. The created system is adaptable and simple to change. The tools and functionalities of Core HTML and CSS have been used to develop the design phase of the software in a neat and uncomplicated manner. The user found the results to be entirely satisfactory. The system is user-friendly because buttons are provided for going to each page, and it has been useful to the developer because it has allowed him to incorporate various fundamental Python ideas while also learning more contemporary ones like

HTML, CSS, Pymongo, and Python Flask. The system is easily expandable and can be improved with subsequent incremental releases of the same.

VI. ACKNOWLEDGEMENT

We would like to acknowledge our appreciation for the guidance and assistance provided by the Department of Computer Science and Engineering faculty at the KMCT College of Engineering for Women during the course of developing software.

VII. RESULT

Here in this project the inputs are given in the forms PDF, Word, Voice, Text formats and output will be a Summarized text along with the questions, answers and The keywords. The algorithms used here are such as YAKE, BERT etc.

References

1. Automatic question-answer pair generation using Deep Learning-Alok Kumar, Aditi Kharadi, Deepika Sign, Mala Kumari, 2021 Third International Conference on Inventive Research in Computing Applications (ICIRCA)
2. Question-Answer Generation for Data Augmentation-Juei-Yian Lin, Jhih-Yuan Huang; Wei-Po Lee, 2021 IEEE International Conference
3. Automation of Question-Answer Generation- Learning-Alok Kumar, Aditi Kharadi, Deepika Sign, Mala Kumari, 2021 Fourth International Conference on Computational Intelligence and Communication Technologies (CCICT)
4. Automatic Question-Answer Generation from Video Lecture using Neural Machine Translation-Sonam Sonia; Praveen Kumar, Amal Saha, 2021 8th International Conference
5. Automatic Question and Answer Generation from Course Materials. A.S.M Nibras, M.F.F Mohamed, I.S.M Arham, A.M.M Mafaris, M.P.A.W Gamage Sri Lanka Institute of Information Technology. A.S.M Nibras, M.F.F Mohamed, I.S.M Arham, A.M.M Mafaris, M.P.A.W Gamage
6. Bottom-Up and Top-Down Attention for Image Captioning and Visual Question Answering Peter Anderson1∗ Xiaodong He2 Chris Buehler3 Damien Teney4 Mark Johnson5 Stephen Gould1 Lei Zhang3
7. BERT: Pre-training of Deep Bidirectional Transformers for Language Understanding Jacob Devlin Ming-Wei Chang Kenton Lee Kristina Toutanova Google AILanguage{jacobdevlin,mingweichang,kentonl,kristout}@google.com
8. Conditional BERT Contextual Augmentation June 2019 ICCS 2019, 19th International Conference, Faro, Portugal, June 12–14, 2019, Proceedings, Part IV (pp.84-95). XingWu, Shangwen Lv, Liangjun Zang, Jizhong Han

Blockchain Based Crowdfunding Application Using Smart Contract

Fathima Shilna
Dept. of CSE
KMCT College of Engineering for Women Calicut, India
shilna6069@gmail.com

Ayisha Safa MK
Dept. of CSE
KMCT College of Engineering for Women Calicut, India
ayishz7869@gmail.com

Arathi M
Dept. of CSE
KMCT College of Engineering for Women Calicut, India
arathim33@gmail.com

Fathima Seja
Dept. of CSE
KMCT College of Engineering for Women Calicut, India
fathimaseja@gmail.com

Dhanya P
Assistant Professor
Dept. of CSE
KMCT College of Engineering for Women Calicut, India
pdhanya984@gmail.com

Abstract— Crowdfunding is a kind of online fund-raising technique which started as a way for people to donate a limited amount money so that innovative people can finance the project. This crowdfunding app differs from similar apps in that it will allow users to donate money while also enabling open communication between them and the charities they support, allowing users to track the progress of their donations. If money is not entirely used for the requirement, it will be returned to the users. Smart contracts even have the ability to automate transactions, which will increase efficiency and hasten the process even more. The transaction or process advances to the following stage when pre-specified requirements are satisfied. All transactions will be recorded and stored as blocks on the block chain. The purposed system is made transparent, trustworthy, and secure via blockchain. The proposed work aims to assist users and organisations in obtaining more financing and building strong interpersonal relationships.

Keywords— Blockchain, Smart Contract, Ethereum.

I. INTRODUCTION

The process of generating funds is difficult because it needs confidence between many parties, including funders, middlemen, or organisations acting as a safe haven for temporary cash to be transferred to the beneficiary of funds. The key capital for fundraising organisations to get donors to offer their finances to receivers of funds is trust.

Crowdfunding is a method of raising small amount of money from a large group of individual investors or businesses. In this charity organization can request for the fund they wanted and the user or the individual can donate funds by checking the details and the purpose of the organization. Currently existing crowdfunding sites accept large sums of money from investors and contributors and then leave them with bogus promises. The blockchain-based crowdfunding model modifies the traditional approach to corporate finance. Three categories of on-screen characters form the foundation of the modern concept of crowdfunding: individuals or investors who invest in the organization, the organization who requests for, and a platform that connects these two characters in order for the venture to succeed.

The Blockchain-Based Crowdfunding Application is a multi-user application that will allow multiple charities to raise funds from users. The charitable organisation can make a charity request that includes who they are raising funds for and send it to the Admin, who is in charge of accepting or rejecting charity requests. This crowdfunding tool is unique in that it does not directly send funds to organisations; rather, the funds are saved in a smart contract (computer programmes that run and stored on a blockchain when specific conditions are met).

In order to verify the usage of the fund, the organizations are required to upload various supporting documents with the spend money details within it. These documents will be uploaded after encryption and will be downloaded and decrypted as per the requirements. If the money has not been fully used the users are guaranteed to receive a return amount as per the ratio of their donation.

II. EXISTING METHODOLOGIES

A. Blockchain

Block chain is a type of database that stores data in blocks, rather than individual pieces of data that must be linked together to form a chain. It differs from regular database in its storage method and involves the creation and maintenance of new records each time they are accessed. A new block is added when new information is received. Once the block is filled with data, the block is chained onto the former block, forming a chronological data chain. A blockchain can store a variety of data, but its most common use has been as a transaction ledger. The blockchain is employed in this situation in a decentralized manner, which means that no single person or group controls the system, rather all users have collective control. Decentralized blockchains are immutable, meaning that the data entered cannot be changed. For this application, it means that transactions are permanently recorded and viewable to anyone.

Blockchain prohibits any modification of the data contained in a block .When the information is recorded, some random block can't be changed without approval of more than half of the nodes in blockchain, that is 51 percent. It is a mutual and unchangeable record and the data in it is open for anybody and everybody to see making it decentralized. Thus, blockchain solves the problem of spending more as there is no need of any central server or trusted authority.

B. Smart Contract

A smart contract is a calculating pact that authorizes us to ease and confirm contract fulfilment. These are activated when sure degree is appeased. These undertakings maybe traced and are unchangeable. Smart contracts outline an understanding's conditions and results same that traditional contracts do. They're repeatedly used to mechanize contract killing for fear that everybody sees the decision as instantly as attainable, without the need for middlemen or idling away time. These smart contracts are buxom utilizing the Solidity prioritize style.

C. Types of Crowdfunding

Crowdfunding is a habit to take for temporary use from a lot of individual financiers or guests.

Donation-Based Crowd funding: There is no fiscal return to subscribers or financial financiers in this in a way crowdfunding. This contains charity, non-political organisations (NGOs), disaster remedy, and medical help.

Rewards-Based Crowd funding: Individuals cause drives in consideration of benefits, that maybe profit or a product under this in a way crowd capital. There are various sites that engage this type of crowdsourcing presently.

Equity-Based Crowd funding: Unlike the premature two types of crowdfunding, one or the other admits you to enhance any of the firm by buying shares. As a result, financiers sustain a return on the party's income.

D. Ethereum

Ethereum, a smart contract computing platform with decentralized open source blockchain. It generates the cryptocurrency token named "ether". On Ethereum blockchain, programmers can create "smart contract" and these contracts are automatically executed according to their code. The "decentralized platform" means anyone can setup and run an Ethereum node, the same way anyone can run a bitcoin node. Anyone who wants to pay the operators of those nodes in ether, which is a cryptocurrency token tied to Ethereum. Thus, people who run ether node provide computing power and are paid in ether, in a similar way to how people who run bitcoin nodes provide hashing power and are paid in bitcoin.

III. RELATED WORK

[1] Trusted Crowdfunding Using Smart Contract

The process of produce earnings is troublesome cause it needs assurance 'tween many bodies, containing funders, middlemen, or organisations be a part of a place of safety for transitory cash expected moved to the recipient of funds. The key capital for fundraising organisations to catch backers to offer their

property to recipients of means is trust. Many non-profit groups symbolize fundraisers, as in the case of the Covid-19 universal. Few non-profit arrangements use electronics to build it smooth for backers to give away resources through bureaucracy. In trust is that the main determinant to urge as many means as likely, science too plays a vast function all along this still. Block chain is associated in nursing incorrupt digital ledger that records each dealing. It's a distributed system so all the records are kept in each node within the localized network. Ethereum permits running applications within the blockchain known as sensible Contracts. All the sensible contracts run on the many frauds are reported. Implementing a crowdfunding strategy in blockchain can facilitate to avoid these sorts of issues. Ethereum Virtual Machine. The matter with this crowdfunding firms is that they are charging high fees and by incorporating blockchain, sensible contract for crowdfunding takes away the normal dealing fees and platforms fees commonly related to alternative crowdfunding platforms.

[2] Venturing Crowdfunding Using Smart Contracts in Blockchain

Crowdfunding is a habit to take for temporary use from a lot of individual financiers or companies. Investors can influence some project they are concerned in and gain if the leadership is profitable. Many crowdfunding sites immediately exist, and they acknowledge big sums of services from financiers and subscribers and before leave ruling class accompanying bogus promises. Blockchain-located crowdfunding alters the typical approach to party finance. In general, when public need to accumulate resources to start a firm, they must first cultivate a policy, statistical surveys, and models, and therefore offer their plans to fascinate crowd or organisations. Banks, sweet financiers, and working capital firms were with the sources of capital. The up-to-date crowdfunding idea is established three types of on-screen types: the task inventor the one presents the plan or venture to be financed, things or financiers the one purchase the plan, and a principle that combines these two characters to guarantee the venture's fame. It is utilised to fund a off-course range of start-boosts and new ideas, to a degree creative actions, medical progresses, travel, and public commerce projects.

[3] Application of Blockchain Technology of Crowd - Funding Using Smart Contract

The blockchain is an unchangeable mathematical book that records all undertakings. Because it is a delivered structure, all records are sustained at each bud of the decentralised network. Smart Contracts are Ethereum-allowed programmes that run on the blockchain. It allows the killing of all Smart contracts. Crowdfunding is a plain approach to raise resources for new project plans. The question accompanying existent crowdfunding groups is that they charge bulky wages and infrequently attract tricks. Implementing a crowdfunding method on blockchain will help to prevent these somewhat troubles. By joining Peer to Peer smart crowdfunding contracts, you may prevent the typical undertaking accounts and platform payments guide additional crowdfunding stages, to a degree Kickstarter. The purpose of our project is to devise a powerful use that will admit each breakthrough plan at hand to existence. We determine to launch a blockchain-located crowdfunding site. We specify a smooth-to-use interface for one to devise and issue their comments about our programme. These beliefs were then told to all. Anyone the one desires to share their plans is welcome to do so. Each of these eras is achieved seemingly.

[4] Smart Contract and Blockchain for Crowdfunding Platform

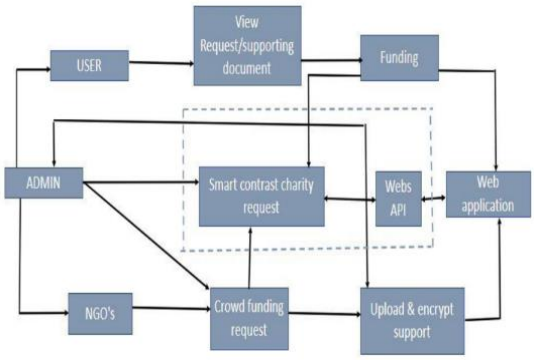

Fig.1. Block Diagram

In contemporary industrial era, practically all industrial sectors, from for-profit to non-profit, use technology to assist their operations. Non-profit organisations (non-profit) have qualities that are nearly identical to profit-oriented organisations (profit), however these two organisations face distinct issues. In the present Covid-19 pandemic crisis, practically every

country faces the same challenge in dealing with this problem, particularly in terms of the cash required. Many techniques have been implemented by the government in order to manage government money in order to combat the Covid-19 disease epidemic. This scenario prompted the community to contribute donations to assist the government in combating the Covid-19 plague epidemic. For fact, raising funds is a difficult process since it involves confidence between many parties, including funders, middlemen, or organisations that serve as a location to hold temporary cash for the beneficiary of funding. That trust is the key capital for fundraising organisations in appealing to funders to deliver their services to fund receivers.

Many non-profit groups present image of fundraisers, as in the case of the Covid-19 universal. Trust is their substantial barrier in persuasive nation to support services to the non-profit. So, from this it maybe decided that apart from trust that is the main determinant to take as many budgets as attainable, science more plays a generous duty in this place also.

IV. PROPOSED METHOD

This item presents a Blockchain-located crowdfunding manifesto that makes use of smart contracts. This will be a multi-consumer use accompanying three sorts of consumers: administrators, Users, and charity organization. Admin must authorise generous groups before they grant permission be included. Charity organisations concede possibility visualize the progress of their request's authorization and gifts elevated in legitimate-opportunity. Users may path the progress of the lenient purpose they are helping, in addition to common news about different generosity requests listed on the request.

The main component of the application is an Admin. The admin can monitor the activities of user and organization (not control them in any way) and can choose to approve or reject the charity request for listing on the application.

The user and organization are the components that form the body of the application. A charity organization creates an account and can create charity request. A user can view different request and can choose to fund them or not. The funded amount is stored in a smart contract which is a set of rules according to which transactions happen. The

web API allows to interact with the Ethereum platform. Blockchain uses the cryptocurrencies for the transaction. Here we use the Ethereum coin. To make the transaction

with Ethereum we use 'Ganache'. Ganache is a private Ethereum blockchain environment that allows to you emulate the Ethereum blockchain so that you can interact with smart contracts in the blockchain. When registering in the Ethereum account we got a secret key. Using the key, we can make transactions. And if the money has not been fully used the users are guaranteed to receive a return amount as per the ratio of their donation.

V. IMPLEMENTATION AND RESULT ANALYSIS

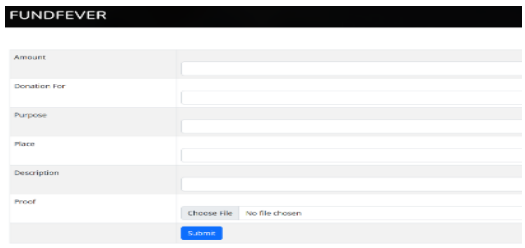

Fig.2. Organization

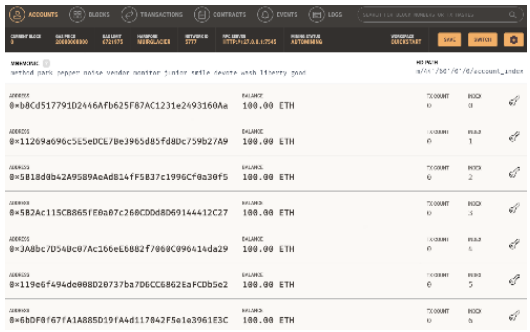

Fig.3. An overview of Ganache environment

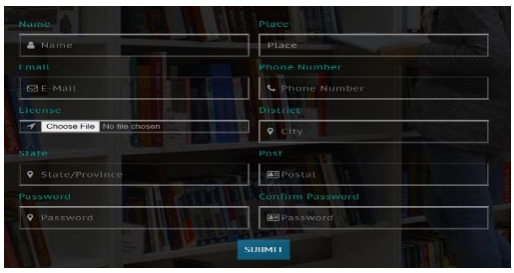

Fig.4. The signup

VI. CONCLUSION

Finally, the interface of this work is user-friendly, the work maintains transparency between the user and the organization. If person engaged in private ownership of business has not existed sufficiently second hand the consumers are insured to accept a return amount as per the percentage of their gift. The money will be amounted to the smart contract only till the point when the necessity of the gift is joined, therefore, guaranteeing that no extra money is moved to the smart contract. The use maybe second hand for secure crowdfunding. Actual financiers can establish services in creative projects that have the potential to evolve marketing.

With the progress of blockchain electronics, the submitted work has a brilliant future and much of range for progress and progress. In the future, the planned research activity can proceed in a more straightforward and secure manner for all concepts realised using the proposed crowdfunding application

REFERENCES

1. Manoharan, Samuel. "Trusted crowdfunding using smartcontract "Journal of Innovative ImageProcessing (JIIP) 2, no. 04 (2020): 175186.
2. N. Yadav and S. V, "Venturing Crowdfunding using Smart Contracts in Blockchain", 2020 Third International Conference on Smart Systems and Inventive Technology (ICSSIT), pp. 192-197, 2020.
3. Smys, S., Abul Basar, and Haoxiang Wang. "Application of blockchain technology of crowdfunding using smart contract" Journal of Artificial Intelligence 2, no. 01 (2020): 42-52
4. Ashari, Firmansyah. (2020). Smart Contract and Blockchain for Crowdfunding Platform. International Journal of Advanced Trends in Computer Science and Engineering. 9. 3036- 3041. 10.30534/ijatcse/2020 /83932020.
5. Juan Garay, Aggelos Kiayias and Nikos Leonardos, "The bitcoin backbone protocol: Analysis and applications", Annual InternationalConference on the Theory and Applications of Cryptographic Techniques, pp. 281-310, 2015
6. H. Halpin and M. Piekarska, "Introduction to Security and Privacy on the Blockchain," 2017 IEEE European Symposium on Security and Privacy Workshops (EuroS&PW), 2017, pp. 13, doi: 10.1109/ EuroSPW.2017.43.
7. S. Gada, A. Dhuri, D. Jain, S. Bansod and D. Toradmalle, "BlockchainBased Crowd funding: A Trust Building Model," 2021 International Conference on Artificial Intelligence and Machine Vision (AIMV), 2021, pp. 1-7
8. S. Pandey, S. Goel, S. Bansla and D. Pandey, "Crowdfunding Fraud Prevention using Blockchain", 2019 6th International Conference on Computing for Sustainable Global Development (INDIACom), pp. 1028-1034, 2019.
9. S. Bansod and L. Ragha, "Blockchain Technology: Applications and Research Challenges", 2020 International Conference for Emerging Technology (INCET), pp. 1-6, Jun. 2020.
10. P. K. Kaushal, A. Bagga and R. Sobti, "Evolution of bitcoin and security risk in bitcoin wallets," 2017 International Conference on Computer, Communications and Electronics (Comptelix), 2017, pp. 172-177, doi: 10.1109/COMPTELIX.2017.8003959.
11. L. Xuefeng and W. Zhao, "Using Crowdfunding in an Innovative Way: A Case Study from a Chinese Crowdfunding Platform," 2018 Portland International Conference on Management of Engineering and Technology (PICMET), 2018, pp. 1-9, doi: 10.23919/PICMET. 2018.8481838.
12. G. Dushnitsky, M. Guerini, E. Piva and C. Rossi-Lamastra, "Crowdfunding in Europe: Determinants of platform creation across countries", California Management Review, vol. 58, no. 2, pp. 44-71, 2016

NLP with User Clustering Behaviour Analysis of People in Whatsapp Message using NLP with user clustering

Fathima Nabeela
Dept.. CSE
KMCT College of Engineering for Women
Kozhiode, India
nabeelato143@gmail.com

Aysha Sherin
Dept. CSE
KMCTCollegeof Engineering for Women
Kozhiode, India
sherinaysha519@gmail.com

Anagha PK
Dept.. CSE
KMCTCollegeof Engineering for Women
Kozhiode,India
anagharajan659@gmail.com

Sangamithra
Dept. CSE
KMCT College of Engineering for Women
Kozhiode,India
sangamithra.p.c.123@gmail.com

Deepthi P
Assistant Professor
Dept. CSE
KMCT College of Engineering for Women
deepthisivaraj@gmail.com

Abstract— These days, the major mode of communication is through messages and WhatsApp with a dynamic user base of over 650 million, WhatsApp is the most popular application for chatting. It has been widely used by all, particularly by businesspeople and teenagers. This project aims to conduct numerous analyses on client chat for a variety of objectives. This research project aims to conduct a time and be a flirt analysis. Sentiment analysis has been carried out for each piece of material using Natural Language Processing (a Deep Learning model). Finding the level of intellect of the chatters depends on this. The number of positive and negative statements in the chat material is calculated using the text mining technique. To categorize users with different types of content, content-based clustering is done.

Keywords— Flirt Analysis, Clustering, Natural Language Processing, Text mining, Time Analysis.

I. INTRODUCTION

These days, the utilization of social media systems presently got to be a common mode to share informations. A wide range of viewers were currently getting used to this mechanical-era show. Social media usage is becoming commonplace for exchanging messages, videos, and photographs. It is also used professionally to share or advertise information linked to businesses, which is now considered to be the norm rather than just for personal use. Currently, most of our chat conversations take place on WhatsApp for the clients' privacy and security, and using sentimental analysis, we can determine whether or not the chat will be secure.

II. PROPOSED METHOD

The system's focus on retrieving WhatsApp messages was taken into account for sentimental analysis using the DL model, or natural language processing.

III. METHODOLOGY

1. Data Collection

Data collection is the practice of acquiring information from various individuals when they are speaking with their friends and acquaintances. WhatsApp allows us to export the chat history as a text file. The exported text file will be converted into a CSV file to aid in analysis. This enables us to collect data for sentimental analysis and keep it.

2. Data Pre-Processing

Pre-processing of the acquired data entails handling missing values, encoding categorical data, eliminating superfluous parameters, scaling parameter values to achieve normal distribution

(zero mean and standard deviation as one), and other tasks. A technique called pre-processing is putting the data through a series of steps so that it may be used for further analysis activities that will be efficient for calculating procedures. The following pre-processing procedures were carried out throughout the process:

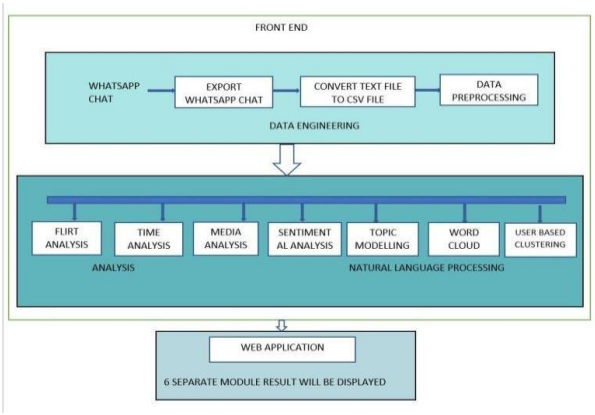

Fig. 1. Block Diagram

Step1: Classification of the time, date, chat, name and text.

Step2: Processing the emoji was made.

Step3: Demojifies the emoji in the pre-processing steps.

Step4: Analyze and removes the excessive gaps in the documents.

3. Flirt Analysis

The flirt analysis method was used to accomplish the majority of the study. By comparing the chat with the list, the module's main objective is to identify verbal flirtation between persons. The flirt analysis will compare the text message and the flirt list. The sum of a person's flirty phrases will be divided by the entire number of flirty phrases. The flirting percentage for each participant in the conversation will be determined.

Flirt Analysis Algorithm:

Step1: First, collect the flirt words.

Step2: Separate the message respective to the name of the chatter.

Step3: Determine how much unique word is used by each of the chatter (U)

Step 4: Determine the total words used in each row (Tw)

Step5: Determine the unique frequency for the each word (Uw)

Step6: Formula:Unique Frequency for a Word is

(Uw)=(U/sum of Tw)* 100

Step7: Determine the total number of flirt list (Fl)

Step8: Check each word with the collected flirt list

Step9: Store the used flirt words by each person as a segregate list(FW)

Step10: Determine the total number of flirt words used by each of the person. (Lf)

Step11: Determine the Unique Flirt frequency of each word for each of the person (Ff)

Step12: Formula for Unique Flirt frequency as

(Ff)= (U/Fl)*100 all text labels in each figure are legible.

Step13: Determine the Total Flirt Percentage as sum of FF/ total number of Fw.

4. Time Analysis

Using time analysis, which separates the date and time of each text, it is feasible to determine the most active hours, the most active day, the most active date, and the average number of messages each day. These kind of choices will be helpful for those who want to peak the date and time of the chat.

5. Media and Call Analysis

Using WhatsApp, you can send someone a picture, a voice message, a video, or an audio file. This decision has advantages and disadvantages. As a result, we can ascertain how many media files each individual has transferred. WhatsApp also offers the ability to delete text, audio, and video messages, making it simple for anyone to communicate with others. We are able to ascertain how many efforts the user has made at calls (both missed voice and video calls) and deleted texts.

6. Topic Modeling

In topic modelling, the entire chat document is analyzed using natural language processing, and based on the specific chat state that we produce, a subject is then generated for the full text.

7. Word cloud

In a Word Cloud, the most popular text words used by character are displayed in decreasing order of font size. This enables us to identify the most frequently used word.

Performance Analysis:

1. The sentimental flirt analysis in a private WhatsApp chat was carried out and the analysis' precise results were provided.

2. The working procedure began with the pre-processing stages, then basically checked the input against the flirt list and processed, before the outcome was to be shown. In this analysing process, what was expected from this methodology for flirt analysis was attained.

3. The methods were developed to logically carry out the associated tasks for the flirt analysis technology.

4. All of the codes provided for obtaining the results were readable and could be used with ease for comprehension, and the progress was organised in accordance with the protocols.

5. A file based graph is plotted depicting what kinds of files are included in the chat.

6. Content-based clustering of user gives the users certain scores and makes them grouped accordingly.

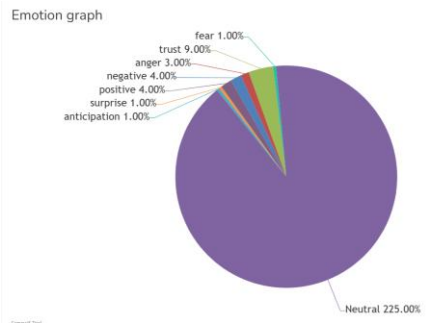

Fig. 2. Emotional graph

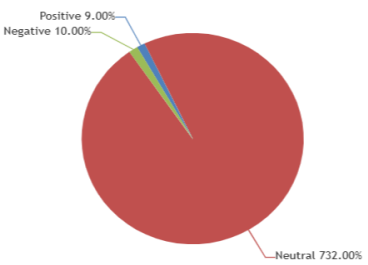

Fig. 3. Sentimental graph

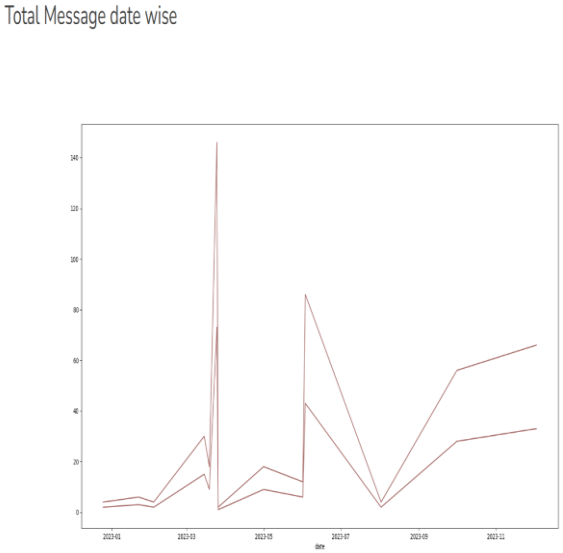

Fig. 4.Time analysis

III CONCLUSION AND FUTURE WORK

The sentimental and flirt analysis techniques were used in this paper's whole chat database, and the corresponding results were distributed. The entire process is implementable, although the cost of using cloud storage for storage was a little high and can be decreased in upcoming projects. With the consent of the relevant users, the appropriate chat messages can be extracted from a variety of users and used productively in subsequent tasks.

REFERENCES

1. P. Garg, H. Garg and V. Ranga, "Sentiment analysis of the Uri terror attack using Twitter", 2017 International Conference on Computing Communication and Automation (ICCCA), pp. 17-20, 2017.
2. B. Liu and L. Zhang, "A survey of opinion mining and sentiment analysis", Mining text data, pp. 415-463, 2012.
3. A. Go, R. Bhayani and L. Huang, "Twitter Sentiment Classification using Distant Supervision", Processing, vol. 150, no. 12, pp. 1-6, 2009.
4. Shikha Tiwari, Anshika Verma, Peeyush Garg and Deepika Bansal, "Social Media Sentiment Analysis On Twitter Datasets", Sentiment analysis using deep learning architectures: a review" Ashima Yadav & Dinesh Kumar Vishwakarma, April 2020.
5. V. Singh and S. K. Dubey, "Opinion mining and analysis: A literature review",

2014 5th International Conference-Confluence The Next Generation Information Technology Summit (Confluence), pp. 232-239, 2014.
6. A. P. Jain and P. Dandannavar, "Application of machine learning techniques to sentiment analysis", 2016 2nd International Conference on Applied and Theoretical Computing and Communication Technology (iCATccT), pp. 628-632, 2016.
7. A.Hassonah Mohammad, Rizik Al-Sayyed, Ali Rodan and Ala' M. Al-ZoubicIbrahimAljarahaHossamFaris, An efficient hybrid filter and evolutionary wrapper approach for sentiment analysis of various topics on Twitter, December 2019.
8. Y. Wang, "Sensing Human Sentiment via Social Media Images: Methodologies and Applications", Arizona State University, 2018.
9. A. O'Connor, R. Balasubramanyan, B. R. Routledge and N. A. Smith, "From tweets to polls: Linking text sentiment to public opinion time series", Icwsm, vol. 11, no. 122, pp. 1-2, 2010.
10. S.-M. Kim and E. Hovy, "Determining the sentiment of opinions", Proceedings of the 20th international conference on Computational Linguistics, pp. 1367, 2004.
11. A. Whitelaw, N. Garg and S. Argamon, "Using appraisal groups for sentiment analysis", Proceedings of the 14th ACM international conference on Information and knowledge management, pp. 625-631, 2005.
12. H. Saif, M. Fernandez, Y. He and H. Alani, "Evaluation datasets for Twitter sentiment analysis", Emot. Sentiment. Soc. Expressive Media, pp. 9, 2013.
13. S.-M. Kim and E. Hovy, "Determining the sentiment of opinions," in Proceedings of the 20th international conference on Computational Linguistics, 2004, p. 1367.
14. A. P. Jain and P. Dandannavar, "Application of W. Chu and S. S. Keerthi, "Support vector ordinal regression," Neural Comput., vol. 19, no. 3, pp. 792–815, 2007.
15. S. Liu, F. Li, F. Li, X. Cheng, and H. Shen, "Adaptive cotraining SVM for sentiment classification on tweets," in Proceedings of the 22nd ACM international conference on Information & Knowledge Management, 2013, pp. 2079– 2088.
16. S. D. Pressman, M. W. Gallagher, and S. J. Lopez, "Is the emotion-health connection a "first-world problem"?," Psychological science, vol. 24, no. 4, pp. 544-549, 2013.
17. M. E. Geisser, R. S. Roth, M. E. Theisen, M. E. Robinson, and J. L. Riley III, "Negative affect, self-report of depressive symptoms, and clinical depression: relation to the experience of chronic pain," The Clinical journal of pain, vol. 16, no. 2, pp. 110-120, 2000.
18. S. Gohil, S. Vuik, and A. Darzi, "Sentiment analysis of health care tweets: a review of the methods used," JMIR public health and surveillance, vol. 4, no. 2, p. e43, 2018.
19. L. Anselin, "Local indicators of spatial association— LISA," Geographical Analysis, vol. 27, no. 2, pp. 93-115, 1995.
20. R. M. Assuncao and E. A. Reis, "A new proposal to adjust Moran's I for population density," Statistics in medicine, vol. 18, no. 16, pp. 2147-2162, 1999.
21. Y. Fan, X. Zhu, B. She, W. Guo, and T. Guo, "Networkconstrained Spatio-temporal clustering analysis of traffic collisions in Jianghan District of Wuhan, China," PLoS One, vol. 13, no. 4, p. e0195093, 2018.
22. M. j. Fortin, M. R. Dale, and J. M. Ver Hoef, "Spatial analysis in ecology," Encyclopedia of environmetrics, vol. 5, 2006.
23. J. D. Morenoff, R. J. Sampson, and S. W. Raudenbush, "Neighborhood inequality, collective efficacy, and the spatial dynamics of urban violence," Criminology, vol. 39, no. 3, pp. 517-558, 2001.
24. L. A. Waller and C. A. Gotway, Applied spatial statistics for public health data. John Wiley & Sons, 2004.
25. S. J. Rey and B. D. Montouri, "US regional income convergence: a spatial econometric perspective," Regional studies, vol. 33, no. 2, pp. 143-156, 1999.
26. B. Ramage, D. Hall, R. Nallapati, and C. D. Manning, "Labeled LDA: A supervised topic model for credit attribution in multi-labeled corpora," in Proceedings of the 2009 Conference on Empirical Methods in Natural Language Processing: Volume 1-Volume 1, 2009: Association for Computational Linguistics, pp. 248-256.
27. M. A. Cabanlit and K. J. Espinosa, "Optimizing N-gram based text feature selection in sentiment analysis for

commercial products in Twitter through polarity lexicons," in Information, Intelligence, Systems and Applications, IISA 2014, The 5th International Conference on, 2014, pp. 94–97.

28. N. R. Kasture and P. B. Bhilare, "An Approach for Sentiment analysis on social networking sites," in 2015 International Conference on Computing Communication Control and Automation, 2015, pp. 390–395.

Covid-19 from Cough Sound and Chest X-Ray Using Machine Learning and Deep Learning

Akshaya P
Dept. of CSE
KMCT College of Engineering for Women, Kozhikode
Kozhikode, India
akshayap894321@gmail.com

Avani Chandran
Dept. of CSE
KMCT College of Engineering for Women, Kozhikode
Kozhikode, India
avanichandran365@gmail.com

Risha Salam
Dept. of CSE
KMCT College of Engineering for Women, Kozhikode
Kozhikode, India
rishadreamz@gmail.com

Sana Basheer
Dept. of CSE
KMCT College of Engineering for Women, Kozhikode
Kozhikode, India
sanabasheerc123@gmail.com

Reshma C V
Assistant Professor
Dept. of CSE
KMCT College of Engineering for Women
reshmaranjucv@gmail.com

Abstract— The official COVID-19 tests are time-consuming, expensive, have a high rate of false negative results, use necessary reagents, and may be in violation of social segregation regulations. Consequently, a quick and dependable alternative remedy. These problems might be resolved by using cough recordings and chest X-rays for preliminary screening. Our architecture for COVID-19 multi-appearance screening makes use of lung area priors collected from CXR images. In order to identify COVID-19 disease, this scoping review examines the use of cough sounds and chest x-rays in artificial intelligence (AI) technologies. Below, we list and describe the features of the identified AI techniques as well as the datasets that were applied to them. The most popular AI architecture was a recurrent neural network, followed by a convolutional neural network. AI models were mostly developed, examined, and utilized on desktop computers rather than mobile apps. In accordance with the findings discussed, AI can help in the detection of COVID 19 using a chest X-ray and cough sound. The suggested approaches may, however, prove to be a useful means of identifying a number of illnesses linked to changes in the human body's respiratory and neurophysiological systems with enough time and appropriate clinical testing.

Keywords— COVID-19, Artificial Intelligence, Machine Learning, Cough sound, Chest X-ray image.

I. INTRODUCTION

The acute respiratory infection Covid-19, which is brought on by the corona virus, can occasionally be fatal ,especially in elderly and immune compromised persons. underlying health issues It was initially found in China in 2019 before spreading to other nations in 2020. Official COVID-19 tests are time- and money-consuming, can yield a high rate of false negatives, consume vital substances, and may result in social harm. As a result, a reliable supplementary test that uses X-ray images for preliminary screening and cough recording may be able to assist in resolving these issues. This scoping study examines the application of machine learning and deep learning to diagnose the covid-19 sickness using chest X-rays, coughing, and other symptoms. This test is multimedia-based.

Here, two datasets—X-ray pictures and covid from cough sound—are present. Datasets are created using the Github and Kaggle repositories. Datasets will typically be consisting of the folders Covid and

Normal. It will be a wave-file format. A wave file that has been transformed into a spectrogram of a signal's frequencies over time. Features of the spectrogram are retrieved using

the mel-frequency ceptral coefficients (MFCC) method. Windowing the signal, applying the DFT, obtaining the log of the magnitude, warping the frequencies on a Mel scale, and finally employing the inverse DCT are the crucial processes in the MFCC features extraction technique.

To determine whether a feature is part of a covid class or a normal class, the feature extraction technique MFCC, which comprises 25 features, is used. That is when created as a csv file. It is learned using the Random Forest Algorithm. Random forest is a well-known machine learning algorithm that makes use of the supervised learning technique. It is applicable to both classification and regression problems in machine learning. It is based on the concept of ensemble learning, which is the process of combining several classifiers to tackle challenging problems and improve model performance.

Accuracy, recall, and precision are used to calculate performance metrics. A training set and a test data set make up the total of two sets. 20% of the test data and 80% of the training set are merged. The random forest method is given the training set data, and models are produced. If the actual result and the predicted result match, the forecast is 100 percent accurate.

Early COVID-19 screening is essential for controlling the pandemic and, as a result, reducing the strain on the healthcare system. Chest X-ray segmentation of the lungs is a possible instrument for early lung disease detection. Recently, supervised lung segmentation has made great strides thanks to deep learning. However, due to domain shift and a dearth of human pixel-level annotations, it is still challenging to understand how to use the lung area in COVID-19 screening.Our framework for COVID-19 multi-appearance screening is built on priors for the lung area that were taken from chest x-ray pictures.

The chest x-ray picture is provided as input. A convolutional neural network is used to train it. In contrast to convolutional neural networks, other neural networks perform better when receiving visual, voice, or audio information.

There are three basic categories of layers in them:

- Convolutional layer
- Pooling layer
- Fully-connected (FC) layer

The top layer of a convolutional network is the convolutional layer.

A. Convolutional layers may be followed by pooling or more convolutional layers, but whole layer connection is always the last layer. The CNN gets increasingly complex and is able to recognise more details in the image with each layer. Early layers highlight simple components like colours and borders. When the visual information advances through the CNN layers and begins to recognise bigger chunks or aspects of the picture, the target object is finally determined.

B. Convolutional Layer: The structural core of a CNN is the convolutional layer, which also houses much of the processing. It needs a few things, like input. data, a feature map, and a filter. Imagine that the input is a 3D pixel matrix representing a colour picture. The input will therefore have three dimensions: height, width, and depth, which match the RGB colour space of a picture. Also, we have a feature detector that will search the image's receptive fields for the feature. This detector is sometimes referred to as a kernel or filter. Convolution is the name given to this.

C. Pooling Layer: Pooling layers, sometimes referred to as down sampling, reduces the number of parameters in the input by conducting dimensionality reduction. A convolutional layer sweeps across the whole input using the pooling technique, similar to how the A filter does, however this filter has no weights. Instead, by using an aggregation function on the values of the receptive field, the kernel creates the output array. Pooling is separated into two groups:

D. Max pooling: When the filter moves over the input, it selects the input pixel with the highest value to deliver to the output array. As a side aside, this approach is typically used more often than standard pooling.

E. Average pooling: When the filter moves over the input, the average value inside the receptive field is calculated and then transferred to the output array. Although the pooling layer sacrifices a lot of information, it also benefits the CNN in a number of ways. They reduce the danger of overfitting, boost efficacy, and reduce complexity.

F. Fully-Connected Layer: The full-connected layer's name accurately summarizes what it accomplishes. As was already established, partly connected layers do not maintain the input image's pixel values. at a short distance of the output layer. Each node in the output layer is, nevertheless, directly linked to a node in the layer below in the totally connected layer. This layer classifies the data based on the characteristics that were obtained by the earlier layers and their corresponding filters. Convolutional and pooling layers commonly utilise ReLu functions to classify inputs, whereas FC layers frequently use a softmax activation function to provide a probability range from 0 to 1..

G. Normalizing image inputs: A critical step that guarantees the data distribution of each input parameter is data normalisation (pixel in this case). This quickens convergence. as the network is being trained. Data is normalised by removing the mean from each pixel and dividing the result by the standard deviation. The data would have a distribution that resembles a Gaussian curve with zero at the centre. Because we need to have positive pixel counts for picture inputs, we could chose to scale the normalised data in the [0, 1] or [0, 255] range.

II. METHOD

Admin provides a cough sound voice dataset, which is subjected to feature extraction using MFCC. Speech recognition is a task that requires supervised learning. The speech recognition task receives a speech signal as input and must predict text from the signal. Because audio signals contain a lot of noise, they cannot be used as input for the model.It has been shown that providing the basic model with features extracted from an audio source rather than the raw audio input results in significantly improved performance.MFCC is a popular method for extracting features from audio signals. The goal of MFCC technology is to create functions from an audio signal.can be used to record a person's voice. However, because there are many sounds in the given audio signal, we divide it into different segments, as shown in the image below.Each segment is 25 ms wide, and the signals are separated by 10 ms. One claims to speak three words into each of four phones at a rate of three states each phone, for a total of 36 states per second, or 28 milliseconds per state. is expected to Near the 25 ms timeframe, this is. Take 39 characteristics from each segment. Furthermore, clipping the signal directly at the signal's edges when interrupting it results in a sharp drop in amplitude at the edges and Noise with a high frequency response. To chop signals that do not produce noise in the high frequency range, we use a Hamming/Hanning window rather than a rectangular window.

In machine learning, these extracted features are trained using the random forest algorithm.

One of the most well-known machines is Random Forest.Algorithms for learning. They are incredibly effective at making predictions, have little overfitting, and have straightforward interpretation. This interpretability is made possible by the ease with which we can deduce the importance of each variable to the tree's choice. As a result, we can immediately ascertain the degree to which each variable affects the choice. 400 to 1200 decision trees, each constructed from a random sampling of observations and attributes from a data collection, make up a random forest.Not all trees exhibit all characteristics or observations. As a result, the trees are uncorrelated and less prone to overfitting. Each tree is also a series of yes-no questions.Questions based on a single trait or a combination of traits. Three nodes (one for each question) divided the dataset into two buckets. Each bucket contains observations that are both similar to and distinct from those in other buckets. The significance of each feature is thus determined by how "pure" each bucket is. The user provides voice input and is subjected to feature extraction. The extracted features are used to make predictions. The user is then presented the result. The administrator provides the picture. 3000 chest X-ray photos from several public image collections were chosen as the standard: Chest X- Ray Pictures(Pneumonia) and Covid-19 Radiography Dataset have repositories on Kaggle. chest radiograph From the Covid-19 Radiography Data Set GitHub repository, 623 COVID-19 images were downloaded. As a consequence, to expand the overall size, we applied picture augmentation.

Convolutional Neural Networks, a deep learning method, is employed with a cap of 2000 pictures. CNNs are a particular kind of network design for deep learning algorithms, and they are particularly useful for image recognition and other

pixel- intensive applications. Although there are other types of neural networks used in deep learning, CNNs are the most effective network design for recognising and classifying objects. Several layers of a CNN are possible, and each one trains the network to recognise various characteristics in the input picture. Every image goes through a filter or kernel, which enhances it incrementally to generate a more detailed result.

Filters can begin as simple functions in the lower layers. The complexity of the filter increases with each successive level, examining and identifying features that distinguish the input object.

As a consequence, the partially recognised picture at the end of each layer, which is the output of each convolutional image, becomes the input of the subsequent layer. On the last layer, the FC layer, the CNN recognises the picture or item it stands for. During convolution, a number of these filters are applied to the input picture. Each filter performs a specific function on the picture, finishes its job, and sends its result to the filter above it..

Eventually, the process is repeated for tens, hundreds, or thousands of layers, during which time each layer learns to recognise different characteristics.Finally, all image data passing through multiple layers of the CNN, the CNN will be able to identify the entire object.The feature is trained and a model is loaded. The x-ray image is input by the user, trained using a convolution neural network, and predictions are made based on the loaded model and the input image.There are two modules available: admin and user. The user can upload both the c-xray and the cough sound. Coughing sounds can be recorded live or pre- recorded.

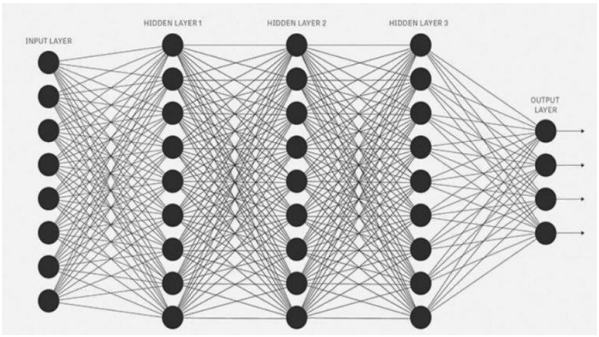

Fig. 1. convolution neural network

Admin has the ability to view feedback, view complaints, and respond.The user can provide feedback, file a complaint, receive a response, upload a c xray, record a cough sound, and view the results. Following the upload of cx-ray and a cough sound are detected, the result is positive; if neither is detected, the result is negative.

III. CONCLUSIONS

We focus on the issue of choosing the optimal classification model while considering eight different assessment criteria. We started by creating characteristics using audio analysis of cough samples. To assess the efficacy of various components of the suggested strategy, we take into account three training procedures with variable parameter values. We then create a choice matrix of

10 ML-driven classifiers with eight assessment criteria for each training technique. The weight of the evaluation criterion is then determined using entropy, and TOPSIS is then added to the proposed approach to rank the models of each training strategy. Next, utilising ensemble approaches, particularly soft ensemble and hard ensemble, the optimal COVID-19 diagnostic model is determined. based on data from quantitative measuring standards (such as average and counting votes corresponding to relative closeness value). To stop the new coronavirus from infecting more people, early diagnosis of the virus is essential. Together with this research, we developed a deep transfer learning technique that automatically recognises the illness from chest X-ray pictures of individuals with COVID-19 and those without the condition. The detection rate of the suggested classification model for COVID-19 is more than 98%.

To enhance our suggested strategy, we will further look into cross-institutional datasets. In addition, we'll apply deep learning models for categorization of the COVID-19 cough. Also, we want to gauge the severity of COVID-19 using cough sounds. In order to provide a better outcome in the future, we are thinking of integrating the three models that were previously suggested in this study and training each layer separately.

IV.ACKNOWLEDGMENT

There should be no numbers in the headings of the acknowledgement or references sections.

The IEEE LaTeX style files that were utilised in the creation of this template were created and maintained by Michael Shell and other contributors, who are thanked by Causal Productions. Please read the contributors list at the start of the file IEEETran.cls in the IEEE LaTeX release for further information.

V. RESULT

Here in this project can detect covid 19 using cough sound and chest x-ray. Two datasets are included:covid from cough sound and X-ray images. This dataset will be in the form of wave-file. The Wave file converted into spectrogram of frequencies of a signal as it varies with time. User can upload both cough sound and c x-ray and if detected, it shows positive result and not detected, it shows negative result.

REFERENCES

1. J. Breckling, Ed., The Analysis of Directional Time Series: Applications to Wind Speed and Direction, ser. Lecture Notes in Statistics. Berlin, Germany: Springer, 1989, vol. 61.
2. S. Zhang, C. Zhu, J. K. O. Sin, and P. K. T. Mok, ―A novel ultrathin elevated channel low-temperature poly-Si TFT,‖ IEEE Electron Device Lett., vol. 20, pp. 569–571, Nov. 1999.
3. M. Wegmuller, J. P. von der Weid, P. Oberson, and N. Gisin,―High resolution fiber distributed measurements with coherent OFDR,‖ in Proc. ECOC'00, 2000, paper 11.3.4, p. 109.
4. R. E. Sorace, V. S. Reinhardt, and S. A. Vaughn, ―High-speed digital- to-RF converter,‖ U.S. Patent 5 668 842, Sept. 16, 1997.
5. (2002) The IEEE website. [Online]. Available: http://www.ieee.org/
6. M. Shell. (2002) IEEEtran homepage on CTAN. [Online]. Available:http:/ /www.ctan.org/tex-archive/macros/latex/ contrib/supported/IEEEtran/
7. FLEXChip Signal Processor (MC68175/D), Motorola, 1996.
8. Y. Oh, S. Park, and J. C. Ye, ―Deep learning COVID-19 features on CXR using limited training data sets,‖ IEEE Trans. Med. Imag., vol. 39, no. 8,pp. 2688–2700, 2020.
9. Laguarta, Jordi, Ferran Hueto, and Brian Subirana. "COVID-19 Artificial Intelligence Diagnosis using only Cough Recordings." IEEE Open Journal of Engineering in Medicine and Biology (2020).
10. Fakhry, Ahmed, et al. " clinically relevant sound-based features in covid-19 identification robustness assessment with a data-centric machine learning pipeline." arXiv preprint arXiv:2103.01806 (2022).
11. Laguarta, Jordi, Ferran Hueto, and Brian Subirana. " convolutional sparse support estimator-based covid-19 recognition from x-ray images " IEEE Open Journal of Engineering in Medicine and Biology (2021).
12. M. Long, Y. Cao, J. Wang, and M. Jordan, ―Learning transferable features with deep adaptation networks,‖ in Proc. 32nd Int. Conf. Int. Conf. Mach. Learn., pp. 97–105, PMLR, 2015.
13. S. Wang, L. Yu, X. Yang, C.-W. Fu, and P.-A. Heng, ―Patch- based output space adversarial learning for joint optic disc and cup segmentation,‖ IEEE Trans. Med. Imag., vol. 38, no. 11, pp. 2485–2495, 2019.
14. G. van Tulder and M. de Bruijne, ―Learning cross- modality representations from multi-modal images,‖ IEEE Trans. Med. Imag., vol. 38, no. 2, pp. 638–648, 2018.A M. Ismael and A. S¸ engur, ―Deep learning approaches for COVID-19
15. ¨ detection based on chest X-ray images,‖ Expert Syst. Appl., vol. 164, p. 114054, 2020.
16. C. Wang, A. Elazab, J. Wu, and Q. Hu, ―Lung nodule classification using deep feature fusion in chest radiography,‖ Comput. Med. Imaging Graph., vol. 57, pp. 10–18, 2017.
17. E. Tzeng, J. Hoffman, K. Saenko, and T. Darrell, Adversarial discriminative domain adaptation,‖ in Proc. IEEE Conf. Comput. Vis. Pattern Recognit., pp. 7167–7176, 2017.

18. M. E. Chowdhury, T. Rahman, A. Khandakar, R. Mazhar, M. A. Kadir,
19. Z. B. Mahbub, K. R. Islam, M. S. Khan, A. Iqbal, N. Al-Emadi, et al., ―Can AI help in screening viral and COVID-19 pneumonia?,‖ IEEE Access, vol. 8, pp. 132665–132676, 2020.
20. B. Van Ginneken, M. B. Stegmann, and M. Loog, Segmentation of anatomical structures in chest radiographs using supervised methods: a comparative study on a public database,‖ Med. Image Anal., vol. 10, no. 1, pp. 19 –40, 2006.

Effective Model to Detect Copy Move Image Forgery Using CNN

Anugraha
Dept of CSE
KMCT College of Engineering for Women, Kozhikode
Kozhikode, India
anugrahapp60@gmail.com

Rasna
Dept of CSE
KMCT College of Engineering for Women, Kozhikode
Kozhikode, India
ransnaponnu@gmail.com

Hiba Fathima
Dept of CSE
KMCT College of Engineering for Women, Kozhikode
Kozhikode, India
hibafathimakp2019@gmail.com

Shyamini
Dept of CSE
KMCT College of Engineering for Women, Kozhikode
Kozhikode, India
shyamilikrishna85@gmail.com

Nasla K
Dept of CSE
KMCT College of Engineering for Women, Kozhikode
Kozhikode, India
nasla.asmal@yahoo.com

Abstract— Digital pictures have recently been employed in a wide variety of applications, where they have drawn the attention of academics studying digital image processing. One popular area that experts are focusing their study on is image forgery. We focus on copy-move picture forgery as a subtopic of misleading forgery. In copy-move image forging, a portion of an original picture is duplicated, then moved to create the fake image. The successful detection of copy-move picture fraud is discussed in this research along with a precise convolutional neural network (CNN) architecture. The suggested design has an appropriate number of convolutional and max-pooling layers and is computationally efficient. Additionally, we offer an efficient testing procedure that takes 0.83 seconds every test. Numerous empirical tests have been performed to make sure.

Keywords— Image forgery detection, machine learning, copy-move, convolutional neural network, image processing.

I. INTRODUCTION

Forensics as courtroom evidence, computer-assisted medical diagnosis systems, social networks, and the military all employ digital photographs as crucial data. given their significance, it is imperative to confirm their legitimacy and maintain the integrity of their contents. digital pictures may be altered using a variety of computer tools, making it challenging for the human eye to recognize phone images. due to the prevalence of fraud tools, it is now necessary to determine if two different types of photos are real or fake. in other words, it's essential to create cutting-edge methods for spotting fake photos.

Fig. 1. illustrates the division of the primary methods for identifying picture fraud into active and passive methods. we may add watermarks and digital signatures to photographs as we create them using the active technique. the passive strategy permits us to slant crucial visuals and transform true information into false information. five categories of digital picture forgery exist: copy-move forgery, image splicing, image retouching, morphing, and enhancement. examples of each of the five categories of digital picture forgeries are shown in Figures 1. One of the most popular methods of forging digital images is the copy-move. There have been several methods developed for identifying copy-move forgeries in digital photographs. In general, we may divide these methods into three major categories: First, well-known local feature extractors like SIFT, SURF, and ORB are used in the conventional copy-move forgery detection method. Second, the features are extracted via the orthogonal moment-based method using geometrically invariant orthogonal moments. The third method is the copy-move forgery detection

strategy based on deep learning, which employs a number of deep learning techniques

A. TRADITIONAL COPY-MOVE FORGERY DETECTION APPROACH

Paragraph With copy-move manipulating, a portion of the image (of any size) is chosen and added to another region of the same image. There will therefore be a strong correlation between these two regions.

The objective of the copy-move tampering detection method is to identify duplicated areas in a certain image. The similarity (correlation) or difference between traits extrapolated from two different areas of the picture demonstrates repetition. Researchers employed the following techniques to extract region-specific features from the image:

(i) As suggested in I the image is divided into tiny pieces known as blocks, and properties for each block are extracted.

(ii) Characteristics for each key point are extracted when all of the image's key points have been identified.

To The retrieved attributes are evaluated block- by-block or key point-by-keypoint to create similar blocks or similar keypoint pairs.

When matching matches between two sites are found the duplicate is validated, and the image is labelled as having been altered These techniques are predicated on the notion that the modified region is sufficiently big to accommodate many blocks or critical points.

Using the Fourier-Mellin Transform (FMT) to extract information from picture frames was suggested by [5]. Also, the use of counting bloom filters by the author helps to reduce reaction time while improving detection performance (CBF). Using the idea of pixel matching, [6] proposed a Discrete Wavelet Transform (DWT) for effective copy-move forgery detection. The method relies on recursively analysing segmented sub-images to find copy-move image forgeries in their geographical and temporal domains.

Fig . 1. Example of copy move : left- original, right- forged image

B. MOMENT-BASED COPY-MOVE FOR GERY DETECTION APPROACH

Currently, various techniques for CMFD have been established. The importance of the concept was projected. Presented a quick and correct algorithm for CMFD set in front Complex epidemics transform the importance of PCETMs. He projected approach showing a high accompanying truthfulness various types of facial deformations. The previous approach has been improved using the appropriate quaternion idea for the color representations Hosny et al.Meena et al. received a very appropriate model for Gaussian based CMFD Hermite Importance GHM. Practical results confirmed the veracity of the proposed approach to discover the copy proposed dummy regions. Good traits of two methods together: accelerate robust Waves and PCET function, was the reason for Wang et al. to present an efficient and correct procedure for CMFD, Waves is used to detect the essential content. Instead, the looks of the representations are drawn using the PCETM. Wang and others absorbed the Single Value Decomposition SVD and PCET Approaches a present the SVD- PCET approach.

II. RELATED WORK

1) Efficient Key point based Copy Move Forgery Detection Method using Hybrid Feature Extraction

Digital photographs are one of the most often used evidence or proof formats in several fields. Forensic analysis, military intelligence, medical imaging, journalism, crime scene investigation, and other fields are only a few examples. With more people using smartphones and affordable Digital picture circulation has expanded as a result of the internet's accessibility.

Having access to a variety of digital picture editing tools has also made altering images more simpler. Such manipulated images provide the wrong message and may be used to sway outcomes, particularly when they are used as the basis for crucial social decisions. The passive image altering technique of copy move has been widely used. In recent years, intensive work has been done to identify such copy move tampering

2) Robust forgery detection for compressed Images using CNN supervision

Images available on online sharing platforms are subject to change and Add global transformations such as compression, resizing and filtering possible changes. Such operations impose many limitations on counterfeit detection algorithms. In this article, we present a framework to improve the robustness of image forgery detection. Many A key step in the framework is to consider the corresponding image quality. Selected application. We therefore relied on a convolution-based camera identification model neural network. Lossy compression like JPEG is considered the most common type of compression. Test your proposals by intentionally or accidentally obfuscating fake images to this operation. Therefore, trained CNNs are supplied with a mix of different qualities. Compressed and uncompressed images. Experimental results demonstrated the importance of this step to improve the effectiveness of our approach.

3) An End-to-End Dense-Inception Net for Image Copy-Move Forgery Detection

This research proposes a novel image copy-move forgery detection method utilizing a Dense-Inception Net. An end-to-end, multi-dimensional, dense- feature connected Deep Neural Network is called a Dense-Inception Net (DNN).

The DNN model is the first to automatically learn the search the potential forgeries snippets using feature correlations and the matching hints. Pyramid Feature Extractor (PFE), Feature Correlation Matching (FCM), and Hierarchical Post- Processing (HPP) modules make up the proposed Dense- Inception Net. To extract multi-dimensional and multi- scale dense features, the PFE module is suggested. Each layer in this extractor module has properties that are directly related to the layers that came before it. Three candidate matching maps are obtained using the FCM module, which is suggested to learn the high correlations of deep features. Last but not least, the HPP module uses three matching

4) A novel deep learning framework for copy-move forgery detection in images

A range of hardware and software technologies can be u sed to create and alter digital images, which are commo n in modern civilization. Copy move faking is a method for altering images that entails obscuring undesirable objects or reconstructing desired objects in the same image. As a result, the necessity for picture content authentic action becomes crucial. This research proposes a novel de ep learning based approach to automatically detect count erfeits on copy migration. Convolutional Neural Network k (CNNs) were created with the goal of detecting counterfeit copies of moves (CMFD).

In order to recognize original and biased images, CNN utilized to learn hierarchical function representation from the input image. Numerous tests demonstrate that the deep CMFD algorithm works significantly better than the typical CMFD systems

III. PRELIMINARIES

A. THE DESCRIPTION OF CNN

Tens or even large group of coatings can be present in a convolutional interconnected system, and each tier maybe prepared to recognize differing facets of an representation.

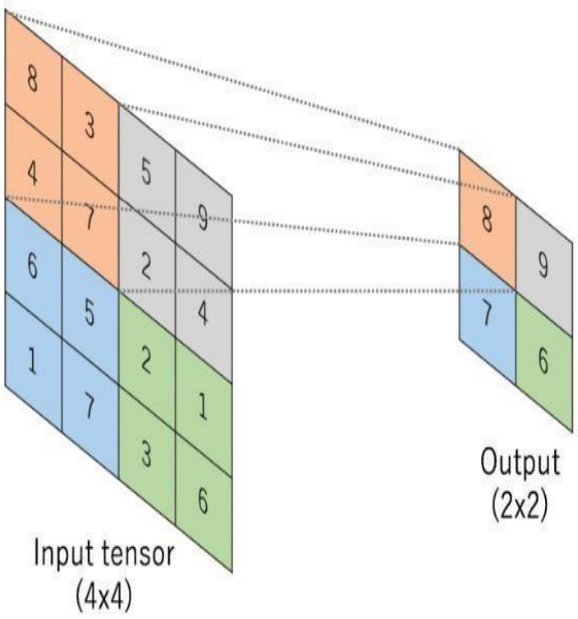

Fig.2.. Layer of CNN

Each training countenance is bear hardshipful miscellaneous determinations, and the result of each convolved image is exploited as the recommendation to the following coating. Beginning with relatively fundamental features like shine and borders, the filters can take more complicated just before they reach traits that expressly identify the object.. A convolutional interconnected system (CNN) is a deep education interconnected system devised to process structured dossier arrays to a degree plots. CNN is excellent at capturing designs in recommendation countenances to a degree lines, gradients, circles, and even eyes and faces. This possessions makes convolutional affecting animate nerve organs networks very healthy to calculating vision. CNN maybe run straightforwardly on the substitute treated images and does not demand some preprocessing. Convolutional affecting animate nerve organs networks are feed-forward neural networks, exceptionally until 20. The substance of convolutional affecting animate nerve organs networks lies in a particular type of coating named a convolutional layer.CNNshold many convolutional tiers shapely intimate, each capable of admitting more intricate shapes. It can identify handwritten digits accompanying 3 or 4 coatings of spiral, and make human faces with 25 coatings. The plan or in general area is for machines to see the realm as persons do, see in a complementary way, and ask their information to miscellaneous tasks such as representation and broadcast acknowledgment, figure inspection and categorization, television renovating, and recommend at in structures to manage accessible robotics, etc.

1. Convolution layer

Convolutional layers are produced by a collection of filters known as kernels and then applied to an input image. The convolutional layer produces a feature map, which is a representation of the input image with the filters applied. In order to create more complex models that can extract finer details from pictures, convolutional layers can be combined.

2. Max pooling layer

A group of filters together referred to as kernels create convolutional layers, which are then applied to an input image. A feature map a representation of the input image with the applied filters is created by the convolutional layer. Convolutional layers can be merged to produce more intricate models that can extract finer details from images.

3. Flattening layer

Creates a one-dimensional matrix from the traits obtained through max-pooling

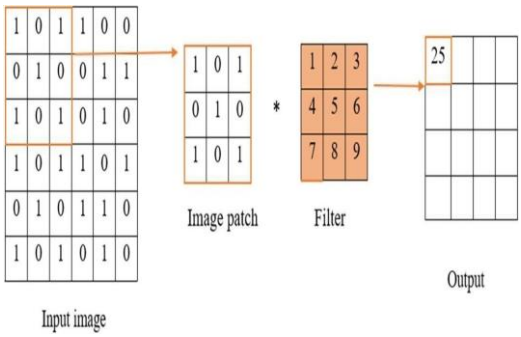

FIGURE 4. Layer of max pooling

3. Fully connected layer

A completely connected neural network is made up of a number of layers, each of which connects every neuron in one layer to every neuron in the other. While being structure agnostic makes fully linked networks very generally applicable, such networks do have a tendency to perform worse than special-purpose networks tailored to the structure of a problem space.

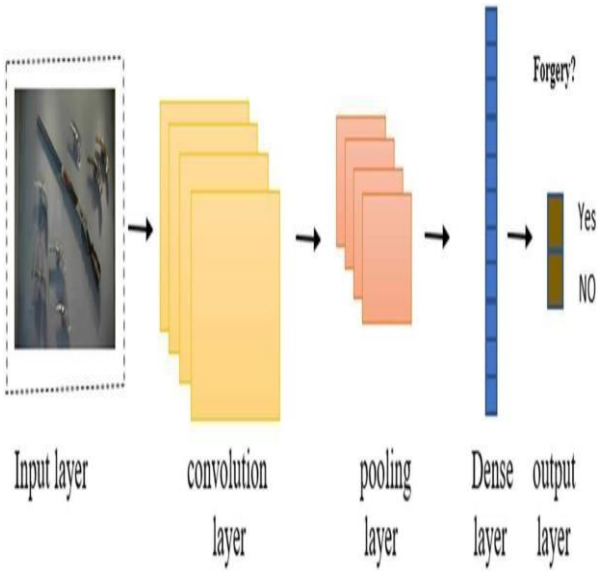

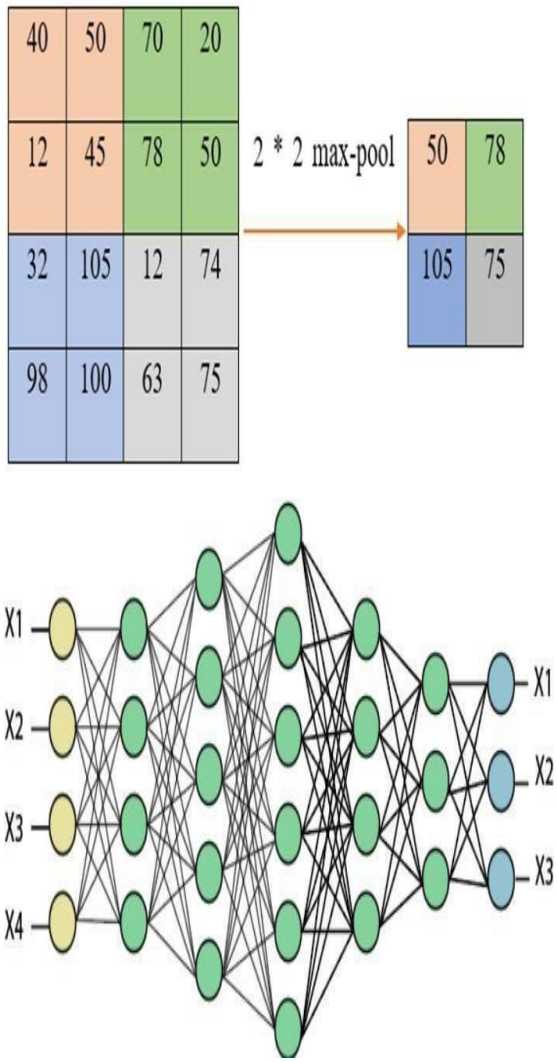

Fig 4. Layer of max pooling

As the term implies, every neuron in a layer that is fully linked has complete connectivity with every other neuron in the layer below. Towards the end of a CNN, fully linked layers are frequently employed when the objective is to use features acquired from earlier levels to produce prediction. Classified as CNNs are commonly used for image recognition and classification tasks. For example, CNNs can be used for identify objects in pictures or classify pictures as cats or dogs. CNNs can also be used for more complex tasks.

IV. PROPOSED METHOD

This paper represented as an accurate deep CNF detection method. The proposed model is based on CNN approach as it shown in figure below. The traditional approaches are work with block-based algorithms, but the CNN approaches is works with the big picture. The bestowed approach has three characteristic steps: Preprocessing, feature origin, and categorization. The input countenance is resized outside coming the next stage Cutting of image parts in the dossier preprocessing stage. Or The feature origin stage holds three convolutional coatings. Followed by a top combining tier. in the end of this aspect A completely related tier connects all physiognomy to a bulk tier. Eventually, the classification stage is named, Dossier in two types (fake or original).Convolutional Tiers as Feature Excavating Convolutional layers create their own feature maps set of filters (namely, ReLU). A working plan created from The first convolutional tier is secondhand in the following top combining Layers for building resized combined feature maps.Recommendation for the next convolutional coating. Final feature picture united accompanying the definitive max combining and formatted as a heading Joined into Sufficiently Connected.the dense layer divides the features obtained from the fully linked layer into two classes (original or forged).

A specific kind of image tampering called copy-move forging involves copying a portion of the image and pasting it somewhere else in the image with the goal of hiding a significant image feature.

The objective of copy-move forgery detection is to identify image regions that are identical or very similar. if it is fake then red sign and if it is not forged then green sign will be displayed.

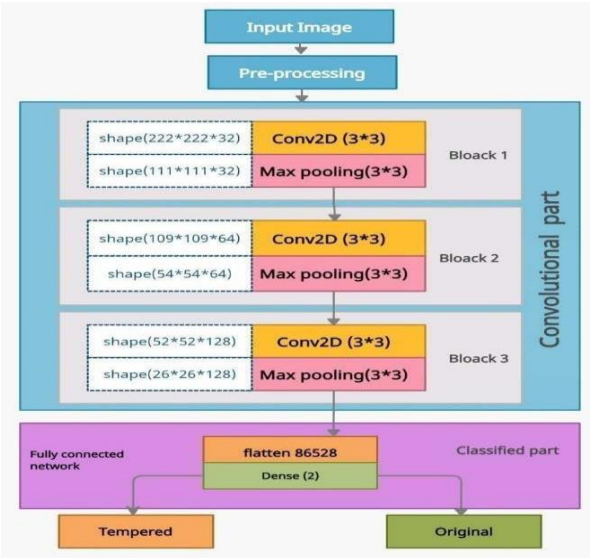

V. CONCLUSION

Finally, this work presented a deep neural learning-based copy-move forgery detection algorithm. The suggested model can detect tampered photos and categorize the candidate's image into two categories: fabricated and original. The suggested system can generate feature vectors from the characteristics of an image. The suggested technique finds feature correspondences and dependencies automatically by utilizing the whole connection layer. To be ready to test and categories the manipulated photos, the proposed model must first be trained.

The suggested model's performance was evaluated using three benchmark datasets: MICC-F2000, MICC-F600, and MICC-F220. The numerical findings of the investigation and comparison with other ways show that the proposed strategy is superior. The proposed method achieved 100% accuracy at no epochs 35 with all datasets in the case of TT, we also obtained good results when compared to existing methods. We found TT values of 47.48sec, 7.73sec, and 0.83sec for the datasets MICC-F2000, MICC-F600, and MICC-F220, respectively. All empirical findings demonstrated that the suggested model outperformed previous published algorithms in terms of accuracy and TT.

VI. RESULT

This part includes a thorough evaluation of the proposed approach's findings. The experiments were carried out on the Google Collaborator server, using the Google compute engine. Memory for the backend (GPU): 2.5GB/12GB. Tensor Flow using Keras as a backend, written in Python 3.0.

The effectiveness of the proposed approach was assessed using three benchmark datasets: MICC-F2000, MICC-F600, and MICC-F220. The numerical findings of the investigation and comparison with other ways show that the proposed strategy is superior. In all datasets, the suggested technique achieved 100% accuracy at no epochs 35. In the case of TT, we also obtained good results when compared to existing methods.

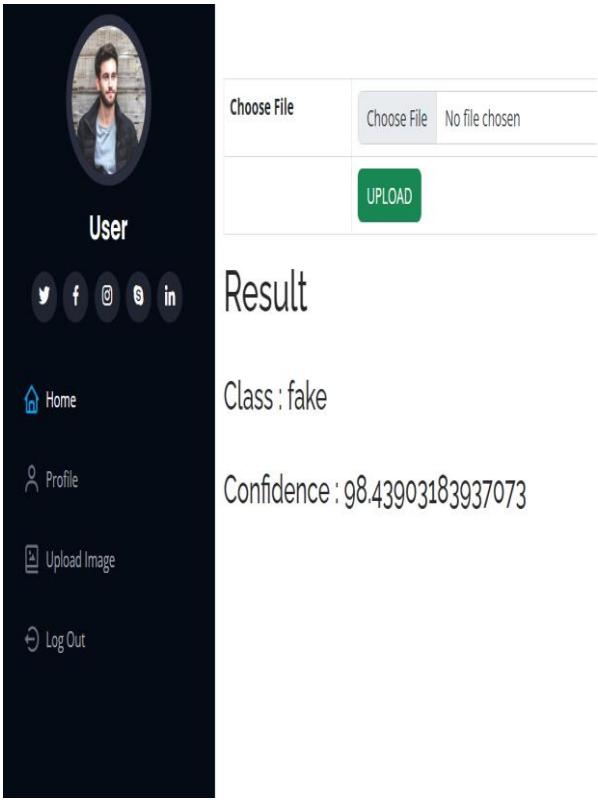

Fig: Output of forged image

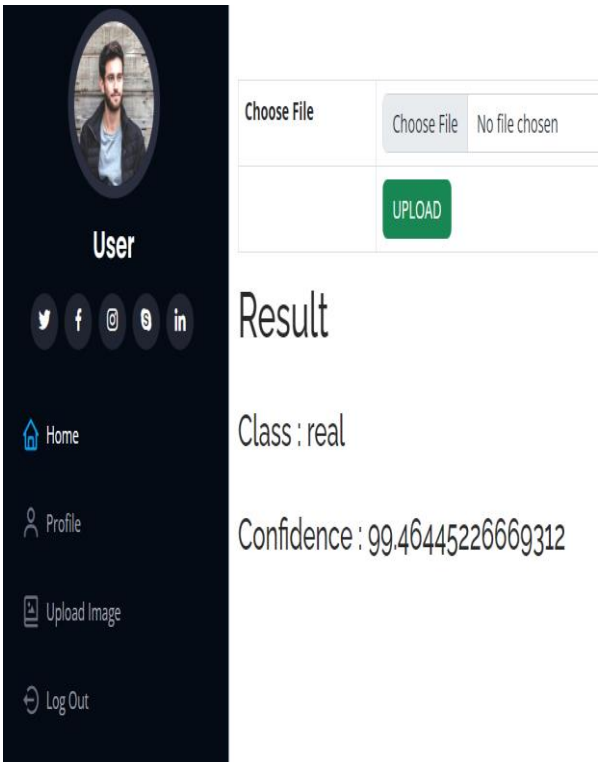

Fig: Output of original image

REFERENCES

1. K. Sunitha and A. N. Krishna, „„Efficient key point based copymoveforgery detection method using hybrid feature extraction, "" inProc. 2 nd
2. T. Chihaoui, S. Bourouis, and K. Hamrouni, „„Copy-move image forgery detection based on SIFT descriptors and SVD-matching,"" in Proc. 1 st Int. Conf. Adv. Technol. Signal Image Process. (ATSIP), Mar.2014,pp.125–129.
3. Amerini, L. Ballan, R. Cardelli, A. Del Bimbo, and G. Serra, A sift based forensic method for copy–move attack detection and transformation recovery,"" IEEE Trans. Inf. Forensics Security, vol. 6, no. 3,pp. 1099–1110,Mar.2011.
4. K. M. Hosny, H. M. Hamza, and N. A. Lashin, „„Copy- move forgery detection of duplicated objects using accurate PCET moments and morphological operators, ""Imag.Sci. J., vol. 66, no. 6, pp. 330–345, Aug.2018.
5. Y. Wang, X. Kang, and Y. Chen, „„Robust and accurate detection of image copy-move forgery using PCET-SVD and histogram of block similarity measures, "" J. Inf. Secure. Appl., vol. 54, Oct. 2020, Art. no. 102536.

Real World Applications of Data Structures

A.P.Jefrina
Department of Computer Science &
Engineering
2nd year, B.E
Coimbatore Institute of Technology
Engineering College
Coimbatore, Tamil Nadu, India.

Abstract— Study, representation and transformation of a data by a digital Technology is defined by computer science. There are two different forms of data type Namely ADT (Abstract Data Type) and Data structure. The logical form of the data type is represented by ADT (Abstract Data Type) and the physical form of the data type is given by the Data structures. A particular data can be organized in logical and mathematical manner. This organization of a data is called the Data structures. It is the building block of software development process and it applies in all disciplines of software development. It gives the efficient method or approach for a given problem. Thus, data structures plays a very important role in data organizing, accessing, sorting etc. Therefore, in this paper we will discuss the applications of various data structures like trees, graphs, stacks, queues, various types of linked lists and arrays.

I. INTRODUCTION

Software development is the major part of a computer science engineering that is accomplished with the help of data structures. We might come across an interesting topic called data structures and algorithms. Overviewing this topic we might think computer science is the study of algorithm. The finite sets of instructions that if followed accomplishes a particular task is said to be an algorithm. But this is not the case, instead computer science deals with the study of data. Data's are raw fact which doesn't gives any specific meaning. These data's are organized and stored in memory by the use of different data structures. Some of the well-known data structures are graphs, trees, linked lists, stacks, queues and arrays. There are many real world applications of data structures in our day-to-day life.

For example: Arrays (i.e. 2D array-matrices) are used in image processing, and in RGB image format n*n*3 dimensional array is used etc. Linked list are used in image viewing software in which the images are linked with one another like a chain so that we can view previous and next images easily. These goes on but still there are problems for which we can't find optimized solutions like travelling sale person problem. An approach to solve the problem is by branch and bound algorithm, dynamic programming, ant colonies optimization etc. The main objective of the paper is to determine the set of data structures for a problem and to arrive at optimized solution. This is accomplished by knowing the applications and usage of data structures in real world entity.

II. DATA STRUCTURES AND ITS APPLICATIONS

The data structures discussed here is arrays, stacks, queues, linked lists, trees and graphs. Let us see them and their applications in real world in a brief manner.

A. ARRAYS:

Arrays is one of the data structures that is used very often and everywhere in real world. Arrays are non-primitive linear data structure since it stores homogeneous elements in consecutive memory locations. Hence, the related data items are stored in an array and processed easily. Its elements are accessed by specifying the index. This is a static data structure because it consists of fixed number of elements or objects and the allocation of memory is done during the compile time. Hence it is a static memory allocation.

a. Representation:

Assuming one word of memory is occupied by each element in the array, then N consecutive word of memory will be occupied by N elements in the array. There are many types of array based on dimensions like 1D, 2D, 3D, ……,ND. D represents dimension of the array.

b. Uses:

Coming to its use 2D arrays are used in image processing and n*n*3D array is used in RGB image. Each speech signal (element) in an array implies the signal of amplitudes hence, it is used in Speech Processing. In recording to remove noise some filters are used which is in the form of array data structure. Strings also uses array to store each of its character. To encrypt/decrypt text we use 2D array of alphabets as a key which is followed in old encrypting algorithm called Playfair-cipher. An application of the array is discussed below.

c. Digital Image Processing:

Processing an image with the help of digital computer is called Digital Image Processing. Input an image and the output is also an image is said to be digital image processing. The main objective of image processing is to automate image-based tasks, extract meaningful information and to enhance the quality of the image. Consider x and y are the spatial coordinates of a two dimensional function F (x, y) which is said to be an image. A digital image is given when the amplitude values of F, x and y coordinates are finite. Hence finite number of elements in which each element have a particular value at a particular location forms a digital image. The intensity of the image at any point is declared as the amplitude of F at any pair of coordinates (x, y). The two-dimensional array arranged in rows and columns forms an image in which the elements of the array is called pixels.

$$f(x,y) = \begin{bmatrix} f(0,0) & f(0,1) & f(0,2) & \dots & f(0,N-1) \\ f(1,0) & f(1,1) & f(1,2) & \dots & f(1,N-1) \\ . & . & . & & . \\ . & . & . & & . \\ . & . & . & & . \\ f(M-1,0) & f(M-1,1) & f(M-1,2) & \dots & f(M-1,N-1) \end{bmatrix}$$

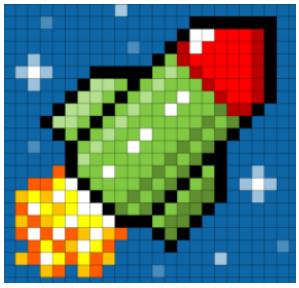

Pixels are also called picture elements or image elements. There are many types of image format we will discuss some of them.

- Binary Image: As we know binary means, it contains only two pixels elements 1 or 0, where 0 represents black and 1 represents white. Thus, Binary Image configures Monochrome.
- Black and White Image: The image, which consists of black and white color alone, is called black and white image.
- 8-bit color format: The widely used image format and also known as greyscale image, which has 256 different shades of colors. In which 0 represents black, 255 represents white, and 127 represents gray.
- 16 bit color format: 65536 shades of colors of a color image format is said to be a 16 bit color format and it has RGB format that uses n*n*3 array which constitutes of three formats red, green and blue.

The image is processed easily with the help of MATLAB. MATLAB is a numeric computing environment and a multi-paradigm programming language developed by Math workers. MATLAB stores images as two-dimensional matrices, in which each element of the matrix corresponds to a single discrete pixel in the displayed image. The representation in MATLAB is represented as

$$f = \begin{bmatrix} f(1,1) & f(1,2) & \cdots & f(1,N) \\ f(2,1) & f(2,2) & \cdots & f(2,N) \\ \vdots & \vdots & & \vdots \\ f(M,1) & f(M,2) & \cdots & f(M,N) \end{bmatrix}$$

Since in MATLAB the indices start form 1 instead of origin. This is the only deviation from normal.

PHASES OF IMAGE PROCESSING:

1. ACQUISITION: Given an image in digital form. It involves scaling and color conversion (RGB to Grey) or vice-versa.
2. IMAGE ENHANCEMENT: It is subjective and it extracts the some hidden details from the image.
3. IMAGE RESTORATION: It is objective and deals with appealing of image based on mathematical model or image degradation.
4. COLOR IMAGE PROCESSING: It deals with full color or pseudo color image processing.
5. WAVELETS AND MULT-IRESOLUTION PROCESSING: The image is represented in various degrees.
6. IMAGE COMPRESSION: It deals with image size or resolution by performing various operations or functions.
7. MORPHOLOGICAL PROCESSING: It deals with description of shape of the image and its representation by the use of various tools.
8. SEGMENTATION PROCEDURE: It partitions the image into different segments or parts where autonomous segmentation is the difficult task in image processing technique.
9. REPRESENTATION AND DESCRIPTION: It takes the output of segmentation task and chooses a representation by which the raw data is transformed into processed data.
10. OBJECT DETECTION AND RECOGNITION: It assigns label to the object as a descriptor.

Finally images are represented as arrays and processed easily. This process improves the image quality, increases the efficiency and accuracy. But the computational cost is high, limitations of algorithms and limited interpretability are the worst part of this process. Considering N*M array where S represent each row and column. Structuring the element as B from image I matrix. Thus, the time complexity is given as O (N*M*B2/S2).

B. LINKED LISTS:

Linked list follows special allocation called linked allocation. Linked allocation is defined as the elements, which are logically adjacent, need not be physically adjacent in memory, which is achieved by the use of pointers or links that point to the elements of the data structures. It is a dynamic data structure with heterogeneous elements. The memory is allocated during execution or run time so dynamic memory allocation.

a. TYPES:

SINGLY LINKED LIST- The data elements are collected linearly by means of nodes. A node consists of 2 parts. Data of the element is stored in the first part of the node called data field and the address of the next node is stored in its second part, which is called as link field or pointer field. The node is represented as

Node

In singly linked list, each node consists of a link field that point to the successor node in the list. Head pointer is a specially designated pointer that points to the first node in the list. The singly linked list is represented as

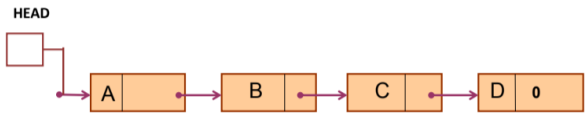

CIRCULAR LINKED LIST- It is similar to a singly linked list except that the last node in the list points the first node. The circular linked list is represented as

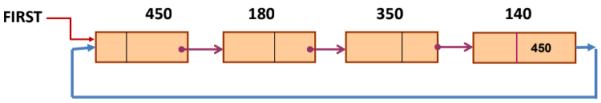

HEADER LINKED LIST- A special node called header node is present in this type of linked list and it points to the beginning of the list. It is of two types known as grounded and circular header linked list. It is represented as

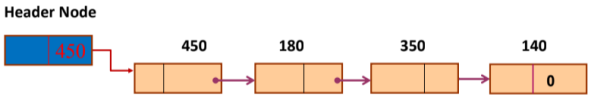

DOUBLY LINKED LIST- Here a node consists of three fields. The address of the predecessor node is stored in the first field and it is said to be as LLINK. The data of the element forms the second field. The address of the successor node is stored in the last field, which is said to be as RLINK. There are two list pointers L

and R, which points to the beginning and end of the list.

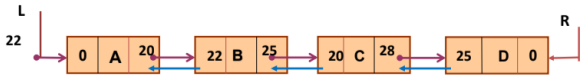

b) APPLICATIONS:

Undo and Redo buttons can be implemented using doubly linked list. It is also used in photo editors, music players, polynomial manipulation etc. It plays a crucial role in Image viewer where there is a previous and next button, which is formed by linking the previous and next image with the help of doubly linked list. Same as in web browser the previous and next buttons are formed so that accessing of previous and next URL can be made. Songs, which plays an important role in our day-to-day life. We loop the songs, rewind the song or else move to next. These are done only with the help of an important data structure known as linked lists.

c) MUSIC PLAYERS:

In day-to-day life linked lists are implemented in music players, similar to Spotify and Sound Cloud. It keeps track on previous and next song to turn to after the current song is done playing. Doubly linked list allows you to move to previous and next song whereas singly linked list allows you to move only to next song. Circular linked lists is used to loop the song i.e. when the last song finishes playing the first song automatically starts playing. These are accomplished by storing the URL of the song in the pointer fields of each node. When the data (song) of the node is executed i.e. when the song is played after its completion, automatically next song specified by the URL in the link field of the node is played. This is how music player uses linked lists to accomplish the task.

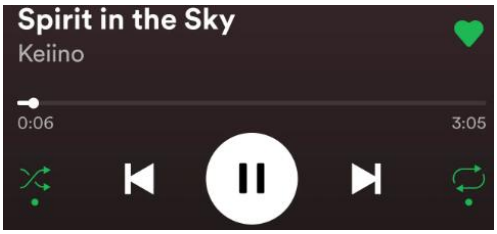

c. STACKS:

Stack is a linear list or linear structure and called as ordered list. It consists of a pointer called top from which the insertions and deletions are made. Given a stack, S= (a1, a2, ……, an), here a1 is the bottom most element and ai is the top element, 1<i<n. It is also called LAST-IN –FIRST-OUT (LIFO) or FIRST-IN –LAST-OUT (FILO) list. This means the last element, which is added to the stack, is the first element to be removed. It can be represented using array or linked list. We have operations like push and pop by which we can add the elements and remove the elements from the stack.

a) APPLICATIONS:

Stack is used in backtracking, for that aim we dig into one path, if the path is inefficient, we can return to the previous state and explore alternate options. For example N-queens problem, web browsers etc. It is also used in activation record of method calls, evaluation of expression.

b) UNDO/REDO BUTTON IN WEB BROWSER:

Whenever a user action is performed, a pair of action structures are pushed onto the undo stack; the pair has the action itself and its inverse. When undo is invoked, a pair is removed from the undo stack and added to the redo stack. When redo is invoked, a pair from the redo stack is popped and added onto to the undo stack. Thus, we can retrieve the last visited page. Thus, stacks are used in undo/redo operations in browser/ text editors.

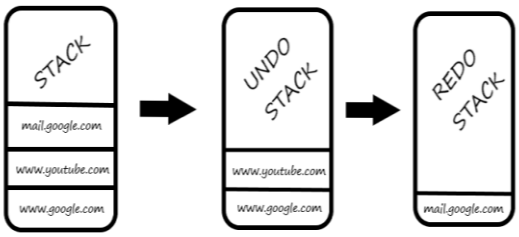

D. QUEUE:

A queue is a linear list or linear structure called as ordered list. It consists of two pointer variables called front and rear. Rear end is used only for the insertion of items. Front end is used only for the deletion of items. It is also known as FIRST-IN-FIRST OUT (FIFO) list. This means that first element which is added to the queue is the first element to be removed. It can be constituted in the form of array or linked list. There are many types of queue like linear, circular, dequeue (double ended queue) and priority queue.

a) APPLICATIONS:

In our daily life queues are used in media playlist to play the song automatically from the artist, album etc. and to handle the website traffic and CPU Scheduling. It is used in task scheduling to schedule the task based on priority or order in which they are received and is used in resource allocation, to manage and allocate resources such as CPU processing time etc.

b) MUSIC STREAMING APPLICATION:

Music streaming applications like Spotify will automatically play the song from the artist, album or playlist from which you have started to play the song. For the implementation of this application, we can use priority queue. When every element of the queue has some priority and the element of higher priority is served first before other elements and elements with same priority is served in the order of queue. This type of queue structure is called priority queue. Queued songs have priority over non-queued songs so, it takes the priority and the song is placed according to it. Priority queue takes a time complexity of O (log n). Thus, once a song is played according to the priority of the song automatically next song will be played.

E. TREES:

A tree consists of finite sets of one or more nodes. The node, which occupies the highest level of any tree structure, is called root node, which is a specially designated node, and it has no parent. The remaining nodes in the tree structure is partitioned into n disjoint sets where each of the set is a tree and is known to be the subtree of the root. A binary tree is similar to a tree but it has disjoint left and right subtree. Each node in the binary tree has no more than two child nodes. A general tree or any tree can be converted into a binary tree by left child right sibling representation. In binary tree the left and right subtrees are differentiated.

a) APPLICATIONS:

In our day-to-day life trees are used in decision, making such tree is called decision tree. A decision tree forms a flowchart like structure. The outcome of the test is held in its branches. The leaf/terminal nodes hold the class label. The internal nodes of the tree represent the test of an attribute. Decision tree used as an important tool for Machine Learning. Trees are also used in predicting the win or lose in the game such game is called game tree. The trees used in many games such as checkers, tic-tac-toe, kalah, chess, nim etc. There are several trees like B tree, B+ tree, Red Black Tree, Tournament tree etc.

b) GAME TREE:

We consider a game called nim in which the toothpicks are arranged in a pile. There are two players A, B and players are asked to move 1 or 2 or 3 tooth picks from the pile at a time. These are the valid moves. The last toothpick removed by a player will be consider as the looser. Thus, the game tree decides which player is going to win/lose the game. Considering a pile has six toothpicks (N=6) then the representation of game tree is given as below:

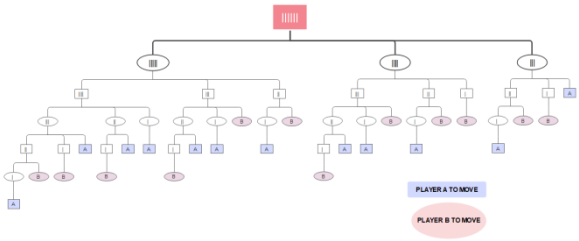

F) GRAPHS:

An example of non-linear data structure is graph. Trees maintains hierarchical relationships whereas relationships are less restricted in graphs. The graph G is represented by G (V, E) where V (G) represents the finite possibly non-empty set of nodes called as vertices and E (G) represents the finite possibly empty set of edges. Adjacency matrix, list and multilists can represent the graphs.

a) APPLICATIONS:

The highway structure of a state or country can be depicted by graph data structure. The vertices of the graph represent the cities in the highway structure and the highway path is represented by the edges of the graph. The weighted edges represents the time or distance required to travel between two cities. It is used in telecommunication to determine the transmission rate and maps to get the shortest path between the two locations, flighting agenda, robotic path, telephone network, IP routing to find the open shortest path first etc.

b) ANDROID MAPS:

Maps, which we are using today, is working based on the data structure Graph. There are many algorithm by which the shortest path can

be found. The algorithms are Dijkstra's algorithm, Floyd's algorithm, Warshall's algorithm etc. One such algorithm is Single Source all destination algorithm or Dijkstra's shortest path algorithm. A Dutch computer scientist in 1956 proposed an algorithm who was known as Dijkkstra. This algorithm has many forms. It finds the distance between two nodes but its variant finds the distance by keeping a node has fixed called as source node and then computing the distance. The main objective of this algorithm is to find the shortest distance between two nodes in a graph G (V, E) using Greedy Strategy and this is used to solve many real world problems like in telecommunication to determine the transmission rate, in maps to get the shortest path between the two locations. Consider a directed graph G = (V, E), a source vertex v0 and the weighted edges w (e). We assume that all weights are positive. The shortest paths from v0 to remaining all the vertices is determined as follows. The directed graph G (V, E) is given as an adjacency matrix, the matrix is chosen such that it is easy to determine the connection of vertices. The graph can also be represented as adjacency lists and adjacency Multilists. The graph representation is as follows

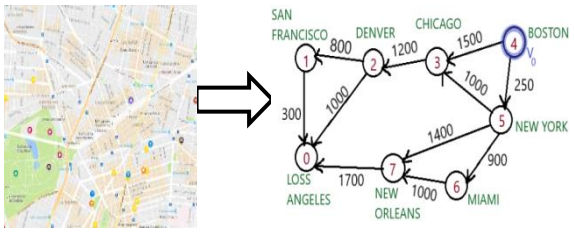

From the shortest path algorithm given by Dijkstra, we examine that if n vertices are present in G then S array maintains the visited and unvisited vertex list. COST adjacency matrix is used to represent G. If COST (i, j) where i=j then assume a non-negative number without affecting the outcome of the algorithm we consider it as 0. COST (i, j) is set as a large number +∞ when it is not in E (G) i.e.; there is no path between the two vertices i and j. The main observation is that the next vertex choose based on min {DIST (w), DIST (u) +COST (u, w)}

Where w is not in S i.e. S (w) =0. The order of time complexity used for this algorithm is O (n2). The actual generation of these paths is a minor extension of this algorithm, which is not discussed here.

III. CONCLUSION

Data structures considered as a tool for collecting, storing and organizing the data. This plays an important role in our real life. By knowing these data structures in detail we can conclude that Where, When and how we can use this in our day-to-day life to solve a real life problem in an effective manner.

REFERENCES

1. Ellis Horowitz, Sartaj Sahni, "Fundamentals of Data Structures", Galgotia Publications, Second Edition, 2008.
2. Introduction to data structure: https://www.scribd.com/
3. Digital Image Processing: https://www.geeksforgeeks.org/digital-image-processing-basics/
4. 2D Image Matrix: wwww.coursehero.com
5. Introduction to Linked lists: https://www.scribd.com/
6. Singly Linked List: https://anandaraj.hpage.com/
7. Application of Linked list: https://speakerdeck.com/
8. Introduction to Stack: https://dokumen.pub/
9. Introduction to Queue: https://www.uou.ac.in/
10. Priority Queue: https://www.slideshare.net/
11. Introduction to trees: https://oms.bdu.ac.in/
12. Introduction to Binary tree: https://www.gangainstitute.com/
13. Introduction to Dijkstra's algorithm: https://en.wikipedia.org/wiki/Dijkstra%27s_algorithm
14. Representation of graph: http://hdl.handle.net/
15. Applications of Graphs: https://www.scribd.com/

Survey on Object Detection using Deep Reinforcement Learning

Najla Musthafa
Department of Computer Science and Engineering
MEA Engineering College, Perinthalmanna
Kerala, India
najlamusthafa@meaec.edu.in

Naseeha Abdullah
Department of Computer Science and Engineering
MEA Engineering College, Perinthalmanna
Kerala, India
naseehaabdullah@gmail.com

Abstract: Deep Reinforcement Learning (DRL) is a method that is a combination of Reinforcement Learning frame work and Deep neural networks. It is observed that DRL achieved a remarkable victory over the fields such as video games, robotics, finance, computer vision, health care etc. Comparing other domains, medicine and health care field has benefitted a lot with DRL. In this paper, we study the role of DRL in object detection using works of various authors. Here we focus on object detection in medicine and healthcare field. It is observed that authors experiences higher speed in the DRL algorithm compared to classic methods. The respective method are more efficient and accurate working on CT/MRI images. Most of authors use an updated DRL algorithm in the stage of feature extraction and also club it with some machine learning techniques. DQN(Deep Q Network), Double DQN, TRPO(Trust Region Policy Optimization) etc are some common DRL algorithms used by researchers. This literature survey emphasize on methodologies of application of DRL algorithms for more efficient object detection. This review helps the futuristic way to develop DRL algorithm for better object detection in healthcare domain and similar ones.

Keywords—Object Detection, Deep Reinforcement Learning, Computer Vision, Medical Imaging, Route navigation

INTRODUCTION

According to Sutton and Barto, reinforcement learning is a framework for finding a series of behaviours that maximise the anticipated result (2018). Deep reinforcement learning is the outcome of combining deep learning and reinforcement learning [1]. Reinforcement learning may now be scaled to previously unsolvable issues thanks to DRL. One of the most cutting-edge frameworks for artificial intelligence currently exists because of the confluence of these two potent technologies. Recent significant performance improvements in a range of industries, including gaming, robotics, natural language processing, and computer vision, can be attributed to the DRL's rapid breakthroughs. The DRL framework, in contrast to supervised learning, can deal with sequential decisions and learn from supervised input that is significantly delayed. Without explicitly modelling how decisions and the world state are distributed, it is not possible to transmit the gradient from rewards to past actions because the world state is affected by the DRL agent's decisions. Because it lacks this explicit modelling, traditional supervised learning is poor for teaching with sequential actions and delayed rewards. Non-differentiable measurements can also be handled by DRL. Figure 1 shows how DRL is structured.

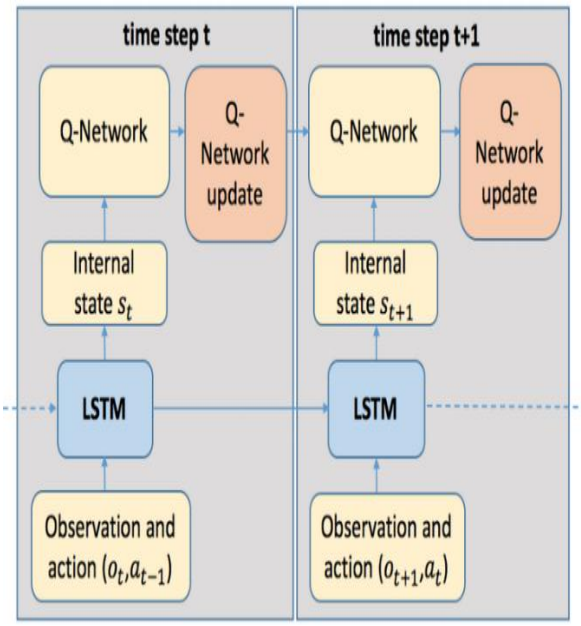

Figure 1. Architecture of DRL (Wang & Chang , 2017)

REINFORCEMENT LEARNING

An agent learns through interacting with its surroundings, which is known as reinforcement learning [5]. Using an RL framework, an agent can learn from errors. Due to the fact that it gets rewarded for participating in the environment, the RL agent learns to select behaviours that maximise the projected cumulative benefit over time. In other words, by seeing the results of the actions it does in the environment, the agent tries to determine the optimum course of action to pursue in order to achieve its goal.

It is possible to model a reinforcement learning agent using a Markov decision process (MDP). If both the state and action spaces are finite, the problem is referred to as a finite MDP. Finite MDPs are essential for RL problems since in literature the environment is frequently believed to be a finite MDP. The following activities are carried out by an RL agent in the finite MDP framework: By taking action, reacting to input, and reaping rewards, the learning agent engages with its surroundings. At each time step t, which is made up of various discrete time intervals, the agent selects one of a set of legal actions A = 1, 2,..., k at state st S, where S is the set of alternative states. The agent's behaviour is described by the policy, which instructs the agent as to which actions should be chosen for each potential state. Following each action, the next state (st+1 S) is observed, and a scalar reward is given (rt R). The probability of each possible next state, st+1, st S, at A, is determined by the transition distribution P(st+1|st, at) (st). Similar to this, the probability (rt) of each potential reward is calculated using the reward distribution (P(rt |st, at); st, S, and at, A) (st). The expected scaler reward, rt, gained by doing action an in the present state s is therefore estimated by EP(rt|st,at) (rt | st = s, at = a). The learning agent's objective is to find the best policy that, over time, maximises discounted rewards overall and establishes the likelihood of selecting either an action or an in-state.The following definition describes the projected discounted return R at time t:

$$R_t = E[r_t + \gamma r_{t+1} + \gamma^2 r_{t+2} + \cdots] = E[\sum_{k=0}^{\infty} \gamma^k r_{t+k}], \quad (1)$$

E[.] stands for the expectation relative to the reward distribution, and the range of the discount factor is 0 to 1. The action-value function Q (s, a) is defined as follows with respect to the transition probabilities and the predicted discounted immediate rewards, which are crucial components for defining dynamics of a finite MDP:

$$Q^{\pi}(s,a) = E_{\pi}[R_t | s_t = s, a_t = a] = E_{\pi}\left[\sum_{k=0}^{\infty} \gamma^k r_{t+k+1} | s_t = s, a_t = a\right]. \quad (2)$$

a function called action-value The predicted outcome is known as A(s, a), where is a mapping from states to actions or distributions over actions, and an agent starts out in state s, s S, performs action a, an A, and then applies policy. The iterative estimation of the action-value function is possible by unrolling Equation 2 to demonstrate that it fulfils a recursive condition as shown below:

$$- E_{\pi}\left[r_t + \gamma \sum_{k=0}^{\infty} \gamma^k r_{t+k+1} \middle| s_t = s, a_t = a\right] = E_{\pi}\left[\begin{matrix} r_t + \gamma Q^{\pi} \\ (s_{t+1} = s', a_{t+1} = a') \end{matrix} \middle| s_t = s, a_t = a\right], \quad (3)$$

Equation 3 establishes a connection between the value of an action in one state and the values of all possible values of s, s' S and a, a' A for its following actions. Also highlighted is the technique for estimating value depending on subsequent values. A reinforcement learning agent seeks to determine the tactic that, when used, gives the greatest potential reward. It must therefore learn a perfect policy, P, that produces a state-value function, Q, and an expected value for all states that is larger than or equal to that of putting other policies into practise (s, a). The following definitions, in particular, are included in an iterative update for choosing the best state-value function:

$$Q_{i+1}(s,a) = E_{\pi}[r_t + \gamma max_{a'} Q_i(s',a') | s,a], \quad (4)$$

It is assumed that s, s' = S in this instance and a, a' = A. This process employs the value iteration method, which converges to the best action-value function Q as I [8]. Since many real-world challenges entail a diverse variety of states and activities, the antiquated method cannot be used (a state-action table to store the values of state-action pairings). One approach to the issue is to use a function approximator as an action-value function estimator.The approximate value function, Q(s, a);, has a parameter vector and has been parameterized. When learning parameters, gradient-descent techniques are frequently used to minimise the mean-squared error in the Q-values loss function.:

$$L(\theta) = E_{\pi}\left[\left(r + \gamma max_{a'} Q_i(s', a'; \theta) - Q(s, a; \theta)\right)^2\right], \quad (5)$$

Where The desired result is equal to r + maxa'Q(s', a');. The gradient shown is produced by differentiating the loss function based on its parameters.

$$Q_{t+1}(s, a) = E_{\pi}|r_t + \gamma max_{a'} Q_t(s'a')|s, a], \quad (6)$$

This makes use of gradient-based approaches. The gradient shown above was frequently optimised using the stochastic gradient descent method. Either a linear or a non-linear function could be used as the parameters' approximation function (such as a neural network). Because of the convergence guarantees they offer, linear function approximators have been used most frequently in reinforcement learning research up until recently. Function approximators for challenging reinforcement learning tasks, such as MLP,CNN, and recurrent neural networks, are frequently used to address the convergence issues

DEEP REINFORCEMENT LEARNING

When DL networks are used to approximate any of the value function, v(s), or q(s, a), policy, and model components of reinforcement learning, deep reinforcement learning methods are produced (state transition function and reward function). The parameters in this instance are deep neural network weights. Shallow RL is created when the function approximator is one of several "shallow" models, such as linear functions, decision trees, tile coding, and others; the parameters in these models are the weight parameters. Remember that a shallow model might not be linear, such as decision trees. The function approximator used to compare "deep" and "shallow" RL is the main distinction between the two. The distinction between "deep" and "shallow" machine learning is analogous to this. The weight parameters in deep RL are often updated using stochastic gradient descent. Instability and divergence may occur when bootstrapping, non-linear function approximation, and off-policy function approximation are connected. Deep Q-Network [10] and AlphaGo, two examples of more recent research, stabilised learning and generated excellent results. Table 1 lists various DRL algorithms in alphabetical order.

Table 1. DRL Algorithms

DRL Algorithm	Illustration
DQN	Deep Q Network
Double DQN	Double Deep Q Network
Dueling DQN	Dueling Deep Q Network
MCTS	Monte Carlo tree sea+rch
UCRL-VTR	Optimistic planning problem
DDPG	DQN with Deterministic Policy Gradient
TRPO	Trust Region Policy Optimization

III. OBJECT DETECTION IN DEEP REINFORCEMENT LEARNING

A DL-based automated glaucoma diagnosis approach was put out by Bander et al. (2017). It is based on CNN, which has shown promising results in diagnosing glaucoma at a far lower computational cost than current equivalent approaches. Without any augmentation or pre-processing, the raw photos are applied directly to CNN with the exception of image scaling to reduce computing costs. From stack layers of the filters convolved along the raw image, the disease's key characteristics are automatically retrieved. This study's usage of transfer learning has shown to be a useful tactic when there aren't enough training data to employ other techniques. They used a dataset of 445 455 high-resolution glaucoma and non-glaucoma pictures to test their

approach. They employ an SVM classifier to categorise the data and a CNN for feature extraction.

Using multi-scale DRL, Ghesu (2017) created a method for real-time 3D land mark recognition in CT scans. In order to enable an artificial agent to systematically learn the most effective techniques for recognising anatomical components, we combine the concept of deep reinforcement learning with multi-scale photo analysis.This is accomplished by reformulating the issue as a general job for behavioural learning. Their approach can be expanded to accommodate the simultaneous detection of many items and gracefully manage the issue of absent objects.

Using CNN, Chen et al. (2015) suggested an automated glaucoma diagnosis system that can distinguish between glaucoma and non-glaucoma patterns for diagnostic judgements. CNN is a deep learning technology. Six learnt layers make up their architecture (figure 2): four convolutional layers and two fully-connected layers. To further improve the effectiveness of glaucoma diagnosis, dropout and data augmentation procedures are used. They made use of well-known datasets like ORIGA and SCES. In order to mitigate the overfitting issue, their suggested model makes use of response-normalization layers and overlapping-pooling layers.

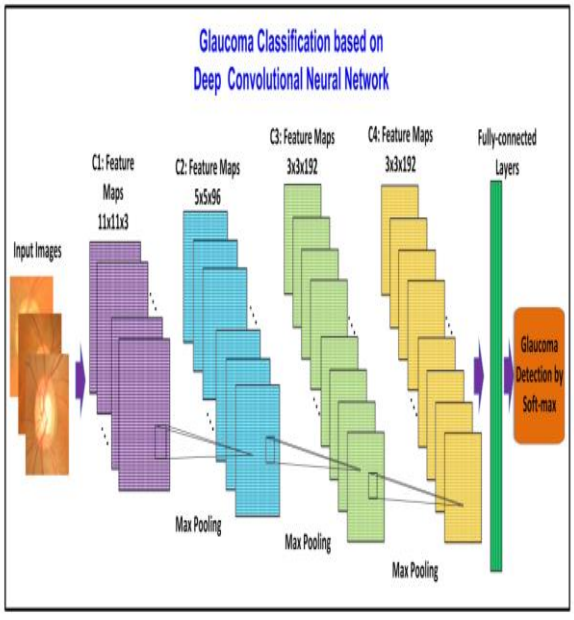

Figure 2. Deep CNN Architecture [Chen et al., 2015]

Table 2. Survey Table

SL.NO	AUTHOR	YEAR	ADVANTAGES	DISADVANTAGES
1	Sutton and Barto	2018	Significant performance improvements	Rapid breakthroughs
2	Bander et al.	2017	Lower computational cost	Less accuracy
3	Al et al.	2019	Provides an accurate and effective localization.	Requires a number of tries to learn the optimal behaviour in RL
4	Tian et al.	2020	Improved fine outcome	Less accuracy
5	Alansary	2019	Automatic landmark detection in medical photos	Less precise
6	Xiang et al.	2015	MDP policy learning, solution may be combined with other object identification, single object tracking, and data association approaches.	Time consuming
7	Zhang et al.	2020	Reduce foetal motion artefacts have the potential to benefit from assessment of foetal position in real time during MRI.	Less precise

Using an MDP with four subspaces of states, Xiang et al. (2015) created an online multi-object tracking framework based on the Markov decision process (Active, Tracked, Lost and Inactive). The birth, death, and presence or absence of an object while it is being tracked are all dealt with naturally by the MDP's state transitions. In the MDP policy with reinforcement learning, a similarity function for data association is also learned. Because it makes use of these methods for MDP policy learning, its solution may be combined with other object identification,

single object tracking, and data association approaches. They put our tracking framework implementation to the test on the demanding MOT Benchmark, and it performed noticeably better than the cutting-edge techniques examined on the benchmark.

Al et al. (2019) created a formulation of the reinforcement learning problem of landmark localisation in 3D medical pictures. Instead of using the value-based approaches that have historically been used to address the problems associated with RL-based localization, they employ a direct policy search strategy that is actor-critic based and framed in a temporal difference learning approach. It is challenging and requires a number of tries to learn the optimal behaviour in RL scenarios with large state and/or action spaces. By learning the best practicable policy on smaller partial domains, they provide a partial policy-based RL that simplifies the challenging localization problem. It improves education. Independent actors can successfully learn the matching partial policies by using each other's independent critiques. With The policy reconstruction from the partial policies provides an accurate and effective localization by using the sub-agents to solve problems of simple binary decision in their respective partial action spaces. Tests using three different localization challenges in 3D CT and MR images show that the proposed reinforcement learning requires much less trials.

Tian et al. (2020) created a multi-step medical image segmentation technique utilising RL. It is an end-to-end segmentation technique for medical images that simulates the multi-step process used by doctors to define a region of interest (ROI). Through a series of steps, performance is steadily improved from a coarse to a fine outcome. The photographs were divided up using the Markov decision process, and the issue was resolved using the DRL algorithm. To determine the ROI, the agent goes through a series of stages. For the experimental evaluation, they used the prostate MR imaging data set and the retinal fundus image data set. They discovered that the suggested model can learn to segment an ambiguous number of distinct regions. However, the intricacy of the foreground regions affects how accurately segments are made.

Several reinforcement learning agents based on DQN architectures were studied by Alansary (2019) for automatic landmark detection in medical photos. By approaching the objective sequentially and methodically, these RL-agents are able to autonomously locate landmarks. However, the background (air) can mask the target landmark by using randomly initialised starting points. They recommended a schema with hierarchical step values to deal with such a situation. Agents have the ability to move at first with big action steps before being scaled back to precisely localise the destination landmark. As an alternative, several agents can be randomly initialised at various sites, with the mean or median of the localised positions being used to determine the eventual target landmark. Finding the best DQN architecture depends on the environment, however choosing the best DQN architecture varies depending on the landmark. The performance of diverse architectures on Atari games demonstrates one of the constraints of RL research, which is evident from the disparate findings. Additionally, they have used methods for fixed- and multi-scale optimal path searches.

In low-resolution 3D MRI during pregnancy, Zhang et al. (2020) suggested incorporating physical foetal skeletal structure to increase DRL to infer landmarks of foetal posture. When inferred foetal motion is combined with online slice prescription with low-latency decision making, predictive methods for detection and to reduce foetal motion artefacts have the potential to benefit from assessment of foetal position in real time during MRI. Deep reinforcement learning (DRL) is currently advancing and offers a revolutionary method for foetal landmark detection. In this position, 15 agents are dispatched to simultaneously locate and identify 15 landmarks using DRL. We recommend an improved DRL that takes into account priors on the physical constitution of the foetal body because optimization is challenging. In order to improve agent communication within a network where each node stands for a landmark on the foetus' body, they first employ graph communication layers. A potential clinical use for online foetal motion detection that guides real-time motion artefact minimization and health diagnostics during MRI of the pregnant lady is illustrated by the suggested DRL (figure 3), which is for foetal pose landmark search. Table 2 depicts the comparison of some literatures.

.

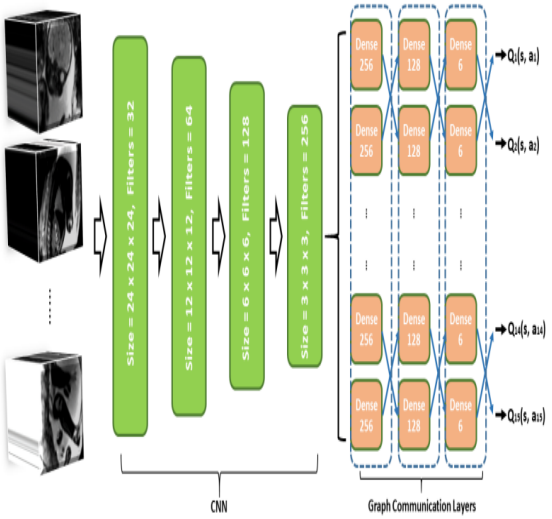

Figure 3. Architecture of DRL Frame work by Zhang et al. (2020)

Table 3. Comparison of Literatures

Author	DRL Algorithm	Bckbone	Dataset used
Bellver et al. (2016)	DQN	5 layer pretrained CNN	Pascal VOC2007 Image Dataset
Bass et l. (2017)		RESNET	T1-weighted anatomical dataset and DCE-MRI is used
Matheetbal. (2016)	Policy sampling and state transition algorithm	Deep Neural Networks	Pascal VOC 2012 dataset
Jie et al. (2016)	DQN	CNN trained with ImageNet	Pascal VOC 2007 and 2012 dataset
Uzkent et al. (2020)		ResNet 32, DarkNet 53	Caltech Pedestrian dataset
Liu et al. (2020)		ResNet 101	KITTI

IV. CONCLUSION

In this survey, we study about the use of DRL in the object detection in healthcare sector. Since DRL is a combination RL and deep neural networks, it has many advantages when compared to traditional supervised learning methods. Compared to CNN, RNN, etc., it has higher computational interferences. Additionally, DRL has small memory footprint, improved scaling up to high picture resolutions, and the best timing between accuracy and speed. We looked through old papers from previous decades for our review (2005-2022). A trend in authors has obtained that replacing ordinary deep learning or machine learning methods with pure DRL algorithms or combinations of DRL and other DL or ML methods. This work helps future researchers to write a better efficient DRL algorithm for object detection in various sectors.

V. FUTURE SCOPE

Deep reinforcement is an efficient method for the object detection in a wide range of sectors , especially in medical object detection. DRL has also used to solve a variety of optimization problems, such as tuning parameters, selecting augmentation strategies, and neural architecture search.

REFERENCES

1. Chen, X., Xu, Y., Wong, D.W.K., Wong, T.Y. and Liu, J., 2015, August. Glaucoma detection based on deep convolutional neural network. In 2015 37th annual international conference of the IEEE engineering in medicine and biology society (EMBC) (pp. 715-718). IEEE
2. Xiang, Y., Alahi, A. and Savarese, S., 2015. Learning to track: Online multi-object tracking by decision making. In Proceedings of the IEEE international conference on computer vision (pp. 4705-4713).
3. Al, W.A. and Yun, I.D., 2019. Partial policy-based reinforcement learning for anatomical landmark localization in 3d medical images. IEEE transactions on medical imaging, 39(4), pp.1245-1255.
4. Alansary, A., Oktay, O., Li, Y., Le Folgoc, L., Hou, B., Vaillant, G., Kamnitsas, K., Vlontzos, A., Glocker, B., Kainz, B. and Rueckert, D., 2019. Evaluating reinforcement learning agents for

anatomical landmark detection. Medical image analysis, 53, pp.156-164.

5. Zhang, M., Xu, J., Abaci Turk, E., Grant, P.E., Golland, P. and Adalsteinsson, E., 2020, October. Enhanced detection of fetal pose in 3D MRI by deep reinforcement learning with physical structure priors on anatomy. In International Conference on Medical Image Computing and Computer-Assisted Intervention (pp. 396-405). Springer, Cham.
6. Alansary, A., Oktay, O., Li, Y., Le Folgoc, L., Hou, B., Vaillant, G., Kamnitsas, K., Vlontzos, A., Glocker, B., Kainz, B. and Rueckert, D., 2019. Evaluating reinforcement learning agents for anatomical landmark detection. Medical image analysis, 53, pp.156-164.
7. Tian, Z., Si, X., Zheng, Y., Chen, Z. and Li, X., 2020. Multi-step medical image segmentation based on reinforcement learning. Journal of Ambient Intelligence and Humanized Computing, pp.1-12.
8. Al, Walid Abdullah, and Il Dong Yun. "Partial policy-based reinforcement learning for anatomical landmark localization in 3d medical images." IEEE transactions on medical imaging 39, no. 4 (2019): 1245-1255.
9. Li, Y., 2017. Deep reinforcement learning: An overview. arXiv preprint arXiv:1701.07274.
10. Esteva, A., Robicquet, A., Ramsundar, B., Kuleshov, V., DePristo, M., Chou, K., Cui, C., Corrado, G., Thrun, S. and Dean, J., 2019. A guide to deep learning in healthcare. Nature medicine, 25(1), pp.24-29.
11. Latif, Jahanzaib, Chuangbai Xiao, Azhar Imran, and Shanshan Tu. "Medical imaging using machine learning and deep learning algorithms: a review." In 2019 2nd International conference on computing, mathematics and engineering technologies (iCoMET), pp. 1-5. IEEE, 2019.
12. Le, Ngan, Vidhiwar Singh Rathour, Kashu Yamazaki, Khoa Luu, and MariosSavvides. "Deep reinforcement learning in computer vision: a comprehensive survey." Artificial Intelligence Review (2021): 1-87.
13. Uzkent, Burak, Christopher Yeh, and Stefano Ermon. "Efficient object detection in large images using deep reinforcement learning." In Proceedings of the IEEE/CVF winter conference on applications of computer vision, pp. 1824-1833. 2020.
14. Pirinen, Aleksis, and Cristian Sminchisescu. "Deep reinforcement learning of region proposal networks for object detection." In proceedings of the IEEE conference on computer vision and pattern recognition, pp. 6945-6954. 2018.
15. Wen, Zhiyao, Wentao Zhang, and Minfeng Qian. "A comprehensive review of deep reinforcement learning for object detection." In 2021 International Symposium on Artificial Intelligence and its Application on Media (ISAIAM), pp. 146-150. IEEE, 2021.
16. Bueno, M.B., Giró-i-Nieto, X., Marqués, F. and Torres, J., 2017. Hierarchical object detection with deep reinforcement learning. Deep Learning for Image Processing Applications, 31(164), p.3.
17. Liu, S., Huang, D. and Wang, Y., 2019. Pay attention to them: deep reinforcement learning-based cascade object detection. IEEE transactions on neural networks and learning systems, 31(7), pp.2544-2556.
18. Mousavi, S.S., Schukat, M. and Howley, E., 2016, September. Deep reinforcement learning: an overview. In Proceedings of SAI Intelligent Systems Conference (pp. 426-440). Springer, Cham.
19. Li, Y., Sycara, K. and Iyer, R., 2018. Object-sensitive deep reinforcement learning. arXiv preprint arXiv:1809.06064.

A New Life For Plastics: Plastic Utilization In Flexible Pavements

Aiswarya Raj
Department of civil engineering APJ Abdul kalam technological university
Kerala, India
aiswaryarajnair2000@gmail.com

Ardra PM
Department of civil engineering APJ Abdul kalam technological university
Kerala, India
ardrazmanoj7306@gmail.com

Manjima NR
Department of civil engineering APJ Abdul kalam technological university
Kerala, India
nrmanjima@gmail.com

Aswathi KV
Assistant professor,
Department of civil engineering APJ Abdul kalam technological university Kerala, India

Abstract— Plastic is a nonbiodegradable materials and hence it's disposal safely and effectively is a major challenge. While disposing there is a chance of releasing various harmful gases, causing environmental pollution. The incorporation of waste plastic in flexible pavement construction not only saves the problem of plastic disposal but also improves the quality of roads compared to conventional ones. The shredded plastic is mixed with aggregates and this is used to prepare bituminous mix and can be used in roads. In this paper we are finding the properties of plastic coated aggregates as well as plastic modified bituminous mix.

Keywords— Plastic coated aggregate, shredded plastic, plastic modified bituminous mix

I. INTRODUCTION

Plastic disposal is a major challenge faced by world today. It is not biologically degradable and can remain on earth for four thousand five hundred years without any change. In present days disposal is done through land filling or incineration or it can be recycled. Land filling and incineration will cause severe negative impact to the environment. So an alternative method for plastic disposal is to be found out. The use of plastic waste in flexible pavement construction is having importance since it improves the quality of roads and shows good durability when compared to conventional one. The coating of plastic waste on aggregate will improve its performance characteristic. The plastic waste were shredded in to small sizes (size range in between 4.75mm and 2.36mm) and is coated on aggregate at specified temperature and this aggregate is used for the preparation of bituminous mix. The properties of plastic modified bituminous mix can be checked by conducting marshall stability test. The plastic waste usage will improve the strength, abrasion and slip resistance of flexible pavement. This process is economical and eco-friendly. In India plastic pavement are of great advantage because of hot and extremely humid climate.

II. LITERATURE SURVEY

Shibani Hota, Abhijith Mangaraj (2022): In this journal paper, about the properties of bitumen with plastic in the design of pavement. They also discussed about two mixing process of plastic in bituminous mix, they are wet process and dry process. In this paper they arrived at a conclusion that plastic enhances the melting point of bitumen.

Rajneesh Kumar, Maaz Allah Khan (2020): In this paper they are replacing bitumen by non-biodegradable material that is plastic. Samples of various proportions of plastics are created and properties are evaluated. It is concluded that polymer coating minimized the voids and will reduces rutting, ravelling and pothole formation.

S.L Hake, R.M. Damgir, P.R Awsarmal (2019): In this paper they use plastic in bituminous blend and utilized as a best layer of adaptable asphalt. They use 5%,7.5%,10%,12.5% and 15% of plastic as substitution pf bitumen and conducted marshall stability test. This paper

conclude that waste plastic increase the properties 0f bitumen and aggregate.

Miss Apurva J Chavan (2013): In this paper waste plastic bags is utilized in bituminous mixes. The plastic waste is coated over aggregate and mixed with bitumen to form polymer modified or plastic modified bituminous mix. This bituminous mix can be utilized for construction of roads and can withstand heavy traffic and shows better durability.

III. OBJECTIVES

The main aim of our project work is to use plastic effectively inflexible pavement construction. For that purpose we need to determine the following;

- To find out the properties of bare aggregates & plastic coated aggregates.
- To find out the properties of bitumen.
- To find out the optimum bitumen content for bituminous mix.
- To find out the properties of conventional bituminous mix & plastic modified bituminous mix.
- To compare conventional bituminous mix properties with plastic modified bituminous mix.

IV. PROPOSED METHODOLOGY

A. TESTS ON AGGREGATES

In order to check the properties of aggregates the following tests were carried out. They are:

- Specific gravity test: This test determines the strength & quality of aggregate.
- Impact value test: This test measures the resistance of aggregate to sudden impact or shock.
- Crushing value test: This test measures the resistance of aggregates sample to crushing under gradually applied compressive load.
- Abrasion test: This test measures the hardness aggregate & check the suitability of aggregate for various constructions.
- Water absorption test: This test measures the water holding capacity of aggregates.
- Stripping test: The stripping is carried out to determine the influence of water in adhesion between bitumen & aggregate.

TABLE 1. RESULTS OF TESTS CONDUCTED,

Sl no	Tests	Results	Ranges
1	Specific gravity	2.68	2.5-3
2	Impact test	28.1%	Max 30%
3	Crushing test	29.09%	Max 30%
4	Abrasion test	37%	Max 40%
5	Water absorption test	0.15%	0.1-2.1%
6	Stripping test	0.3%	Max 25%

B. TESTS ON BITUMEN

In order to check the properties of bitumen the following tests were carried out. They are:

- Penetration test: This test measures the hardness or softness of bitumen by measuring the depth of penetration of loaded needle.
- Ductility test: This test measures the elongation of bitumen when it pulled by standard specimen at specified speed and temperature.
- Softening test: This test determines the temperature at which bitumen melts.
- Flash & fire point test

TABLE 2. RESULTS OF TESTS CONDUCTED

Sl no	Tests	Results	
1	Penetration test	8.5mm	2-22.5mm
2	Ductility test	71	Min 40
3	Softening test	38^0c	35-60^0c

C. TESTS ON BITUMINOUS MIX

In our project work we conducted marshall stability test in order to find out the bituminous mix properties. This test measures the ability of bituminous mix to resist the load. Marshall stability machine records the stability value (the maximum load that it can carry) & Flow value (the maximum deflection occurs under this load).

The following tests and analysis were conducted in marshall method for each specimen in the order listed below.

- Determination bulk density
- Conduct stability and flow test
- Analysis of density and voids

TABLE 3. GRADATION FOR BITUMINOUS CONCRETE

Is sieve size (%)	Cumulative %of weight of total aggregate passing	Mid value	Cumulat ive % retained	% weight retained	For 1200 g sample
26.5	100	100	0	0	0
13.2	79-100	89.5	10.5	10.5	126
9.5	70- 88	79	21	10.5	126
4.75	53 -71	62	38	17	204
2.36	42-58	50	50	12	144
1.18	34-48	41	59	9	108
0.600	26-38	32	68	9	108
0.300	18-28	13	77	9	108
0.150	12-20	16	84	7	84
0.075(filler)	4-10	7	93	9	108
Pan			100	7	84

TABLE 4. OBSERVATION TABLE FOR MARSHALL STABILITY AND FLOW VALUE

Bitumen content (%)	Stability value measured (KN)	Stability value corrected (KN)	Flow value (mm)
4.5	10.45	10.45	13.8
5	12.78	12.78	16.51
5.5	8.26	8.26	16.98
6	8.01	8.01	12.9

TABLE 5. OBSERVATION TABLE FOR DENSITY AND VOIDS

Bitumen content(%)	Weight in air(g)	Weight in water (g)	G_m	G_t	V_v	V_b	V M A	VFB
4.5	1208.3	704.3	2.397	2.48	3.467	10.12	13.587	74.483
5	1210.8	708.3	2.409	2.4	3.136	11.25	14.386	78.2
				87				
5.5	1215.6	705.2	2.387	2.447	2.451	12.19	14.641	83.259
5	1230	736.7	2.386	2.431	1.851	13.2	15.091	87.469

The following graphical plots were prepared from the properties found above:

- Bitumen content versus corrected Marshall stability
- Bitumen content versus Marshall flow
- Bitumen content versus percentage of void (Vv) in the total mix
- Bitumen content versus voids filled with bitumen (VFB)
- Bitumen content versus unit weight or bulk specific gravity (Gm)

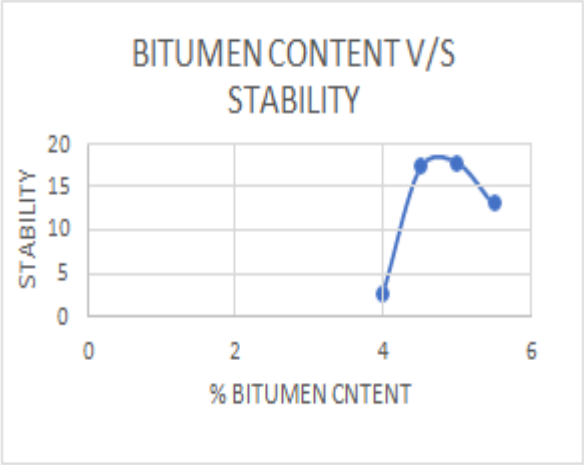

Fig. 1. Bitumen content v/s stability graph

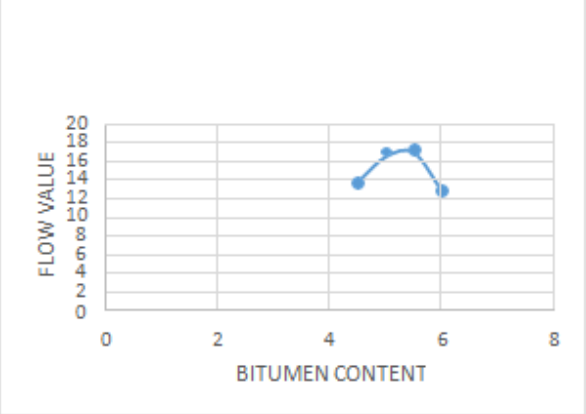

Fig. 2. Bitumen content v/s flow value graph

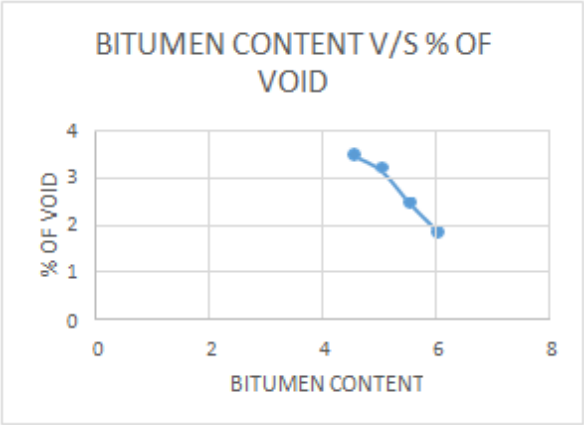

Fig. 3. Bitumen content v/s % of void graph

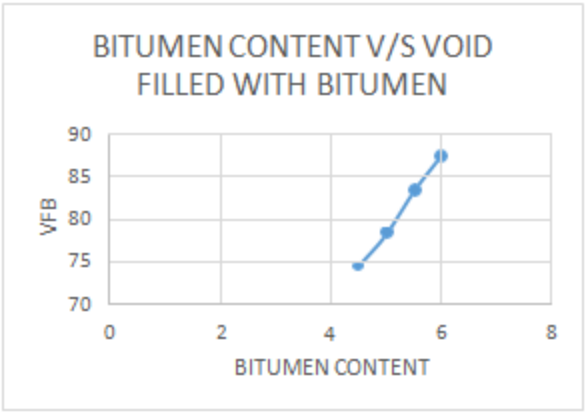

Fig. 4. Bitumen content v/s VFB graph

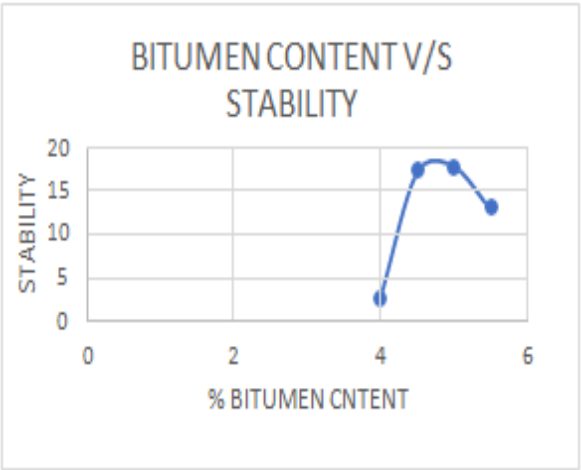

Fig. 5. Bitumen content v/s bulk specific gravity graph

To determine the optimum binder content for the mix design we need to take the mean value of the following three bitumen contents corresponding to :

- Maximum stability
- Maximum bulk specific gravity
- Median of designed limits of percent of air voids in the total mix (4%)

Which was found from the graphs obtained above. Results:

Optimum bitumen content = 4.6 %

At bitumen content:

- Marshall Stability = 10.116 KN
- Marshall flow = 14.3mm
- Voids in total mix = 3.4%
- Voids in mineral aggregate filled with bitumen = 75.23%

V. CONCLUSIONS

The waste plastic has the ability to modify the properties of bitumen & aggregate. The properties of aggregates are improved by the incorporation of plastic. The usage of plastic waste in flexible pavement shows better results when compared to conventional one & also it reduces the need of bitumen & thereby decreasing the cost of construction. These modified roads can withstand heavy traffic. It also shows good durability. This method not only improves the quality of the road but also helped to use the plastic waste generating day by day. This method is eco friendly and shows good results & easy method for plastic disposal.

REFERENCES

1. Miss Apurva Chavan J, " Use of plastic waste in flexible pavements", Volume 2, Issue 4, April 2013.
2. Nabin kumar sahoo et.al , "Project on preparation of Plastic road using single used waste plastic" , Volume 10 Issue 5, May 2022.
3. Dr.S.L.Hake, Dr.R.M.Damgir, P.R. Awsarmal, "Utilizati on of plastic waste in bitumen for flexible pavements", 3779-3785, 2020.
4. Rajnesh kumar, Maaz Allah Khan, "Use of plastic waste along with bitumen in construction of flexible pavement Volume 10,Issue 1, 2020.

An Investigation Of The Performance Of Coconut Husk And Watermelon Peel As Activated Carbon For Treatment Of Wastewater

Fathima Hanna P
Student, Department of Civil Engineering
APJ Abdul Kalam Technological University, Kerala
hannabubu782@gmail.com

Nida hanan k
Student, Department of Civil Engineering
APJ Abdul Kalam Technological University, Kerala
hanannida4@gmail.com

Aswathi k
Student, Department of Civil Engineering
APJ Abdul Kalam Technological University, Kerala
aswathikrajan01@gmail.com

Fathima Rinsha P
Student, Department of Civil Engineering
APJ Abdul Kalam Technological University, Kerala
fathimarinshap2001@gmail.com

Reena Abraham
Assistant Professor, Department of Civil Engineering
APJ Abdul Kalam Technological University, Kerala
reenacr5@gmail.com

Abstract— The wastewater produced cause a very bad effect on environment (surroundings) and it reduce the standard of water on the top layer of water bodies. This investigation assess the performance of activated carbon which is produced from coconut husk and watermelon peel to reduce the contaminants in wastewater. The wastewater sample is collected from college canteen and carwash and characterized, later the activated carbon was produced using chemical agent ZnCl2. The wastewater effluents from carwash and canteen is collected and a batch experiment has been done and observed for specific time and the results for BOD, COD, pH , turbidity and TSS were tested

KeyWords: Wastewater, activated carbon, coconut husk, watermelon peel, ZnCl2,BOD, COD, pH, turbidity,TSS

I. INTRODUCTION

The world population is growing rapidly every year Garbage has a severe impact on the surrounding area Reduced surface water quality. Wastewater treatment is one way to remove this substance pollutants in wastewater and ensure Discharged water harms the environment and humans, not Aquatic organisms. Activated carbon adsorption process can be taken as one of the most efficacious in removing contaminantts in wastewater. Manufacture of Activated Carbon Made using cheap and renewable materials such as Banana peel, orange peel, watermelon peel, rice husks and coconut husk. This research Emphasize the performance of coconut husk and watermelon peel acts as activated carbon to treat the effluent. Here's how activated carbon made from coconut husk performs and watermelon peel and coconut husk and Watermelon peel will be evaluated in wastewater treatment. Determination using different concentrations of AC Percentage of contaminants removed after each experiment.

II. METHODOLOGY

A .Waste Water Effluent Collection

The wastewater effluents were collected from the college canteen (KMCTCEW, Calicut) and from carwash at koduvally. Tests were conducted to determine pH, temperature, dissolved oxygen, turbidity, biological oxygen demand (BOD), chemical oxygen demand (COD)

B. Activated Carbon Preperation From Coconut Husk

Coconut husk were carbonised at 600°C for 1 hour in a furnace. An aqueous Solution of 100 ml consisting of 10 grams of zinc chloride (ZnCl2) was used. The char produced was then Added to the aqueous solution of zinc chloride. After 1 hour of proper mixing, the Apparatus was allowed to cool. Later, the oven was switched on and set up at 105°C, and the blend Materials were let to dry in the oven for 24 hours. After that, the

activated product was then cooled at Room temperature, and these materials were washed with distilled water to remove any undiluted residue Of zinc chloride (ZnCl2).

C. Activated Carbon Preperation From Water Melon Peel

The watermelon peel samples gathered were sundried for 5-7 days to drastically reduce their moisture content, the dried watermelon peel were crushed into powdered form later the powdered sample were introduced into hot zone of a muffle furnace and were carbonized at a temperature of 300C and the sample were held for 60 minutes. The content was removed from the muffle furnace after the set period and cooled in an open air for one hour. An aqueous Solution of 100 ml consisting of 10 grams of zinc chloride (ZnCl2) was used. The char produced was then Added to the aqueous solution of zinc chloride. After 1 hour of proper mixing, the Apparatus was allowed to cool. Later, the oven was switched on and set up at 105°C, and the blend Materials were let to dry in the oven for 24 hours. After that, the activated product was then cooled at Room temperature, and these materials were washed with distilled water to remove any undiluted residue Of zinc chloride (ZnCl2).

D. Collection Of Waste Water

The canteen wastewater and carwash is collected from college canteen and koduvally respectively.

E. Batch Adsorption Studies On Adsorbents

A batch experiment setup is put in order to treat the wastewater effluents and activated carbon from coconut husk and watermelon peel. The experiment is carried out using the jar test method. The beakers of 2L capacity is taken and 1L of sample is taken in each beaker (wastewater effluent from canteen in first 3 beakers and wastewater effluent from carwash in other 3 beakers) the activated carbon from water melon peel is added in the order 2g, 4g, and 6g respectively in canteen wastewater and 2g, 4g, 6g respectively in carwash wastewater and allow mixing for 30 minutes in 20-30 rpm. The adsorption occurs in the jar test method, which allowed the activated carbon to be mixed with the effluent samples. Then all the parameters were evaluated. Later in similar manner 8g, 10g and 12g is added respectively to canteen wastewater and 8g, 10g and 12g is added respectively to carwash wastewater. Then similarly all parameters are analysed

III. RESULT AND DISCUSSION

Characteristics of wastewater sample from canteen (KMCTCEW, Calicut) and Carwash (Koduvally)

TABLE 1: CHARACTERISTICS OF UNTREATED WASTEWATER FROM COLLEGE CANTEEN (KMCTCEW, CALICUT)

Parameters	
BOD	24.53 mg/L
COD	391.88 mgO_2/L
Ph	3.69
Turbidity	49NTU
TSS	1000 mg/L

TABLE 2: CHARACTERISTICS OF UNTREATED WASTEWATER FROM CARWASH (KODUVALLY)

Parameters	
BOD	13.799 mg/L
COD	403.52 mgO_2/L
Ph	5.57
Turbidity	35 NTU
TSS	2000 L

A. Wastewater Treated With Watermelon Peel

TABLE 3: PH OF THE TREATED CANTEEN WASTEWATER WITH ACTIVATED CARBON FROM WATERMELON PEEL

Amount of AC/L	Day 1	Day5	Day10	Day15
2g	4.89	5.13	5.52	5.52
4g	5.3	5.48	5.53	5.53
6g	5.46	5.69	5.81	5.81
8g	6.23	6.4	6.53	6.53
10g	5.79	5.86	5.97	5.97
12g	5.65	5.46	5.34	5.34

As shown in TABLE 3 the pH increases upto the addition of 8g of activated carbon and then decreases. The table 3 also shows the increment in the pH after 5 and 10 days.

TABLE 4: PH OF THE TREATED CARWASH WASTEWATER WITH ACTIVATED CARBON FROM WATER MELON PEEL

Amount of AC/L	Day 1	Day5	Day10	Day15
2g	6.43	6.44	6.45	6.45
4g	6.44	6.46	6.47	6.47
6g	6.47	6.49	6.5	6.5
8g	6.52	6.55	6.58	6.58
10g	6.18	6.2	6.21	6.21
12g	6.16	6.19	6.2	6.2

TABLE 5: BOD OF THE TREATED CANTEEN WASTEWATER WITH ACTIVATED CARBON FROM WATERMELON PEEL

Amount of AC/L	Day 1 (mg/L)	Day5 (mg/L)	Day10 (mg/L)	Day15 (mg/L)
2g	20.85	19.36	18.97	18.97
4g	15.10	14.9	13.4	13.4
6g	12.65	12.49	12.16	12.16
8g	9.92	9.9	9.45	9.45
10g	10.27	10.13	10.05	10.05
12g	10.29	10.25	10.19	10.19

TABLE 6: BOD OF THE TREATED CARWASH WASTEWATER WITH ACTIVATED CARBON FROM WATERMELON PEEL

Amount of AC/L	Day 1 (mg/L)	Day5 (mg/L)	Day10 (mg/L)	Day15 (mg/L)
2g	12.15	11.52	11.09	11.09
4g	10.62	10.14	9.27	9.27
6g	10.13	9.95	9.54	9.54
8g	9.26	9.15	9.12	9.12
10g	9.71	9.67	9.27	9.27
12g	9.97	9.85	9.49	9.49

TABLE 7: COD OF THE TREATED CANTEEN WASTEWATER WITH ACTIVATED CARBON FROM WATERMELON PEEL

Amount of AC/L	Day 1 (mgO_2/L)	Day5 (mgO_2/L)	Day10 (mgO_2/L)	Day15 (mgO_2/L)
2g	356.96	349.2	341.44	341.44
4g	322.04	314.28	306.52	306.52
6g	291	283.24	275.48	275.48
8g	240.56	232.8	228.92	228.92
10g	263.84	259.96	256.08	256.08
12g	271.6	267.7	263.84	263.84

TABLE 8: COD OF THE TREATED CARWASH WASTEWATER WITH ACTIVATED CARBON FROM WATER MELON PEEL

Amount of AC/L	Day 1 (mgO_2/L)	Day5 (mgO_2/L)	Day10 (mgO_2/L)	Day15 (mgO_2/L)
2g	341.44	337.56	325.92	325.92
4g	325.92	318.16	302.94	302.94
6g	294.88	287.12	275.48	275.48
8g	248.32	244.44	240.56	240.56
10g	271.6	267.72	263.84	263.84
12g	275.48	271.6	267.72	267.72

TABLE 9: TURBIDITY OF THE TREATED CANTEEN WASTEWATER WITH ACTIVATED CARBON FROM WATERMELON PEEL

Amount of AC/L	Day 1 (NTU)	Day5 (NTU)	Day10 (NTU)	Day15 (NTU)
2g	30	30	29	29
4g	28	27	27	27
6g	27	27	26	26
8g	23	21	20	20
10g	26	25	24	24
12g	28	27	27	27

TABLE 10: TURBIDITY OF THE TREATED CARWASH WASTEWATER WITH ACTIVATED CARBON FROM WATER MELON PEEL

Amount of AC/L	Day 1 (NTU)	Day5 (NTU)	Day10 (NTU)	Day15 (NTU)
2g	33	33	32	32
4g	33	31	30	30
6g	25	25	24	24
8g	23	22	21	21
10g	24	23	22	22
12g	24	23	23	23

TABLE 11: TSS OF THE TREATED CANTEEN WASTEWATER WITH ACTIVATED CARBON FROM WATERMELON PEEL

Amount of AC/L	Day 1 (mg/L)	Day5 (mg/L)	Day10 (mg/L)	Day15 (mg/L)
2g	500	500	500	500
4g	500	500	500	500
6g	500	500	500	500
8g	500	500	500	500
10g	500	500	500	500
12g	500	500	500	500

TABLE 12: TSS OF THE TREATED CARWASH WASTEWATER WITH ACTIVATED CARBON FROM WATER MELON PEEL

Amount of AC/L	Day 1 (mg/L)	Day5 (mg/L)	Day10 (mg/L)	Day15 (mg/L)
2g	1000	1000	1000	1000
4g	500	500	500	500
6g	500	500	500	500
8g	500	500	500	500
10g	500	500	500	500
12g	500	500	500	500

B .Wastewater Treated With Coconut Husk

TABLE 13: PH OF THE TREATED CANTEEN WASTEWATER WITH ACTIVATED CARBON FROM COCONUT HUSK

Amount of AC/L	Day 1	Day5	Day10	Day15
2g	4.57	5.11	5.39	5.39
4g	5.02	5.39	5.98	5.98
6g	5.36	5.78	5.86	5.86
8g	5.91	5.99	6.13	6.13
10g	6.35	6.46	6.52	6.52
12g	5.93	5.95	5.98	5.98

TABLE 14: PH OF THE TREATED CARWASH WASTEWATER WITH ACTIVATED CARBON FROM COCONUT HUSK

Amount of AC/L	Day 1	Day5	Day10	Day15
2g	6.41	6.43	6.44	6.44
4g	6.43	6.45	6.47	6.47
6g	6.45	6.47	6.49	6.49
8g	6.47	6.48	6.49	6.49
10g	6.5	6.52	6.53	6.53
12g	6.11	6.26	6.27	6.27

TABLE 15: BOD OF THE TREATED CANTEEN WASTEWATER WITH ACTIVATED CARBON FROM COCONUT HUSK

Amount of AC/L	Day 1 (mg/L)	Day5 (mg/L)	Day10 (mg/L)	Day15 (mg/L)
2g	20.68	18.91	18.36	18.36
4g	14.89	14.7	14.31	14.31
6g	12.6	12.36	11.96	11.96
8g	10.35	10.17	10.05	10.05
10g	9.52	9.23	9.15	9.15
12g	10.46	10.36	10.25	10.25

TABLE 16: BOD OF THE TREATED CARWASH WASTEWATER WITH ACTIVATED CARBON FROM COCONUT HUSK

Amount of AC/L	Day 1 (mg/L)	Day5 (mg/L)	Day10 (mg/L)	Day15 (mg/L)
2g	12.26	12.12	11.95	11.95
4g	10.83	10.62	10.41	10.41
6g	10.26	10.12	9.97	9.97
8g	9.87	9.72	9.15	9.15
10g	9.58	9.34	9.17	9.17
12g	10.21	10.19	9.88	9.88

TABLE 17: COD OF THE TREATED CANTEEN WASTEWATER WITH ACTIVATED CARBON FROM COCONUT HUSK

Amount of AC/L	Day 1 (mgO_2 /L)	Day5 (mgO_2/L)	Day10 (mgO_2/L)	Day15 (mgO_2/ L)
2g	349.2	333.68	329.8	329.8
4g	318.16	306.52	302.64	302.64
6g	279.36	271.6	263.84	263.84
8g	263.84	259.96	256.08	256.08
10g	252.2	248.3	244.4	244.4
12g	263.84	256.08	252.2	252.2

TABLE 18: COD OF THE TREATED CARWASH WASTEWATER WITH ACTIVATED CARBON FROM COCONUT HUSK

Amount of AC/L	Day 1 (mgO_2 /L)	Day5 (mgO_2/L)	Day10 (mgO_2/L)	Day15 (mgO_2/ L)
2g	341.44	337.56	333.68	333.68
4g	322.04	314.28	306.52	306.52
6g	287.12	275.48	267.72	267.72
8g	263.84	256.08	252.2	252.2
10g	256.08	252.2	248.32	248.32
12g	271.6	267.72	263.84	263.84

TABLE 19: TURBIDITY OF THE TREATED CANTEEN WASTEWATER WITH ACTIVATED CARBON FROM COCONUT HUSK

Amount of AC/L	Day 1 (NTU)	Day5 (NTU)	Day10 (NTU)	Day15 (NTU)
2g	42	40	36	36
4g	35	33	30	30
6g	30	29	28	28
8g	28	27	26	26
10g	25	24	23	23
12g	28	27	26	26

TABLE 20: TURBIDITY OF THE TREATED CARWASH WASTEWATER WITH ACTIVATED CARBON FROM COCONUT HUSK

Amount of AC/L	Day 1 (NTU)	Day5 (NTU)	Day10 (NTU)	Day15 (NTU)
2g	33	32	30	30
4g	30	29	27	27
6g	28	27	26	26
8g	26	25	24	24
10g	24	23	22	22
12g	27	26	25	25

TABLE 21: TSS OF THE TREATED CANTEEN WASTEWATER WITH ACTIVATED CARBON FROM COCONUT HUSK

Amount of AC/L	Day 1 (mg/L)	Day5 (mg/L)	Day10 (mg/L)	Day15 (mg/L)
2g	1000	1000	1000	1000
4g	500	500	500	500
6g	500	500	500	500
8g	500	500	500	500
10g	500	500	500	500
12g	500	500	500	500

TABLE 22: TSS OF THE TREATED CARWASH WASTEWATER WITH ACTIVATED CARBON FROM COCONUT HUSK

Amount of AC/L	Day 1 (mg/L)	Day5 (mg/L)	Day10 (mg/L)	Day15 (mg/L)
2g	1000	1000	1000	1000
4g	500	500	500	500
6g	500	500	500	500
8g	500	500	500	500
10g	500	500	500	500
12g	500	500	500	500

From the **TABLE 11,12,21** and **22** it is clear that TSS cannot be reduced by the treatment of activated carbon from watermelon peel and coconut husk.

IV. CONCLUSIONS

- The entailment of this study is to reduce the water pollution faced by water bodies.
- Activated carbon is prepared using ZnCl2
- It has been concluded that the materials used for activated carbon can be substituted to low-cost material
- Optimum dosage of activated carbon from watermelon peel is 8g and optimum dosage of activated carbon from coconut husk is 10 g.
- The BOD, COD, pH, Turbidity can be treated using activated carbon from watermelon peel and coconut husk but TSS cannot be reduced efficiently,

References

1. Anina James et. al (2021),"Valorization of coconut waste for facile treatment of contaminated water: A comprehensive review (2010–2021)"https://doi.org/10.1016/j.eti.2021.102075
2. Abdulkareem, A.S et. al (2014): "Production of Activated Carbon from Watermelon Peel"International Journal of Scientific & Engineering Research, Volume 5, Issue 2, February-2014 ISSN 2229-5518
3. N Kasmuri et.al (2021): "An investigation of a mixture of coconut husk and rice husk as activated carbon for treatment of wastewater"IOP Conf. Ser.: Earth Environ. Sci. 1019 012048
4. Mohammad Sarmadi et. al (2021): "Carwash wastewater characteristics - a systematic review study" doi: 10.5004/dwt.2021.26972

Planning, Analysis And Design Of School Building At Vadakara

Sruthakeerthi S
Department of civil engineering
KMCT College of engineering for Women
Kerala, India
srukeerthis@gmail.com

Athira V M
Department of civil engineering
KMCT College of engineering for Women
Kerala, India
athiravm0801@gmail.com

Akshayamrutha E K
Department of civil engineering
KMCT College of engineering for Women
Kerala, India
akshayamruthaek@gmail.com

Prof. U.C Ahammed Kutty
Department of civil engineering
KMCT College of engineering for Women
Kerala, India
ucakutty@gmail.com

Abstract—This project aims at planning, analysis and design of a high school building. The proposed site is located at Mayyannur in Villiappally GramaPanchayath. The building is four storeyed and is designed as framed structures. The provision is to accommodate 480 students. The functional planning is done according to KPBR and Indian Standard Codes. The plan is drafted using Auto CAD software and analysis is done for different load cases and load combinations. Analysis is done using Kanis method in order to compare various results obtained via manual analysis with more defined computer solutions. Frame is modeled in STAAD Pro and Limit State Method is followed for designing

Keywords— Category, objective, field survey, plan, analysis, design

I. INTRODUCTION

Educational institutions are that space where students transform both socially and culturally. It includes structures used as schools, colleges, institutions for education or research. Education being the fundamental right of each child educational institutions is to be constructed such that it full fills the needs and requirements of each child. Constructing such a building is only possible by going to a set of rigidly interconnected columns and beams. The aim of this project is to plan, analyse and design a four storied high school building. The planning is carried out as per Kerala Panchayath Building Rules (KPBR). The building is designed as a framed structure. The plan is drafted using Auto Cad software and analysed using STAAD Pro software. All the structures and structural elements are to be designed according to the Limit State Method.

The aim of this design is to establish a structure that full fills all the requirements and performs satisfactorily during its intended life, with an appropriate degree of freedom. The proposed site for the establishment of the project is located at Mayyannur in Viliiappally GramaPanchayath. The area of the plot is about 4526.49m2

II. CATEGORY

As per KMBR the school building come under group B. It Includes all educational buildings or part there of exceeding 150 sq. meters floor area, used for schools, college, institution, education and or research.

III. OBJECTIVES OF THE PROJECT

The main objectives of the project are:

- To plan the building as per KPBR thus satisfying the functional requirements.
- To analyze the structure manually and by using software.
- To design the building components as per IS code.
- To familiarize AutoCAD and STAAD Pro software's.

IV. SCOPE OF THE PROJECT

- To provide better education facilities for students.
- To gain more knowledge about building construction.
- To achieve basic idea and skill to use STAAD Pro and Auto Cad.

V. METHODOLOGY

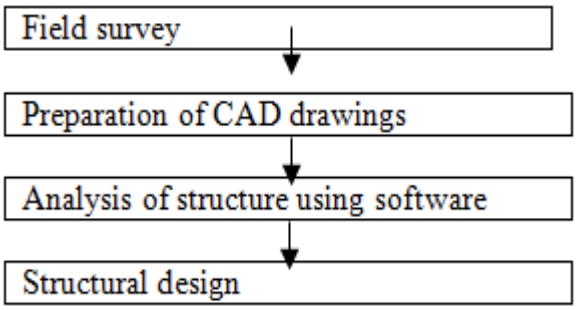

A. Field Survey

Surveying is the art of determining the relative positions of an object on the surface of the earth and taking measurements and drawing them to a convenient scale. Reconnaissance and detailed survey were carried out to determine the boundary and the area of the plot is calculated and all the details obtained from the site are also noted carefully.

B. Preparation Of CAD Drawings

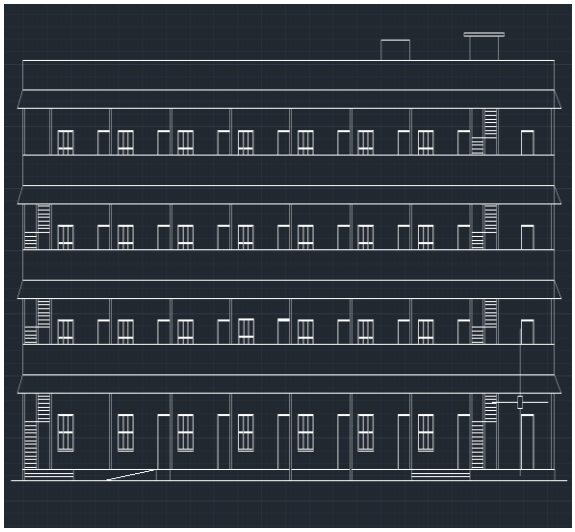

Fig .1. Elevation

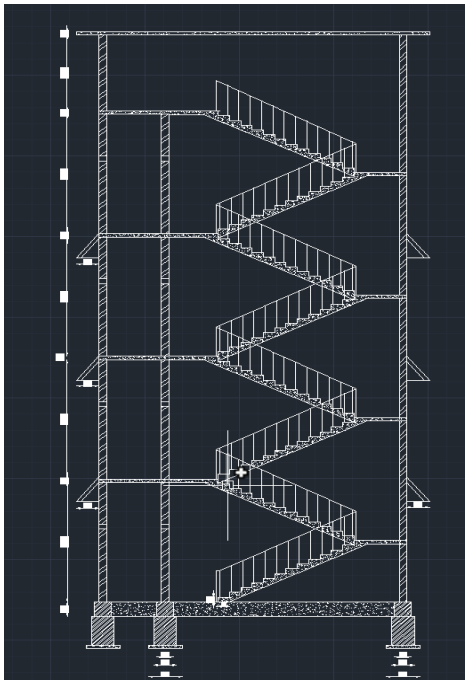

Fig. 2. Section

C. Analysis

Manual analysis of frames was done using Kani's method and is compared with the results obtained from STAAD Pro. The analysis of frames was done as follows:

- A new file was created by opening STAAD. Pro Advanced Connect edition.
- The frame was created by snap beam method.
- Property tab was selected and by using define command, the width and depth values were assigned.
- By selecting material tab materials were assigned.
- Then support page was opened by clicking on support tab. Fixed support was created and assigned.
- By selecting loading tab, load case details were added. Then the required loads and combinations were created and assigned.
- In the analysis tab provide analysis commands as perform analysis and no print. Then analysis was done by selecting Run analysis.
- Results are then obtained from post processing mode.

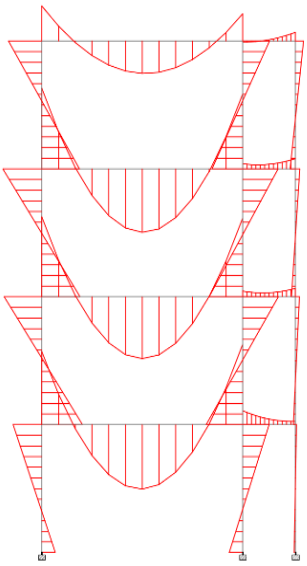

Fig. 3. Sample frame 1

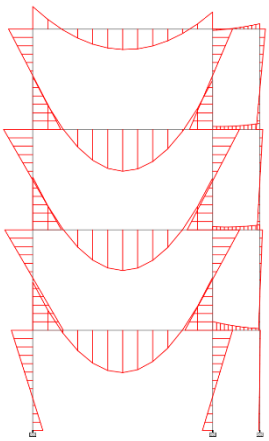

Fig. 4. Sample frame 2

VI. CONCLUSION

The school building was planned according to KPBR. The building plan was prepared by using AutoCAD software and analysed using Staad.Pro for various load combinations. There are 16 classrooms and the provision is to accommodate 480 students.

VII. FURTHER PROCEEDINGS

We are expecting to design the structure as per Limit State method such that it satisfies all the requirements.

REFERENCES

1. AtulKurezkar (2021), Analysis and design of a residential building by using STAAD Pro
2. Basil Varghese, et.al (2021), planning of school building- Kadavoor Gov.VHSS
3. P. GuruswamyGoud (2020), Analysis and design of hostel building (G+4) using ETABS
4. AparnaVijaykumar et al (2019), Design and analysis of G+2 hostel building
5. S Brhama Naidu, et al (2018), planning, designing and analysis of hostel building
6. Raiyan Mansoori et.al (2016), Application of building information modelling to civil engineering projects

Effects of Silica Fume in Papercrete

Gowri Nandakumar
Department of civil engineering
KMCT College of Engineering for Women
Calicut, India
gowrinand2001@gmail.com

Muhsina
Department of civil engineering
KMCT College of Engineering for Women
Calicut, India
tmuhsinathiruthimmal@gmail.com

Aleena. A
Department of civil engineering
KMCT College of Engineering for Women
Calicut, India
aleenaalungal@gmail.com

Bana Jasmin. P
Department of civil engineering
KMCT College of Engineering for Women
Calicut, India
banajsminp@gmail.com

Mubeena Banu E
Department of civil engineering
KMCT College of Engineering for Women
Calicut, India
mubeenabanu8492@gmail.com

Abstract—The waste materials are nowadays used as a usefulbuilding-materials all over the world. It leads to good disposal of these waste material and therefore it reduces its impact on environment. Concrete is the important building material. Waste materials are used to replace various concrete constituent material to reduce its cost and make them more environment friendly. Papercrete is newly used material it consists of the mixture of paper, cement and sand. The availability of raw materials and its properties such as fire resistant and sound insulation makes papercrete more famous. This paper mainly aims to study the effect of silica fume in papercrete.

Keywords—Papercrete, Paper pulp, Silica fume, Strength, Light weight

I. INTRODUCTION

The building and other structure construction become more expensive these days because of the cost of raw materials and less availability of constituent materials. This became a major challenge to the engineers to discover new alternative materials for the construction. They use different waste materials as a building material and most of them have good properties and strength. Thesetypes of building material are also reduced the building construction cost. Papercrete is one of the newly discovered construction material made by using paper pulp along with cement and sand.

A. Papercrete

Papercrete is mainly a light weight concrete and have good fire resistant and sound insulation property. The pulp of waste paper such as newspapers, old magazine, carboardetc. are the main constituent of papercrete. The use of papercrete block reduce the paper waste. Its light weight is the main problem in construction industry. There are different types of material used to improve the properties of construction materials such as concrete. Silica fume is one of them. Silica fume is an abundant Material and it's also had less cost compared to other material. This experiment investigates the effect of silica fume in papercrete especially aims to check the difference in strength of papercrete before and after adding silica fume.

B. Silica fume

Amorphous silicon dioxide is the main constituent of silica fume. Silica fume is a by-product, formed through the production process of silicon metal. It's chemical properties and physical properties helps to increasing the strength of concrete when it is used in concrete mix. Concrete containing silica fume also require less finishing

work than conventional concrete. Silica fume is available in both dry form and wet form.

II. EXPERIMENTAL STUDY

The constituent materials cement and fine aggregate were tested in the lab.

A. Cement

We use Zuari cement's ordinary Portland cement. The cement used complied with the IS:269-1989 specification.

1) Standard consistency test

This test is used to determine how much water should be added to cement to make a standard acceptable cement paste. To conduct the test, a Vicat apparatus conforming to IS:5513:1998 is used. We found out the percentage of water required to achieve normal consistency is 32%.

2) Fineness test

The test is run to find-out the fineness of the cement sample. According to IS:4031-1996 part 1 residue shall not exceed 10% in the case of ordinary Portland cement. Here, we must obtain 8% fines of cement sample.

3) Initial and final setting time

This test is run according to IS:4031-1988 part 5.Vicat apparatus is used in this experiment. The obtained initial and final setting time of cement paste are 45 minutes and 7 hours respectively.

4) Specific gravity of cement

Thecement's specific gravity was determined using a Le-chateliers flask in accordance with IS:4031-1988 part 11.WE Found out the specific gravity as 3.15.

B. Fine aggregate

1) Sieve analysis

The purpose of sieve analysis is to determine the aggregate particle size distribution.This isdone in accordance with IS:2386 (part 1) -1963. Here, wedetermined that the fineness modulus is 2.93.

2) Specific gravity of fine aggregate

The significant specific gravity of sand is around 2.65, and this test is performed in accordance with IS:2386 (part3) 1963. The specific gravity obtained from the experiment is 2.47.

3) Bulk density test

Bulk density is defined as the mass of the material's many particles divided by the total volume that they occupy. The bulk deny is carried out in accordance with IS:2386 part 3. The bulk density must be 1.397kg/m3 in this case.

C. Tests on Harden papercrete

1) Compressive strength test on cube

Here, we must conduct a comprehensive strength text on concrete, which is dependent on many factors such as cement strength, concrete material quality, quality control during the manufacturing process, and so on. The text was written in accordance with IS:516-1959.

2) Split tensile strength on cylinder

It is performed to determine the tensile strength of concrete. This test is carried out in accordance with IS:5816-1999

3) Flexural strength on beam

The flexural strength test is used to indirectly evaluate the tensile strength of concrete. IS:516-1956 conducts this test.

III.CASTING PROCEDURE

A. Preparation of paper pulp

The papers are gathered but they can't be used right now. Prior to combining it with other materials, it should be turned into paper pulp. The steps that go into creating pulp are as follows. The paper was first torn into tiny bits. Next, fill a bucket with water until it is 2/3 full. The tiny bits of paper were then placed in the bucket. To get the paper totally wet, the pieces were submerged one at a time, not all at once. The papers were weighed before they were submerged in water. For two to three days, the papers were left in the bucket until they turned into a paste-like substance. The paper was then removed from the water and converted into paperpulp.

B. Mixing

The paper pulp which made from waste paper is taken and all dry mixes like cement, Fine aggregate is taken according to its proportions and mix it thoroughly to form uniform mix

C. Casting

We use cubical, cylindrical, and rectangular moulds for casting cubes, cylinders, and beams, respectively. Before filling the moulds with the mix, they are cleaned and greased. Fill the material in three equal layers and compact each layer 25 times with a standard tamping rod. After filling the moulds, strike extra material to level the surface.

D. Water curing

Curing is the process in which the concrete keeps in moisture for certain period of time to complete the hydration process. Concrete's potential strength and durability will only be fully realised if it is properly cured. The specimen is removed from the mould after 24 hours. The specimen was sun-dried for three days before being immersed in water for curing. After three days of drying, the specimen is immersed in water until it is tested.

E. Testing of sample

After seven and twenty-eight days of curing, the samples are evaluated in the compression testing apparatus. After seven and twenty-eight days, three cubes underwent testing. After 28 days of curing, the beams and cylinder underwent testing.

IV. RESULT AND DISCUSSION

A. Compressive strength test

After three days of sun drying and curing for a certain period of time, that is 7 days and 28 days the Papercrete cubes were tested to find out the compressive strength in compression testing machine.

TABLE 1. RESULT OF COMPRESSIVE STRENGTH TEST ON 7th DAY

	0%	5%	10%
Average load (KN)	51.67	66.67	75
Compressive strength(N/mm^2)	0.73	0.94	1.06

TABLE 2. RESULT OF COMPRESSIVE STRENGTH TEST ON 28th DAY

	0%	5%	10%
Average load (KN)	23.33	56.67	71.67
Compressive strength(N/mm^2)	1.04	2.52	3.18

B. Split tensile strength test

The cylinder is made by papercrete mix is tested after the curing for a period of 28 days.

TABLE 3 .RESULT OF SPLIT TENSILE STRENGTH ON 28th DAY

	0%	5%	10%
Average load (KN)	45	64.33	86.67
Compressive strength(N/mm^2)	2	2.85	3.85

C. Flexural strength test

Flexural test is conducted after 28 days of curing.

TABLE 4. RESULT OF FLEXURAL STRENGTH ON 28th DAY

	0%	5%	10%
Average load (KN)	5	10	13.33
Compressive strength(N/mm^2)	2.5	5	6.67

VI. CONCLUSIONS

In this study we replaced the cement in papercrete by 0%, 10% and 15% silica fume. Paper pulp was prepared by using old news paper and prepared papercrete mix and casted cube, cylinder and beam for various tests. Compressive strength test conducted after 7 days and 28 days of curing. Split tensile test and flexural test was conducted after 28 days of curing.

V. FUTURE WORK

Supposed to conduct the test of specimen with 15% silica fume.

REFERENCES

1. YD Shermale et.al "Papercrete : An efficient use of waste paper" Recent trends in civil engineering & technologyISSN:2249_8753(online),ISSN: 2321_6476(print)Volume5,Issue3 www.stmjournals.com, 2015
2. AnokhaShilin et.al (2016), "Papercrete" International Journal of Engineering Research & Technology (IJERT) ISSN: 2278-0181Published by, www.ijert.org, Special Issue - 2016
3. H. M zaki et.al "Properties of Papercrete" ARPN Journal of Engineering and Applied SciencesWWW.arpnjournals.com ISSN 1819_6608VOL.12 NO. 24,2017
4. Akinwumi et al " Experimental study on some mechanical properties of papercrete concrete "ISSN: 2327-2503 (Print); ISSN: 2327-252X (Online), 2014

Complete Replacement Of Fine Aggregate With Granite Powder And Partial Replacement Of Coarse Aggregate With Crushed Ceramic Tile

Jaseera
Dept. of Civil Enginnering
KMCT College of Engineering for Women
Calicut, India
jaseeraabdullah@gmail.com

Jinsha KK
Dept. of Civil Enginnering
KMCT College of Engineering for Women
Calicut, India
minnjinu@gmail.com

Namitha Salim
Dept. of Civil Enginnering
KMCT College of Engineering for Women
Calicut, India
namithasalim97@gmail.com

Resmina P
Dept. of Civil Enginnering
KMCT College of Engineering for Women
Calicut, India
resminalkmw18ce028@gmail.com

Deepa V
Dept. of Civil Enginnering
KMCT College of Engineering for Women
Calicut, India
deepamaniyur@gmail.com

Abstract—As a result of modernization andadvancement in construction field, the use of traditional aggregates is at its peak. But due to over exploitation of the traditional aggregates availability is decreasing and their mining also effect our environment negatively.So it has become crucial to find an alternative source for the aggregates. Thus the purpose of construction rubbish in modern construction.we can use demolition rubbish from construction field such as broken tiles, graniteetc. as a replacement for aggregates. Also waste granite and tile from different industries can be used for replacement of conventional aggregates in concrete.In this project we are using broken tiles as coarse aggregate and powdered granite as fine aggregate.The broken tiles were replaced in place of coarse aggregates by 5%, 10%, 15%, 20% and Granite powder were replaced in place of fine aggregate by 100% without changing the mix design. M20 grade concrete was calculated tomake the ordinary mix. Without altering the current mix different types of mixes were formed by substituting the coarse aggregates and fine aggregate at different percentages of broken tiles and granite powder.Different tests like Compressive strength test, split tensile strength test and Flexural strength test, multiple concrete mixes with varying percentages of broken tiles and granite powder after 7 and 28 days curing period.

Keywords—ceramic tiles, granite powder, tensile strength, Compressive strength, flexural strength

I. INTRODUCTION

Generally in design of concrete mix, cement, fine aggregate and coarse aggregate are using from a long years back. These three materials only play a crucial role in designing of a particular grade of concrete. But nowadays there's a scarcity in aggregates. So, some new materials which are very near to our surroundings and some type of materials have to be introduced for replacing fine and coarse aggregate as well as cement to get the same strength as that these basic materials can give.

In the present study we have to replace the waste tiles and granite powder were collected from the surroundings. Crushed tiles are replaced in place of coarse aggregate by the percentage of 5%, 10%, 15%, and 20% and complete replacement of fine aggregate by granite powder. After 7 and 28 days of curing period the compressive strength, split tensile strength, flexural strength are calculated.

For conducting compressive strength test specimens are prepared in form of cubes and in the form of cylinders for split tensile test, and beam for flexural strength test. Specimens were prepared by hand, casted and then cured. Workability of concrete was measured by carrying out slump test of concrete mix. Moreover Compression Testing Machine (CTM) was used for carrying out compression, split tensile, flexural strength tests.

II. EXPERIMENTAL STUDY

The study on different materials have to be conducted before we start to cast the specimens to determine their different properties.

A. Cement

Cement forms the most important ingredient of concrete which acts as a binder material to keep the fine and coarse aggregate together by filling the void spaces between the aggregate. Portland slag cement with conforming to BIS (IS: 455- 1989) was used in the entire experimental study. Here we used zuvari cement.

TABLE- 1.

Properties	Test values	Standard values
Specific gravity	3.15	3.1 -3.16
Consistency test	32%	25%-35%
Fineness test	7%	< 10%
Initial setting time	30 minutes	30 minutes
Final setting time	6 hours	10 hours

B. Fine aggregate

Fine aggregates consist of natural sand or any crushed stone particles that are smaller than 4.75mm .here we are using crushed hard granite powder which is a waste product from construction industry.

TABLE-2.

Properties	Test values
Fineness modulus	3.592
Specific gravity	2.47
Bulk density	1397 kg/m^3

C. Coarse aggregate

Coarse aggregates refers to irregular and granular materials such as sand, gravel or crushed stone. They are used for making concrete. Generally particles which retain on 4.75mm are considered as coarse aggregates. Here we are using crushed stone and waste tiles from construction industry as coarse aggregates.

TABLE 3.

Properties	Test values
Fineness modulus	7.14
Specific gravity	2.966
Bulk density	1603 kg/m^3

D. Granite powder

Granite powder will be collected from industry and it is passed through 4.75 mm sieve. Granite powder is an industrial byproduct obtained from crushing of granite stone and granite polishing industry in a powder form.it is also generated from recycling demolition waste of granite.

TABLE 4.

Properties	Test values
Fineness modulus	2.4
Specific gravity	2.53
Bulk density	1597 kg/m^3

E. Crushed tiles

Crushed tiles which are collected from ceramic manufacturing unit. That are of appropriate size or are made into needed size using a crusher. Which retain on 4.75 mm size sieve act as a replacement for coarse aggregate in concrete.

TABLE-5.

Properties	Test values
Fineness modulus	3.12
Specific gravity	2.78
Water absorption	2%

III. CASTING

Beams, cylinders, and cubes. In common steel moulds, cubes with dimensions of 150mm x 150mm x 150mm and cylindrical specimens with dimensions of 10mm in diameter and 20mm in height were both cast. Before pouring concrete into the moulds, the surfaces of the moulds were cleaned and lightly oiled to make it easier to remove the specimens from the moulds. The test cube specimens were created as soon as possible after mixing and in a manner that would fully compact the concrete while preserving segregation. The moulds were filled with layers of concrete that were each about 5 cm thick. With a tamping rod, compaction was accomplished. If the mould is excessively full, do not finish off the concrete's surface with the extra concrete.

A. Test on fresh concrete

Slump test

The slump test was done by using slump cone. It is performed to check the workability of fresh concrete mix. This test is according to Indian standard code IS: 1199-1959.

TABLE-1. SLUMP TEST

Description	Slump values
5% replaced mix	75mm
10% replaced mix	78mm
15% replaced mix	78mm
20% replaced mix	79mm

B. Test on hardened concrete

- **Compressive strength test**

The examination followed IS: 516:1959. Three specimens measuring 150x150 mm were subjected to compressive strength tests, and the average strength was used to determine the concrete's cube compressive strength. An apparatus for assessing compression was used for the tests.

- **Flexural strength test**

This test is done by IS: 516: 1956.

- **Split tensile test**

It is done to obtain tensile strength of concrete

IV. RESULT AND DISCUSSION

- Compressive strength test

TABLE-2. COMPRESSIVE STRENGTH TEST

Mix type	7 days	28 days
0% replacement	14.81 N/mm^2	21.90 N/mm^2
5% C.agg & 100% F.agg replacement	15.27 N/mm^2	23.28 N/mm^2
10% C.agg & 100% F.agg replacement	17.18 N/mm^2	25.10 N/mm^2
15% C.agg & 100% F.agg replacement	19.25 N/mm^2	27.31 N/mm^2
20% C.agg & 100% F.agg replacement	18.88 N/mm^2	26.48 N/mm^2

- Split tensile strength test

TABLE-3. SPLIT TENSILE STRENGTH TEST

Mix type	28 days
0% replacement	2.70 N/mm^2
5% C.agg& 100% F.agg replacement	2.65 N/mm^2
10% C.agg& 100% F.agg replacement	2.60N/mm^2
15% C.agg& 100% F.agg replacement	2.59N/mm^2
20% C.agg& 100% F.agg replacement	2.56N/mm^2

- Flexural strength test

TABLE-4. FLEXURAL STRENGTH TEST

Mix type	28 days
0% replacement	3.50 N/mm^2
5% C.agg& 100% F.agg replacement	3.38 N/mm^2
10% C.agg& 100% F.agg replacement	3.30 N/mm^2
15% C.agg & 100% F.agg replacement	3.28 N/mm^2
20% C.agg& 100% F.agg replacement	3.25 N/mm^2

V. CONCLUSION

Since that material waste is steadily rising with rising urbanisation and population, research on the use of waste construction materials is crucial. Because ceramic tile aggregate is readily available and less expensive than natural aggregates, it has been the subject of several studies and analyses. Mining is necessary for natural aggregates, however tile aggregate can skip this step. Based on research using a mixture of ceramic-granite waste material on newly-poured and cured concrete, it was discovered that:

1. Based on their characteristics, ceramic tile aggregates make suitable concrete components that can replace coarse aggregates in concrete.

2. It is feasible to substitute used ceramic tile for some of the regular 20 mm aggregates in concrete of grade M20.

3. Using tile aggregates is more cost-effective than using regular concrete.

Savings of 16% of the entire sum are possible.

4. Concrete's compressive strength increases when up to 15% of the coarse aggregate is replaced with crushed ceramic tile rather than the traditional mix.

5. There is no significant difference in split tensile strength and tensile strength.

VI .ACKNOWLEDGMENT

We would like to express ours inceregr attitude to our faculty guide Miss Deepa forher expertise, guidance and supervision. We would also like to thank KMCT college of engineering for women, Calicut, India for giving us this wonderful opportunity and providing us the required equipment and facilities.

References

1. Binici, Effect of crushed ceramic and basaltic pumice as fine aggregates on concrete mortars properties, Construction and Building Materials 21 (2007) 1191–1197.
2. Brito j.de., pereira a.s., correia j.r., (2005), mechanical behaviour of non-structural concrete made with recycled ceramic aggregates, cement & concrete composites, pp 429-4331.
3. Use of waste ceramic tile aggregates as an alternative material of coarse aggregates in cement concrete(jaspreet singh, gurpreet singh bath , amanpreet singh virk)(2017)
4. An partial replacement of aggregates with granite powder and ceramic tiles in concrete(dr.k.chandramouli, j.sree naga chaitanya, dr.d.vijaya kumar)(2022)
5. Characteristic studies on concrete by partial replacement of fine aggregate with waste granite powder (molakani pavan kumar and smt. K. Chandrakala)(2019)
6. Impact of replacement of coarse aggregates with ceramic tile waste on the strength characteristics of concrete (s.o. Ajamu1 , j. R. Oluremi2 and e. S. Ogunyemi)(2018)
7. Partial replacement of sand by granite powder in concrete (narmatha.m vishali, noveena.s ,uthra megala.r (2018)
8. Replacement of fine aggregates by mixture of ceramic and marble powder in concrete (shabnum qayoom, ravi kumar) (2017)

Pedestrian Level of Service Analysis at Unsignalised Intersections

Diya Mariyam
Dept. of Civil Enginnering
KMCT College of Engineering for Women
Kozhikode,India
diyamariyamclt@gmail.com

Naja TA
Dept. of Civil Enginnering
KMCT College of Engineering for Women
Kozhikode,India
kmw19ce024@gmail.com

Raniya Rahman
Dept. of Civil Enginnering
KMCT College of Engineering for Women
Kozhikode,India
raniyarahman1924@gmail.com

AthiraPS
Dept. of Civil Enginnering
KMCT College of Engineering for Women
Kozhikode,India
athirasasi58@gmail.com

AparnaS
Dept. of Civil Enginnering
KMCT College of Engineering for Women
Kozhikode,India
aparnas@kmctcew.ac.in

Abstract—LOS classifies traffic flow to study roadways and intersections. The average vehicle control delay is used by the Highway Capacity Manual to define LOS. The analysis of unsignalized junction stakes in to account each possible movement. The goal of the study is to increase pedestrian safety by enhancing current road conditions and planning for future road design. To determine how safe that road was for pedestrians, the pedestrian level of service (PLOS) was taken in to consideration. As per HCM, 2000, LOS seems to be a quality statistic that depicts the operational circumstances present within a traffic stream, particularly in terms of administrative metrics like speed and trip duration, mobility, movement obstructions, and comfort and convenience. The HCM has established six service categories that rank activities through best to worst. Two unsignalised four-legged intersections in Kozhikode, Kerala, with heavy traffic volumes were chosen for LOS analysis.

Keywords—Intersections, Level of Service, Pedestrian, Traffic, Unsignalised.

INTRODUCTION

In India, walking is one of the most popular forms of transportation. A person who travels by walking is referred to asapedestrian. Although they pose the mostsusceptibleroaduser and are consistentlydisregardedintransportationplanning, construction, and administration, pedestrians play an inevitable part in Indian traffic. At cross roads, where traffic from many routes utilizes a same place to cross, there is a particularly high risk of conflict between diverse roadusers. The immenselyvaried nature of Indian traffic makes it difficult for pedestrians to pass through it. The operating conditions that are available within stream of traffic as seen by drivers and any other user are referred to as the level of service (LOS) in this context. The phrase "LOS" was created by high way capacity manual (HCM) to characterize the level of amenities a user can acquire from a road under varied operational circumstances and traffic volume. According to HCM, LOS A to LOS F denotes the best to poorest service levels.The pedestrian level of service (PLOS) gauges how well pedestrian needs for safety, comfort, continuity, and speed are met by road amenities. Road facilitie sincludecross walks, walkways, RefugeeIsland, side walk sand soon. Atthespecified unsignalized intersections, the effectiveness of the crosswalks is the main focus of our study. The reason to use an unsignalized intersection was made for this reason:

Unsignalized intersections provide worse pedestrian safety than signalized intersections.

A. Pedestrian Level of Service

The pedestrian level of service serves as a benchmark for such creation of pedestrian facilities and outlines the amenities offered for walkers in road traffic services. Six levels of

services are outlined in the PLOS definition as follows:

1. LOSAisapedestrianenvironmentwithoptimalcircumstancesandfewelementsthatadversely affectped estrian LOS.
2. LOS B implies that there is a reasonable pedestrian environment, but only a few aspects have an impact on the security and comfort of pedestrians. LOS B seems to be a suitable benchmark when compared to LOS A.
3. According to LOS C, there are several fundamental conditions for pedestrians, although a sizable number of variables affect their safety and comfort.
4. LOS D denotes the poor pedestrian environment as well as numerous or especially significant elements with anadverseinfluenceonPLOS.Thereareobvioussafetyconcernsamongpedestriansandlittleroomforcomfort.
5. Such pedestrian nature is unacceptable, according to LOS E. This problem develops when all or nearly all of the PLOS-affecting factors are lacking.
6. Every walk able velocity is severely constrained at LOS F, and the only forward motion possible is shuffling. There is usually unavoidable touch with other pedestrians .Movements that cross or reverse the flow are essentially impossible.

II. OBJECTIVES

The investigation's goal is:-

- To identify the critical variables that affect PLOS at the chosen unsignalized junctions.
- Toenhancepedestriansafetybyimprovingtheconditionoftheroadsandplanningthemin thefuture.

III. METHODOLOGY

1. Identification of Factors

The identification of elements that significantly affect the level of service provided at crosswalks for pedestrians is crucial for boosting the level of safety and comfort felt by users and for improving the crosswalk facilities' quality of service. The facility can only be improved by taking action after these factors have been identified. The amount of service provided by crosswalk stoped estrians has been examined in the literature, and important factors have been discovered. We referred more than ten literatures based on the PLOS of different intersection and analyses each of them. From these studies we identified the factors that influence the PLOS of an intersection.

2. Reconnaissance Survey

The reconnaissance survey is a thorough examination of a large region that could be utilized as a road or an airport. Its goal is to find the more promising routes or places while eliminating the impractical or unworkable ones. Aerial photos and existing maps could be very useful. Maps with contours display the topography and relief of a region. Aerial images display the most recent plan metric information.

3. Pilot Survey

A pilot survey is a brief questionnaire that a researcher delivers to a smaller sample size than the intended audience. You can forecast people's response patterns and adjust your research accordingly by gathering data from a convenience sample.

4. Questionnaire Survey

Questionnaire survey is based on safety and comfort of pedestrian on both the selected unsignalised intersections and is asked to the pedestrians. The questionnaire was created to measure the comfort level of pedestrians because most qualitative PLOS studies employed questionnaires and direct observations to evaluate how pedestrians perceived the state of the sidewalks.

5. Video Graphic Survey

A video-graphic survey was used to gather information about the pedestrian, traffic, and geometry conditions at unsignalized intersections. At a few crosswalks in each intersection, cameras were installed to record pedestrian movement in both the upstream and downstream directions. The video-graphic survey covered the chosen crossing and captured foot traffic all around the research area. In the lab, the necessary data were manually extracted; this process takes longer, but it has the advantage of providing more accurate data and a permanent record of events.

6. Data Analysis

The data are obtained from questionnaire survey as well as video graphic survey. These data collected were analyzed by using the pie chart and tables. Thus by analyzing we abstained corresponding PLOS for the junctions.

7. Pedestrian LOS Assessment

Making sure that people can move around safely and securely requires the assessment of pedestrian level of service(PLOS). It can be seen that the pedestrian facility's safety and security is the most significant element for PLOS assessment. There is a wealth of literature on the subject of PLOS evaluation, but little study has been done on the integration of qualitative and quantitative criteria for PLOS assessment for unsignalized junctions.

8. Pedestrian Facilities Improvement

This is to improve the pedestrian facilities. There are many ways for improving the junction. These can be done by Channelization, providing traffic signals wherever necessary, by making speed humps and speed cushions, zebra crossing, markings, round about etc.

IV. STUDY AREAS

Two junctions in Kozhikode district are taken as the study area for this project work, namely Chindhavalappu and Chungam.

A four-legged crossroads is present in one of the research areas for the project work, at Chungam, Kozhikode district, Kerala, India. The Chindhavalappu intersection also meet with four major roads.

V. DATA COLLECTION AND ANALYSIS

1. Identification of Factor

The initial step is to identify the factors affecting the particular study areas. The factors may vary according to the traffic flow, environmental conditions, crossing facilities, delays etc. After conducting proper literature studies based on the pedestrian LOS at various intersection

2. Reconnaissance Survey

In reconnaissance survey we analyze two junctions in Kozhikode district ,namely Chungam and Chindhavalappu as per the pedestrian flow and traffic flow. The selected stretch of Chungam junction (NH-17) has the widthof14.72meter and length of 45.43 meter and selected Chindhavalappu junction stretch has 14.8-meter width and 61.26-meter length.

3. Pilot Survey

To help obtain specific and pertinent input from respondents, it can also include some of the questions from the pilot survey in addition to the real survey questions. This inquiry enables researchers to determine whether survey questions were clear to respondents or whether they needed to be made simpler. From various angles, this question provides a good indication of survey response time. Additionally, you may combine the available data and interpret the results to determine whether you need to add more questions or abbreviate your survey. The selected junctions are Chungam junction and Chindhavalappu junction, Kozhikode with 4 legged. These two junctions are included in urban area with high traffic flow .The questionnaire consists of 7 multiple choice questions.

Comparison of pilot survey at Chungam and Chindhavalappu junctions

Factors	Chungam	Chindhavalappu
Speed of vehicle	Very high speed	High speed
Traffic congestion	Very high	Very high
Delay of trip	Average	Very high
Crossing path	Zebra crossing	Random
Factors influencing the crossing	No signal	No signal
Type of vehicle	Bus	Two-wheeler
Crossing time	Low	Average

4. Questionnaire Survey

Questionnaire survey is based on safety and comfort of pedestrian on both the selected unsignalised intersections and are asked to the pedestrians by online and offline mode. We'll probably use 11 multiple-choice questions to build this poll. Shop owners, pedestrians, including students, daily workers, those near bus stops, etc .were all included in the poll.

Total of 70 peoples responded in Chungam junction and a total of 48 people werer esponded in Chindhavalappu junction.

Factors	Chungam	Chindhavalappu
Crossing analysis	Average	Good
Travel mode	Walking	Not walking
Usage of cross walk	Everyday	More than once a day
Self-alertness	Alert	Alert
Criterion to cross	vehicle's approaching speed	Vehicle's approaching distance.
Confusion on gap analysis	Never	Most of time
Accident	No	No
Crossing factors	Hand signals	Hand signals
Unsafe conditions	Less priority given by drivers	No signal
Crossing path	Zebra crossing	Policeman

5. Video graphic Survey

Some of the major factors that affect junctions are pedestrian volume, pedestrian delay, pedestrian crossing time, pedestrian age and gender restrictions, impediments when crossing, vehicle speed, etc. The values for each of the variables were determined via video graphic surveys conducted at a few selected unsignalized junctions during rush hour. Cameras have been installed on either side of the two cross roads, Chunghamand Chindhavalappu, in order to do this.

6. Pedestrian LOS Assessment

- **LOS A**

LOS A is a pathway where people walk along desired paths without changing their strides in response to other people. There is no restriction on walking pace, and collisions between pedestrians are unusual.

- **LOS B**

At LOS B, there is enough room for pedestrians to select their walking speeds freely in order to avoid other pedestrians and avoid crossing problems. At this stage, people on the street start to notice other people on the street and react to their presence while choosing a walking path.

- **LOS C**

There is sufficient space at LOSC for normal walking speeds as well as for largely unidirectional streams of pedestrians to pass. Movement sinthereverse direction or when crossing can resultinmin or conflicts, and the flow rate and speeds are a little slower.

- **LOS D**

The flexibility to choose one's own walking pace and to avoid other walkers is constrained at LOS D. Asubstantia llikelihood of conflict exists during crossing or reverse-flow movements, necessitating frequent adjustments to speed and position. Although the LOS allows for a rather smooth flow, pedestrian conflict and contact are likely.

- **LOS E**

Nearly all pedestrians at LOS E slowdown from their usual walking pace and frequently change their gait. Only shuffling allows for forward motion at the lower range. There is not enough room for slower pedestrians to pass. Cross-or reverse flow movements are only very difficultly possible. As design volumes get close to the maximum capacity of the walkway, there are halts and flow pauses.

- **LOSF**

At LOSF, all walking speeds are imperceptibly restricted, making forward motion impossible.

7. Junction Facilities Improvement

The overall location where two or more roads converge or diverge is known as a junction. Junction design is essential since it directly affects the operation's efficiency, safety, speed, cost of operation, and capacity. A junction's scientifically out can prevent accidents, promote orderly traffic flow, and reduce delays in various directions.

A. Junction Improvement Methods

These are the basic techniques employed to enhance the junction facilities and hence enhance pedestrian line of sight.

- **Channelization**

The division of conflicting traffic flows in to separate lanes of travel using pavement markings or raised islands, channelization

promotes the safe and orderly flow of both cars and pedestrians.

Channelization helps with:

1. Distinguishing conflicts
2. Control of angle of conflict
3. Managing speed
4. Pedestrian protection
5. Protection for vehicles exiting or navigating main lanes of traffic.
6. Reducing the number of intersections.
7. Refusal of unlawful behavior.
8. Where to find traffic control equipment

- **Roundabouts**

Roundabouts will significantly minimize the number of accidents that happen at intersections where four different roundabouts converge. For turning traffic hat must cross and integrate with traffic streams, roundabouts offer good facility.

- **Traffic Signals**

By allocating precedence to different traffic movements, traffic signals regulate both car and pedestrian traffic signals are designed to keep traffic moving smoothly, provide vehicles and pedestrians an opportunity to cross an intersection, and reducecollisions between vehicles entering crossings from different directions.

- **Speed Hump and Speed Cushions**

It was obvious that there were neither speed humps nor speed cushions at the junction. This has led to cars approaching the cross roads very quickly, which is a major factor in the incidents that have happened there. Speed bumps can beused to slow down traffic and make it easier for pedestriansto cross the intersection.

- **Zebra crossing**

Only on streets with little traffic do you see zebra crossings, which are never at signalized crossings. Zebra crossings have poles that are black and white and have orange globes on top of them that flash. The zigzag lines in front of the crossing prohibit parking as well as passing a moving vehicle that is close to the crossing or a moving vehicle that has stopped to let pedestrians pass.

VI. RESULTSANDDISCUSSION

A. Questionnaire Survey

Following the completion of the questionnaire surveys at both intersections, it was discovered that there is a conflict between pedestrians and vehicles, which poses a risk to their safety and comfort.

- **Chungam Junction.**

Pedestrians are having issues because there are no signals. By doing the survey, it became evident that the signals existed previously but were suppressed. Al though there is a zebra crossing at NH, most pedestrians cross at random. These result in numerous accidents and incorrect vehicle speed estimations. Here, because of the close proximity of the bus stops to the cross roads ,it can occasionally be difficult for pedestrians to cross the street because of the buses. And they feel average for passing through ,In particular.

- **Chindhavalappu Junction**

Most of them ask police officers at Chindhavalappu for assistancein crossing the street. As they pass at Chindhavalappu, they feel at ease and at ease. Through this intersection, they travel by vehicle. Most pedestrians only utilize the crosswalk once every month.

B. Video Graphic Survey

The PLOS at both junctions is calculated using video graphic survey details. From this, we can determine the pedestrian crossing patterns, behavior, timing, delays, conflicts, etc. At both cross roads, crossing habits were initially examined in respect to gender. At the bypass road at the Chungam intersection, female pedestrians wait an average of 25 seconds while male pedestrians wait an average of 18 seconds. Only 31% of men and 69% of women used the crosswalks that were available in Chungam, and only 25% of men and 75% of women used the crosswalks that were available in Chindhavalappu.

C. PLOS Assessment

The main benefit of the HCM pedestrian LOS methodology is how straightforward it is. The process of gathering information and figuring out a location's pedestrian LOS is not too difficult. The only information required for the mid-block pedestrian LOS is a count of pedestrians, the

effective sidewalk width, and a statement about whether ornotplatooning was taking place.

Sl.No	Junction	Stretch	PLOS level
1	Chungam	National Highway	A
2		Beach road	E
3		Bypass road	E
4	Chindhavalappu	Stadium road	E
5		Jail road	F
6		Palayam road	F

The HCM technique also generalizes the features of the research population without giving much thought to specific pedestrian traits. For instance, a pedestrian's comfort level and pace on various sidewalk portions may be greatly influenced by their gender, age, and trip purpose. The LOS of the sidewalk may vary according on the time of day, other land users, and the weather.

D. Junction Improvement Facilities

The overall location where two or more roads converge or diverge is known as a junction. For the safety and comfort of pedestrians, several junction improvements at the Chungam intersection are required. As we have shown, PLOS in NH is below A due to the possibility of a zebra crossing; thus, similar improvements should also be made at the beach and on the bypass road so that PLOS can be raised from E to A. It is also important to install traffic signals at this crossroads, which will lessen traffic and improve pedestrian safety.

VII. CONCLUSION

According to the study, pedestrian LOS at unsignalized crossings was significantly impacted by the presence of the median, competing motor vehicle traffic, and conflicting non-motorized vehicle traffic. It can be applied to assist in managing and enhancing pedestrian amenities. The study found that despite the variation of traffic environments, pedestrians' perceptions of convenience and safety remained constant. Based on the average of the safety and convenience scores, it was established that the volume of motor vehicle traffic had a negative impact on the LOS of pedestrians.

- The results of this study allow us to draw the conclusion that a variety of factors, including vehicle speed, the type of approaching vehicle, traffic congestion, pedestrian age and gender, vehicular obstruction, and crossing behaviour, affect the safety and comfort of pedestrians through intersections.
- According to the findings at Chungam Junction, the Bypass Road and Beach Road are classified as PLOS E levels, while the NH Road falls into the PLOS A level group.
- The Stadium Road is classified under PLOS E at Chindhavalappu Junction, while Palayam Road and Jail Road are classified under PLOS F.
- At the Chungam and Chindhavalappu intersections, we can additionally offer channelization, roundabouts, zebra crossings, speed bumps or speedcushions, and traffic signalsas junction improvement services for both pedestrians and vehicles. For enhancing pedestrian level of service, we advise installing a roundabout in Chungam and a footo verbridgein Chindhavalappu intersections.

REFERENCES

1. Archana G, Reshma E K, "Analysis of Pedestrian Level of Service for Crosswalk at Intersections for Urban Condition," International Journal of Students Research in Technology & Management (IJSRTM), vol. 1, December 2013.
2. Arunabha Banerjee, Akhilesh Kumar Maurya, Gregor Lammel, A Review of Pedestrian Flow Characteristics and Level of Service Over Different Pedestrian Facilities, Collective Dynamics 3, A17, June 2018.
3. K.V.R Ravi Shankar, Parvathy Maheswari Nair, "Pedestrian Risk Analysis at Uncontrolled Mid block and Unsignalised Intersections," Journal of Traffic and

Transportation Engineering (JTTE), volume 5, issue2, April 2018.

4. Lalam Govinda, Dodappaneni Abhigna, Parvathy MNair, K.V.R Ravi Shankar, "Comparative Study of Pedestrian Crossing Behaviour atUncontrolled Intersection and Midblock Locations," Transportation Research Procedia, vol.48, May2019.
5. Raghuram Bhadradri Kadali, P Vedagiri, "Evaluation of PedestrianAccepted Vehicle Gaps with Varied Roadway Width Under MixedTraffic Conditions," International Journal of Transportation Research (IJTR), vol.11, November 2017.
6. RimaSahani, P K Bhuyan, "Modelling Pedestrian Perspectives in Evaluating Satisfaction Levels of Urban Roadway Walking Facilities," Transportation Research Procedia 48, May 2019.
7. V Indumathy, Shifamol K, Henna Beegam M K, Libin Laiju, Anitta Aloysious, "Pedestrian LOS at Unsignalised Intersection and JunctionImprovement" IOSR Journal of Dental and Medical Sciences (IOSR-JDMS), vol.19, issue7, July2020.

Soil Stabilization Using Geo fiber (Coir Fiber)

Mahbooba yasmin
Dept. of Civil Enginnering
KMCT College of Engineering for Women Kerala, India
mahboobayasmin786@gmail.com

Najimunisha SP
Dept. of Civil Enginnering
KMCT College of Engineering for Women Kerala, India
najimunishasp@gmail.com

Hana Fathima
Dept. of Civil Enginnering
KMCT College of Engineering for Women Kerala, India
hanasaleem20@gmail.com

Athira K
Dept. of Civil Enginnering
KMCT College of Engineering for Women Kerala, India
athiramohan729@gmail.com

Shamila T
Dept. of Civil Enginnering
KMCT College of Engineering for Women Kerala, India
shamilat12@gmail.com

Abstract—Fiber reinforced soils are now a common building material in the civil engineering industry. Due to the clayey soil's weakening qualities and geotechnical limitations, It is extremely risky to construct buildings and other civil engineering structures on it. It could be necessary to treat the soil to enhance its engineering properties. This investigation's goal is to recognize and measure the impact of coir fiber on the functionality of fiber-reinforced soil specimens. In this study, clayey soil and coir fiber were combined in a variety of ratios to examine the relative strength gained in terms of compaction CBR

Keywords—clayey soil, geo-fiber(coir fiber)

INTRODUCTION

The earth's top most layer is thought to be the soil, particularly where plants thrive. The primary natural cause of it in the cosmos is the breakup of rocks. It is one of the most affordable and accessible building materials, but on the other hand, its behavior is some what complex. Since it is a naturally occurring material, we are unable to accurately predict how it would be have under various circumstances. In two different situations, the same type of soil exhibits diverse behaviour. Here, a civil engineer's work is of the utmost importance since they must determine whether the superstructure's load can be supported by the existing earth..The use of additives to soften soils in the field is referred to as soil stabilization. The properties of the soil are improved mechanically or chemically in this treatment. Soil stabilization has always been an intriguing topic for researchers. Materials have evolved over time Clay soils, for example, are used to stabilize weak soils. The utilization of waste products to enhances of soils is a current trend. Lower costs and a fresh approach to trash disposal are two advantages of utilizing waste materials in building.

II. E XPERIMENTAL STUDY

A. Coir Fiber

Coir was cut in to lengths ranging from 30 mm to 50 mm.

B. Sieve Analysis

Sand and gravel proportions in the soil sample are determined by sieving, which was done to determine the soil's coarser content. This controls the ratio of sand and gravel in the soil. According to IS:2720 (PartIV) -1985, sieving was carried out using a variety of sieves ranging from 4.75mmto.075mm.

C. Consistency Limits

In order to conduct soil tests, IS:2720 (PartV)-1985 was consulted. The liquid limit is measured in the laboratory using Casagrande's apparatus. The liquid limit is the lowest water content at which soil has a tendency to flow, and all soil has a minimal shear strength at the liquid limit. The term "plastic limit" describes the amount of water at which a soil sample would just start to crumble when rolled into a thread about 3mmindiameter.

D. Specific Gravity

According to IS: 2720 (Part III) 1980 instructions, the soil fraction was estimated by

measuring the amount of soil that passed through a 4.75mm IS sieve with the use of a pycnometer. It is described as the ratio of the weight of an equivalent amount of water at 4 degrees Celsius to a certain volume of solids.

E. Standard Proctor Compaction Test

To analyse the geotechnical properties of soil, such as unconfined compressive strength and CBR value, it is necessary to ascertain the water content at which compactive effort can yield the maximum value of dry density. This water content is referred to as optimum moisture content (OMC) and dry density as maximum dry density (MDD), and standard proctor tests were carried out in the laboratory to as certain these values. Used was a 1000 cc cylindrical mould with a 100mm diameter and 127.3 mm height, a detachable base, and a collar with a 50 mm height. Three layers of the dirt were compacted, each getting 25 hits from a 2.6 kg rammer that was dropped from a height of 310mm.

F. Unconfined Compressive Strength Test

It is one of the quick stand simplest tests that is frequently performed for cohesive soil to assess the shear strength of the soil. Unconfined compression tests were conducted in line with IS:2720 (PartX) -1991 to investigate the impact of coir fiber on the strength behavior of soil. The preparation of cylindrical test specimens involved using a mould with dimensions of 50 mm by 100 mm (height). Samples were loaded into a compression testing machine to determine their strength, and a strain rate of 1.25 mm per minute was applied until the sample failed by cracking or the strain reached more than 20% of the sample's length. That is among the quickest and easiest things.

G. California Bearing Ratio Test

The ratio of the test load to the standard load, expressed in percentage terms for a specific plunger penetration, combined with load penetration and an empirical chart, allows us to calculate the pavement's thickness. to research whether coir fiber can increase soil's CBR value. On soil compacted to their MDD at OMC in a mould with a diameter of 150 mm and a height of 175 mm, provided with a 50 mm height collar and a 50 mm deep displacement disc to keep in the mould during penetration, a California bearing ratio test in an unsaturated condition was carried out in accordance with IS 2720 (PartXVI)-1987.A surcharge was also maintained to stimulate the effect of over lying pavement. A plunger with a diameter of 50mm may be penetrated at a rate of 1.25 mm per minute, and load reading sat various intervals are recorded. For un soaked CBR, CBR values are determined for penetration of 2.5 mm and 5 mm, respectively.

III. RESULT AND DISCUSSION

A. Specific Gravity

Specific gravity is a crucial aspect of soil that is required for geotechnical applications and other purposes. IS claims that the soil's specific gravity was calculated in 1980 and was 2720 (Part III/Sec II). On average, three samples are taken. The specific gravity of the soil sample is discovered to be 2.65.

B. Consistency Limit

According to IS: 2720 (Part V) 1985, the consistency limit tests were conducted. The liquid limit of the soil was discovered to be 26.5%. The plastic limit for the soil sample was 21%. 5.5% of soil has a plasticity index. (PI).

C. Compaction Test

The outcomes of the compaction tests performed on soil containing various amounts of coir fiber are shown in Table1.

TABLE 1. COMPACTION TEST

Sl. No.	Materials	OMC (%)	MDD (KN/m^3)
1	0%coirfiber +soil	10.96	17.78
2	0.5% coir fiber +soil	12.16	17.04
3	1%coir fiber+ soil	13.96	16.47
4	1.5% coir fiber +soil	14.56	14.56

D. Unconfined Compressive Strength Test

In soil that had various amounts of coir fiber, UCS tests were conducted. Table2 shows the results for various mixes.

TABLE 2. UCC TEST

% of coir fiber	Strength (kg/cm^2)
0	0.295
0.5	0.312
1	0.334
1.5	0.338

E. California Bearing Ratio Test

The result of the California bearing ratio test performed on the soil containing various amount of coir fiber are shown inTable3.

TABLE 3. CBR TEST

%of coir fiber	CBR Value
0	1.24
0.5	1.95
1	2.68
1.5	2.55

IV. CONCLUSION

- As the amount of coir fiber increases, maximum dry density decreases. 14.56 KN/m3 is now the value, down from 17.78KN/m3.
- The reduction in Maximum Dry Density is caused by the addition of Coir fiber to the soil in amounts ranging from 0.25to1%.
- The optimal moisture level rose from 10.96% to14.56% as the ratio of coirfiber to soil increased.
- When the percentage of Coir fiber in the soil grew, the unconfined compression strength increased up to 1.5% coir content.
- The amount of Coir fiber that should be incorporated into the soil should be 1.0%, according to the results of several laboratory tests, it increases from 0.295 to 0.388Kg/cm2
- Increases in CBRValuesfrom1.24 to2.68
- Coir fiber is added to boost CBR Value.
- The ideal amount of fiber was discovered to be 1%, with a CBR Value that was2.16 times greater than that of virgin soil.

REFERENCES

1. Effect of coir fiber on the stress-strain behavior of are constituted fine-grained soil, Dasaka, S.M. & Sumesh, K.S. (2011). Natural History189–204 in Fibers, 8(3).
2. Performance of coir fiber reinforced clayey soil. Chaple, P.M., & Dhatrak, A.I.,2013. Engineering International Journal and Science, 2(4), 54-65.
3. Soil mechanics and foundation engineering, S.Chandand Company Limited , New Delhi, Dr.K.R Arora,2010
4. [1:15am,25/03/2023] Aadira Kmct: G.Ayininuola [1:16am, 25/03/2023] Aadira Kmct: Geotechnical properties of coconut coir fiber soil mixture, Ayininuola, G.M., & Oladotun, P.O. (2016). Civil Engineering Journal Research, 6(4), 79-85.
5. Soil stabilization utilizing natural coir fiber.UpadhyayP &Singh Y.

Soil Stabilization: Comparative Study Using Silica Fume and Fly Ash

Fathima Nusrin
Dept. of Civil Enginnering
KMCT College of Engineering for Women Kerala, India
fnusrin1@gmail.com

Varsha Sadanandhan
Dept. of Civil Enginnering
KMCT College of Engineering for Women Kerala, India
varshasadanadankm@gmail.com

Arya P
Dept. of Civil Enginnering
KMCT College of Engineering for Women Kerala, India
arya901kgm@gmail.com

Nihma Kabeer
Dept. of Civil Enginnering
KMCT College of Engineering for Women Kerala, India
nihmakabeer@gmail.com

Sindhu V
Dept. of Civil Enginnering
KMCT College of Engineering for Women Kerala, India

Abstract– The use of waste resources as building material due to their applications, causes serious concern for engineers in various fields. In light of this, studies on the usage of waste products will assist in resolving several environmental issues and lead to innovative, practical engineering discoveries. Clayey soils or expansive soils can pose difficulties for civil engineering projects as they do not have enough strength to withstand the loads imposed on them during construction or during the structure's operational life. This paper reviews different studies done on the impacts of silica fume and fly ash on clayey soils. The researches reveal that silica fume and fly ash performs well to improve the properties of clayey soils.

I. INTRODUCTION

Engineers frequently have to build structures on or in soils that are insufficiently strong to handle the stresses placed on them during construction or for the duration of the structure's service life.

A variety of techniques could be utilized to enhance the performance of subpar soils. The type of soil that has to be improved, its features, and the kind and level of improvement needed in a given application all play a role in the decision of which method to use.

The performance of pavement systems and the qualities of soil can both be improved through soil stabilization. Any stabilizing method utilized aims to improve the soil's workability and constructability as well as its strength, durability, and erosion management. Instead of removing and replacing the material, stabilization may be more successful in improving the soil's characteristics for any given soil. The stabilizing agent may also be chosen based on criteria such as availability or budgetary considerations. This scenario alters the characteristics of certain soils, making them unsuitable as building material. One of the best ways to enhance the qualities of soil is soil stabilization.

The category of reinforced earth technology for soil stabilization includes the inclusion of plastic waste strips. Cement, lime, or waste materials like slag, silica fume, fly ash, etc. have traditionally been used to improve subgrade soils.

II. MATERIALS

Materials used are clay, fly ash and silica fumes.

A. Clay

Clay is difficult to work with because of its low strength, great compressibility, and considerable volumetric changes. Clay needs to be improved before it can be used to construct runways, airports, dams, slurry walls, and landfills. Clay is often improved for stability by improved gradation, a decrease in swelling potential and flexibility, as well as an improvement in strength and workability.

Property	Property value
Water content	8.29
Liquid limit	63.5
Plastic limit	17.27
Plasticity index	46.23
Specific gravity	2.69
Maximum dry density(g/cc)	1.46
Optimum Moisture Content(%)	20
Free swell index	46.5

B. Silica Fume

Silica fume is obtained as a byproduct from production of silicon metal or ferrosilicon alloys. More than 95% of the silica fume particles are smaller than 1 μm, making them incredibly tiny. The major component of silica fume is unprocessed, pure silica. The amount of amorphous silicon dioxide in silica fumes is very high, and the particles are all very small and spherical. Alkali oxides, iron, and magnesium are also present in trace levels. Silica fume is a highly reactive pozzolanic material owing its extreme fineness and extremely high amorphous silicon dioxide concentration.

C. Fly Ash

Fly ash is a byproduct of coal combustion that is made up of the flu vapors and particulates (fine particles of burned fuel) which are driven out of coal-fired boilers. Fly ash is made up of spherical particles that range in size from 0.5 to 100 pm. Fly ash mostly consists of silicon dioxide, which comes in two different forms: amorphous and crystalline. Fly ash contains various environmental toxins such arsenic, barium, beryllium, chromium, lead, manganese, and other heavy metals.

III. METHODOLOGY OF EXPERIMENT

The literature review was conducted for the thorough understanding of properties and behavior of the soils and tests to be conducted. The soil which was known to be weak was collected from Mavoor. Samples were collected within a depth of about 1.5m from the existing ground surface. The collected soil was kept in a large polythene bag and dried in air for about 7 days. After drying the soil's physical and index properties of the soil have been determined by sieve analysis specific gravity and atterberg's limit test. It is seen that the soil contains a high liquid limit, low unit weight, and high water content. Also, compaction test, california bearing ratio test, unconfined compressive strength test and direct shear test are conducted to analyze the strength of the native soil.

Into this soil, 5%, 10%, 15%, 20%, 25%, 30% of Fly Ash by dry weight of soil were mixed with the natural soil sample in order to investigate the utilization of the material and improvement of the engineering properties of the clay soil itself. The maximum dry density (MDD) values and the optimum moisture content (OMC) of the samples were obtained by using the normal compaction test. To determine the strength of the mixtures, Unconfined Compression Test (UCT), California bearing ratio test and direct shear test has been conducted. Finally, for each sample, Atterberg Limits have been determined. The optimum dosage of the fly ash is determined. Further, to the clayey soil Silica fume is mixed on a percentage basis i.e. 0%, 5%, 10%, 15% and 20% by weight of dry soil. The compaction test, california bearing ratio test, unconfined compressive strength test and direct shear test were conducted on soil and Silica Fume mixes ;as per relevant IS Code. Atterberg's limit tests are also conducted to determine the index properties. Also, the optimum dosage is determined. After the soil is treated with both silica fumes and fly ash, a comparative study is carried out to study the behavioral differentiation and determine the best additive.

IV. RESULTS AND DISCUSSION

A. Effect of Silica Fume

TABLE 1. HEAVY COMPATION TEST

% of Silica fume	Max. dry density (g/cc)	Optimum moisture content (%)
5	1.42	22
10	1.39	23
15	1.37	24
20	1.35	26
25	1.32	27

TABLE2. CALIFORNIA BEARING RATIO TEST

% of Silica fume	CBR value
5	3.76
10	3.99
15	5.04
20	6.09
25	6.68

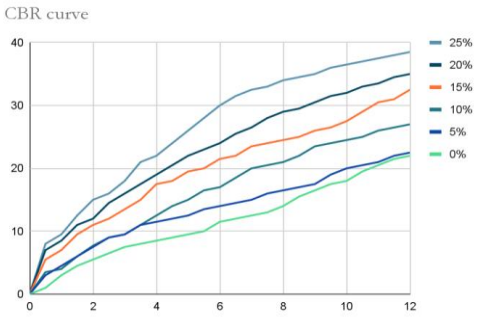

Fig. 1.CBR curve

TABLE 3. UNCONFINED COMPRESSION TEST

% of Silica fume	Compressive strength (kg/cm^2)	Cohesion (kg/cm^2)
5	1.42	0.71
10	1.57	0.785
15	1.76	0.88
20	1.87	0.935
25	1.92	0.96

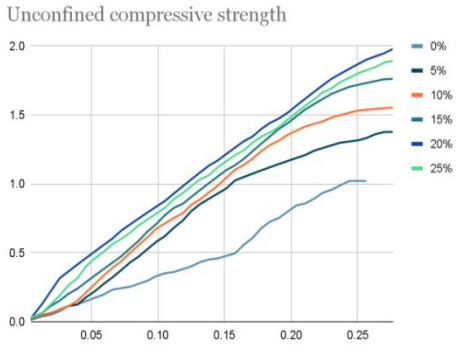

Fig. 2. UCC curve

B. Effect of Fly Ash

TABLE 1. HEAVY COMPACTION TEST

% of Fly ash	Max. dry density (g/cc)	Optimum moisture content(%)
5	1.48	22
10	1.465	24
15	1.44	25
20	1.414	26

TABLE 2. CALIFORNIA BEARING RATIO TEST

% of Fly ash	CBR value
5	3.97
10	5.22
15	6.269
20	7.10

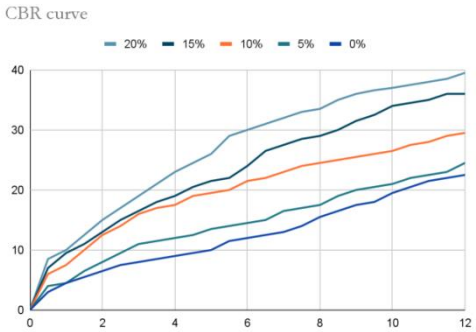

Fig. 1. CBR curve

TABLE 3. UNCONFINED COMPRESSION TEST

% of Fly ash	Compressive strength (kg/cm^2)	Cohesion (kg/cm^2)
5	1.51	0.755
10	1.65	0.825
15	1.78	0.89
20	1.95	0.975

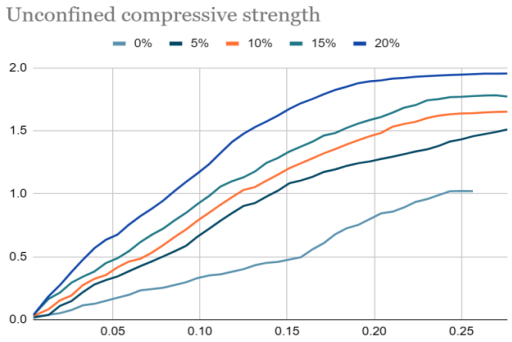

Fig. 2. UCC curve

V. CONCLUSION

- With increase in percentage of additives (silica fume and fly ash) the maximum dry density decreases and optimum moisture content increases.
- On addition of silica fume the maximum dry density went down from 1.42 g/cc to 1.32 g/cc and corresponding optimum moisture content rose from 22% to 27%.
- Addition of fly ash resulted in a decrease in the highest dry density from 1.48 g/cc to 1.414 g/cc and an increase in the optimum moisture content from 22% to 26%.
- The CBR value of the soil on addition of silica fume increases from 3.76 to 6.68
- Addition of fly ash exhibits a better results by increasing the CBR value from 3.97 to 7.10
- UCC value on addition of silica fume increased from 1.42 kg/cm2 to 1.92 kg/cm2 and cohesion from 0.71 kg/cm2 to 0.96 kg/cm2
- When fly ash was added UCC value improved from 1.51 kg/cm2 to 1.95 kg/cm2 and cohesion from 0.755 kg/cm2 to 0.975 kg/cm2

VI. FUTURE WORKS

- Direct shear test for native soil, stabilized soil with varying percentages of silica fume, stabilized soil with varying percentages of fly ash
- Determination of bearing capacity using Rankine's formula.
- Comparative study.

Partial Replacement of Cement by Cow Dung Ash and Fine Aggregate by Sawdust in Concrete

Agishlya s suresh
Dept. of Civil Enginnering
KMCT College of Engineering for Women Kerala, India
agishlya434@gmail.com

Dilna NV
Dept. of Civil Enginnering
KMCT College of Engineering for Women Kerala, India
dilnanair533@gmail.com

Ilfadiya KV
Dept. of Civil Enginnering
KMCT College of Engineering for Women Kerala, India
ilfadiyash@gmail.com

Hibamariyam M
Dept. of Civil Enginnering
KMCT College of Engineering for Women Kerala, India
hibalenu@gmail.com

Chithra UT
Dept. of Civil Enginnering
KMCT College of Engineering for Women Kerala, India

Abstract--The population in the 21st century increased day by day, which require many buildings around the world. Due to this the demand of concrete has been increased. Concrete has high strength and durability so that, it is mostly used for the building construction work. Cement is the most important component used to produce concrete. This study focuses on compressive, flexural, split tensile strength of concrete containing different percentages of cow dung ash and sawdust as a partial replacement of cement and fine aggregate.

Keywords—cow dung ash, sawdust

INTRODUCTION

Concrete is the mixture of composite materials such as cement, fine, coarse aggregate, and water. It is second most constituent used in the world after water, and mostly used for the construction work. The expense of building construction work increasing daily as the result of increasing the amount of material. Due to this, there is a need to examine the use of different materials which are commonly available in nature. The reduction in the expense of concrete manufacturing will reduce the cost of construction and open a way for law income earner to become a house owner. Cow dung, sawdust are locally available and can be used for the production of concrete. These concretes are cost effective and environment friendly.

A. Cow Dung Ash

Cow dung is a mixture of indigestible plant, water and other materials that are released from animal intestine. The cowdung was collected and dried under sunlight at high temperature and cooled it. Then these crushed in to a powder form.

B. Sawdust

Sawdust is generated in the wood industry. It is a waste material of wood. Small irregular chips are produced when wood logs of different sizes are chopped.

II. EXPERIMENTAL STUDY

A. Cement

One of the most important constituent of concrete is cement, which act as a binder material in concrete. It keeps the fine and coarse aggregate together by filling the void spaces between the aggregate. In the entire experimental study, Portland slag cement with conforming to BIS (IS: 455-1989), Zuari cement was used for this experiment.

1) Specific gravity of cement

It is the ratio between the weight of a given volume of material and weight of equal volume of water. The specific gravity of Portland cement is around 3.15. Le Chaterliers flask is used to check the specific gravity.

2) Standard consistency test

The test was conducted by using Vicat apparatus conformed to IS: 5313: 1998 is used to conduct the test. The test is usually used to decide the consistency. 32%water is mandatory to

achieve the normal consistency. This test was performed according to IS 4031: 1988 part 4.

3) Initial and final setting time

To determine vicat apparatus is used. For OPC initial setting time is 30 minutes and final setting time is 600 minutes as per IS 4031 part 5. Here we obtained initial setting time as 45 minutes and final setting time as 7 hrs.

4) Fineness test

For the ordinary Portland cement the residue shall not increase 10%.The fineness is measured by sieving cement through standard sieve. Here we obtained 8% as fineness of cement.

B. Fine Aggregate

1) Sieve analysis

Sieve analysis is calculated by using set of standard sieves. As per IS: 2386 (part 1) 1963. Here we obtained fineness modulus is 2.93.

2) Specific gravity of fine aggregate

The specific gravity of sand considered as around 2.711. Apparatus is pycnometer. As per IS:2386 (part3)-1963 the test is conducted. The obtained specific gravity is 2.47.

3) Bulk density

It is the mass of many particle of material divided by the total volume of the occupied.It is done as per IS: 2386 part 3. Here we obtained the bulk density is 1397 kg/m3.

C. Coarse Aggregate

Coarse aggregate means irregular granular material of crushed stone. Here obtained specific gravity is 2.966 and bulk density is 1603kg/m3

D. Cow Dung Ash

The obtained specific gravity is 2.89.

E. Fresh Concrete Mix

1) Slump test

The test was done by using slump cone. The test is performed to find out the workability of fresh concrete mix. This test is according to Indian standard code IS: 1199-1959.

F. Harden Concrete

1) Compressive strength

As per IS:516:1956,the test was conducted by using three specimens having size 150x150 mm and the average strength was taken as the cube compressive strength of concrete. The tests were carried out by using compression testing machine.

2) Flexural strength

The test was done by IS:516:1956. The test was conducted on beam specimens.

3) Split tensile strength

It is used to discover tensile strength of concrete. Cylinder specimens are used. Test conducted by using compressive testing machine.

III. CASTING PROCEDURE

Cement was mixed with the fine aggregate along with cow dung ash, sawdust and coarse aggregate were added to the mix proportion for each mix. Water-cement ratio is taken as 0.5. It is being mixed well for obtaining a mixture of uniform color and consistency.Hence it is ready for casting. Then concrete mix is filled into cube, cylinder, beam mold which has been cleaned and oiled. Mold get filled in 3 layers and each layer should compacted 25 times. Then they were kept in water tank for curing to maintain the moisture on the surface of the specimen for desired age.

IV. RESULT AND DISCUSSION

TABLE 1. SLUMP TEST

Mix type	Slump(cm)
0% Replacement	5
6%Cowdung ash & 5% sawdust	8
6%Cowdung ash & 10% sawdust	10
6% Cowdung ash & 15% sawdust	10.5
6% Cowdung ash & 15% sawdust	11

TABLE 2. COMPRESSIVE STRENGTH

The cubes were after 7 days of curing. The test was conducted. On CTM machine. 4.3 split tensile strength & flexural strength

Mix type	**7 days**	**28 days**
0% replacement	14.814N/mm^2	21.9N/mm^2
6% cowdung ash & 5% sawdust	15.2N/mm^2	22.4 N/mm^2
6% cowdung ash & 10% sawdust	15.39N/mm^2	23.14N/mm^2

6% cowdung ash & 15% sawdust	15.68N/mm^2	23.46N/mm^2
6% cowdung ash & 20% sawdust	15.01N/mm^2	21.3N/mm²

TABLE 3. SPLIT TENSILE STRENGTH & FLEXURAL STRENGTH

Mix type	28 days split tensile strength	28 days flexural strength
0% Replacement	2.70N/mm^2	3.5N/mm^2
6% Cow dung ash & 5% sawdust	2.81N/mm²	3.31N/mm²
6% Cow dung ash & 10% sawdust	2.68N/mm²	3N/mm²
6% Cow dung ash & 15% sawdust	2.5N/mm^2	2.89N/mm^2
6% Cow dung ash & 20% sawdust	2.48N/mm^2	2.55N/mm^2

V. CONCLUSIONS

In M20 grade concrete, the fine aggregate and cement was replaced by 5%, 10%, 15%, 20% of sawdust and 6% cow dung ash respectively. It is observed that compressive strength increased in 5%,10%,15% of sawdust replacement and got decreased in 20% replacement. At 5% replacement split tensile strength increases,10%, 15%, 20% got decreased. The flexural strength decreases at 5, 10,15,20% replacement.

REFERENCES

1. Agbede O. I. &Monash J. (2009) Suitability of Periwinkle Shell as Partial Replacement for Gravel in Concrete
2. Ayeni October [2015] Investigation of properties of concrete using saw dust as partial replacement of sand
3. L. O. Ettu variation of OPC – Sawdust ash composite strength with mix proportion.

ABOUT RAiSE '23

An engineer is a professional concerned with applying scientific knowledge, mathematics, and innovation to develop solutions for the technological and societal problems. The International Conference on Recent Advancements in Science and Engineering (RAiSE '23) will be a remarkable international congregation for sharing expertise in innovations and demands in engineering technology. The RAiSE '23 provides a forum for a strong and sophisticated interaction between academia and industry to showcase their contribution and opportunities for evolution in the research work for improved outcomes thereby bridging the gap in the research being carried out in the academia and the industry. The industry, in turn, benefits from the exposure to cutting-edge problems that require future research and deployment of industrial-scale resources through interaction with the academic researchers. The conference mainly focuses on the advancements in the areas Science, Technology, Engineering and Management. The RAiSE '23 aims to bring up numerous ideas and solutions to address the present-day challenges in the fields of science, engineering and technology.

Dr. D. Jerline Sheebha Anni *received B.Tech. degree in Information Technology and Master of Engineering in Computer Science and Engineering from Anna University, India and she received her Ph. D degree in 2019 from VIT University, India. She had more than 15 years of experience in various reputed institutes in three different states of south India. She is currently working as Principal in KMCT College of Engineering for Women, Kozhikode, Kerala. She has published more than 9 SCI indexed Journals and Book Chapters. She has organised and participated various seminars and conferences. Her areas of interest are in Wireless Sensor Networks, Network Security and Soft Computing. She is a member of IEEE, IE(I), and ISTE. She had successfully completed AICTE funded MODROBS Project as the Co-Principal Investigator. Under her mentorship, students got the funding in Karnataka State Council for Science and Technology. She has received Best Researcher Award-2020 from International Research Awards on New Science Inventions (NESIN-2020).*

ISBN 978-93-5515-988-5
9 789355 159885